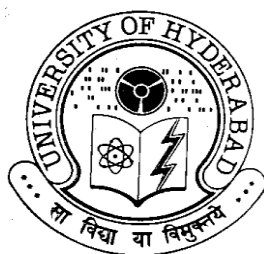


POLYMORPHISM AND SOLUBILITY OF SELECTED ACTIVE PHARMACEUTICAL INGREDIENTS

**A Thesis Submitted for the work carried out during 2009-2014 to
the University of Hyderabad in partial fulfillment of the award of
a Ph.D. degree in Chemistry**

By

S. SUDALAI KUMAR



**School of Chemistry
University of Hyderabad
Central University P.O., Gachibowli
Hyderabad 500 046
Telangana
India**

August 2014

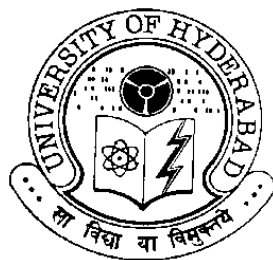
Dedicated to the Celebration of

***International Year of
Crystallography (IYCr 2014)***

*“The important thing in science is not so much to obtain new facts as to discover
new ways of thinking about them.” -Sir William Henry Bragg (1862–1942)*

My parents and Brother

சுப்பிரமணியன், பேச்சியம்மாள் மற்றும் வடிவேல்



CERTIFICATE

This is to certify that the thesis entitled **“Polymorphism and Solubility of Selected Active Pharmaceutical Ingredients”** submitted by **S. Sudalai Kumar** bearing Regd. No. 09CHPH38 in partial fulfillment of the requirements for the award of Doctor of Philosophy in Chemistry is a bonafide work carried out by him under my supervision and guidance.

The thesis has not been submitted previously in part or in full to this or any other University or Institution for the award of any degree or diploma.

Dean
School of Chemistry

Prof. Ashwini Nangia
Thesis Supervisor

DECLARATION

I am **S. Sudalai Kumar** hereby declare that this thesis entitled **“Polymorphism and Solubility of Selected Active Pharmaceutical Ingredients”** submitted by me under the guidance and supervision of **Professor Dr. Ashwini Nangia** is a bonafide research work. I also declare that it has not been submitted previously in part or in full to this University or any other University of Institution for the award of any degree or diploma.

Name: **S. Sudalai Kumar**

Date:

August 2014

Hyderabad

Signature of the Student

Regd. No. 09CHPH38

Education is what survives when what has been learned has been forgotten.
- B. F. Skinner (US psychologist, 1904 - 1990)

Preface

Chemistry, the study of the formation and properties of molecules and materials, is central to the advancement of science and technology. Chemistry deals with the properties that distinguish one substance from another. In Chemistry, there are several different branches including organic chemistry, inorganic chemistry, physical chemistry, analytical chemistry and biochemistry. It's a science in its own right that supports and interacts with other scientific disciplines. In connection with biology, physics, medicine, materials science and other core disciplines, it offers effective solutions to problems facing the world today and renders mankind the essentialities for tomorrow. By discovering the world of molecules and ways to synthesize them, chemists profoundly influence and enable science and technology and shape the world as we know it today. Chemistry can be broadly defined as the study of matter and the changes that it undergoes. Many people think of chemistry as the chemical changes in terms of mysterious experiments conducted in chemical laboratories with strange chemicals and complex apparatus. This is only one aspect of chemistry. Chemical changes are also natural processes and take place all about us. The burning of coal, gas, and wood; the cooking of meat and other foods; the rusting of a kitchen knife and the tarnishing of silver-all these things which we take for granted involve chemical changes. Life processes such as growth, digestion, and breathing are also examples of chemical change. Many of these changes, which take place in our bodies, are so complex that they cannot yet be duplicated in chemical laboratories.

The emergence of supramolecular chemistry is a great evolution of human knowledge and is an effort to understand and analyze the

supermolecules and their important scientific findings. Advancement of this field along with crystal engineering paves the way for the growth of X-ray crystallography in organic chemistry, a branch of chemistry. The crystal engineering approach is also used in the design of molecules prior to synthesis is more convenient, insightful and cost effective and useful in designing new candidates with desired physical and chemical properties. In recent years polymorphs, cocrystals, salts, eutectics and solid solutions have progressed into the direct applications in the pharmaceutical industry because they exhibit different properties i.e., stability, solubility, dissolution and bioavailability. These strategies are used to understand the very subtle but weak non-covalent interactions that guide many complex biological processes to design the drug molecules and solve the issues associated with marketed drugs. The present thesis work is such an attempt focusing on the designing of molecules for sulfa drugs, amphoteric drugs, fenamates, amino acids and fibrates.

Chapters 2, 3 and 4 are dealing with the polymorphism that exhibit different properties of bio-active sulfonamides, amphoteric molecules and *N*-acetyl-L-cysteine drug respectively. These sulfonamides with well analyzed crystal structures have been taken for the present study in order to compare the molecular conformations with solubility and dissolution trends of six sulfonamides. Therefore in chapter 2, the solubility properties of twisted molecular conformations are responsible for the high solubility behavior due to the less packing of molecules in the crystal lattice. Hence the functional group modification can be used to solve the solubility issues via chemical modification in the drug discovery step. Chapter 3 is just opposite to the above one, the functional group modification was done by using the crystal engineering strategy of optimizing the zwitterionic polymorphs for the better solubility and stability. We proved it through the structure-solubility relationship and apply the same trend in other drugs

without any more chemical modification. The chapter 4 is interesting one that deals with identification of novel polymorphs of NAC and the comparison of structure-stability relationship. The thermal stability and thermodynamic stability of polymorphs were investigated in this chapter and recommending the NAC form I as the suitable form for the formulation from the comparison of hydrogen bonding and other noncovalent interactions with stable modification.

Moving from polymorphs to designing molecules for drugs to pharmaceutical materials, a complete understanding of the strong and weak intermolecular interactions that stabilize the complex/ multi-component systems is essential for me to expand the idea of understanding the structure-property relationship studies into it. Realizing the promise these studies have by leading to new idea for engineering novel cocrystals and salt materials are the complex formation drugs substances with GRAS coformers (chapter 5 and 6). A complete solid state characterization of all cocrystals and salts is done in this thesis to understand the effect of these multi-component systems on solubility and dissolution rate. The competencies of salts and cocrystals towards solubility have been studied in chapter 5 and found that salts are high soluble and stable compared to the cocrystals. Therefore, salt formation techniques are extended to the chapter 6 for some of the BCS class II drugs to address the solubility issues. Successfully, these salts are well characterized in terms of improving the drug properties and interestingly the solubility is 10 times more for all drug salts. The mineral salt and molecular salts are of having equal advantage of solubility and dissolution properties. Out of all these works, six papers have been published and one more are in a ready to submit. The published results, after minor modifications have been straight-away adapted as chapter 2, 3, 4 and 5. Chapter I describe the background of the several solid forms, characterization and structure-property relationship, along with a brief note

on supramolecular synthons. Scope of the thesis is appended at the end of chapter 1 and 7. Description about polymorphs, cocrystals, salts and eutectics is avoided in the introduction section of every chapter since it has been discussed in the introduction of chapter 1. All crystallographic details related to polymorphs, salts and cocrystals are mentioned in the tables in the appendix at the end of the 7 chapters.

"Life is Chemistry: Dilute your Sorrow, Evaporate your Worries, Filter your Mistakes and Boil your Ego. "You will get the Crystal of Happiness"

திரு. சு. சுடலை குமார்

(S. Sudalai Kumar)

ACKNOWLEDGEMENT

With a profound sense of gratitude, I thank my supervisor **Prof. Dr. Ashwini Nangia** for his constant cooperation, encouragement and kind guidance, and it is my immense pleasure to thank UGC Networking Resource Centre for introducing me to this research field. It has been great pleasure and fortune to have such a summer project work with my guide before my PhD joining. I am also indebted to him for the work freedom he has given me during the summer project work and my entire PhD tenure. I am also thankful to the former Coordinator of UGC networking centre and the former Dean, School of Chemistry, Prof. M. V. Rajasekharan for my UGC summer fellowship and help.

I would like to thank the former and present Dean, School of Chemistry, for their constant inspiration and for allowing me to avail the available facilities. I am extremely thankful individually to the entire faculty and staff members of the school for their various help and cooperation in recording X-ray diffractometers and solid state NMR facility especially instrument operators Mr. Kumar, Mr. Ramana, Mr. Srilakshmi, Mr. Vijayalakshmi, Mr. Turabudhin, Mr. Sathyanarayana and Mr. Durgesh in School of Chemistry.

I wish to record my thanks to CSIR for fellowship and contingency support. I also would like to record my thanks to DST-SERB for ITS grant, CICS and CSIR for travel fellowship grant for funding my conference visit to ICCOSS 2013 conference at St. Catherine College, Oxford, UK for delivering the lecture.

My sincere thanks to Dr. Palash Sanphui for guiding and teaching me single crystal X-ray machine operation, Dr. R. Thakuria for voriconazole drug and Dr. N. K. Nath for project works. I thank Dr. B. Sarma and Dr. N. Jagadessh Babu for the encouragement and Dr. S. Cherukuvada for lab instruments.

I express my heartiest thanks to all my teachers from my school especially Science teachers from Concordia school (Vallioor), especially Mr. K. Natarajan (Kamaraj Municipal Higher Secondary School, Pettai), my UG Professors especially Dr. S. J. A. Diraviam and Dr. A. Thomas (St. Xavier's College,

Palayamkottai) and PG Professors Dr. V. S. S. Srinivasan, Dr. K. Nagarajan, Dr. A. Prince and Dr. S. Muniraj (Ramakrishna Mission Vivekananda College, Mylapore) for their wonderful teaching and education throughout my academics. I am also thankful to Prof. Dr. R. Raghunathan and my project senior Dr. Purusothaman for their research helps and support during my M. Sc. summer project in University of Madras. Kindness and concern of my professors for their students is an innate trait of them that deserves to be acknowledged here.

I express my sincere thanks to acknowledge my lab seniors Dr. B. K. Saha, Dr. S. Aitipamula, Dr. S. Reddy, Dr. M. Reddy, Dr. B. K. Reddy, Dr. S. Roy, Mr. S. Chandran and Dr. R. Goud and other lab seniors Dr. Arunbabu Dhamodaran, Dr. Tanneeru, Dr. Ellendula, Dr. Bharath, Dr. Anjaneyalu, Dr. Ganesan, Dr. Tammineni, Dr. Ramesh, Dr. Viji, Dr. Kishore, Dr. Kodiyath, Patida, Rishi da, Raghaviah, Basak, Sandhanam, Mandava, Sathish and Sai Arun for their help and encouragement at various stages of my Ph. D. My sincere thanks to my labmates Kalyan, Maddileti, Geetha, Suresh, Suryanarayana, Swagath, Sharath, Chaitanya, Kranthi, Billa Kishore, A. Madhavi, Simarpreet Kaur, Srikanth Reddy, Raghavender, Babu, Anilkumar, Harish, Abdul, Satyanarayana, Jaiboon, Moumita, Naveen, Himanshu, Kanishka, Sumanth, Uday, Sreenu, Gita, Uma, Dinesh, Kiran and Swarupa for maintaining a friendly and cooperative atmosphere in the lab.

My appreciation, gratitude earnest feelings to my mother S. Petchiyammal for giving me her constant mental support and suggestions thought out my entire Ph.D life. I should thank my friends Mr. S. Manojveer, Mr. N. Ram Kumar, Dr. B. J. Ganesh Kumar, Dr. Vignesh Babu and Dr. C. Gupta for encouraging me in research. My pleasant association with HCU friends Tamilarasan, Justin, Mohanraj, Raja, Nayan, Sanathan, Raju, Prakash, Praveen, Satyajit, Ashok, Ajay, Naveen, Chandra, Raj Kumar, Moorthy, Murali, Shakthi Devi, Suresh, Nanda, Jeevandham, Prasad, Suman, Varul, Chandhu, Murugananth, Shanmugaraja, Thirupathi, Tridib, Mehboob, Reddy and Tanmay is unforgettable. I would like to acknowledge few of my beloved seniors and friends outside HCU are Arun,

Vasu, Ramsankar, Robinson James, Dr. Vijay Solomon, Mothish, Kalaivanan, Anand, Balan, Ramesh, Pradeep, Subramanian, Venkat, Shyam, Kannan, Ravi, Arumugam, Kodama, Helene, Johmoto, Sasaki, Ida, Marivel, Grecu, Roots, Vysakh, Vijay, Prasanna, Mani, Senthil, Rajamoorthy, Ritesh, Srinu, Stanly, Sachin, Sudhir, Chaitrali, Tamal, Periyasami, Kumaraguru, Karthik, Saravanan, Ekambaram, Anandhan and Simon. Finally, I take great pleasure in expressing my thanks to my father V. Subramanian, younger brother S. Vadivel and cousins Kannan, Raja, Mahalaxmi, Kumar and Malathi for their support and encouragement. Eventually, I thank Prof. Joly Puthussery, Prof. N. Naveen Kumar and Prof. Y. A. Sudhakar Reddy for the moral support in HCU campus.

I can't imagine my current position without the support from the Tamil Nadu government officials and so I thank Thiru. T. Udhayachandran IAS (TNPSC), Thiru. R. Natraj IPS (TNPSC) and Thiru. K. S. Sripathi IAS (TNSIC) for their help and advice and finally Mr. P. Balasubramanian, social activist (Mylapore) for the moral support and appreciation. The blessings and best wishes of my parents are to keep me active throughout my life and hereafter. They teach me what I am and I owe everything to them. Dedicating this thesis to my parents is a minor recognition for their invaluable support and encouragement.

S. Sudalai Kumar

ABOUT THE AUTHOR

Thiru. S. Sudalai Kumar, eldest son of Thiru. V. Subramanian and Tmt. S. Petchiyammal, was born in Pattarpuram, Nanguneri Taluk, Tirunelveli District of Tamil Nadu, India, in 1987. He received his primary education from Pattarpuram Government Primary School, CMS Mary Arden School (Palayamkottai) and Concordia High Sec. School (Vallioor) in Tirunelveli District and completed his secondary school and higher secondary education at Kamaraj Municipal Higher Secondary School, Pettai, Tirunelveli. He then completed his B. Sc. in Chemistry from St. Xavier's College (Manonmaniam Sundaranar University), Palayamkottai, Tamil Nadu. After the completion of his M.Sc. in Chemistry from Ramakrishna Mission Vivekananda College (University of Madras), Chennai, Tamil Nadu, he then joined the School of Chemistry, University of Hyderabad to pursue his PhD in Chemistry (Crystal engineering and X-ray Crystallography) in 2009 under the supervision of Prof Ashwini Nangia. He qualified CSIR-UGC-National Eligibility Test for Junior Research Fellowship (JRF) as CSIR JRF (59th rank in 2009 NET exam) held in June 2009 and was awarded research fellowship by the Council of Scientific and Industrial Research (CSIR) during 2010-2015 periods.

திரு. சு. சுடலை குமார் 1987ல் தமிழ்நாட்டில் திருநெல்வேலி மாவட்டத்தில் உள்ள பட்டர்புரம் என்ற கிராமத்தில் பிறந்தார். அவரது பெற்றோர்கள் திரு. சுப்பிரமணியன் மற்றும் திருமதி. பேச்சியம்மாள் ஆவர். அவருக்கு ஒரு இளைய சகோதரர் திரு. எஸ். வடிவேல் என்பவரும் இருக்கிறார். அவர் தனது முதன்மை பள்ளி கல்வியை பாளையங்கோட்டை மேரிஸ் பள்ளியிலும் மற்றும் கன்காந்தியா மேல்நிலைப்பள்ளியிலும் பின்னர் இரண்டாம் நிலை கல்வியை திருநெல்வேலி மாவட்டத்தில் உள்ள பேட்டை காமராஜ் நகராட்சி மேல்நிலைப்பள்ளியிலும் பயின்றார். அதன் பின்னர் இளநிலை அறிவியல் வேதியியல் பட்டப்படிப்பை புனித சேவியர் கல்லூரியிலும் (மனோன்மணியம் சுந்தரனார் பல்கலைக்கழகம்) தனது முதுகலை வேதியியல் அறிவியல் பட்டப்படிப்பை ராமகிருஷ்ணா மிஷன் விவேகானந்தா கல்லூரியிலும் (சென்னை பல்கலைக்கழகம்) படித்தார். ஜூன் மாதம் 2009ல் நடைபெற்ற சிஎஸ்ஐஆர் இளநிலை ஆராய்ச்சியாளர் நெட் தேர்வில் 59 வது ரேங்க் எடுத்ததன் மூலம் அவர் பேராசிரியர் அஸ்வினி நாங்கியா மேற்பார்வையின் கீழ் 2009ல் இரசாயனவியல் டாக்டர் பட்டம் தொடர், ஹைதராபாத் மத்திய பல்கலைக்கழகத்தில் சேர்ந்தார். 2010 முதல் 2012 வரை இளநிலை ஆராய்ச்சியாளருக்கான அறிவியல் மற்றும் தொழில்நுறை ஆராய்ச்சி கவுன்சில் (சிஎஸ்ஐஆர்) மூலம் ஆராய்ச்சி உதவித்தொகையும் வழங்கப்பட்டது. பின்னர் அந்த உதவியும் சிஎஸ்ஐஆர் மூலம் 2014 வரை நீடிக்கப்பட்டது.

Synopsis

This thesis entitled “**Polymorphism and Solubility of Selected Active Pharmaceutical Ingredients**” consists of seven chapters.

CHAPTER ONE

Introduction

Chemistry is an evolving subject and it is traditionally divided into four categories as organic, inorganic, physical and analytical chemistry. A new classification in the modern era is the (supramolecular) solid state chemistry which is different from the molecular chemistry (liquids and gases). It has now reached the immense importance in the level of identification, separation and characterization of different crystalline forms of the same molecule or of aggregates of molecules with other molecules due to the difference in their physical and chemical properties. Physical properties are an intrinsic part of solid state chemistry since the broad area of structure-property relationship needs the identification of new solid crystalline forms such as polymorphs, solvates/hydrates, salts and cocrystals (Figure 1) and their characterization to understand their properties to control their activity. The importance of identifying these crystalline materials is to investigate their physico-chemical issues of active pharmaceutical ingredients (APIs) and address the solubility, stability and hydration problems using the crystal engineering approach. Crystal engineering of APIs through cocrystallization has gained an immense interest among the academicians, pharmaceutical scientists and US-FDA regulating as means of optimizing the physical properties and/or stability of solid dosage forms.

McCrone defined the term polymorphism as “*a solid crystalline phase of a given compound resulting from the possibility of at least two different crystalline arrangements of the molecules of that compound in the solid state*”. It can be classified as conformational polymorph (due to flexible rotation of molecule), synthon polymorph (due to difference in hydrogen bonding patterns) and packing polymorph (because of changes in the crystal packing of molecules)

in 2D or 3D. The term Pharmaceutical Cocrystal can be defined as “*the crystalline complex of two or more neutral molecules is constituted including API, bonding together in the crystal lattice through non-covalent interactions such as hydrogen bonding*”. Polymorphism and Cocrystallization has great importance in pharmaceutical industry, dyes and pigment, agrochemicals, explosive materials etc. due to its ability to alter the melting point, color, compressibility, filterability, stability, solubility etc. of the challenging solid materials. Salt formation is an acid base reaction and a compound having an acidic or basic group can crystallize in salt preparation in solution crystallizations. The traditional approach of salt formulation to improve drug solubility is unsuccessful with the molecules that lack of ionisable functional groups, have sensitive moieties that are prone to decomposition/ racemisation and/or are not sufficiently acidic /basic to enable salt formation.

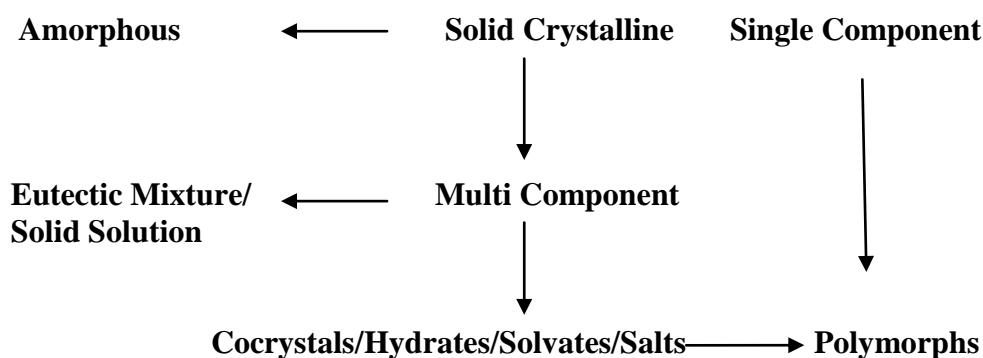


Figure 1 Various solid forms based on structure and composition variations.

Solubility is one of the most important physicochemical properties when evaluating compounds as potential drug candidates. The thermodynamic solubility of a compound in a solvent is the maximum amount of the most stable crystalline form of the compound that can remain in solution under equilibrium conditions. Kinetics is a time-dependent phenomenon, and thermodynamics is, by definition, time independent. Poor aqueous solubility of any drug is likely to result in poor absorption, even if the permeation rate is high, since the flux of a drug across the intestinal membrane is proportional to the concentration gradient between the intestinal lumen and the blood. Again high concentrations of poorly

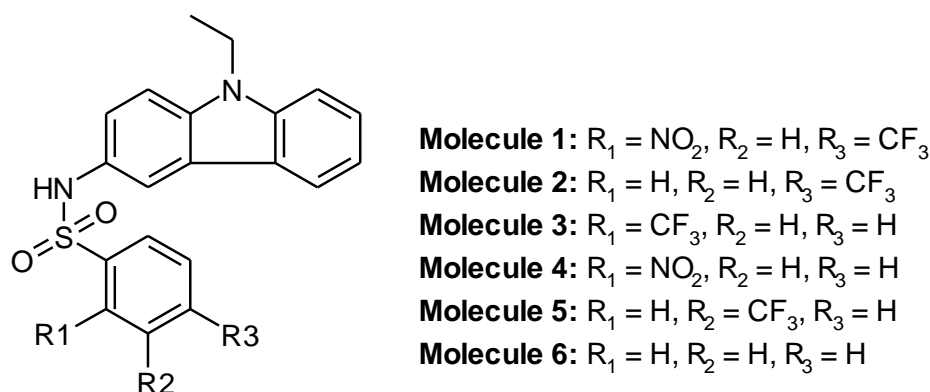
soluble drugs in organisms may result in crystallization and acute toxicity. There is need to balance between solubility and dosage form of a drug. Overall, poor solubility of drug candidates has been identified as the main cause of numerous drug development failures at the final stages of formulations. We addressed these issues in some of the active compounds by correlating the differences in conformation, changes in functional groups in polymorphs and this study provides a guide in drug delivery for solubility optimization. In this thesis, we have chosen few drugs or biologically active compounds to study their polymorphic behaviours and cocrystal/salt formation using high throughput screening and highlighted their solubility and stability differences with respect to the structure modifications such as cocrystals and salt formation.

CHAPTER TWO

Polymorphism in Cardiosulfa and Its Analogs

Cardiosulfa is a biologically active sulfonamide molecule which induces abnormal heart development in zebrafish embryo through activation of the aryl hydrocarbon receptor (AhR). The present report is a systematic study of polymorphic search of cardiosulfa (more active) and its biologically active analogs (moderate and less active) belong to the *N*-(9-ethyl-9H-carbazol-3-yl)benzene sulfonamide skeleton (Scheme 1). Cardiosulfa (molecule **1**, $R_1 = \text{NO}_2$, $R_2 = \text{H}$, $R_3 = \text{CF}_3$), molecule **2** (H , H , CF_3), molecule **3** (CF_3 , H , H), molecule **4** (NO_2 , H , H), molecule **5** (H , CF_3 , H), and molecule **6** (H , H , H) were synthesized and subjected to a polymorph search and solid state characterization by X-ray diffraction, DSC, VT-PXRD, FT-IR and ss-NMR. Molecule **1** was obtained in a single crystalline modification which is sustained by $\text{N-H}\cdots\pi$ and $\text{C-H}\cdots\text{O}$ interactions, but devoid of strong intermolecular $\text{N-H}\cdots\text{O}$ hydrogen bonds. Molecule **2** showed a $\text{N-H}\cdots\text{O}$ catemer *C*(4) chain in Form I whereas a second polymorph was characterized by PXRD. The dimorphs of molecule **3** contain $\text{N-H}\cdots\pi$ and $\text{C-H}\cdots\text{O}$ interactions but no $\text{N-H}\cdots\text{O}$ H bonds. Molecule **4** is trimorphic with $\text{N-H}\cdots\text{O}$ catemer in Form I, and $\text{N-H}\cdots\pi$ and $\text{C-H}\cdots\text{O}$ interactions in Form II, and a third polymorph was characterized by PXRD. Both

polymorphs of molecule **5** contain the N–H···O catemer C(4) chain, whereas the sulfonamide N–H···O dimer synthon $R_2^2(8)$ was observed in polymorphs of **6**. Differences in the strong and weak hydrogen bond motifs were correlated with the substituent groups and the solubility and dissolution rates with the conformation in the crystal structure of **1-6** (Figure 2). Higher solubility compounds, such as **2** (10.5 mg/mL) and **5** (4.4 mg/mL), adopt a twisted confirmation whereas less soluble **1** (0.9 mg/mL) is nearly planar. This study provides practical guides for functional group modification of drug lead compounds for solubility optimization.



Scheme 1 Molecular structures of Cardiosulfa and its analogs.

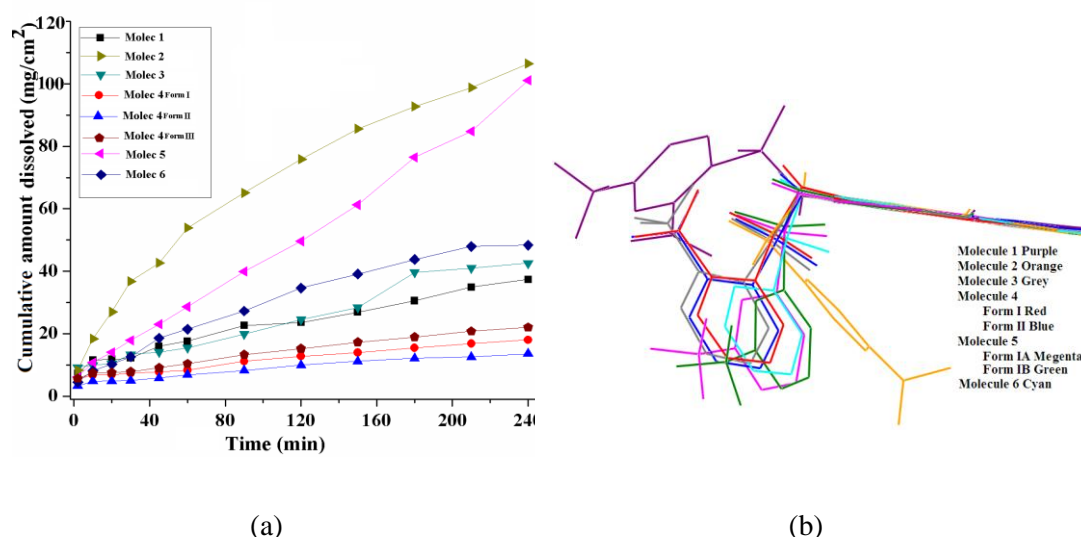
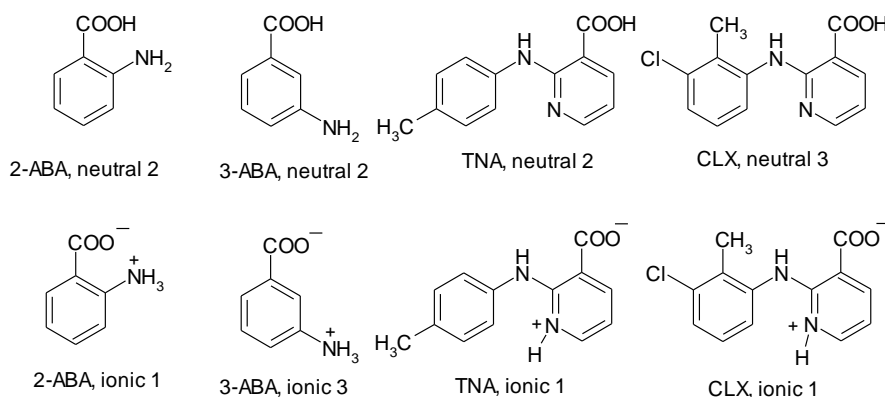


Figure 2 (a) Dissolution profiles of sulfonamides **1-6** in 80% ethanol–water mixture at 37 °C. (b) Overlay of molecular conformations of molecules **1-6**.

CHAPTER THREE

Structure-property Comparison of Neutral and Zwitterionic Polymorphs

Several amphoteric model compounds and drugs, such as isomers of aminobenzoic acids (ortho, meta, and para), *N*-aryl-2-amino-nicotinic acids (three isomers), drugs such as aminosalicyclic acids (meta and para), clonixin, and niflumic acid were selected to obtain their reported zwitterionic and neutral polymorphs (Scheme 2) with the objective to correlate their X-ray crystal structures with solubility and dissolution rate, and stability. We were successful in crystallizing neutral and ionic polymorphs for 2- and 3-aminobenzoic acid (ABA), 2-(*p*-tolylamino)nicotinic acid (TNA), and clonixin (CLX), as well as 4- and 5-aminosalicylic acid (4-ASA as neutral and 5-ASA in ionic form). The neutral and zwitterionic crystalline polymorphs were differentiated by their distinctive powder XRD, FT-IR, Raman and ss-NMR spectroscopy, and further quantified by Hirshfeld surface analysis. Phase transitions were monitored by DSC and VT-PXRD. The difference in solubility and dissolution rates of the neutral and zwitterionic polymorphs were correlated with their hydrogen bonding, see Figure 3a-c, (O–H···O, O–H···N and N⁺–H···O[–]). The faster dissolution rates of the ionic forms were ascribed to stronger, attractive interactions between the solvent molecules and the zwitterionic functional groups (Figure 3d). Even as there is no general strategy yet to crystallize ionic polymorphs of amphoteric molecules, the present study shows the advantages of zwitterionic forms for solubility enhancement.



Scheme 2 Neutral and Zwitterionic crystal structures in CSD (Feb 2014 update).

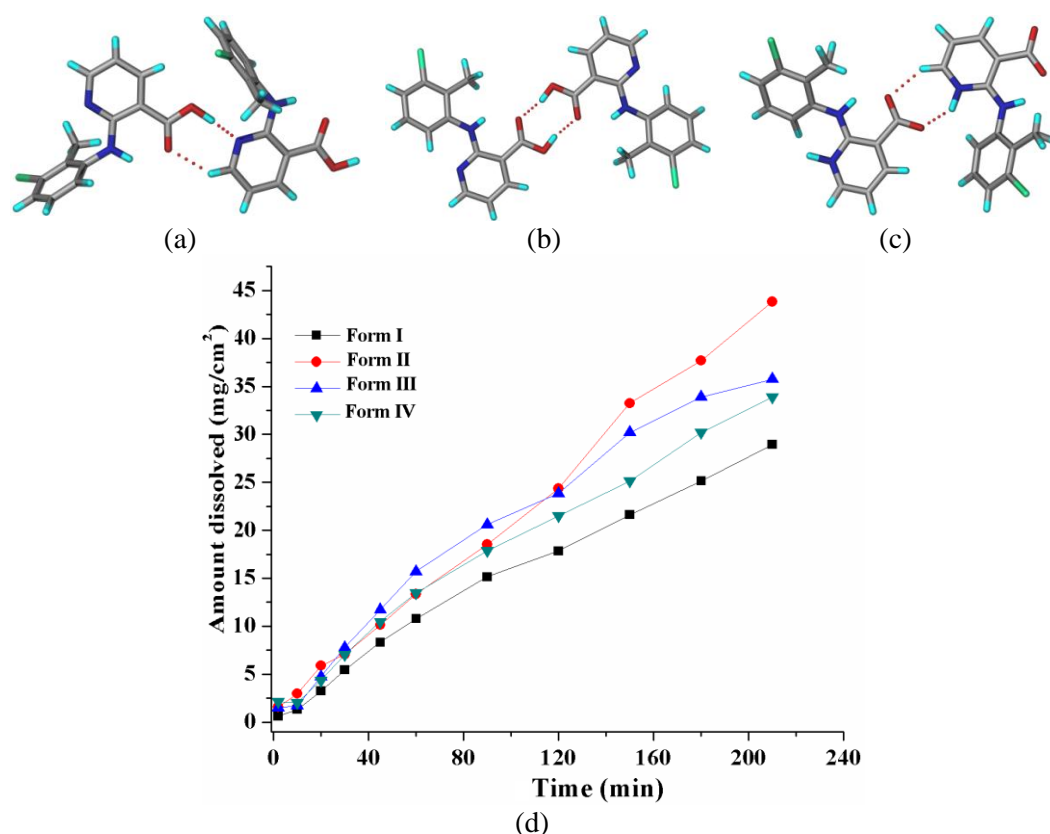


Figure 3 Clonixin polymorphs. (a) Strong acid–pyridine O–H...N synthon in neutral form I (a), acid dimer O–H...O $R_2^2(8)$ motif in neutral form III (b), acid–pyridine ionic $N^+-H...O^-H$ bond in zwitterionic form II (c), Dissolution profile of CLX polymorphs in 60% EtOH–water.

CHAPTER FOUR

Conformational Polymorphs of *N*-Acetyl-L-cysteine

A novel polymorph of *N*-acetyl-L-cysteine (NAC) is identified after three decades of the first report on the X-ray crystal structure of this bioactive compound. The crystal structure of the new orthorhombic polymorph (form II in $P2_12_12_1$ space group) is characterized by X-ray diffraction compared to the triclinic structure of form I (NALCYS02 and NALCYS10 in $P1$ space group). Both polymorphs contain a $C(7)$ chain of $COOH...O=C-CH_3$ hydrogen bonds except that the $COOH$ group is rotated by 180° in form II to make an auxiliary $C-H...O$ interaction with the methyl group in a $R_2^2(8)$ ring motif. The known form I contains weak $S-H...O=C-OH$ and $N-H...S$ hydrogen bonds whereas the new

form II has only N–H···S interaction (Figure 4). The conformational polymorphs of NAC were compared by Hirshfeld surface analysis (d_{norm}) and XPac methods, and spectroscopically characterized by FT-IR and Raman. The bulk phases were distinguished by their ^{13}C ss-NMR and powder X-ray diffraction line patterns. The two polymorphs are enantiotropically related (form I has higher melting temperature and lower enthalpy of fusion). However, no phase transition was observed in DSC. The metastable form II converted to stable form I in solid-state grinding, slurry medium, and storage in ambient conditions for 3 months.

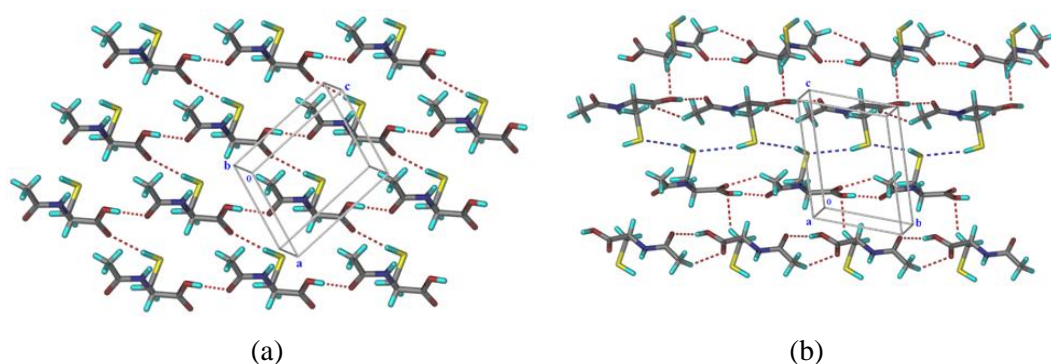


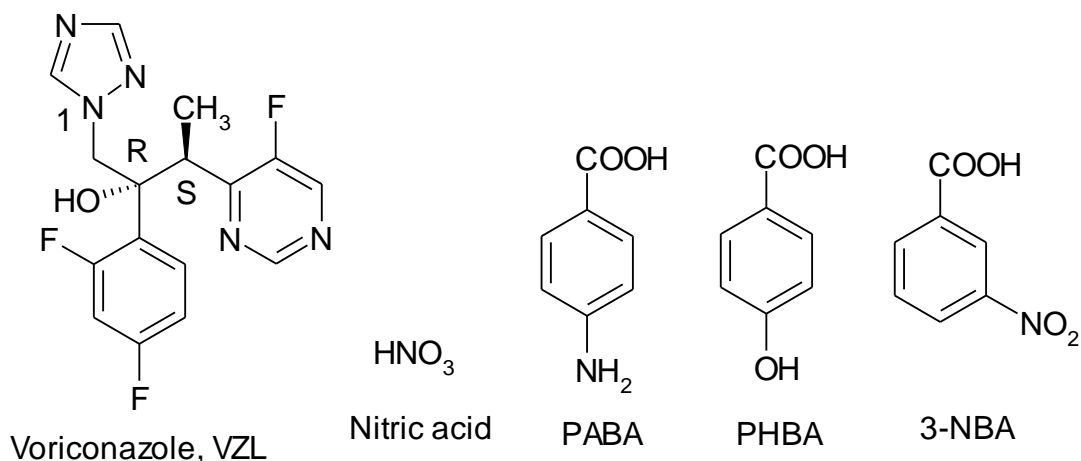
Figure 4 NAC polymorphs (a) 2D network of S–H···O and O–H···O hydrogen bonds in form I. (b) C–H···O hydrogen bonds (red dots) and S–H···S short contacts (blue dots) in form II.

CHAPTER FIVE

Pharmaceutical Cocrystals of Voriconazole

Voriconazole ((2R,3S)-2-(2,4-difluorophenyl)-3-(5-fluoropyrimidin-4-yl)-1-(1H-1,2,4-triazol-1-yl)butan-2-ol, VZL) is an antifungal drug with low aqueous solubility of 0.71 mg/mL and it is a BCS class II drug (Biopharmaceutics Classification System) of the azole family. We have prepared a nitrate salt and three cocrystals of VZL with p-hydroxybenzoic acid, p-aminobenzoic acid (both are GRAS compounds) and m-nitrobenzoic acid cofomers (Scheme 3) to improve aqueous solubility and stability. All the four multi-component crystals of voriconazole were obtained by solution crystallization as well as solid-state grinding and their structures were confirmed by X-ray diffraction, FT-IR, Raman, and NMR spectroscopy, and thermal techniques. VZL–PHBA and VZL–PABA are 3D isostructural by XPac calculations and molecular packing arrangement. A

notable result from a crystal engineering viewpoint is that the supramolecular synthon between the basic drug and the acidic coformer undergoes a switch based on the pK_a of the acid. The solubility of Voriconazole-nitrate salt is 10 times higher soluble than the API in acidic medium (0.1 N HCl), see Figure 5.



Scheme 3 Voriconazole and its successful coformers in cocrystallization method.

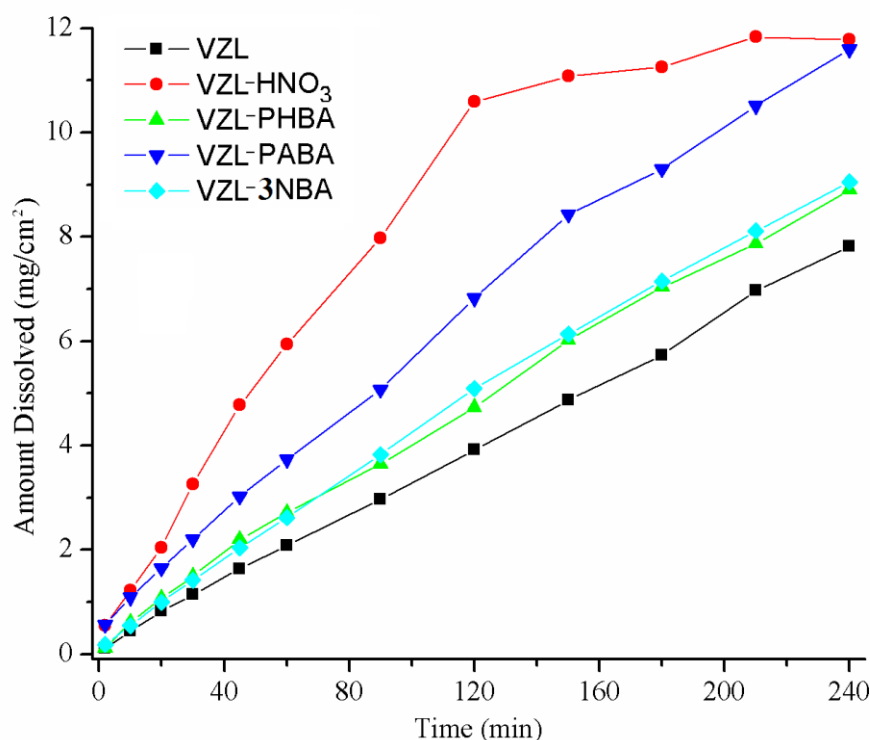
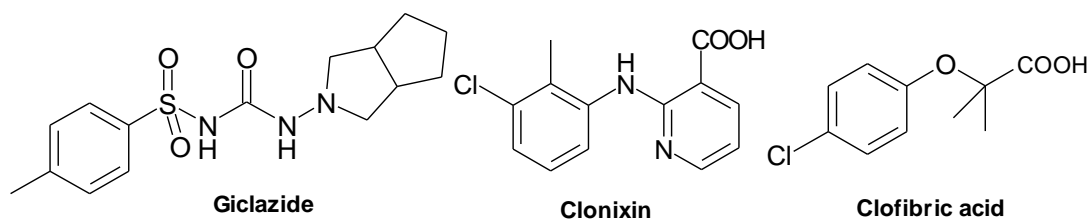


Figure 5 Dissolution profile of voriconazole pure base and its solid forms in 0.1N HCl solution in 4 h at 37 °C.

CHAPTER SIX

Pharmaceutical Salts of Active Compounds

Almost half of the drugs are marketed as salts and reported as they have improved the performance of drug product in clinical usage. This is well established solid formulation in pharmaceutical field in respect to improving drug properties of BCS class II using cocrystallization technique. Gliclazide (GLZ), Clonixin (CLX) and Clofibric acid (CLF) are the low aqueous soluble drugs selected for salt screening experiments in an attempt to improve their solubility (Scheme 4).



Scheme 4 Molecular structures of selected APIs for salt screen.

Gliclazide (GLZ) *N*-(hexahydrocyclopenta[*c*]pyrrol-2(1*H*)-ylcarbamoyl)-4-methylbenzene- sulfonamide, is a second-generation sulphonylurea drug used in the treatment of type II diabetes. Gliclazide is categorised in BCS II classification as it is a low aqueous soluble drug. Hence, it was crystallized with sodium hydroxide and other bases in EtOH solvent to improve the solubility during our attempt to design novel salts of sulphonylurea functional group. A new solid form of sodium gliclazate (GLZ-Na) is crystallized in $P2_1/c$ space group that was also confirmed by DSC and PXRD. Both the solid forms are characterized by ^{13}C ss-NMR spectroscopy. As expected, the solubility (19.6 mg/mL) is 10 times higher and faster dissolution rate ($1.0 \text{ mg/cm}^2/\text{min}$) observed for GLZ-Na salt than the reference drug GLZ (2.2 mg/mL, $0.32 \text{ mg/cm}^2/\text{min}$) in 50% EtOH-water mixture (Figure 6.1).

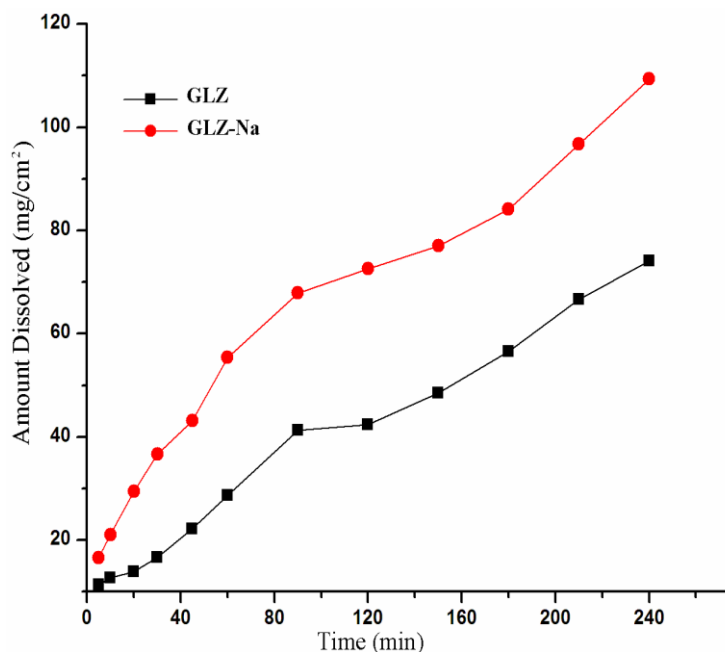


Figure 6.1 Dissolution profile of GLZ and GLZ-Na in 50% EtOH-water mixture at 37 °C.

Clonixin, 2-[(3-chloro-2-methylphenyl)amino]-3-pyridinecarboxylic acid is a non-steroid analgesic drug. Clonixin (CLX), 2-[(3-chloro-2-methylphenyl)amino]-3-pyridinecarboxylic acid It belongs to the fenamate group and although structurally similar to mefenamic acid it is more potent as an analgesic than as an anti-inflammatory, suggesting that clonixin may act on the central nervous system. The piperazinum-clonixate (CLX-PIP) and cytosinium-clonixate salts (CLX-CYT) were the successful solid forms obtained after many trials in solution crystallization and further confirmed by single crystal and powder X-ray diffraction methods. The stacking of CLX molecules are sustained by the $N^+-H \cdots O^-$ (1.59 Å, 173° and 2.53 Å, 127°) and $N^+-H \cdots N$ (1.92 Å, 158°) hydrogen bonding networks with ionized piperazine (Figure 6.2a). Two molecules of CLX are interacting through the $N^+-H \cdots O^-$ (1.68 Å, 172°) and $C-H \cdots N$ (2.69 Å, 106°) interactions with cytosinium ions in CLX-CYT. Both salts showed significant differences in solid state NMR and DSC analysis with respect to the CLX. These organic salts exhibit high solubility (CLX-PIP, 21.8 mg/mL; CLX-CYT, 14.1 mg/mL) and dissolution rate (0.47 mg/cm²/min, 0.40

mg/cm²/min) than the clonixin drug (1.9 mg/mL, 0.14 mg/cm²/min). Two salts are found to more soluble than the stable zwitterionic form (2.0 mg/mL, 0.20 mg/cm²/min) of CLX (Fig 6.3).

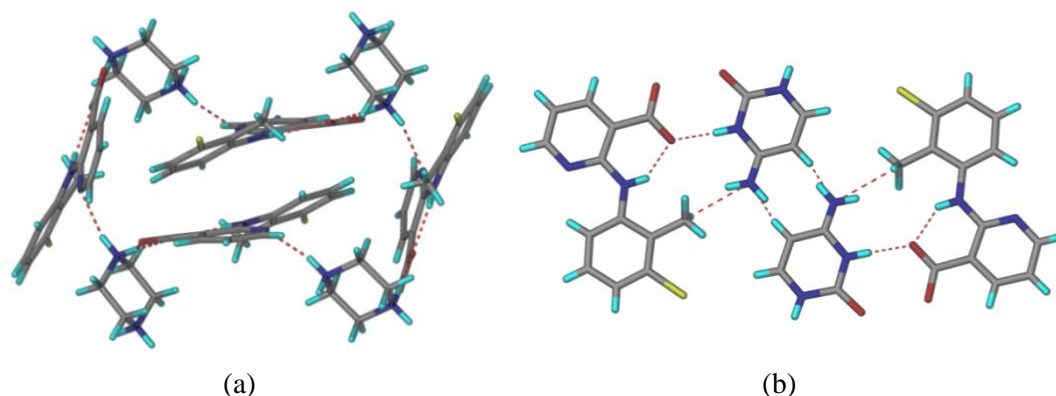


Figure 6.2 (a) N-H...O and N-H...N interaction in CLX-PIP (b) N-H...O and C-H...N interactions in CLX-CYT.

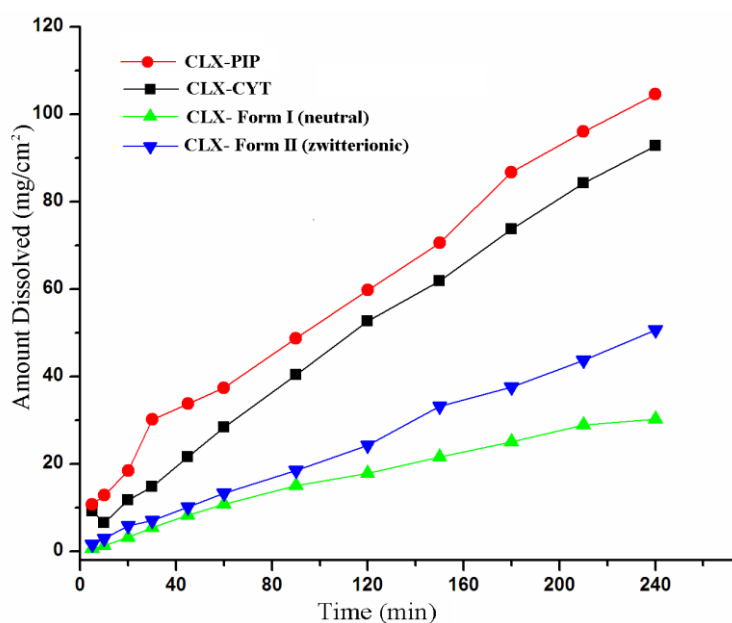


Figure 6.3 Dissolution profiles of CLX and CLX-PIP and CLX-CYT salts in 60% EtOH-water mixture at 37 °C.

Clofibric acid (CLF), 2-(4-Chlorophenoxy)-2-methylpropanoic acid, is an antihyperlipidemic drug; pharmaceutically active metabolite of lipid regulators fibrates and the recent literature indicate that clofibric acid produces potent antitumor effects against ovarian cancer in conjunction with a reduction of

angiogenesis and induction of apoptosis (fibrate; fenofibrate). GRAS molecules as the coformers such as Piperazine, Cytosine etc. were used to obtain new salt solid forms of CLF using the solution crystallization techniques. Piperazinium-clofibrate (CLF-PIP) salt and Cytosinium-clofibrate-cytosine monohydrate (CLF-CYT) confirmed by only single crystal XRD and refined in $P2_1/n$ and $C2$ space groups respectively. The CLF molecule is interacting with piperazine molecule via two strong hydrogen bond $N^+-H\cdots O^-$ (1.68Å, 176°, 1.72 Å, 163°) and one $N^+-H\cdots O^-$ weak hydrogen bonds (2.53Å, 119°) in CLF-PIP (Figure 6.4a). In case of CLF-CYT, two neutral cytosine molecules are interacting via two point $N-H\cdots O$ synthon (1.84 Å, 169°) where as the ionic cytosine were connected by two point ionic synthon $N^+-H\cdots O^-$ (1.81Å, 174°) interactions. The neutral cytosine is connected directly to two different clofibric acid molecules by only $N1-H1\cdots O2$ (1.83Å, 174°) and $N3-H3B\cdots O3$ (2.01Å, 159°) interactions. The weak hydrogen bonds $O6-H6B\cdots O3$ (1.84Å, 161°) and $O6-H6C\cdots O2$ (2.12Å, 136°) is connecting the water molecules with CLF and the $N4-H4B\cdots O6$ (1.93Å, 160°) interactions is bound by cytosinium ions. CLF-PIP salt is easily reproducible compared to cytosinium salt and it exhibits the highest solubility of 18.3 mg/mL and two times improvements in dissolution rate of 0.98 mg/cm²/min with respect to the solubility 2.7 mg/mL and dissolution rate 0.42 mg/cm²/min of CLF drug in 20% EtOH-water mixtures (Figure 6.5).

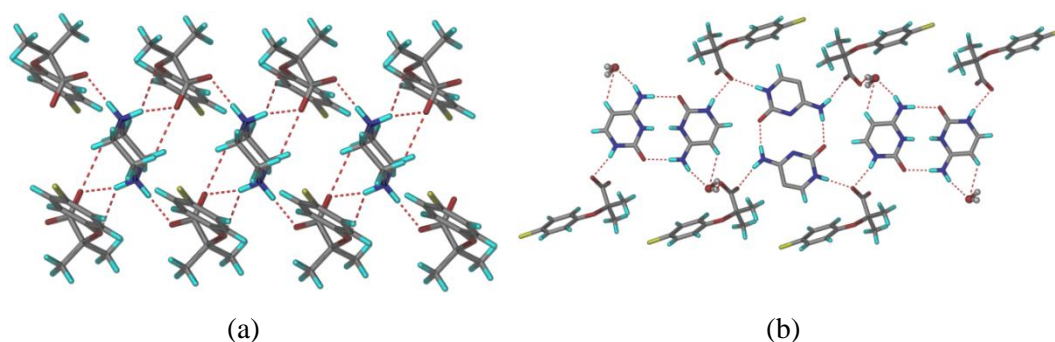


Figure 6.4 (a) $N^+-H\cdots O^-$ interactions between the piperazinium ion and CLF (b) two point $N-H\cdots O$ synthon between the neutral and ionic cytosine in CLF-CYT hydrate complex.

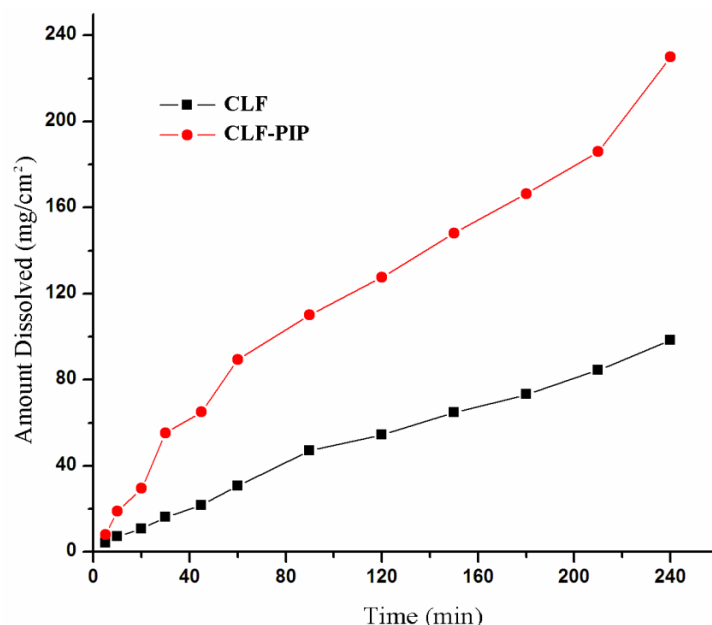


Figure 6.5 Dissolution profiles of CLF and CLF-PIP salts in 20% EtOH-water mixture at 37 °C.

CHAPTER SEVEN

Conclusions and Future Prospects

APIs can exist in different solid forms, such as polymorphs, pseudopolymorphs (solvates and hydrates), salts, co-crystals and amorphous solids. Almost 50% of all the APIs are shown to be polymorphic. Polymorphs are possible for each of these solid forms if money and time spend rigorously. Each form may possess its own unique mechanical, thermal, physical and chemical properties that can remarkably affect the solubility, bioavailability, hygroscopicity, melting point, stability, compressibility and other performance characteristics of the drug. A thorough understanding of the relationship between a particular solid form and its functional properties are crucial for selecting the most suitable form of the API for scale up, formulation activities, clinical trials, and finally manufacturing. This exercise requires inputs about crystallization, pharmacology and formulation. Hence several new polymorphs were identified and their phase transitions and stability order was established in chapter 2 for cardiosulfa and its similar molecules. Moreover, general relationship between molecular twist and higher solubility for aryl sulfonamides emerged from six

sulfonamide molecules. Planar sulfonamide molecules pack more efficiently in the crystal lattice and hence are less soluble; molecules with a bent molecular conformation were found to have higher solubility. Finally, Cardiosulfa appears to be the best candidate in the series studied because despite its lower solubility there is no evidence of polymorphs. In chapter 3, the structural-cum-solubility study of neutral and zwitterionic polymorphs of selected four ampholytes provides methods for their preparation and a comparison of solubility–stability characteristics. Generally solubility and stability are inversely related for drug polymorphs. We show that the twin characteristics of high solubility and good stability may be jointly optimized in the same zwitterionic polymorph for amphoteric drugs. The selective crystallization of zwitterionic forms could be possible through crystallization promoter additives such as ionic liquids, polymer-induced heteronucleation, and seeding with ionic structural mimics. In chapter 4, the stability of form II is compared with the weak interactions to understand the hydrogen bonding-crystal stability relationship.

More than 80% drugs are marketed as solid formulations and 90% of them are crystalline in nature. Hence, pharmaceutical scientists constantly strive to improve physical properties of active pharmaceutical ingredients (APIs) using several formulation techniques such as cocrystal, salt formation and eutectic mixture preparation. API is a substance (mostly solid crystal) that is pharmaceutically active in a drug and are delivered to the patients in the solid-state as part of dosage forms (e.g. tablets, capsules, granules, powders, etc.) because of their easy uptake in the body. Much of the research is being focussed to improve the physical properties of API crystals using pharmaceutical cocrystallization/salt formation technique since the efficiency of the dosage form is often strongly related to API and the desired improvements in terms of crystallinity, solubility, hygroscopicity, stability, particle size, flow, filterability, density and taste can be often achieved by these methods. In chapter 4 and 5, a nitrate salt and three cocrystals of voriconazole with PHBA, PABA and 3-NBA, sodium-gliclazate, piperazinium-clonixate and cytosinium-clonixate were

prepared in bulk as well as by solution crystallization and therefore the solubility (10 times more soluble) and dissolution rates (3 times faster dissolving) of selected drugs voriconazole, gliclazide and clonixin were improved almost by the salt formation. Novel salts of clofibric acid with piperazine and cytosine were also identified. Some of the cocrystals VZL-PABA etc. of voriconazole are more soluble (3 times) than the reference drug. Identifying the optimum solid form of an active pharmaceutical ingredient (API) using cocrystallization/salt formation and solid solution/eutectic composition is a challenging task towards thickening the pipeline of high solubility drugs.

CONTENTS

Certificate	i
Declaration	ii
Preface	iii-vi
Acknowledgement	vii-ix
About the Author	x
Synopsis	xi-xxv

CHAPTER ONE

INTRODUCTION	1-80
1.1 Supramolecular Chemistry	2
1.2 Solid State Chemistry	3
1.3 Crystal Engineering	5
1.4 Classification of Crystalline Forms	6
1.4.1 Polymorphism	7
1.4.1.1 Conformational Polymorphism	9
1.4.1.2 Pseudopolymorphism	12
1.4.1.3 Desmotropism and Tautomeric Polymorphism	14
1.4.1.4 Zwitterionic and Neutral Polymorphism	17
1.4.1.5 Concomittant and Disappearing Polymorphs.....	18
1.4.1.6 Color Polymorphs	23
1.4.1.7 Crystallization of Polymorphs	25
1.4.1.8 Characterization of Polymorphs	27
1.4.1.9 Thermodynamics of Polymorphs	29
1.4.2.0 Prediction Rules for Polymorphs	30
1.4.2.1 Properties of Polymorphs	34
1.4.2.2 Cocrystals and Salts	35

1.4.2.3	Cocrystal/ Salt Polymorphs	38
1.4.2.4	Solid Solution and Eutectic Composition	41
1.5	Solubility and Dissolution	43
1.6	Structure-property Relationships.....	47
1.6.1	Compression Behavior	49
1.6.2	Mechanical Behavior	51
1.6.3	Solid-state Emission Behavior	53
1.6.4	Solubility Behavior	56
1.7	CSD and Supramolecular Synthon	60
1.8	Conclusions	65
1.9	References	66

CHAPTER TWO

POLYMORPHISM IN CARDIOSULFA AND ITS ANALOGS		81-139
2.1	Introduction	82
2.2	Results and Discussion	88
2.2.1	Crystal Structures of Sulfonamides	89
2.2.2	Conformational Analysis	100
2.2.3	Differences in Sulfonamide Polymorphs	103
2.2.4	Solid state ¹³ C NMR and FT-IR	104
2.3	Polymorphic Transformations	109
2.3.1	Cryogenic Temperature Phase Transitions	110
2.3.2	High Temperature Phase Transitions	115
2.4	Dissolution and Solubility	124
2.5	Conclusions	129
2.6	Experimental Section	130
2.7	References	134

CHAPTER THREE

STRUCTURE-PROPERTY COMPARISON OF NEUTRAL AND ZWITTERIONIC POLYMORPHS 140-195

3.1	Introduction	141
3.2	Results and Discussion	145
3.2.1	Neutral and Zwitterionic Polymorphs	146
3.2.2	Crystallization and Structural Analysis of Ampholytes	147
3.2.3	Molecular Conformations of Clonixin	154
3.3	ΔpK_a Calculation for Ampholytes	159
3.4	Characterization of Neutral and Zwitterionic Polymorphs	162
3.5	Thermal Stability and Phase Transition Study	172
3.6	Solubility and Dissolution	179
3.7	Conclusions	187
3.8	Experimental Section	188
3.9	References	190

CHAPTER FOUR

CONFORMATIONAL POLYMORPHS OF *N*-ACETYL-L-CYSTEINE 196-220

4.1	Introduction	197
4.2	Results and Discussion	198
4.2.1	Crystal Structural Analysis	199
4.2.2	Characterizations of NAC Phases	207
4.2.3	Stability of Polymorphs	211
4.3	Conclusions	215
4.4	Experimental Section	215
4.5	References	219

CHAPTER FIVE

PHARMACEUTICAL COCRYSTALS AND A NITRATE SALT 221-258 OF VORICONAZOLE

5.1	Introduction	222
5.2	Results and Discussion	223
5.2.1	Structural Analysis	226
5.2.2	Supramolecular Synthon and CSD Search	234
5.2.3	Conformation of VZL	238
5.2.4	Characterization of VZL Crystalline Forms	239
5.2.5	DSC Analysis	246
5.3	Solubility and Dissolution	247
5.4	Conclusions	249
5.5	Experimental Section	250
5.6	References	254

CHAPTER SIX

NEW PHARMACEUTICAL SALTS OF GLICLAZIDE, 259-304 CLONIXIN AND CLOFIBRIC ACID

6.1	Introduction	260
6.2	Results and Discussion	263
6.2.1	Crystal Structural Analysis	264
6.2.2	Conformational Analysis	271
6.3	CSD Search and pK_a Calculation	274
6.4	Characterization of Pharmaceutical Salts	278
6.4.1	Spectroscopy Analysis	282
6.4.2	Thermal Analysis	289
6.5	Solubility and Dissolution Study	292

6.6	Conclusions	296
6.7	Experimental Section	297
6.8	References	301

CHAPTER SEVEN

CONCLUSIONS AND FUTURE PROSPECTS 305-310

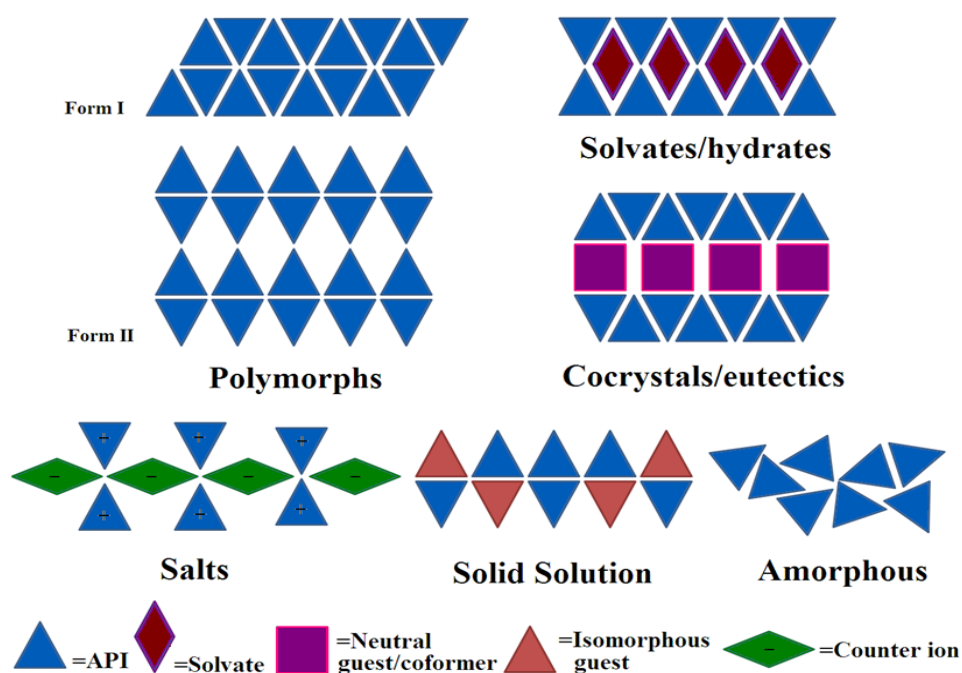
7.1	Solid Dosage Forms.....	306
	List of Publications	311
	Events Attended	312

APPENDIX A1-A8

	Crystallography Tables	A1
--	------------------------------	----

Chapter One

Introduction: Pharmaceutical Solids



Schematic representation of the possible crystalline modifications (polymorphs, solvates, cocrystals, salts, solid solution and eutectic composition) and amorphous phase of any single and multi-solid component systems.

1.1 Supramolecular Chemistry

Jean-Marie Lehn (1969) defined the term supramolecular chemistry¹ as the chemistry of molecular assemblies and of the intermolecular bond, and was awarded the Nobel Prize for his work in the same area in 1987. He expressed supramolecular chemistry as ‘chemistry beyond the molecule’ and this is extended by other chemists as the chemistry of non-covalent interactions and non-molecular chemistry.² But simply and originally, it is described as the non-covalent interactions between a guest and a host molecule and product host-guest complex (Fig. 1.1) or supermolecule.³ The host is a molecular entity which provides the hydrogen bond donors (convergent binding sites) and the guest provides the hydrogen bond acceptors (divergent binding sites) for the inclusion of one molecule in another. Initially, this field began with the discovery of chlorine hydrate by Davy in 1810 and it has grown from the further development of macrocyclic ligands for metal ions by Curtis in 1961.⁴ Modern supramolecular chemistry is not limited only to host-guest systems but also includes molecular devices, molecular recognition, self assembly and self organization (self processes) and it has become interdisciplinary which includes complex matter and nanochemistry.⁵ Furthermore development of such devices requires the design of molecular components performing a given application and function such as photoactive, electroactive, ionoactive, thermoactive, or chemoactive, and suitable for assembly into an organized array.⁶ Light-conversion devices and charge-separation centers have been developed with photoactive cryptates formed by receptors having photosensitive groups. It is extended in technological devices and is due to the functions of supermolecular recognition, catalysis and transport.^{3,7}

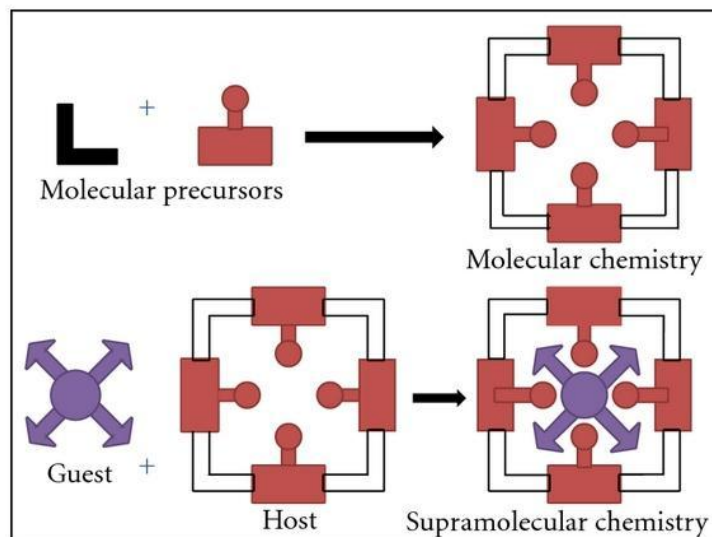


Figure 1.1 Comparison between the scope of molecular and supramolecular chemistry (Lehn).

1.2 Solid State Chemistry

When we intend to understand the solid state chemistry, we need to have some perceptiveness about the solids, structures and the forces that hold them together in the solid-state.⁸ Indeed, the chemical bonding in solids is not well understood even today, in fact there is wide variation in the chemical properties of crystalline solids.⁹ Many difficult challenges and expectations remain in predicting the composition, structure, and the properties of some new materials.¹⁰ So the synthesis and design of novel solids with desired functions is as much an art as a science.¹¹ Solid state chemistry is concerned mainly with the crystalline inorganic and organic materials, synthesis, characterizations, crystal structures, properties and applications in devices.¹² Recently materials chemistry has emerged as a new distinctive branch of chemistry from solid state chemistry which covers molecular, non-molecular and solid materials.^{9,13} So these materials give overwhelming interests

in new chemistry, new structures and improved understanding of structure-property relationships.¹⁴

The crystal structures are usually determined by X-ray crystallography and this technique relies on the fact that the distance between the atoms in the crystals are of the same order of magnitude as the wavelength (1 Å) of X-rays. Dunitz expressed the crystal as a supermolecule par excellence of macroscopic dimensions, millions of molecules held together in a long and periodic arrangement by the non-covalent bond interactions.¹⁵ A crystal thus behaves as a three dimensional diffraction grating to X-rays and the diffraction pattern can give the internal positions of atoms in the crystal very clearly. Throughout history, scientists have worked on the slow and serendipitous trial-and-error crystallization process for discovering and developing new crystalline materials using different laboratory crystallization techniques. However, an emerging theme in modern crystalline science is the notion of intelligent design of crystals such as molecular and non-molecular complexes with desired chemical and physical properties.¹⁶ The pharmaceutical industry is adapted for the purposes of materials science and crystal engineering and the combinatorial approach represents a watershed in the process of accelerated discovery, development and optimization of pharmaceutical materials using different crystal engineering strategies. Therefore, the crystallization process itself is an impressive model of supramolecular self assembly in solid state chemistry field involving specific molecular recognition.¹⁷ This is the advantage of crystalline solids in materials science and it differs from the other phases such as liquids and gases. The crystal property of phase transition differs from the liquids is due to the cooperativity of molecules in the crystal lattice otherwise the local effects in the liquids. Within a crystal, every displacement of a molecule from the equilibrium conformation, position and orientation in the crystal packing is immediately communicated to its immediate and distant neighboring molecules through the coupling of molecular motions in a set of lattice vibrations that extend through the entire crystal.¹⁸

1.3 Crystal Engineering

Crystal engineering is an emergent subject in solid state chemistry for the design of new crystal structures with the same or different molecules as building blocks. This began with Robertson's work to systematically correlate the molecular structures of organic compounds with their crystal structures.¹⁹ It demands a detailed understanding of intermolecular interactions because they act as the supramolecular glue that binds molecules into crystals.²⁰ This became active and under investigation to analyze the interactions for around 30 years from the Bragg's discovery of X-ray crystallography study for naphthalene and anthracene. Pepinsky introduced the term crystal engineering in 1955 as the crystallization of organic ions with metal complexes results the crystals with advantageous properties that can be engineered. Schmidt was also pioneered in this field in around 1950s for the systematic published works and topochemistry of crystalline alkenes.^{20b,c} Now the concepts of crystal engineering are applicable to any kind of intermolecular assembly such as protein ligand recognition, the design of supramolecular polymers, molecular complexes for drug delivery. Now this field has expanded its wide scope in many disciplines including organic chemistry, inorganic chemistry, physical chemistry, X-ray crystallography, materials sciences and computational chemistry.²¹

Recently, Desiraju (1989) added the term crystal engineering as *the understanding of intermolecular interactions in the context of crystal packing and the utilization of such understanding in the design of new solids with desired physical and chemical properties*.¹⁰ This is well understood by many students because of the trio attributions such as analysis, design and functions was taken together in the definition. It has been further described as the careful understanding and the exploitation of non-covalent interaction between molecular or ionic components for the rational design of solid-state structures that could exhibit interesting electrical, magnetic, and optical properties.²² It is now recognized by

many scientists and it is becoming increasingly evident that the specificity, directionality, and predictability of intermolecular hydrogen bonds can be utilized to assemble supramolecular structures of controlled dimensionality to achieve the solids with the desired functions.²³ Crystal engineering approaches are now potentially applied to a wide range of crystalline materials that offers an alternative and potentially fruitful solution for improving the solubility, dissolution rate and subsequent bioavailability of poorly soluble drugs in the market.²⁴

1.4 Classification of Crystalline Forms

Several novel crystalline forms are identified for organic and inorganic compounds in the recent literatures and they supposed to show different physical and chemical properties. These solid forms include polymorphs, solvates, cocrystals, salts, solid solution and eutectic mixtures (Fig. 1.2) are now modern solution to many solid state issues.²⁵ Many crystallization techniques and different conditions are available for screening these solid forms to achieve the desired physical properties for some of the solids such as stability, solubility, hygroscopicity, and melting point to increase the bioavailability for weak acids and bases or neutral and zwitterionic compounds.²⁶ The available techniques are solution crystallization, grinding, milling, sublimation and heating experiments are generally used to screen new crystalline solid forms.²⁷ In this approach, the discovery and optimization of solid forms of pharmaceuticals are essential to achieve the optimal properties. In conclusion, we collect the right information of relevant solid forms for direct comparison and recommend the best solid form based on the improved properties of the material or else and next development plan of our ideas on finding alternative forms and other formulation methods for long term strategic considerations.²⁸

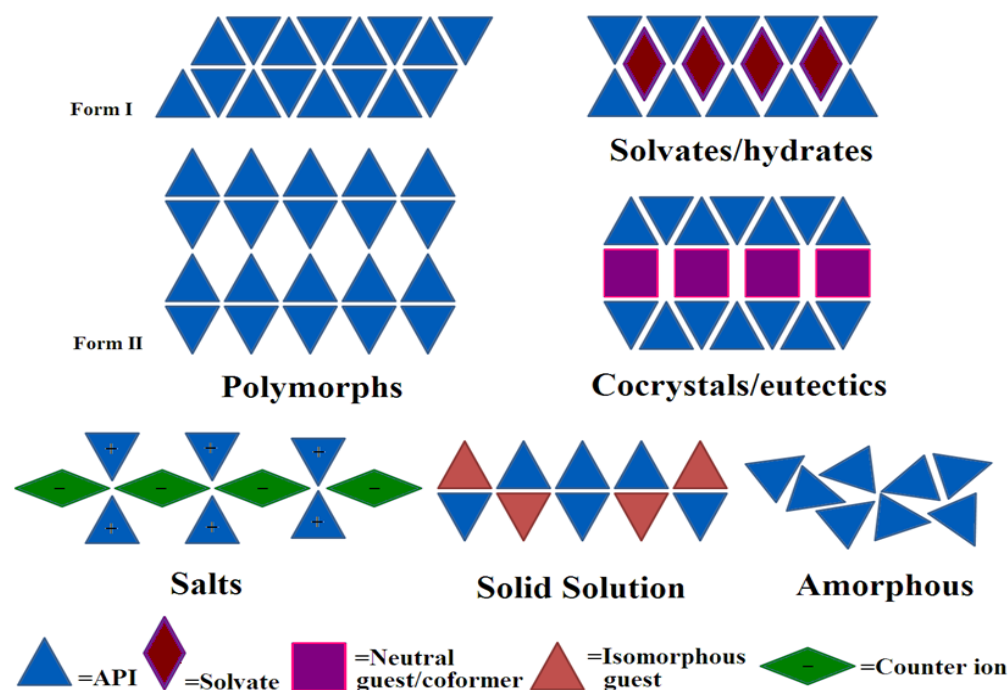


Figure 1.2 Pictures displaying the more common solid-state strategies and their respected components.

1.4.1 Polymorphism

Polymorphism is the usual occurrence in which same chemical substance exhibits different crystalline arrangements in the crystal lattice for any solid materials.²⁷ In 1965, McCrone defined the *polymorph* as *it is a solid crystalline phase of a given compound resulting from the possibility of at least two different arrangements of the molecules of that compound in the solid state*.²⁹ Then it was simplified as “*if these solids can exist in different crystal lattices, then we speak of polymorphism*”.³⁰ Polymorphism is a passionate research topic that covers the research interests of physical, organic, inorganic, metal-organic, supramolecular, computational, pharmaceutical and solid material scientists. It started with Robertson and Ubbelohde work in 1938 with determination of the crystal structures of two polymorphs of resorcinol as the first example after the first discovery of

polymorphism in sodium phosphate arsenate (1820) and benzamide (1832).³¹ Allotropes and polymorphs are closely related terms but they are different in terms of elements and molecules. In brief the word polymorph is used for structural differences in molecular compounds (paracetamol) whereas allotrope is for the structural variations in elements such as C, Sn and Se.³² For example carbon has three well known allotropes called diamond, graphite and fullerenes. Interestingly, Tin pest is the allotropic transformation from metallic allotrope of β -form- white tin to brittle, nonmetallic, α -form-grey tin upon cooling ($13.2\text{ }^{\circ}\text{C}$). Selenium allotropes exhibit distinctive color variations of black and red colors and they can be visually identified (Fig. 1.3).



Tin medal affected by tin disease Black and red colored allotropes of Se

Figure 1.3 Allotropes of tin and selenium elements exhibiting different characteristics (Adapted from Wikipedia, Ref. 32)

Polymorphism can occur because of the change in differences in the packing of molecules in the crystal lattice, conformational flexibilities, and supramolecular synthon competitions. They are classified accordingly with respect to changes called packing, conformational, and synthon polymorphism respectively.³³ Polymorphism in organic compounds is very often and of course fundamental importance since its ability to change the physical and chemical properties such as solubility, dissolution, toxicity and bioavailability for different crystal forms (Ritonavir: solubility $I > II$ and Mebendazole: toxicity $B > A \approx C$).³⁴ There is no

limit for number of polymorphs to obtain for any compounds but the Flufenamic acid is the only example having nine polymorphs^{34c} (graphical Fig. 1.4) having solved crystal structures in the CSD after second most 5-Methyl-2-[(2-nitrophenyl)amino]-3-thiophenecarbonitrile, known as ROY for its red, orange, and yellow crystals, heptamorphic crystal structures.⁷⁰

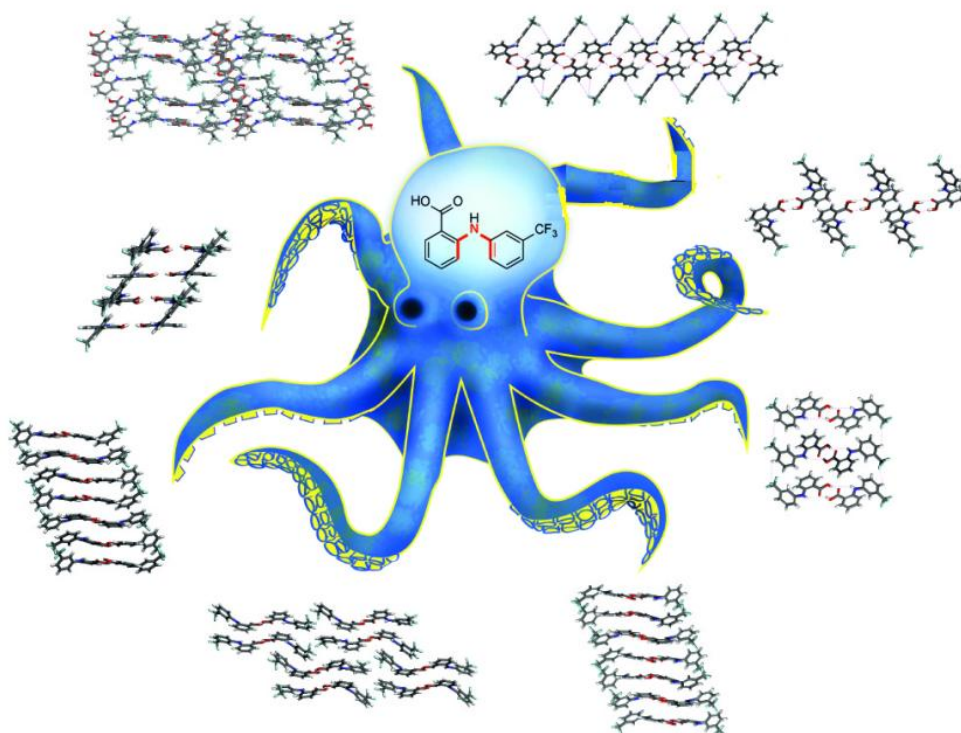


Figure 1.4 Nonamorphism in Flufenamic acid (FFA) and a new world record for a polymorphic compound with solved structures (Adapted from Re. 34c).

1.4.1.1 Conformational Polymorphism

According to IUPAC definitions, a conformation is “*the spatial arrangement of the atoms affording distinction between stereoisomers which can be interconverted by rotations about formally single bonds*”, whereas a conformer “*is one of a set of stereoisomers, each of which is characterized by a conformation corresponding to a distinct potential energy minimum*”.³⁵ Bernstein likened it with

Dunitz's thoughts to define the conformer as *any change in a given single rotatable bond of a molecule always affords a new conformation, but it affords a new conformer only if the conformational change goes through a potential energy barrier into a different potential energy well.*³⁶ Finally, any organic molecule with flexible torsions and low energy conformations in the crystal structures will have a greater likelihood of displaying polymorphism because (1) different conformations will lead to new hydrogen bonding and close packing modes and (2) the exchange of energy that reduces the total energy difference between alternative crystal structures. Molecular conformation is able to make noticeable distinctions but make significances in the property related to the chemistry of the organic solid state. The rotations are about single bonds worth of 1-3 kcal mol⁻¹ but can be as high as 8 kcal mol⁻¹ due to restricted rotation in organic molecules.³³ The consequent compensation of Gibb's free energy for these changes in conformer destabilization process by the crystal environment increases the propensity of polymorphism in organic molecules with flexible torsions. The study of conformational polymorphism is the reasonable one in crystal engineering approach and it has become improved further through the various crystallization methods to find various crystal forms and the correlation of their properties by techniques such as single crystal X-ray crystallography, powder X-ray diffraction, differential scanning calorimetry, infrared and Raman spectroscopy and rarely terahertz spectroscopy.³⁷ A conformational polymorph renaissance have been developed for number of reasons: (1) different conformational polymorphs of the same substance can exhibit very different physical and chemical properties than the other polymorphs (2) the possibility of using those polymorphs as the ideal systems for the comparison and the study of structure–property correlations (3) the immense interest for carrying out single crystal structure determinations is the structural characterization and comparison of the polymorphs (4) the recognition of their purpose in pharmaceutical industries and the high-profile patenting on polymorphism (5) the ease of publishing these polymorphs having color and

solubility differences in the mainstream scientific literatures (6) some conformational polymorphs might be harder to crystallize because their conformers are less accessible experimentally.³⁸

For instance, two polymorphs are conformational polymorphs only when their conformations are related by changes in torsion angles of those two crystal structures. These changes can be identified through the energy calculations because this change requires a change of gas-phase conformer and crossing of an energy barrier. Though the energy differences associated with conformational variations of small organic molecules in different polymorphs are usually small, higher energy conformations in crystalline polymorphs are rare but for few possible cases listed here, (i) molecules that are able to break an intramolecular interaction in favor of a strong intermolecular interaction to attain the new conformation i.e., polymorphism in cardiosulfa and its analogs^{39a} and (ii) molecules that crystallize in special symmetry positions i.e., C_2 and C_i in dimorphs of phenyl-2-pyridyl-ketone-azine^{39b} (iii) Zwitterionic molecules i.e., tetramorphs of cysteine.^{39c} If a change in conformations in any crystal structures, conformational adjustment and conformational change are the two postulated possibilities.³⁸ Conformational adjustment always observed for any conformationally flexible molecule in a crystal to some extent of minimal and a small conformational energy penalty is paid for intermolecular interactions in the crystal. Therefore, the flexible molecule adjusts to the crystal environment by changing slightly its conformation to minimize the lattice energy of that particular crystal. In other case, conformational change involves a change of gas-phase conformer and so that it requires high energy over the energy barriers. Two conformations are related by conformational change then the torsion changes would be $\max(\Delta\theta) > 95^\circ$ otherwise it is a conformational adjustment. Additionally, the *rmsd[r]-crystal* cutoff of 0.375 Å is an indication for the type of conformational flexibilities when comparing two conformations and it is a very

convenient approximation for the large set of polymorphs and molecules of different nature (Fig. 1.5a). In similar way, there are thirty six percent of polymorphic compounds in the CSD showed conformational polymorphism and the best example is Chlorpropamide^{40a-e} drug. It has been reported as the largest number of conformational polymorphs (pentamorphs overlay, Fig. 1.5b) after Tolbutamide drug (tetramorphs) in the CSD.^{40f-g}

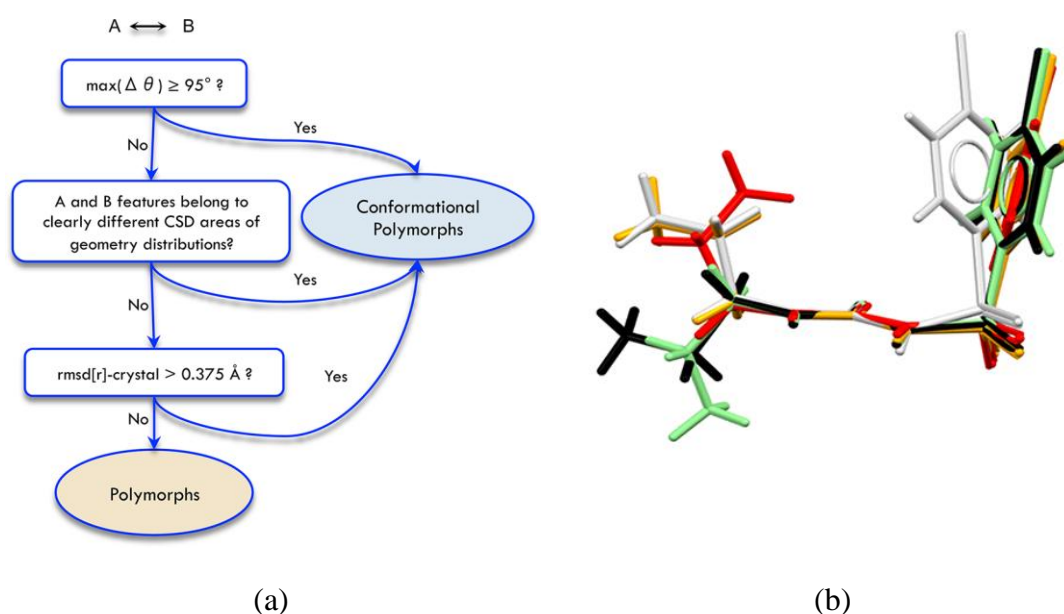


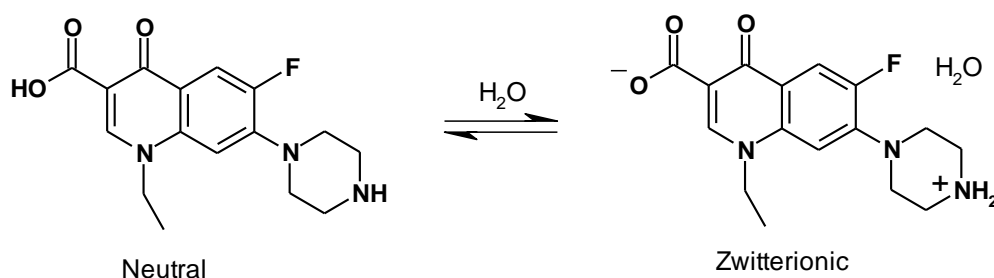
Figure 1.5 (a) Decision tree to identify the conformational polymorphs A and B with structural data. (b) Overlay of five different conformers in chlorpropamide polymorphs (Adapted from Ref. 38).

1.4.1.2 Pseudopolymorphism

Solvatomorphism or pseudopolymorphism arises due to the multi-point recognition with strong and weak intermolecular interactions between solvent and solute molecules facilitate the retention of aqueous or organic solvents in crystals during the nucleation step. The phenomenon *pseudopolymorphism is the major occurrence wherein a compound is obtained in crystalline forms that differ in the*

*nature or stoichiometry of included solvent molecules.*⁴¹ The process of crystallization is bringing the solute and the solvent together to interact first and forms the aggregates in the nucleation step. This whole aggregate contains solute–solute, solute–solvent and solvent–solvent interactions in the initial crystallization process.⁴² The supramolecular synthons or intermolecular non-covalent interactions between the solute and solute provides an adequate driving force for nucleation and crystallization to overcome the solvent-solute interactions when there is simultaneous entropic gain in eliminating solvent molecules from these aggregates into the bulk solution and enthalpic gain in forming stable solute species as the crystals.⁴³ This thermodynamic change results that most organic crystals are unsolvated in CSD. In solvates, the interaction are in multi-point manner through either strong O/N–H···O or weak C–H···O intermolecular hydrogen bonds with solvent molecules are present so the extrusion of solvent from the aggregates into the bulk solution becomes thermodynamically unfavorable. Hence, the solvent remains an integral part of the crystals during the nucleation step itself.⁴⁴ Practically, the unsolvated forms is not possible to obtain in normal crystallization of solvated compounds such as fluoroquinone derivatives (norfloxacin, ciprofloxacin etc). Unfortunately, one third of pharmaceutical solids are prone to form or transform to hydrate species depending on the external environmental and other conditions.^{42b} This solid-state transformation will have vigorous effects on the physical and chemical properties of drugs and eventually modify the drug stability and biological properties such as solubility, dissolution and bioavailability.⁴³ So the identification, characterization of solvates and understanding of their interactions of water and drugs is so important to control the transition and assure the quality of the drug products.⁴⁴⁻⁴⁵ In contrast to the solvates, the drug norfloxacin hydrates showed better solubility and stability compared to the anhydrous forms. The main functional groups of norfloxacin changed from COOH to COO[−] and NH to NH₂⁺ in hydrated structures and the proton transfer from COOH group to NH group caused by the

water molecules (Scheme 1.1). This suggests that the hydration can induce the interaction between norfloxacin molecules from hydrogen bonding to ionic bonding by a intramolecular proton-transfer process in the solid state.⁴⁶ We found that water molecules is not only induced the proton transfer reaction between norfloxacin molecules in the solid state, but also changed the solid character from a neutral state to ionic state to make a higher dissolution rate of norfloxacin after hydration.



Scheme 1.1 Norfloxacin hydration involves the intra-proton transfer in the solid state

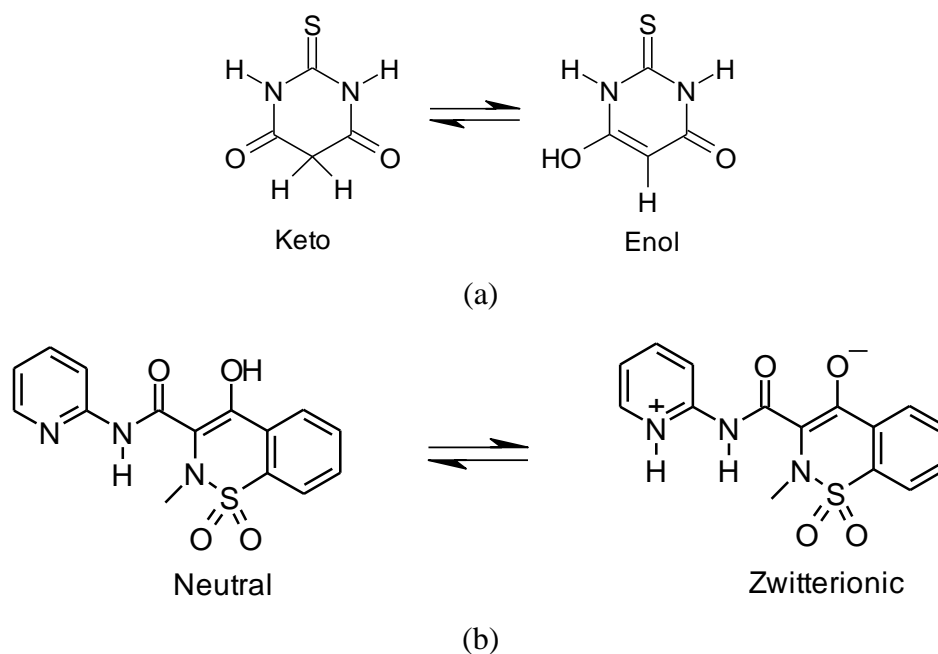
1.4.1.3 Desmotropism and Tautomeric Polymorphism

Desmotropy is a German term introduced by Jacobson in 1887 and it was formed from the Greek language meaning change of bonds.⁴⁷ It was later explained as tautomers are constitutional isomers of organic compounds that readily interconvert by a chemical reaction called tautomerization.⁴⁸ These interconversion reactions deal with the migration of a hydrogen atom or proton which is accompanied by a switch of a single bond in conjugation with adjacent double bonds. Desiraju said that a crystal structure with a particular tautomer is polymorphic to a different crystal structure that contains another tautomer. If they are different in nature of tautomer in different crystal structures then they are not polymorphs at all but crystals of different compounds.⁴⁹ If there are structures of different molecules but they are isometric in nature in the same crystal structure. Then this phenomenon is called as *synthomorphism*⁵⁰ means there is local similarity in the internal crystalline arrangement of atoms in structures because of the local similarity in the

crystal structure. The other important terms in the crystalline studies are *isomorphism*, *isotypism*, *isostructuralism*, *homostructuralism*, and *approximate isomorphism*.⁵¹ Isomorphism is originally defined by Mitscherlich^{51e} in 1819 and it refers only to morphological similarities but in later isostructurality implies similar close packing within similar unit cells. Now the isomorphous crystals which differ by only one substituent have high degree of structural similarity. Isostructural crystal pairs formed by molecules differing only in the chirality of one atom are termed as configurationally isostructural.⁵¹ According to IUCr online dictionary,⁵² two crystals are said to be Isomorphous (isometric) if (a) both have the same space group and unit-cell dimensions and (b) the types and the positions of atoms in both are the same except for a replacement of one or more atoms in one structure with different types of atoms in the other (isomorphous replacement), such as heavy atoms, or the presence of one or more additional atoms in one of them (isomorphous addition).⁵² When the related molecules differing by substitutions on more than one atomic site have similar packing, it is called homeostructural crystals. In order to avoid the confusion with other important terms with respect to crystalline arrangements, the Conformational isomorphism and Conformational synmorphism are two phenomena are also are discussed here. Conformational isomorphism which may arise due to conformational differences present in the flexible molecules having more than one molecule in the asymmetric unit.³¹ The existence of different conformers of the same molecule in the same crystal structure represents conformational isomorphism for $Z' > 1$ type of molecules. Conformational synmorphism refers to a random distribution of different conformers within the crystal structure for $Z' > 1$ cases.³¹

Solid-state tautomeric inter-conversion and tautomeric polymorphs are strictly related but they involve confusions to address in a general way of differentiating them. For tautomers, rapidly interconverting species in solution or in the melt would be accepted as polymorphs (2-thiobarbituric acid, Scheme 1.2a) and

called tautomeric polymorphs, although slowly interconverting species would be excluded. This is now little meaningful when we see the “safe” criterion for classification of a system as polymorphic would be if the crystal structures were different but lead to identical liquid and vapor state.⁵³ Gavezzotti illustrated the polymorphs as polymorphs are a set of crystals (a) with identical chemical composition; (b) made of molecules with the same molecular connectivity, but allowing for different conformations by rotations about single bonds; (c) with distinctly different three-dimensional translationally periodic symmetry operations.⁵⁴ Hantzsch and Herrmann insisted that if a substance could be isolated in two stable forms it should be called desmotropic (Piroxicam, Scheme 1.2b), while if it could not be isolated it should be termed tautomeric.⁵⁵ Although there are no examples of desmotropy involving three tautomeric structures in different crystal structures but limited to only two isomeric structures in the literatures.⁵⁶

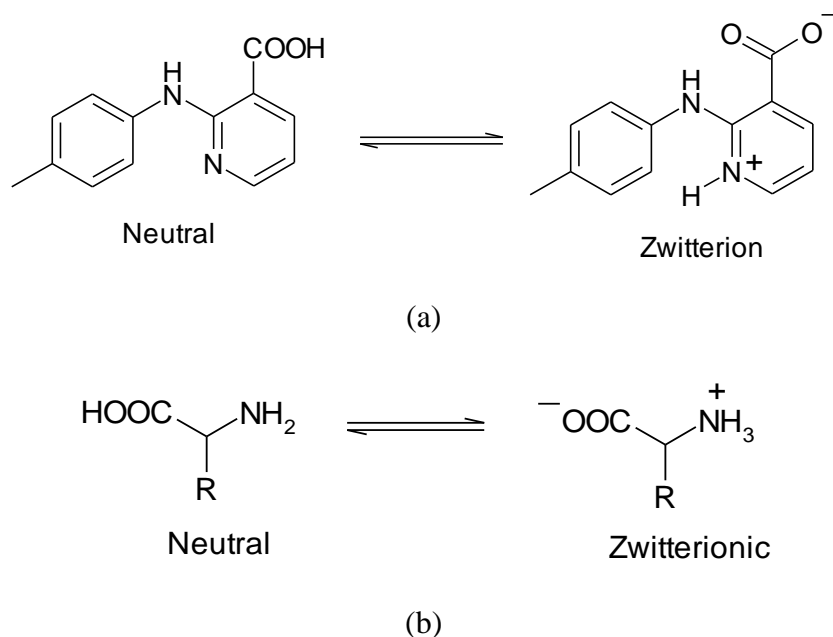


Scheme 1.2 (a) Tautomeric pentamorphs of 2-thiobarbituric acid, (b) Two desmotropes of piroxicam

1.4.1.4 Zwitterionic and Neutral Polymorphism (Desmotropism)

In chemistry, a zwitterion (in German word *zwitter* means *hybrid*) is a neutral molecule with a positive and a negative electrical charge simultaneously present in the same molecule.⁵⁷ Amino acids and some of the ampholytes are the well known examples for zwitterions. Some of the ampholytes are crystallized as neutral polymorph in one crystal structure and zwitterionic polymorph in another crystal structure for the same molecule. There is an intramolecular proton transfer in nucleation and crystallization steps (2-(*p*-tolylamino)nicotinic acid, Scheme 1.3a).⁵⁸ These polymorphs are not common for all organic amphoteric molecules and even in amino acids. Very few drug examples in the literature are reported as neutral and zwitterionic polymorphs including the amphoteric drugs ciprofloxacin, norfloxacin, torsemide, clonixin and tianeptine and remaining amphoteric drugs are reported as either neutral or zwitterionic in their crystal structures. Generally, the solubility and stability are inversely related for any drug polymorphs. However, the zwitterionic polymorphs are highly stable and soluble compared to neutral polymorphs. This is the main advantage of these ionic forms in the pharmaceutical industries to optimize the physical property without any chemical modification of drugs. Recently, Nangia et al proved experimentally in model and drug compounds that the twin characteristics of high solubility and good stability may be jointly optimized in the same zwitterionic polymorph for marketed amphoteric drugs.⁵⁹ Thus, the drug property can be improved by zwitterionic polymorph optimization method for any amphoteric drug without altering the original drug formula. When we are able to separate these neutral and zwitterionic isomers in the crystal structures then they can be called as desmotropes. Surprisingly, there were no reports on the neutral polymorphs of 20 amino acids in the literatures; ten of those amino acids are resulting only zwitterionic polymorphic crystal structures till date (Scheme 1.3b). Once we optimize and understand the neutral polymorphs formation from amino

acids in crystallizations and may be the zwitterionic forms from the ampholytes could be explored further in applications. The optimization and control of zwitterionic polymorphs would be utilized in pharmaceutical industry because of the twin characteristics of these ionic polymorphs.



Scheme 1.3 (a) Two isomers of 2-(p-tolylamino)nicotinic acid for neutral and zwitterionic polymorphs (desmotropes) (b) Isomeric amino acids but only zwitterionic polymorphs present (no desmotropy in amino acids)

1.4.1.5 Concomittant and Disappearing Polymorphs

Bernstein and Davey elaborated the term ‘concomitant polymorphs’ in crystallization experiments that yield crystals of different polymorphic structures simultaneously and potentially offer both structural and thermodynamic information, not available when only one phase crystallizes.⁶⁰ Crystallization is a remarkable process that brings approximately 10^{20} molecules or ions into an essentially ordered array, and results in the same structure or limited number of structures, in the case of polymorphism for every crystal. In this process, the regions in which there is overlap of occurrence domains in nucleation one may expect that two or more polymorphs

would crystallize under essentially identical conditions thus leading to this concomitant polymorphism.⁶¹ The occurrence domain can be the solvent, temperature, rate of evaporation or cooling, and other conditions under which a material will crystallize for any substances. It is of more meaning when we discuss this with energy functions. The free energy associated with any chemical reaction is a transition state and an activation free energy which can decide the relative rates of formation of the two structures. Crystallization is not well understood by the nature of the activated state because it relates to a large collection of self-assembled molecules with precise packing arrangement a new separate nucleate or solid phase (Fig. 1.6).

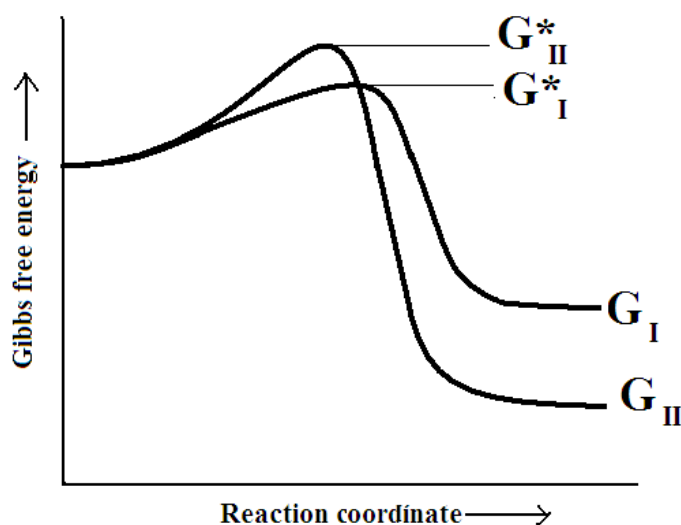


Figure 1.6 Crystallization energy profile of two polymorphs (Ref. 60).

The concept of critical size in which an assembly of molecules must have in order to be stabilized by further growth is the main part here to include in the crystallization process. The higher the operating level of supersaturation, the smaller this size is typically a few tens of molecules. In Figure 1.6, the supersaturation with respect to form I is simply $G_0 - G_I$ and is lower than $G_0 - G_{II}$ for structure II. However,

it can now be seen that if the critical size is lower for I than for II for a particular solution composition then the activation free energy for nucleation is lower and kinetics will favor form I. Finally form I will have to transform to form II, Overall the probability that a particular form will appear is explained by Equation (1),

$$P(i) = f(\Delta G, R) \dots \dots \dots (1)$$

in which ΔG is the free energy for forming the i th polymorph and R is the rate of some kinetic process associated with the formation of a crystal by molecular self aggregation in Equation (2).

$$G = H - TS \dots \dots \dots (2)$$

Thus, if we follow the above reasoning we could equate the rate process with J , the rate of nucleation of the form. If all polymorphs had the same rates of nucleation then their appearance probability would be dominated by the relative free energies of the possible crystal structures.

$$J = A_n e^{\left(\frac{-16\pi\gamma^3\theta^2}{3k^3T^3\sigma^2}\right)} \dots \dots \dots (3)$$

The rates of nucleation is as expressed by the classical expression of Volmer related to various thermodynamic and physical properties of the system such as bulk and surface free energy (γ), temperature (T), degree of supersaturation (σ), solubility (hidden in the pre-exponential factor A_n) in Equation (3).⁶²

Figure 1.7 shows three possible simultaneous solutions of the nucleation equations which involve the careful control of the occurrence domain, there may be conditions in which the nucleation rates of the two forms are equal and hence their appearance probabilities are nearly equal. Under these conditions we might expect the polymorphs to crystallize concomitantly. Many polymorphs are reported as concomitant polymorphs and For example, polymorphs I, II and III of 6-chloro-2,4-

dinitroaniline are concomitantly crystallized from CH_2Cl_2 resulted the needles (Form II) and indistinguishable I and III polymorphs (Fig. 1.8) amongst the chunks.¹¹⁹

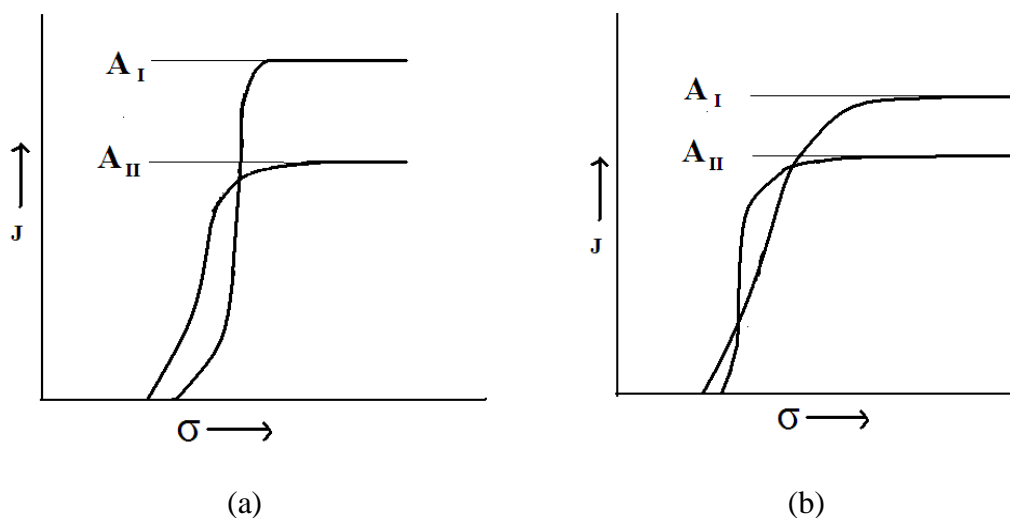
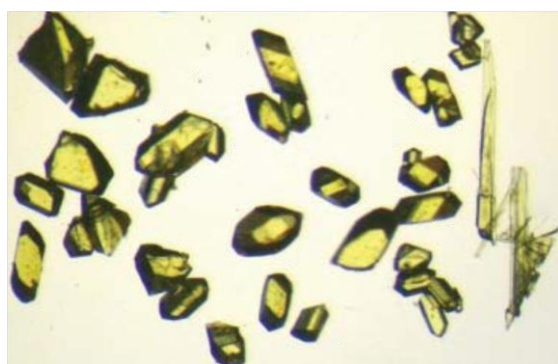
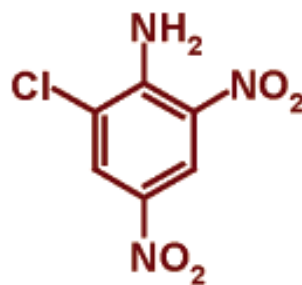


Figure 1.7 Rates of nucleation (J) are plotted as functions of supersaturation (σ) for the dimorphic system and simultaneous nucleation of the forms at supersaturation levels corresponding to the (a) crossover (b) two crossovers of the curves (Ref 60).



(a)



(b)

Figure 1.8 (a) Mixture of polymorphs I, II and III of 6-chloro-2,4-dinitroaniline concomitantly from CH_2Cl_2 : needles (Form II) and indistinguishable I and III polymorphs amongst the chunks (b) Molecular structure of 6-chloro-2,4-dinitroaniline (Ref 119).

Disappearing polymorphs are unfortunate events where the polymorph was previously considered to be stable and easy to make, suddenly becomes very difficult to obtain. The reasons for these problems may be poor understanding of mechanism involved in nucleation and crystallizations. The phenomenon of ‘disappearing polymorphs’ where a previously apparently stable form can no longer be routinely produced, is a scientific anathema.^{63a} Indeed it should be possible to reproduce any metastable polymorph by reproducing the appropriate crystallization conditions but not. The new outcome suffers from a ‘disappearing polymorph’, which can be found to our surprise that a second polymorph of maleic acid was obtained 124 years after evidence of the first crystal form was reported (Fig. 1.9).^{63b} To avoid this we need to understand the mechanism involved in the stabilization of crystallites in the nucleation and the proper solvent selection enables the solute solvent interaction to be tuned to promote: (i) the desired conformation, (ii) the mode of molecular assembly and (iii) modify the growth kinetics of the crystal as reflected in the crystal habit and the transformation of one phase to another. Further an effective crystal engineering strategy for polymorph isolation requires: (i) isolation or prediction of polymorphs, (ii) analysis of the similarities and differences between polymorphs, (iii) identification of functionality required by the additive or solvent, (iv) analysis of solvent or additive interaction with host lattice, and (v) experimental verification of selectivity.⁶⁴

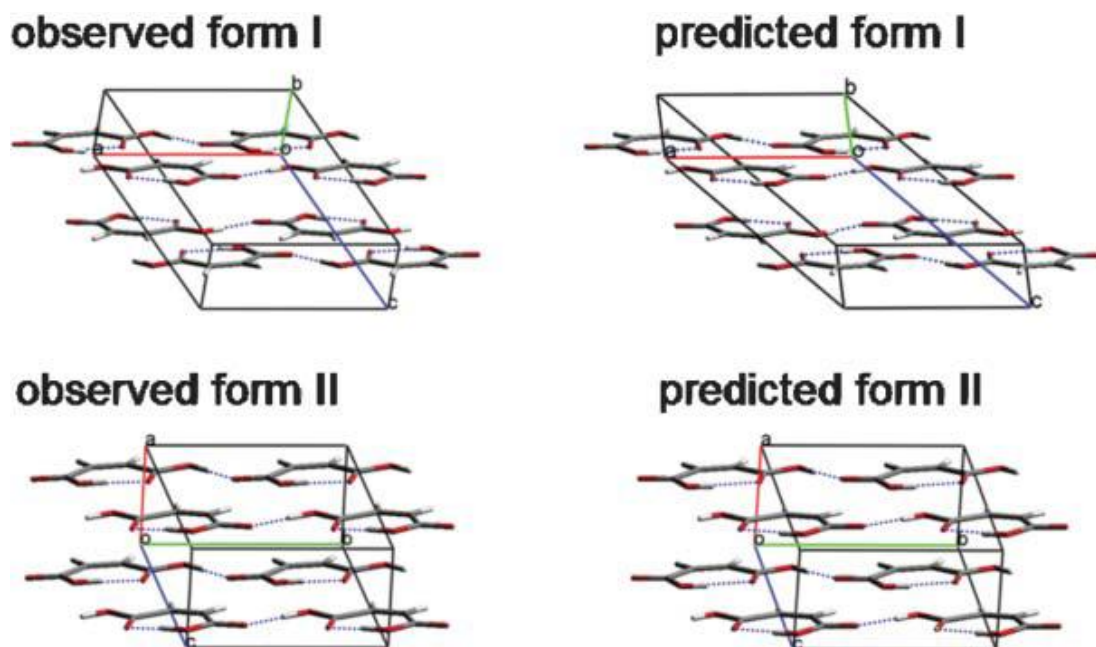


Figure 1.9 Observed and predicted polymorphs of maleic acid (Ref. 63b).

1.4.1.6 Color Polymorphs

Organic solid-state luminescent materials are now attracting interest in various application fields and in fact the tuning of solid-state luminescence by controlling the mode of molecular packing, instead of the commonly used synthetic modification of molecules, has attracted great interest. The related potential application in the development of new organic luminescent materials based on the crystal engineering concept, which would lead to applications in novel photonic, photoelectronic, and sensory materials.⁶⁵ In the beginning, Byrn et al described colorless and yellow forms of a terephthalic acid derivative 3,6-dichloro-2,5-dihydroxyterephthalat in 1972.⁶⁶ Interestingly, many on this topic, “*polymorph-dependent luminescence*”, have appeared recently. In these systems, modification of inter-luminophore interactions or packing-induced conformational changes of any molecules are allowing for tuning the luminescence properties.⁶⁷ However, development of such methods are still remains a challenging task because of the lack

of understandings in mechanisms that allow for alteration of molecular packing with different luminescence properties. A detailed study and plan on the relationships between the molecular packing modes and the luminescence properties are the topic of interest in dealing with multiple polymorph-dependent luminescence is desirable for the study of the structure–property relationships. 5-Methyl-2-[(2-nitrophenyl)amino]-3-thiophene-carbonitrile has been crystallized in heptamorphs as yellow prisms (Y), red prisms (R), orange needles (ON), orange plates (OP), yellow needles (YN), orange-red plates (ORP), and red plates (RPL). It is named as ROY⁷⁰ for its red, orange, and yellow crystal colors (Fig. 1.10a). The related interesting topic is photochromism. Light-induced reversible color change of substances is known as ‘*photochromism*’ and organic photochromic compounds have attracted much attention over the past decades for their applications in optic data storage, electronic display systems, optical switching devices, ophthalmic glasses, this in turn leads to changes in the physicochemical properties of such compounds including absorption, fluorescence, refraction index and electric permittivity.⁷¹ *N*-Salicylideneanilines exhibit photochromism in solution and in the solid state respectively. The trimorphs alpha, beta, gamma forms were formed in the crystallization of *N*-3,5-di-*tert*-butylsalicylidene-3-carboxyaniline (SCA). When the crystals were irradiated with UV light, alpha and beta showed photochromism whereas gamma was unchanged (Fig. 1.10b). Moreover, the lifetimes of the colored species of alpha and beta forms were quite different.^{71a}

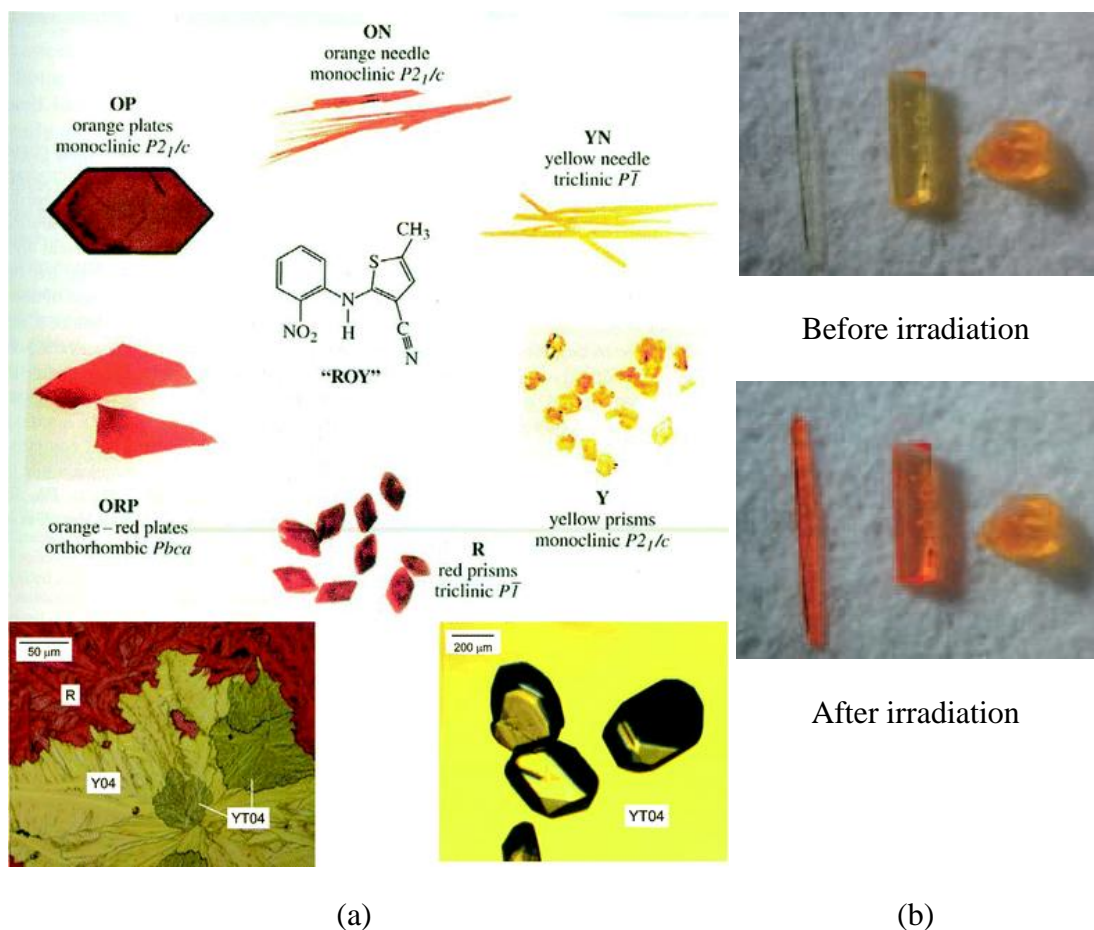


Figure 1.10 (a) Seven polymorphs: yellow prisms (Y), red prisms (R), orange needles (ON), orange plates (OP), yellow needles (YN), orange-red plates (ORP), and red plates (RPL), and Color changes of trimorphs alpha, beta and gamma forms (SCA); Ref. 70 (b) before UV irradiation, after UV irradiation; Ref. 71.

1.4.1.7 Crystallization of Polymorphs

A large number of controllable and uncontrollable factors can influence the outcome of polymorphic crystallization, including supersaturation, temperature, solution concentration, cooling rate, solvent, agitation, pH, additive, impurity, seeding, interface, etc.⁷² Kitamura came up with idea of grouping the controlling factors for polymorphic crystallization into two group of categories and it depends mainly on systems and crystallization methods. The primary factors are the operation

of the polymorphic crystallizations including supersaturation, temperature, seeds, the stirring rate, the addition rate of antisolvent, the cooling rate, the mixing rate of reactant solutions, etc. On the other hand, other factors are solvents, additives, interfaces, etc. are grouped in the secondary factor group.⁷³ Both factors impart thermodynamic and kinetic effects on polymorphic crystallization. Nevertheless, the mechanism of the effect and the quantitative relationship between the operational factors and the crystallization characteristics of polymorphs is not well understood as usual.⁷⁴ The modern techniques and methods that generally used to obtain the polymorphs are *control of supersaturation level*, *control of nucleation temperature*, *solvent screening*,⁷⁵ *Heating and sublimation of the materials*,⁷⁶ *low temperature and high temperature evaporation*,³¹ *roto vapor fast evaporation*,⁷⁷ *seeding technology*,⁷⁸ *capillary crystallization*,⁷⁹ *introduction of additives*,⁸⁰ *polymer-induced heteronucleation*,⁸¹ *nucleation confined in nanopores*,⁸² *heteronucleation on substrates such as ionic liquids and gels*,⁸³ *laser-induced nucleation*⁸⁴ and *crystal structure prediction*.⁸⁵

The new concept of high-throughput (HT) screening and combinatorial synthesis are applied recently to the development of drugs, high-throughput (HT) crystallization systems have recently been developed and are emerging as an accelerator for the discovery and screening of solid forms of an API.⁸⁶ After a particular form at small scale is identified in the HT screening, scale-up studies will be conducted to further optimize the process for laboratory scale production. The HT crystallization has been applied to discover solid forms for a series of APIs, such as acetaminophen, sulfathiazole. Peterson *et al.* discovered the highly unstable form III of acetaminophen by use of the HT crystallization technique.^{86b} In experimental and industrial practice, it has been commonly observed that the metastable form appears first and then transfer into a more stable structure. From this phenomenon, Ostwald⁸⁷ concluded that “when leaving a metastable state, a given chemical system does not

seek out the most stable state, rather the nearest metastable one that can be reached without loss of free energy.” That is, in a crystallization from the melt or from solution, the solid first formed will be that which is the least stable of the polymorphs, the one with the largest Gibbs free energy (Fig. 1.11). As a result, the crystallization of the least stable form is expected to predominate at high levels of supersaturation. Meanwhile this effect is also dependent upon the solvent-solute interactions and other important factors.

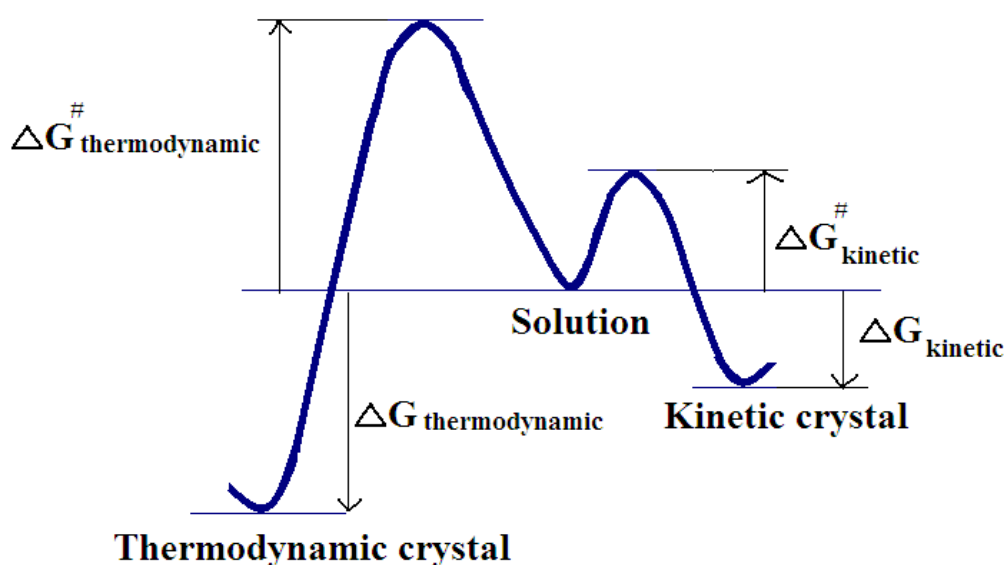


Figure 1.11 Hypothetical transitions from solution to thermodynamic and kinetic crystals. Difference between $\Delta G^{\#}_{\text{thermodynamic}}$ and $\Delta G^{\#}_{\text{kinetic}}$ determines the ease of formation of kinetic crystals (Ref. 87)

1.4.1.8 Characterization of Polymorphs

In the pharmaceutical industry, identification and discovery of polymorphism during early stage development is critical, as unanticipated appearance of polymorph and polymorphic transitions of a drug substance can affect chemical and physical stability, solubility, morphology, hygroscopicity, and, ultimately, bioavailability. A number of analytical techniques have been employed for characterizing polymorphs

and *in-situ* monitoring the formation and transformation of polymorphs during the process.³¹ The analytical techniques and the information extracted from those instruments are available in the Table 1.1 below.

Table 1.1 Analytical techniques and the observation for polymorphs

Category	Techniques	Information
X-ray diffraction	Powder and Single crystal X-ray diffractions	Structure, crystallinity, chemical and phase composition, molecular weight, etc.
Vibrational spectroscopy	FT-Raman and Infrared spectroscopy	Structure, molecular conformation, chemical and phase composition, hydrogen bonding, etc.
Microscopy	Optical, Scanning electron	Crystal size and habit, etc.
	and Atomic force microscopy	Surface properties, interactions between particles, etc.
Thermal methods	Hot-stage Microscopy	Melting point, transitions, etc.
	Thermogravimetric analysis	Melting point, transitions, etc.
	Differential scanning calorimetry	Thermal transitions. Melting point, transitions, heat capacity, crystallinity, etc.
	Differential thermal analysis	Heat and rate of transition, crystallinity, etc.
NMR Spectroscopy	Isothermal calorimetry	
	Solid-state nuclear magnetic resonance spectroscopy (¹³ C and ¹⁵ N NMR)	Chemical and phase composition, structure, crystallinity, intermolecular interaction, conformational change, etc.

1.4.1.9 Thermodynamics of Polymorphs

The thermodynamic and kinetic properties of the polymorphic system is essential for the control of polymorphs accompanied by crystallization process and it requires a full understanding of the nucleation, crystal growth, and phase transformation in the crystallization.³¹ The Gibbs free energy change ΔG_c of a crystallization process at constant temperature and pressure is (4),

$$\Delta G_c = \Delta H_c - T\Delta S_c \dots\dots\dots(4)$$

Where $\Delta H_c, \Delta S_c$ are the enthalpy change and the entropy change of the crystallization process respectively. From the thermodynamic viewpoint, for a polymorphic system, the minimization of ΔG_c is the classical thermodynamic driver (eqn 5), which leads to the formation of stable form, whilst the maximization of the rate of entropy production is the driver in irreversible thermodynamics, which will lead to the formation of less stable form.

$$\Delta G_T = \Delta H_T - T\Delta S_T \dots\dots\dots(5)$$

Meanwhile, the relative thermodynamic stability of polymorphs and the driving force for a transformation at constant temperature and pressure is also determined by the difference in Gibbs free energy between the polymorphs ΔG_T . Where ΔH_T the enthalpy difference between the polymorphs, reflects the lattice or structural energy differences and the entropy difference; ΔS_T the entropy difference between the polymorphs, is related to the disorder and lattice vibrations. When $\Delta G_T < 0$, the transformation can occur spontaneously; $\Delta G_T = 0$, the free energy of the two phases is the same; $\Delta G_T > 0$, the spontaneous transformation is not possible under the specific conditions. According to the corresponding thermodynamic relationships, polymorphs can be classified as either enantiotropes or monotropes, depending on one form can transform reversibly to another or not.

1.4.2 Prediction Rules for Polymorphs

Burger and Ramberger proposed a series of rules for predicting the relative thermodynamic stability of polymorphs and the nature of polymorphic system because the exact course of G isobars cannot be followed experimentally, since the entropy cannot be determined.³⁰ At a given temperature, the thermodynamically stable modification has always the lowest Gibbs free energy.^{31a} Fig. 1.12a represents an enantiotropically related system of two modifications (polymorphs). Modification II shows the lowest Gibbs free energy until the T_p is reached and is therefore thermodynamically stable from absolute zero up to T_p . Beyond T_p , the Gibbs free energy of mod. II is higher than for mod. I; therefore, the mod. II is thermodynamically unstable from T_p up to its melting point. At T_p polymorphs I and II have equal Gibbs free energy and equal thermodynamic stability. The two modifications are enantiotropically related. ΔH_t represent the enthalpy of transition for the transformation II/I, $\Delta H_{f,I}$ and $\Delta H_{f,II}$ represent the enthalpy of fusion for modifications I and II respectively. Figure 1.12c gives an energy/temperature diagram for tedisamil dihydrochloride demonstrating that its three polymorphic forms are enantiotropically related. Fig. 1.12b describes the relations in a monotropic system. Modification II shows a larger Gibbs free energy than mod. I and is therefore thermodynamically unstable compared with mod. I from absolute zero up to M_p . There is no T_p over this temperature region, but a transition in the solid state of mod II into mod. I is possible; however, the reverse transition never occurs.^{31c} It is worth noting that such a monotropic transition is always exothermic, as has been known for a long time but now is often forgotten in the interpretation of new experimental results. Fig. 1.12d gives an Energy/ Temperature diagram for flurbiprofen demonstrating that its polymorphic forms are monotropically related.^{31d,e} Of course there are many reasons why during preparation of a solid substance polymorphic modifications are transformed.

Heat-of-Transition Rule: This rule generalizes that, if an endothermic enthalpy of phase transition between two crystal forms is observed at a specific temperature, so then there is a transition point below this temperature and the two polymorphs are enantiotropically related.^{28c,30} If an exothermic enthalpy of phase transition is observed at a particular temperature, and there is no transition at higher temperatures, the two polymorphs may be monotropically related.

Heat-of-Fusion Rule: The heat-of-fusion rule indicates that in an enantiotropic system the higher-melting polymorph of a pair will have the lower enthalpy of fusion. If the higher-melting polymorph also has the higher enthalpy of fusion, the two polymorphs are monotropically related.^{28c,30} The rule will be valid so long as the Gibbs energy profiles of dimorphic systems can be described.

Enthalpy-of-Sublimation Rule: If the polymorph with the higher melting point has the lower enthalpy of sublimation, the two polymorphs are enantiotropic. Monotropism is realized if the lower melting form shows the lower enthalpy of fusion.^{28c,30}

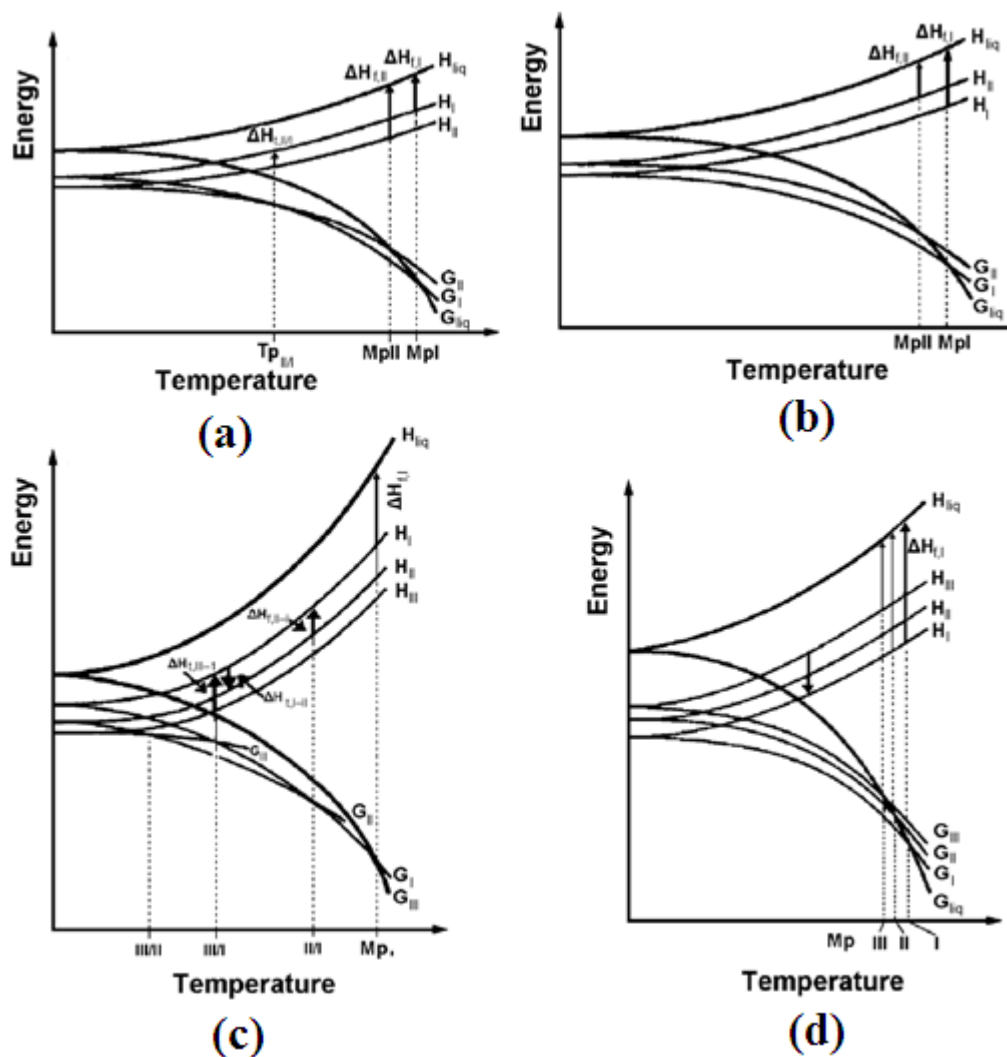


Figure 1.12 Energy–temperature diagrams. *Enantiotropy*: (a) general principles (G , Gibbs free energy; H , enthalpy; ΔH_f , enthalpy of fusion; *liq*, melt; M_p , melting point; T_p , thermodynamic transition point; ΔH_t , enthalpy of transition); (c) example of enantiotropic behaviour: three modifications of tedisamil dihydrochloride (G , Gibbs free energy and H , enthalpy of the melt (*liq.*); mod I (I), mod II (II); mod. III (III); (M_p) melting point; (III/II, III/I, II/I) thermodynamic transition points; ΔH_f , enthalpy of fusion; ΔH_t , enthalpy of transition) *Monotropy*: (b) general principles (G , Gibbs free energy; H , enthalpy; ΔH_f , enthalpy of fusion; *liq*, melt; M_p , melting point); (d) example of monotropic behaviour: crystalline modifications of flurbiprofen (symbols the same as in b), (Adapted from ref 31c).

Entropy-of-Fusion Rule: The melting point is defined as the temperature at which the liquid is in equilibrium with the solid so that the difference in Gibbs free energy between the two phases is zero. According to the rule, if a polymorph has the higher melting point but has the lower entropy of fusion, the two polymorphs are enantiotropically related. Monotropism is inherent if the lower melting polymorph has the lower entropy of fusion.^{28c,30} The entropy of fusion ΔS_f can then be expressed as $\Delta S_f = \frac{\Delta H_f}{T_f}$

Heat-Capacity Rule: At a given temperature, if one polymorph has both the higher melting point and the higher heat capacity than another polymorph, these two polymorphs are enantiotropically related.^{28c,30} For a pair of polymorphs, if the polymorph with the higher melting point also has a higher heat capacity at a given temperature, there exists an enantiotropic relationship between them. Otherwise, the system is monotropic.

Density Rule: If the polymorph with the higher melting point has the lower enthalpy of sublimation, the two polymorphs are enantiotropic. Monotropism is realized if the lower melting form shows the lower enthalpy of fusion. The most energetically stable structure is expected to correspond to the one that has the most efficient packing. The two polymorphs are monotropically related if the polymorph with higher melting point possesses the higher density. Otherwise they are enantiotropically related. This rule is quite general for ordered molecular solids that are dominated by van der Waals interactions. Exceptions such as acetazolamide, are not unexpected when other interactions, such as hydrogen bonds, dominate the packing, since some energetically favourable hydrogen-bond dominated packing arrangements can lead to large voids in the crystal structure with correspondingly lower density.³¹

Infrared Rule: The rule is normally for the hydrogen-bonded crystals and the highest frequency infrared absorption band in polymorphic structures containing strong hydrogen bonds.³¹ The formation of strong hydrogen bonds is associated with a reduction in entropy and an increase in the frequency of the vibrational modes of those same hydrogen bonds. The hydrogen bonded polymorphic structure with the higher frequency in the bond stretching modes may be assumed to have the larger entropy.

Solubility Rule: Since the solubility is directly proportional to the free energy of a polymorph, determination of solubility is the most reliable method of assessing ΔG_T between polymorphs. Generally the stable form has a lower solubility.³¹ It is important to note that although the absolute solubility of a polymorph will be solvent dependent, the relative solubility of different forms will not depend on the solvent used. If one form with a higher melting point has a higher solubility at temperatures above the transition temperature, polymorphs are enantiotropic.^{28c,30} When the polymorphs are monotropic, the solubility of one form with the higher melting point is always lower than another form with the lower melting point.

1.4.2.1 Properties of Polymorphs

The particular advantage of polymorphism is that the chemical identity and utility of the materials remains unchanged from one polymorph to another, so that a direct correlation between activity and solid state structure are made for better understanding in the solid state.³¹ Polymorphism is very important in those areas of chemical research that covers characterization of a material has a pivotal role in determining its ultimate use of pharmaceutical, pigment, agrochemical, explosive and fine chemicals in industries. It is interesting to note that polymorphism has left an impression even on the history of our world (Ex. Sn allotropes).³⁸

Packing properties: Molar volume, Density, Refractive index, Optical properties conductivity, Electrical, Thermal and Hygroscopicity.

Mechanical properties: Hardness, Tensile strength, Compactibility, Tabletability, Handling, Flow and Blending.

Surface properties: Surface free energy, Interfacial tensions and Habit.

Thermodynamic properties: Melting and Sublimation temperatures, Internal energy, Enthalpy

Heat capacity, Entropy, Free energy and Chemical potential, Thermodynamic activity, Vapour pressure and Solubility.

Kinetic properties: Dissolution rate, Rates of solid state reactions and Stability.

Spectroscopic properties: Electronic transitions, Ultraviolet-visible spectra, Vibrational transitions, Infrared and Raman spectra, Rotational transitions and Nuclear Magnetic Resonance chemical shifts.

1.4.2.2 Cocrystals and Salts

Solid-state chemists are focusing on different strategies when attempting to alter the chemical and physical solid-state properties of APIs or any materials, namely, the formation of salts, polymorphs, hydrates, solvates, cocrystals, eutectics and solid solution.⁸⁸ Salt formation is the first and one of the primary solid-state approaches to modify the physical properties of APIs, and it is estimated that over half of the medicines on the market are administered as salts. However, a major drawback with this salt formation approach is that the API must possess a suitable basic or acidic ionizable site.⁸⁹ The other immediate idea is that the cocrystals in which the multicomponent assemblies held together by freely reversible non-covalent interactions offer a different pathway where any API regardless of acidic, basic, ionizable groups could potentially be cocrystallized. Aakeröy^{89a} defined the term *cocrystal* as *the structurally homogeneous crystalline material that contains two or more neutral building blocks that are present in definite stoichiometric amounts*. Again Jones elaborated cocrystal as “*a crystalline complex of two or more neutral molecular constituents bound together in the lattice through non-covalent*

interactions, often including hydrogen bonding.” Furthermore, the use of pharmaceutical cocrystal is a common platform and usually applied when an API is one of the molecules in the multicomponent crystalline system. In cocrystallization, evaluation of the API should be carried out with number and arrangement of hydrogen bond donors and acceptors whereas in salt forming ability that depends on ΔpK_a rule, conformational flexibility, and solubility requirements.⁹⁰ The compounds including APIs that are rigid, highly symmetrical, possess strong non-bonded interactions, and low molecular weight are more apt to cocrystallize with GRAS conformers (Generally Regarded as Safe Molecules). Suitable coformers are selected based on hydrogen bonding rules, probable molecular recognition events and toxicological profiles.⁹¹ To extend this idea of selection of the conformers based on the charge distribution, many prediction were made in the last two decades to understand the cocrystal synthesis and mechanism. The first one is that the Hammett substituent constants were used as the basis to model the formation of cocrystal products.⁹² By this way, 32 acid/acid combinations of substituted benzoic acids in the attempted cocrystallization it was interestingly found that 90% of the systems formed cocrystals if the Hammett constants of the coformers were of opposite sign, while only 25% of the systems where the constants were of the same sign yielded cocrystals.⁹³ It was noted in the paper that a direct relationship exists between the Hammett constant and the ionization constant of the carboxylic acids, and hence systems characterized by large differences in substituent constants.⁹⁴ The Hammett constant approach is successful in major level. Another approach for studying the salt-cocrystal continuum has involved the evaluation of protonation states using X-ray photoelectron spectroscopy, where the shifting in energy of the nitrogen 1s spectrum of theophylline was used to evaluate the degree of proton transfer. In the formation of an adduct with citric acid, and the equivalence in energies of the nitrogen 1s spectra in theophylline and its citric acid adduct was the substantial existence of a cocrystal formation and the lack of salt formation.⁹⁵ Cocrystal eutectic

constants are calculated as the ratio of the solution-phase concentrations at the eutectic point of the compounds making up a cocrystal species which are the indicators of phase behavior. These constants were shown to be capable of providing guidance to the selection and synthesis of cocrystals.⁹⁶ The third approach is Hansen solubility parameters, and it was used as part of an interaction study of 30 coformers with indomethacin, and it was proved to improve the efficiency of cocrystal screening.⁹⁷ The degree of proton transference in a hydrogen-bonded synthon determines whether a particular solid should be classified as a cocrystal or as a salt or else continuum between salts and cocrystals retain their property. The fourth one is the degree of transfer between substituted pyridine derivatives and a series of carboxylic acids were evaluated using molecular electrostatic potential surface (MEPS) calculations,⁹⁸ and it was reported that the calculated charges on the *N*-heterocyclic base bond acceptor could be used to predict the existence of a salt or a cocrystal. Formation of the salt was inevitable once the charge on the hydrogen-bond acceptor exceeded a critical value, while the intended cocrystal could not form if the charge was too low.

By converting APIs into pure salts/cocrystals if they are liquids at or below body temperature, some problems typically associated with solid APIs such as low solubility and polymorphism, may have to overcome. The non-covalent modification of APIs has become the immense interest in their regulatory and intellectual property ramifications, as well as the technological aspects. Already the new crystalline salts and solvates of a known API are considered as patentable new forms. But the cocrystals could also be considered as patentable but it can be the novel forms if they improve upon drug properties. Cocrystals are not yet approved and marketed as drugs but there is a lot of scope and reason for optimism. Much recognition for one of the first studies of comparing the pharmacokinetic profile of a novel carbamazepine: saccharin cocrystal⁹⁹ to a marketed drug carbamazepine (Tegretol®)

drew the industrial attention with economic aspects of this field. Indeed, some APIs currently marketed as salts such as caffeine citrate may assumed to be cocrystals. The co-crystals of fluoxetine·HCl (Prozac) and various organic acids reported by Childs et al. are the well known examples for ionic cocrystals.¹⁰⁰ Co-crystals would be considered analogous to API-excipient systems such as inclusion compounds of drugs and so would not be considered new drugs as per the FDA norms. Rather, they would be eligible for approval under an Accelerated New Drug Application (ANDA), which only requires proving bioequivalence to a market drug (CBZ:SAC can be taken). However, the FDA regulates novel salts of an API as entirely new drugs which must undergo full testing. It means the full biological test is needed to prove the equivalence of drug activity with the new cocrystal and it requires several screening test to be approved as drugs. So the Selection of an appropriate salt or cocrystal form for a new drug entity provides the pharmaceutical and formulation scientist to modify the characteristics of the potential drug substance and to permit the development of dosage forms with good bioavailability, stability, manufacturability, and patient compliance. Salts are most commonly employed for modifying aqueous solubility. However, the salt form selected will influence a range of other properties such as melting point, hygroscopicity, chemical stability, dissolution rate, solution pH, crystal form, and mechanical properties.¹⁰¹

1.4.2.3 Cocrystal/ Salt Polymorphs

Polymorphs offer a unique way to study the structure–property relationships of the drug compound of single or multi component systems resulted from the different crystalline environments. As we know that characterizing and analyzing the polymorphic property of an API is important in the drug developments. It is estimated that more than 50% of drug molecules are polymorphic and studies concerning polymorphism in cocrystals and salts are not so explored well and very few studies are available for identifying novel polymorphs of cocrystals.¹⁰² As per

the recent report, polymorphs of 17 cocrystals have been found to crystallize concomitantly out of the 114 polymorphic cocrystals reported. Cocrystallization experiments can be conducted from solvents of different polarities and solvent mixtures and a number of polymorphs were reported for cocrystals by conventional crystallization techniques.^{102b,c} Parallel to solvent-based cocrystallization technique, solid state grinding is used extensively for cocrystal screening. Forms I and II of the 1:1 cocrystal of caffeine–glutaric acid was crystallized concomitantly from evaporative crystallization but form I was obtained by neat grinding or grinding with a few drops of non-polar solvents and then form II can be obtained by grinding with a few drops of polar solvents.¹⁰³ Trask et al. have shown that the two polymorphs of the cocrystal of caffeine with glutaric acid showed differences in stability property under elevated relative humidity (RH) conditions.^{103ba} Goud and Nangia have recently reported two polymorphs of a cocrystal of a sulfonamide antibiotic, SACT with ACT with improved solubility and dissolution rates. The crystal structure analysis revealed that these two polymorphs were distinguished by N–H···O sulfonamide and N–H···O carbonyl hydrogen bonds and thus can be classified as synthon polymorphs.^{104a} Desiraju coined the term supramolecular synthon and defined it as *structural units within supermolecules which can be formed and/or assembled by known or conceivable intermolecular interactions*.²¹ A different conformational polymorphism has been observed by Braga et al. for 1:1 cocrystal of pimelic acid with BP, which forms three polymorphs that show minor differences in their overall crystal packing but feature differences in the conformations of pimelic acid.^{104b} When different tautomers of a compound crystallize in different crystal forms, they are termed as tautomeric polymorphs. In general, tautomerism occurs when the constitutional isomers of different hydrogen-atom connectivities are in dynamic equilibrium with one another. A 1:1 cocrystal of a nonsteroidal anti-inflammatory drug, piroxicam with 4-HBA represents a rare case of tautomeric polymorphism in cocrystals.^{104c} Saha recently reported a methanol solvate of a

cocrystal of 1,3,5-benzenetricarboxylic acid (BTA) with 4,4'-methylenebis-(2,6-dimethylaniline) (MBDA) in a 1 : 1 : 1 molar ratio which exists in two polymorphic forms.^{104d} Ma et al found that cocrystallization of C-methylcalix[4]resorcinarene (CMCR) with BP in the presence of benzil resulted in concomitant crystallization of two polymorphs of a 1 : 1 : 1 ternary cocrystal, CMCR–BP–benzil.^{104e} In another ternary system, the crystal structures of two polymorph is shown to have 10 independent molecules in the asymmetric unit of trimesic acid (benzene-1,3,5-tricarboxylic acid, TMA), *tert*-butylamine (TBA), and methanol. Among polymorphic systems reported previously, there are very few examples for which two polymorphs have 10 or more independent molecules in the asymmetric unit and very few examples of co-crystals comprising three or more distinct organic molecules.^{104f}

Salt polymorphs are also reported and limited to very few in the literatures. A second polymorphic form of a 1 : 2 : 3 pamoate : DABCO : water salt has been obtained by liquid-assisted grinding, and it is shown that interconversion between this salt and a salt with 1 : 1 : 2 stoichiometry is facile via liquid-assisted grinding with additional amounts of pamoic acid.^{104g} In other case, A metastable polymorph of metformin hydrochloride is identified in capillary crystallization technique and characterized by thermal microscopy.⁷⁹ The stability relationship between the two polymorphs of metformin–embonate can be inferred from the solubility and dissolution measurements at room temperature in the aqueous medium. The above results indicate that form II is more stable at RT, which therefore has a lower solubility and lower dissolution rates compared to the less stable form I.^{105a} Both hydrochloride and hydrobromide carbamazepine salts (CBZHCl and CBZHBr) were initially isolated as metastable polymorphs that subsequently spontaneously transformed to the more favorable isomorphic forms, CBZ.HCl (II) and CBZ.HBr (II).^{105b} Six structures of new salt forms of CBZ and

CYT are reported and their occurrence and structural similarities discussed by Kennedy et al. Piperazinium meclofenamate salt (1:1) crystallized as monoclinic ($P2_1/c$) and orthorhombic ($P2_12_12_1$) polymorphs concomitantly from acetonitrile solvent.^{105c} Many other salt polymorphs are reported elsewhere and related the structural importance in deciding the solid state characteristics with polymorphs.¹⁰⁶

1.4.2.4 Solid Solution and Eutectic Composition

Solid solution are possible only between the materials that should have isomorphous⁵² that means same space group and unit cell dimensions and/or almost same type and position of atoms or functional groups or isostructural having same structure but not necessarily the same unit cell dimensions present in the materials.¹⁰⁷ Hume-Rothery rules says that solid solution is often formed by isomorphous crystals where the crystal structures having the same space group and unit cell dimensions.¹⁰⁸ These solid solutions are sustained by strong cohesive interactions and retain the lattice structure of the parent (major) component as the inclusion of the second (minor) component happens substitutionally or interstitially in the parent crystal lattice. This topic is not explored so well for organic and pharmaceutical materials to understand their structure property relationships.²⁵ Thus, the distinction of components as solvent and solute is superficial in continuous solid solutions, since they can mix in any proportion. When the interacting materials have similar size and crystal structures, they can have unlimited solubility and accommodate and distribute well in the crystal lattice, either substitutionally or interstitially, without disturbing the parent lattice structure and thus form continuous solid solutions (Cu-Ni).^{108c} They can form a homogeneous phase or solid solution throughout the lattice wherein no interface exists between the copper and nickel atoms, non-isomorphous crystals can give rise to a eutectic. Solid solutions are possible to characterize by single crystal X-ray diffraction as the site occupancy factor (s.o.f.) of atoms and it can be used to determine the integrity and stoichiometry of the components.²⁵ When the materials

have atomic/molecular size/shape mismatch and asymmetry in the crystal structures, they have limited solubility and thus cannot fit beyond a threshold in the crystal lattice of each other, since this will cause strain and disorganization of the lattice structure. Such systems cannot form continuous solid solutions and instead tend to form eutectics (Pb-Sn).^{108c}

The components of eutectic solid solutions can be differentiated as solvent/solute because of limited solubility in one another. Therefore, *a eutectic can be envisaged as an ensemble of many/different solid solutions which are discontinuous.*²⁵ The individual components retain their crystal structures as discontinuous solid solutions and form the eutectic crystal lattice. A eutectic's microstructure may be more precisely defined as '*a conglomerate of solid solutions*' or '*a conglomerate of lattice structures of different materials.*'²⁵ Fortunately, the atomic pair distribution function PDF is available to estimate the instantaneous atomic arrangements and reveals the local structure (low r region) from the average crystallographic structure. The utility of pair distribution function (PDF) in the characterization of felodipine–eutragit E solid dispersion is an early pharmaceutical example.^{108d} The characterization of eutectics is really a challenge because depression in melting point by thermal methods DSC, Kofler's hot stage microscope, heat–cool–reheat is the only indicator of eutectic formation. Anti-tuberculosis combination drugs are found to form eutectics upon thermal treatment (pyrazinamide–isoniazid and rifampicin–isoniazid).^{109a} Apart from the fusion and solvent-based methods, eutectics can also be prepared by compaction (acetaminophen–propylphenazone) and grinding (curcumin–hydroquinone). Aspirin eutectics are reported by melting and grinding techniques.^{109b,c} To exploit the full potential of eutectics as novel organic materials, advances in XRD techniques must dovetail into the preparatory and property studies on eutectics. The several reports of

unsuccessful cocrystallization experiments could actually be latent eutectics, after a thorough analytical study.

1.5 Solubility and Dissolution

Solubility is a thermodynamic property while dissolution is a kinetic process.¹¹⁰ The equilibrium solubility of a compound is defined as *the maximum quantity of that substance which can be completely dissolved at a given temperature and pressure in a given amount of solvent, and is thermodynamically valid as long as a solid phase exists which is in equilibrium with the solution phase.*¹¹¹ Drug bioavailability depends on adsorption that can be assessed by Fick's First law, $J = PC$ where the flux (J) of a drug through the gastrointestinal wall depends on the permeability coefficient (P) of the gastrointestinal barrier for the drug and the drug concentration (C). Generation and maintenance of the metastable supersaturated state is a strategy to improve intestinal absorption of poorly water soluble drugs.¹¹² Two essential steps need to be considered and they are termed the “spring and parachute” approach¹¹³ (Fig. 1.13). A thermodynamically unstable, supersaturated solution of a drug can only be generated starting from a high energy form of a drug which is known as the “spring”. An example might be an amorphous API which is much more soluble than the crystalline material. A combination of excipients such as co-solvents, lipids, or polymer-based formulations can deliver the drug in solution as high energy solid forms that can easily provide an accelerated dissolution or a higher apparent solubility and is known as the “parachute effect”. The apparent solubility is the apparent equilibrium between drug in solution and a solid whose structure is in the high energy state. A high energy form of the drug (the spring) provides the driving force to solubilize the drug at a concentration greater than its equilibrium solubility level and a similar effect resulted by the combination of excipients (the parachute) by inhibiting or retarding precipitation. For a pure solid to be in equilibrium with a solution containing, the chemical potential of solid, μ_0 , must be

the same in the solid (s) and liquid (l) phases; f^* –solubility. So the chemical potential of solid and liquids are same in equilibrium condition is given as follows (eqn 6),

$$\mu_{solid} = \mu_{solution}$$

$$\mu_{0 solid} = \mu_{0 solution} + RT f^* \dots\dots\dots(6)$$

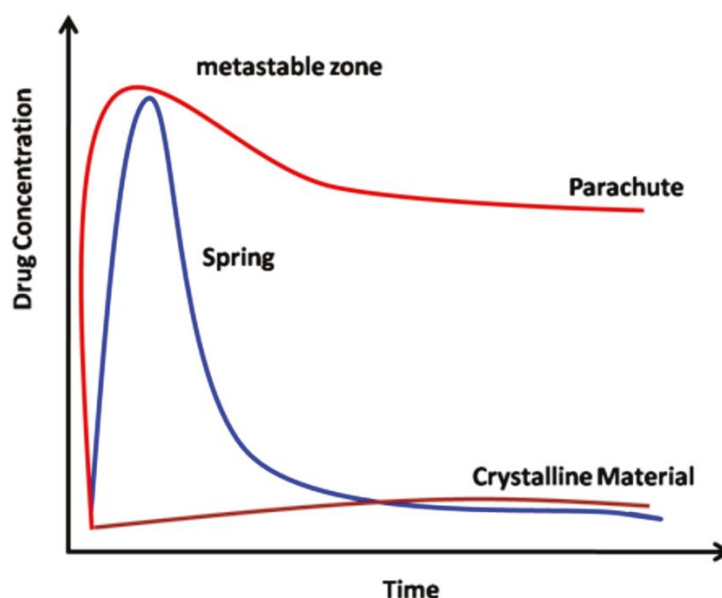


Figure 1.13 “Spring and parachute” approach to promote and maintain supersaturation of poorly soluble drugs (Ref. 113).

Kinetics is a time-dependent term and the dissolution rate of a solid in solvent is written by Noyes–Whitney equation, as follows (eqn 7),

$$\frac{dC}{dt} = \frac{DS_w}{Vh} (C_s - C) \dots\dots\dots(7)$$

where C and C_s represent the concentration of the dissolved substance at a given time t and the solubility concentration of the substance, respectively. The D , S_w , V , and h represent the diffusion coefficient of the substance, the surface area of exposed solid, the volume of solution, and the thickness of the diffusion layer, respectively.

For drugs that undergo phase change during the solubility experiment, the IDR of the drug must be measured (designated J_m and J_s for metastable and stable polymorphs), and these values in turn are used to estimate the apparent solubility of the metastable species. Equation 8 can be derived from the Noyes Whitney Nernst equation,

$$C_m = C_s \left(\frac{J_m}{J_s} \right) \dots\dots\dots(8)$$

The origins of the concept of dissolution impacting the absorption of a drug substance from the GI tract were attributed to a publication by Edwards in 1951 in an excellent historical perspective on dissolution by Dokoumetzidis and Macheras.¹¹⁴ However, the working apparatus and underlying concepts used by scientists to routinely assess the dissolution characteristics of drug substance and dosage forms have not evolved significantly over the same period. Indeed, the USP I/II apparatus typically used around the globe to measure product performance can trace its origins back to the 1960s with formal adoption of the basket stirred flask test by the USP and NF in 1970.^{114b} The simple basket or paddle stirred USP I/II systems provide a well-stirred, medium-rich environment in which dosage form disintegration and dissolution can be evaluated. Such a static, closed environment is limited by the absence of an absorptive sink and the relevance of the resulting hydrodynamics is also questionable given the continuous stirring and large volumes of media often deployed. *In vivo* solubility and dissolution rates are affected by the unique physicochemical properties of the drug and dosage form and by physiological factors such as pH, fluid composition and hydrodynamics. The composition of intestinal fluids is likely to vary considerably due to meal ingestion, diet, gastric emptying, secretion, intestinal transit and motility. All of which can impact both saturation solubility and dissolution rate.^{117a-b} A key exemplar of this class of system is the artificial stomach duodenal model (ASD) which has been used to evaluate the effect of gastric emptying on API dissolution, solubilization and precipitation in a separate

duodenal compartment (Fig. 1.14).^{115c} The *in vivo* relevance of ASD dissolution profiles is based on the assumption that the concentration of dissolved drug in the simulated duodenum is proportional to its bioavailability. The simplicity of this technique combined with biorelevant fluid transfer makes it a powerful tool to understand dynamic dissolution issues for compounds if they are subject to physical chemistry processes such as precipitation, dissolution or solubilization.¹¹⁵

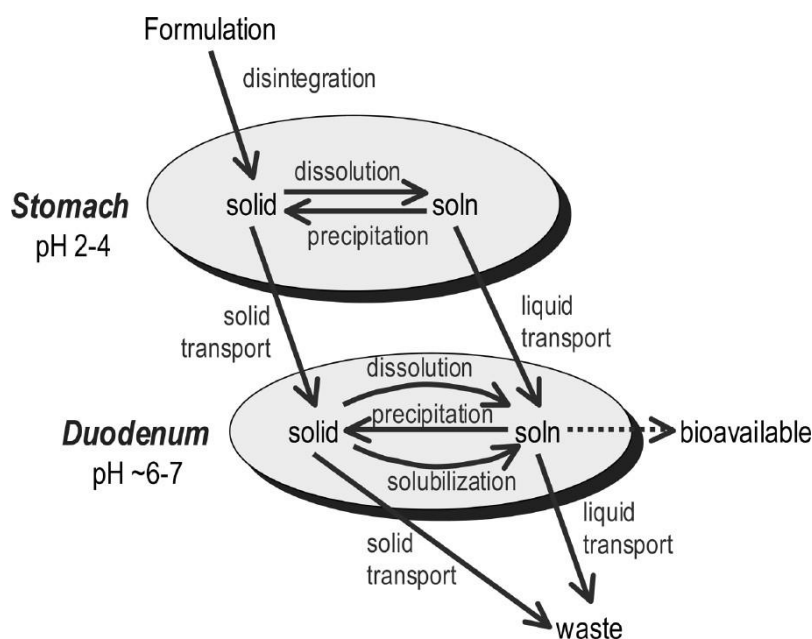


Figure 1.14 Dynamic processes present in the artificial stomach duodenal model (ASD, Ref. 115a).

Maximum Dose Strength. For WHO oral drugs formulated in immediate-release dosage forms, values for maximum dose strength and lowest dose strength (milligrams) were obtained from the WHO Essential Medicines Core List. For the oral drugs in immediate-release dosage forms in the top 200 U.S. list, this information was obtained from the Orange Book (online version updated June 2003).

$$Do = \left(\frac{M_0}{V_0} \right) Cs \dots\dots\dots(9)$$

The above equation 9 was used to calculate the dose number, where M_0 is the highest dose strength (milligrams), C_s is the solubility (milligrams per milliliter), and $V_0 = 250$ mL. A Do value of <1 means a highly soluble drug whereas Do is >1 for low solubility compounds. In simple terms, Do is the number of glasses of water required to dissolve the tablet at its highest dose. Do values of 25-100 are considered low solubility drugs and this number can even exceed 1000.^{113c}

1.6 Structure-property Relationships

Crystal engineering has reached the immense level of developments over few decades as a new subject of the interaction between crystallography and chemistry. Chemistry deals with molecules while crystallography has to do with crystals in which they are extended and long ordered assemblies of molecules in the crystal lattice. The interplay between chemistry and crystallography is just interaction between the structure and properties of molecules on one hand and those of extended assemblies of molecules on the other.¹¹⁶ Polymorphism can cause direct impact on physical properties, melting point (T_m), density (ρ), elastic modulus (E), and hardness (H) of the molecular crystals. In the structure-property context, the variation in the crystal packing or conformations of polymorphs can lead to variations in dissolution, solubility, grindability, and tabletability. So they affect the pharmaceutical industrial processes such as industrial scale ups and formulations.³¹ A new mechanochemical approach that is stress-induced phase transformations of polymorphs from one crystalline form to another during milling and tableting are generally undesirable in drug products. Nanoindentation provides useful information on the mechanical properties of polymorphic drugs, which in turn allows for developing an understanding of their stability in the solid state. Higher hardness, H , and elastic modulus, E , This can be addressed by seeking the correlation between H and solubility of molecular crystals. Both H and solubility depend broadly on crystal structure and the intermolecular interactions. Desiraju has found an inverse linear

correlation between H and solubility (i.e., the higher the H , the lower the solubility) in curcumin and sulfathiazole polymorphs (Fig. 1.15) and confirmed the Gibbs free energy of the polymorphs are close to one another in this study.^{117a}

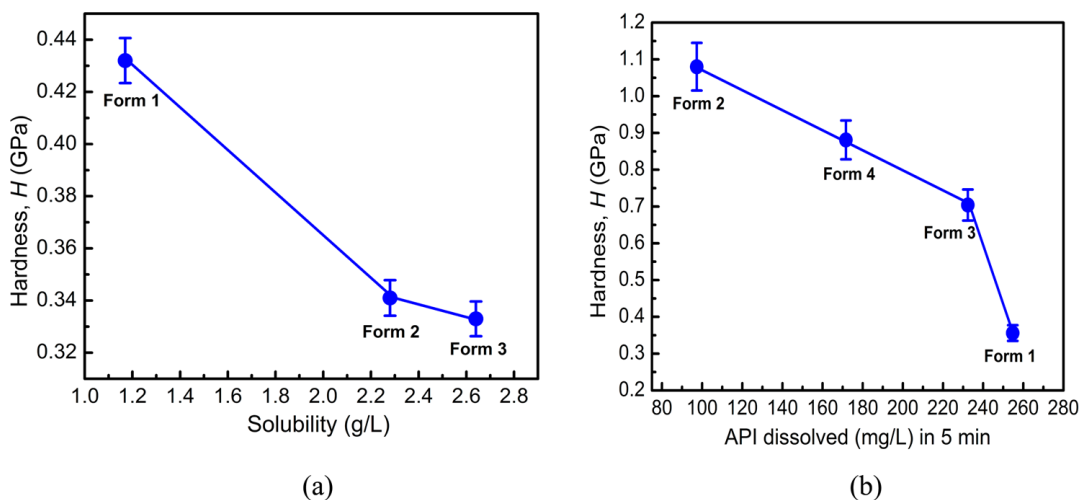


Figure 1.15 inverse correlations of hardness and solubility in (a) curcumin and (b) sulfathiazole polymorphs (Adapted from Ref. 117a).

In the similar way, Desiraju showed the correlation of elastic modulus, E , of the single crystals with T_m measured by the nanoindentation technique and that both E and T_m are strongly dependent on solid state molecular conformations.^{117b} A crystal with a higher E has a similarly larger set of restoring forces between molecules that may be measured with nanoindentation. The melting temperature T_m depends on two thermodynamic factors called enthalpic and entropic factors.^{117c} A higher T_m is associated with efficient three dimensional close packing and higher density. The even diacids have a crystal packing that is dominated by alkyl chain close packing and the melting points and E values are correspondingly high. In the odd acids, the packing follows from a high-energy strained conformation. Relief of this strain energy is provided by melting or by mechanical flexing. This accounts for their anomalously low T_m and E values (Fig. 1.16). Nanoindentation may be used as a direct measure of molecular and crystal energies in molecular crystals.

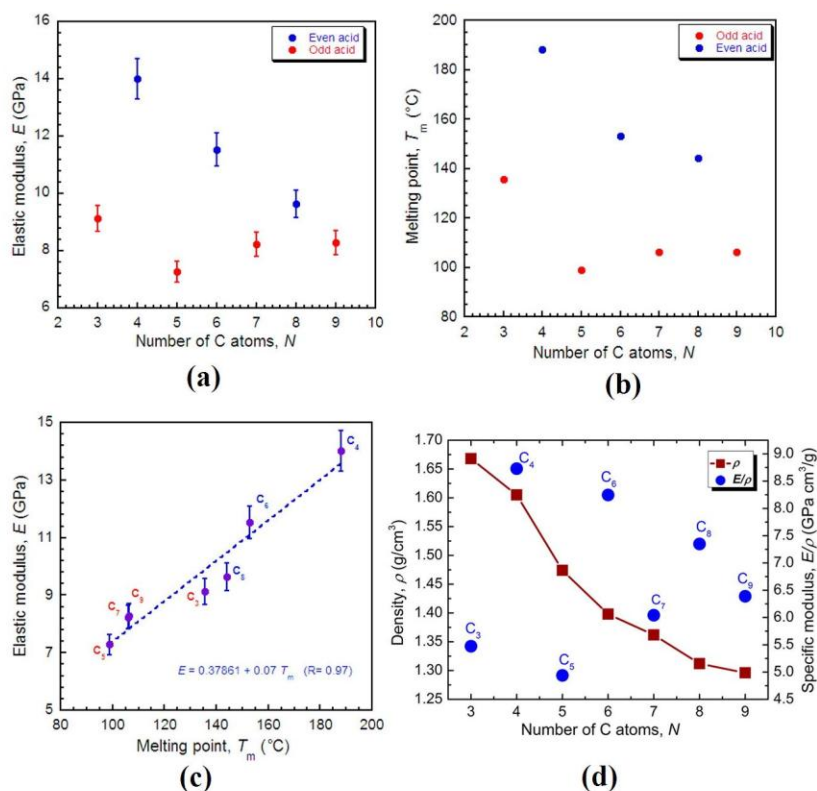


Figure 1.16 Variation of (a) E and (b) T_m with N in α,ω -alkane dicarboxylic acids. (c) Linear correlation between E and T_m , (d) E/ρ vs N and variation in ρ and E with N (Adapted from Ref. 117b).

1.6.1 Compression Behavior

Crystal engineering can be an effective means in rectifying among many other properties, including the poor mechanical properties of a drug for smooth development of tablet dosage forms. The Influence of crystal structures and intermolecular interactions on the tableting properties of paracetamol and sulfamerazine polymorphs is compared here.^{118a} The purpose of this study was to investigate the compression behavior of orthorhombic polymorph and to compare with the monoclinic paracetamol. There are sliding planes present in the orthorhombic form responsible for an increase in crystal plasticity. Tableability of the orthorhombic crystals was observed to be far better than that of the monoclinic

ones. Orthorhombic paracetamol from II exhibited greater fragmentation at low pressure, increased plastic deformation at higher pressure, and lower elastic recovery during decompression compared to form I. A structure analysis of two polymorphs showed that the nature of intermolecular bonds was similar in two polymorphs and the number of bonds is being greater for orthorhombic paracetamol. The crystalline structure accounts for its better compression behavior, because of the presence of sliding planes and orthorhombic paracetamol is suitable for the direct compression process.

Recently the compression behavior of acetaminophen salt was compared with the monoclinic form I and protonated of Acetaminophen hydrochloride monohydrate is discovered to solve these compaction problems associated with paracetamol polymorphs.^{118b} This exhibits improved mechanical properties and superior tableting behavior as expected which can address the poor compaction in ACM polymorphs (Fig. 1.17). Like form II, the flat-layered structure in salt which allows facile plastic deformation of crystals when stressed and a much lower force is needed to make an indent of the same size on the crystal of salt. It is concluded that acetaminophen HCl monohydrate demonstrate its excellent tableting properties to the polymorphs.

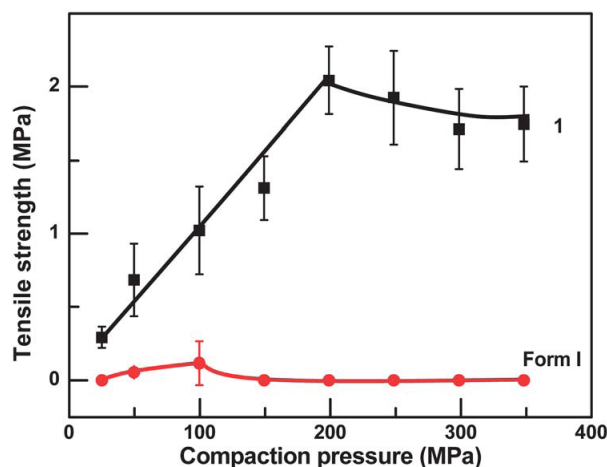


Figure 1.17 Tableability plots of Form I acetaminophen Vs acetaminophen salt (Adapted from Ref. 118b)

Bulk powders of sulfamerazine polymorph I and of two batches II(A) and II(B) of different particle size of polymorph II were crystallized for understanding the compression behavior. The powders were compressed to form tablets of known porosity and tensile strength. The tableability of these polymorphs are following the order of $I \gg II(A) > II(B)$ and compressibility follows the order, $I \ll II(A) < II(B)$. Therefore, the increased tableability of form I over forms II(A) or II(B) is attributed to its greater compressibility. The crystal structure analysis reveals that the slip planes in crystals of I is the reason for good compressibility but this was absent in form II. Slip planes provide I crystals greater plasticity and therefore greater compressibility and tableability.^{118a} Thus, the slip planes confer greater plasticity to crystals of acetaminophen salt than polymorphs, and sulfamerazine polymorphs I than II and therefore greater tableability achieved by using the crystal engineering strategies.

1.6.2 Mechanical Behavior

Polymorphs are quite different in terms of their mechanical hardness/softness, and this is a property of interest in the pharmaceutical and material industry, because the harder form will have better granularity, filterability and flowability properties. For example, the compound 6-chloro-2,4-dinitroaniline has three polymorphs which are obtained concomitantly from a variety of solvents.^{119a} All of them are visually indistinguishable chunks in crystallization flask (Fig. 1.8a) and it is accomplished by picking them by their ability to withstand (Form III) or collapse (Form I) on application of mechanical shear. Form I has Layer structure to show $N-H\cdots O$, $C-H\cdots O$, $C-H\cdots Cl$ and $C-Cl\cdots O$ interactions in the crystal structure and forms the stacking in a [010] plane (Fig. 1.18). Significantly, Forms I and III are quite different in terms of their mechanical hardness/softness in this study and may open an interest in mechanical property. In conclusion, the strength of a tablet is expected to be directly proportional to the strength of intermolecular

interactions in the lowest energy slip planes in the corresponding crystal form. The established relationship between the presence of a thin flat 2D layer structure and high plasticity in molecular crystals of Form I showed that the bending type crystals have an alternate packing type for achieving high plasticity in crystals.

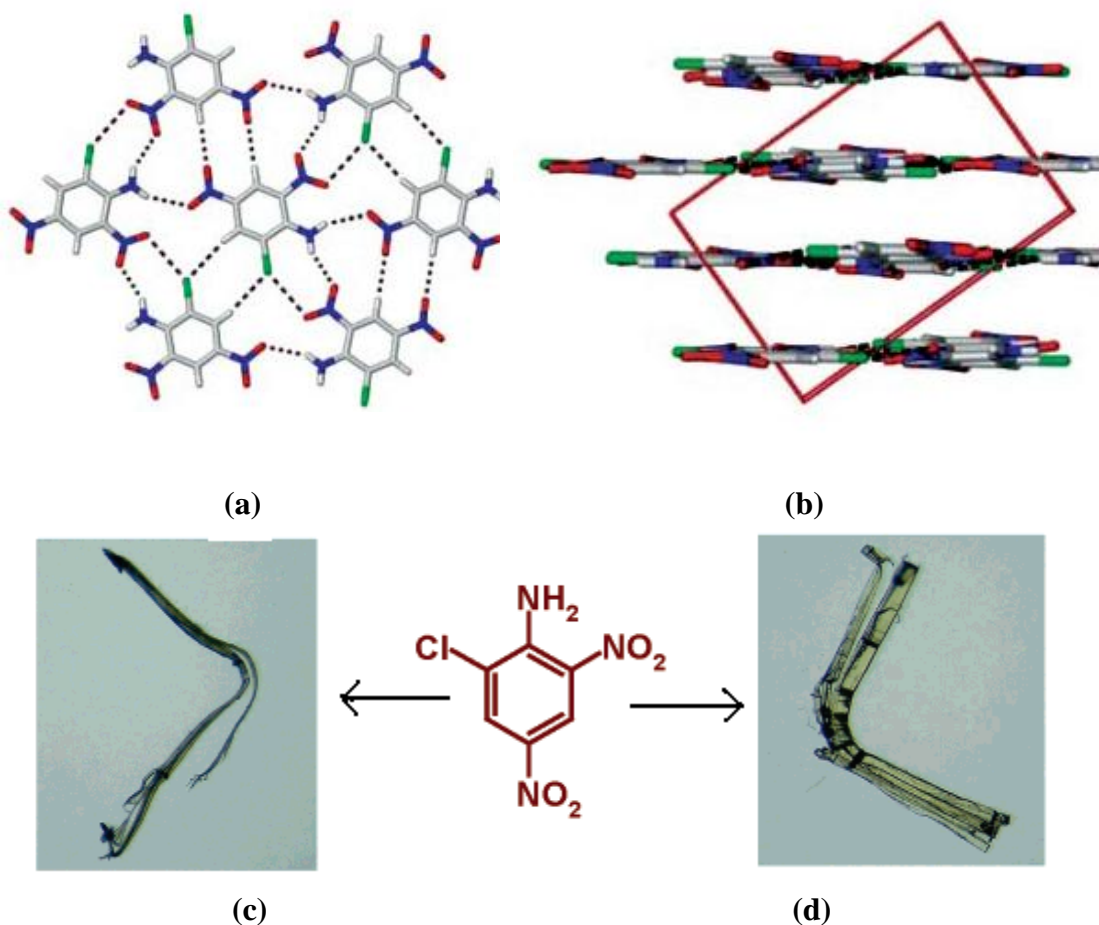


Figure 1.18 Crystal structure of Form I of 6-chloro-2,4-dinitroaniline (CDA), (a) Layer structure to show N-H...O, C-H...O, C-H...Cl and C-Cl...O interactions. (b) View down [010] to show stacking of antiparallel layers (c) Two different crystals of form I that are not only bent but are also cracked along the crystal length. Middle: Molecular structure of CDA (Adapted from 119ab).

Another interesting example is the crystals of C₆Cl₆ and it was deformed into Ω and \cap shapes^{119c} (Fig. 1.19a), depending on the direction and the points of

applying the support and stress on the crystals. When a crystal of C_6Cl_6 (Fig. 1.19b) was compressed carefully along its needle length [010] a bending deformation takes place. It is just continued in extreme level of bending the crystals can even be flattened upon themselves and reaches the zero bend radius. The reason for this extreme level bending nature is that the interactions among halogen atoms between the stacks are weaker and/or less specific than the $\pi \cdots \pi$ interactions within a stack.

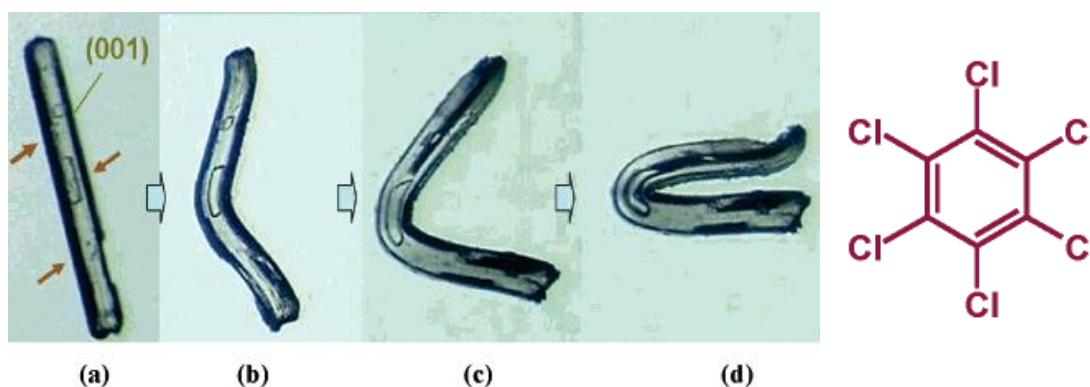
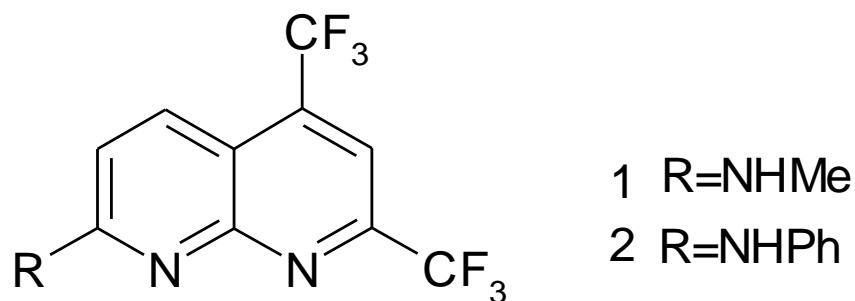


Figure 1.19 Bending of C_6Cl_6 crystal. (a) Before bending. Arrows show the point and direction of the stress applied. (b-d) Different snapshots in the bending process. Notice the very low bend radius (close to zero) in Figure d. Right hand side: Molecular structure of C_6Cl_6 (Ref. 119c)

1.6.3 Solid-state Emission Behavior

Many organic molecules and metal-containing hybrid ligands exhibit solid-state emissions in the field of fundamental research on photophysical properties and applications for electroluminescent devices, light-emitting diodes (LED), solid state dye lasers, and light-emitting electrochemical cells. Basically, this field originated from the intramolecular charge-transfer (ICT) state, excited-state intramolecular proton transfer (ESIPT), aggregation-induced enhanced emission (AIEE).¹²⁰ The characteristics of solid-state emission are that the emitting behavior strongly depends on the molecular structure and molecular arrangement in crystal structures. In the course of development of emitting molecules, polymorph-dependent emissions were

proposed as a promising approach to control the emission properties.^{121a-b} For example, the quinoline derivatives with donor and acceptor substituents as new fluorophores were screened for polymorphic single crystals that could emit different colors.^{121c} Surprisingly, the crystals demonstrated SC-to-SC transformations between the polymorphs in response to heat, and the thermal alteration of molecular rearrangements in the single crystal polymorphs. They were successfully confirmed by X-ray diffraction and X-ray crystallography. The compound N-methyl and N-phenyl derivatives of 2,4-tri-fluoromethyl-7-aminoquinoline (1 and 2 in Scheme 1.4) and their absorption and emission properties in the solution and the crystalline state were compared and the emission change with the thermal SC-to-SC phase transition is also accounted. The absorptions for the powder and the emission spectra for the crystal samples of 1 namely polymorph GB and YG and 2 polymorphs B and G are shown in Figure 1.20. The large red shifts of emission maxima $\lambda_{\text{max}}^{\text{f}}(c)$ and reduction of emission intensity $\Phi^{\text{f}}(c)$ observed in the solid-state emission might be due to the intermolecular $\pi \cdots \pi$ interaction and the intermolecular hydrogen bond. Although the $\pi \cdots \pi$ interaction at distances between the quinoline rings greater than 3.6 Å were limited. The $\pi \cdots \pi$ interaction was considered to stabilize the photoexcited state and led to the red shift of $\lambda_{\text{max}}^{\text{f}}(c)$ and the reduction of $\Phi^{\text{f}}(c)$ in the solid state. In addition, the intermolecular hydrogen bonding might lead the non-radiative decay process. The crystal structure analysis showed the herringbone arrangements for polymorphs (1), slipped parallel and slipped-columnar modes for polymorphs G and B (2) respectively. The herringbone, slipped-columnar, and slipped-parallel modes showed partial overlapping of the quinoline rings with J-aggregate form. In this study, thermal SC-to-SC transformation between the crystal polymorphs that emitted different colors was successfully monitored in irradiation process. However, the observed thermal emission color changes were irreversible.



Scheme 1.4 Molecular structural unit of 2,4-tri-fluoromethyl-7-aminoquinoxaline

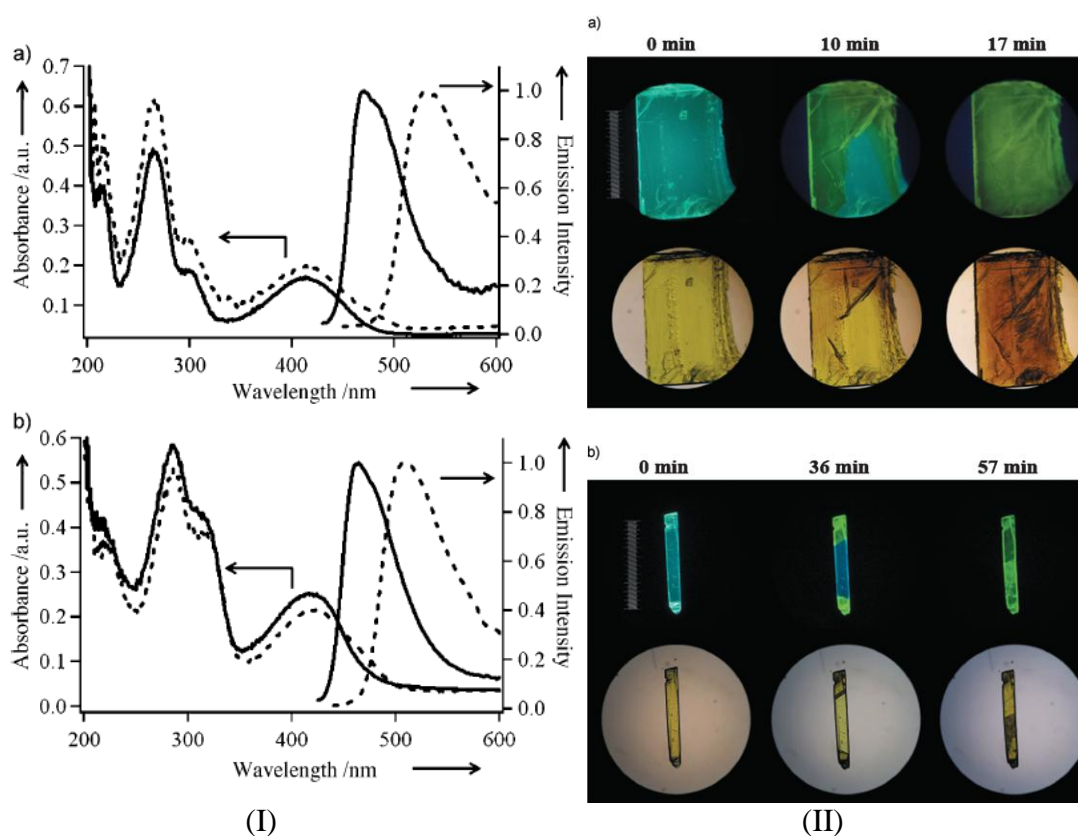


Figure 1.20 (I) Spectra of absorption for the powder and emission for the crystal samples of a) 2 (polymorph GB: solid line, and polymorph YG: dashed line), and b) 3 (crystal B: solid line, and crystal G: dashed line). Arrows in the spectra indicate the vertical axes. II. Time dependence of the views of a) crystal GB of 2 at 90.8 °C and b) crystal B of 3 at 110.8 °C. Top: irradiation at 365 nm. Bottom: Under ambient lighting. Scale bar beside 0 min indicates 1 mm (Adpated from Ref. 121c).

1.6.4 Solubility Behavior

In general, the aqueous solubility of small molecules depends on mainly their hydrophobicity (log P). The partition coefficient log P (eqn 10) can be defined as follows:

$$\log P = \log \left[\frac{\text{solute in octanol}}{\text{solute in water}} \right] \dots\dots\dots(10)$$

Increase of aqueous solubility leads to an increase of the denominator of the above equation and a decrease of log P. To decrease the value of log P by chemical modification, i.e., substitution of hydrophilic group(s) into molecules is a general strategy for improving aqueous solubility of organic compounds. But this approach is limited when we have hydrophilic group(s) in the substitution because sometimes this interferes with the target protein drug interaction and affects purpose of the lead compounds. This strategy is also not effective when both solubility and hydrophobicity need to be increased in special cases to improve the oral bioavailability of highly hydrophilic compounds having insufficient solubility. Furthermore, compounds with poor solubility in both octanol and water sometimes retain poor absolute values of aqueous solubility despite a decrease of log P values, because log P values are just the ratios of two parameters. So there is special focus to find a novel and general strategy to increase the aqueous solubility of drug and bio active candidates that would have a great impact on drug discovery and medicinal chemistry.^{122a} Polymorphism can make an increase in dissolution rate and a temporary or apparent increase of solubility.^{122b} But it cannot produce a permanent alteration of solubility issues. The undissolved solute particles in the solution will revert to its most stable crystal form at any time and therefore the solubility will approach the true thermodynamic solubility. Hence, the role of crystal modification/polymorph is confined to increasing the dissolution rate of drugs. Finally, some of the solubility scientists collectively introduced an alternative

strategy for improving aqueous solubility by means of disruption of molecular planarity and symmetry. Molecular planarity and symmetry are known to influence crystal packing, and disruption of molecular planarity is expected to decrease the efficiency of crystal packing and the melting point.

By following this general strategy to address this solubility, Yalkowsky (1980) came up with the idea of general solubility equations (GSEs) derived on the basis of semi-empirical analysis (eqn 11).^{122c} GSE includes not only log P but also melting point:

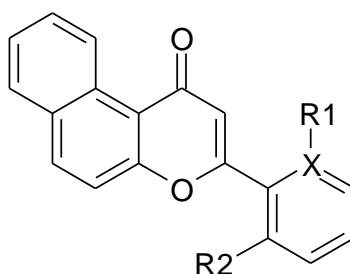
$$\text{Log [solubility (M)]} = 0.5 - (\log P) - 0.01\{[\text{melting point (}^{\circ}\text{C)}] - 25\} \dots (11)$$

The melting point and solubility is closely related to crystal lattice and crystal packing energies. In general, the solubility of a solid solute in water is dependent on two important factors: (a) the crystallinity of the solute and (b) the ability of the solute to interact with water molecules.^{122d} Therefore, the disruption of crystal packing would be an alternative solution for improving aqueous solubility of the drugs. A few chemical modifications focused on crystal packing have been discussed here to compare structure-property relationships. Gavezzotti emphasized that *the melting point is one of the most difficult crystal properties to predict*, and Lipinski mentioned that *the prediction of crystal packing energies is at present extremely difficult*.¹²³ There is a wide scope to make a concrete and general strategy to decrease melting point and disrupt the crystal packing to address these issues by analyzing the crystal packing through crystal structure and melting point determination for solid state chemists. Recently, Lovering analyzed the drug and clinical candidate database and reported that an increase in the fraction of sp³ hybridized carbons is associated with a decrease in melting point.^{124a} In 1995, Gavezzotti noted that *a very old rule of thumb says that symmetrical molecules pack in a three-dimensional periodic lattice more easily than less symmetrical ones and hence form more stable, higher-melting and less soluble crystals*.^{124b} In 1996, Yalkowsky also reported a statistical study

showing that the entropy of melting of organic compounds is related to molecular symmetry number.^{124c} Thus, the relationship between molecular planarity and melting point could provide the basis for a strategy to increase solubility of drug candidates.

In this discussion, we will have to focus on chemical modification of bicyclic lead molecules in different ways to disrupt molecular planarity/symmetry by increasing the dihedral angle. In fact Dihedral angles are considered here for improving the solubility because (i) little is known about the effect of increased dihedral angle on solubility, and (ii) dihedral angle is a convenient numerical parameter that can be obtained by calculation or X-ray crystal analysis among parameters of molecular planarity. For example, β -Naphthoflavone¹²⁵ (Scheme 1.5) was reported to be a more potent aryl hydrocarbon receptor (AhR) agonist than the usual AhR agonist TCDD. Its hydrophobicity is found to be lower than that of other AhR agonists that could make a potentially more useful tool for AhR research. The structural developmental studies of (1) were aimed to obtain AhR ligands with more potent activity and improved solubility. The structure of 1 includes a rotatable biaryl moiety to decrease the planarity of the molecule and later introduced substituent(s) (2-6) on the phenyl group of 1 to understand the structure-solubility relationships. The thermodynamic aqueous solubility of 1-6 was carried in phosphate buffer (pH 7.4) solution. The aqueous solubility of 1 was quite low ($<0.15 \mu\text{g/mL}$) compared to other derivatives. EtOH was used as an aqueous medium for the evaluation of thermodynamic solubility in addition to the buffer solution. The solubility improved to $84.6 \mu\text{g/mL}$. Ortho-substituted derivatives 2-5 showed better solubility than 1 as expected. Indeed, dimethyl analogue 3 was 15 times more soluble ($1270 \mu\text{g/mL}$) than 1. Difluoro analogue 5 showed 3 times greater solubility ($248 \mu\text{g/mL}$) than 1. On the other hand, methoxy analogue 6 was less soluble than 1 (Table 1.2). Compounds 2, 3, and 4 possess increased hydrophobicity, larger dihedral angle, lower melting

point, and improved aqueous solubility compared with 1. These results suggest that introduction of substituent into 1 disrupted the planarity by increasing the dihedral angle in turn to decreased crystal packing energy. This results in lower of melting point and increasing of solubility after this modification. Lack of molecular symmetry of 4 might lead to a lower melting point and greater solubility, or the changes of electron density arising from the introduction of fluorine might have resulted in increased solubility. In the first chapter we expanded this study of comparing the molecular planarity with solubility and dissolution study of cardiosulfa and its analogs to validate this new strategy to make modification in low aqueous soluble drugs for further improvements.



Scheme 1.5 Molecular structure of β -Naphthoflavone AhR agonist

Table 1.2 Thermodynamic solubility of β -Naphthoflavone derivatives

Compound	R1	R2	X	Dihedral angle	Melting point (°C)	Solubility (μg/mL)	CLogP
1	H	H	C	17.8	165	84.6	4.7
2	H	Me	C	37.9	135	262	4.9
3	Me	Me	C	70.0	92	1270	5.1
4	F	H	C	9.1	157	153	4.8
5	F	F	C	40.5	150	248	4.9
6	OMe	H	C	18.5	192	45.8	4.1

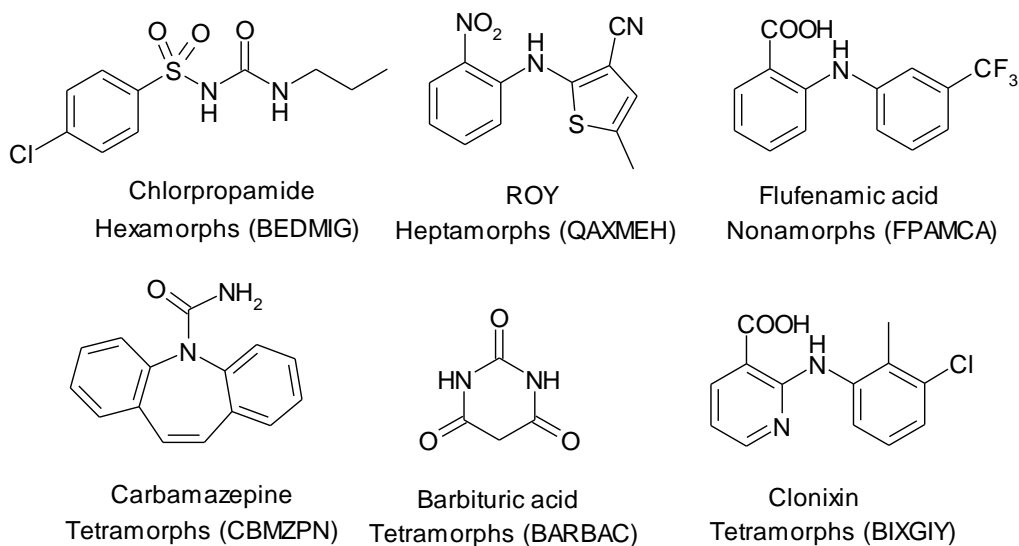
1.7 CSD and Supramolecular Synthon

The Cambridge Structural Database CSD (1965) currently has structural information on over 700000 (2014)^{126a} crystal structures of organic molecules as polymorphs, cocrystals, salts and solvates, and also many organometallic complexes. In the CSD, all crystal structures are differentiated by unique refcode codes having six letters. Any new crystal structure is to be reported that will have this refcode family. In future if any further changes in the structures of the same chemical compound like redeterminations under the same or different conditions or, specifically in the current context, those structures will be given same those six letters plus additionally two more numbers. If there are no accurate structures in redetermination with proper refinement factor then only the unique structure with the lowest R factor will be kept. In addition to redeterminations, potentially wrong structures are also eliminated including structures with R factors of >10% together with structures exhibiting positional disorder of heavy atoms. Therefore, the resulting list contains only structures of high quality with no disorder. Thus, any refcode family containing more than one refcode within the best-R-factor list corresponds to a polymorphic family.³⁸

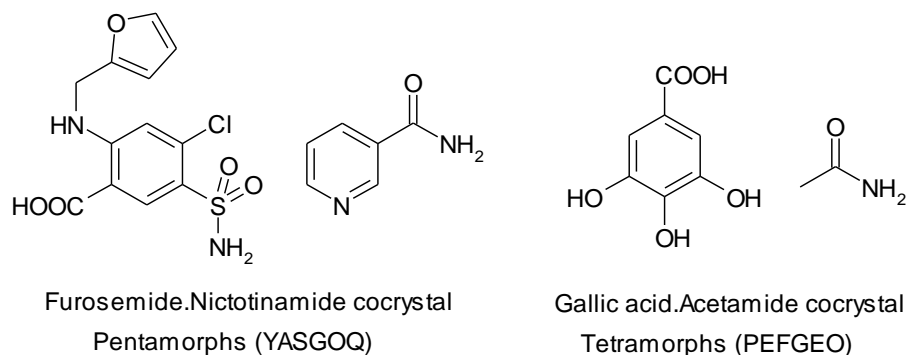
Polymorphs: Only structures with all of their three-dimensional atomic coordinates determined with the exception of hydrogen atoms were retrieved, and polymeric structures were removed. The search returned 2935 different crystal structures containing 1366 polymorphic molecules. Gavezzotti stated that “*structures without a substantial change in the three dimensional symmetry operations should strictly be referred to not as polymorphs but as modulations or phases.*”^{126b} A 2011 data analysis set revealed that 1297 out of 1366 are originally polymorphic retrieved through COMPACK algorithm, 1157 (89.2%) have two polymorphs, 114 (8.8%) have three polymorphs, and only 26 (1.4%) molecules have four polymorphs. Six molecules are there in the pentamorphic systems where as only one molecule has

hexamorph and heptamorph category.³⁸ A new record of polymorphic molecule, Flufenamic acid (FFA), reported by Matzger is the example of nonamorphism in the CSD having nine solved crystal structures. However, there are some families of related molecules, such as the sulphonamides, ROY derivatives, barbiturates, carbamazepine derivatives, and fenamates, which appear to have a strong tendency for polymorphism. A new concept of a *polymorphophore*, first introduced by Matzger as a structural element that, when incorporated into a molecule, favors the formation of polymorphic crystal forms.^{126c} This is analogous to “*pharmacophores*” as particular structures which are particularly useful in finding new leads in drug discovery, especially when the three-dimensional (3D) structure of the receptor is unknown. The concept recognizes that there are families of molecules containing a common substructure (polymorphophore) where many members exhibit polymorphism (Scheme 1.6). These common substructures to several polymorphic molecules have been referred to as polymorphophores.

For cocrystals, polymorphism in 114 of cocrystal cases is a result of conformational flexibility and/or minor structural changes in the packing out of many organic co-crystals in the CSD. Synthon polymorphism in a co-crystal is more specific, and occurs when the primary synthons in the forms are different.^{102a} Five polymorphs (FUR-NCT)^{102b} reported for a cocrystal of a loop diuretic drug, furosemide (FUR), and nicotniamide (NCT) and four polymorphs (GA-ACT)^{102c} for cocrystal of gallic acid with acetamide in the CSD (Scheme 1.7). Dimorphs of ternary cocrystal has also been reported for C-methylcalix[4]resorcinarene (CMCR)^{104e} compound in CSD.



Scheme 1.6 Polymorphophores (substructure for polymorphic molecules) in CSD



Scheme 1.7 Highly polymorphic cocrystals of furosemide and gallic acid in the CSD

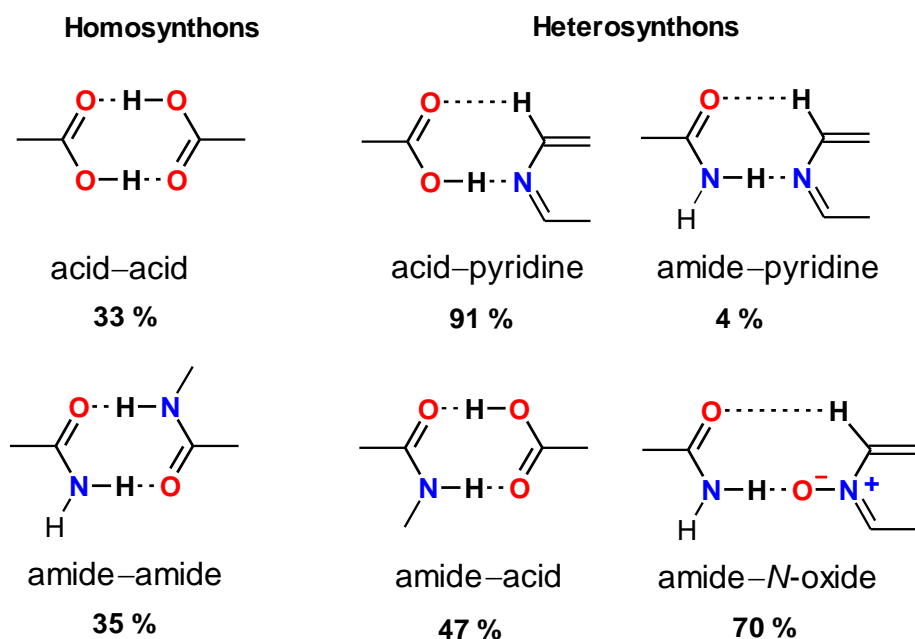
Intermolecular bonds: A bond brings together atoms, molecules, or ions in chemically acceptable and meaningful ways though different modes of orientation with the help of covalent bonds, ionic bonds, metallic bonds, and hydrogen bonds. In IUPAC Gold book, a hydrogen bond is defined as a form of association between an electronegative atom and a hydrogen atom attached to a second, relatively electronegative atom. It is best considered as an electrostatic interaction by hydrogen which permits proximity of the interacting dipoles or charges. Hydrogen bonds can

be inter-molecular or intramolecular. Generally, it is involving fluorine, the associated energies are less than 20-25 kJ/mol. The H atom is the seat of bonding of hydrogen bridge in $X-H\cdots Y-Z$ because it is the key ingredient that brings atoms X and Y together. Hydrogen bonds of the typically $N-H\cdots O$, $O-H\cdots O$, $O-H\cdots X$, $F-H\cdots F$ (Pauling's definition)^{127a} do not violate the definition because they are short, linear, energetically very favorable, and can be identified spectroscopically. This strength follows from the electronegativities of the elements X and Y. Typical "new" hydrogen bonds are the $C-H\cdots O$, $C-H\cdots N$, $O-H\cdots \pi$, $N-H\cdots \pi$, and $C-H\cdots \pi$ interactions^{127e} and still in the controversy to name them as hydrogen bonds. All these weak and strong bonds are mentioned in the table 1.3 for more information.

Table 1.3 Characteristics of Hydrogen bonds

Interactions $X-H\cdots Y-Z$	Strong	Moderate	Weak
$X-H\cdots Y$	Mainly covalent	Mainly electrostatic	Electrostatic
Bond energy (kJ/mol)	60-20	16-60	<12
Bond Lengths (Å)			
$H\cdots Y$	1.2-1.5	1.5-1.2	2.2-3.2
$X\cdots Y$	2.2-2.5	2.5-3.2	3.2-4.0
Bond angles $X-H\cdots Y$ (°)	175-180	130-180	90-150
IR stretching	25%	10-25%	<10%
NMR shift	14-22	<14	-
Examples	Gas phase dimers	Acids	C-H H and π -bonds

The systematic analysis on the probabilities of formation of supramolecular synthons and the Etter's hydrogen ring motifs constructed from O–H...O, O–H...N, N–H...O and N–H...N hydrogen bonds in the crystal structures.^{21,127a-d} The maximum probabilities of formation of 75 bimolecular hydrogen-bonded ring motifs in organic crystal structures were determined to the robust supramolecular synthons. Among all of 34 different hydrogen bond acceptors (O, N, S, halogen and π -acceptors) for the strong carboxyl donor, carboxylic groups are among the best investigated hydrogen bond functionalities possess a hydrogen bond donor as well as an acceptor site that can readily form cyclic dimers (85%) or open arrays or catemer (15%).^{128a-b} However, the probability drops to 33% for dimer and 2.8% for catemer in presence of other functional groups. Zaworotko^{128c} showed 84% probability for amide dimers and 14% for catemers in the absence of competing hydrogen bond donors/acceptors. Again the probability of formation of amide dimer and catemer comes down to 35% and 18% respectively when there are competing groups such as carboxylic acid, secondary amide, aminopyridine, pyridine, water, alcohol, amines etc are present. For example, presence of pyridyl-N as a competitor makes the probability of formation of acid–pyridine heterosynthon 91% than a carboxylic acid dimer or catemer. Hence it is known as the highly robust synthon that can be utilized for crystal design. Zaworotko^{128d} classified synthons as homosynthons and heterosynthons based on the interacting functional groups. Classified synthons as homosynthons and heterosynthons based on the interacting functional groups are given in Scheme 1.8. The known hydrogen bonds are acid–pyridine,¹²⁹ phenol–pyridine,¹³⁰ phenol–amine,¹³¹ acid–amide,¹³² aminopyridine–acid and amide–pyridine-*N*-oxide¹³³ are robust heterosynthons.



Scheme 1.8 Supramolecular synthons with their probabilities calculated from CSD statistical study.

1.8 Conclusions

Polymorphism plays an important role in pharmaceutical and other industries and therefore knowing the possible forms will help to choose the best form for development, determine the most stable form, develop a robust crystallization process, develop a suitable formulation process, avoid processing conditions that could produce another form, prevent latent polymorphs from appearing late in development or in marketed products, prepare an acceptable regulatory package, expand intellectual property for the compound and assess lifecycle management. The identification of zwitterionic polymorphs for amphoteric drugs may open a new way of modifying the drug property suitable for dosage forms without any chemical modification. The crystal engineering strategies are still useful to find out these polymorphs and need some more attention of understanding the mechanism to develop the method to stabilize this new category of polymorphs.

Cocrystals, salts and eutectic compositions are multi components used in the developmental stage of drug properties and it requires the specific strategies to select the conformer which can form cocrystals with API. Salts are the better formulation techniques compared to the cocrystals because of the FDA restrictions on the approval of cocrystal as drugs. It is believed to conduct many biological experiments on cocrystal would help us to reach the next level of marketing the cocrystal products. So the eutectics mixtures and cocrystals are in the clinical stage and now expected to show the equal or more efficiency in clinical performance.

Solubility is the main issue for many drugs in the drug discovery stage and it requires the novel strategies to predict the solubility of new molecules before it come to the synthesis stage. Either chemical modification or crystal engineering techniques should be focused more on this aspect to improve the solubility of lead molecules. This will save the time and investment on working with insoluble drug/lead molecules. This area is now interdisciplinary to biological testing for engineered materials and that would expand the wide scope of crystal engineering in many ways. The structure-property relationships would be useful to develop the material properties by using crystal structure analysis and theoretical predictions of cocrystals and polymorphs.

1.9 References

1. J.-M. Lehn, *Angew. Chem. Int. Ed. Engl.*, **1988**, 27, 89.
2. J.-M. Lehn, *Angew. Chem. Int. Ed. Engl.*, **1990**, 29, 1304.
3. (a) J. W. Steed and J. L. Atwood *Supramolecular Chemistry*, 2nd Ed., John Wiley and Sons **2009**; (b) M. D. Ward, *Science*, **2003**, 300, 1104 ; (c) H. K. Chae, D. Y. Siberio-Perez, J. Kim, Y. Go, M. Eddaoudi, A. J. Matzger, M. O. Keeffe, O. M. Yaghi, *Nature* **2004**, 427, 523.
4. (a) The collected works of sir Humphry Davy, ed. by J. Davy, Vol. VI, London, **1840**; (b) N.F. Curtis, *Coord. Chem. Rev.*, **1968**, 3, 3; (c) N. F. Curtis *J. Chem. Soc.*, **1960**, 4409; (d) N. F. Curtis, R. W. Hay, *J. Chem. Soc. Chem. Commun.*, **1960**, 4409.

5. (a) B. Moulton and M. J. Zaworotko *Chem. Rev.*, **2001**, 101, 1629; (b) A. Nangia, *J. Chem. Sci.* **2010**, 122, 295; (c) I. Rafols, M. Meyer and J.-H. Park, *Hybrid Nanomaterials Research: Is It Really Interdisciplinary?*, in *The Supramolecular Chemistry of Organic-Inorganic Hybrid Materials* eds K. Rurack and R. Martínez-Máñez, John Wiley and Sons, **2010**; (d) O. M. Yaghi, M. O'Keeffe, N. W. Ockwig, H. K. Chae, M. Eddaoudi and J. Kim, *Nature*, **2003**, 423, 705.
6. (a) V. Balzani, M. Venturi, A. Credi, *Molecular Devices and Machines*, Wiley-VCH, **2003**; (b) E.W. Meijer, *Chem. Rev.* **1999**, 99, 1665; (c) M.D. Ward, *Chem. Soc. Rev.* **1997**, 26, 365; (d) A. Poggi, *Chem. Soc. Rev.* **1995**, 24, 197; (e) E. Drexler and C. Peterson *Unbounding the Future: The Nanotechnology Revolution*, **1991**.
7. (a) V. Balzani, *Chem. Rev.* **1996**, 96, 759-778; (b) G. M. J. Schmidt, *Pure. Appl. Chem.* **1971**, 27, 647; (c) G. R. Desiraju *Nature*, **2001**, 412, 397.
8. (a) G. R. Desiraju, *The Crystal as a Supramolecular Entity*, John Wiley and Sons, **2008**; (b) Desiraju, G. R. *Nature*, **2000**, 408, 407.
9. A. R. West, *Solid State Chemistry and its Applications*, 2nd Edition: Student Edition John Wiley and Sons, **2013**.
10. (a) G. R. Desiraju, *Crystal Engineering. The Design of Organic Solids, Materials Science Monographs 54*, Elsevier, Amsterdam, **1989**; (b) A. Gavezzotti, *Curr. Opin. Solid State Mater. Sci.*, **1996**, 1, 501.
11. F. J. DiSalvo *Science*, **1990**, 247, 649.
12. C. N. R. Rao, *New Directions in Solid State Chemistry* C. N. R. Rao and J. Gopalakrishnan, Cambridge University Press, **1997**.
13. (a) L. E. Smart, E. A. Moore, *Solid State Chemistry: An Introduction*, 4th Edition CRC Press, **2012**; (b) G. M. J. Schmidt, *J. Chem. Soc.*, **1964**, 2014.
14. (a) G. R. Desiraju, J. J. Vittal and A. Ramanan, *Crystal Engineering: A Textbook*, World Scientific, **2011**; (b) G. R. Desiraju, *Nature*, **2001**, 412, 397.
15. (a) S. Subramanian and M. J. Zaworotko, *Can. J. Chem.* **1995**, 73, 414; (b) G. R. Desiraju, *J. Appl. Cryst.* **1991**, 24, 265.
16. (a) E. Weber, *Design of Organic Solids*, Springer, **1998**; (b) G. A. Jeffrey, *An Introduction to Hydrogen Bonding* Oxford Univ. Press, New York, **1997**.
17. (a) S. I. Stupp and L. C. Palmer, *Chem. Mater.*, **2014**, 26, 507; (b) R. Bishop *Chem. Soc. Rev.*, **1996**, 25, 311.
18. G. R. Desiraju, *Organic Solid State Chemistry, Studies in Organic Chemistry 32*, Elsevier, Amsterdam, **1987**.

19. (a) J. M. Robertson, *Proc. R. Soc. (London) Ser. A* **1951**, 207, 101; (b) G. R. Desiraju, *J. Chem. Sci.*, **2010**, 122, 667.
20. (a) W. H. Bragg, *Proc. Phys. Soc. (London)*, **1921**, 34, 33; (b) R. Pepinsky *Phys. Rev.* **1955**, 100, 971; (c) G. M. J. Schmidt, *In Solid State Photochemistry*, Ginsburg, D., Ed.; Verlag Chemie: New York, **1976**.
21. (a) G. R. Desiraju, *Angew. Chem., Int. Ed. Engl.*, **1995**, 34, 2311; (b) M. C. Etter, J. C. MacDonald and J. Bernstein *Acta Crystallogr.* **1990**, B46, 256.
22. G. R. Desiraju, *Chem. Commun.* **1997**, 1475.
23. L. Brammer, *Hydrogen Bonds in Inorganic Chemistry: Applications to Crystal Design. In Crystal Design. Structure and Function*; G. R. Desiraju Ed.; Wiley: Chichester. **2003**, 1.
24. (a) Ö. Almarsson and M. J. Zaworotko *Chem. Commun.*, **2004**, 1889; (b) P. Vishweshwar, J. A. McMahon, J. A. Bis and M. J. Zaworotko, *J. Pharm. Sci.* **2006**, 95 499; (c) S. L. Childs and M. J. Zaworotko *Cryst. Growth Des.* **2009**, 9, 4208; (d) N. Schultheiss, and A. Newman, *Cryst. Growth Des.* **2009**, 9, 2950.
25. S. Cherukuvada and A. Nangia *Chem. Commun.*, **2014**, 50, 906.
26. J. J. Novoa, D. Braga and L. Addadi, *Engineering of Crystalline Materials Properties*, **2008**.
27. R. Hilfiker, *Polymorphism: In the Pharmaceutical Industry*, John Wiley and Sons, **2006**.
28. (a) C. P. Price, A. L. Grzesiak, and A. J. Matzger *J. Am. Chem. Soc.*, **2005**, 127, 5512; (b) M. Kitamura, *J. Cryst. Growth*, **2002**, 237, 2205; (c) B. Rodríguez-Spong, C. P. Price, A. Jayasankara, A. J. Matzger, N. Rodríguez-Hornedo, *Adv. Drug Deliv. Rev.*, **2004**, 56241.
29. (a) W.C. McCrone, *Polymorphism. In Physics and Chemistry of the Organic Solid State*, Vol. II (ed. D. Fox, M. M. Labes, and W. A.), Interscience, **1965**; (b) W.C. McCrone, *Polymorphism. Phys. Chem. Org. Solid State* 2, **1965**, 725; (c) W.C. McCrone, *Microscopy held to be prime problem-solver. Quality Assurance*, **1965**.
30. A. Burger, *The relevance of polymorphism. In Topics in pharmaceutical Science* ed. D. D. Breimer and P. Speiser, Elsevier, Lausanne **1983**, 3, 347–58.
31. (a) J. Bernstein *Polymorphism in Molecular Crystals*, Oxford University Press, **2002**; (b) S. R. Byrn, R. R. Pfeiffer, G. Stephenson, D. J. W Grant, W. B. Gleason, *Solid-State Chemistry of Drugs SSCI*, West Lafayette, IN, **1999**;

- (c) J.-O. Henck and M. Kuhnert-Brandstatter, *J. Pharm. Sci.*, **1999**, 88, 103; (d) J.-O. Henck, E. Finner and A. Burger, *J. Pharm. Sci.*, **2000**, 89, 1151; (e) S. L. Randzio *Annu. Rep. Prog. Chem., Sect. C: Phys. Chem.*, **2002**, 98, 157.
32. (a) R. Purohit, P. Venugopalan, *Reson*, **2009**, 14, 882; (b) http://en.wikipedia.org/wiki/Tin_pest.; (c) A. Eckert, *Mater. Corros.* **2008**, 59, 253.
33. (a) A. Nangia, *Acc. Chem. Res.*, **2008**, 41, 595; (b) N. J. Babu, S. Cherukuvada, R. Thakuria and A. Nangia *Cryst. Growth Des.*, **2010**, 10, 1979.
34. (a) S. R. Chemburkar, J. Bauer, K. Deming, H. Spiwek, K. Patel, J. Morris, R. Henry, S. Spanton, W. Dziki, W. Porter, J. Quick, P. Bauer, J. Donaubauer, B. A. Narayanan, M. Soldani, D. Riley, K. McFarland, *Org. Process Res. Dev.*, **2000**, 4, 413; (b) F. Rodriguez-Caabeiro, A. Criado-Fornelio, A. Jimenez-Gonzalez, L. Guzman, A. Igual, A. Perez, M. Pujol, *Chemotherapy*, **1987**, 33, 266; (c) V. López-Mejías, J. Kampf, A. Matzger, *J. Am. Chem. Soc* **2012**, 134, 9872.
35. IUPAC Gold Book, <http://goldbook.iupac.org/C01258.html>, <http://goldbook.iupac.org/C01262.html>.
36. J. D. Dunitz, *X-ray Analysis and the Structure of Organic Molecules*; Cornell University Press: Ithaca, NY, **1979**.
37. (a) D.E. Bugay, *Adv. Drug Deliv. Rev.*, **2001**, 48, 43; (b) J.D. Dunitz and J. Bernstein, *Acc. Chem. Res.*, **1995**, 28, 93; (c) H-B. Liu, Y. Chen, X. C. Zhang, *J. Pharm. Sci.*, **2007**, 96, 927.
38. A. J. Cruz-Cabeza and J. Bernstein *Chem. Rev.* **2014**, 114, 2170.
39. (a) S. S. Kumar, S. Rana, and A. Nangia, *Chem. Asian J.*, **2013**, 8, 1551; (b) E. Amadei, M. Carcelli, S. Ianelli, P. Cozzini, P. Pelagatti, C. Pelizzi, *J. Chem. Soc., Dalton Trans.* **1998**, 1025; (c) S. A. Moggach, A. R. Lennie, C. A. Morrison, P. Richardson, F. A. Stefanowicz and J. E. Warren, *CrystEngComm*, **2010**, 12, 2587.
40. (a) A. P. Ayala, M. W. C. Caetano, S. B. Honorato, J. M. Filho, H. W. Siesler, S. N. Faudone, S. L. Cuffini, F. T. Martins, C. C. P. daSilva, J. Ellena, *J. Raman Spectrosc.* **2012**, 43, 263; (b) T. N. Drebuschak, Y. A. Chesalov, E. V. Boldyreva, *Acta Crystallogr. Sect. B Struct. Sci.* **2009**, 65, 770; (c) T. N. Drebuschak, N. V. Chukanov, E. V. Boldyreva, *Acta Crystallogr. Sect. C Cryst. Struct. Commun.* **2008**, 64, o623; (d) T. N. Drebuschak, N. V. Chukanov, E. V. Boldyreva, *Acta Crystallogr. Sect. C Cryst. Struct. Commun.* **2007**, 63, o355; (e) T. N. Drebuschak, N. V.

- Chukanov, E. V. Boldyreva, *Acta Crystallogr. Sect. E Struct. Rep.* **2006**, 62, o4393; (f) S. Thirunahari, S. Aitipamula, P. S. Chow, R. B. H. Tan, *J. Pharm. Sci.* **2010**, 99, 2975; (g) N. K. Nath and A. Nangia, *CrystEngComm*, **2010**, 13, 47.
41. A. Nangia and G. R. Desiraju, *Chem. Commun.*, **1999**, 605-606.
 42. (a) T. L. Threlfall, *Analyst*, **1995**, 120, 2435; (b) H. B. Stahl, *The problem of drug interactions with excipients. Towards better safety of drugs and pharmaceutical products*. In: Braimer DD, editor, New York: Elsevier/North-Holland: pp 265–280.
 43. P. Sanphui, S. S. Kumar, A. Nangia, *Cryst. Growth Des.*, **2012**, 12, 4588.
 44. (a) A. L. Gillon, N. Feeder, R. J. Davey, R. Storey, *Cryst. Growth Des.*, **2003**, 3, 663; (b) J. Lu1, J. Wang, Z. Li and S. Rohani, *African J. of Pharm. Pharmacol.*, **2012**, 6, 269; (c) R. K. Khankari, D. J. W. Grant, *Thermochim. Acta.*, **1995**, 248, 61.
 45. H. G. Brittain, *J. Pharm. Sci.*, **2012**, 101, 464; (b) M. R. Caira, E. C. Tonder, M. M. Villiers, A. P. Lotter, *J. Inclus. Phenom Mol. Recognit. Chem.* **1983**, 31, 1–16.
 46. T. -C. Hu, S-L. Wang, T-F. Chen, S-Y. Lin. *J. Pharm. Sci.*, **2002**, 91, 1351.
 47. (a) T. Holczbauer, L. Fábian, P. Csomós, L. Fodor, A. Kálmán, *Cryst. Eng. Comm.* **2010**, 12, 1712; (b) P. Jacobson, *Ber. Dtsch. Chem. Ges.* **1887**, 20, 1732; P. Jacobson, *Ber. Dtsch. Chem. Ges.* **1888**, 21, 2624.
 48. IUPAC Gold Book <http://goldbook.iupac.org/T06252.html>
 49. (a) G. R. Desiraju, *Cryst. Growth Des.* **2008**, 8, 3; (b) P. M. Bhatt, G. R. Desiraju, *Chem. Commun.* **2007**, 2057.
 50. (a) H. Karfunkel, H. Wilts, Z. Hao, A. Iqbal, J. Mizuguchi and Z. Wu, *Acta Crystallogr.*, **1999**, B55, 1075; (b) V. R. Vangala, A. Nangia and V. M. Lynch *Chem. Commun.*, **2002**, 1304.
 51. (a) A. Kálmán, L. Fábián, Gy. Argay, G. Bernáth and Zs. Gyarmati, *J. Am. Chem. Soc.*, **2003**, 125, 34; (b) A. Kálmán, L. Fábián and Gy. Argay, *Chem. Commun.*, **2000**, 2255; (c) A. Kálmán, L. Párkányi and Gy. Argay, *Acta Crystallogr., Sect. B*, **1993**, 49, 1039; (d) C. M. Reddy, M. T. Kirchner, R. C. Gundakaram, K. A. Padmanabhan, and G. R. Desiraju, *Chem. Eur. J.*, **2006**, 12, 2222; (e) Evan M. Melhado, *Mitscherlich's Discovery of Isomorphism*, **1980**, 87-123.
 52. http://reference.iucr.org/dictionary/Isomorphous_crystals

53. (a) G. R. Desiraju, *Cryst. Growth Des.*, **2008**, 8, 3; (b) M. R. Chierotti, L. Ferrero, N. Garino, R. Gobetto, Luca Pellegrino, D. Braga, F. Grepioni, and L. Maini *Chem. Eur. J.* **2010**, 16, 4347.
54. A. Gavezzotti, *J. Pharm. Sci.* **2007**, 96, 2232.
55. A. Hantzsch, W. A. Herrmann, *Ber. Dtsch. Chem. Ges.* **1887**, 20, 2803.
56. (a) B. Kojic-Prodic, Z. Ruzic-Toros, *Acta Crystallogr. Sect. B* **1982**, 38, 2948; (b) G. Reck, D. Dietz, G. Laban, W. Günther, G. Bannier, E. Höhne, *Pharmazie* **1988**, 43, 477; (c) F. Vrecer, S. Srcic, S. J. mid-Korbar, *Int. J. Pharm.* **1991**, 68, 35; (d) T. P. Shakhtshneider, M. A. Vasilchenko, A. A. Politov, V. V. Bodyrev, *J. Therm. Anal.* **1997**, 48, 491; (e) T. P. Shakhtshneider, *Solid State Ionics* **1997**, 101-103, 851.
57. IUPAC Gold Book <http://goldbook.iupac.org/Z06752.html>
58. (a) N. K. Nath, S. S. Kumar and A. Nangia, *Cryst. Growth Des.* **2011**, 11, 4594; (b) P. A. Williams, C. E. Hughes, G. K. Lim, B. M. Kariuki, K. D. M. Harris, *Cryst. Growth Des.*, **2012**, 12, 3104; (c) L. Orola, M. Veidis, I. Sarcevic, A. Actins, S. Belyakov, A. Platonenko, *Int. J. Pharm.* **2012**, 432, 50; (d) A. Trask, N. Shan, W.D. S. Motherwell, W. Jones, S. Feng, R. Tan, K. Carpenter, *Chem. Commun.* **2005**, 880; (e) M. Takasuka, H. Nakai, M. Shiro, *J. Chem. Soc., Perkin Trans. 2* **1982**, 1061; (f) G. E. Hardy, W. C. Kaska, B. P. Chandra, J. I. Zink, *J. Am. Chem. Soc.* **1981**, 103, 1074; (g) W. H. Ojala, M. C. Etter, *J. Am. Chem. Soc.* **1992**, 114, 10288; (h) P. W. Carter, M. D. Ward, *J. Am. Chem. Soc.* **1994**, 116, 769; (i) C. J. Brown, M. Ehrenberg, *Acta Crystallogr., Sect. C* **1985**, C41, 441; (j) H. Takazawa, , S. Ohba, Y. Saito, *Acta Crystallogr., Sect. C* **1986**, C42, 1880; (k) A. O. Surov, I. V. Terekhova, A. Bauer-Brandl, G. L. Perlovich, *Cryst. Growth Des.* **2009**, 9, 3265; (l) P. Moser, A. Sallmann, I. Wiesenberger, *J. Med. Chem.* **1990**, 33, 2358; (m) G. L. Perlovich, A. O. Surov, L. K. Hansen, A. B. Brandl, *J. Pharm. Sci.* **2007**, 96, 1031.
59. S. S. Kumar and A. Nangia *Cryst. Growth Des.* **2014**, 14, 1865.
60. J. Bernstein, R. J. Davey, and J.-O. Henck, *Angew. Chem. Int. Ed.* **1999**, 38, 3440 - 3461.
61. K. Sato, R. Boistelle, *J. Cryst. Growth.* **1984**, 66, 441.
62. M. Volmer, *Kinetik der Phasenbildung*, Steinkopf, Leipzig, **1939**.
63. (a) J. D. Dunitz and J. Bernstein, *Acc. Chem. Res.* **1995**, 28, 193; (b) G. M. Day, A. V. Trask, W. D. S. Motherwell and W. Jones *Chem. Commun.*, **2006**, 54; (c) L. Yu *J. Am. Chem. Soc.*, **2003**, 125, 6380.

64. L. Yu, S. M. Reutzel-Edens and C. A. Mitchell *Org. Proc. Res. Develop.* **2000**, *4*, 396.
65. (a) H. Sasabe and J. Kido, *Chem. Mater.*, **2011**, *23*, 621; (b) S. J. Yoon, J. W. Chung, J. Gierschner, K. S. Kim, M. G. Choi, D. Kim and S. Y. Park, *J. Am. Chem. Soc.*, **2010**, *132*, 13675; (c) G. A. Stephenson, T. B. Borchardt, S. R. Byrn, J. Bowyer, C. A. Bunnell, S. V. Snorek, L. Yu, *J. Pharm. Sci.* **1995**, *84*, 1385; (d) T. Mutai, H. Shono, Y. Shigemitsu and K. Araki *CrystEngComm*, **2014**, *16*, 3890.
66. (a) S. R. Byrn, D. Y. Curtin, C. I. Paul, *J. Am. Chem. Soc.* **1972**, *94*, 890; (b) J. Bernstein, I. Izak, *J. Chem. Soc., Perkin Trans. 2* **1976**, 429.
67. (a) E. Csikós, G. G. Ferenczy, J. G. Ángyán, Z. Böcskei, K. Simon, C. Gönczi, I. Hermecz, *Eur. J. Org. Chem.* **1999**, 2119.
68. (a) T. Shida, T. Mutai and K. Araki, *CrystEngComm*, **2013**, *15*, 10179; (b) X. L. Luo, J. N. Li, C. H. Li, L. P. Heng, Y. Q. Dong, Z. P. Liu, Z. S. Bo and B. Z. Tang, *Adv. Mater.*, **2011**, *23*, 3261.
69. (a) G. R. Krishna, M. S. R. N. Kiran, C. L. Fraser, U. Ramamurty and C. M. Reddy, *Adv. Funct. Mater.*, **2013**, *23*, 1422–1430; (b) S. P. Anthony, *Chem. Asian J.*, **2012**, *7*, 374; (c) Y. Abe, S. Karasawa and N. Koga, *Chem. – Eur. J.*, **2012**, *18*, 15038.
70. (a) L. Yu. *Acc. Chem. Res.*, **2010**, *43*, 1257; (b) L. Yu, G. A. Stephenson, C. A. Mitchell, C. A. Bunnell, S. V. Snorek, J. J. Bowyer, T. B. Borchardt, J. G. Stowell, S. R. Byrn, *J. Am. Chem. Soc.* **2000**, *122*, 585; (c) C. A. Mitchell, L. Yu, M. D. Ward, *J. Am. Chem. Soc.* **2001**, *123*, 10830; (d) S. Chen, I. A. Guzei, L. Yu, *J. Am. Chem. Soc.* **2005**, *127*, 9881; (e) S. Chen, H. Xi, L. Yu, *J. Am. Chem. Soc.*, **2005**, *127*, 17439.
71. (a) K. Johmoto, A. Sekine, H. Uekusa, and Y. Ohashi, *Bull. Chem. Soc. Jpn.* **2009**, *82*, 50; (b) H. Duerr, H. Bouas-Laurent, *Photochromism Molecules and Systems*. Amsterdam: Elsevier, **1990**; (c) T. Fukaminato, T. Sasaki, T. Kawai, Tamai, M. Irie, *J. Am. Chem. Soc.*, **2004**, *126*, 14843.
72. (a) L. Yu, S. M. Reutzel-Edens and C. A. Mitchell, *Org. Process Res. Dev.*, **2000**, *4*, 396; (b) Q. Jiang and M. D. Ward, *Chem. Soc. Rev.*, **2014**, *43*, 2066; (c) A. Newman *Org. Process Res. Dev.*, **2013**, *17*, 457.
73. (a) M. Kitamura *J. Cryst. Growth*, **2002**, *237–239*, 2205; (b) N. Blagden, R. J. Davey, H. F. Lieberman, L. Williams, R. Payne, R. Roberts, R. Rowe, R. Docherty, *J. Chem. Soc., Faraday Trans.* **1998**, *94*, 1035; (c) A. Gavezzotti, G. Filippini, *Chem. Commun.* **1998**, 287; (d) I. Weissbuch, R. Popovitzbiro,

- M. Lahav, L. Leiserowitz, *Acta Crystallogr., Sect. B: Struct. Sci.* **1995**, *51*, 115.
74. (a) A. S. Myerson, *Handbook of Industrial Crystallization*; Butterworth-Heinemann Ltd: Oxford, **1993**; (b) A. Y. Lee, I. S. L. Lee, A. S. Myerson, *Chem. Eng. Technol.* **2006**, *29*, 281; (c) T. Friscic, S. L. Childs, S. A. A. Rizvi, W. Jones, *CrystEngComm*, **2009**, *11*, 418.
 75. (a) J. M. Miller, B. M. Collman, L. R. Greene, D. J. W. Grant, A. C. Blackburn, *Pharm. Dev. Technol.* **2005**, *10*, 291; (b) Y. Marcus, *The Properties of Solvents*; Wiley: New York, **1998**, p 95.
 76. (a) D. P. McNamara, S. L. Childs, J. Giordano, A. Iarriccio, J. Cassidy, M. S. Shet, R. Mannion, E. O'Donnell, A. Park, *Pharm. Res.* **2006**, *23*, 1888; (b) D. J. Berry, C. C. Seaton, W. Clegg, R. W. Harrington, S. J. Coles, P. N. Horton, M. B. Hursthouse, R. Storey, W. Jones, R. Friscic, N. Blagden, *Cryst. Growth Des.* **2008**, *8*, 1697; (c) N. K. Nath, H. Aggarwal and A. Nangia *Cryst. Growth Des.*, **2011**, *11*, 967–971.
 77. (a) P. P. Bag and C. M. Reddy *Cryst. Growth Des.* **2012**, *12*, 2740; (b) J. Anwar, S. E. Tarling, and P. Barnes, *J. Pharm. Sci.*, **1989**, *78*, 337; (c) N. K. Nath, S. Nilapwar, and A. Nangia *Cryst. Growth Des.*, **2012**, *12*, 1613.
 78. (a) R. Spruijtenburg, *Org. Process Res. Dev.* **2000**, *4*, 403; (b) W. Beckmann *Org. Process Res. Dev.* **2000**, *4*, 372; (b) D. Braga, F. Grepioni, L. Maini, M. Polito, K. Rubini, M. R. Chierotti, and R. Gobetto, *Chem. Eur. J.*, **2009**, *15*, 1508; (c) A. Lemmerer, J. Bernstein U. J. Griesser, V. Kahlenberg, D. M. Többs, S. H. Lapidus, P. W. Stephens, and C. Esterhuysen, *Chem. Eur. J.*, **2011**, *17*, 13445; (d) S. Ferlay and W. Hosseini *Chem. Commun.*, **2004**, 788.
 79. S. L. Childs, L. J. Chyall, J. T. Dunlap, D. A. Coates, B. C. Stahly, and G. P. Stahly, *Cryst. Growth Des.*, **2004**, *4*, 441.
 80. (a) E. H. Lee, S. X. M. Boerrigter, A. C. F. Rumondor, S. P. Chamrathy and S. R. Byrn *Cryst. Growth Des.*, **2008**, *8*, 91; (b) A. W. Xu, W. F. Dong, M. Antonietti, H. Colfen, *Adv. Funct. Mater.* **2008**, *18*, 1307; (c) G. Mehta, S. Sen and K. Venkatesan *CrystEngComm*, **2007**, *9*, 144; (d) E. H. Lee, S. R. Byrn, and M. T. Carvajal, *Pharm. Res.*, **2006**, *23*, 2375; (e) M. T. Kirchner, D. Bläser, R. Boese, and G. R. Desiraju *CrystEngComm*, **2009**, *11*, 229.
 81. (a) C. P. Price, A. L. Grzesiak, A. J. Matzger, *J. Am. Chem. Soc.* **2005**, *127*, 5512; (b) V. Lopez-Mejias, J. W. Kampf, A. J. Matzger, *J. Am. Chem. Soc.* **2009**, *131*, 4554; (c) A. Munroe, D. Croker, B. K. Hodnett, C. C. Seaton, *CrystEngComm*, **2011**, *13*, 5903; C. A. Mitchell, L. Yu, M. D. Ward, *J. Am. Chem. Soc.* **2001**, *123*, 10830.

82. (a) H. Jeong-Myeong, J. H. Wolf, M. A. Hillmyer, and M. D. Ward *Chem. Soc. Rev.*, **2014**, 43, 2066; (b) J-M. Ha, J. H. Wolf, M. A. Hillmyer, and M. D. Ward, *J. Am. Chem. Soc.*, **2004**, 126, 382; (c) Q. Jiang, C. Hu, and M. D. Ward, *J. Am. Chem. Soc.*, **2013**, 135, 2144; (d) J-M. Ha, B. D. Hamilton, M. A. Hillmyer, and M. D. Ward *Cryst. Growth Des.*, **2012**, 12, 4494; (e) B D. Hamilton, J-M. Ha, M. A. Hillmyer, and M. D. Ward, *Acc. Chem. Res.*, **2012**, 45, 414; (f) B. D. Hamilton, M. A. Hillmyer, and M. D. Ward *Cryst. Growth Des.*, **2008**, 8, 3368.
83. (a) A. Y. Lee, A. Ulman, A. S. Myerson, *Langmuir*, **2002**, 18, 5886; (b) J. F. Kang, J. Zaccaro, A. Ulman, A. S. Myerson, *Langmuir*, **2000**, 16, 3791; (c) C. A. Mitchell, L. Yu, and M. D. Ward *J. Am. Chem. Soc.*, **2001**, 123, 10830; (d) M. Lackinger, S. Griessl, W. M. Heckl, M. Hietschold, and G. W. Flynn, *Langmuir*, **2005**, 21, 4984; (e) J.-H. An, J.-M. Kim, S.-M. Chang and W.-S. Kim, *Cryst. Growth Des.*, **2010**, 10, 3044; (f) A. Cojocaru, A. Siriwardana, G. Gurau, and R. D. Rogers, *Pharmaceutically Active Supported Ionic Liquids, in Supported Ionic Liquids: Fundamentals and Applications* (eds R. Fehrmann, A. Riisager and M. Haumann), Wiley-VCH Verlag GmbH Co. K. Ga. A, Weinheim, Germany. **2014**; (g) Y. Diao, K. E. Whaley, M. E. Helgeson, M. A. Woldeyes, P. S. Doyle, A. S. Myerson, T. A. Hatton, and B. L. Trout, *J. Am. Chem. Soc.*, **2012**, 134, 673.
84. (a) J. Zaccaro, J. Matic, A. S. Myerson, and B. A. Garetz, *Cryst. Growth Des.*, **2001**, 1, 5; (b) B. A. Garetz, J. E. Aber, N. L. Goddard, R. G. Young, A. S. Myerson, *Phys. Rev. Lett.* **1996**, 77, 3475.
85. (a) A. T. Hulme, S. L. Price, and D. A. Tocher *J. Am. Chem. Soc.*, **2005**, 127, 1116; (b) W. I. Cross, N. Blagden, and R. J. Davey, *Cryst. Growth Des.*, **2003**, 3, 151.
86. (a) A. J. Alvarez, A. Singh and A. S. Myerson, *Cryst. Growth Des.*, **2009**, 9, 4181; (b) M. L. Peterson, S. L. Morissette, C. McNulty, A. Goldsweig, P. Shaw, M. LeQuesne, J. Monagle, N. Encina, J. Marchionna, A. Johnson, J. Gonzalez-Zugasti, A. V. Lemmo, S. J. Ellis, M. J. Cima, and Ö. Almarsson, *J. Am. Chem. Soc.*, **2002**, 124, 10958.
87. W. Ostwald, *Z. Phys. Chem.* **1897**, 22, 289.
88. (a) S. L. Morissette, Ö. Almarsson, M. L. Peterson, J. F. Remenara, M. J. Read, A. V. Lemmo, S. Ellis, M. J. Cima, C. R. Gardner, *Adv. Drug Deliv. Rev.*, **2004**, 56, 275; (b) B. Sarma, J. Chen, H.-Y. His, and A. S. Myerson, *Korean J. Chem. Eng.*, **2011**, 28, 315.
89. (a) C. B. Aakeröy, M. Fasulo, J. Desper, *Mol. Pharmaceutics*, **2007**, 4, 317; (b) Stahl, P. H.; Nakano, M. *Pharmaceutical Aspects of the Drug Salt Form.*

- In Handbook of Pharmaceutical Salts: Properties, Selection, and Use*; Stahl, P. H., Wermuth, C. G., Eds.; Wiley-VCH: New York, **2002**.
90. S. Aitipamula, R. Banerjee, A. K. Bansal, K. Biradha, M. L. Cheney, A. R. Choudhury, G. R. Desiraju, A. G. Dikundwar, R. Dubey, M. Duggirala, P. P. Ghogale, S. Ghosh, P. K. Goswami, N. R. Goud, R. K. R. Jetti, P. Karpinski, P. Kaushik, D. Kumar, V. Kumar, B. Moulton, A. Mukherjee, G. Mukherjee, A. S. Myerson, V. Puri, A. Ramanan, T. Rajamannar, C. M. Reddy, N. Rodriguez-Hornedo, R. D. Rogers, T. N. G. Row, P. Sanphui, N. Shan, G. Shete, A. Singh, C. C. Sun, J. A. Swift, R. Thaimattam, T. S. Thakur, R. K. Thaper, S. P. Thomas, S. Tothadi, V. R. Vangala, N. Variankaval, P. Vishweshwar, D. R. Weyna and M. J. Zaworotko, *Cryst. Growth Des.*, **2012**, *12*, 2147.
 91. (a) G. Stahly, *Cryst. Growth Des.*, **2007**, *7*, 1007; (b) S. Childs and K. Hardcastle, *Cryst. Growth Des.*, **2007**, *7*, 1291; (c) N. Shan and M. J. Zaworotko, *Drug Discov. Today*, **2008**, *13*, 440; (d) W. Jones, W. D. S. Motherwell and A. V. Trask, *MRS Bull.*, **2006**, *341*, 875.
 92. (a) J. Wouters, L. Quere and D. E. Thurston *Pharmaceutical Salts and Co-crystals*, Royal Society of Chemistry, **2011**; (b) L. P. Hammett, *J. Am. Chem. Soc.* **1937**, *59*, 96; (c) Hammett, L. P. *J. Chem. Educ.* **1966**, *43*, 464.
 93. (a) C. C. Seaton, K. Chadwick, G. Sadiq, K. Guo, and R. J. Davey *Cryst. Growth Des.*, **2010**, *10*, 726; (b) S. N. Black, E. A. Collier, R. J. Davey, R. J. Roberts, *J. Pharm. Sci.* **2007**, *96*, 1053.
 94. (a) K. Chadwick, G. Sadiq, R. J. Davey, C. C. Seaton, R. G. Pritchard, A. Parkin, *Cryst. Growth Des.* **2009**, *9*, 1278; (b) C. C. Seaton, *CrystEngComm*, **2011**, *13*, 6583.
 95. (a) J. S. Stevens, S. J. Byard, C. A. Muryn, and S. L. M. Schroeder, *J. Phys. Chem. B*, **2010**, *114*, 13961; (b) Stevens, J. S., Byard, S. J. and Schroeder, S. L.M. (2010), *J. Pharm. Sci.*, *99*: 4453–4457; (c) J. S. Stevens, S. J. Byard, C. C. Seaton, G. Sadiq, R. J. Davey and S. L. M. Schroeder, *Phys. Chem. Chem. Phys.*, **2014**, *16*, 1150.
 96. (a) D. J. Good and N. Rodríguez-Hornedo, *Cryst. Growth Des.*, **2010**, *10*, 1028; (b) D. J. Good, *Pharmaceutical Cocrystal Eutectic Analysis: Study of Thermodynamic Stability, Solubility and Phase Behavior*, PhD thesis, University of Michigan, USA. **2010**.
 97. (a) M. A. Mohammad, A. Alhalaweh, S. P. Velaga, *Int. J. of Pharm.*, **2011**, *407*, 63; (b) M. A. Mohammad, A. Alhalaweh, M. Bashimam, M. A. Al-Mardini, S. Velaga, *J. Pharm. Pharmacol.*, **2010**, *62*, 1360.

98. (a) C. B. Aakeröy, A. Rajbanshi, Z. J. Li, J. Desper, *CrystEngComm*, **2010**, *12*, 423; (b) C. B. Aakeröy, J. Desper and M. M. Smith, *Chem. Commun.*, **2007**, 3936; (c) T. Grecu, C. A. Hunter, E. J. Gardiner, and J. F. McCabe, *Cryst. Growth Des.*, **2014**, *14*, 165.
99. M. B. Hickey, M. L. Peterson, L. A. Scoppettuolo, S. L. Morrisette, A. Vetter, H. Guzmán, J. F. Remenar, Z. Zhang, M. D. Tawa, S. Haley, M. J. Zaworotko, Ö. Almarsson, *Eur. J. Pharm. Biopharm.* **2007**, *67*, 112.
100. S. L. Childs, L. J. Chyall, J. T. Dunlap, V. N. Smolenskaya, B. C. G. P. Stahly, *J. Am. Chem. Soc.*, **2004**, *126*, 13335.
101. S. S. Kumar, R. Thakuria and A. Nangia *CrystEngComm*, **2014**, *16*, 4722.
102. (a) S. Aitipamula, P. S. Chow and R. B. H. Tan *CrystEngComm*, **2014**, *16*, 3451; (b) T. Ueto, N. Takata, N. Muroyama, A. Nedu, A. Sasaki, S. Tanida and K. Terada, *Cryst. Growth Des.*, **2012**, *12*, 485; (c) R. Kaur and T. N. G. Row, *Cryst. Growth Des.*, **2012**, *12*, 2744.
103. (a) A. V. Trask, W. D. S. Motherwell and W. Jones, *Chem. Commun.*, **2004**, 890; (b) A. V. Trask, W. D. S. Motherwell and W. Jones, *Cryst. Growth Des.*, **2005**, *5*, 1013; (c) R. Thakuria, M. D. Eddleston, E. H. H. Chow, G. O. Lloyd, B. J. Aldous, J. F. Krzyzaniak, A. D. Bond and W. Jones, *Angew. Chem., Int. Ed.*, **2013**, *52*, 10541.
104. (a) N. R. Goud and A. Nangia, *CrystEngComm*, **2013**, *15*, 7456; (b) D. Braga, G. Palladino, M. Polito, K. Rubini, F. Grepioni, M. R. Chierotti and R. Gobetto, *Chem.–Eur. J.*, **2008**, *14*, 10149; (c) S. L. Childs and K. I. Hardcastle, *Cryst. Growth Des.*, **2007**, *7*, 1291; (d) F. Wöhler and J. Liebig, *Ann. Pharm.*, **1832**, *3*, 249; (e) B.-Q. Ma, Y. Zhang and P. Coppens, *J. Org. Chem.*, **2003**, *68*, 9467; (f) Y. Yan, C. E. Hughes, B. M. Kariuki, and K. D. M. Harris, *Cryst. Growth Des.*, **2013**, *13*, 27; (g) L. Loots, H. Wahl, L. van der Westhuizen, D. A. Haynes and T. le Roex, *Chem. Commun.*, **2012**, *48*, 11507.
105. (a) J. B. Nanubolu, B. Sridhar, K. Ravikumar, K. D. Sawant, T. A. Naik, L. N. Patkar, S. Cherukuvada and B. Sreedhar, *CrystEngComm*, **2013**, *15*, 4448; (b) A. R. Buist, A. R. Kennedy, K. Shankland, N. Shankland, and M. J. Spillman, *Cryst. Growth Des.*, **2013**, *13*, 5121; (c) P. Sanphui, G. Bolla and A. Nangia, *Cryst. Growth Des.* **2012**, *12*, 2023.
106. (a) A. Lemmerer, J. Bernstein and M. A. Spackman, *Chem. Commun.*, **2012**, *48*, 1883; (b) V. André, M. T. Duarte, D. Braga and F. Grepioni, *Cryst. Growth Des.*, **2012**, *12*, 3082.

107. (a) A. I. Kitaigorodskii, *In Mixed Crystals*, Springer-Verlag: Berlin, Heidelberg, **1984**. (b) J. A. R. P. Sarma, G. R. Desiraju, *J. Am. Chem. Soc.* **1986**, *108*, 2791; (c) A. Anthony, M. Jaskólski, A. Nangia, G. R. Desiraju, *Chem. Commun.* **1998**, 2537; (d) F. C.; Pigge, V. R.; Vangala, D. C. Swenson, *Chem. Commun.* **2006**, 2123; (e) N. K. Nath and A. Nangia, *Cryst. Growth Des.*, **2012**, *12*, 5411.
108. (a) A. I. Kitaigorodsky, *Mixed Crystals*, Springer-Verlag, Berlin, **1984**; (b) W. F. Smith and J. Hashemi, *Foundations of Materials Science and Engineering*, McGraw-Hill, New York, 4th edn, **2006**; (c) D. R. Askeland and P. P. Fulay, *Essentials of Materials Science and Engineering*, Cengage Learning, 2nd edn, **2000**; (d) K. Nollenberger, A. Gryczke, CH. Meier, J. Dressman, M. U. Schmidt and S. Brühne, *J. Pharm. Sci.*, **2009**, *98*, 1476.
109. (a) S. Cherukuvada and A. Nangia, *CrystEngComm*, **2012**, *14*, 257; (b) N. R. Goud, K. Suresh, P. Sanphui and A. Nangia, *Int. J. Pharm.*, **2012**, *439*, 63; (c) M. Bi, S.-J. Hwang and K. R. Morris, *Thermochim. Acta*, **2003**, *404*, 213.
110. (a) Y. Ran, and S. H. Yalkowsky *J. Chem. Inf. Comput. Sci.* **2001**, *41*, 354; (b) Serajuddin, A. *Adv. Drug Del. Rev.*, **2007**, *59*, 603; (c) Llinàs, A.; Glen, R. C; Goodman, J. M. *J. Chem. Inf. Model.* **2008**, *48*, 1289; (d) J. Alsenz, M. Kansy *Adv. Drug Del. Rev.* **2007**, *59*, 546; (e) D. Giron, *Thermochim. Acta* **1995**, *248*, 1.
111. (a) A. Avdeef, *Solubility in Absorption and Drug Development: Solubility, Permeability, and Charge State*, 2nd Eds. John-Wiley, USA, **2012**, p. 251; (d) C. Lipinski, F. Lombardo, B. Dominy, P. Feeney, *Adv. Drug Del. Rev.* **2001**, *46*, 3.
112. (a) C. Lipinski, *J. Pharmacol. Toxicol. Methods*, **2000**, *44*, 235; (b) K. Urakami, Y. Shono, A. Higashi, K. Umemoto, M. Godo *Bull. Chem. Soc. Jpn.* **2002**, *75*, 1241; (c) Y. A. Abramov, K. Pencheva, *Thermodynamics and Relative Solubility Prediction of Polymorphic Systems, In Chemical Engineering in the Pharmaceutical Industry: R&D to Manufacturing*, (Ed. D. J. am Ende), John-Wiley, USA, **2010**, p. 477.
113. (a) H. Guzmán M. Tawa Z. Zhang P. Ratanabanangkoon P. Shaw P. Mustonen C. Gardner H. Chen J. Moreau O. Almarsson J. Remenar *AAPS J.*, **2004**, *6*, 189; (b) H. Guzmán M. Tawa Z. Zhang P. Ratanabanangkoon P. Shaw P. Mustonen C. Gardner H. Chen J. Moreau O. Almarsson J. F. Remenar 2007. *J Pharm Sci.*, **1996**, 2686; (c) N. J. Babu, A. Nangia, *Cryst. Growth Des.*, **2011**, *11*, 2662; (d) J. Chen, B. Sarma, J. M. B. Evans, and A. S. Myerson *Cryst. Growth Des.*, **2011**, *11*, 887.

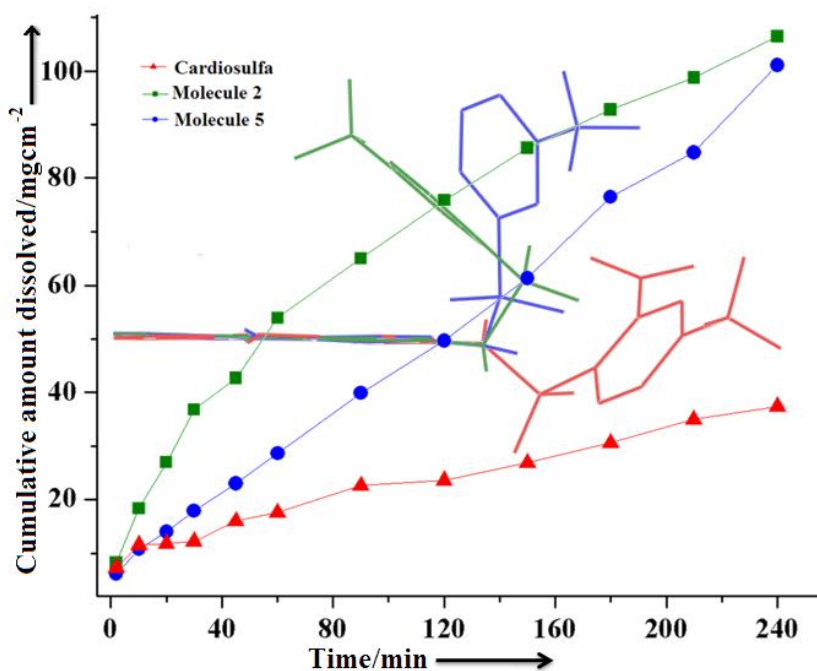
114. (a) L. Edwards, *J. Trans. Faraday Soc.*, **1951**, 47, 1191; (b) A. Dokoumetzidis, P. Macheras, *Int. J. Pharm.* **2006**, 321, 1.
115. (a) M. McAllister, *Mol. Pharmaceutics*, **2010**, 7, 1374; (b) H. Lennernas, *Curr. Drug Metab.* **2007**, 8, 64; (c) S. R. Carino, D. C. Sperry, M. Hawley, *J. Pharm. Sci.* **2006**, 95, 116.
116. (a) C. B. Aakeröy, *Acta Crystallogr.* **1997**, B53, 569; (b) D. Braga, F. Grepioni, and G. R. Desiraju, *Chem. Rev.* **1998**, 98, 1375.
117. (a) M. K. Mishra, P. Sanphui, U. Ramamurty, and G. R. Desiraju, *Cryst. Growth Des.* **2014**, 14, 3054; (b) M. K. Mishra, S. Varughese, U. Ramamurty, and G. R. Desiraju, *J. Am. Chem. Soc.*, **2013**, 135, 8121; (c) A. R. Ubbelohde, *The Molten State of Matter*; Wiley Interscience: Chichester, **1978**.
118. (a) C. Sun and D. J. W. Grant, *Pharm. Res.*, **2001**, 18, 274; (b) S. R. Perumalla, L. Shi and C. Calvin Sun *CrystEngComm*, **2012**, 14, 2389.
119. (a) C. M. Reddy, S. Basavoji and G. R. Desiraju, *Chem. Commun.*, **2005**, 2439; (b) P. P. Bag, M. Chen, C. C. Sun and C. M. Reddy, *CrystEngComm*, **2012**, 14, 3865; (c) C. M. Reddy, K. A. Padmanabhan, and G. R. Desiraju, *Cryst. Growth Des.* **2006**, 6, 2720; (d) S. Ghosh and C. M. Reddy *Angew. Chem. Int. Ed.*, **2012**, 51, 10319.
120. (a) M. K. Nazeeruddin, A. Kay, I. Rodicio, R. Humphry-Baker, E. Muller, P. Liska, N. Vlachopoulos, M. Grätzel, *J. Am. Chem. Soc.*, **1993**, 115, 6382; (b) C.-H. Zhao, A. Wakamiya, Y. Inukai, S. Yamaguchi, *J. Am. Chem. Soc.*, **2006**, 128, 15934; (c) T. Mutai, H. Tomoda, T. Ohkawa, Y. Yabe, K. Araki, *Angew. Chem.* **2008**, 120, 9664; *Angew. Chem. Int. Ed.* **2008**, 47, 9522; (d) B.-K. An, S. H. Gihm, J. W. Chung, C. R. Park, S.-K. Kwon, S. Y. Park, *J. Am. Chem. Soc.*, **2009**, 131, 3950.
121. (a) T. Mutai, H. Tomoda, T. Ohkawa, Y. Yabe, K. Araki, *Angew. Chem.* **2008**, 120, 9664; *Angew. Chem. Int. Ed.* **2008**, 47, 9522; (b) R. Davis, N. P. Rath, R. Das, *Chem. Commun.*, **2004**, 74; (c) Y. Abe, S. Karasawa, and N. Koga, *Chem. Eur. J.* **2012**, 18, 15038.
122. (a) M. Ishikawa, and Y. Hashimoto, *J. Med. Chem.*, **2011**, 54, 1539; (b) S. H. Yalkowsky, *Solubility and Solubilization in Aqueous Media*; American Chemical Society: Washington, DC, **1999**; (c) S. Banerjee, S. H. Yalkowsky, S. C. Valvani, *Environ. Sci. Technol.* **1980**, 10, 1227; (d) N. Jain, S. H. Yalkowsky, *J. Pharm. Sci.* **2001**, 90, 234.
123. (a) A. Gavezzotti, *Acc. Chem. Res.* **1994**, 27, 309; (b) C. A. Lipinski, F. Lombardo, B. W. Dominy, P. J. Feeney, *Adv. Drug Deliv. Rev.* **2001**, 46, 3.

124. (a) F. Lovering, J. Bikker, C. J. Humblet, *Med. Chem.*, **2009**, 52, 6752; (b) A. Gavezzotti, *J. Chem. Soc., Perkin Trans. 2*, **1995**, 1399; (c) R.-M.; Dannenfelser, S. H. Yalkowsky, *Ind. Eng. Chem. Res.* **1996**, 35, 1483.
125. Y.; Fujita, M.; Yonehara, M.; Tetsuhashi, T.; Noguchi-Yachide, Y.; Hashimoto, Ishikawa *Bioorg. Med. Chem.* **2010**, 18, 1194.
126. (a) C. R. Groom, and F. H. Allen, *Angew. Chem. Int. Ed.*, **2014**, 53, 662; (b) A. Gavezzotti, *J. Pharm. Sci.* **2007**, 96, 2232; (c) K. M. Lutker, Z. P. Tolstyka, A. J. Matzger, *Cryst. Growth Des.*, **2008**, 8, 136.
127. (a) G. R. Desiraju, *Angew. Chem. Int. Ed.* **2011**, 50, 52 ; (b) M. C. Etter, *J. Am. Chem. Soc.* **1982**, 104, 1095; (c) M. C. Etter, *Acc. Chem. Res.* **1990**, 23, 120; (d) M. C. Etter, *J. Phys. Chem.* **1991**, 95, 4601; (e) G. R. Desiraju, T. Steiner, *The Weak Hydrogen Bond in Structural Chemistry and Biology*; Oxford University Press: Oxford, **1999**.
128. (a) F. H. Allen, W. D. S. Motherwell, P. R. Raithby, G. P. Shields, R. Taylor, *New. J. Chem.* **1999**, 25; (b) T. Steiner, *Acta. Crystallogr.* **2001**, B57, 103; (c) J. A. McMahon, J. A. Bis, P. Vishweshwar, T. R. Shattock, O. L. McLaughlin, M. J. Zaworotko, *Z. Kristallogr.* **2005**, 220, 340; (d) R. D. B. Walsh, M. W. Bradner, S. Fleishman, L. A. Morales, B. Moulton, N. Rodríguez-Hornedo, M. J. Zaworotko, *Chem. Commun.* **2003**, 186.
129. (a) C. B. Aakeröy, D. J. Salmon, *CrystEngComm* **2005**, 7, 439; (b) B. R. Bhogala, S. Basavoju, A. Nangia, *CrystEngComm* **2005**, 7, 551; (c) B. R. Bhogala, S. Basavoju, A. Nangia, *Cryst. Growth Des.* **2005**, 5, 1683; (d) A. V. Trask, W. D. S. Motherwell, W. Jones, *Cryst. Growth Des.* **2005**, 5, 1013; (e) X. Gao, T. T. Friščić, L. R. MacGillivray, *Angew. Chem. Int. Ed.* **2004**, 43, 232; (f) B. R. Bhogala, A. Nangia, *Cryst. Growth Des.* **2003**, 3, 547; (g) C. B. Aakeröy, A. M. Beatty, B. A. Helfrich, *Angew. Chem. Int. Ed.* **2001**, 40, 3240; (h) B. R. Bhogala, A. Nangia, *New. J. Chem.* **2008**, 32, 800; (i) P. Vishweshwar, A. Nangia, V. M. Lynch, *J. Org. Chem.* **2002**, 67, 556; (j) B. R. Bhogala, P. Vishweshwar, A. Nangia, *Cryst. Growth Des.* **2002**, 2, 325; (k) N. Shan, A. D. Bond, W. Jones, *New J. Chem.* **2003**, 27, 365; (m) B. R. Bhogala, A. Nangia, *Cryst. Growth Des.* **2002**, 2, 325; (n) Ö, Almarsson, M. J. Zaworotko, *Chem. Commun.* **2004**, 1889; (o) C. V. K. Sharma, G. A. Broker, G. J. Szulczewski, R. D. Rogers, *Chem. Commun.* **2000**, 1023; (p) M. Tomura, Y. Yamashita, *Chem. Lett.* **2001**, 532; (q) N. Shan, E. Batchelor, W. Jones, *Tetrahedron Lett.* **2002**, 43, 8721; (r) B. Olenik, T. Smolka, R. Boese, R. Sustmann, *Cryst. Growth Des.* **2003**, 3, 183; (s) A. D. Bond, *Chem. Commun.* **2003**, 250; (t) S. Varughese, V. R. Pedireddi, *Chem. Eur. J.* **2006**, 12, 1597; (u) M. Du, Z. H. Zhang, X. J. Zhao, chapter 6, 195; (v) H. Cai, *Cryst. Growth Des.* **2006**, 6, 114; (v) C. M. Grossel, A. N. Dwyer, M.

- B.Hursthouse, J. B. Orton, *CrystEngComm* **2006**, 8, 123; (w) B. R. Bhogala, A.Nangia, *New J. Chem.* **2008**, 32, 800; (x) R. Santra, N. Ghosh, K. Biradha, *New J. Chem.* **2008**, 32, 1673.
130. (a) P. Vishweshwar, A. Nangia, V. M. Lynch, *CrystEngComm* **2003**, 5, 164; (b) K. Biradha, M. J. Zaworotko, *J. Am. Chem. Soc.* **1998**, 120, 6431; (c) J. A. Bis, O. L. McLaughlin, P. Vishweshwar, M. J. Zaworotko, *Cryst. Growth Des.* **2006**, 6, 2648.
131. (a) V. R. Vangala, R. Mondal, C. K. Broder, J. A. K. Howard, G. R. Desiraju, *Cryst. Growth Des.* **2005**, 5, 99; (b) O. Ermer, A. Eling, *J. Chem. Soc. Perkin Trans. 2* **1994**, 925; (c) S. Hanessian, M. Simard, S. Roelens, *J. Am. Chem. Soc.* **1995**, 117, 7630; (d) F. H. Allen, V. J. Hoy, J. A. K. Howard, V. R. Thalladi, G.R. Desiraju, C. C. Wilson, G. J. McIntyre, *J. Am. Chem. Soc.* **1997**, 119, 3477; (e) V. R. Vangala, B. R. Bhogala, A. Dey, G. R. Desiraju, C. K. Broder, P. S. Smith, R. Mondal, J. A. K. Howard, C. C. Wilson, *J. Am. Chem. Soc.* **2003**, 125, 14495; (f) S. Hanessian, R. Saladino, R. Margarita, M. Simard, *Chem. Eur. J.*, **1999**, 5, 2169; (g) A. Dey, G. R. Desiraju, R. Mondal, J. A. K. Howard, *Chem. Commun.* **2004**, 2528.
132. (a) P. Vishweshwar, A. Nangia, V. M. Lynch, *Cryst. Growth Des.* **2003**, 3, 783; (b) L. S. Reddy, P. M. Bhatt, R. Banerjee, A. Nangia, G. J. Kruger, *Chem. Asian J.* **2007**, 2, 505; (c) J. A. Bis, M. J. Zaworotko, *Cryst. Growth Des.* **2005**, 5, 1169.
133. (a) L. S. Reddy, N. J. Babu and A. Nangia, *Chem. Commun.* **2006**, 1369; (b) N. J. Babu, L. S. Reddy and A. Nangia, *Mol. Pharma.* **2007**, 4, 417; (c) N. R. Goud, N. J. Babu and A. Nangia *Cryst. Growth Des.*, **2011**, 11, 1930.

Chapter Two

Polymorphism in Cardiosulfa and Its Analogs



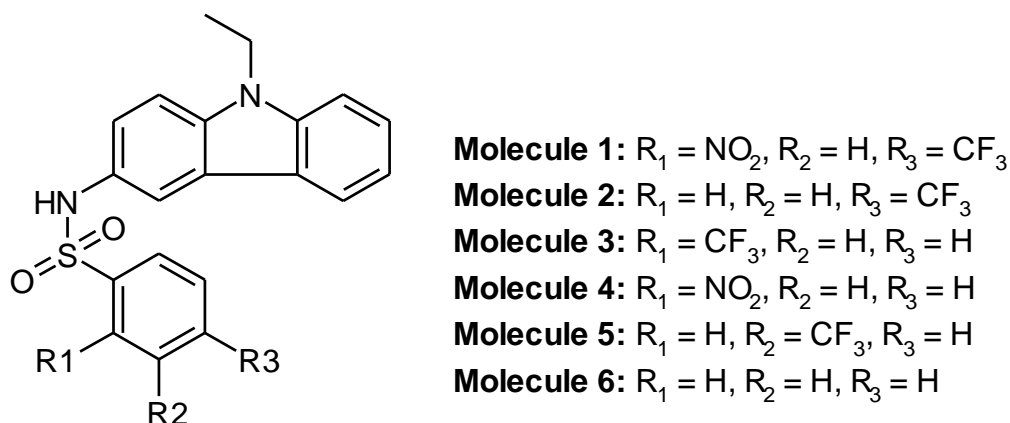
*A twist to solubility: The more soluble and polymorphic compounds **2** (green) and **5** (blue) adopt twisted conformations in the crystal structures unlike a near-planar conformation of less soluble and non-polymorphic cardiosulfa **1** (red).*

2.1 Introduction

Cardiosulfa^{1a} is defined as a small molecule that induces abnormal heart developments in zebra fish. It is a biologically active sulfonamide molecule which was recently shown to induce abnormal heart development in zebrafish embryo through activation of the aryl hydrocarbon receptor (AhR).¹ It's action is agonist like property towards the aryl hydrocarbon receptor^{1b} (AhR), a transcription factor and a member of the nuclear receptor family, whose primary function is to regulate xenobiotic metabolism and mediate the toxic response of dioxin like environmental pollutants.^{1c,d} In zebrafish models,^{1e} cardiosulfa **1** and its derivatives molecules **2** to **6** (Scheme 2.1) were able to impair cardiovascular function by modulating the AhR signaling pathway, which evoked edema like responses in pericardial and yolk sac.^{1c}

However, AhR signaling in humans can be tissue specific,^{2a} depending upon whether it is localized in liver, kidney, lungs, ovary or breast.^{2b} Numerous studies have illuminated the other side of AhR signaling, eliciting a more defined cell biological response, ranging from cell growth, proliferation, differentiation to apoptosis. For example, agonistic activation of AhR and downstream signaling in MCF-7 breast cancer cell line cause DNA damage and possibly an alternative therapy for breast cancer.^{2b} AhR agonists can up regulate caspase-8^{2c} and enhanced apoptosis via receptor signaling. Similarly, it has been shown that AhR agonist can inhibit pancreatic cancer cell growth in a dose dependent manner.^{2d} It is suggested that agonist dependent AhR activation can regulate both Treg and Th17 cell differentiation, which play a key role in immune response.^{2e,f} It is therefore important to study synthetic agonists of AhR and small molecule polymorphism. From quantitative structure activity relationship (QSAR) studies, it is apparent that planar molecules with dimensions limiting to $14 \text{ \AA} \times 12 \text{ \AA} \times 5 \text{ \AA}$ interact with the AhR ligand binding domain, even as the effectiveness of the binding can be contingent upon certain molecular functionality.^{2g} The binding of cardiosulfa to AhR triggers

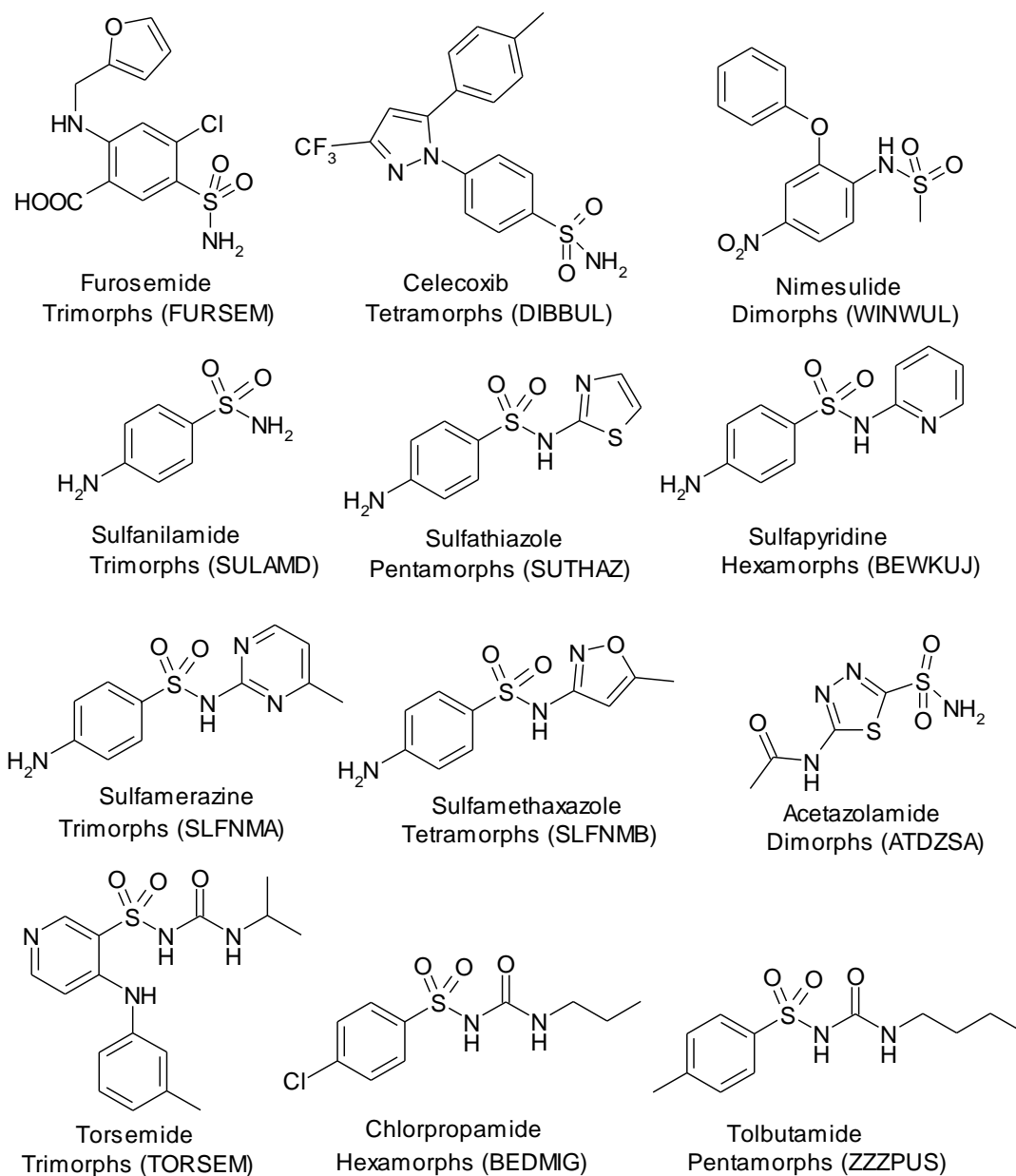
cardiovascular impairment in zebrafish, suggesting that cardiosulfa can serve as a biological probe in understanding heart growth and development. On the other side, cardiosulfa's role on AhR signaling in human tissues is currently unknown and it is quite possible that cardiosulfa might display therapeutically beneficial pharmacology in humans. Exploring the solid-state forms of AhR binding molecules evokes interest because AhR is involved in several cell biological responses. A better understanding of the crystal structures and physicochemical properties of cardiosulfa analogs is necessary to exploit its potential as a bioactive molecule in structure-based drug design.



Scheme 2.1 Molecular structures of cardiosulfa and its analogs

Moreover, sulfa drugs^{3a,b} are an important class of molecules containing the flexible sulfonamide moiety ($\text{R-SO}_2\text{-NH-Ar}$). The polymorphism of sulfa drugs/sulfonamides was well known in the early 1940 when sulfonamide chemotherapy was at its peak rising in the anti-microbial drugs. The discovery of new crystal forms of sulfonamides were the serendipity results during those early periods and the study was not well established at that time. The first report of polymorphism in a sulfonamide was reported by Zyp in 1938 for sulfanilamide sulfa drug that displayed several distinct crystalline forms from a drop of water

crystallization technique and examined by the microscope.^{3c} In 1941, Watanabe reported three polymorphic modifications of sulfanilamide drug by the X-ray diffraction patterns.^{3d} Yakowitz confirmed the reported refractive indexes and heats of solution for the three forms of sulfanilamide.^{3e} X-ray crystal structure of fourth form of sulfanilamide was reported by McLach-Ian in his book.^{3f} The second sulfonamide studied is sulfathiazole polymorphism where Grove and Keenan discovered two polymorphs of sulfathiazole and found the difference in phase transition between the two polymorphs.^{3g} Then the third form was also identified by X-ray diffraction patterns for these polymorphs.^{3h} Later, Milosovich compared the dissolution rate of two polymorphs.³ⁱ All these sulfa drugs (Scheme 2.2) display a wide range of biological activities and a high success rate in therapeutic medicines.^{3j} Given the estimate that fully one-third of all organic compounds are likely to exhibit polymorphism, a frequency of >50% for more than one crystalline modification in sulfonamides are the second best candidates to display polymorphism where as the top drug category is being barbiturates at 70% as carboxamides.⁴



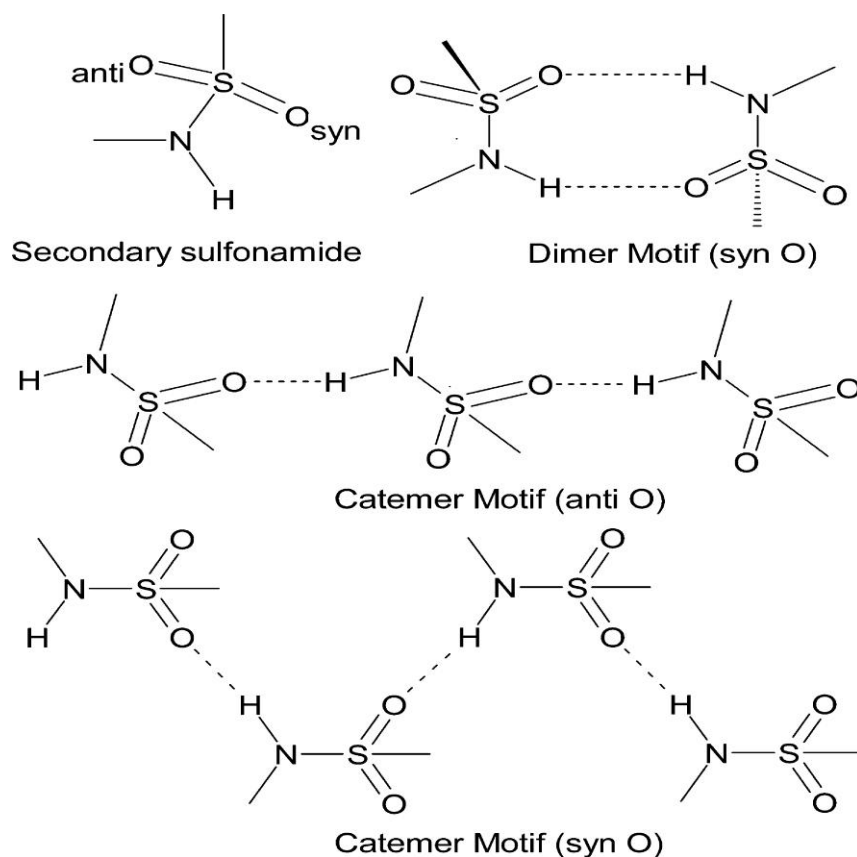
Scheme 2.2 Selected list of sulfa drugs reported for the polymorphism in the CSD

The biological action of a drug molecule can change in different polymorphic states from therapeutic to toxic due to sudden changes in dissolution rate for the given dose, e.g. as for mebendazole and chloramphenicol.⁵ Thus lead molecules may

be optimized from a larger set of sulfonamides synthesized by combinatorial technology in medicinal chemistry programs.⁶ Such an approach recently lead to the discovery of Cardiosulfa or *N*-(9-ethyl-9H-carbazol-3-yl)-2-nitro-4-(trifluoromethyl) benzene sulfonamide (molecule **1** in Scheme 2.1).^{1a} Based on the biological relevance to crystal structures and frequent occurrence of polymorphs in sulfonamides, we synthesized cardiosulfa analogs **1-6** (Scheme 2.1) and carried out a systematic solid form hunt and characterization using X-ray diffraction, FT-IR, ¹³C ss-NMR, and solubility experiments.¹⁹ Polymorphic phase transformations were monitored by DSC and VT-XRPD to establish thermodynamic relationship and thermal stability of polymorphs in this chapter.²¹⁻²²

Shortly, a systematic comparison of solid-state forms of cardiosulfa and its biologically active analogs belonging to the *N*-(9-ethyl-9H-carbazol-3-yl)benzene sulfonamide skeleton. The sulfa compounds (Scheme 2.1) were prepared by the amide coupling of 9-ethyl-9H-carbazol-3-amine with the appropriate benzenesulfonyl chloride (Scheme 2.4). Cardiosulfa (molecule **1**, R₁ = NO₂, R₂ = H, R₃ = CF₃), molecule **2** (H, H, CF₃), molecule **3** (CF₃, H, H), molecule **4** (NO₂, H, H), molecule **5** (H, CF₃, H), and molecule **6** (H, H, H) were synthesized and subjected to a polymorph search and solid form characterization by X-ray diffraction, DSC, VT-PXRD, FT-IR and ss-NMR. Normally, sulfonamides exhibit sulfonamide N-H···O catemer and dimer synthons (Scheme 2.3) in the crystal structures during the polymorphism. In contrast, Molecule **1** was obtained in a single crystalline modification which is sustained by N-H···π and C-H···O interactions but devoid of strong intermolecular N-H···O hydrogen bonds. Molecule **2** displayed a N-H···O catemer C(4) chain in Form I whereas a second polymorph was characterized by PXRD. The dimorphs of molecule **3** contain N-H···π and C-H···O interactions but no catemer/dimer N-H···O bonds present in the crystal structures. Molecule **4** is trimorphic with N-H···O catemer in Form I, and N-H···π and C-H···O interactions

in Form II, and a third polymorph was characterized by PXRD. Both polymorphs of molecule **5** contain the N–H···O catemer $C(4)$ chain, whereas the sulfonamide N–H···O dimer synthon $R_2^2(8)$ was observed in molecule **6**. Differences in the strong and weak hydrogen bond motifs were correlated with the substituent groups and the solubility and dissolution rates with the different conformation in the crystal structures of molecules **1-6**. Higher solubility compounds, such as **2** (10.5 mg/mL) and **5** (4.4 mg/mL), adopt a twisted confirmation whereas less soluble cardiosulfa **1** (0.9 mg/mL) is nearly planar. This study provides practical guides for functional group modification of drug lead.



Scheme 2.3 Common supramolecular synthons in sulfonamides: Dimer and catemer hydrogen bond synthons of the sulfonamide group. The chain motif formed with anti and syn O acceptor atoms (Adapted from Ref. 17c).

2.2 Results and Discussion

2.2.1 Crystal structures of sulfonamides

Molecule 1. Among the six sulfonamides,^{1a} cardiosulfa (molecule **1**) is the most active^{1c} in zebrafish heart deformation compared to molecules **2**, **3** and **4**, whereas molecules **5** and **6** are only weakly active. The purpose of the present solid form screening was to explore the polymorphic behavior as well as determine the aqueous solubility of molecules **1-6** and their novel polymorphs. Cardiosulfa was crystallized from acetone–methanol (1:1) and the structure was solved and refined in the monoclinic space group $P2_1/n$ (See Appendix for crystallographic information). The crystallization condition for six sulfonamides and its polymorphs are given in Table 2.1. In the crystal structure analysis, the molecular conformation is locked by an intramolecular N–H \cdots O hydrogen bond (2.44 Å, 108°) of $S(7)$ motif. N–H $\cdots\pi$ interaction is present instead of strong intermolecular N–H \cdots O catemer/dimer hydrogen bond (H bonds listed in Table 2.2). An N–H $\cdots\pi$ interaction is quite uncommon in sulfonamides⁷ given the opportunity for strong N–H \cdots O hydrogen bonding (Scheme 2.3). The molecular arrays are assembled via N1–H1 $\cdots\pi$ (3.04 Å) and S1–O1 $\cdots\pi$ (3.06 Å) interactions (Figure 2.1a). Weak interactions such as C3–H3 \cdots O3 (2.47 Å, 159°), C20–H20A \cdots F2 (2.48 Å, 132°), and C5–H5 $\cdots\pi$ (2.82 Å) are involved in the overall crystal packing (Figure 2.1b). The presence of two electron-withdrawing groups, CF₃ and NO₂, decrease the propensity for N–H \cdots O hydrogen bonding by weakening the O acceptor capability. We noted previously in diaryl urea crystal structures^{7e} that the NO₂ group can significantly alter the molecular conformation and strong hydrogen bond network. Conformational rigidity due to the intramolecular N–H \cdots O and the lack of strong H bonding capability gave only one crystal structure (i.e. no polymorphs were found for **1**). Attempts with several different crystallization methods and conditions, such as solvent evaporation,

melting, sublimation, slow cooling, flash cooling to obtain a second polymorph of cardiosulfa was unsuccessful.

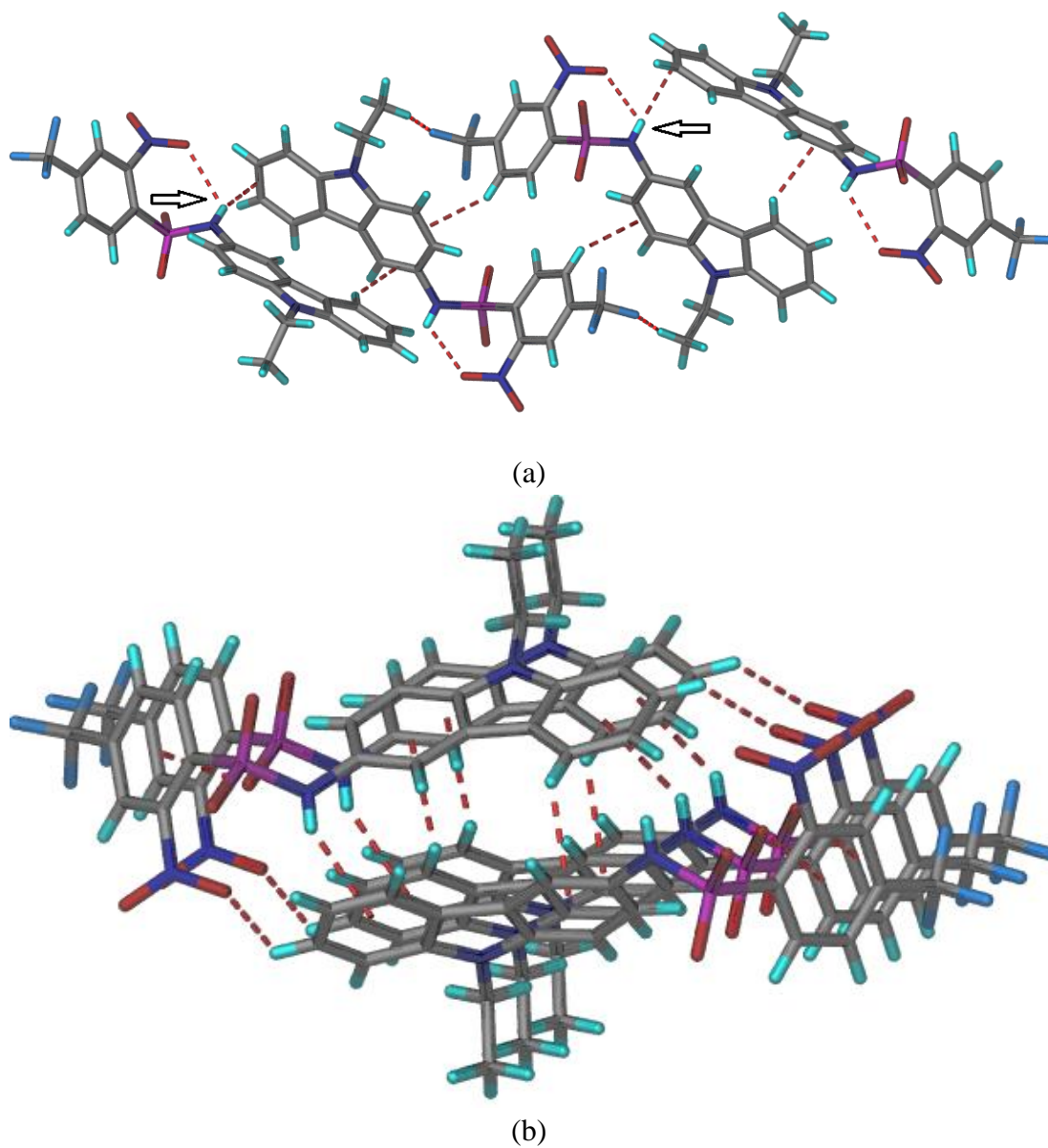


Figure 2.1 (a) N-H... π and C-H... π interactions persist, compared to strong N-H...O H bonding, in cardiosulfa **1**. The intramolecular (sulfonamide) N-H...O (nitro) H bond S(7) is highlighted by an arrow. (b) C-H...O (nitro) and C-H... π interactions in the crystal structure.

Table 2.1 List of crystallization solvents and methods for polymorph screening.

Molecules	Melting/Heating	Amorph to crystalline	Methanol	Ethanol	Acetone	Tetrahydrofuran	Nitromethane	Dimethyl sulfoxide	Ethyl acetate	Acetonitrile	Benzene	Hexane-EtOAc	Toluene	Anisole	Chloroform	Diethylether	Hexane	Acetic acid
1	A	I	I	I	I	I	I	I	I	I	I	I	I	I	I	I	I	I
2	A	I	I	I	I	I	I	I	I	I	I	I	I	I	I	I	I	I/ II
3	A	II	I	I	I	I	I	I	I	I	I	I	I	I	I	I	I	I
4	A	I	II	II	I/I I	I	II	II	I	II	II	I	I/I I	I	I	II	I	II
5	A	I	II	II	I/I I	II	I	I	I	I/I I	II	I	II	II	I	I	I	I
6	A	I	I		I	I	I	I	I	I	I	I	I	I	I	I	I	I

Table 2.2 Hydrogen bonds in crystal structures (neutron-normalized distances).

Crystal forms	Interaction	H...A /Å	D...A /Å	∠D-H...A /°	Symmetry code
1_Form I	N1-H1...O3	2.44	2.920(3)	108	Intramolecular
	C3-H3...O3	2.47	3.496(3)	159	3/2-x, 1/2+y, 1/2-z
	C6-H6...O2	2.34	2.808(4)	104	Intramolecular
	C20-H20A...F2	2.48	3.302(4)	132	1-x, 1-y, -z
2_Form I	N1-H1...O2	2.07	2.947(7)	144	x, -1+y, z
	C2-H2...O1	2.51	2.912(8)	101	Intramolecular
	C2-H2...O1	2.49	3.199(8)	122	1-x, -1/2+y, 1-z

3_Form I	N1–H1···F1	2.22	2.920(2)	125	Intramolecular
	C5–H5···O2	2.46	3.298(3)	134	$-1+x, y, z$
	C6–H6···O1	2.32	2.792(3)	105	Intramolecular
	C20–H20C···O1	2.51	3.487(3)	150	$x, 1+y, z$
	C12–H12···F2	2.46	3.472(3)	154	$x, y-1, +z$
4_Form I	N1–H1···O1	2.01	2.955(3)	154	$1/2-x, -1/2+y, z$
	N1–H1···O4	2.50	3.063(3)	113	Intramolecular
	C3–H3···O2	2.49	3.253(3)	126	$1/2+x, 1/2-y, -z$
	C6–H6···O1	2.39	2.830(3)	103	Intramolecular
	C17–H17···O3	2.35	3.254(4)	139	$x, 1/2-y, 1/2+z$
4_Form II	N1–H1···O3	2.23	2.962(3)	128	Intramolecular
	C7–H7B···O2	2.36	2.807(4)	103	Intramolecular
	C5–H5···O1	2.59	3.410(4)	132	$x+1, y, z$
	C14–H14···O2	2.58	3.558(3)	149	$-x+1, -y+1, -z+1$
5_Form I	N1–H1···O4	1.97	2.971(3)	172	x, y, z
	N3–H3···O2	1.92	2.929(3)	179	$-1+x, y, z$
	C6–H6···O2	2.48	2.884(3)	101	Intramolecular
	C8–H8···O2	2.48	3.136(3)	118	Intramolecular
	C17–H17···F6	2.39	3.471(2)	173	$1+x, -1+y, z$
	C27–27···O4	2.48	2.889(3)	101	Intramolecular
	C29–H29···O4	2.44	3.077(3)	117	Intramolecular
	C19–H19B···O3	2.49	3.267(3)	127	$1-x, -y, -z$
5_Form II	N1–H1···O2	1.96	2.965(3)	176	$1/2-x, 1/2+y, 1/2-z$
	C6–H6···O2	2.43	2.852(4)	101	Intramolecular
	C8–H8···O1	2.43	3.486(3)	165	$1/2-x, -1/2+y, 1/2-z$

	C17–H17···F2	2.32	3.405(5)	177	$1/2+x, 1/2-y, -1/2+z$
6_Form I	N1–H1···O2	2.08	3.046(5)	160	$1/2-x, -1/2-y, -z$
	C2–H2···O2	2.41	3.421(8)	155	$1/2-x, -1/2-y, -z$
	C6–H6···O1	2.49	2.904(8)	101	Intramolecular

Molecule 2. This molecule is dimorphic. Form I was crystallized in chiral space group $P2_1$ as thin colorless plate-type crystals from a 1:1 acetone–methanol solution. The sulfonamide catemer synthon (N1–H1···O2, 2.07 Å, 144°) of $C(4)$ chain runs along the b -axis (Figure 2.2a). Layers of molecules are connected by C–H···O (2.49 Å, 122°) and C–H··· π interactions (2.86 Å) (Figure 2.2b).

A second polymorph (form II) was obtained concomitantly⁸ from acetic acid along with form I. The crystal quality of this minor polymorph was not so good. These hair morphology crystals (thin fibers) were characterized by powder XRD (diffractogram is shown in Figure 2.11).

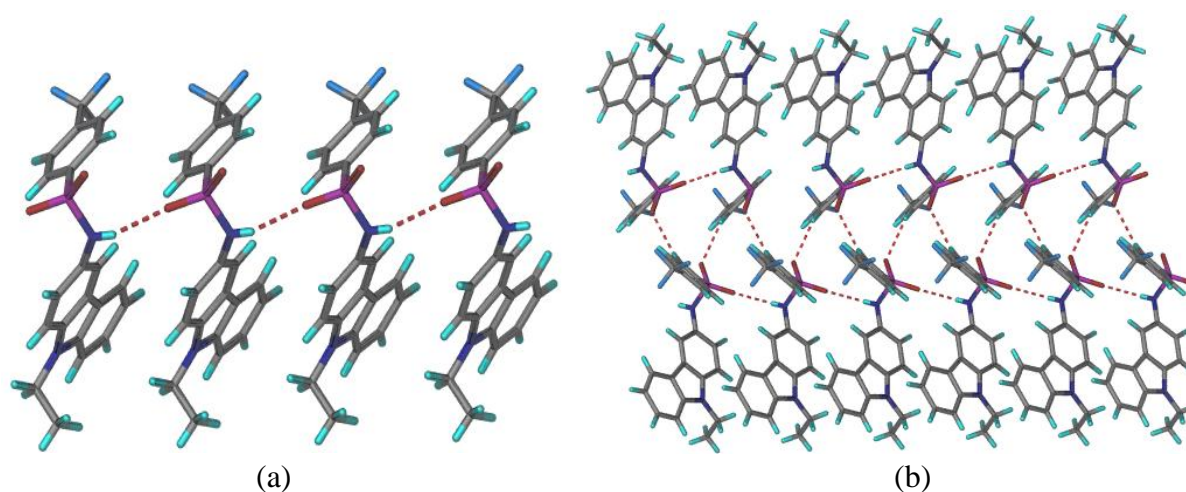


Figure 2.2 Hydrogen bonds in the crystal structure of molecule **2** form I. (a) Sulfonamide N–H···O catemer and (b) C–H···O interactions.

Molecule 3. Molecule **3** is also dimorphic. Colorless crystals of plate and block morphology were obtained from acetone and it was solved in the triclinic space group $P\bar{1}$. Similar to cardiosulfa **1**, molecules of **3** are connected via N–H $\cdots\pi$ (2.76 Å) and $\pi\cdots\pi$ stacking (3.52 Å) interactions (Figure 2.3a). Auxiliary C–H \cdots O interactions complete the overall packing in 3D arrangements (Figure 2.3b).

An amorphous phase of **3** was obtained by melting form I at 180 °C. Crystallization of form II occurred between the recrystallization (81 °C) and melting temperature (162 °C) of this amorphous phase by heating it at 150 °C for 20–30 min. The resulting powdery material was confirmed to be a new polymorph by PXRD (Figure 2.11). It was not possible to grow single crystals of form II by solvent evaporation.⁹

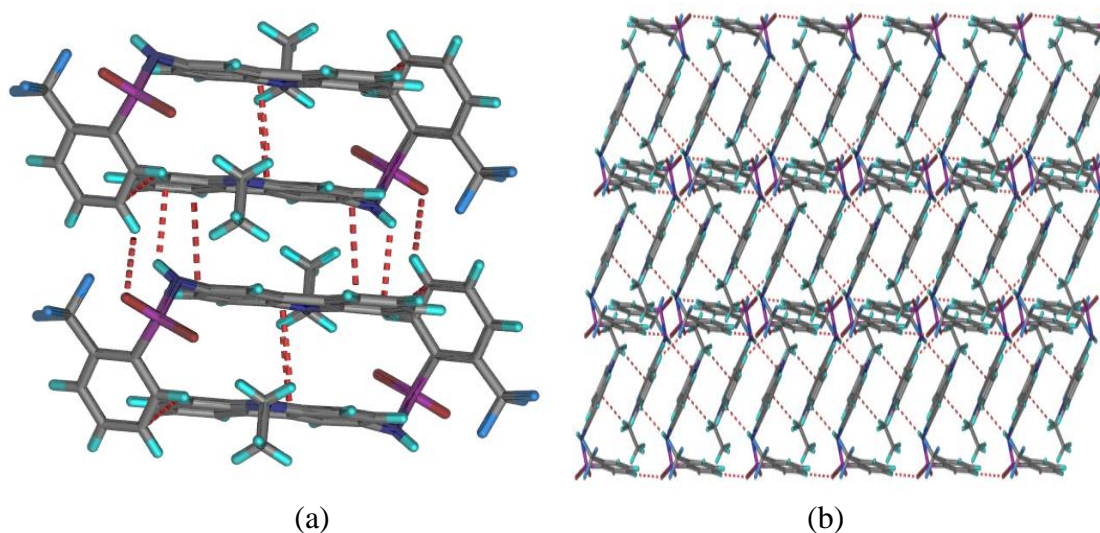


Figure 2.3 (a) N–H $\cdots\pi$ interactions in crystal structure **3**. No strong N–H \cdots O hydrogen bonds, similar to cardiosulfa **1**. (b) N–H $\cdots\pi$ and C–H $\cdots\pi$ interactions in molecule **3**.

Molecule 4. This trimorphic compound belongs to the category of conformational and color polymorphs.¹⁰ Form I was crystallized from acetone as

colorless crystals of thin and long plate morphology. In the crystal structure (space group *Pbca*), two molecules interact via N–H \cdots O C(4) chain (2.01 Å, 154°) along the *b*-axis (Figure 2.4a). The layers are cross-linked by weak C–H \cdots O hydrogen bonds (Figure 2.4b). There is an intramolecular N–H \cdots O bond with a nitro O (2.50 Å, 113°) and an N–H \cdots π interaction (2.82 Å).

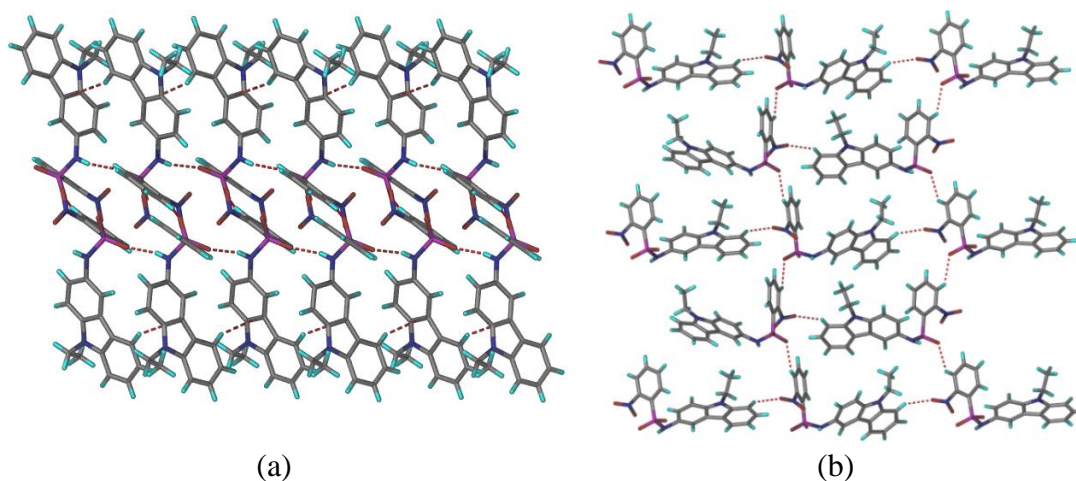


Figure 2.4 (a) Sulfonamide N–H \cdots O catemer synthon in form I of molecule **4**, and (b) C–H \cdots O (to NO₂ and SO₂ acceptors) interactions.

Form II was crystallized from methanol as brown-yellow crystals of thick, long plate morphology, which was solved in the triclinic space group $P\bar{1}$. The molecules are stacked via N–H \cdots π (2.82 Å) and C–H \cdots O (2.59 Å, 132°) interactions (Figure 2.5a-b) but there are no strong intermolecular hydrogen bonds in the crystal structure. An intramolecular N1–H1 \cdots O3 (2.23 Å, 128°) is present in form II, which is stronger than that in cardiosulfa. Polymorph II of this molecule is different from form I in three important aspects: (1) conformational difference in C–S–N–C (SO₂NH) and C–N–C–C bond (N-ethyl group) torsions, (2) major N–H \cdots O/ N–H \cdots π interactions between the molecules, and (3) color differences in crystals and powdered samples.¹⁰ (Figure 2.5c-e)

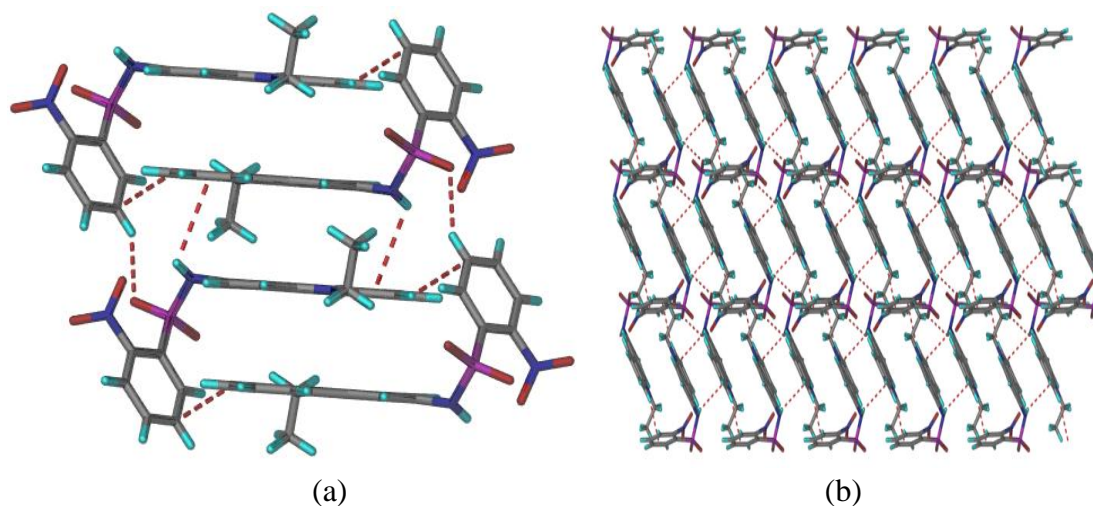


Figure 2.5 The main differences in intermolecular interactions between form I and form II of molecule **4**. (a) N-H... π and C-H...O interaction in form II, (b) C-H...O (SO₂) interactions between the layers of form II. The NO₂ acceptor is not involved in intermolecular H bonding.

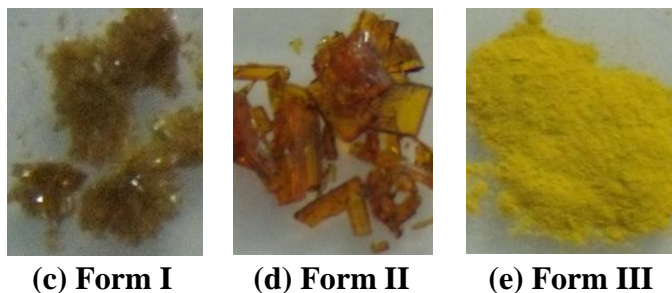


Figure 2.5 Color differences in polymorphs (Form I-colorless; Form II-brown; Form III-yellow) of molecule **4**.

There is no example of X-ray crystal structures for polymorphic sulfonamides that differ by a N-H...O catemer/dimer synthon in one structure and N-H... π interaction in the second polymorph, based on a survey of the Cambridge Structural Database¹¹ (ver 5.33, ConQuest 1.13, May 2012 update). The closest example we could find is the p-tosylhydrazone derivative of bis(p-methyl)benzophenone, for which polymorph 1 has N-H...O dimer synthon while forms 2 and 3 have no such strong hydrogen bonds even though the molecule

contains an SO₂NH group.^{7a} A list of H bonds and synthons in molecules **1-6** is presented in Table 2.2 and 2.4. Such examples of unconventional hydrogen bonds in crystal structures of sulfonamides are rare in the CSD. Crystallization of form **3** of **4** is detailed in the next section on cryogenic conditions.

Molecule 5. It was crystallized as two polymorphs, form I ($Z' = 2$) from nitromethane as plate type crystals and form II ($Z' = 1$) from methanol as block/plate type crystals. The crystal structure of form I is solved in space group $P\bar{1}$ whereas form II is in $P2_1/n$ space group (Figure 2.6). A third polymorph (form III) was identified by DSC and VT-PXRD, and it was reproduced by heating form I/II at the transition temperature (about 170 °C). Two symmetry-independent conformers A and B¹² are present in form I, which interact through N–H···O catemer synthon (Figure 6a, N1–H1···O4 of molecule A, 1.97 Å, 172°; and N3–H3···O2 of molecule B, 1.92 Å, 179°) in a layer structure. Crystal structures of form I and form II are 2D isostructural^{13a-d} (Figure 2.6). The CF₃ group in conformer A is a by-stander but the CF₃ in conformer B molecules makes intermolecular F···F interactions (2.87, 2.88 Å) in form I.

Only a single molecule in the asymmetric unit of form II is similar to conformer B of form I. The catemer synthon (N1–H1···O2, 1.96 Å, 176°) and weak hydrogen bonds (C17–H17···F2, 2.32 Å, 177°; and C8–H8···O1, 2.43 Å, 165°) in form II crystal structure are also similar to form I. Their 2D similarity was quantified by XPac^{13e-g} (Figure 2.6), which showed that the inter-layer packing is different. Two neighboring layers in form I are connected by C–H···O(SO₂) hydrogen bonds (red color arrow) and C–H···F (blue color arrow) interactions, whereas in form II only C–H···F interactions (blue color arrow only) are present. The CF₃ group is shown as spheres to the good clarity.

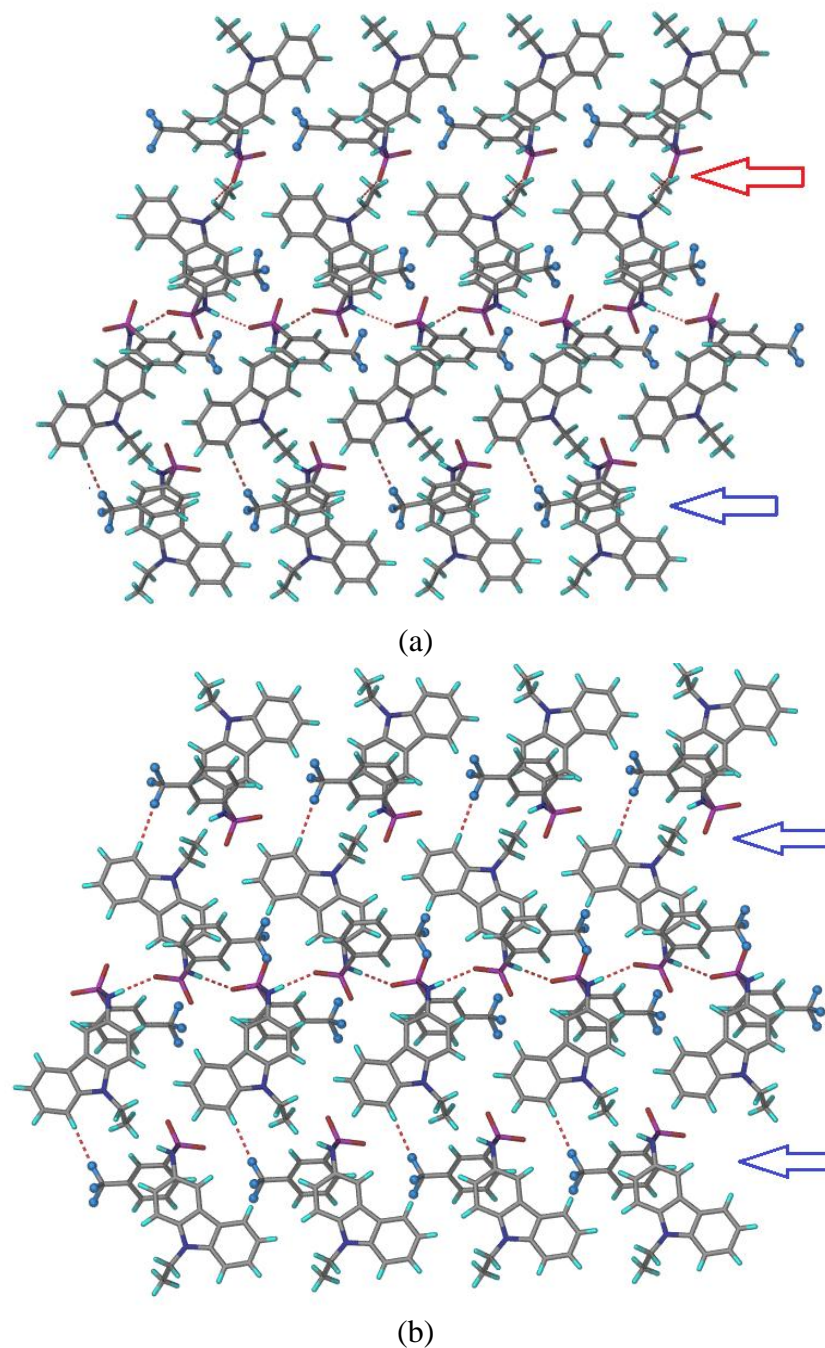
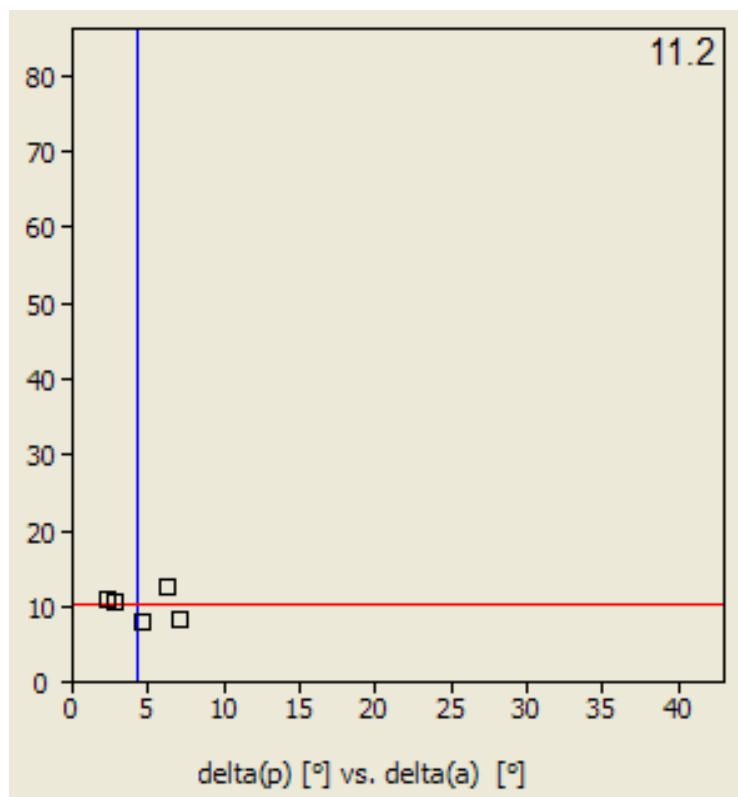


Figure 2.6 2D similarity of form I and form II in molecule **5**. The N-H...O catemer synthon is common but weak interactions are different; C-H...F and C-H...O interactions in form I (a) but only C-H...F interaction in form II (b)



(c)

Figure 2.6 Similarity index of 11.2 in XPac indicates that two polymorphs of molecule **5** are dissimilar (c).

The 3D packing is different in molecule **5** polymorphs (Figure 2.7a and 2.7b) because the CF_3 group participates in different interactions; $\text{F}\cdots\text{F}$ in form I but $\text{C-H}\cdots\text{F}$ in form II. Surprisingly, form I with $\text{F}\cdots\text{F}$ interactions and $Z' = 2$ is more stable than form II having $Z' = 1$ and $\text{C-H}\cdots\text{F}$ interaction. Cryo-milling¹⁴ (milling of materials at low temperature by cooling the metal jar with liquid nitrogen) of crystalline form II at 200 K transformed it to stable polymorph I. Polymorph I has higher crystal density (1.45 vs. 1.42 g cm^{-3}) and lower cell volume per molecule (920 vs. 957 Å^3). Recent pharmaceutical examples of high Z' polymorphs in the stable state are discussed elsewhere.¹⁴ Crystallization of a third form of molecule **5** is detailed in the next section on VT-PXRD.

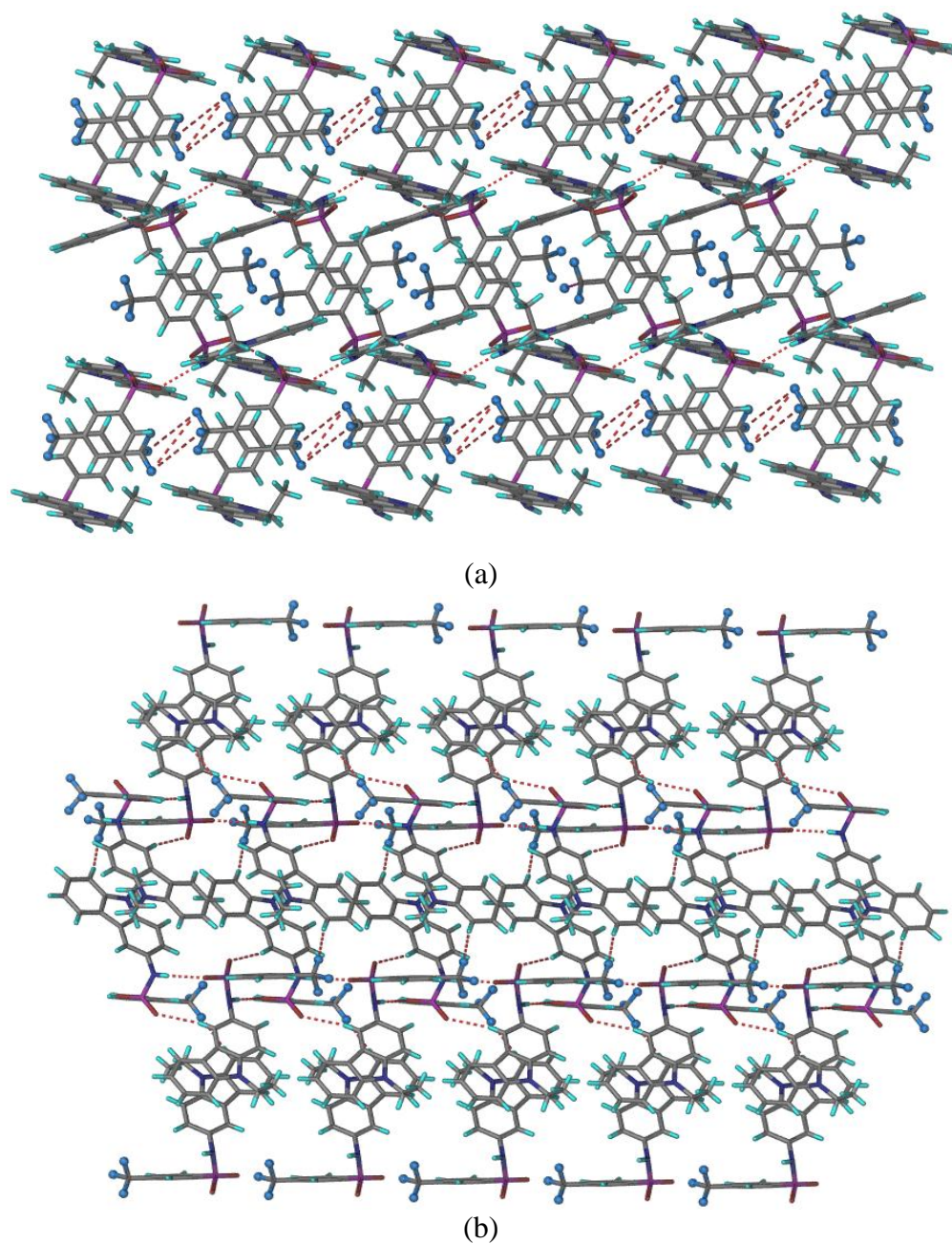


Figure 2.7 Differences between form I and II of molecule **5**. (a) The CF₃ group in one layer of form I make F...F inter-halogen interactions, whereas the CF₃ group in the next layer is idle. (b) CF₃ group participates in C-H...F interaction only and F...F contacts are absent in form II.

2.2.2 Conformational Analysis

The molecular conformation is a subtle yet important parameter in the organic solid-state.¹⁵ Rotations about single bonds (intramolecular torsions) are worth 1-3 kcal mol⁻¹ but can be as high as 8 kcal mol⁻¹ due to steric factors.¹⁶ Cardiosulfa showed much greater variation in torsion angles at the sulfonamide *N*-ethyl group (the most flexible terminal group in the molecule) compared to the other sulfonamides (Figure 2.8, torsion angles are listed in Table 2.3). The difference in torsion angles at the ethyl group was 18° and the sulfonyl moiety was 7° between the dimorphs of **4**. Conformer A and B (of form I) differ from form II by about 8° at the ethyl and sulfonyl groups in molecule **5** (Figure 2.9a and 2.9b).

Table 2.3 Torsion angles of sulfonamides.

Sulfonamides	Torsion angle (°)	Torsion angle (°)
	τ_1 (C1–S1–N1–C7)	τ_2 (C10–N2–C19–C20)
1 Form I	84.0(2)	85.9(3)
2 Form I	67.0(5)	86.8(8)
3 Form I	61.5(2)	87.3(2)
4 Form I	52.6(2)	106.3(3)
4 Form II	59.4(2)	88.3(2)
5 Form I A	51.2(2)	98.0(3)
Form I B	55.7(2)	90.8(3)
5 Form II	47.7(2)	89.9(3)
6 Form I	55.2(3)	89.9(6)

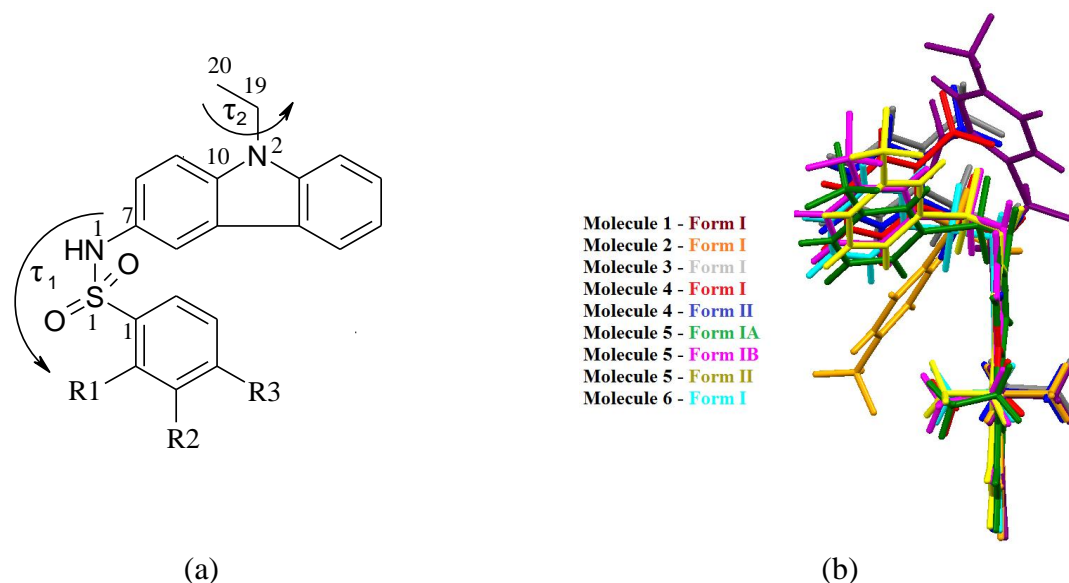


Figure 2.8 (a) Two main torsion parameters in sulfonamides. (b) Overlay of sulfonamides (including polymorphs) extracted from the crystal structure to visualize the difference in molecular conformation at the C1–S1–N1–C7 and C10–N2–C19–C20 portions of the molecule.

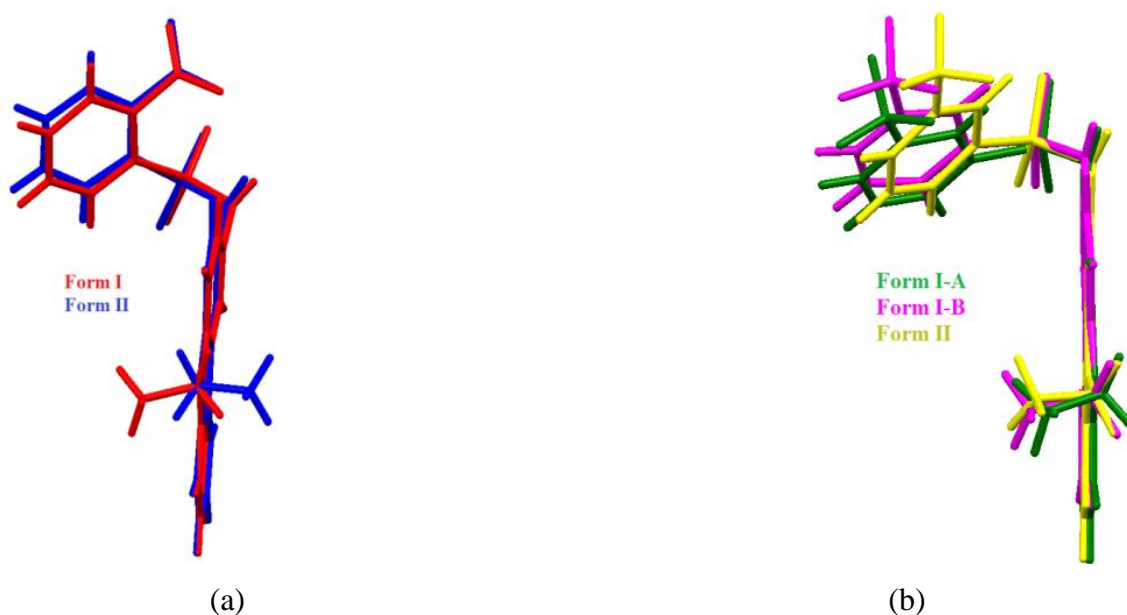


Figure 2.9 The differences in conformation of polymorphs at the sulfonamide and *N*-ethyl functionality in molecule (a) 4 and (b) 5.

Molecule 6. It was crystallized from acetic acid as diamond morphology crystals and the structure was solved in the monoclinic space group $C2/c$. This is the only cardiosulfa derivative to exhibit the sulfonamide $N-H\cdots O$ dimer synthon¹⁷ ($N1-H1\cdots O2$, 2.08 Å, 160°; Figure 2.10). The same crystalline form was obtained from several organic solvents, i.e. no polymorphs.

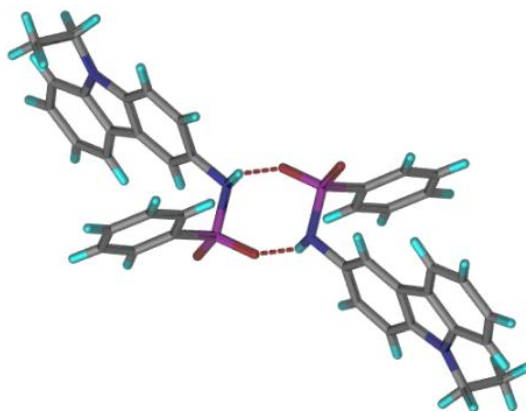


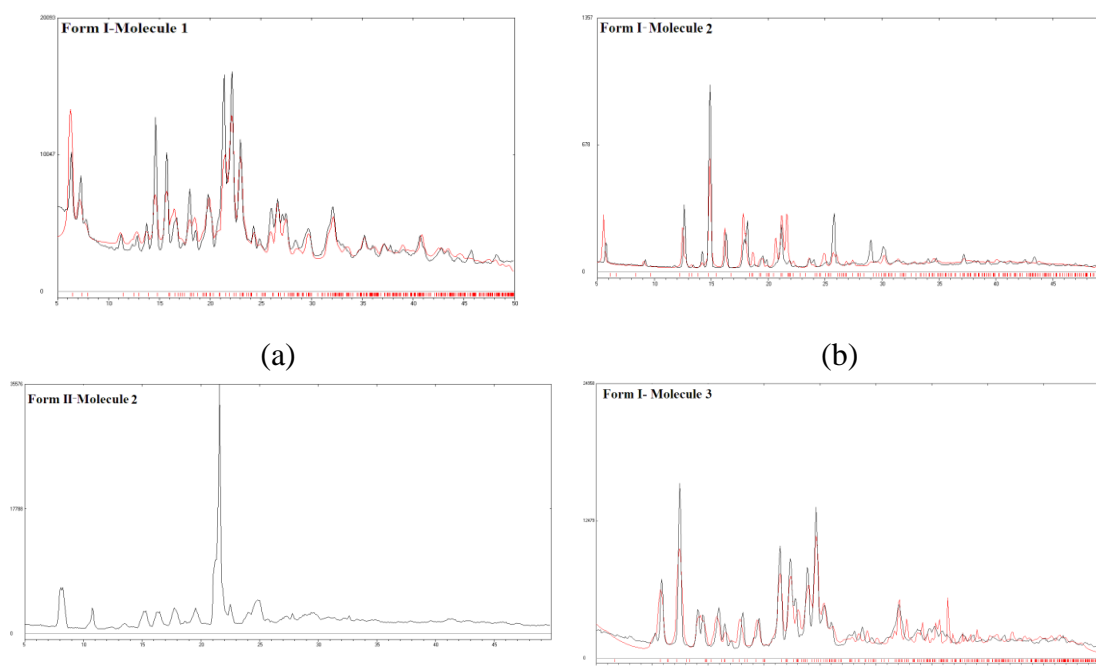
Figure 2.10 Sulfonamide $N-H\cdots O$ dimer in molecule 6.

Table 2.4 Catemer/dimer $N-H\cdots O$ synthon and weak $N-H\cdots\pi$ interaction in 1–6.

Molecule	Form I	Form II	Remarks
1	$N-H\cdots\pi$	---	No polymorphs
2	$N-H\cdots O$ catemer	---	Two polymorphs
3	$N-H\cdots\pi$	---	Two polymorphs
4	$N-H\cdots O$ catemer	$N-H\cdots\pi$	Three polymorphs
5	$N-H\cdots O$ catemer	$N-H\cdots O$ catemer	Three polymorphs
6	$N-H\cdots O$ dimer	---	No polymorphs

2.2.3 Differences in sulfonamide polymorphs

Our previous experience^{17c} with sulfonamides suggested that N-H \cdots O dimer and catemer synthons of graph set notations⁹ $R_2^2(8)$ and $C(4)$ are frequent in these crystal structures. On the other hand, when the SO₂NH group is flanked by aromatic rings on both sides, there is possibility of weak N-H $\cdots\pi$ and C-H \cdots O hydrogen bonds in the crystal structure,^{7a} instead of strong N-H \cdots O bonds. Sulfonamides **1-6** are expected to exhibit polymorphism because (1) they belong to the polymorph promiscuous aromatic sulfonamide class;⁷ (2) they can make N-H \cdots O dimer or catemer to give synthon polymorphs,^{16c,17d-f} (3) conformational flexibility in the molecule will increase the likelihood of polymorphism,^{8,15} and (4) the presence of NO₂ and CF₃ groups that introduces competing hydrogen bond motifs in the crystal structures, and consequently polymorphism. The sulfonamide products were crystallized from suitable solvents and the bulk purity in the solid-state^{10a} was ascertained by powder XRD and ¹³C ss-NMR^{10b,c} (Figure 2.11-2.12).



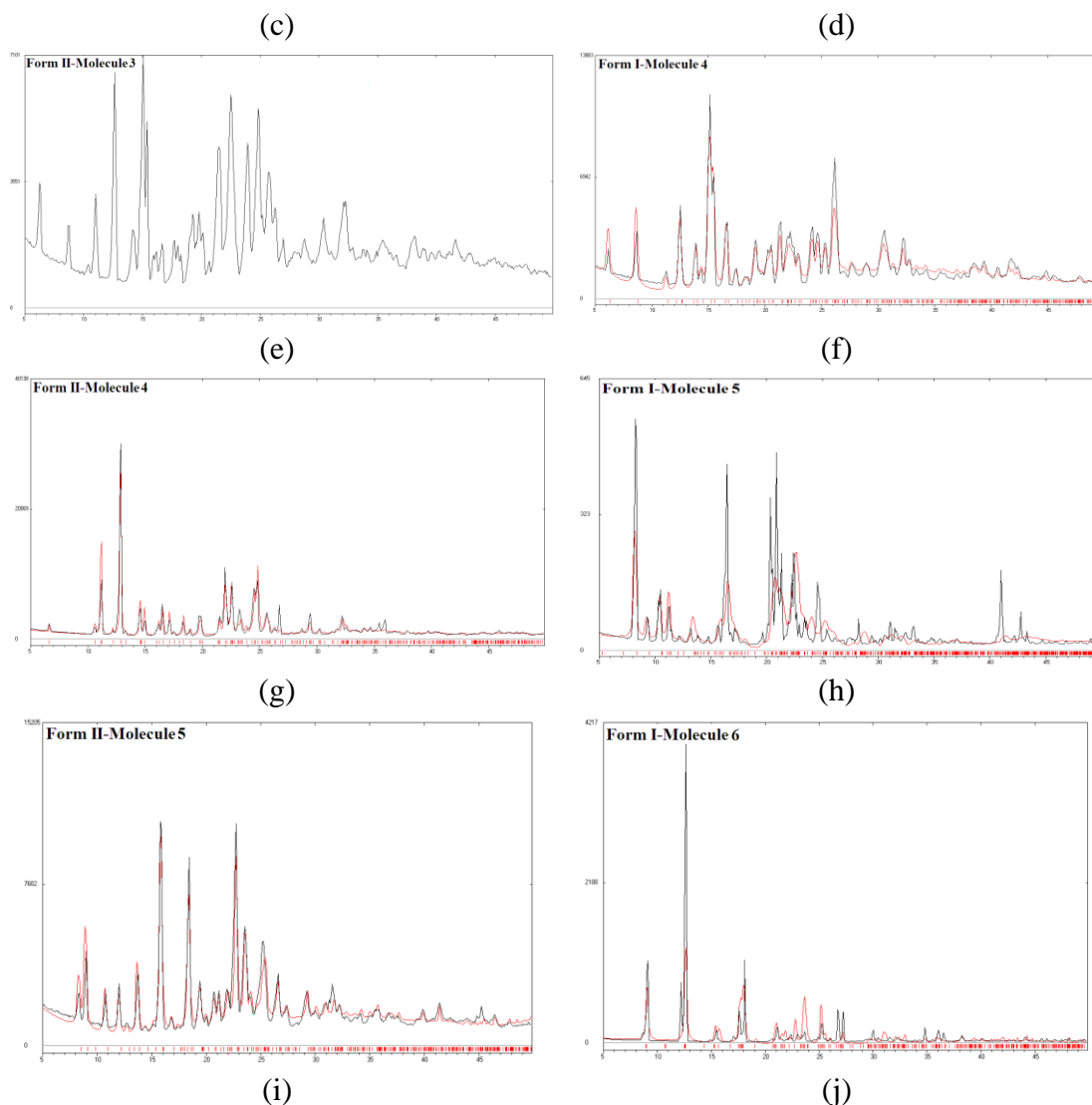
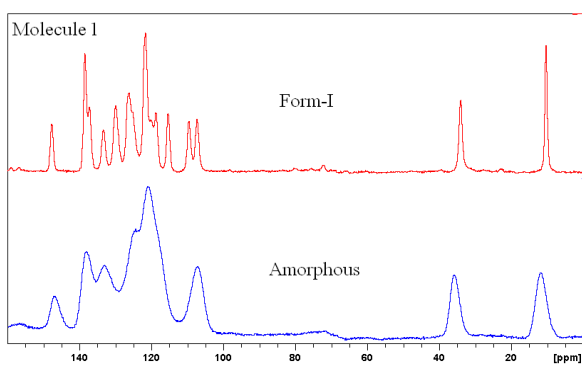


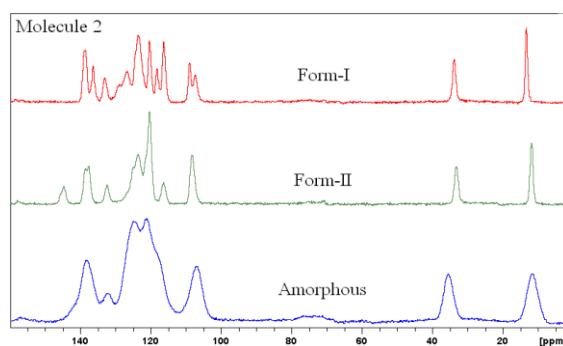
Figure 2.11 Experimental (black) and calculated (red) PXRD line patterns. (a) Form I of molecule 1. (b) Form I of molecule 2. (c) Form II of molecule 2. (d) Form I of molecule 3. (e) Form II of molecule 3. (f) Form I of molecule 4; (g) Form II of molecule 4. (h) Form I of molecule 5; (i) Form II of molecule 5; and (j) Form I of molecule 6. The excellent overlay confirms the purity of the bulk phase with the single crystal X-ray structure.

2.2.4 Solid state ^{13}C NMR and FT-IR. Differences between the polymorphs and amorphous phases were identified by ^{13}C ss-NMR and ^{13}C chemical shifts of

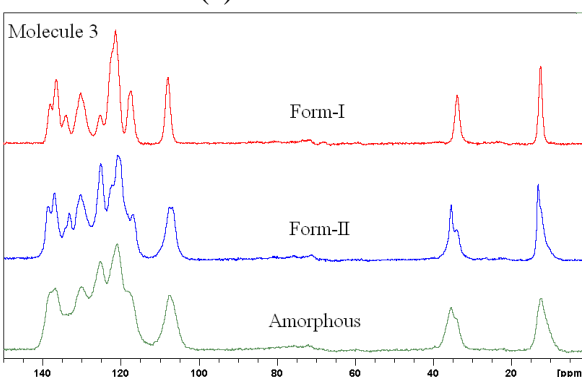
polymorphs are listed in Table 2.5. The different chemical environments of the carbon atoms due to different intermolecular interactions and short range order resulted in up/down-field shifts for the polymorphs. The crystalline and amorphous phases were differentiated by the broadness of peaks (typical hump) for the amorphous phase. Chemical shifts of the terminal ethyl group were used to differentiate polymorphs. For example, in molecule **2**, the N-ethyl group resonates at δ 13.2 and 33.7 ppm for form I and at δ 11.8 and 33.2 ppm in form II (see NMR spectra in Fig. 2.12). Further characterization was carried out by FT-IR^{10d} (Figure 2.13, Table 2.6).



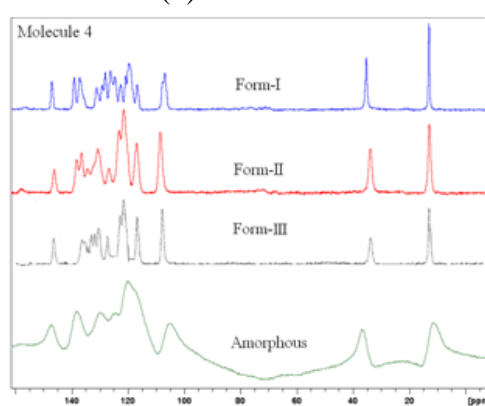
(a) Molecule **1**



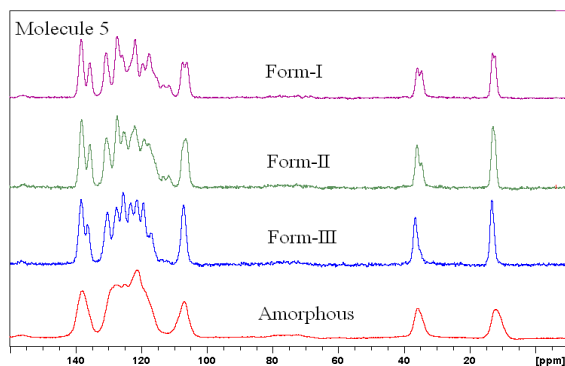
(b) Molecule **2**



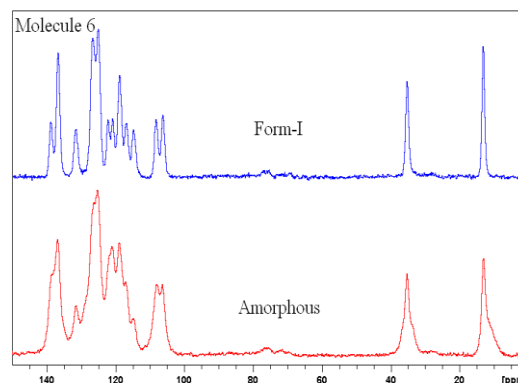
(c) Molecule **3**



(d) Molecule **4**



(e) Molecule 5



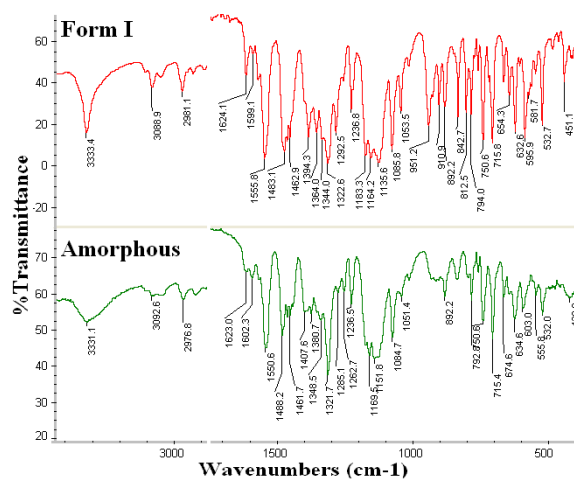
(f) Molecule 6

Figure 2.12 ^{13}C ss-NMR spectra of molecules 1-6 polymorphs shown as stacked overlay plot.

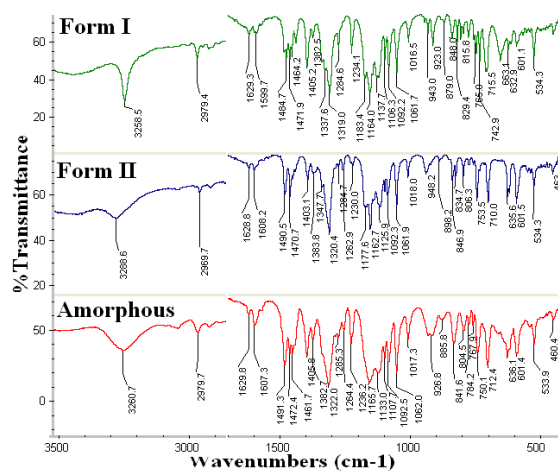
Table 2.5 ^{13}C chemical shift δ values (ppm) of polymorphs for compounds 1–6.

S.No	Molecule 2		Molecule 3		Molecule 4			Molecule 5		
Carbon label	Form I	Form II	Form I	Form II	Form I	Form II	Form III	Form I	Form II	Form III
C21	120.3	123.6	121.3	120.8	-	-	-	121.7	120.1	120.1
C20	13.2	11.8	12.4	13.0	12.8	12.7	14.0	12.0 12.8	12.7	13.0
C19	33.7	33.2	33.8	35.3	35.1	33.6	34.8	34.9 35.7	34.7	36.4
C18	108.9	108.2	107.9	106.8	106.7	108.3	109.6	106.0 107.2	106.3	106.9
C17	120.3	123.6	125.1	122.3	122.4	122.9	124.2	121.7	120.1	122.0
C16	120.3	123.6	125.1	122.3	120.6	121.2	122.5	119.3	119.0	119.3
C15	118.1	116.2	121.3	120.8	119.4	116.8	117.8	117.5	117.7	117.5
C14	131.5	131.5	125.1	125.1	125.5	122.9	124.2	125.6	125.2	123.0
C13	130.8	116.2	121.3	120.8	119.4	116.8	117.8	117.5	117.7	117.5
C12	130.8	132.3	117.3	116.9	116.6	116.8	117.8	113.0	113.1	117.0
C11	131.5	132.3	130.2	130.1	128.9	130.5	131.5	130.5	130.4	130.1

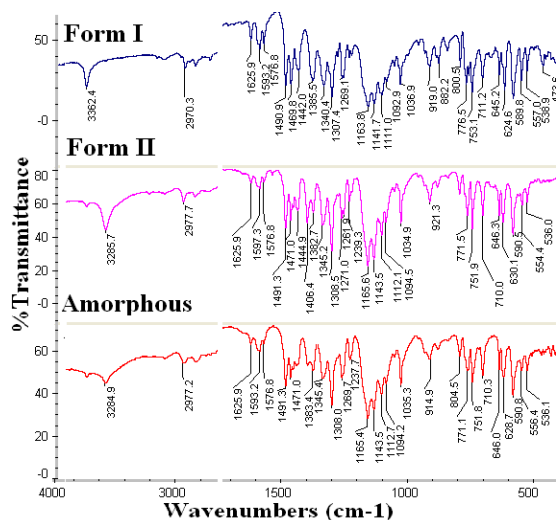
C10	130.8	124.9	130.2	130.1	130.9	130.5	131.5	130.5	130.4	130.1
C9	116.3	116.2	117.3	116.9	116.6	116.8	117.8	111.5	111.5	106.9
C8	128.3	124.9	107.9	106.8	106.7	108.3	109.6	107.2	106.3	106.9
C7	131.5	131.5	134.0	133.1	127.9	130.5	131.5	127.1	127.2	127.4
C6	136.3	137.6	134.0	133.1	136.5	134.2	135.2	135.5	135.5	136.2
C5	133.0	137.6	134.0	133.1	136.5	134.2	135.2	135.5	135.5	136.2
C4	138.5	144.7	134.0	133.1	126.1	126.5	127.7	127.1	127.2	127.4
C3	133.0	137.6	136.5	136.9	137.1	136.2	137.8	138.1	138.0	138.1
C2	136.3	137.6	136.5	136.9	146.8	146.0	147.2	135.5	135.5	13.2
C1	138.5	138.4	138.6	138.6	138.9	138.1	138.8	138.1	138.0	138.1



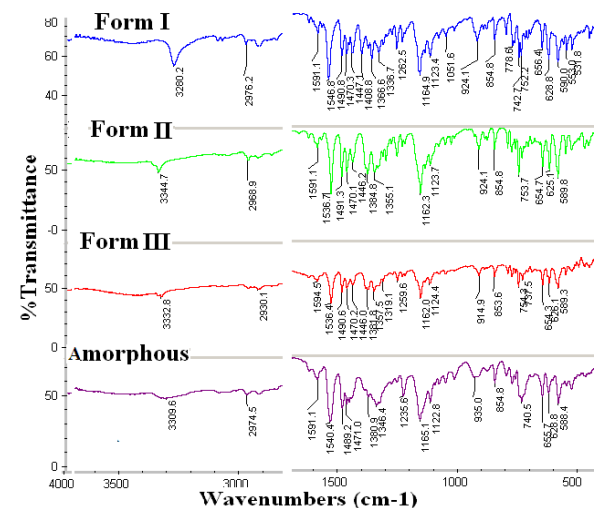
(a) Molecule 1



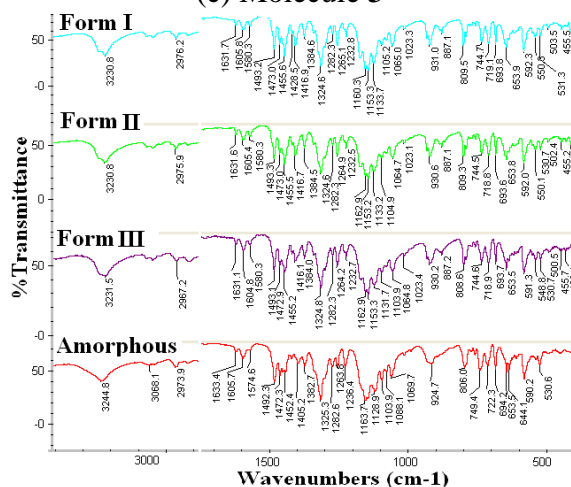
(b) Molecule 2



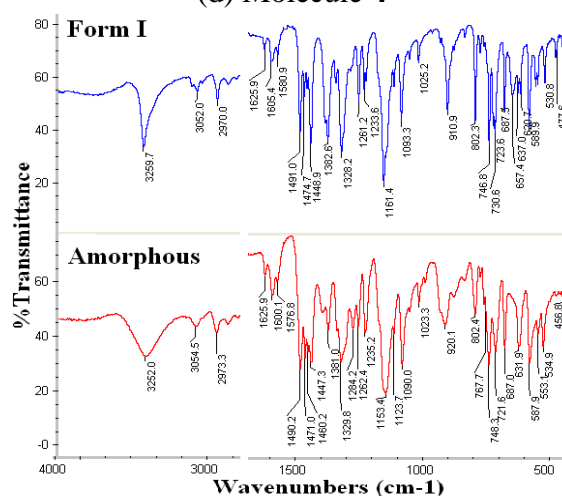
(c) Molecule 3



(d) Molecule 4



(e) Molecule 5



(f) Molecule 6

Figure 2.13 FT-IR spectra of molecules 1–6.

Table 2.6 FT-IR stretching frequencies of polymorphs of 1–6.

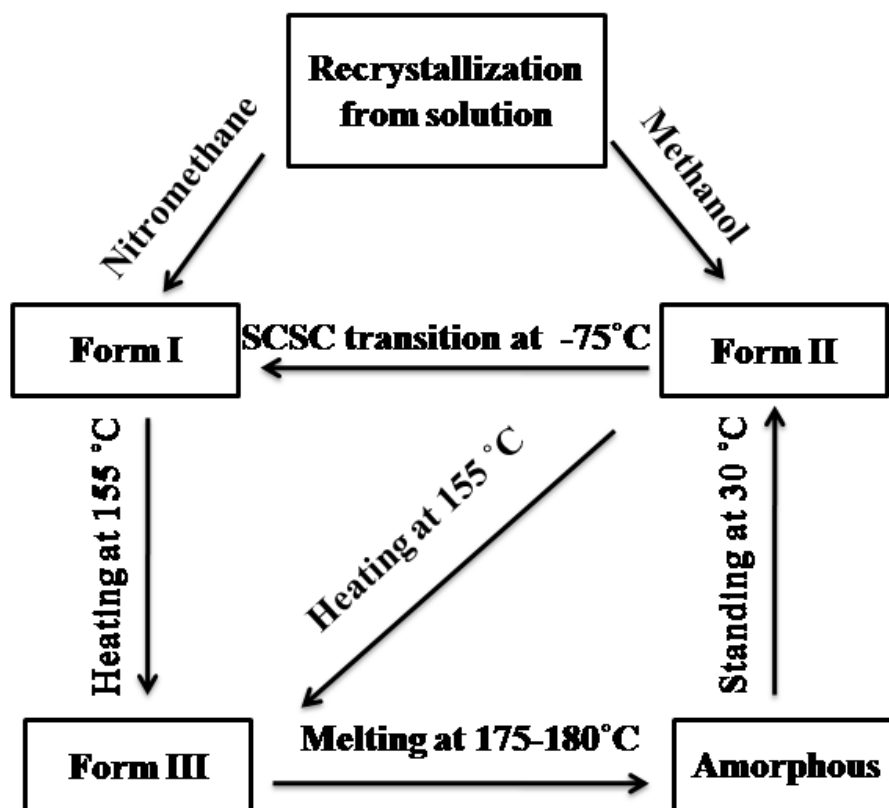
Molecules	N–H stretch cm ⁻¹	N–H bend cm ⁻¹	S=O asym/ sym stretch cm ⁻¹
Molecule 1 Form I	3333.4	1483.1	1364.0/ 1164.2
Molecule 1 amorphous	3331.1	1488.8	1380.7/ 1169.5
Molecule 2 Form I	3258.5	1484.7	1382.5/1164.0

Molecule 2 Form II	3288.6	1490.5	1383.8/1162.7
Molecule 2 amorphous	3260.7	1491.3	1382.7/1165.7
Molecule 3 Form I	3362.4	1490.9	1385.5/ 1163.8
Molecule 3 Form II	3285.7	1491.3	1382.7/ 1165.6
Molecule 3 amorphous	3284.9	1491.3	1383.4/1165.4
Molecule 4 Form I	3280.2	1490.8	1381.1/1164.9
Molecule 4 Form II	3344.7	1491.3	1384.8/1162.3
Molecule 4 Form III	3332.8	1490.6	1381.8/1162.0
Molecule 4 amorphous	3309.6	1489.2	1380.9/1165.1
Molecule 5 Form I	3230.8	1493.2	1384.6/1160.3
Molecule 5 Form II	3230.8	1493.3	1384.5/1162.9
Molecule 5 Form III	3231.5	1493.1	1384.0/1162.9
Molecule 5 amorphous	3244.8	1492.3	1382.7/1163.7
Molecule 6 Form I	3245.2	1491.0	1382.6/1161.4
Molecule 6 amorphous	3259.7	1490.2	1381.0/1153.4

2.3 Polymorphic Transformations

2.3.1 Cryogenic cooling conditions. Molecule **5** exhibited phase transformations under cryogenic and high temperature conditions as summarized in Figure 2.14a. A single-crystal-to-single-crystal transition¹⁸ was observed for form II of molecule **5**. The crystal structure of form II was collected at room temperature, because it transformed to form I at low temperature (100 K). The single crystal of form II is unstable at 0 °C. These transformations were analyzed by collecting X-ray reflections at different temperatures (Table 2.7). The peaks extracted from the area detector frames of the 200 K data set viewed in RLATT (Bruker-AXS crystallographic software to view the reciprocal lattice) did not show a periodic pattern, and so the structure solution was aborted. Reflections on the same crystal were recollected at 100 K and the crystal structure solved satisfactorily (the *R*-factor

improved from 0.1354 at 200 K to $R = 0.0393$ at 100 K and 0.0536 at 298 K). The unit cell parameters matched with that of form I, molecule **5**. The cryogenic transition of form II was studied by variable-temperature PXRD in the T range 298–173 K (Figure 2.14b). Cryogenic milling¹⁴ of form II at liquid N₂ temperature and slurry grinding of form III gave stable form I (Figure 2.15).



(a)

Figure 2.14 (a) Schematic of solid-to-solid phase transitions in molecule **5**.

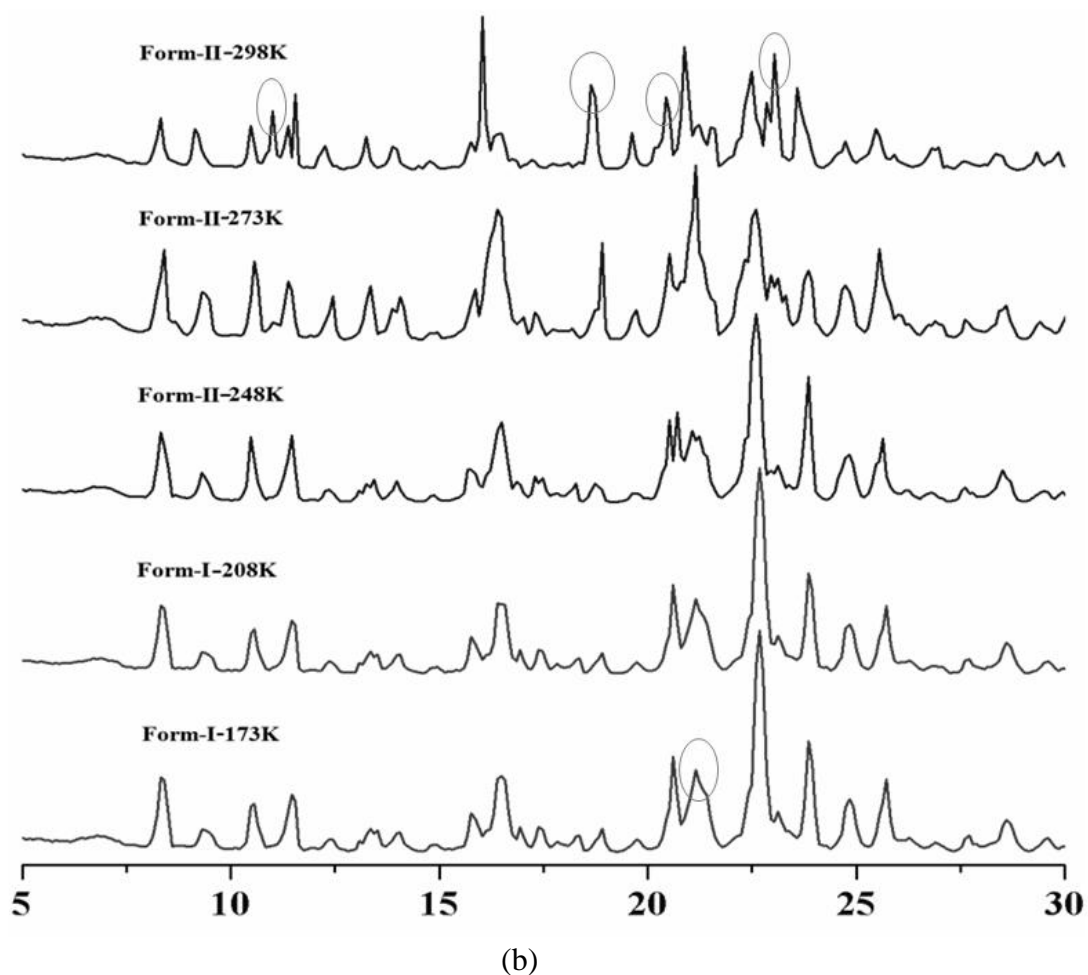


Figure 2.14 (b) VT-PXRD patterns confirm the transformation of molecule **5**, form II to form I upon cooling from 298 K to 173 K. T range of phase transition is 210-250 K. The diagnostic peaks for each polymorph are circled

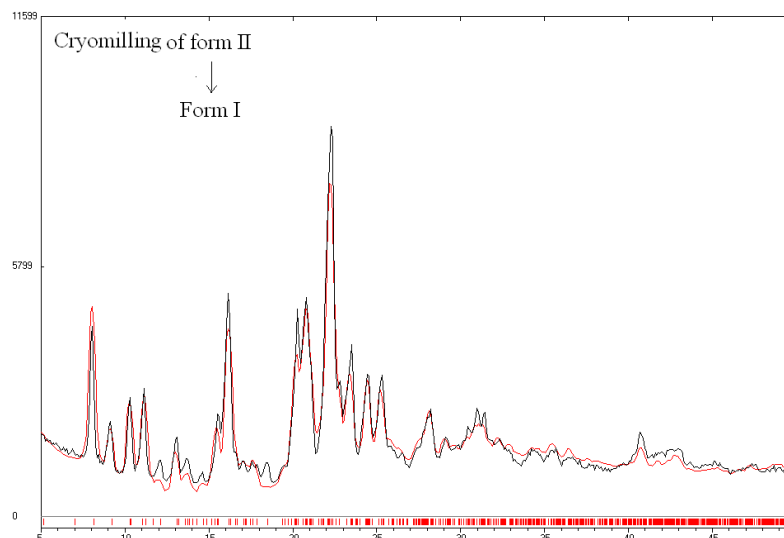


Figure 2.15 Cryogenic-milling of form II resulted in form I, as confirmed by the overlay of the experimental PXRD pattern (black) on the calculated diffraction lines of form I (red) from the X-ray crystal structure.

Table 2.7 Single-crystal-to-single-crystal transformations of molecule **5**.

Crystallographic parameters	At 298 K Form II	At 200 K	At 100 K	At 100 K Form I
		Form II → I beginning	Form II → I complete	
Crystal system	Monoclinic	Triclinic	Triclinic	Triclinic
a (Å)	12.0002(10)	8.894	8.747(9)	8.7343(8)
b (Å)	9.0708(7)	12.916	12.929(13)	12.9486(12)
c (Å)	18.0591(13)	17.091	17.16(2)	17.1899(15)
α (°)	90.00	80.77	79.69(2)	79.7680(10)
β (°)	94.164(7)	81.56	80.121(16)	80.3670(10)
γ (°)	90.00	76.57	75.080(16)	74.9410(10)
V (Å ³)	1960.6(3)	1872	1828(3)	1832.4(3)
Z/Z'	4/1	---	4/2	4/2
Space group	$P2_1/n$	$P\bar{1}$	$P\bar{1}$	$P\bar{1}$
R-factor	0.0628	High	0.1354	0.0393

Molecule 4 under cryogenic conditions. When a crystal of form II of molecule **4** was rapidly cooled by dipping in liquid nitrogen, it got fractured. Such a breakage upon sudden cooling was observed for molecule **4** only; the fractured crystal matched with form II by DSC. The powder pattern of this broken material is named form III, which is different from that of form I and II by PXRD (Figure 2.16). FT-IR analysis showed clear differences between the three polymorphs of molecule **4** in the N–H stretching frequency region at 3280.2, 3344.7 and 3332.8 cm^{-1} for form I, II and III respectively (Figure 2.13, Table 2.6). Neat grinding of form II (N–H $\cdots\pi$) or form III of molecule **4** for 30 min gave form I (N–H \cdots O) in independent experiments by PXRD match (Figure 2.16). Even though there was no phase change observed for form I and II in slurry crystallization, form III transformed to form II upon slurry grinding in 80% ethanol–water after 24 h (solubility measurement conditions, see Figure 2.17f).

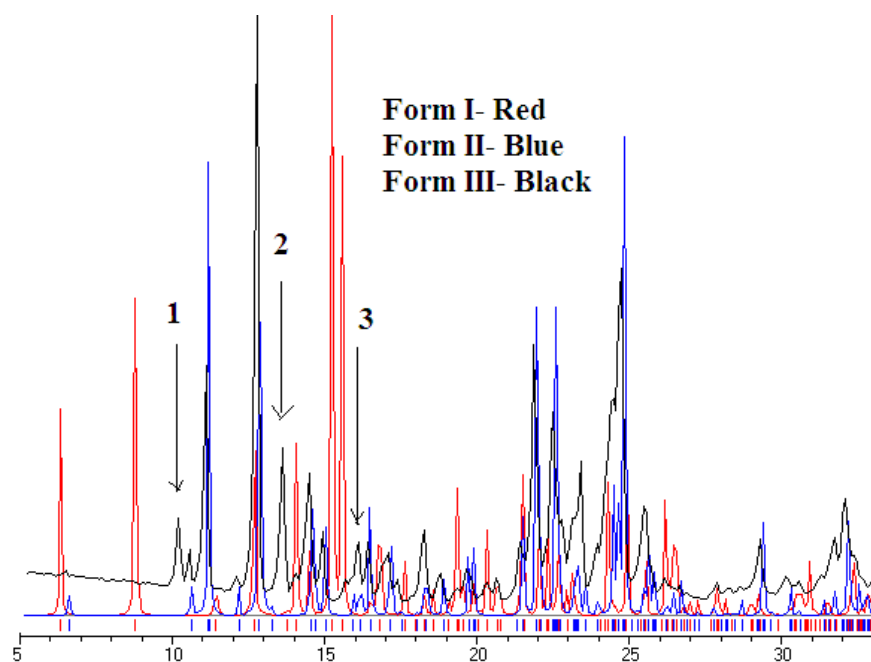


Figure 2.16 Overlay of calculated PXRD peaks of form I and form II with the experimental pattern of form III of molecule **4**. New diffraction peaks are highlighted with arrows.

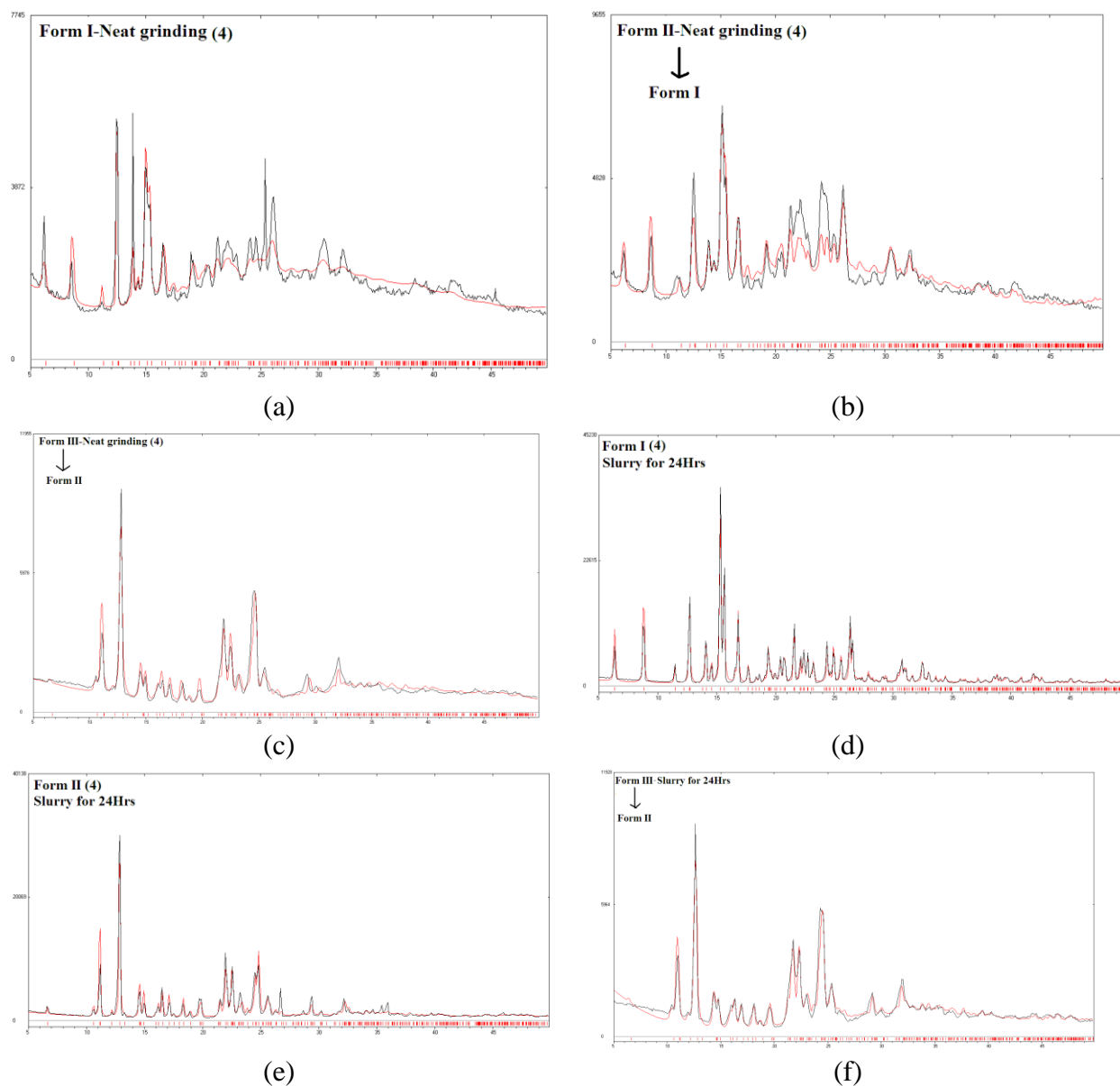


Figure 2.17 Comparison of experimental calculated PXPD line patterns for molecule 4. (a) Form I, neat grinding for 30 min, no change; (b) Form II, neat grinding for 30 min, transforms to form I; (c) Form III, neat grinding for 5 min gave form II; (d) Form I, slurry grinding for 24 h, no change, (e) Form II, slurry grinding for 24 h, no change; (f) Form III, slurry grinding for 24 h, transforms to form II.

2.3.2 High temperature phase transitions. All polymorphs and amorphous phases were studied by DSC.¹⁹ The crystalline form of cardiosulfa **1** exhibited a melting endotherm at 171.5 °C (Figure 2.18a). The glass transition temperature of the amorphous phase ($T_g = 54.1^\circ\text{C}$) was followed by recrystallization (starting at 104.6 °C) and then melting of the crystalline phase (at 169.2 °C).²⁰ The amorphous form of **6** similarly transformed to the crystalline phase during the DSC measurement (Figure 2.18b). Both **1** and **6** exist in a single crystalline form. A combination of DSC and VT-PXRD²¹ measurements (Figure 2.20-2.22) gave an idea of the thermal stability of polymorphs (low and high temperature phases, Table 2.8) and the heat of transition rule^{21e} enabled assignment of **2**, **3**, **4** and **5** as enantiotropic systems. The stable polymorph in these polymorphic systems was identified by slurry and neat grinding experiments at ambient conditions^{19f,21f} (Table 2.9).

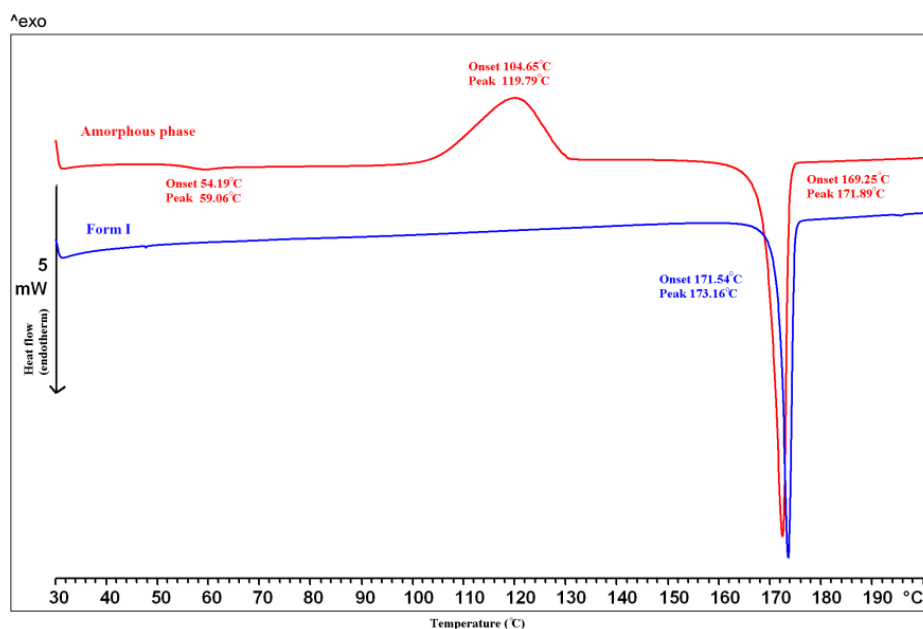


Figure 2.18 (a) Thermal behavior of the stable crystalline form I and amorphous phase of cardiosulfa **1** in DSC, There is no indication of a phase transition.

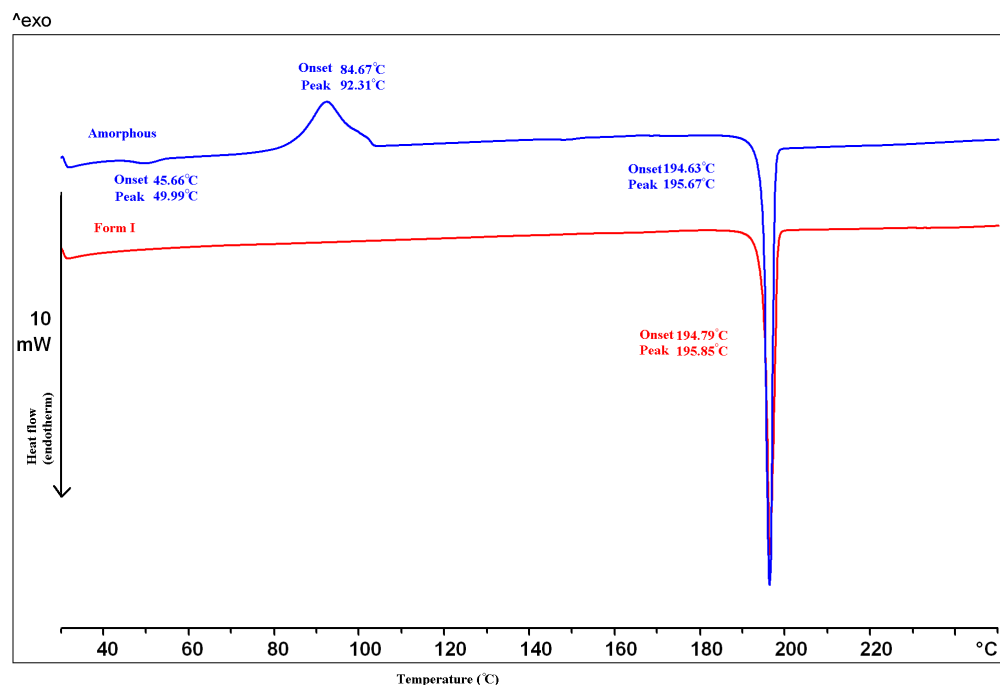
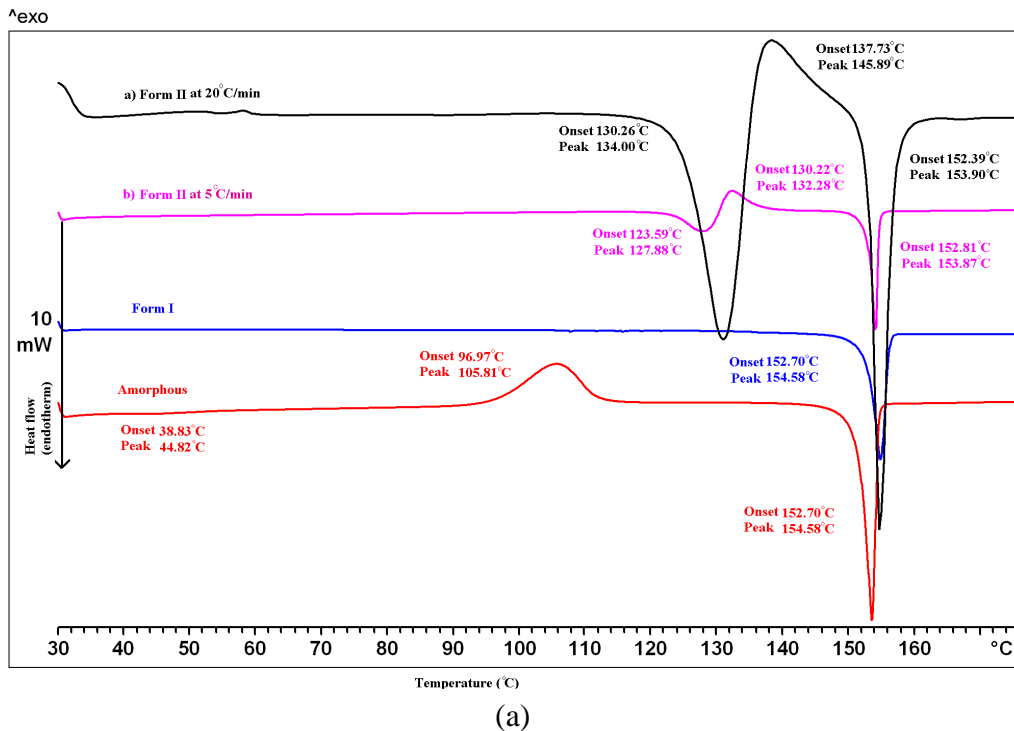


Figure 2.18 (b) Thermal behaviors of the crystalline and amorphous phases of molecule **6** by DSC.



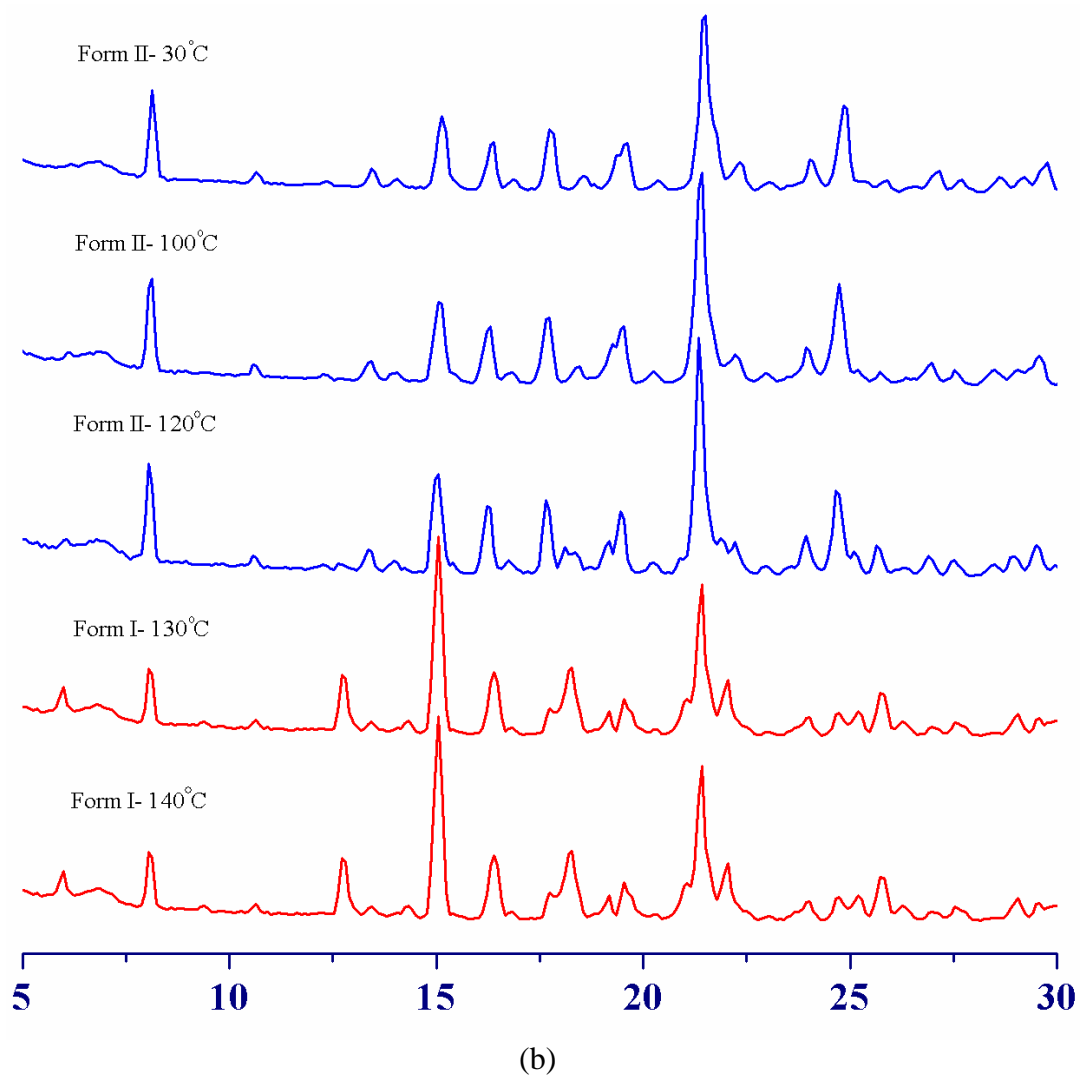


Figure 2.19 (a) The thermal behavior of the polymorphs of molecule 2. (b) VT-PXRD shows the phase transition from Form II to Form I for molecule 2 in the range 120-130 °C.

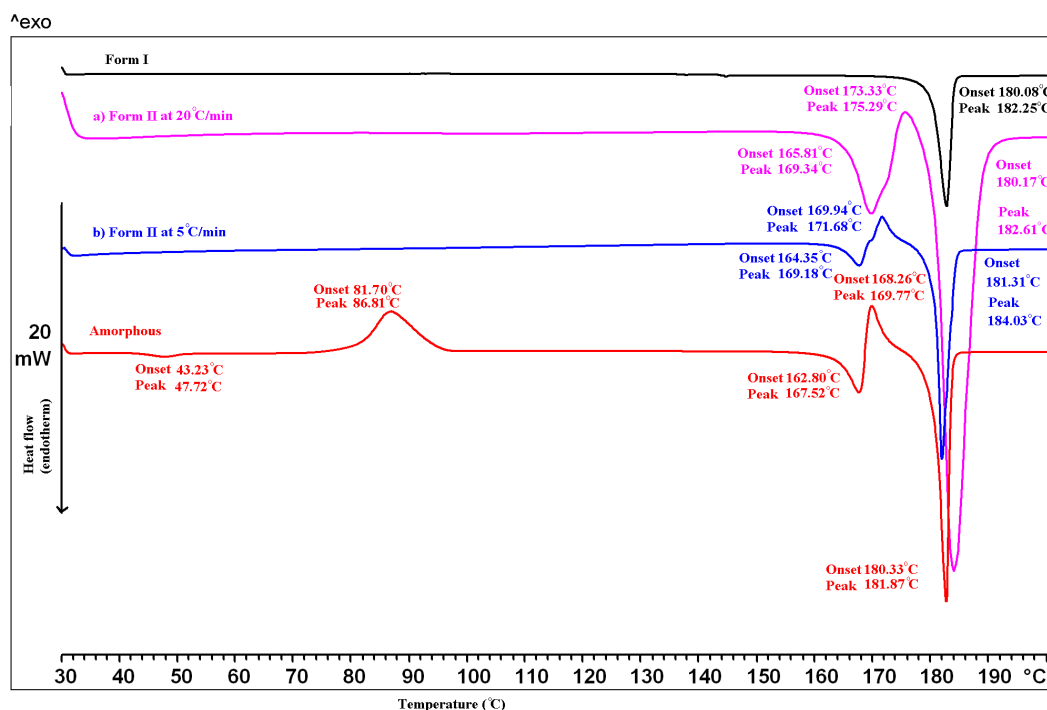


Figure 2.20 (a) Phase transition and melting points of polymorphs for molecule 3 by DSC.

Table 2.8 Thermal analysis and phase transitions of sulfonamide polymorphs (DSC).^a

Sulfonamide polymorphs	Melting and phase transition onset (°C)			Amorphous phase of sulfonamide		
	Form I	Form II	Form III	Glass transition Onset (°C)	Recrystallization Onset (°C)	Melting Onset (°C)
Molecule 1	171.54	---	---	54.19	104.65	169.25
Molecule 2	152.70 (HTP)	123.59 (LTP)	---	38.83	96.97	152.70
Molecule 3	180.08 (HTP)	164.35 (LTP)	---	43.23	81.70	180.33
Molecule 4	193.09 (HTP)	186.91 (LTP)	187.52 (LTP)	Below RT	93.01	187.31

Molecule 5	147.30 (LTP)	155.98 (LTP)	174.70 (HTP)	Below RT	76.15	173.31
Molecule 6	194.79	---	---	45.66	84.67	194.63

^a HTP = high temperature phase, LTP = low temperature phase

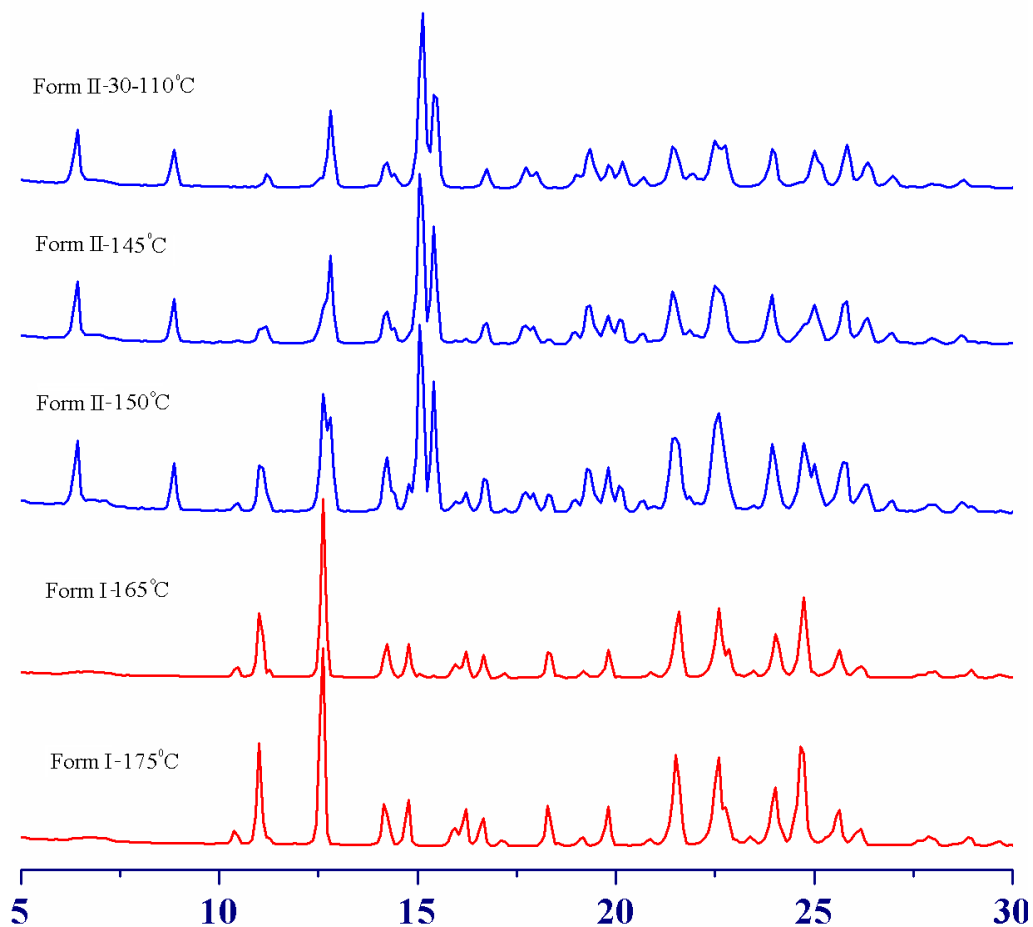


Figure 2.20 (b) VT-PXRD of the phase transition from form II to form I in the range of 150-165 °C for molecule **3**.

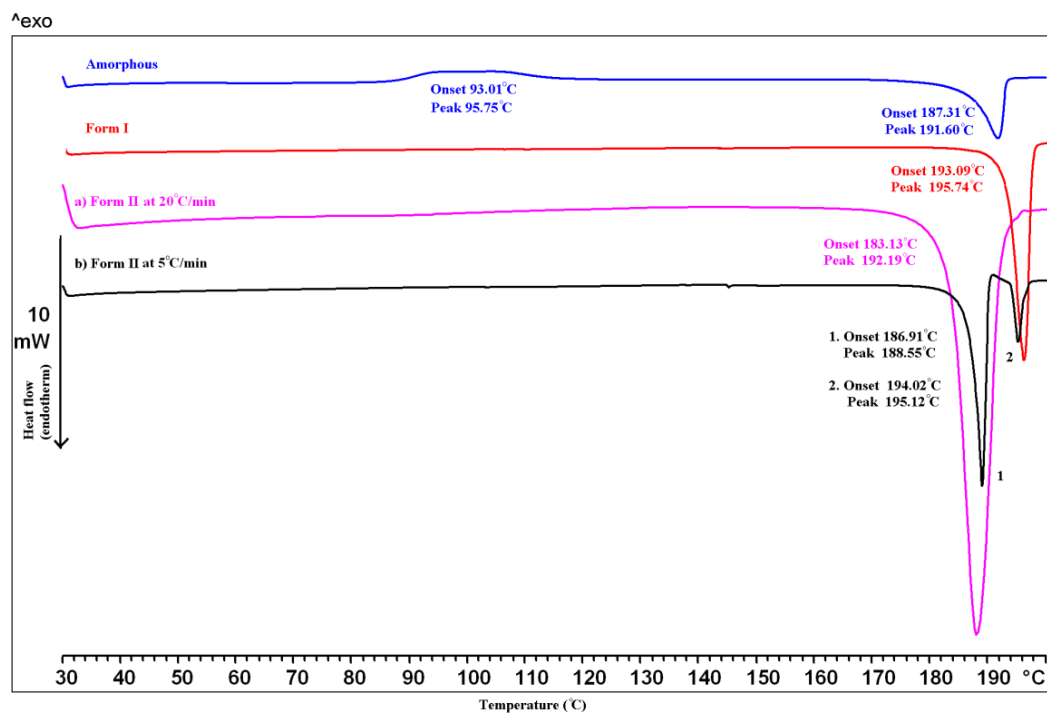


Figure 2.21 (a) The thermal behavior of form I and form II of molecule **4** by DSC.

Table 2.9 Stability and thermodynamic relationships between polymorphs of **1-6**.

Molecules	Density (g cm ⁻³)		Packing fraction (%)		Enthalpy of fusion/ Enthalpy of transition (kJ/mol)			Thermodynamic relationship and identification of the stable polymorph by slurry and neat grinding at ambient conditions
	Form I	Form II	Form I	Form II	Form I	Form II	Form III	
1	1.58	---	71.8	---	42.1	---	---	No polymorphs, stable form I
2	1.38	---	64.0	---	28.5	15.3 -14.5	---	Form I and form II are Enantiotropic, stable form I
3	1.52	---	71.5	---	41.9	5.3 -4.6	---	Form I and form II are Enantiotropic, stable form I

4	1.34	1.42	64.4	68.6	34.7	36.4	36.2	Form I and II, I and III are Enantiotropic, stable form I
5	1.45	1.41	67.5	65.7	1.6	0.2 -0.4	33.8	Form I and III, II and III are Enantiotropic, stable form I
6	1.30	---	65.7	---	36.7	---	---	No polymorphs, stable form I

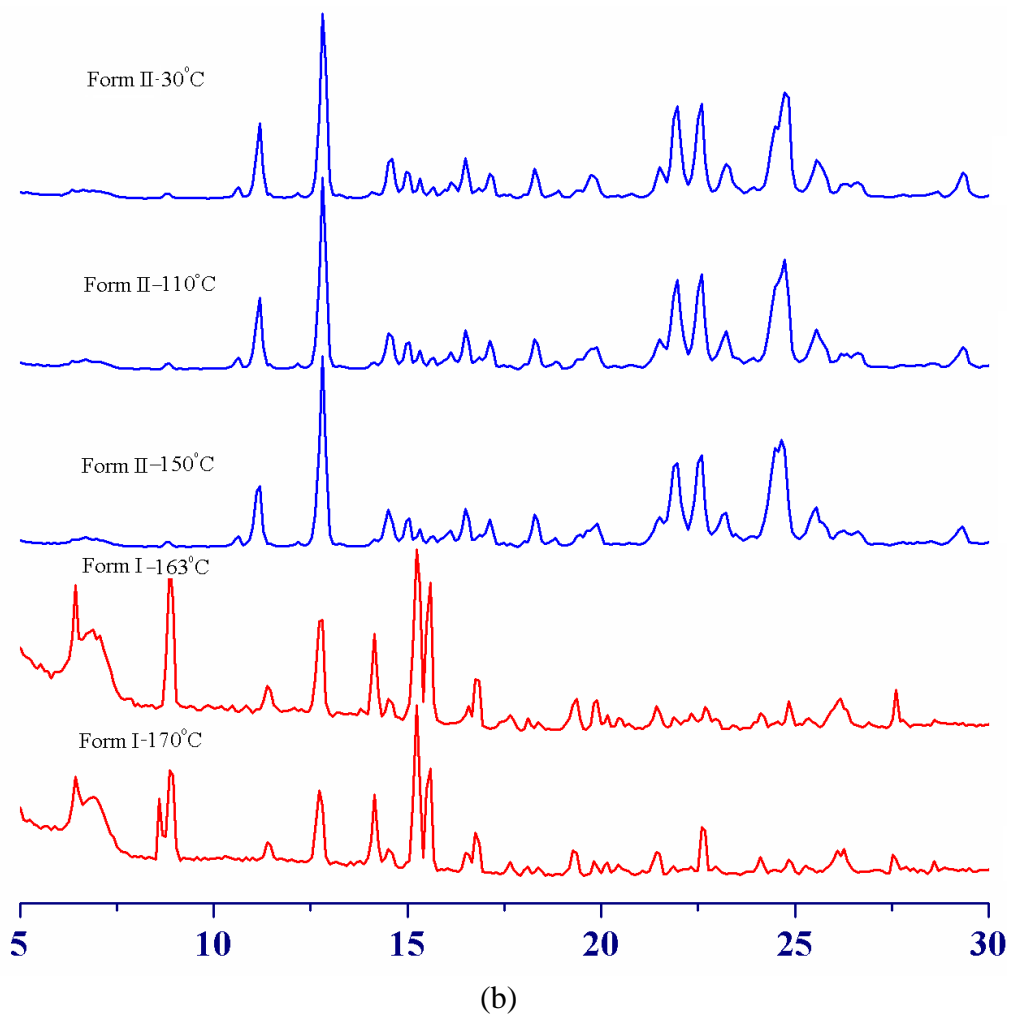
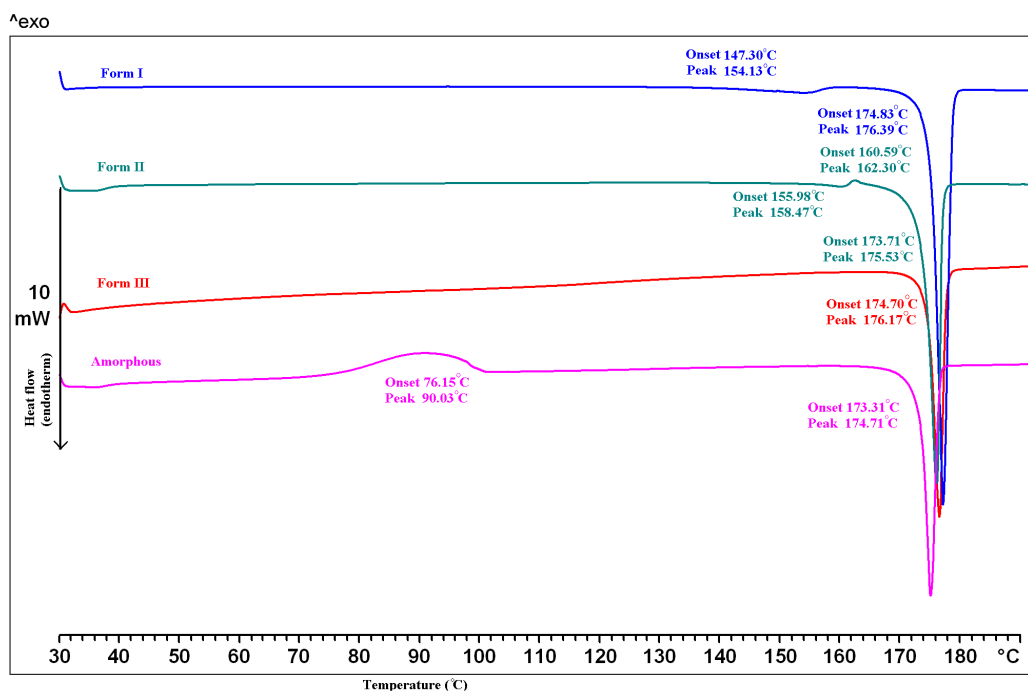


Figure 2.21 (b) VT-PXRD shows the phase transition from form II to form I in the range 150-165 °C for molecule **4**.



(a)

Figure 2.22 (a) The thermal behavior of trimorphs of molecule **5** by DSC.

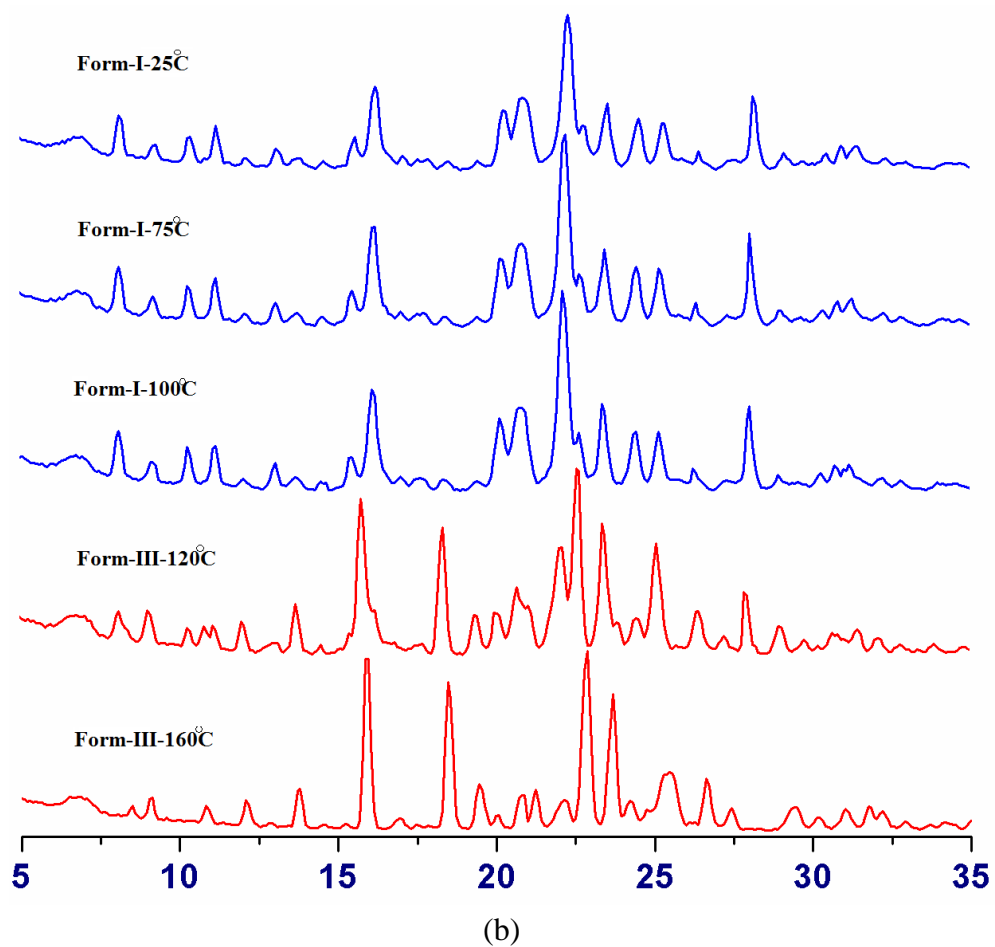


Figure 2.22 (b) VT-PXRD shows the phase transition from form I to form III in the range of 100-120 °C for molecule **5**.

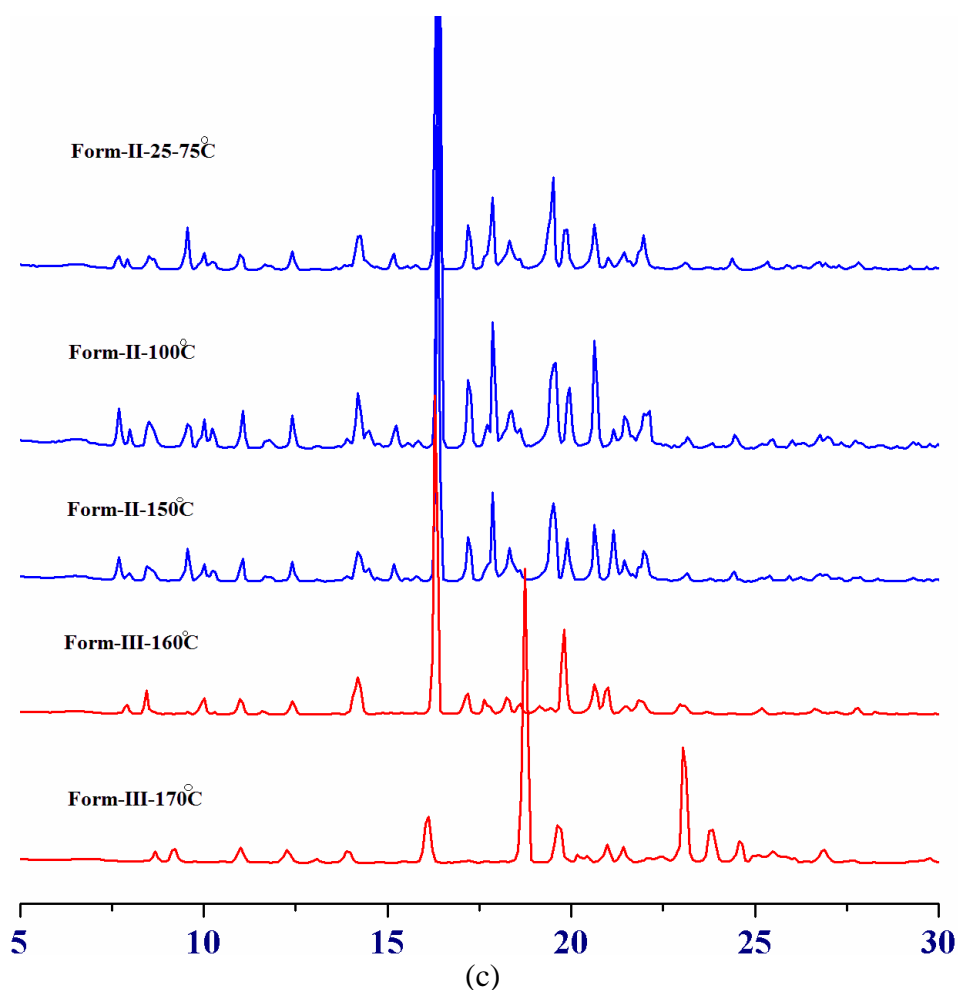


Figure 2.22 (c) VT-PXRD shows the phase transition from form II to form III in the range of 150-160 °C for molecule **6**.

2.4 Dissolution and Solubility

The crystalline phases of molecules **1-6** were subjected to solubility and dissolution studies^[20] in order to rationalize the relationship with molecular conformation, crystal structure, and melting point.²² Solubility and dissolution experiments were performed in 80% ethanol–water mixture (Figure 2.23a, values are listed in Table 2.10). Cardiosulfa has solubility (0.96 mg/mL) and IDR (0.14 mg/cm²/min) in the middle zone of the series **1-6**. Molecule **2** is highly soluble

(10.54 mg/mL) and fast dissolving (0.90 mg/cm²/min) compared to cardiosulfa and other molecules. The variation in solubility/ dissolution rate was analyzed from the molecular conformation (twisted or and planar)²³ in the crystal structure. Cardiosulfa molecule is rigidified due to the intramolecular N–H···O hydrogen bond and maintains pseudo-planarity in the crystal structure. In contrast, molecule **2** lacks the NO₂ group and adopts a twisted conformation in the crystal structure. The pseudo-planarity and conformational rigidity in cardiosulfa may account for the observed difference in solubility and dissolution rate compared to molecule **2**. A planar conformation favors efficient crystal packing and better stability compared to a twisted confirmation which will result in less dense packing, e.g., $D_{\text{calc}} = 1.58 \text{ g cm}^{-3}$ (cardiosulfa) and $D_{\text{calc}} = 1.38 \text{ g cm}^{-3}$ (molecule **2**). The extreme difference in the planar to twisted conformation (see Figure 23b) of molecule **1** and **2** could account for the observed difference in their melting point (171 °C cardiosulfa **1**, and 152 °C molecule **2**), density, solubility, and dissolution rates.^{23c} Molecule **5** adopts an intermediate molecular conformation and density ($D_{\text{calc}} = 1.45 \text{ g cm}^{-3}$), between that of cardio sulfa and molecule **2** (see torsion angles in Table 2.3), and its solubility (4.40 mg/mL) and dissolution rate (0.44 mg/cm²/min) lie in between those for molecule **1** and **2**. Molecule **3** ($D_{\text{calc}} = 1.52 \text{ g cm}^{-3}$) and **6** ($D_{\text{calc}} = 1.30 \text{ g cm}^{-3}$) similarly follow the solubility–conformation trend. Thus *functional group modification may be used as a handle to control molecular conformation in the solid-state and consequently drug solubility*. All solubility and dissolution measurements were done in triplicate and the mean of best two values is reported in Table 2.10. A better understanding of the factors that correlate molecular conformation in the crystal structure to the solubility of pharmaceutical compounds is of current interest.²² The amorphous phases were not considered for solubility measurements because they were found to transform to the stable crystalline form (by PXRD) within 1-2 days under ambient conditions and almost immediately (few minutes) in the aqueous slurry medium.

Even though, molecule **3** (Form I) and molecule **4** (Form II) are isomorphous, their solubility and dissolution rates are different. Molecule **3** with a CF_3 substituent has higher solubility and dissolution rate than **4** with a NO_2 group. Normally it is expected that the CF_3 group will increase lipophilicity and hence aqueous solubility should decrease. In fact **3** ($\text{R}_1 = \text{CF}_3$) has slightly lower solubility and dissolution than **6** ($\text{R}_1 = \text{H}$, Table 10). However, there are examples of drug molecules for which solubility increases on perfluorination or CF_3 group addition, and a plausible reason could be the high electronegativity and strong electron-withdrawing capability of the fluorine atom.^{23g} This explains the better aqueous solubility of **3** compared to **4**. Moreover, both **2** and **5** which are high in solubility ranking have a CF_3 substituent.

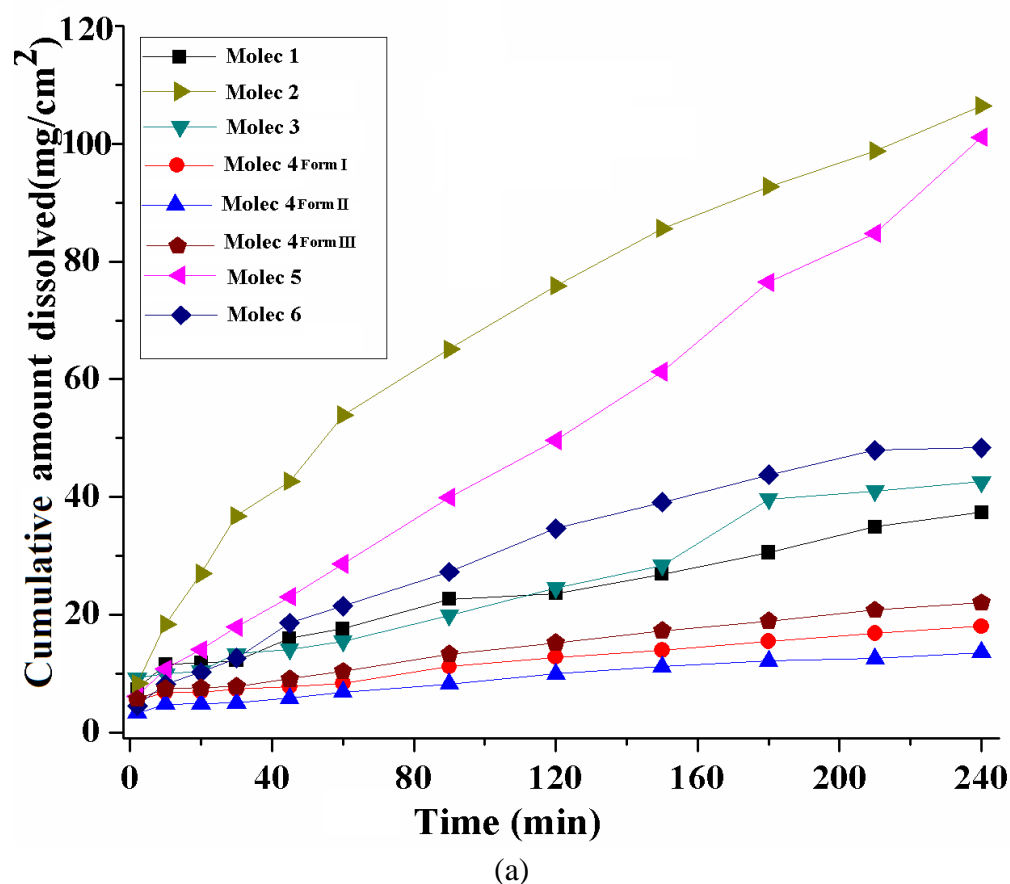


Figure 2.23 (a) Dissolution profiles of sulfonamides **1-6** in 80% ethanol–water

mixture at 37 °C.

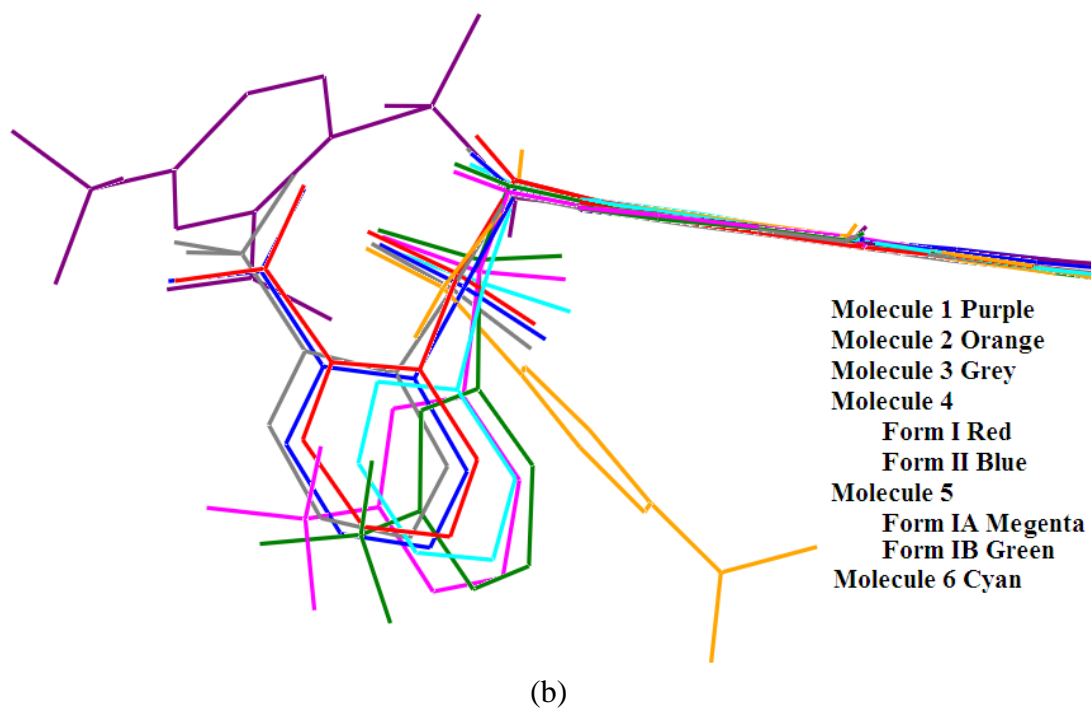


Figure 2.23 (b) Overlay of molecular conformations of molecules **1-6**.

Table 2.10 Solubility and dissolution rate of **1-6** in 80% ethanol–water system.

Compounds	Solubility at 37 °C (24 h) (mg/mL)	IDR at 37 °C (up to 4 h) (mg/cm ² /min)
Molecule 1 (Cardiosulfa)	0.96 (±0.17)	0.14 (±0.03)
Molecule 2	10.54 (±0.19)	0.90 (±0.09)
Molecule 3	1.58 (±0.03)	0.20 (±0.01)
Molecule 4	0.62 (±0.12)	0.05 (±0.00)
Molecule 5	4.40 (±0.11)	0.44(±0.02)
Molecule 6	1.48 (±0.18)	0.25 (±0.03)

We next compared the solubility and dissolution properties of two polymorphs of molecule **4**, which exhibit different hydrogen bonding motifs. The secondary amino group (SO₂-NH) in form I participates in sulfonamide N-H···O catemer synthon, whereas form II has weak N-H··· π / C-H···O interactions. The strong hydrogen bonds of form I are able to better interact with the solvent water/ethanol molecules and the solubility and dissolution rate of form I are higher than those of form II (0.62 mg/mL, 0.05 mg/cm²/min vs. 0.43 mg/mL, 0.04 mg/cm²/min). Thus, molecule **4** provides further insight into structure–property relationship. Form I with N-H···O hydrogen bond catemer has lower density ($D_{\text{calc}} = 1.34 \text{ g cm}^{-3}$) compared to form II ($D_{\text{calc}} = 1.42 \text{ g cm}^{-3}$) with N-H··· π interaction. We are not aware of such a study on strong vs. weak hydrogen bonding in drug polymorphs on solubility and dissolution rate. We confirmed in independent experiments (Figure 2.17d and 2.17e) that there is no inter-conversion between polymorphs I and II of **4** during dissolution and solubility measurements (Figure 2.24), but form III transformed to form II at the end of the solubility experiment (Figure 2.17f). The bent conformation of molecule **4** is similar (Figure 2.23b) in both structures and so their solubility difference may be attributed to hydrogen bonding. This explanation offers yet another reason for the low solubility of cardiosulfa, the only crystal structure in this family without strong N-H···O hydrogen bonding. The higher solubility of form III of molecule **4** (0.56 mg/mL, 0.06 mg/cm²/min) is difficult to rationalize in the absence of crystal structure details.

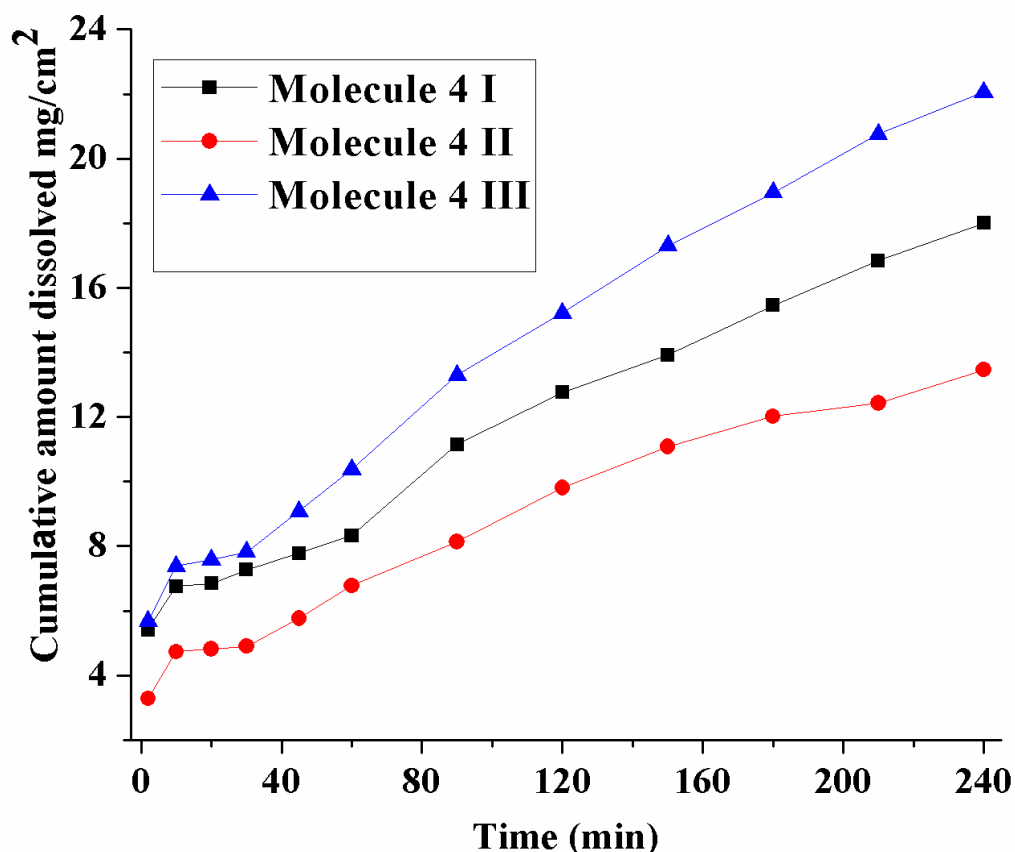


Figure 2.24 Dissolution profiles of form I (N–H···O), form II (N–H··· π), and form III of molecule **4** in 80% ethanol–water. Form III curve is the highest but there is no information about hydrogen bonding in this crystal structure.

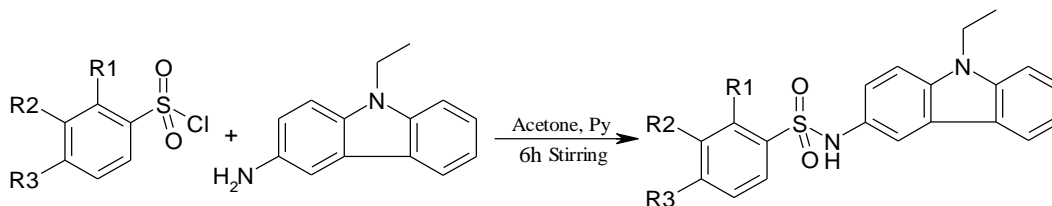
2.5 Conclusions

The X-ray crystal structures of a new class of synthetic AhR agonist molecules based on the cardiosulfa lead were systematically studied and analyzed for solubility trends. Several new polymorphs were identified and their phase transitions and stability order was established. The crystal structures of polymorphs were analyzed in terms of strong N–H···O and weak N–H··· π , C–H···O hydrogen bonds. A relationship between molecular twist and higher solubility for aryl sulfonamides emerged from this study. Planar molecules pack more efficiently in the crystal lattice and hence are less soluble; molecules with a bent molecular conformation were

found to have higher solubility. Thus functional groups should be loaded on to the drug molecule so that there is opportunity for strong hydrogen bonding because crystal structures sustained by N–H···O bonds exhibited higher solubility. The CF₃ group is preferable in lead optimization because it offers the added benefit of increased solubility and a bent molecular conformation due to no possibility for intramolecular hydrogen bonding. Finally, multiple crystalline forms can often complicate drug formulation, and in this sense molecule **1** appears to be the best candidate in the series because despite its lower solubility there was no evidence of polymorphism. Given the importance and involvement of the AhR receptor in several biological processes, we expect that these structure–property trends will offer a rational strategy for the pharmaceutical development of cardiosulfa analogs as novel drugs.

2.6 Experimental Section

Synthesis. The starting materials for sulfonamide synthesis were purchased from Sigma-Aldrich (Hyderabad, India). Sulfonamides (**1-6**) were prepared by mixing 1.0 equiv of 3-amino-9-ethylcarbazole and 1.2 equiv of the appropriate benzenesulfonyl chloride in 20 mL of freshly distilled acetone under inert N₂ atmosphere in 100 mL round bottom flask. Pyridine (2 mL) was added drop wise and the reaction mixture was stirred overnight at RT. The product was washed with water and extracted with ethyl acetate. The product was purified by recrystallization from methanol.



Scheme 4 Synthesis of Cardiosulfa and its analogs.

Molecule 1: Yield 76 %. M.p. 171-173 °C. ^1H NMR (500 MHz, CDCl_3) δ 8.13 (s, 1 H), 8.03 (d, 1 H, $J = 7.5$ Hz), 7.87-7.92 (m, 2 H), 7.71 (d, 1 H, $J = 9$ Hz), 7.46 (m, 1 H), 7.41 (d, 1 H, $J = 8.5$ Hz), 7.24-7.31 (m, 4 H), 4.33 (q, 2H, $J = 7.5$ Hz), 1.42 (t, 3 H, $J = 7.5$ Hz). ^{13}C NMR (125 MHz, CDCl_3) δ 148.5, 140.5, 138.9, 136.1, 135.7, 135.4, 133.0, 129.1, 126.5, 125.8, 123.4, 123.0, 122.9, 122.3, 120.6, 119.3, 117.3, 109.0, 108.8, 37.2, 13.7.

Molecule 2: Yield 80%. M.p. 127-129 °C. ^1H NMR (500 MHz, CDCl_3) δ 8.09 (d, 1 H, $J = 7.5$ Hz), 7.68-7.85 (m, 3 H), 7.51 (d, 2 H, $J = 7.6$ Hz), 7.49 (m, 1 H), 7.41 (d, 1 H, $J = 10$ Hz), 7.15 (m, 2 H), 7.12 (m, 1 H), 6.98 (s, 1 H), 4.33 (q, 2 H, $J = 9$ Hz), 1.41 (t, 3 H, $J = 9.5$ Hz). ^{13}C NMR (125 MHz, CDCl_3) δ 142.6, 140.4, 138.6, 134.5, 134.2, 127.9, 126.4, 126.3, 126.0, 123.3, 122.3, 121.8, 120.6, 119.2, 117.2, 108.9, 108.7, 37.7, 13.8.

Molecule 3: Yield 76%. M.p. 181-182 °C. ^1H NMR (500 MHz, CDCl_3) δ 9.06 (s, 1 H), 7.78 (d, 2 H, $J = 7.5$ Hz), 7.40 (d, 2 H, $J = 8.5$ Hz), 7.31 (m, 1 H), 7.24 (m, 1 H), 7.18 (m, 1 H), 6.99 (m, 3 H), 4.0 (q, 2 H, $J = 7$ Hz), 1.15 (t, 3 H, $J = 7$ Hz). ^{13}C NMR (125 MHz, CDCl_3) δ 140.2, 138.5, 137.8, 132.3, 131.9, 131.6, 127.8, 127.6, 125.95, 123.9, 122.8, 122.2, 122.0, 121.7, 120.3, 118.7, 115.6, 108.6, 108.5, 30.7, 13.6.

Molecule 4: Yield 72%. M.p. 198-200 °C. ^1H NMR (500 MHz, CDCl_3) δ 7.71 (d, 1 H, $J = 7.5$ Hz), 7.64 (m, 2 H), 7.52 (m, 1 H), 7.49 (m, 1 H), 7.47 (m, 3 H), 7.36 (m, 1 H), 7.22 (m, 2 H), 4.31 (q, 2 H, $J = 9$ Hz), 1.41 (t, 3 H, $J = 9$ Hz). ^{13}C NMR (125 MHz, CDCl_3) δ 148.3, 140.4, 138.7, 133.6, 132.4, 132.4, 132.0, 126.5, 126.3, 125.1, 123.3, 123.1, 122.3, 120.6, 119.2, 117.2, 108.8, 108.7, 37.7, 13.8.

Molecule 5: Yield 56%. M.p. 170-172 °C. ^1H NMR (500 MHz, CDCl_3) δ 8.07 (d, 1 H, $J = 8.5$ Hz), 7.9 (d, 1 H, $J = 7.5$ Hz), 7.87 (d, 1H, $J = 7.5$ Hz), 7.83 (d, 1 H, $J = 2$ Hz), 7.72 (d, 1 H, $J = 8$ Hz), 7.46 (m, 2 H), 7.38 (d, 1 H, $J = 8$ Hz), 7.21 (m, 2 H), (dd, 1 H, $J = 8$ Hz, $J = 2$ Hz), 4.27 (q, 2 H, $J = 7$ Hz), 1.37 (t, 3 H, $J = 7$ Hz). ^{13}C

NMR (125 MHz, CDCl₃) δ 140.6, 140.4, 138.4, 131.5, 131.2, 130.6, 129.4, 129.0, 127.0, 126.2, 124.5, 124.4, 124.3, 123.3, 122.9, 122.4, 122.1, 120.6, 119.0, 117.0, 108.7, 108.6, 30.8, 13.6.

Molecule 6: Yield 40%. M.p. 190-192 °C. ¹H NMR (500 MHz, CDCl₃+DMSO-D₆) δ 9.30 (m, 1 H), 7.98 (d, 1 H, J = 7.5 Hz), 7.67 (m, 3 H), 7.30 (m, 5 H), 7.0 (m, 3 H), 4.19 (q, 2 H, J = 7.5 Hz), 1.28 (t, 3 H, J = 7 Hz). ¹³C NMR (125 MHz, CDCl₃+DMSO-D₆) δ 140.2, 139.8, 137.8, 132.2, 128.6, 127.1, 125.9, 122.9, 122.4, 122.3, 120.4, 118.7, 115.7, 108.6, 37.5, 13.7.

CSD Search. The CSD (version 5.33, May 2012; August 2012 update)¹¹ was searched using the following fragments SO₂NXH...C (105 hits) and SO₂NXH...Ph (25 hits) in the distance range 2.5-3.5 Å, all organic compounds with the word “form”, “polymorph”, “modification”, and “phase” in the qualifier, excluding the entries for which 3D coordinates are not available. These searches did not result in any polymorphic set for a single component organic sulphonamide having short contacts (N–H... π) in one crystal structure and catemer N–H...O hydrogen bond in another crystal structure.

X-ray Crystallography. X-ray reflections for molecule 1, 3 and form I of molecule 5 (LT data) were collected on a Bruker SMART APEX CCD diffractometer equipped with a graphite monochromator and Mo-K α fine-focus sealed tube (λ = 0.71073 Å). Data integration was done using SAINT.^{24a} Intensities for absorption were corrected using SADABS. Structure solution and refinement were carried out using Bruker SHELX-TL.^{24b} X-ray reflections for polymorphs of molecules 2, 4, 5 and 6 were collected on an Oxford Xcalibur Gemini Eos CCD diffractometer using Mo-K α , radiation. Data reduction was performed using CrysAlisPro (version 1.171.33.55). OLEX2-1.0 and SHELX-TL 97 were used to solve and refine the data.^{24c,d} All non-hydrogen atoms were refined anisotropically, and C–H hydrogens

were fixed. N–H was located from difference electron density maps and C–H hydrogens were fixed. N–H protons for molecule 1 and 2 were fixed by DFIX by 0.85 Å to remove some of the alerts. Packing diagrams were prepared in X-Seed. Crystallographic .cif files (CCDC Nos. 913656 – 913663) are available at www.ccdc.cam.ac.uk/data_request/cif or as part of the Supporting Information.

Vibrational Spectroscopy. Nicolet 6700 FT-IR spectrometer with an NXR FT-Raman module was used to record IR spectra. IR spectra were recorded on samples dispersed in KBr pellets.

¹³C ss-NMR Spectroscopy. Solid-state NMR spectra were recorded on a Bruker Advance spectrometer operating at 400 MHz (100 MHz for ¹³C nucleus). ss-NMR spectra were recorded on a Bruker 4 mm double resonance CP-MAS probe in zirconia rotors at 5.0 kHz spin rate with a cross-polarization contact time of 2.5 ms and a recycle delay of 8 s. ¹³C CP-MAS spectra recorded at 100 MHz were referenced to the methylene carbon of glycine and then the chemical shifts were recalculated to the TMS scale ($\delta_{\text{glycine}} = 43.3$ ppm).

Thermal Analysis. DSC was performed on Mettler Toledo DSC 822e module. Samples were placed in crimped but vented aluminum sample pans. The typical sample size was 3–4 mg, and the temperature range was 30–250°C at heating rate of 5 °C/min and 20 °C/min. Samples were purged by a stream of dry nitrogen flowing at 150 mL/min.

Dissolution and Solubility Measurements. Intrinsic dissolution rate (IDR) and solubility measurements were carried out on a USP certified Electrolab TDT-08 L dissolution tester (Electrolab, Mumbai, MH, India). A calibration curve was obtained for molecules **1–6** and polymorphs of molecule **4** by plotting absorbance vs. concentration UV-vis spectra curves on a Thermo Scientific Evolution EV300 UV-vis spectrometer (Waltham, MA) for known concentration solutions in 80% EtOH–

water medium. The mixed solvent system (EtOH-water) was selected for its higher solubility of cardiosulfa molecules in this medium. The slope of the plot from the standard curve gave the molar extinction coefficient (ϵ) by applying the Beer-Lambert's law. Equilibrium solubility was determined in 80% EtOH-water medium using the shake-flask method. To obtain equilibrium solubility, 100 mg of each solid material was stirred for 24 h in 5 mL of 80% EtOH-water at 37 °C, and the absorbance was measured at 237-238 nm. The concentration of the saturated solution was calculated at 24 h, which is referred to as the equilibrium solubility of the stable solid form. The dissolution rates are obtained from the IDR experiments.

Powder X-ray Diffraction. PXRDs were recorded on a SMART Bruker D8 Advance X-ray diffractometer (Bruker-AXS, Karlsruhe, Germany) in the Bragg-Brentano geometry using Cu-K α X-radiation ($\lambda = 1.5406 \text{ \AA}$) at 40 kV and 30 mA. Diffraction patterns were collected over the 2θ range of 5-50° at a scan rate of 1°/min. The appearance of polymorphs for all the molecules was monitored by the appearance of new diffraction peaks. Powder Cell 2.359^{24e} was used for overlaying the experimental XRPD pattern on the calculated lines from the crystal structure. Variable temperature mode fixed on the same instrument and recorded the phase transition with 600-1200 s delay time at a heating rate of 2 °C/min.

Ball Mill Grinding. Retsch-MM400 ball mill used for cryogenic milling of form II of molecule 5 in 10 min and frequency 20 Hz for the complete conversion to form I.

2.7 References

1. (a) S.-K. Ko, H. J. Jin, D.-W. Jung, X. Tian, I. Shin, *Angew. Chem. Int. Ed.* **2009**, *48*, 7809; (b) J. Abel, T. Haarmann-Stemmann, *Biol. Chem.* **2010**, *391*, 1235; (c) S.-K. Ko, I. Shin, *ChemBioChem* **2012**, *13*, 1483; (d) http://glxxxlabs.com/chemical-products/drugsdrug-candidates_p3/ cardiosulfa; (e) L. D'amico, C. Li, E. Glaze, M. Davis, W. L. Seng, *Zebrafish: A Predictive Model for Assessing Cancer Drug-Induced Organ Toxicity*, P. McGrath, Ed. John Wiley & Sons, **2011**; (f) J.-Y. Winum, A.

- Maresca, F. Carta, A. Scozzafava, C. T. Supuran, *Chem. Commun.* **2012**, 48, 8177.
2. (a) Jr. J. P. Whitlock, *Annu. Rev. Pharmacol. Toxicol.* **1999**, 39, 103; (b) M. A. Callero, A. I. Loaiza-Pérez, *Int. J. Breast Cancer*, **2011**, DOI:10.4061/2011/923250; (c) K. Stolpmann, J. Brinkmann, S. Salzmann, D. Genkinger, E. Fritsche, C. Hutzler, H. Wajant, A. Luch, F. Henkler, *Cell Death Dis.* **2012**, e388, DOI:10.1038/cddis.2012.127; (d) A. Koliopanos, J. Kleeff, Y. Xiao, S. Safe, A. Zimmermann, M. W. B. Chler, H. Friess, *Oncogene* **2002**, 21, 6059; (e) N. P. Singh, U. P. Singh, B. Singh, R. L. Price, M. N. Nagarkatti, P.S. Nagarkatti, *PLoSOne* **2011**, 6, e23522; (f) E. A. Stevens, J. D. Mezrich, C. A. Bradfield, *Immunology*, **2009**, 127, 299; (g) M. S Denison, A. Pandini, S. R. Nagy, E. P. Baldwin, L. Bonati, *Chem. Biol. Interact.* **2002**, 141, 3.
3. (a) I. Gardner, R. S. Obach, D. A. Smith, Z. Miao, A. A. Alex, K. Beaumont, A. Kalgutkar, D. Walker, D. Dalvie, C. Prakash, V. Alf, *Metabolism, Pharmacokinetics and Toxicity of Functional Groups: Impact of Chemical Building Blocks on ADMET*, Chapter 5, Ed. D. A. Smith, Royal Society of Chemistry, **2010**, pp. 210; (b) J. E. Lesch, *The First Miracle Drugs: How the Sulfa Drugs Transformed Medicine*, Oxford University Press, **2007**; (c) C. V. Zyp, *Pharm. Weekhl.*, **1938**, 75, 585; (d) A. Watanabe, *Naturwissenschaften*, **1941**, 29, 116; Watanabe and H. Kamis, *J. Pharm. Soc. Jap.*, **1942**, 62, 501; (e) M. Yakowitz, *J. Ass. Ofic. Agr. Chem.*, **1948**, 31, 656; (f) D. McLachlan, "X-ray Crystal Structure," McGraw-Hill, New York, **1957**, p. 138; (g) D. C. Grove and G. L. Keenan, *J. Amer. Chem. Soc.*, **1941**, 63, 97; (h) H. Miyazaki, *Jap. J. Pharm. Chem.*, **1947**, 19, 133; (i) G. Milosovich, *J. Pharm. Sci.*, **1964**, 53, 484; (j) S. S. Yang and J. K. Guillory, *J. Pharm. Sci.*, **1972**, 61, 26.
4. (a) C. P. Price, A. L. Grzesiak, A. J. Matzger, *J. Am. Chem. Soc.* **2005**, 127, 5512–5517; (b) D. J. W. Grant, *Theory and Origin of Polymorphism: Polymorphism in Pharmaceutical Solids*, Ed. H. G. Brittain, Marcel Dekker, **1999**, pp. 1; (c) S. R. Bryn, R. R. Pfeiffer, J. G. Stowell, *Solid-State Chemistry of Drugs*, SSCI, **1999**, pp. 160; (d) N. Blagden, R. J. Davey, H. F. Lieberman, L. Williams, R. Payne, R. Roberts, R. Rowe, R. Docherty, *J. Chem. Soc., Faraday Trans.*, **1998**, 94, 1035; (e) D. S. Hughes, M. B. Hursthouse, R. W. Lancaster, S. Tavener, T. L. Threlfall, *Chem. Commun.* **2001**, 603.
5. (a) J. Bernstein, *Polymorphism in Molecular Crystals*, Clarendon, **2002**; (b) R. Hilfiker, Ed. *Polymorphism in the Pharmaceutical Industry*, Wiley-VCH, **2006**; (c) F. T. Martins, P. P. Neves, J. Ellena, G. E. Cami, E. V. Brusau, G. E. Narda, *J. Pharm. Sci.* **2009**, 98, 2336; (d) J. Bauer, S. Spanton, R. Henry,

- J. Quick, W. Dziki, W. Porter, J. Morris, *Pharm. Res.* **2001**, *18*, 859; (e) S. R. Byrn, R. R. Pfeiffer, G. Stephenson, D. J. W. Grant, W. B. Gleason, *Chem. Mater.* **1994**, *6*, 1148; (f) J. D. Dunitz, *Acta Cryst.* **1995**, *B51*, 619; (g) F. Rodriguez-Caabeiro, A. Criado-Fornelio, A. Jimenez-Gonzalez, L. Guzman, A. Igual, A. Perez, M. Pujol, *Chemotherapy* **1987**, *33*, 266; (h) M.C. Gamberini, C. Baraldi, A. Tinti, C. Rustichelli, V. Ferioli, G. Gamberini *J. Mol. Struct.*, **2006**, 785, 216.
6. J. E. Torr, J. M. Large, E. McDonald *Comb. Chem. High Throughput Screening*, **2009**, *12*, 275.
7. (a) S. Roy, A. Nangia, *Cryst. Growth. Des.* **2007**, *7*, 2047; (b) F.-E. Shi, *Acta Cryst.* **2007**, *E63*, 4372; (c) H. V. R. Dias, S. Singh, *Dalton Trans*, **2006**, 1995; (d) S. Tsuzuki, K. Honda, T. Uchimar, M. Mikami, K. Tanabe, *J. Am. Chem. Soc.* **2000**, *122*, 11450; (e) L. S. Reddy, S. K. Chandran, S. George, N. J. Babu, A. Nangia, *Cryst. Growth. Des.* **2007**, *7*, 2675.
8. (a) F. T. Martins, M. D. Bocelli, R. Bonfilio, M. B. de Araújo, P. V. de Lima, P. P. Neves, M. P. Veloso, J. Ellena, and A. C. Doriguetto, *Cryst. Growth. Des.* **2009**, *9*, 3235; (b) N. J. Babu, S. Cherukuvada, R. Thakuria, A. Nangia, *Cryst. Growth. Des.* **2010**, *10*, 1979; (c) S. Tothadi, B. R. Bhogala, A. R. Gorantla, T. S. Thakur, R. K. Jetti, G. R. Desiraju, *Chem. Asian J.* **2012**, *7*, 2330; (d) N. K. Nath, S. Nilapwar, A. Nangia, *Cryst. Growth. Des.* **2012**, *12*, 1613.
9. (a) M. C. Etter, *Acc. Chem. Res.* **1990**, *23*, 120; (b) J. Bernstein, R. E. Davis, L. Shimon, N.-L. Chang, *Angew. Chem., Int. Ed. Engl.*, **1995**, *34*, 1555; (c) D. A. Adsmond, D. J. W. Grant, *J. Pharm. Sci.* **2001**, *90*, 2058; (d) J. D. Dunitz, J. Bernstein, *Acc. Chem. Res.*, **1995**, *28*, 193.
10. (a) L. Yu, *J. Phys. Chem. A* **2002**, *106*, 544; (b) S. Chen, H. Xi, L. Yu, *J. Am. Chem. Soc.* **2005**, *127*, 17439; (c) K. Johmoto, A. Sekine, H. Uekusa, Y. Ohashi, *Bull. Chem. Soc. Jpn.*, **2009**, *82*, 50; (d) L. N. Kuleshova, B. B. Averkiev, D. V. Gusev, K. Y. Suponitskiĭ, M. Y. Antipin, *Cryst. Reports*. **2004**, *49*, 798; (e) S. Matsumoto, Y. Uchida, M. Yanagita, *Chem. Lett.* **2006**, 35, 654.
11. Cambridge Structural Database, ver. 5.33, ConQuest 1.13, May 2012 release, Cambridge Crystallographic Data Center; <http://www.ccdc.cam.ac.uk>.
12. (a) J. Bernstein, J. D. Dunitz, A. Gavezzotti, *Cryst. Growth. Des.* **2008**, *8*, 2011; (b) S. Roy, P. M. Bhatt, A. Nangia, G. J. Kruger, *Cryst. Growth. Des.* **2007**, *7*, 476; (c) T. S. Thakur, R. Sathishkumar, A. G. Dikundwar, T. N. G.

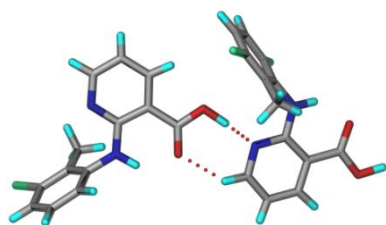
- Row, G. R. Desiraju, *Cryst. Growth. Des.* **2010**, *10*, 4246; (d) B. Rodríguez-Spong, C. P. Price, A. Jayasankar, A. J. Matzger, N. Rodríguez-Hornedo, *Adv. Drug Deliv. Rev.* **2004**, *56*, 241; (e) A. J. Florence, K. Shankland, T. Gelbrich, M. B. Hursthouse, N. Shankland, A. Johnston, P. Fernandes, C. K. Leech, *CrystEngComm* **2008**, *10*, 26.
13. (a) C. M. Reddy, M. T. Kirchner, R. C. Gundakaram, K. A. Padmanabhan, G. R. Desiraju, *Chem. Eur. J.* **2006**, *12*, 222; (b) D. Cinčić, T. Friščić, W. Jones, *Chem. Mater.* **2008**, *20*, 6623; (c) N. K. Nath, B. K. Saha, A. Nangia, *New J. Chem.* **2008**, *32*, 1693; (d) A. Kálmán, *Acta Cryst.* **2005**, *B61*, 536–547; (e) F. P. A. Fabbiani, B. Dittrich, A. J. Florence, T. Gelbrich, M. B. Hursthouse, W. F. Kuhs, N. Shankland, H. Sowa, *CrystEngComm* **2009**, *11*, 1396; (f) N. K. Nath, S. S. Kumar, A. Nangia, *Cryst. Growth. Des.* **2011**, *11*, 4594; (g) T. Gelbrich, T. L. Threlfall, M. B. Hursthouse, *CrystEngComm* **2012**, *14*, 5454.
14. (a) T. N. Drebuschak, V. A. Drebuschak, E. V. Boldyreva, *Acta Cryst.* **2011**, *B67*, 163; (b) T. N. Drebuschak, A. A. Ogienko, E. V. Boldyreva, *CrystEngComm*, **2011**, *13*, 4405; (c) J. B. Nanubolu, B. Sridhar, V. S. P. Babu, B. Jagadeesh, K. Ravikumar, *CrystEngComm*, **2012**, *14*, 4677.
15. (a) J. Bernstein, *Conformational Polymorphism in Organic Solid-State Chemistry*, G. R. Desiraju, Ed. Elsevier, **1987**, pp. 471; (b) A. Nangia, *Models, Mysteries and Magic of Molecules*, J. C. A. Boeyens, J.F. Ogilvie, Eds. Springer, **2008**, pp. 63.
16. (a) A. Nangia, *Acc. Chem. Res.*, **2008**, *41*, 595; (b) S. SeethaLekshmi, T. N. G. Row, *Cryst. Growth. Des.*, **2012**, *12*, 4283; (c) S. Aitipamula, P. S. Chow, R. B. H. Tan, *Cryst. Growth. Des.*, **2011**, *11*, 4101; (d) P. Sanphui, N. R. Goud, U. B. R. Khandavilli, S. Bhanoth, A. Nangia, *Chem. Commun.* **2011**, *47*, 5013; (e) R. J. Davey, N. Blagden, G. D. Potts, R. Docherty, *J. Am. Chem. Soc.*, **1997**, *119*, 1767; (f) L. Yu, S. M. Reutzel-Edens, C. A. Mitchell, *Org. Proc. Res. Dev.*, **2000**, *4*, 396.
17. (a) S. Terada, K. Katagiri, H. Masu, H. Danjo, Y. Sei, M. Kawahata, M. Tominaga, K. Yamaguchi, I. Azumaya *Cryst. Growth. Des.*, **2012**, *12*, 2908; (b) S. Murugavel, N. Manikandan, D. Kannan M. Bakthadoss, *Acta Cryst.* **2012**, *E68*, 1009; (c) P. Sanphui, B. Sarma, A. Nangia, *Cryst. Growth. Des.*, **2010**, *10*, 4550; (d) N. Nagel, H. Bock, P. Eller, *Acta Cryst.* **2000**, *B56*, 234; (e) S. Roy, A. J. Matzger, *Angew. Chem. Int. Ed.* **2009**, *48*, 8505; (f) B. R. Sreekanth, P. Vishweshwar, K. Vyas, *Chem. Commun.* **2007**, 2375.

18. (a) D. Das, D.; E. Engel, L. J. Barbour, *Chem. Commun.* **2010**, 46, 1676; (b) M.-L. Cao, H.-J. Mo, J.-J. Liang, B.-H. Ye, *CrystEngComm* **2009**, 11, 784; (c) S. Takahashi, H. Miura, H. Kasai, S. Okada, H. Oikawa, H. Nakanishi, *J. Am. Chem. Soc.* **2002**, 124, 10944; (d) Q. Chu, D. C. Swenson, L. R. MacGillivray, *Angew. Chem. Int. Ed.* **2005**, 44, 3569.
19. (a) N. Zencirci, T. Gelbrich, D. C. Apperley, R. K. Harris, V. Kahlenberg, U. J. Griesser, *Cryst. Growth. Des.* **2010**, 10, 302; (b) D. Mangin, F. Puel, S. Veessler, *S. Org. Proc. Res. Dev.* **2009**, 13, 1241; (c) J. Li, S. A. Bourne, M. R. Caira, *Chem. Commun.* **2011**, 47, 1530; (d) K. Fucke, N. Qureshi, D. S. Yufit, J. A. K. Howard, J. W. Steed, *Cryst. Growth. Des.* **2010**, 10, 880; (e) P. Sanphui, B. Sarma, A. Nangia, *J. Pharm. Sci.* **2011**, 100, 2287; (f) S. Cherukuvada, R. Thakuria, A. Nangia, *Cryst. Growth. Des.* **2010**, 10, 3931.
20. (a) J. Bernstein, J. D. Dunitz, A. Gavezzotti, *Cryst. Growth. Des.* **2008**, 8, 2011; (b) S. Roy, P. M. Bhatt, A. Nangia, G. J. Kruger, *Cryst. Growth. Des.* **2007**, 7, 476; (c) T. S. Thakur, R. Sathishkumar, A. G. Dikundwar, T. N. G. Row, G. R. Desiraju, *Cryst. Growth. Des.* **2010**, 10, 4246; (d) B. Rodríguez-Spong, C. P. Price, A. Jayasankar, A. J. Matzger, N. Rodríguez-Hornedo, *Adv. Drug Deliv. Rev.* **2004**, 56, 241; (e) A. J. Florence, K. Shankland, T. Gelbrich, M. B. Hursthouse, N. Shankland, A. Johnston, P. Fernandes, C. K. Leech, *CrystEngComm* **2008**, 10, 26.
21. (a) H. Wu, N. Reeves-McLaren, J. Pokorny, J. Yarwood, A. R. West, *Cryst. Growth. Des.* **2010**, 10, 3141; (b) D. Braga, F. Grepioni, L. Maini, M. Polito, *Struct. Bonding* **2009**, 132, 25; (c) M. Karjalainen, S. Airaksinen, J. Rantanen, J. Aaltonen, J. Yliruusi, *J. Pharm. Biomed. Anal.* **2005**, 39, 27; (d) E. V. Boldyreva, T. N. Drebuschak, T. P. Shakhtshneider, H. Sowa, H. Ahsbahs, S. V. Goryainov, S. N. Ivashevskaya, E. N. Kolesnik, V. A. Drebuschak, E.B. Burgina, *ARKIVOC* **2004**, 12, 128; (e) A. Burger, R. Ramberger, *Mikrochim. Acta II* (Vienna), **1979**, 273; (f) A. Trask, N. Shan, W. D. S. Motherwell, W. Jones, S. Feng, R. B. H. Tan, K. Carpenter, *Chem. Comm.* **2005**, 880.
22. (a) M. R. Yadav, A. R. Shaikh, V. Ganesan, R. Giridhar, R. Chadha, *J. Pharm. Sci.* **2008**, 97, 2637; (b) Y. Qiu, Y. Chen, L. Liu, G. G. Z. Zhang, *Developing Solid Oral Dosage Forms: Pharmaceutical Theory and Practice*, 1st Ed., Academic Press, **2009**, pp. 75; (c) M. McAllister, *Mol. Pharmaceutics* **2010**, 7, 1374–1387; (d) J. Halebian, W. McCrone, *J. Pharm. Sci.* **1969**, 58, 911.
23. (a) Y. Fujita, M. Yonehara, K. Kitahara, J. Shimokawa, Y. Hashimoto, M. Ishikawa, *Heterocycles* **2011**, 83, 2563–2575; (b) Y. Fujita, M. Yonehara, M.

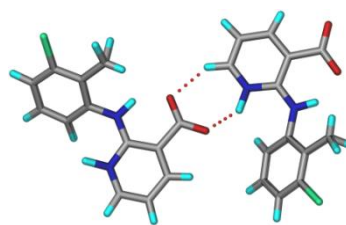
- Tetsuhashi, T. Noguchi-Yachide, Y. Hashimoto, M. Ishikawa, *Bioorg. Med. Chem.* **2010**, *18*, 1194; (c) M. Ishikawa, Y. Hashimoto, *J. Med. Chem.* **2011**, *54*, 1539; (d) J. Kasuga, M. Ishikawa, M. Yonehara, M. Makishima, Y. Hashimoto, H. Miyachi, *Bioorg. Med. Chem.* **2010**, *18*, 7164; (e) B. Kuhn, P. Mohr, M. Stahl, *J. Med. Chem.* **2010**, *53*, 2601; f) G. Lewin, A. Maciuk, A. Moncomble, J. P. Cornard, *Planta Medica* **2012**, *78*, 1080; (g) S. Purser, P. R. Moore, S. Swallow and V. Gouverneur *Chem. Soc. Rev.* **2008**, *37*, 320.
24. (a) *SAINT-Plus*, version 6.45, Bruker-AXS Inc., **2003**; (b) G. M. Sheldrick, *SADABS, Program for Empirical Absorption Correction of Area Detector Data*, University of Göttingen, Germany, **1997**; (c) *SMART* (Version 5.625) and *SHELX-TL* (Version 6.12), Bruker-AXS Inc., **2000**; (d) G. M. Sheldrick, *SHELXS-97* and *SHELXL-97*, University of Göttingen, Germany, **1997**; (e) Powder Cell, A program for structure visualization, powder pattern calculation and profile fitting, www.ccp14.ac.uk.

Chapter Three

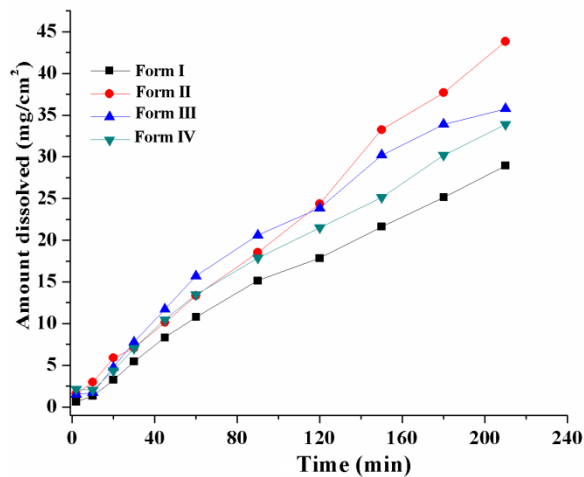
Structure-property Comparison of Neutral and Zwitterionic Polymorphs



Neutral polymorph (CLX-I)



Zwitterionic polymorph (CLX-II)



Solvent evaporation and melt solidification methods are used here and hence zwitterionic polymorphs were found to be more soluble and fast dissolving in aqueous medium compared to the neutral polymorphs.

3.1 Introduction

Polymorphism is a solid-state phenomenon exhibited by more than 33% of organic compounds and over half the pharmaceuticals. Polymorphs differ in their X-ray crystal structures, physicochemical properties such as stability, solubility, dissolution and bioavailability, as well as filterability, compaction, tableting, etc.¹ The differences in these properties arise due to the differences in crystal packing, molecular conformation, morphology, and stability of polymorphs.² For example, the conformational difference in the polymorphs of Ritonavir and Nimesulide causes differences in their solubility and dissolution rates.^{3a,b} Differences in crystal packing can induce different solubility and dissolution rates of polymorphs.^{3c-e} The solubility and dissolution rates of drug forms are related inversely with their stability, i.e. metastable polymorphs are more soluble whereas the thermodynamic form is the least soluble.⁴ The higher solubility of metastable polymorphs is due to their higher thermodynamic functions and free energy.^{2,3} In case of ampholytes, i.e. molecules with both acidic and basic groups in the same structure, they can exist in neutral, zwitterionic, or dual states. Amino acids are the simplest examples of ampholytes, but they exist in the zwitterionic form only in the crystal structure.⁵ We initiated a study of amphoteric model compounds and drugs to study neutral and zwitterionic solid-state forms, proton state of acidic/ basic groups in these structures, and the solubility and dissolution rate of such neutral/ zwitterions polymorph pairs.^{6,7} Over 40 drug molecules are amphoteric (see Table 1.1) with high/ moderate solubility and low permeability, and thus selection of the optimal crystalline form for solubility optimization⁸ is an end goal in such studies. A disadvantage with zwitterionic drug forms could be that their low permeability will affect druggability and bioavailability.⁹ However, because of facile proton transfer as a function of pH, some zwitterionic drugs are more permeable than their neutral structures.¹⁰

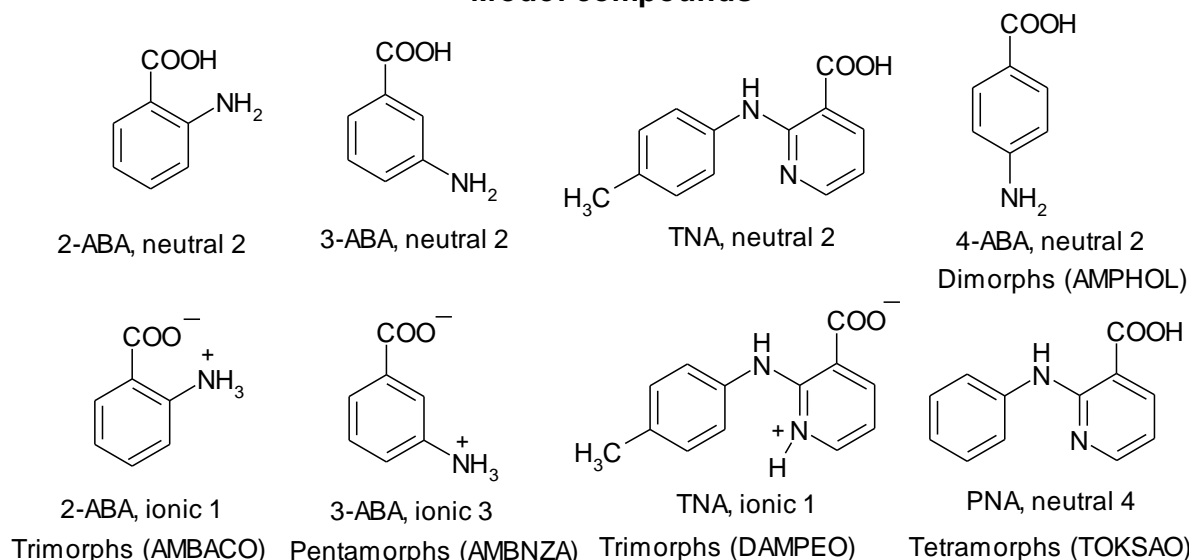
Table 3.1 List of marketed amphoteric drugs in the market

S. No	Amphoteric/zwitterionic drugs	S. No	Amphoteric/zwitterionic drugs
1	Acyclovir	21	Meloxicam
2	Ganciclovir	22	Isoxicam
3	Torsemide	23	Amdinocillin
4	5-Aminosalicylic acid/Mesalamine	24	Benazepril
5	4-Aminosalicylic acid	25	Ceftazidime
6	Clonixin	26	Cerivastatin
7	Ciprofloxacin	27	Cetirizine
8	Enoxacin	28	Chlortetracycline
9	Lomefloxacin	29	Daunorubicin
10	Gatifloxacin	30	Demeclocycline
11	Sparfloxacin	31	Doxycycline
12	Norfloxacin	32	Famotidine
13	Ofloxacin	33	Fexofenadine
14	Pefloxacin	34	Levocarnitine
15	Levofloxacin	35	Lisinopril
16	Trovafoxacin	36	Melphalan
17	Tenoxicam	37	Minocycline
18	Piroxicam	38	Tetracycline
19	Lornoxicam	39	Flunixin
20	Droxicam	40	Tianeptine

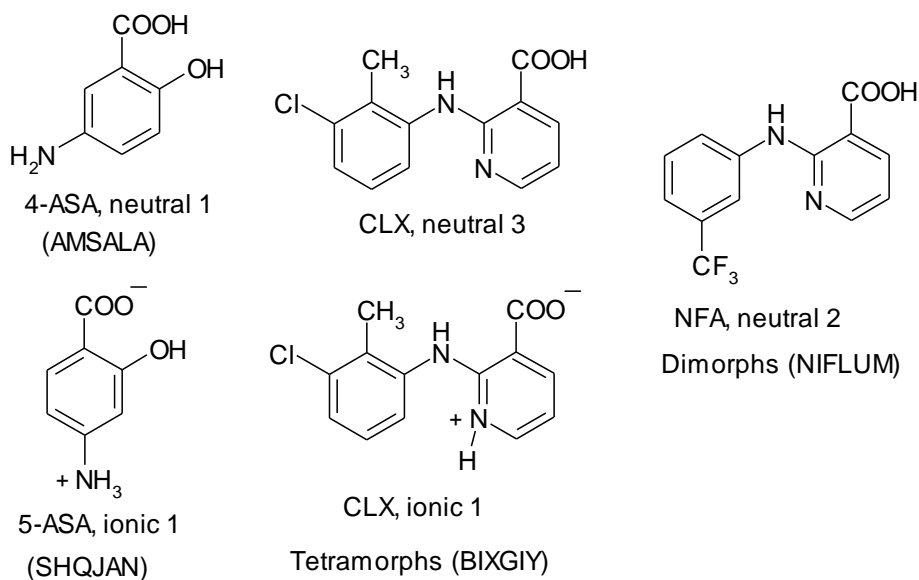
Based on the above idea and the importance of amino acids and diarylamines in medicine and solid-state chemistry, a few amphoteric molecules (Scheme 3.1) were selected and screened by several crystallization techniques to obtain neutral and/or zwitterionic crystal structures.^{7,11,12} The drugs include clonixin (CLX, anti-

inflammatory), 4-aminosalicylic acid (4-ASA, anti-tuberculosis), mesalazine (5-ASA, anti-inflammatory), along with 2-aminobenzoic acid (2-ABA) and 3-aminobenzoic acid (3-ABA) as model compounds, whose crystal structures were recently reported.^{6,7,12} The known polymorphs for these ampholytes are three neutral forms and one zwitterionic form of CLX, two neutral forms and one zwitterionic form for TNA, a neutral form for 4-ASA, a zwitterionic structure of 5-ASA, one zwitterionic-neutral and two neutral forms of 2-ABA, and three zwitterionic forms plus two neutral forms of 3-ABA (Scheme 3.1). We were successful in reproducing three of the reported cases to obtain one zwitterionic and another neutral polymorph for the same molecule (2-ABA, 3-ABA, TNA and CLX). These sets of neutral and zwitterionic polymorphs were characterized by FT-IR, Raman, solid-state ¹³C NMR, and powder X-ray diffraction. Thermal phase transitions between the neutral and zwitterionic polymorphs were studied by VT-PXRD and DSC.¹³ Attempts to crystallize a novel polymorph of 4-ASA and 5-ASA was not successful (both are available in single crystal structure drugs), so these isomeric drugs were used as such to compare solubility trends between neutral and zwitterionic isomeric compounds. The difference in solubility and dissolution rates of the neutral and zwitterionic polymorphs were correlated with their hydrogen bonding (O–H···O, O–H···N and N⁺–H···O[–]). The faster dissolution rates of the ionic forms were ascribed to stronger, attractive interactions between the solvent molecules and the zwitterionic functional groups. Even as there is no general strategy yet to crystallize ionic polymorphs of amphoteric molecules, the present study shows the advantages of zwitterionic forms for solubility enhancement.

Model compounds



Amphoteric drugs

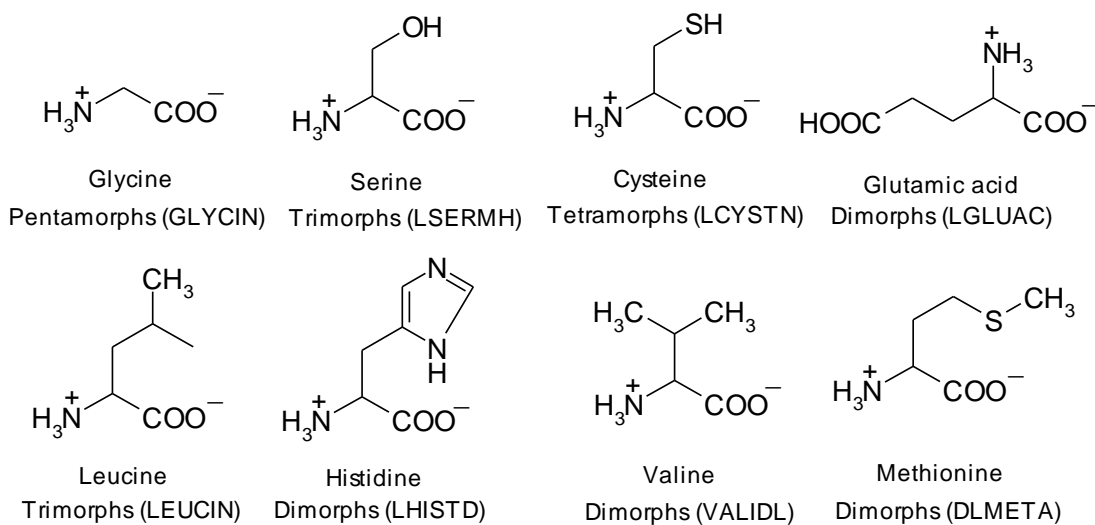


Scheme 3.1 Polymorphic neutral and zwitterionic crystal structures discussed in this study. 4-ASA and 5-ASA are monomorphic but isomeric structures. The X-ray crystal structures are reported in refs. 6a,b,e, 7a,d,e, and 12a,e. The number of reported polymorphs is mentioned in parenthesis below the compound for each type.

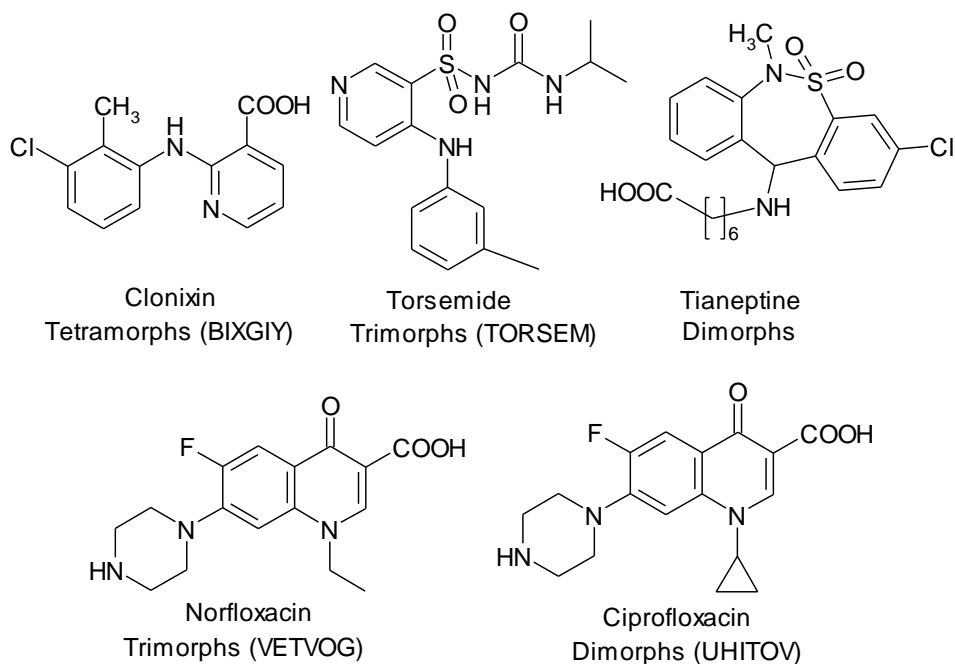
3.2 Results and Discussion

3.2.1 Neutral and zwitterionic polymorphs

Polymorphism in amino acids is common but the existence of both neutral and zwitterionic forms has so far not been observed in the crystal structures of these biomolecules. Glycine, leucine, serine, histidine, cysteine, and glutamic acid are enantiomerically pure crystalline zwitterionic polymorphs (Scheme 3.2), and valine, serine, cysteine, and methionine are racemic crystalline polymorphs known among the 20 proteinogenic amino acids. Among the amphoteric drugs, a few examples were extracted as neutral and zwitterionic crystal structure sets from the Cambridge Structural Database (CSD ver. 5.34, May 2013 update). Notably Clonixin, Ciprofloxacin, Norfloxacin, Torsemide and Tianeptine (Scheme 3.3) are examples of neutral and zwitterionic drug polymorphs.⁶ Moreover, three of the model organic compounds studied in recent papers,^{6,7} namely 2-aminobenzoic acid, 3-aminobenzoic acid, and 2-(p-tolylamino)nicotinic acid fall in the category of zwitterionic/ neutral polymorph pairs (Scheme 3.1). The intramolecular proton transfer in these molecular crystals suggested the possibility to control solubility and stability based on proton-transfer mediated polymorphism.⁶ Given the small number of marketed drugs in this category, we expanded the case studies to model compounds as well. 2-(p-Tolylamino)nicotinic acid was reported recently by us^{6a} and anthranilic acids by Harris et al.^{6b} A recent study suggests that crystallization of the zwitterionic polymorph of Tianeptine was controlled by pH.^{6c} We crystallized ampholyte compounds under different crystallization conditions to obtain neutral and ionic polymorphs for studying their physicochemical properties. We were unable to develop a general protocol for the controlled crystallization of neutral or ionic polymorph.



Scheme 3.2 Zwitterionic polymorphs of eight amino acids in the CSD (May 2013 update).



Scheme 3.3 Neutral and zwitterionic polymorphs of five drugs in the CSD (May 2013 update).

3.2.2 Crystallization and structural analysis of ampholytes

2-Aminobenzoic acid (2-ABA) polymorphs: The trimorphs of 2-ABA were reproduced by solvent crystallization and melting/heating techniques.^{7a} Form I was crystallized from methanol or ethanol. Form II was produced in polar solvents such as EtOAc, i-PrOH and nitromethane. Form III was obtained by melt crystallization at 135 °C for 30 min. The bulk purity of all three polymorphs was checked by powder XRD and DSC. The crystalline forms of 2-ABA have been reported by different groups.⁷ Hardy et al.^{7a} studied luminescent behavior of three polymorphs collectively and identified the ionic Form I as triboluminescent whereas the two neutral forms were non-triboluminescent based on their polarity. Ojala and Etter^{7b} reexamined all three polymorphs in terms of phase transition and reported the single-crystal to single-crystal transformation of form II to I. Carter and Ward^{7c} demonstrated the importance of surface functionality on polymorph selectivity and growth orientation in anthranilic acid polymorphs. Neutral O–H···N and ionic N⁺–H···O[−] hydrogen bonds stabilize the solid-state structures (Figure 3.1; the cif files were extracted from the CSD; Refcodes AMBACO01, AMBACO05 and AMBACO08).¹⁴ Form I (Z'=2) and II (Z'=1) are reported as orthorhombic structures in *P2₁cn* and *Pbca* space groups (a=12.868, b=10.772, c=9.325 Å; and a=15.992, b=11.624 c=7.160 Å) whereas the third form (Z'=1) is in *P2₁/c* space group (a=6.537, b=15.351, c=7.086 Å; β=112.64°). Form I has one neutral and one zwitterionic molecule in the asymmetric unit. Form I contains neutral (N–H···O) and ionic (N⁺–H···O[−] and N⁺–H···N) H bonds in the R₆⁴(12) ring motif whereas form II and form III contain centrosymmetric carboxylic acid O–H···O dimer synthon of R₂²(8) notation in the crystal structure¹⁵ (Figure 3.1).

The contribution of intermolecular interactions was quantified by Hirshfeld surface analysis¹⁶ and 2D fingerprint plots to differentiate the two distinct asymmetric unit molecules (A and B) of form I compared to those in form II and III (Figure 3.2). The sharp spikes in the 2D fingerprint plot of form I, II and III at $d_e = d_i \approx 1.0$ Å indicates short $\text{N-H}\cdots\text{O}/\text{N}^+-\text{H}\cdots\text{O}^-$ interactions. The sharp spikes for form IA, II and III at $d_e = d_i \approx 1.6$ and 2.2 Å indicates the presence of $\text{N}^+-\text{H}\cdots\text{N}$ interactions in the neutral structures of form IA, II and III. The absence of sharp spikes for $\text{N-H}\cdots\text{N}$ interactions in form IB is a clear indication of protonated amine which does not accept hydrogen bonds.

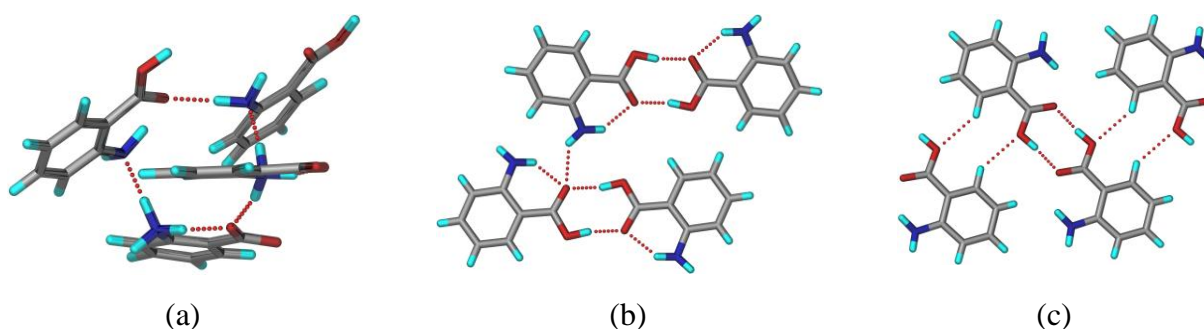
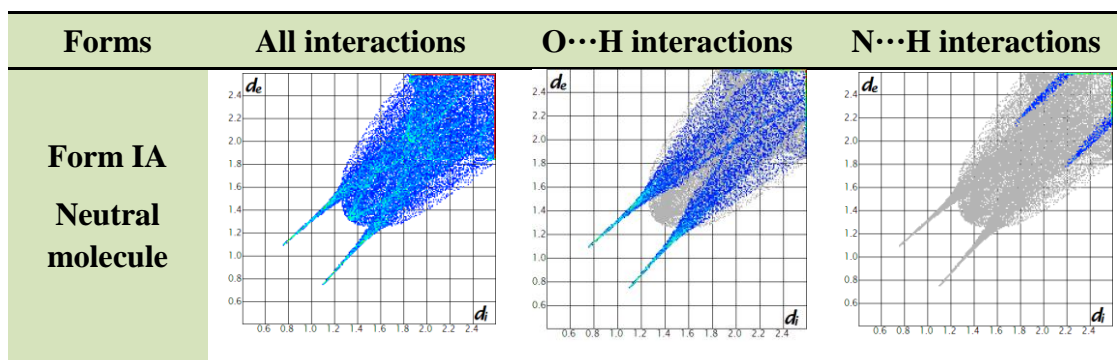


Figure 3.1 2-Aminobenzoic acid polymorphs. Neutral ($\text{N-H}\cdots\text{O}$) and ionic ($\text{N}^+-\text{H}\cdots\text{O}^-$ and $\text{N}^+-\text{H}\cdots\text{N}$) hydrogen bonds in form I having $\text{R}_6^4(12)$ motif (a), and $\text{O-H}\cdots\text{O}$ carboxylic acid dimer synthon of $\text{R}_2^2(8)$ notation in form II (b) and form III (c).



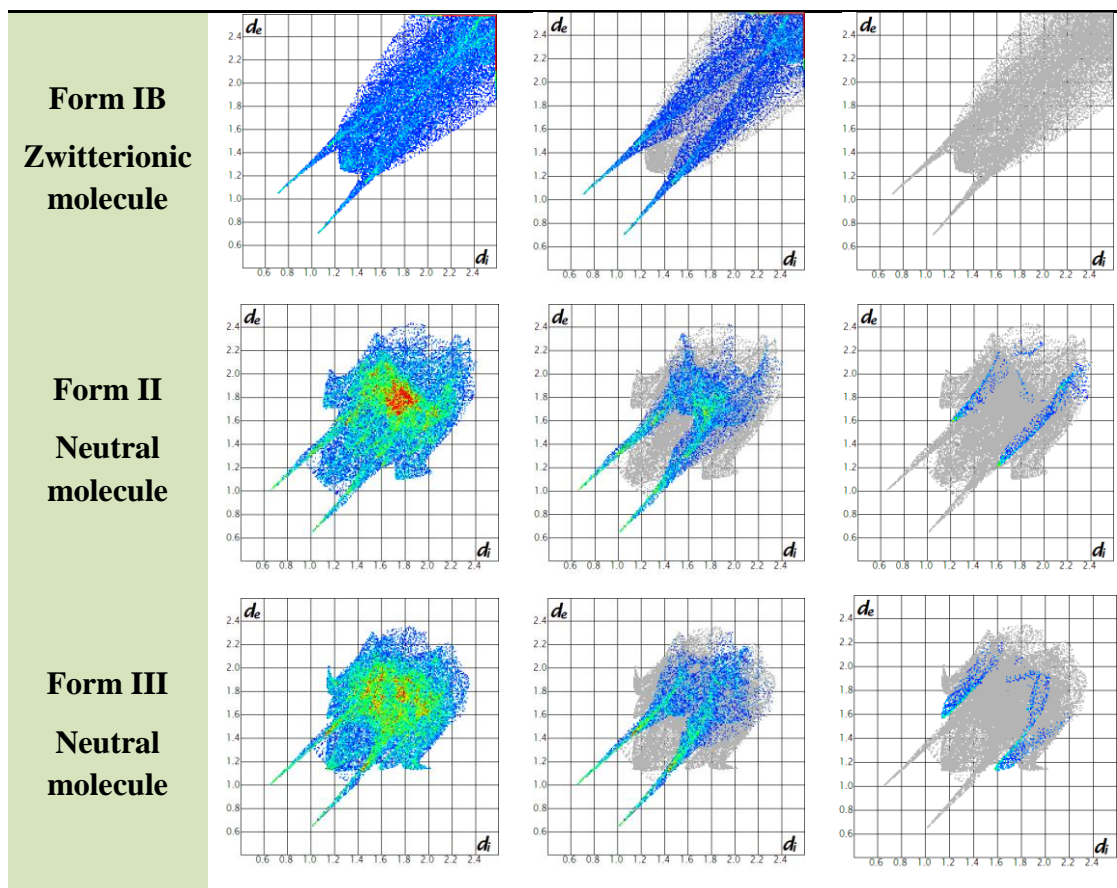


Figure 3.2 Hirshfeld 2D fingerprint plot for differentiating neutral N–H···O interactions from the ionic $\text{N}^+\text{--H}\cdots\text{O}^-$ and $\text{N}^+\text{--H}\cdots\text{N}$ interactions for 2-ABA trimorphs.

3-Aminobenzoic acid (3-ABA) polymorphs: The three polymorphs were reproduced by crystallization through solvent evaporation and melting. We are unable to reproduce polymorphs I and V by the reported method of solvent evaporation from methanol and melting of form III, respectively.^{6b} Form II was produced by melt crystallization at 170 °C for 30 min and form III was crystallized in acetonitrile solvent while form IV was crystallized using EtOAc solvent in our hands. The bulk purity of the polymorphs was checked by PXRD and DSC. Harris et al.^{6b} reported recently the crystal structures of three new polymorphs, form III (AMBNZA01), form IV (AMBNZA02), and form V (AMBNZA03), determined by

powder XRD data structure solution. They compared the crystal structures and thermal stability of these new polymorphs with the reported polymorph I (no crystal structure in CSD) and II (AMBNZA). Form II ($Z'=2$, $P2_1/c$, $a=5.047$, $b=23.06$, $c=11.790$ Å, $\beta=105.47^\circ$) and V ($Z'=1$, $P2_1/a$, $a=14.787$, $b=4.956$, $c=9.081$ Å, $\beta=95.21^\circ$), respectively. Form III ($Z'=1$, $P2_1/a$, $a=21.339$, $b=7.296$, $c=3.777$, $\beta=94.82^\circ$), and IV ($Z'=2$, $P\bar{1}$, $a=3.800$, $b=11.55$, $c=14.633$ Å, $\alpha=110.50^\circ$, $\beta=92.74^\circ$, $\gamma=96.59^\circ$) were crystallized as zwitterionic forms. Two molecules in the asymmetric unit of neutral form II interact through O–H \cdots O acid dimer of $R_2^2(8)$ ring motif (Figure 3.3). The zwitterionic molecules in form III contains ionic N $^+$ –H \cdots O $^-$ H bonds in a $R_4^4(8)$ ring motif. Two independent molecules of zwitterionic form IV are forming a linear $C(7)$ chain through ionic N $^+$ –H \cdots O $^-$ interactions. The crystal structure of form I is not disclosed so far and form V crystal structure is excluded from this discussion due to disorder. The wings expected at $d_e = d_i \approx 1.6$ and 2.4 Å for N–H \cdots N interactions are absent in the Hirshfeld 2D fingerprint plots (Figure 3.4) for 3-ABA zwitterionic polymorphs, which means the absence of zwitterionic interactions in form III and IV due to a protonated amine/iminium ion.

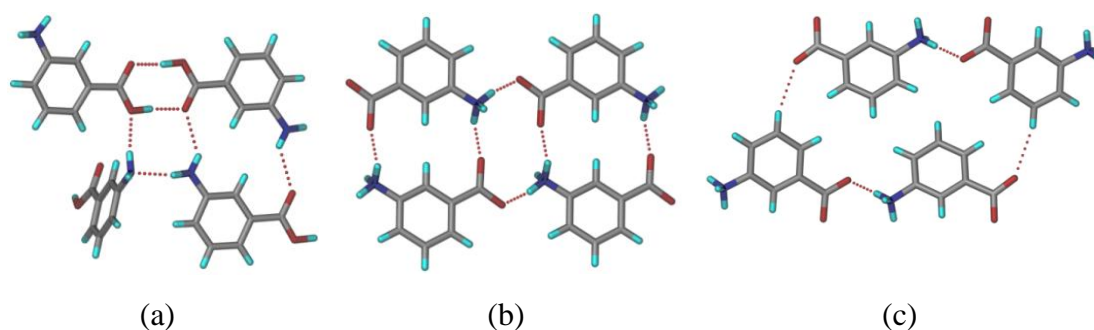
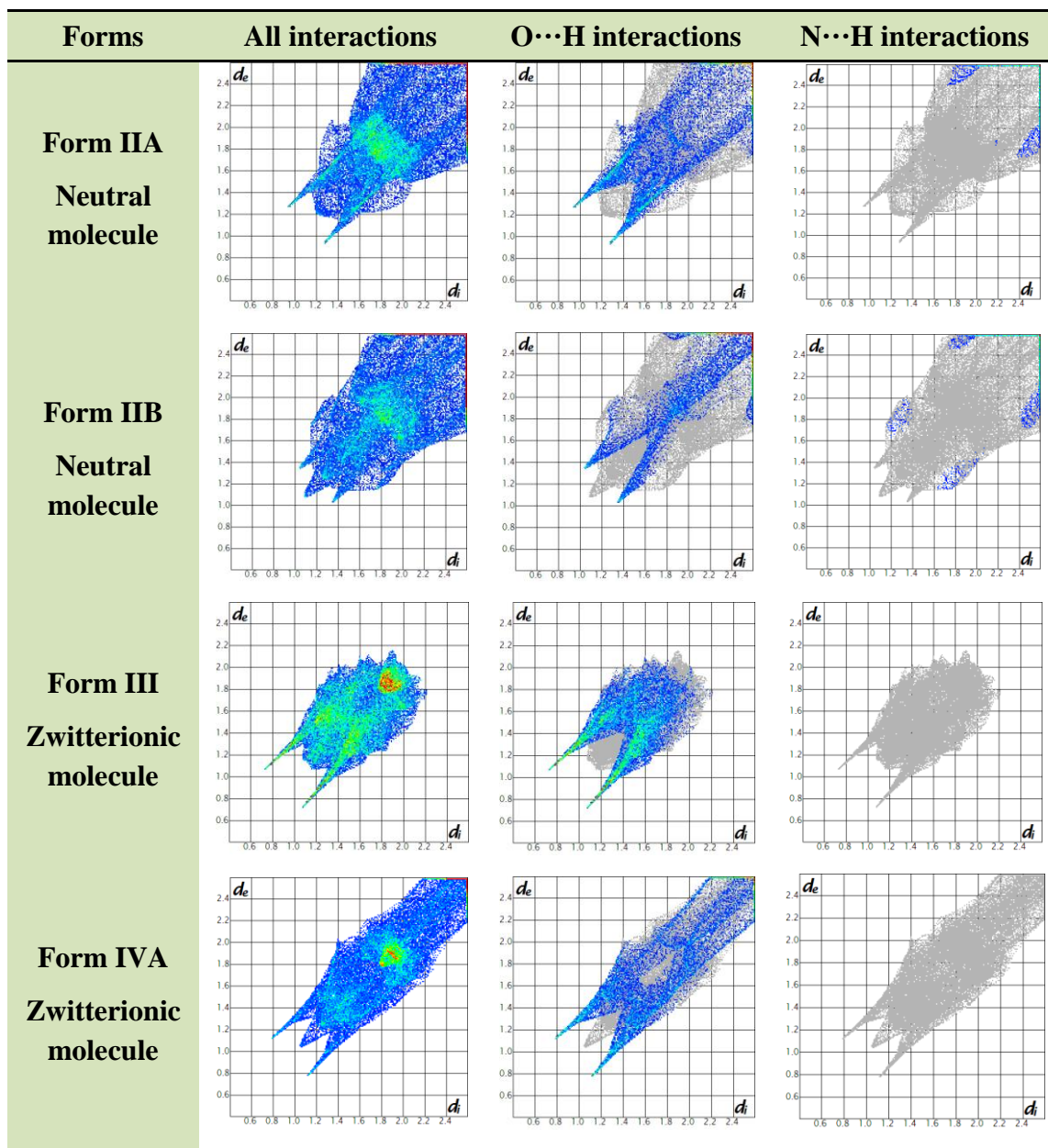


Figure 3.3 3-Aminobenzoic acid polymorphs. Acid dimer O–H \cdots O synthon $R_2^2(8)$ motif, neutral N–H \cdots O bonds in form II (a), and ionic N $^+$ –H \cdots O $^-$ in form III (b) and form IV (c).



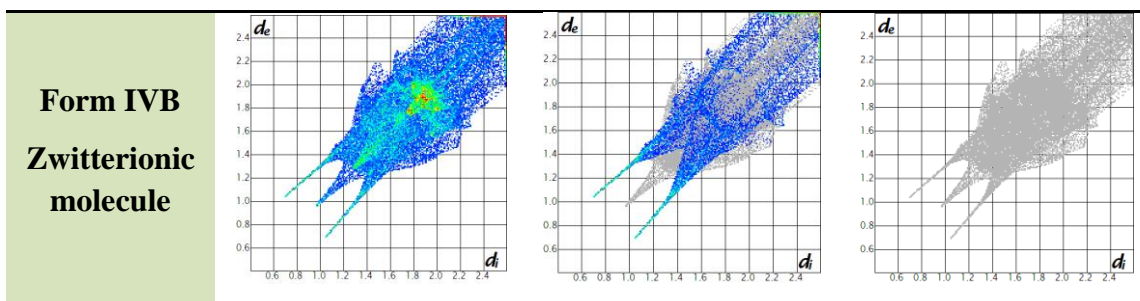


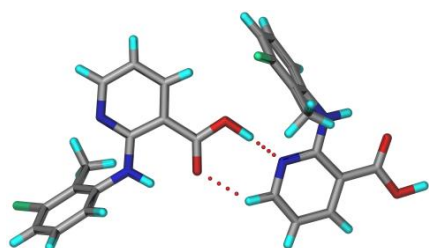
Figure 3.4 Hirshfeld 2D fingerprint plot for differentiating the O–H···O and N⁺–H···O[–] H bonds in neutral and ionic structure of 3-ABA trimorphs.

Clonixin (CLX) polymorphs: Clonixin polymorphs^{6e} are reported in the literature. We recently synthesized this compound and crystallized it from different organic solvents.^{6a} The reproducibility of crystallization on a bulk scale for solubility measurements posed challenges under the reported conditions of single crystal growth. After some experimentation, we crystallized Form I from acetone, EtOAc and nitromethane; form II from acetic acid; and the other two neutral forms were produced in toluene and MeOAc, respectively. The purity and stability of these polymorphs was monitored by PXRD and DSC. Form I neutral structure contains strong acid–pyridine synthon (O–H···N) whereas form II ionic structure contains acid–pyridine ionic N⁺–H···O[–] H bond in the crystal structure (Figure 3.5). The Hirshfeld 2D finger plot for form I and II are different for these neutral and ionic polymorphs (Figure 3.6). The sharp spike at $d_e = d_i \approx 1.0 \text{ \AA}$ is for N···H contribution in form I but this spike is absent in form II fingerprint plot. The third and fourth neutral forms of clonixin have the centrosymmetric O–H···O carboxylic acid dimer synthon. The reported unit cell values of these tetramorphs are listed in Table 3.2.

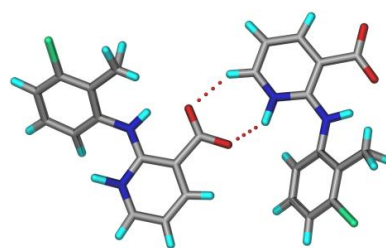
Table 3.2 Crystallographic parameters reported in the CSD for clonixin polymorphs.

2-(2-Methyl-3-chloroanilino)-nicotinic acid	Form I	Form II	Form III	Form IV
CSD Refcode ¹⁴	BIXGIY	BIXGIY04	BIXGIY02	BIXGIY03

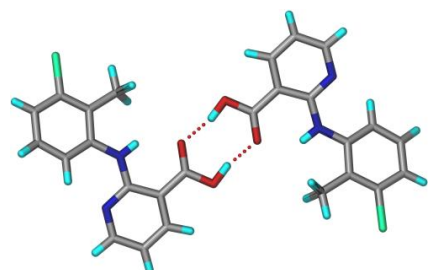
Formula Weight	C ₁₃ H ₁₁ Cl N ₂ O ₂	C ₁₃ H ₁₁ ClN ₂ O ₂	C ₁₃ H ₁₁ Cl N ₂ O ₂	C ₁₃ H ₁₁ Cl N ₂ O ₂
Crystal system	Monoclinic	Orthorhombic	Triclinic	Triclinic
Space group	<i>P</i> 2 ₁ / <i>c</i>	<i>Pca</i> 2 ₁	<i>P</i> $\bar{1}$	<i>P</i> $\bar{1}$
<i>a</i> (Å)	7.625(1)	23.597(6)	13.810(1)	7.670(1)
<i>b</i> (Å)	14.201(1)	4.042(1)	3.858(1)	7.254(1)
<i>c</i> (Å)	11.672(1)	12.127(3)	10.984(2)	10.882(1)
α (°)	90	90	94.98(1)	100.66(1)
β (°)	101.65(1)	90	94.42(1)	102.02(1)
γ (°)	90	90	95.57(1)	86.97(1)
<i>V</i> (Å ³)	1237.8	1156.6	578.1	581.8
<i>D</i> _{calcd} (g cm ⁻³)	1.41	1.51	1.51	1.50
<i>Z</i> / <i>Z'</i>	4/1	4/1	2/1	2/1
<i>wR</i> ₂ (all)	5.2	6.5	7	4.8
<i>T</i> (K)	298	298	298	298



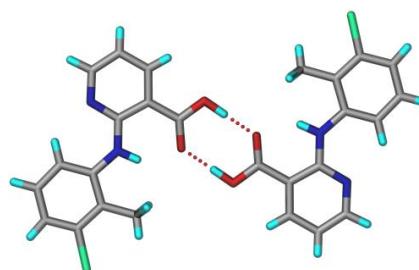
(a)



(b)



(c)



(d)

Figure 3.5 Clonixin polymorphs. Strong acid–pyridine O–H···N synthon in form I (a), acid–pyridine ionic N⁺–H···O[−]H bond in form II (b), and acid dimer O–H···O R₂²(8) motif in form III (c) and form IV (d).

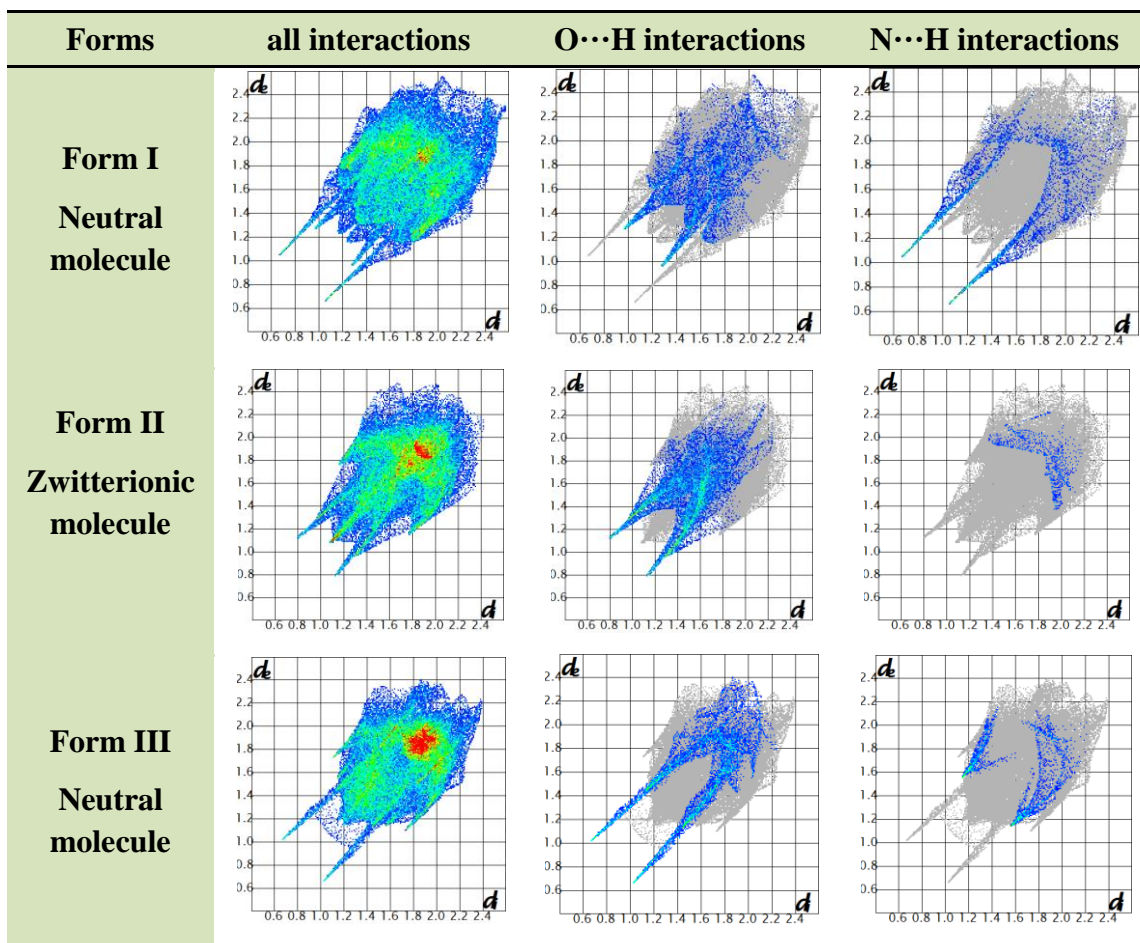


Figure 3.6 Hirshfeld 2D fingerprint plots for differentiating the neutral acid–pyridine O–H···N hydrogen bond from the ionic N⁺–H···O[−] and O–H···O in clonixin polymorphs. Form IV is not included because H atoms could not be located in the crystal structure.

3.2.3 Molecular conformations of Clonixin: The molecular conformation is different in neutral and zwitterionic polymorphs of clonixin at the flexible C2–N2–C6–C7 bonds. This fluxional change in clonixin molecule results in conformational polymorphs¹⁷ (see Table 3.3 for torsion angles and overlay diagram in Figure 3.7) along with the synthon changing from carboxylic acid dimer to acid–pyridine in four

polymorphs. The influence of molecular conformation on drug solubility and dissolution rate were discussed in a recent paper: in general, twisted conformation gave a more soluble crystalline form compared to the planar state.¹⁸ The twisted and planar conformations of clonixin polymorphs could tune drug solubility.

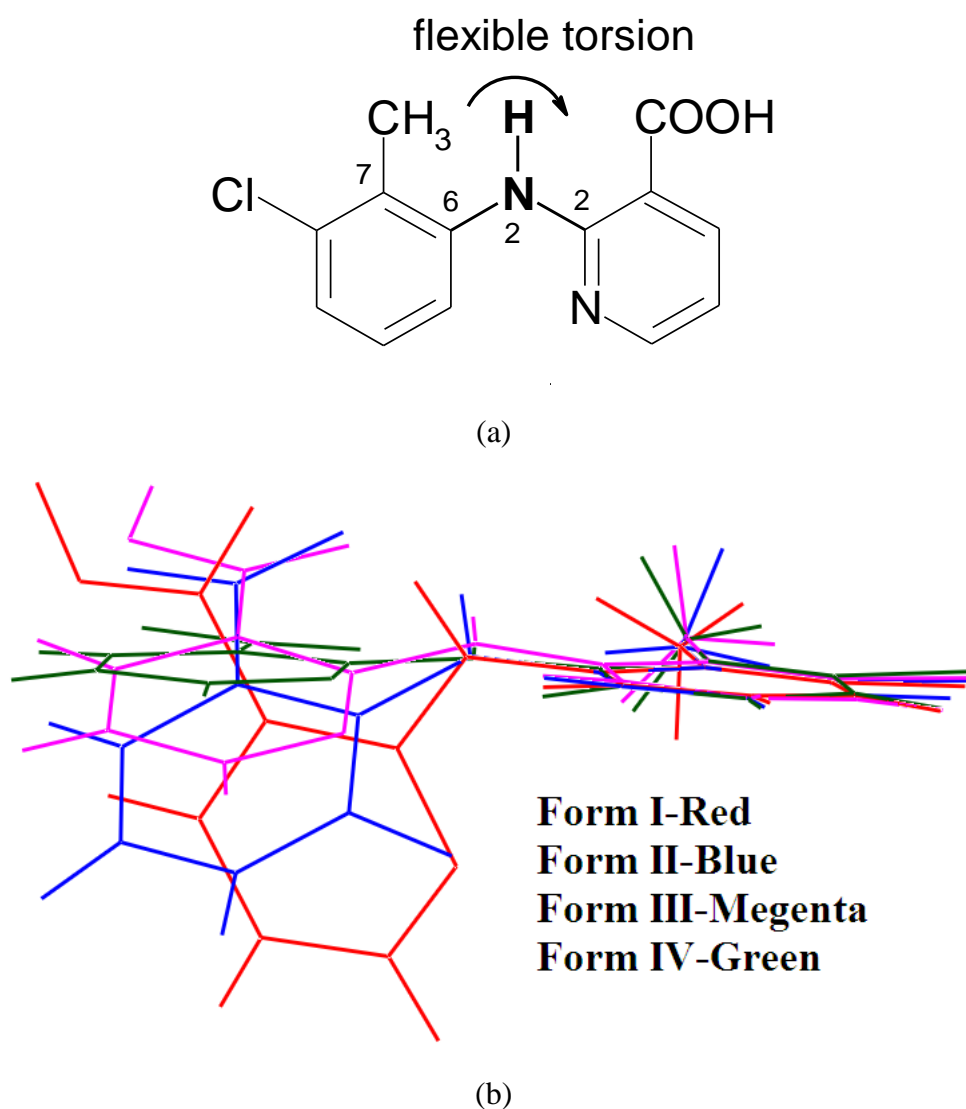


Figure 3.7 (a) Torsional flexibility in clonixin tetramorphs, and (b) the overlay of different molecular conformations in CLX tetramorphs.

Table 3.3 Torsion angles for molecular conformations of clonixin tetramorphs.

Clonixin polymorph	Torsion angle C2-N2-C6-C7 (°)
Form I	71.27
Form II	140.26
Form III	160.24
Form IV	178.81

Aminosalicylic acid isomers: 4-Aminosalicylic acid (4-ASA) was crystallized in several organic solvents to obtain a new zwitterionic polymorph under ambient and freeze evaporation conditions. However only the known neutral form was crystallized in all experiments.¹² 5-Aminosalicylic acid (5-ASA) has limited solubility in organic solvents. It is freely soluble in water and tends to degrade under ambient conditions. The color change of the solution indicated degradation to 3-aminophenol upon heating/boiling the solution to dissolve more of the compound for crystallization.¹² Carboxylic acid dimer O–H···O synthon of $R_2^2(8)$ ring motif with N–H···O interaction in 4-ASA structure are different from the ionic $N^+–H···O^-$ interactions of $R_4^4(12)$ ring motif^{15b} in 5-ASA structure (Figure 3.8). The Hirshfeld surface 2D fingerprint plot shows the difference between the crystal structures of the neutral and ionic isomers (Figure 3.9).

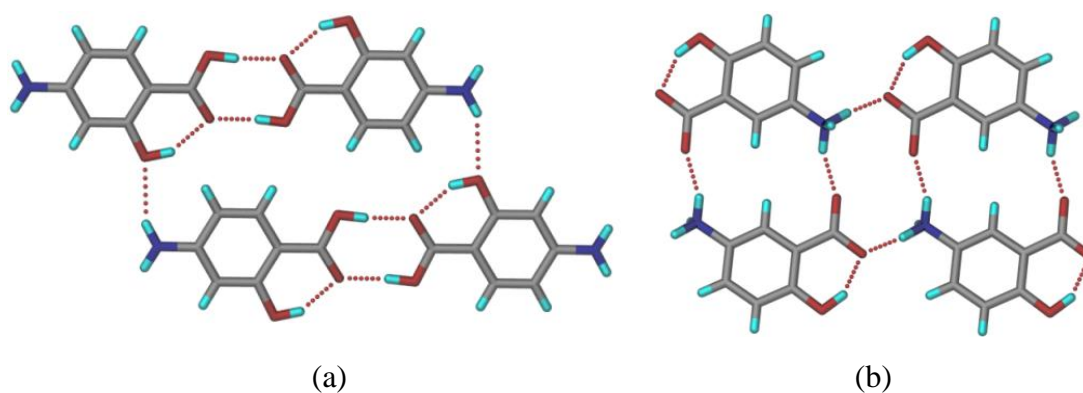


Figure 3.8 Carboxylic acid dimer O–H···O synthon of $R_2^2(8)$ ring motif and neutral N–H···O interactions in 4-ASA (a) are replaced by ionic $N^+–H···O^-$ interactions in $R_4^4(12)$ ring motif for 5-ASA (b).

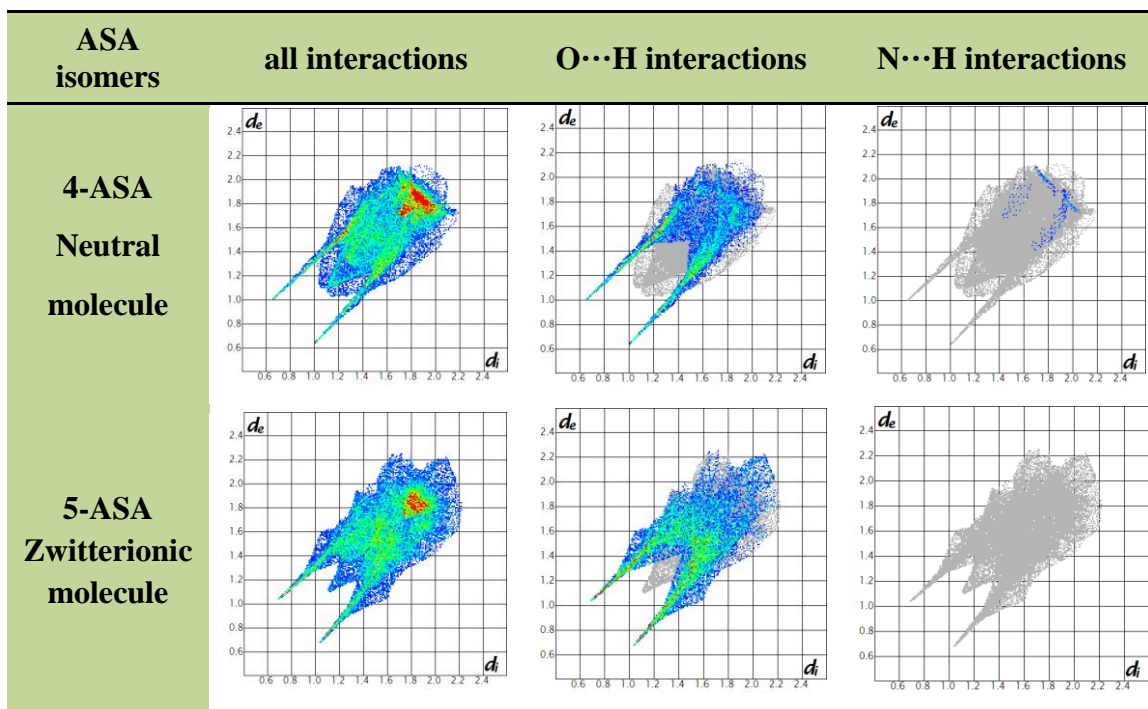


Figure 3.9 Hirshfeld surface 2D fingerprint plots show unionized N···H interactions in 4-ASA (a) the absence of ionized N···H interactions in 5-ASA (b).

2-(*p*-Tolylamino)nicotinic acid (TNA): TNA was synthesized and crystallized in different organic solvents to obtain three polymorphs.^{6a} The neutral forms were reproducible using normal solvent crystallization techniques and melting methods. TNA-I and TNA-II mostly crystallized concomitantly from acetone, methanol, ethanol, ethyl acetate, acetonitrile, chloroform and THF. TNA-II was obtained exclusively by melt crystallization. Zwitterionic form TNA-III was obtained when TNA was cocrystallized with 2-bromo-3-hydroxy pyridine, 2-amino pyridine, isonicotinic acid and nicotinic acid in CH_3CN solvent. The neutral and zwitterionic polymorphs were compared with their hydrogen bonding (O–H···O, O–H···N and $N^+–H···O^-$) in figure in Figure 3.10 and correlated with 2D finger print plot to quantify the neutral and ionic interactions in the crystal structures. Indeed, the

zwitterionic form, which crystallized previously only in the presence of pyridine coformers and the separation of zwitterionic form as bulk material was difficult from the mixture of coformers and concomitant polymorphs.¹³ Thus comparison of solubility for neutral vs. ionic polymorphs could not be conducted for lack of pure polymorphic material. Form I and II contain the acid–pyridine synthon whereas form III has ionic H bonds.^{6a}

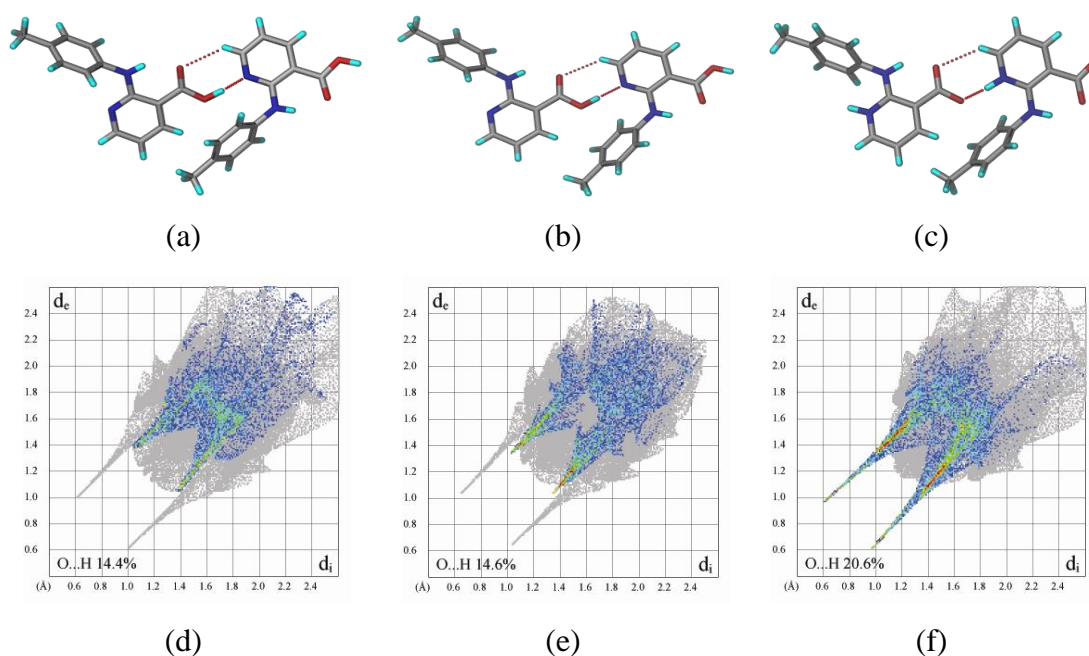


Figure 3.10 2D fingerprint plots for Hirshfeld surface show clear differences of O...H interactions of neutral polymorphs TNA-I (a), TNA-II (b) and zwitterionic form TNA-III (c).

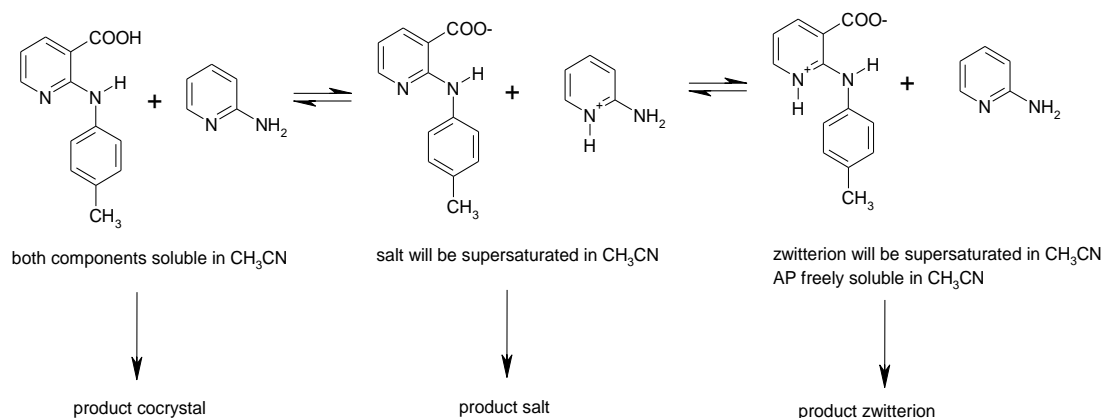
Other amphoteric compounds chosen for this polymorphic study comparison are 2-phenylaminonicotinic acid (PNA), 2-(*o*-tolylamino)nicotinic acid (*o*-TNA), 4-aminobenzoic acid (PABA). But we were unsuccessful in obtaining neutral and zwitterionic crystal structures for these compounds. Our studies continued with the structurally similar niflumic acid. Attempts to crystallize neutral and zwitterionic forms of niflumic acid by solvent evaporation and heating techniques gave the neutral form of niflumic acid only. A new form II recently identified by PXRD^{7g}

appears to be very close to the known neutral form I by IR spectroscopy, and hence it is unlikely to be a zwitterionic structure.

3.3 ΔpK_a calculation for ampholytes

The crystallization of TNA-III in presence of pyridine type coformer is the first instance of a zwitterionic polymorph being crystallized in the presence of a basic coformer as an additive. There are many reports for additive induced polymorph generation but a general protocol for this phenomenon is still unknown. In our previous work, the crystallization of a salt structure with 2-aminopyridine wherein the TNA molecule exists as a carboxylate anion and the AP is a pyridinium cation gave answer. If the pK_a of pyridine base is closely related then the Py moiety is present in TNA or AP, suggests that there could be a dynamic equilibrium between several species in solution (Scheme 3.4), a few neutral ones and others ionic. Nangia has concluded that depending on the solvent of co-crystallization, temperature, coformer additive, supersaturation, etc, the concentration of the neutral adduct, salt and zwitterion will vary depending on the solubility of that species as part of the equilibrium in the crystallization medium. Since the species that is most supersaturated in a given solvent will precipitate first, the product of such a co-crystallization experiment will strongly depend upon the supersaturation conditions, and consequently on the crystallization parameters such as solvent, temperature, concentration, rate of cooling, etc. Could a general recipe to obtain the zwitterionic polymorph of acid–base compounds be to use coformers whose acidic/basic functional groups are of similar pK_a to the molecule? Those solvents in which the ionic form is likely to supersaturate will be preferred. The crystallization of zwitterionic polymorphs for acid–base drugs will have an immediate application for solubility improvement. We carried out some of the experiments with CLX, 2-ABA, 3-ABA etc to control the desired zwitterionic polymorph under different pH conditions using different acid and base coformers. However, we couldn't come with

any general protocol for this polymorphs and anyway the experiments are currently under way to establish a general protocol for those amphoteric drugs. We expect this experimental design parameters will best operate in the grey zone of pK_a between 0 and 3 for all ampholytes. When $\Delta pK_a < 0$ or > 3 , the outcome can be predictable.



Scheme 3.4 Equilibrium between soluble and supersaturated components, TNA and AP, in CH_3CN Solvent. This kind of equilibrium situation will most probably be present in solution when $0 < \Delta pK_a < 3$.

Based on the above idea, the pK_a values were calculated for all the molecules to know the ΔpK_a rule validity ($\Delta pK_a = pK_a \text{ BaseH}^+ - pK_a \text{ Acid}$) for intramolecular proton transfer in the solid-state for these amphoteric compounds. Recently, Cruz-Cabeza¹⁹ studied the ΔpK_a rule for 6465 multi-component systems in the CSD and concluded that ionized acid–base complexes are detected exclusively for $\Delta pK_a > 4$ and non-ionized species for $\Delta pK_a < -1$, with only a few exceptions. For acid–base complexes whose ΔpK_a is between -1 to 4 , which is the majority category for organic acid–base complexes and amphoteric molecules, a linear relationship between the probability of salt formation and the pK_a difference was noted. The calculated ΔpK_a values for amphoteric molecules (Table 3.4) were compared with the observed proton state in the crystal structure. $\Delta pK_a < -2$ for aminobenzoic acids 2-ABA and 3-ABA, and $\Delta pK_a > 3.5$ for aminonicotinic acids (TNA and CLX), ΔpK_a is -1.4 and -1.7 for zwitterionic 5-ASA and Torsemide drugs, and 3.8 and 2.9 for 4-

ASA and Ciprofloxacin and Norfloxacin. There seems to be no particular trend here for neutral vs. zwitterionic structure and ΔpK_a for amphoteric drug molecules, in what is perhaps the first systematic analysis of this issue.

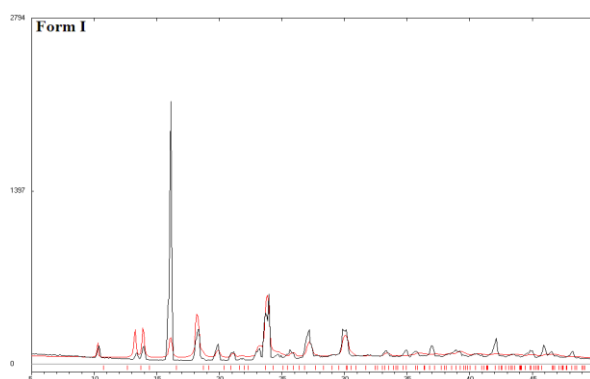
Table 3.4 ΔpK_a of a few amphoteric molecules and drugs^{a,b} and proton transfer in the crystal structure.

S. No.	Amphoteric compound	Neutral crystal structure	Zwitterionic crystal structure	Calculated pK_a of acid and conjugate acid of the base	ΔpK_a
1	2-Aminobenzoic acid (2-ABA)	Form II and III	Form I	4.89 (COOH) 1.95 (NH ₂)	-2.94
2	3-Aminobenzoic acid (3-ABA)	Form II and V	Form I, III and IV	4.81 (COOH) 3.27 (NH ₂)	-2.86
3	2-(p-Tolylamino) nicotinic acid (TNA)	Form I and II	Form III	1.89 (COOH) 5.52 (Py N)	3.63
4	Clonixin (CLX)	Form I, III and IV	Form II	1.88 (COOH) 5.51 (Py N)	3.63
5	Tianeptine	Form A	Form B	4.22 (COOH) 8.10 (NH)	3.88
6	Torsemide	Form II	Form I and III	5.92 (-CONHCO-) 4.20 (Py N)	-1.72
7	Norfloxacin	Form B and C	Form A	5.77 (COOH) 8.68 (Pip NH)	2.91
8	Ciprofloxacin	Form II	Form I	5.76 (COOH) 8.68 (Pip NH)	2.92
9	4-Aminosalicylic acid (4-ASA)	Form I	Not known	2.02 (COOH) 5.87 (NH ₂)	3.85
10	5-Aminosalicylic acid (5-ASA)	Not known	Form I	3.68 (COOH) 2.19 (NH ₂)	-1.49

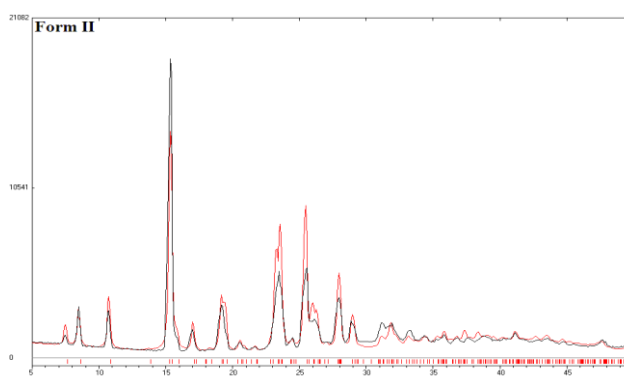
^a pK_a values are calculated using ChemAxon (Marvin 6.0.1, 2013, ChemAxon software <http://www.chemaxon.com>). ^b For reference, the experimental pK_a of pyridine in water is 5.22 (calc. 5.12) and that of aniline is 4.58 (calc. 4.64).

3.4 Characterization of neutral and zwitterionic polymorphs

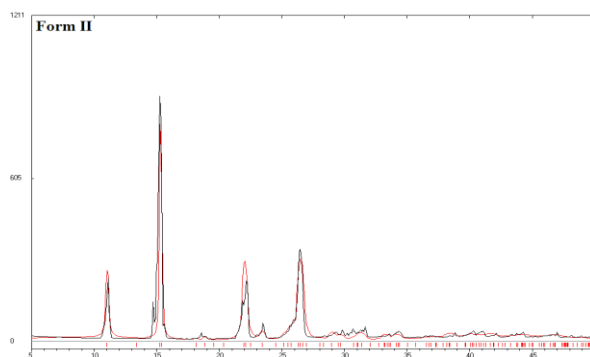
3.4.1 Powder XRD: Neutral and zwitterionic polymorphs of 2-ABA, 3-ABA and CLX were characterized for bulk purity by powder XRD.²⁰ The calculated powder pattern from the X-ray crystal structure of these polymorphs matched with the experimental powder X-ray line profile (Figure 3.11).



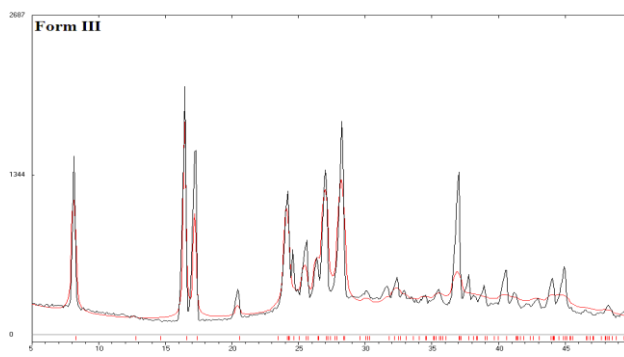
(a) Form I-2-ABA



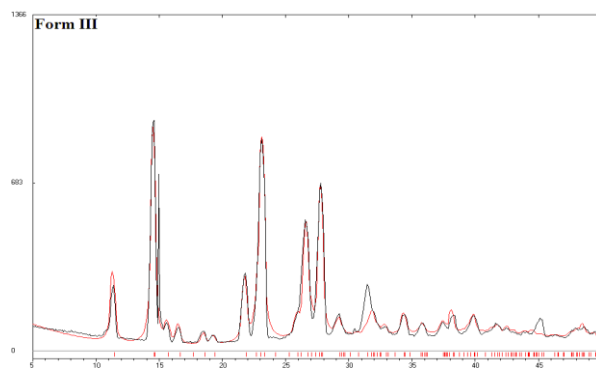
(d) Form II-3-ABA



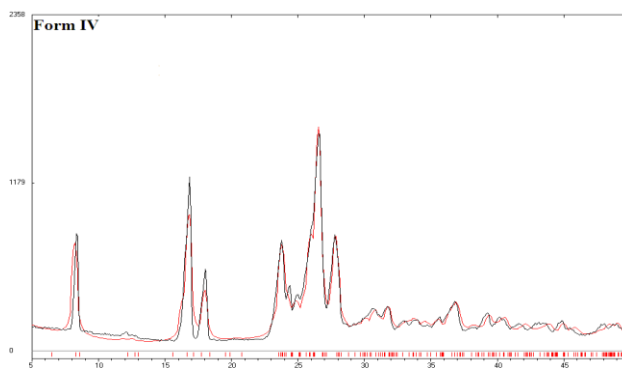
(b) Form II-2-ABA



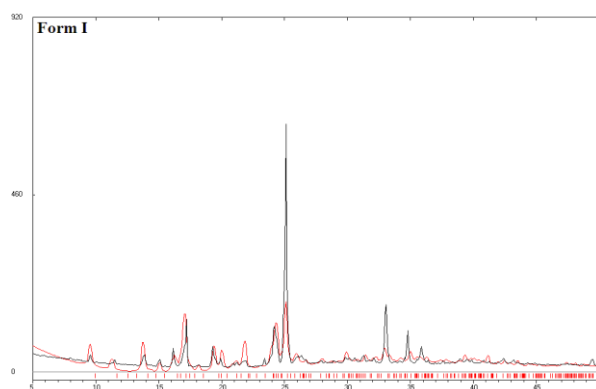
(e) Form III-3-ABA



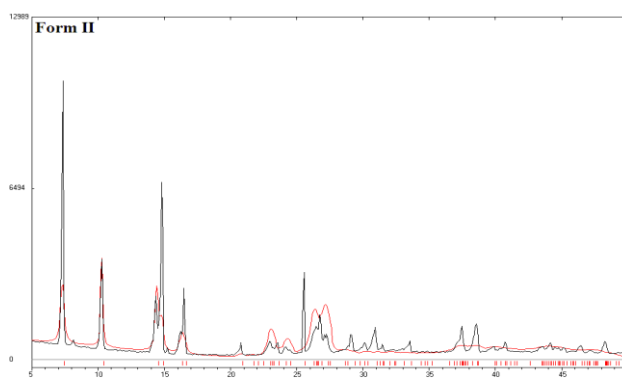
(c) Form III-2-ABA



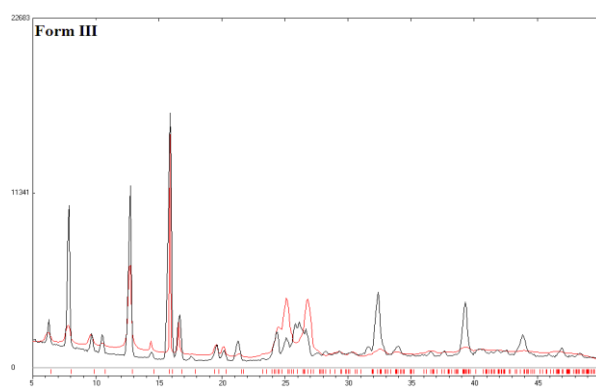
(f) Form IV-3-ABA



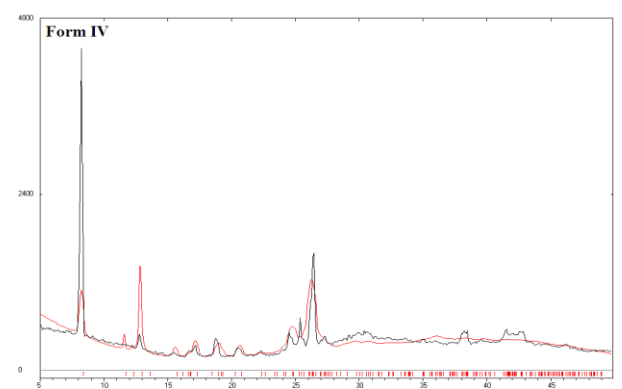
(g) Form I-CLX



(h) Form II-CLX



(i) Form III-CLX

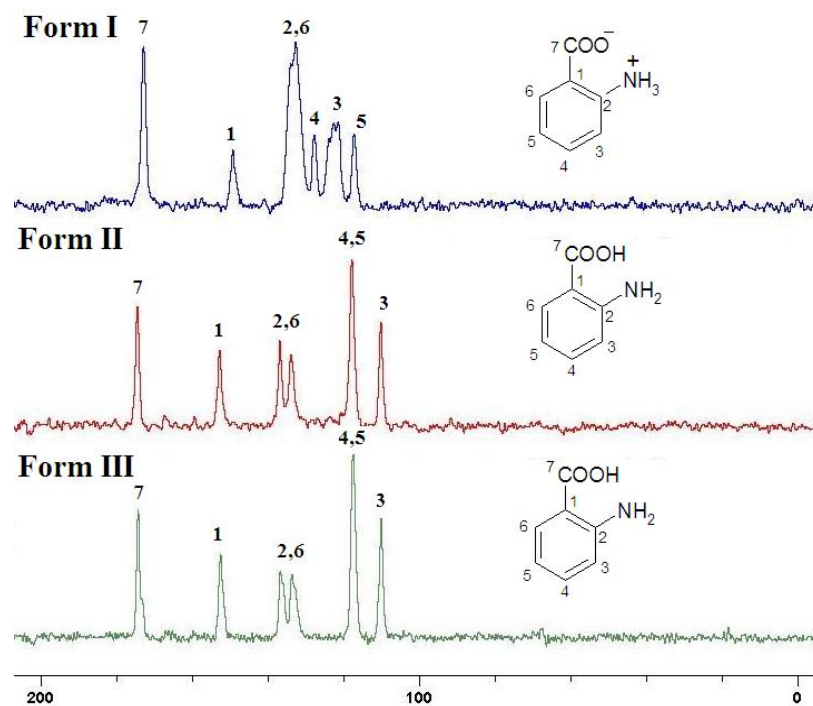


(k) Form IV-CLX

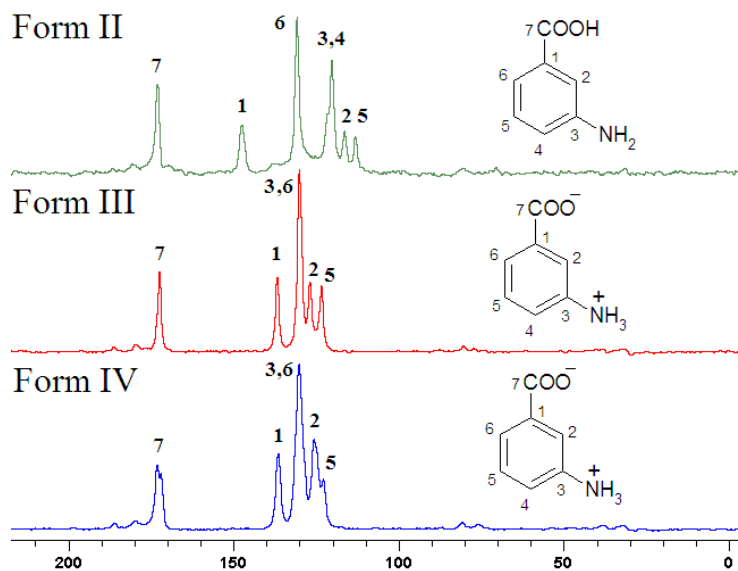
Figure 3.11 Overlay of experimental (black) and calculated (red) powder X-ray line pattern of polymorphs.

3.4.2 Solid state-NMR: Solid state ^{13}C NMR is a powerful technique to identify neutral and zwitterionic polymorphs, e.g. of 2-ABA and 3-ABA.^{6,7} The neutral forms of clonixin were characterized by ss-NMR.²¹ The chemical shift of the carboxylic acid carbon of anthranilic acid (2-ABA) and 3-aminobenzoic acid showed significant difference between the neutral and zwitterionic forms. The chemical shift value of COOH for 2-ABA (form I, half zwitterionic, 172.76 ppm) is shifted up field compared to the neutral forms II and III (174.35 and 174.16 ppm), as would be expected from the higher electron density present on the carboxylate group. The up field drift in the chemical shift of C1 in form I (149.13 ppm) compared to form II (152.58 ppm) and III (152.26 ppm) may be due to electron delocalization at the carboxylate group in the zwitterionic forms (see Figure 3.12).

The chemical shift values of form III (172.7 ppm), form IV (172.1 ppm) and form II (172.75 ppm) are very close for 3-ABA, and a reason may be the meta-effect of the electron-donating amino group. The chemical shift of C1 in form III (136.54 ppm) and IV (136.23 ppm) is up field because of electron delocalization in the carboxylate group compared to the form II (147.29 ppm). The ss-NMR of clonixin form II could not be recorded for comparison because of limited sample and difficulty to crystallize the zwitterionic form II (see Figure 3.12c). The chemical shift values for all polymorphs are listed (Table 3.5).



(a) 2-ABA



(b) 3-ABA

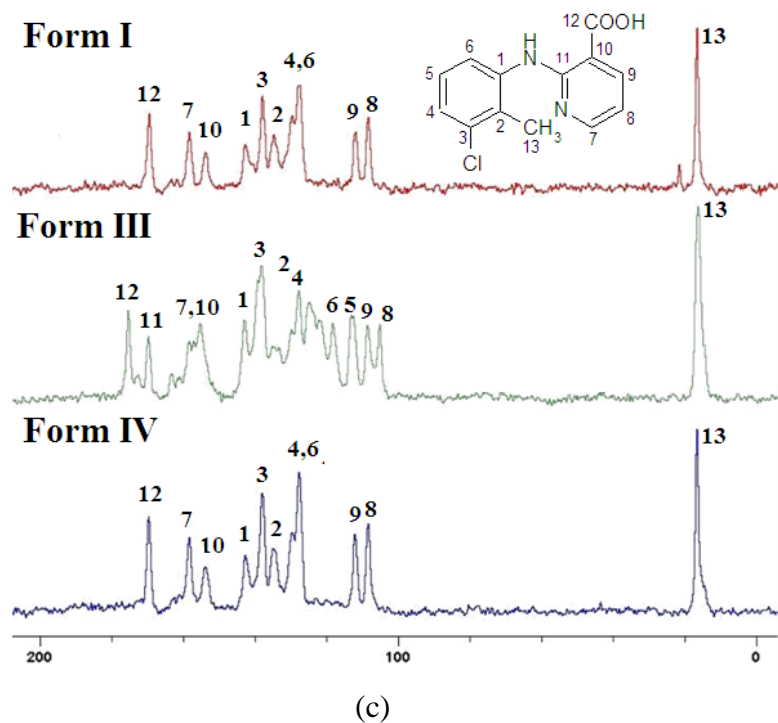


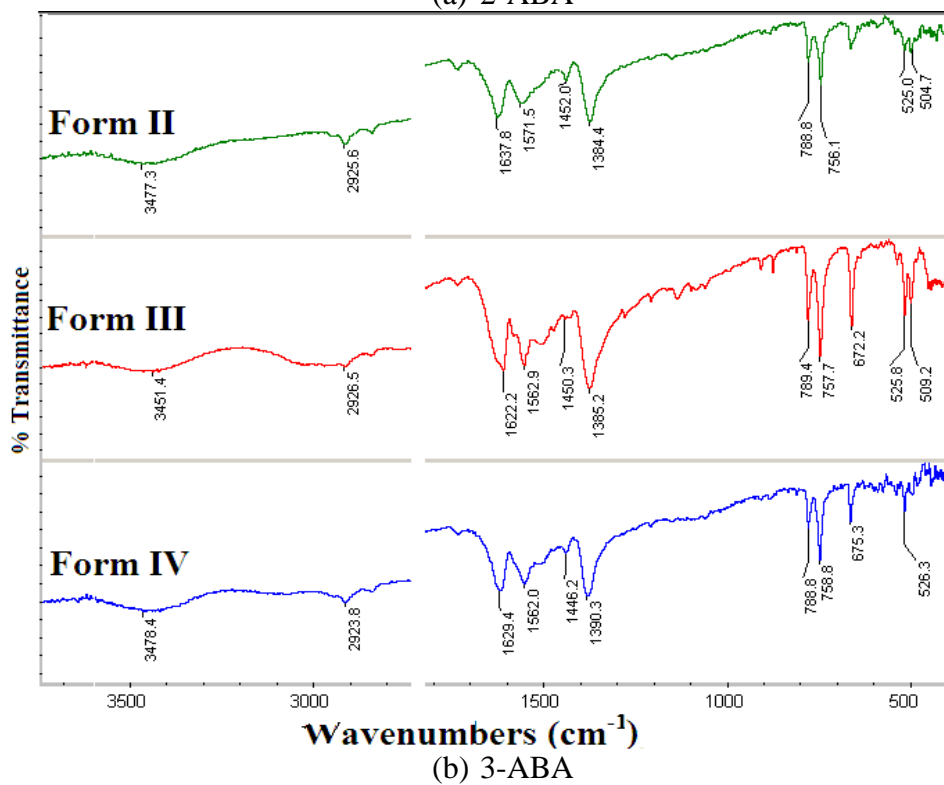
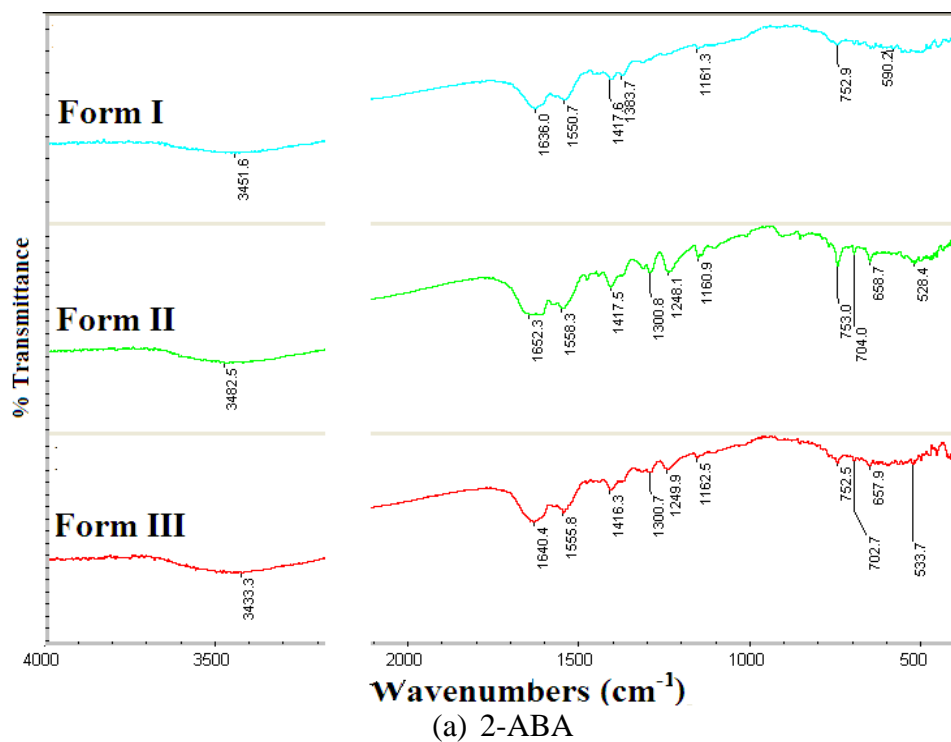
Figure 3.12 ^{13}C ss-NMR spectra of polymorphs of molecules (a) 2-ABA, (b) 3-ABA and (c) CLX

Table 3.5 Chemical shift values for polymorphs

Carbon atoms	2-ABA			3-ABA			CLX		
	I	II	III	II	III	IV	I	III	IV
C1	149.1	152.5	152.2	147.2	136.5	136.2	142.5	142.7	142.6
C2	133.8	133.7	133.2	116.1	126.6	125.3	129.5	129.6	129.6
C3	122.5 , 121.3	109.9	109.8	119.9	129.7	129.8	137.8	137.9	137.8
C4	127.5	117.6	117.4	119.9	-	-		123.3	
C5	117.1	117.6	117.4	112.8	123.1	122.5	158.2	121.4	158.1
C6	133.8	133.7	133.2	130.5	129.7	129.8		118.1	
C7	172.7	174.3	174.2	172.7	172.1	172.8	108.1	157.0	108.18
C8	-	-	-	-	-	-		105.0	

								9	
C9	-	-	-	-	-	-	111.5	112.3	111.8
C10	-	-	-	-	-	-	153.3	155.0	153.9
C11	-	-	-	-	-	-	-	172.4	169.4
C12	-	-	-	-	-	-	169.3	175.1	
C13	-	-	-	-	-	-	16.49	16.0	16.5

3.4.3 FT-IR: FT-IR technique has been used to differentiate neutral and zwitterionic polymorphs of ampholytes.^{20,22} For example, the stretching frequency of the carbonyl group in the zwitterionic form (Form I, half zwitterionic, 1636.0 cm^{-1}) of anthranilic acid (2-ABA) is less than that of the other two neutral forms (Form II, neutral, 1652.3 cm^{-1} ; form III, neutral, 1640.0 cm^{-1}). The decrease in the stretching frequency of zwitterionic form is a result of delocalization of electron cloud over the caboxylate group, e.g. also in the zwitterionic structure of m-aminobenzoic acid (3-ABA). The stretching frequency of the C=O group in carboxylic acid in two zwitterionic polymorphs (Form III and IV, 1622.2 , 1629.4 cm^{-1}) is less than that of the reported neutral form (1637.8 cm^{-1}). Similarly clonixin showed a difference between the neutral and zwitterionic polymorphs (Form II, zwitterionic, 1646.7 cm^{-1} ; Form I, III, neutral, 1677.3 and 1665.8 cm^{-1}). The forth form of clonixin showing a broad peak in the FT-IR (not discussed). FT-IR and Raman spectral details are displayed in Figure 3.13 and 3.14 and Table 3.6 and 3.7.



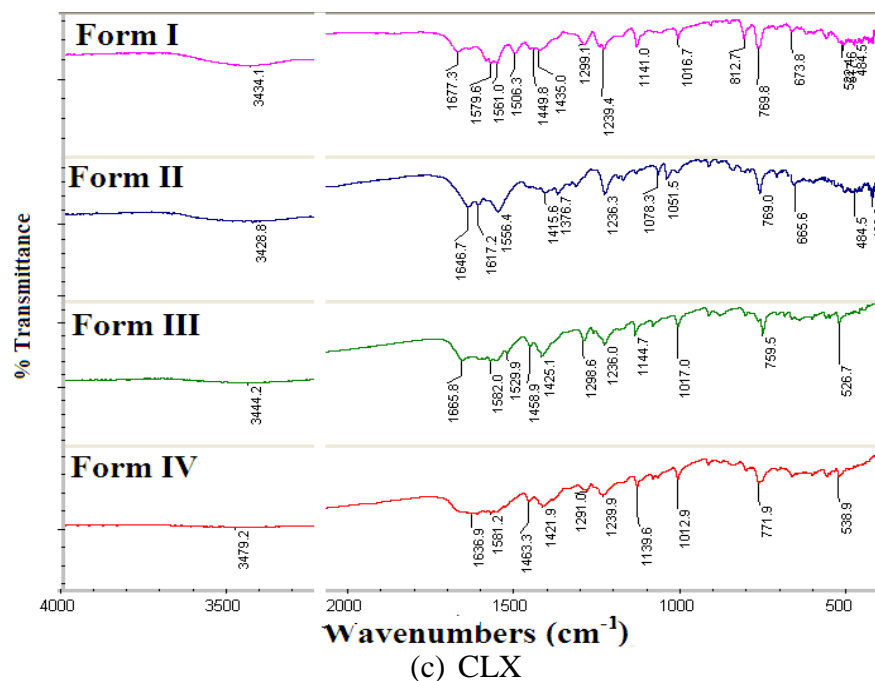
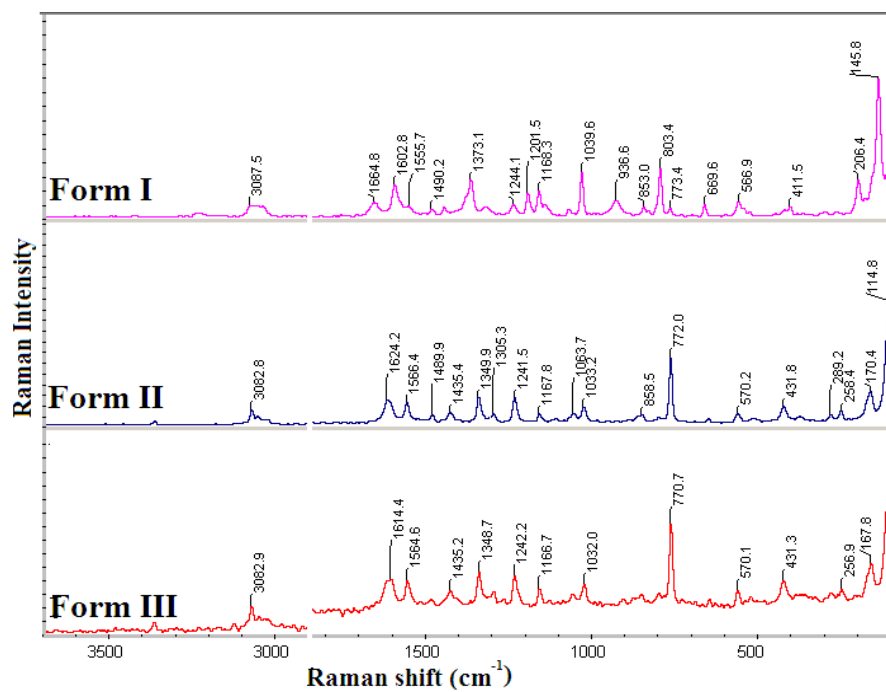


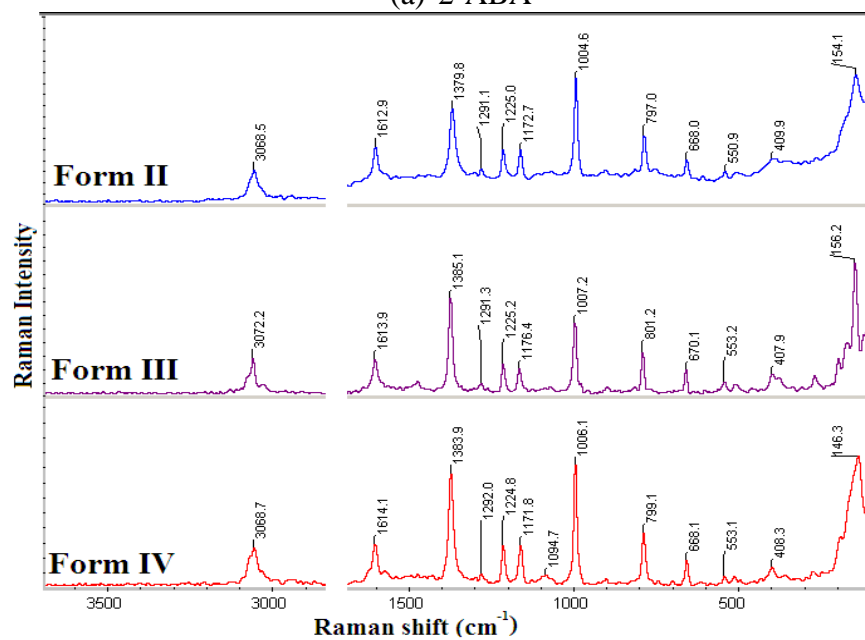
Figure 3.13 FT-IR comparison of polymorphs of (a) 2-ABA, (b) 3-ABA and (c) CLX

Table 3.6 FT-IR stretching frequencies for polymorphs

Molecules	N–H stretch (broad) cm^{-1}	N–H bend cm^{-1}	C=O asym/ sym stretch cm^{-1}
Form I (2-ABA)	3451.6	1550.7	1636.0
Form II (2-ABA)	3482.5	1558.3	1652.3
Form III (2-ABA)	3433.3	1555.8	1640.0
Form II (3-ABA)	3477.3	1571.5	1637.8
Form III (3-ABA)	3451.4	1562.9	1622.2
Form IV (3-ABA)	3478.4	1562.0	1629.4
Form I (CLX)	3434.1	1579.6	1677.3
Form II (CLX)	3428.8	1617.2	1646.7
Form III (CLX)	3444.2	1582.0	1665.8
Form IV (CLX)	3479.2	1581.2	1636.9 (broad)



(a) 2-ABA



(b) 3-ABA

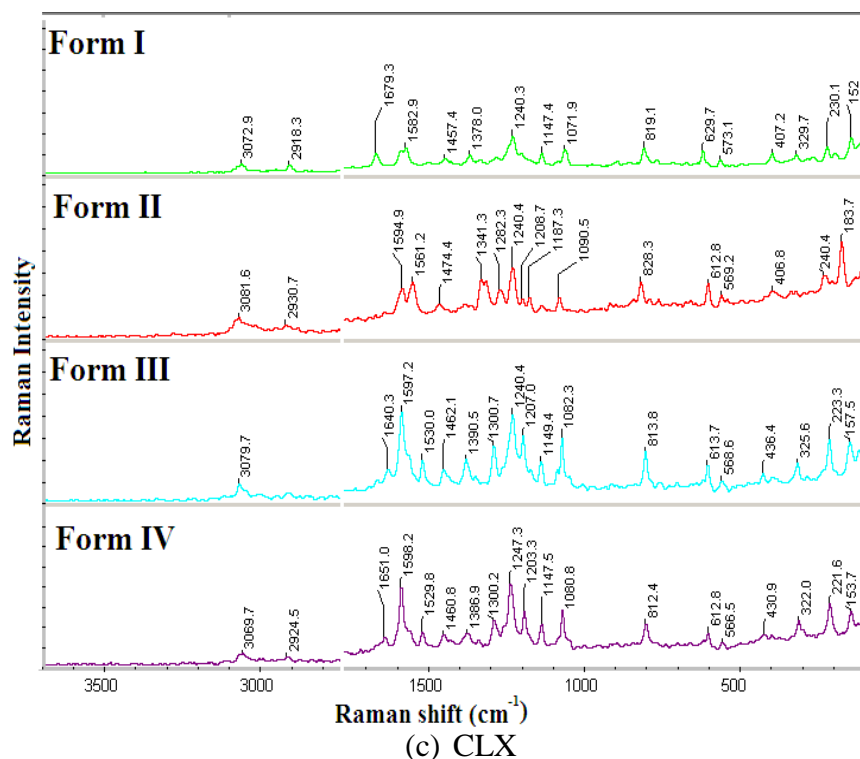


Figure 3.14 FT-Raman comparison of polymorphs of (a) 2-ABA, (b) 3-ABA and (c) CLX

Table 3.7 Raman stretching frequencies for polymorphs

Molecules	Aromatic C–H stretch cm^{-1}	N–H bend cm^{-1}	C=O asym/ sym stretch cm^{-1}
Form I (2-ABA)	3087.5	1555.7	1664.8
Form II (2-ABA)	3082.8	1566.4	1624.2
Form III (2-ABA)	3082.9	1614.4	1614.4
Form II (3-ABA)	3068.5	-	1612.9
Form III (3-ABA)	3072.2	-	1613.9
Form IV (3-ABA)	3068.7	-	1614.1
Form I (CLX)	3072.9	1582.9	1679.3
Form II (CLX)	3081.6	1561.2	1594.9
Form III (CLX)	3079.7	1597.2	1640.3
Form IV (CLX)	3069.7	1598.2	1651.0

3.5 Thermal stability and phase transition study

The neutral and zwitterionic forms of three ampholyte molecules exhibited extensive phase transitions by DSC and variable-temperature powder X-ray diffraction.²³ The zwitterionic polymorph of 2-ABA transformed to neutral the form III at 95.9 °C and finally melted at 144 °C. The zwitterionic form and the neutral forms are enantiotropic, with form I being the low temperature phase and form III is the high temperature phase. DSC and VT-PXRD for such phase transitions between neutral and zwitterionic forms of anthranilic acid is displayed in Figure 3.15. Form I is stable up to 24 hours of slurry grinding in aqueous medium but form II and III transformed to form I in those slurry conditions.^{6d} Our thermal analysis is consistent with the study of Ojala and Etter^{7b} on 2-ABA polymorphs.

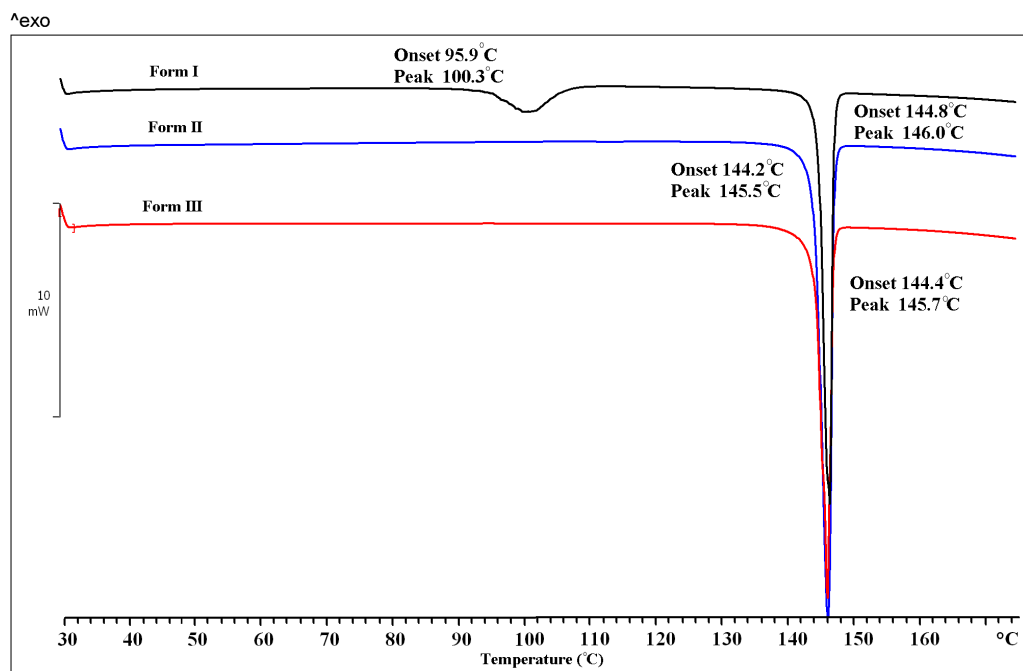
The zwitterionic form III of m-aminobenzoic acid (3-ABA) transformed to another second zwitterionic form IV at 161.9 °C and melts at 177.1 °C. VT-PXRD suggested that the transformation of zwitterionic form III to form IV occurred via neutral form I as an intermediate phase (Figure 3.16b), based on PXRD match with the diffraction lines for reported form I. The zwitterionic form IV transformed to the neutral form II at 166.7 °C and the melted at 176.4 °C. We identified form III as the lower temperature phase and form II as the higher temperature phase in this study. Form II is unstable at room temperature transformed to the stable form III. Our measurements qualify the studies of Harris et al^{6b} wherein they reported III and IV as stable based on the DSC and the density rule. We confirmed zwitterionic form III as the stable polymorph by slurry experiments (Figure 3.19). Form III and form IV are enantiotropically related to form II as reported in previous work^{6b} (Figure 3.16).

For clonixin (CLX) tetramorphs, the zwitterionic form II is first transformed to form I at 149.2 °C and then melted at 233.6 °C. Form III underwent a phase transition at 142.4 °C and melted at 233.6 °C. Form II and form III are

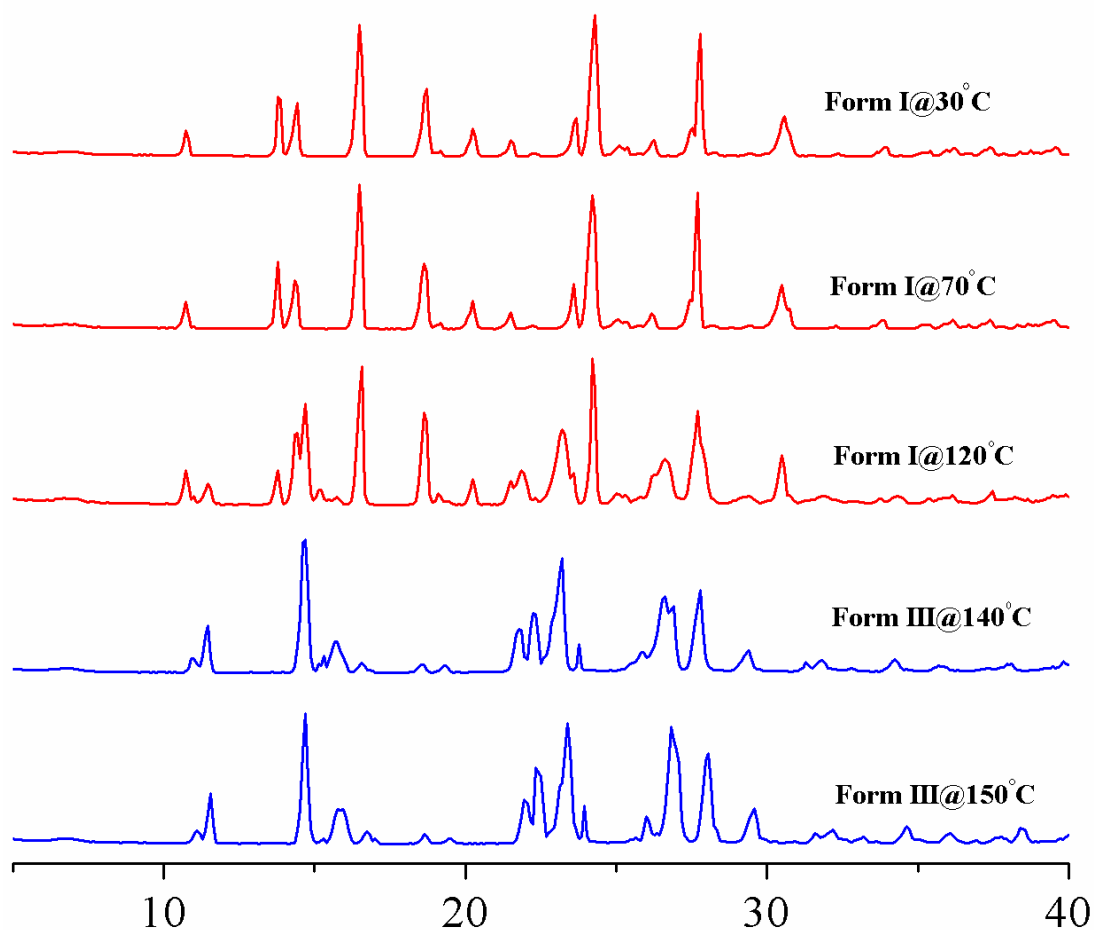
enantiotropically related to form I (see DSC and VT-PXRD in Figure 3.17). The zwitterionic forms transform to the neutral polymorph upon heating for the above mentioned three molecules. These data are summarized in Table 3.8.

Table 3.8 Thermodynamic parameters of polymorphic systems.

Molecule	2-Aminobenzoic acid			3-Aminobenzoic acid			Clonixin			
Polymorphs	I	II	III	II	III	IV	I	II	III	IV
Melting and phase transition onset	95.9	144	144	177	161	166	236	149	142	224
Enthalpy of fusion/ Enthalpy of transition (kJ mol ⁻¹)	23, 5	23	22	28	30, 1.8	21, 10	27	29, 5	21, 1.5	21
Density (g cm ⁻³)	1.40	1.37	1.39	1.37	1.55	1.53	1.41	1.51	1.51	1.49
Packing fraction (%)	72.4	68.5	70.2	69.6	78.2	77.1	67.8	72.8	72.7	71.6
Thermodynamic relationship and stable polymorph	Enantiotropic and stable half-zwitterionic form I			Enantiotropic and stable zwitterionic form III			Enantiotropic and stable neutral/ionic form I \approx II			

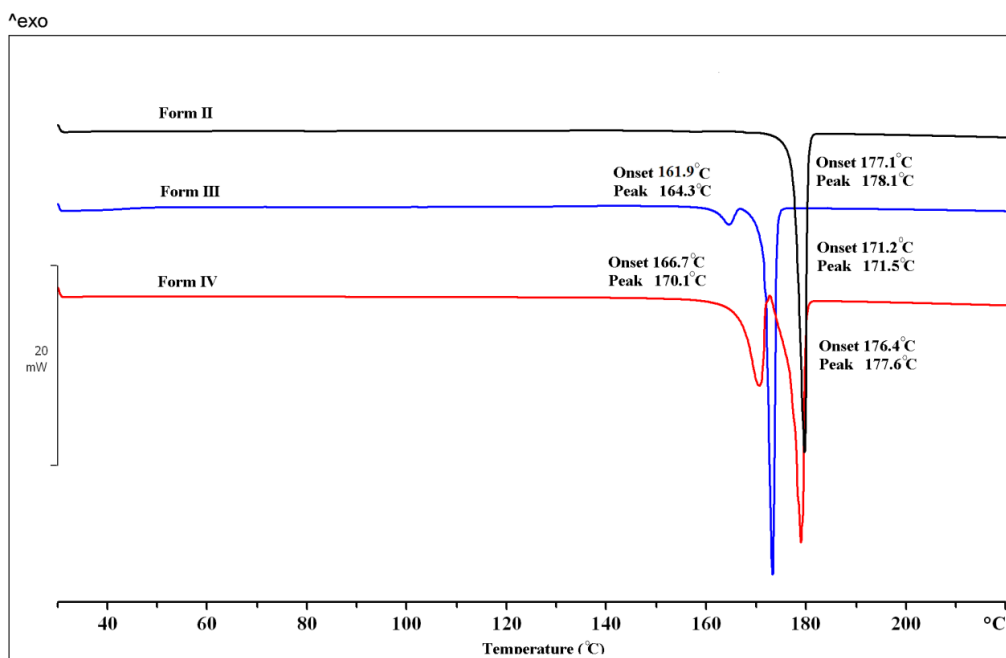


(a) DSC of 2-ABA

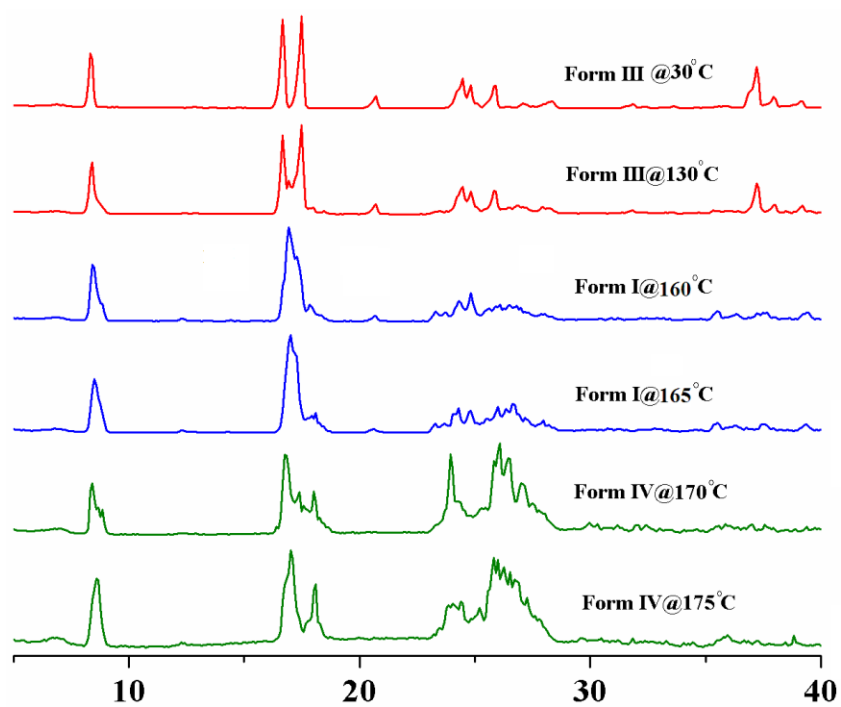


(b) VT-PXRD-Form I, 2-ABA

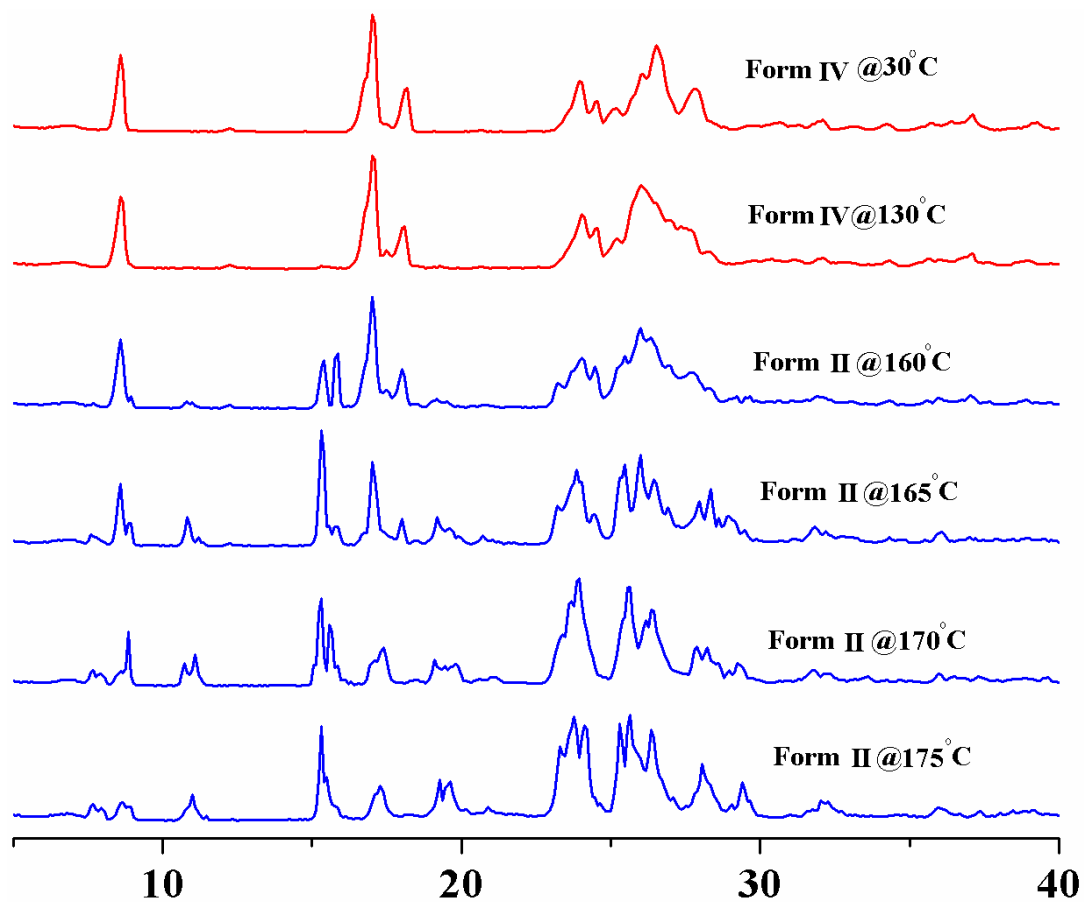
Figure 3.15 (a) Thermal analysis by DSC and (b) VT-PXRD shows the phase transition of neutral and zwitterionic form I to form III of 2-ABA at 120 °C.



(a) DSC of 3-ABA

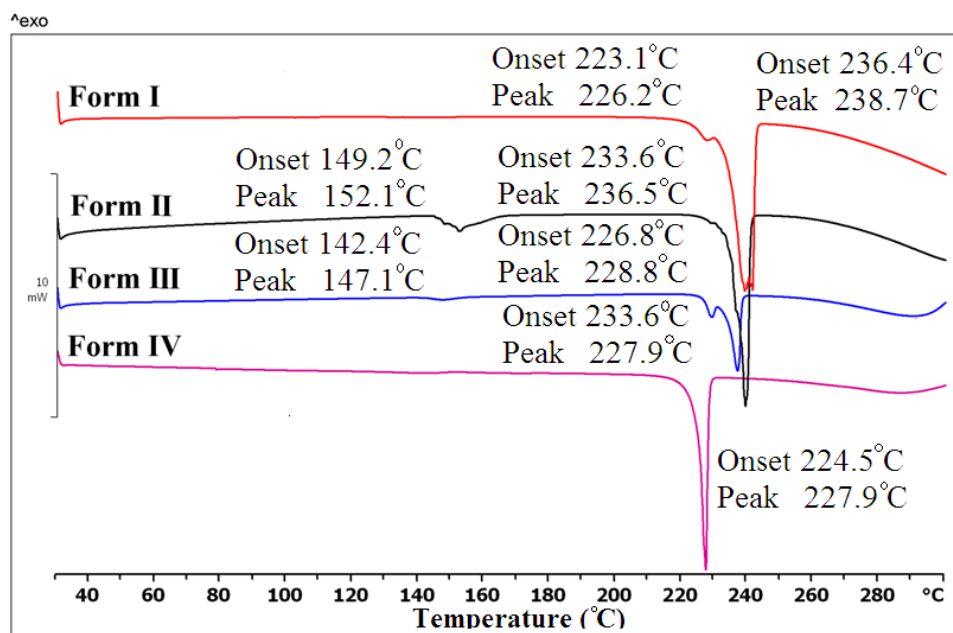


(b) VT-PXRD of form III of 3-ABA

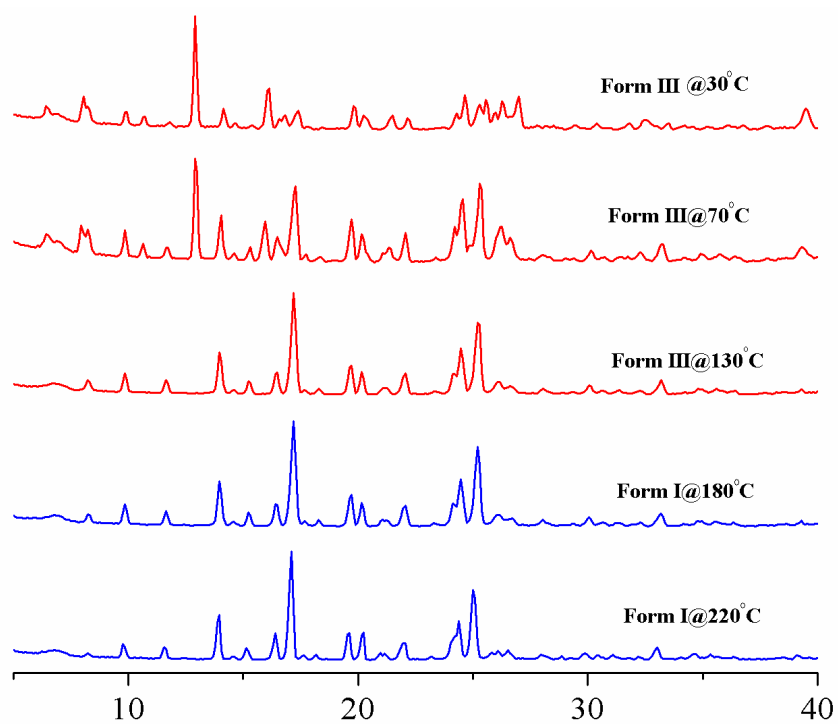


(c) VT-PXRD of form IV of 3-ABA

Figure 3.16 Thermal behavior of 3-ABA trimorphs. (a) DSC; (b) Form III to form I at 160 °C, and form I to form IV at 165 °C; and (c) Form IV to form II at 160 °C by VT-PXRD.



(a) DSC of CLX



(b) VT-PXRD of form III of CLX

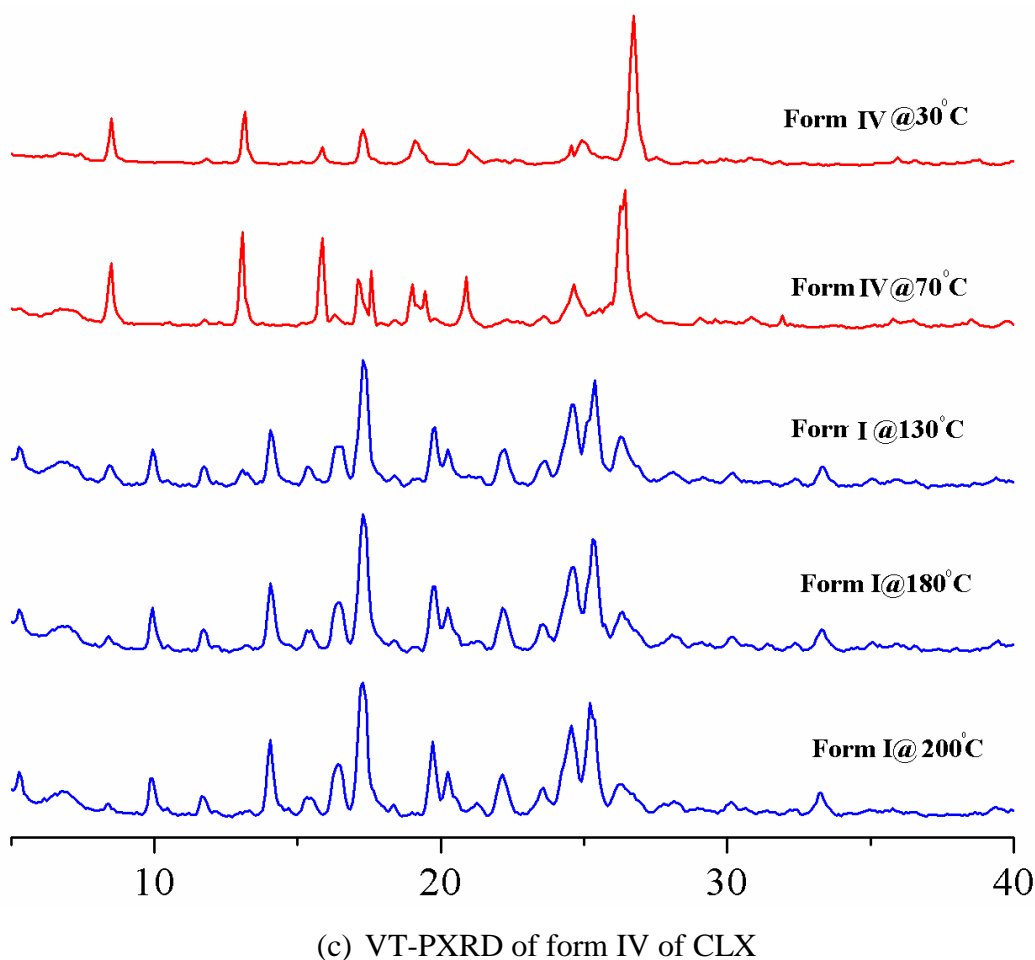


Figure 3.17 Thermal behavior of tetramorphs of clonixin by (a) DSC, (b) Form III to form I at 130 °C and (c) Form IV to form I at 130 °C by VT-PXRD.

3.6 Solubility and dissolution study

The main motivation of this study was to compare the dissolution rate and solubility of zwitterionic and neutral polymorphs and make structure–solubility correlations. The solubility of 2-ABA, 3-ABA and CLX polymorphs are tabulated (Table 3.9). Generally, metastable polymorphs exhibit higher solubility and dissolution rate compared to the stable form, in line with the inverse solubility–stability trend.^{2,24} Among neutral and zwitterionic polymorphic sets, we observed that the solubility of the zwitterionic form was higher, even when it is the more

stable modification compared to the neutral form. In effect, *a zwitterionic form can combine the twin criteria of high solubility and good stability in the same crystalline polymorph*, which is a desirable optimization in pharmaceutical development. The reason for the higher solubility is that the ionic functional groups in the zwitterionic crystal structure expose the charged ends of the functional groups to the water and polar solvents, e.g. the charged acidic/ basic groups are able to hydrogen bond better with water and alcohol-like solvents. Among the structures studied, the stable form of 2-ABA is half zwitterionic/ neutral (form I), and its solubility is higher (10.33 mg/mL) than the neutral forms (form II; 6.37 mg/mL, form III; 3.97 mg/mL) in water medium. The stability of form I was confirmed in a slurry experiment at ambient conditions, and there was no inter-conversion to the neutral forms after 24 h. The neutral forms II and form III of 2-ABA transformed to the stable ionic form I under the same slurry conditions. The density and packing fraction of form I (1.40 g cm^{-3} , 72.4%) is greater than form II (1.37 g cm^{-3} , 68.5%) and form III (1.39 g cm^{-3} , 70.2%), consistent with the observed stability order. The solubility trends for 3-ABA in water is form IV (zwitterionic, most stable) 7.69 mg/mL > form III 6.07 mg/mL (zwitterionic) > form II 4.34 mg/mL (neutral; least stable). The density and packing fraction of zwitterionic form III (1.55 g/cm^3 , 78.2%) and form IV (1.53 g/cm^3 , 77.1%) of 3-ABA are higher than that of neutral form II (1.37 g/cm^3 , 69.6%). That the zwitterionic form is more stable than the neutral form was confirmed in slurry experiments over 24 h. For CLX, the solubility of metastable forms III and IV is higher than that of the ionic stable forms in 60% EtOH-water mixture. The solubility of zwitterionic form II (2.01 mg/mL) is slightly higher than the stable neutral form I (1.93 mg/mL) for CLX. The higher solubility of the zwitterionic forms is similar to the solubility trend followed in aminobenzoic acid polymorphs and varies inversely with crystal density and packing fraction (Form I: 1.41 g/cm^3 , 67.8%; Form II: 1.51 g/cm^3 , 72.8%). The apparent solubility of neutral, metastable polymorphs of CLX, form III and IV (2.32 mg/mL and 2.25 mg/mL), is higher than that of stable form I

and zwitterionic form II (1.93 mg/mL and 2.01 mg/mL). The solubility of these two metastable forms is not consistent with their higher crystal density and packing efficiency (form III 1.51 g cm^{-3} , 72.7%; form IV 1.49 g cm^{-3} , 71.6%). The higher density perhaps arises from the planar conformation in these metastable polymorphs III and IV which results in a denser packing of molecules. Even though we recently concluded that planar a molecular conformation tends to give low solubility,¹⁸ the present results appear to be an oddity with the planar confirmation and higher density polymorphs III and IV of CLX exhibiting higher solubility. The neutral forms III and IV of CLX transformed to the stable neutral form I in slurry experiments, whereas zwitterionic form II and neutral form I are stable to the same aqueous solution (Figure 3.19).

The dissolution rates of zwitterionic forms of 2-ABA, 3-ABA and CLX are higher than the neutral forms (Table 3.9 and Figure 3.18). The IDR of zwitterionic form I of 2-ABA is $1.36 \text{ mgcm}^{-2}\text{min}^{-1}$ and it dissolves faster than the neutral forms (form II $0.82 \text{ mgcm}^{-2}\text{min}^{-1}$, form III $0.67 \text{ mgcm}^{-2}\text{min}^{-1}$). The dissolution rate of form III ($1.51 \text{ mgcm}^{-2}\text{min}^{-1}$) and form IV ($1.56 \text{ mgcm}^{-2}\text{min}^{-1}$) is almost two times faster than that of neutral form II for 3-ABA. The dissolution rate of zwitterionic form II ($0.20 \text{ mgcm}^{-2}\text{min}^{-1}$) of CLX is higher than that of neutral polymorphs I ($0.14 \text{ mgcm}^{-2}\text{min}^{-1}$) and III ($0.19 \text{ mgcm}^{-2}\text{min}^{-1}$) and IV ($0.16 \text{ mgcm}^{-2}\text{min}^{-1}$).

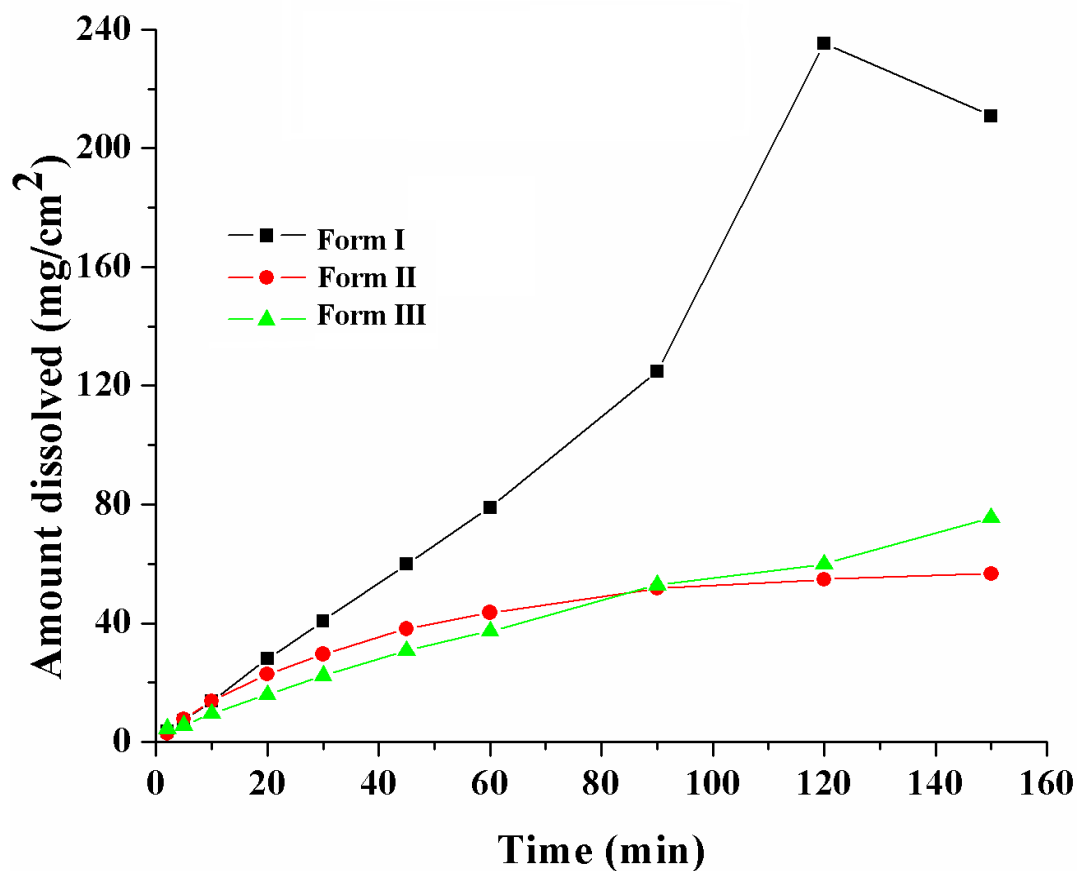
The dissolution rate of the two isomers of aminosalicic acid was taken here to compare the solubility difference between the ionic and neutral isomers of APIs. The neutral structure of 4-ASA exhibited higher dissolution rate than the zwitterionic structure of 5-ASA. The density and melting point of 5-ASA (m.p. 283°C , D_c 1.56 g cm^{-3}) is higher than that for 4-ASA (m.p. 150°C , D_c 1.48 g cm^{-3}) and the lower solubility of zwitterionic 5-ASA with strong ionic $\text{N}^+\text{--H}\cdots\text{O}^-$ hydrogen bonds is again counter-intuitive. In any case, these isomeric structures are not truly polymorphic but have similar molecular structures.

Table 3.9 Solubility and dissolution rate of polymorphs.

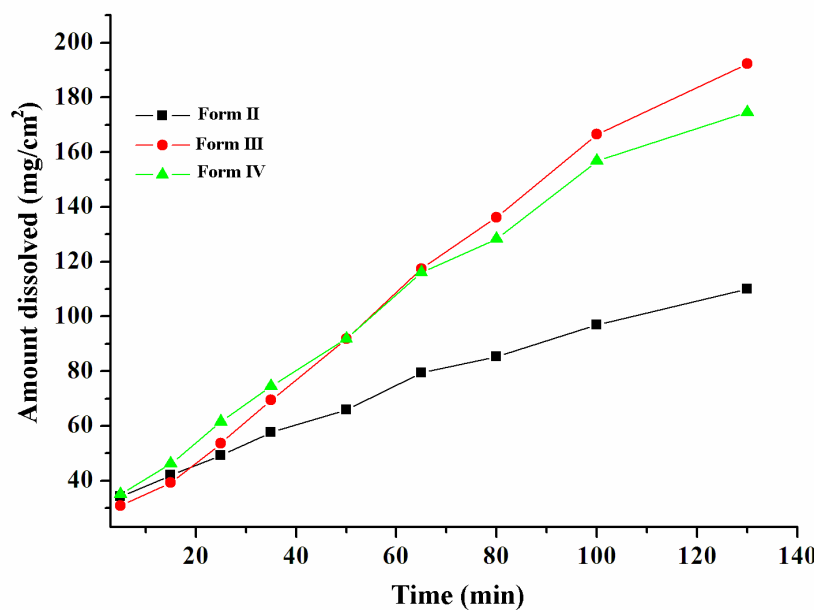
Polymorph	Nature in solid state	Absorption coefficient (ϵ), (M ⁻¹ cm ⁻¹)	Solubility (mg/mL)	Intrinsic Dissolution rate (mgcm ⁻² min ⁻¹)
2-Aminobenzoic acid polymorphs				
Form I	Half zwitterionic/ neutral	12.26	10.33	1.36
				1.75
Form II	Neutral	13.60	9.25	0.82
			6.37 ^a	0.93
Form III	Neutral	12.39	8.01	0.67
			3.97 ^a	
3-Aminobenzoic acid polymorphs				
Form II	Neutral	6.22	7.81	0.84
			4.34 ^a	
Form III	Zwitterionic	6.22	6.07	1.51
Form IV	Zwitterionic	6.25	7.69	1.56
Clonixin polymorphs				
Form I	Neutral	68.36	1.93	0.14
			2.01	
Form II	Zwitterionic	69.27	3.12	0.19
			2.32 ^a	
Form III	Neutral	57.58	2.51	0.16
			2.25 ^a	
Form IV	Neutral ^b	98.36	2.51	0.16
			2.25 ^a	
Aminosalicylic acid isomers				
4-ASA	Neutral	60.49	2.54 ^c	0.25
5-ASA	Zwitterionic	22.32	1.43 ^c	0.17

^a For these metastable forms the apparent solubility was measured. ^b The neutral nature of COOH was derived from the C=O, C–O distances (1.23 Å, 1.31 Å) in .cif

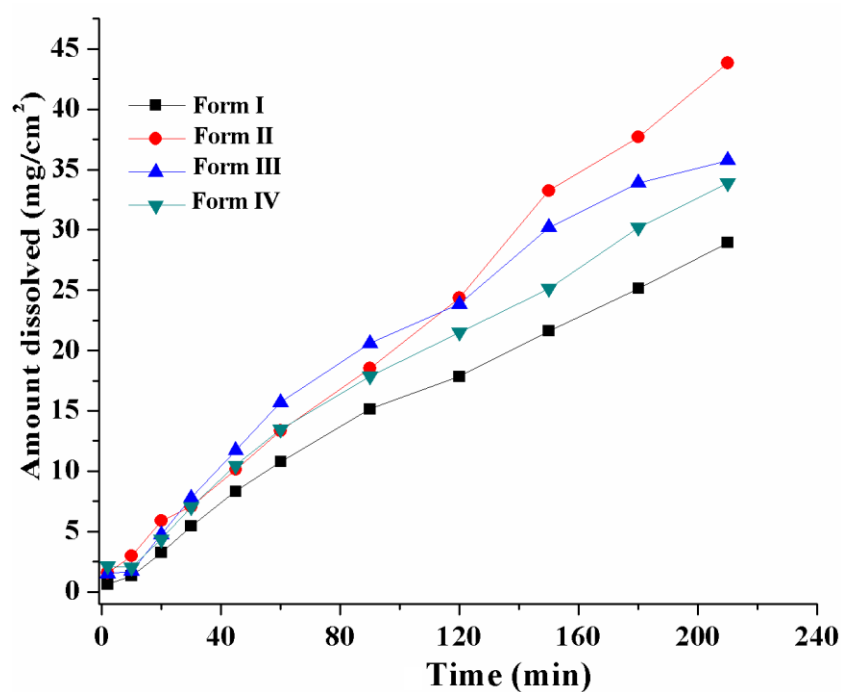
file BIXGIY03. ^c Solubility is reported in ref. 12g and 12h. The compound suffered degradation in long term solubility experiments (24 h).



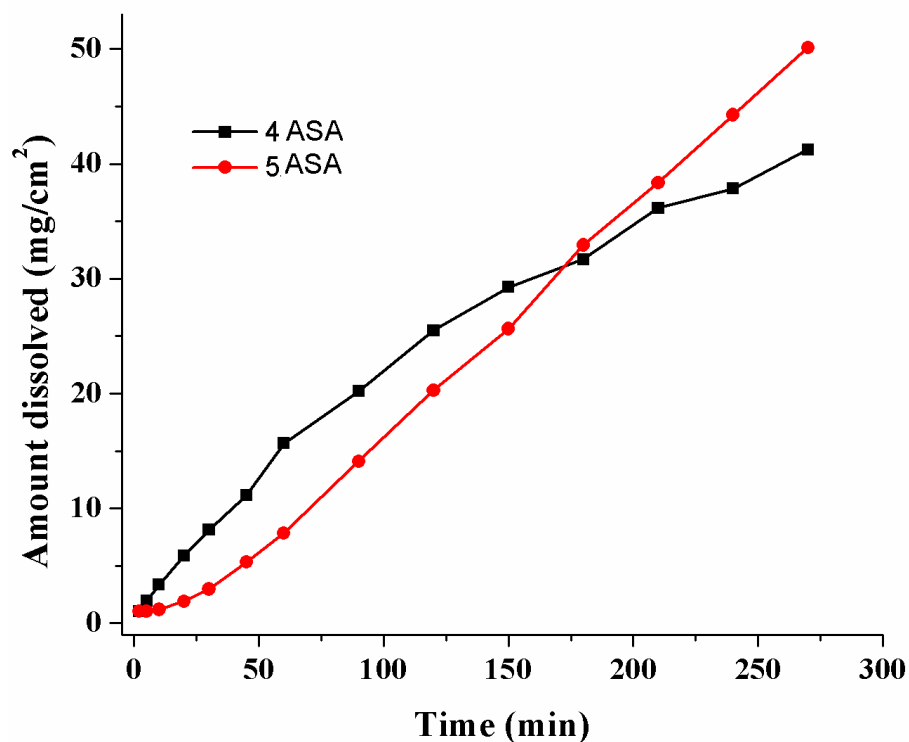
(a) Dissolution profile of 2-ABA polymorphs in water: Form I is half zwitterionic and form II and III are neutral. The pellet completely dissolved after 120 min for form I.



(b) Dissolution profile of 3-ABA polymorphs in water: Form II is neutral and form III, IV are zwitterionic

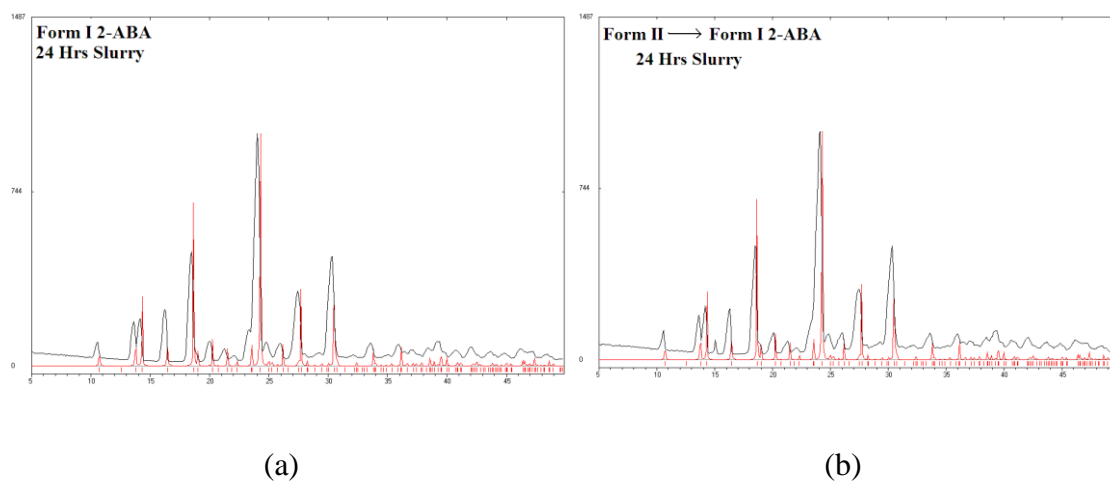


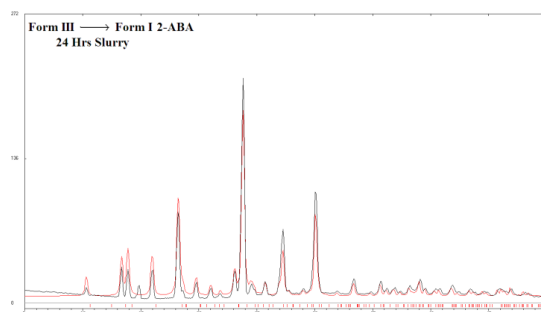
(c) Dissolution profile of CLX polymorphs in 60% EtOH-water: Form I, III and IV are neutral and form II is zwitterionic



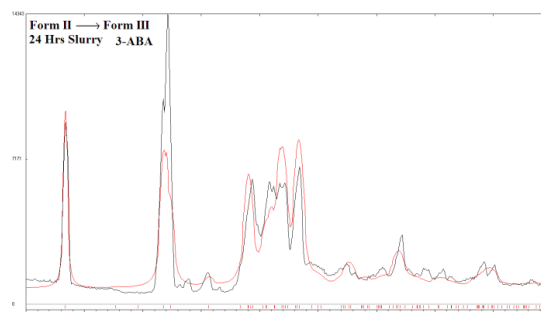
(d) Dissolution profile of isomeric drugs in water: 4-ASA is neutral and 5-ASA is zwitterionic

Figure 3.18 Dissolution profiles of neutral and zwitterionic polymorphs of drugs at 30 °C.

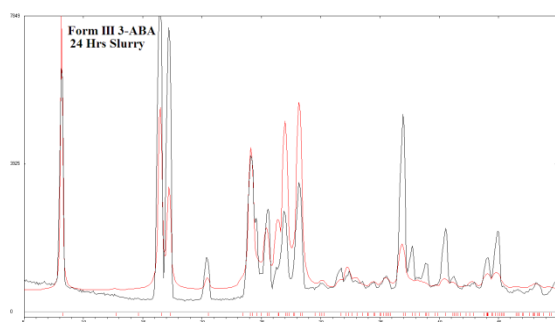




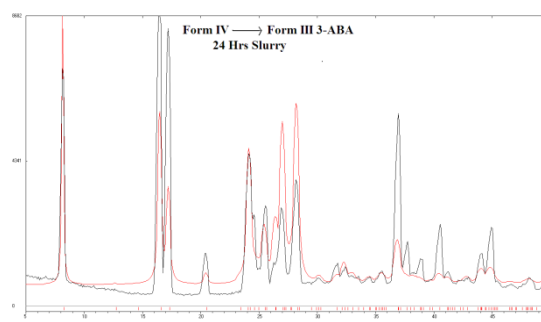
(c)



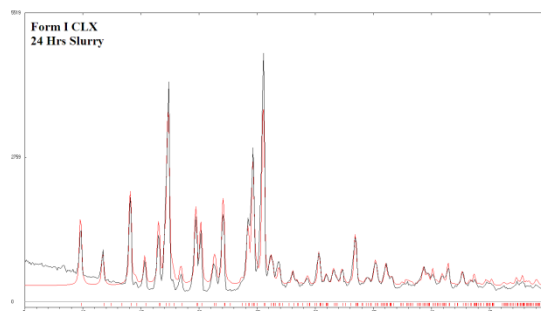
(d)



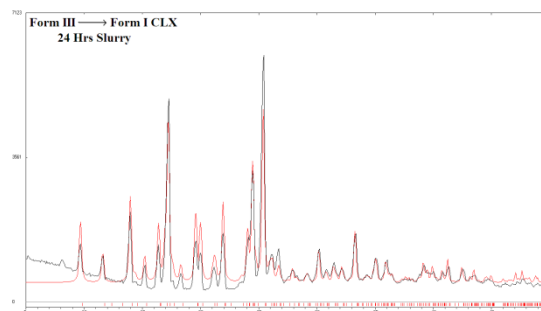
(e)



(f)



(g)



(h)

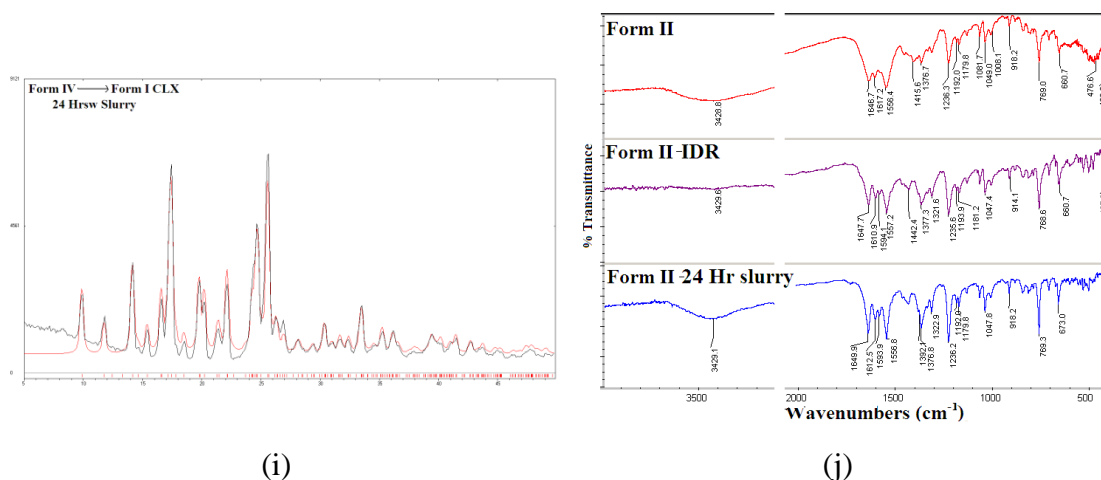


Figure 3.19 PXRDs of (a) form I (b) form II (c) form III of 2-ABA, (d) form II (e) form III (f) form IV of 3-ABA, and (g) form I (h) form III (i) form IV of CLX and (j) FT-IR of form II after 24 hours slurry experiments in aqueous medium for equilibrium solubility experiments

3.7 Conclusions

Several drugs are amphoteric in nature. This structural-cum-solubility study of neutral and zwitterionic polymorphs provides methods for their preparation and a comparison of solubility–stability characteristics. Normally solubility and stability are inversely related for drug polymorphs. We show that the twin characteristics of high solubility and good stability may be jointly optimized in the same zwitterionic polymorph for amphoteric drugs. The high polarity and ionic nature of acidic/ basic groups promote hydrogen bonding with water (for higher solubility) as well as a tighter crystal lattice of ionized molecules (polymorph stability). All the crystal structures were fully characterized by FT-IR, Raman and ss-NMR as well as powder X-ray diffraction line pattern. The thermodynamic relationships and phase transition between the neutral and zwitterionic polymorphs was analyzed by DSC and VT-PXRD. This study provides a new direction to crystallize ionic polymorphs of amphoteric drugs for solubility enhancement. The selective crystallization of zwitterionic forms could be possible through crystallization promoter additives such

as ionic liquids,²⁵ polymer-induced heteronucleation,²⁶ and seeding with ionic structural mimics.²⁷

3.8 Experimental Section

General. 2-ABA, 3-ABA, 4-ASA, 5-ASA and NFA were purchased from Sigma-Aldrich, Hyderabad, India. All other solvents, reagents and coformers were purchased from commercial sources and used without further purification.

Synthesis. Clonixin, PNA, o-TNA and p-TNA were synthesized by refluxing *o*-chloronicotinic acid (315.3 mg, 2 mmol) and an equivalent amount of the appropriate aromatic amine (1.1 equiv). The precipitated product was filtered and purified by crystallization from acetone to obtain pure clonixin (CLX), 2-(phenylamino)nicotinic acid, 2-(*o*-tolylamino)nicotinic acid, and 2-(*p*-tolylamino)nicotinic acid which were characterized by NMR and single crystal XRD.

Vibrational Spectroscopy. Nicolet 6700 FT-IR spectrometer with an NXR FT-Raman module was used to record IR spectra. IR spectra were recorded on samples dispersed in KBr pellet.

CSD search. A search of the CSD (version 5.34, November 2012)¹⁴ was performed by drawing the amine and the acid groups as search criteria all organic compounds with the word "form", "polymorph", "modification" and "phase" in the qualifier, excluding the entries for which 3D coordinates are not available. These searches resulted in only four drugs and three model compounds having zwitterionic and neutral polymorphic sets for single component organic molecules with solved X-ray crystal structures. Another search on amino acids gave 223 hits but only eight zwitterionic polymorphs of amino acids resulted from this search. There are no neutral–zwitterionic polymorph sets for amino acids at the present time in the CSD.

^{13}C ss-NMR Spectroscopy. Solid-state NMR spectra were recorded on a Bruker Advance spectrometer operating at 400 MHz (100 MHz for ^{13}C nucleus). ss-NMR spectra were recorded on a Bruker 4 mm double resonance CP-MAS probe in zirconia rotors at 5.0 kHz spin rate with a cross-polarization contact time of 2.5 ms and a recycle delay of 8 s. ^{13}C CP-MAS spectra recorded at 100 MHz were referenced to the methylene carbon of glycine and then the chemical shifts were recalculated to the TMS scale ($\delta_{\text{glycine}} = 43.3$ ppm).

Thermal Analysis. DSC was performed on Mettler Toledo DSC 822e module. Samples were placed in crimped but vented aluminum sample pans. The typical sample size was 3-4 mg, and the temperature range was 30-250 °C at heating rate of 5 °C/min. Samples were purged by a stream of dry nitrogen flowing at 150 mL/min.

Dissolution and Solubility Measurements. Intrinsic dissolution rate (IDR) and solubility measurements were carried out on a USP certified Electrolab TDT-08 L dissolution tester (Electrolab, Mumbai, MH, India). A calibration curve was obtained for all aminobenzoic acids molecules and its polymorphs by plotting absorbance vs. concentration UV-vis spectra curves on a Thermo Scientific Evolution EV300 UV-vis spectrometer (Waltham, MA) for known concentration solutions in water and 60% EtOH–water medium. The mixed solvent system (EtOH–water) was selected for its higher solubility of CLX polymorphs in this medium. The slope of the plot from the standard curve gave the molar extinction coefficient (ϵ) by applying the Beer-Lambert's law. Equilibrium solubility was determined in water for 2-ABA, 3-ABA and salicylic acids and 60% EtOH–water medium for CLX polymorphs using the shake-flask method. To obtain equilibrium solubility, 100 mg of each solid material was stirred for 24 h in 5 mL of water for ABA polymorphs and 60% EtOH–water for CLX polymorphs at 37 °C, and the absorbance was measured at 318 nm and 327 nm for 2-ABA and 3-ABA polymorphs, and 289 nm for CLX polymorphs. The concentration of the saturated solution was calculated at 24 h, which is referred to as

the equilibrium solubility of the stable solid form. The dissolution rates are obtained from the IDR experiments.

Powder X-ray Diffraction. PXRDs were recorded on a SMART Bruker D8 Advance X-ray diffractometer (Bruker-AXS, Karlsruhe, Germany) in the Bragg-Brentano geometry using Cu-K α X-ray radiation ($\lambda = 1.5406 \text{ \AA}$) at 40 kV and 30 mA. Diffraction patterns were collected over the 2θ range of $5\text{--}50^\circ$ at a scan rate of $1^\circ/\text{min}$. The appearance of polymorphs for all the molecules was monitored by the appearance of new diffraction peaks. Powder Cell 2.359²⁸ was used for overlaying the experimental XRPD pattern on the calculated lines from the crystal structure. Variable temperature mode fixed on the same instrument and recorded the phase transition with 600-1200 s delay time at a heating rate of $2^\circ\text{C}/\text{min}$.

pK_a Calculation. pK_a values were calculated using ChemAxon software for all the ampholytes. These values are calculated theoretically in aqueous medium. This software is available in free of cost in this website <http://www.chemaxon.com> as Marvin 6.0.1, 2013, ChemAxon software.

3.9 References

1. (a) V. López-Mejías, J. Kampf, A. Matzger, *J. Am. Chem. Soc.* **2012**, *134*, 9872; (b) J. Haleblan, W. C. McCrone, *J. Pharm. Sci.* **2006**, *58*, 911; (c) S. R. Byrn, R. R. Pfeiffer, J. G. Stowell, *Solid-State Chemistry of Drugs*. 2nd ed.; SSCI Inc.: West Lafayette, **1999**; (d) J. Dunitz, A. Gavezzotti, *J. Phys. Chem. B*, **2012**, *116*, 6740; (e) K. Allen, R. J. Davey, E. Ferrari, C. Towler, G. J. T. Tiddy, M. Jones, R. G. Pritchard, *Cryst. Growth Des.* **2002**, *2*, 523; (f) M. Kitamura, *CrystEngComm* **2009**, *11*, 949; (g) F. H. Allen, *Acta Crystallogr., Sect. B* **2002**, *B58*, 380; (h) D. J. W. Grant, *Polymorphism in Pharmaceutical Solids*, H. G. Brittain, Ed. Marcel Dekker Inc.: New York, **1999**, pp 1-32; (i) J.W. Mullin, *Crystallization*, 4th Ed. Butterworth-Heinemann: Oxford, U.K., **2001**; (j) W. C. McCrone, *Polymorphism in Physics and Chemistry of the Organic Solid-State*, Vol. 2, Eds. D. Fox, M. M. Labes, and A. Weissberger, Wiley-Interscience, New York, **1965**, p. 725; (k) D. Braga, F. Grepioni, *Making Crystals by Design*, John-Wiley, **2007**, p. 348.

2. (a) A. Maher, Å. C. Rasmuson, D. M. Croker, B. K. Hodnett, *J. Chem. Eng. Data.* **2012**, *57*, 3525; (b) M. Bartolomei, P. Bertocchi, M. C. Ramusino, N. Santucci, L. Valvo, *J. Pharm. Biomed. Anal.* **1999**, *21*, 299; (c) A. Avdeef, *Solubility, in Absorption and Drug Development: Solubility, Permeability, and Charge State*, 2nd Eds. John-Wiley, USA, **2012**, p. 251. (d) C. Lipinski, F. Lombardo, B. Dominy, P. Feeney, *Adv. Drug Del. Rev.* **2001**, *46*, 3; (e) C. Lipinski, *J. Pharmacol. Toxicol. Methods*, **2000**, *44*, 235; (f) K. Urakami, Y. Shono, A. Higashi, K. Umemoto, M. Godo, *Bull. Chem. Soc. Jpn.* **2002**, *75*, 1241; (g) Y. A. Abramov, K. Pencheva, *Thermodynamics and Relative Solubility Prediction of Polymorphic Systems, In Chemical Engineering in the Pharmaceutical Industry: R&D to Manufacturing*, (Ed. D. J. am Ende), John-Wiley, USA, **2010**, p. 477.
3. (a) J. Bauer, S. Spanton, R. Henry, J. Quick, W. Dziki, W. Porter, J. Morris, *Pharm. Res.* **2001**, *18*, 859; (b) P. Sanphui, B. Sarma, A. Nangia, *J. Pharm. Sci.* **2011**, *100*, 2287; (c) S. Cherukuvada, R. Thakuria, A. Nangia, *Cryst. Growth. Des.* **2010**, *10*, 3931; (d) S. R. Johnson, X.-Q. Chen, D. Murphy, O. Gudmundsson, *Mol. Pharm.*, **2007**, *4*, 513; (e) R. Lalit, P. Sanphui, G. R. Desiraju, *Cryst. Growth. Des.*, **2010**, *13*, 3681.
4. (a) N. J. Babu, A. Nangia, *Cryst. Growth Des.* **2011**, *11*, 2662; (b) A. Serajuddin, *Adv. Drug Del. Rev.*, **2007**, *59*, 603; (c) A. Llinàs, R. C. Glen, J. M. Goodman, *J. Chem. Inf. Model.* **2008**, *48*, 1289; (d) J. Alsenz, M. Kansy *Adv. Drug Del. Rev.* **2007**, *59*, 546. (e) D. Giron, *Thermochim. Acta* **1995**, *248*, 1.
5. (a) H. Bordallo, E. Boldyreva, A. Buchsteiner, M. Koza, S. J. Landsgesell, *Phys. Chem. B* **2008**, *112*, 8748; (b) B. D. Hamilton, M. A. Hillmyer, M. D. Ward, *Cryst. Growth Des.*, **2008**, *8*, 3368; (c) J. Huang, L. Yu, *J. Am. Chem. Soc.*, **2006**, *128*, 1873; (d) S. A. Moggach, S. Parsons, P. A. Wood, *Cryst. Rev.*, **2008**, *14*, 143; (e) M. Jamróz, J. Rode, S. Ostrowski, P. Lipiński, J. Dobrowolski, *J. Chem. Inf. Model.* **2012**, *52*, 1462; (f) T. Luker, R. Bonnert, S. Paine, J. Schmidt, C. Sargent, A. Cook, A. Cook, P. Gardiner, S. Hill, C. Weyman-Jones, *J. Med. Chem.* **2011**, *54*, 1779; (g) R. Flaig, T. Koritsanszky, B. Dittrich, A. Wagner, P. Luger, *J. Am. Chem. Soc.* **2002**, *124*, 3407.
6. (a) N. K. Nath, S. S. Kumar, A. Nangia, *Cryst. Growth Des.* **2011**, *11*, 4594; (b) P. A. Williams, C. E. Hughes, G. K. Lim, B. M. Kariuki, K. D. M. Harris, *Cryst. Growth Des.*, **2012**, *12*, 3104; (c) L. Orola, M. Veidis, I. Sarcevic, A. Actins, S. Belyakov, A. Platonenko, *Int. J. Pharm.* **2012**, *432*, 50; (d) A. Trask, N. Shan, W. D. S. Motherwell, W. Jones, S. Feng, R. B. H. Tan, K. Carpenter, *Chem. Commun.* **2005**, 880; (e) M. Takasuka, H. Nakai, M. Shiro,

- J. Chem. Soc., Perkin Trans. 2* **1982**, 1061; (f) S. Long, S. Parkin, M. A. Siegler, A. Cammers, T. Li, *Cryst. Growth Des.* **2008**, *8*, 4006; (g) S. Long, T. Li, *Cryst. Growth Des.* **2009**, *9*, 4993; (h) S. Mahapatra, K. N. Venugopala, T. N. G. Row, *Cryst. Growth Des.* **2010**, *10*, 1866; (i) F. P. A. Fabbiani, B. Dittrich, A. J. Florence, T. Gelbrich, M. B. Hursthouse, W. F. Kuhs, N. Shankland, H. Sowa, *CrystEngComm*, **2009**, *11*, 1396.
7. (a) G. E. Hardy, W. C. Kaska, B. P. Chandra, J. I. Zink, *J. Am. Chem. Soc.* **1981**, *103*, 1074; (b) W. H. Ojala, M. C. Etter, *J. Am. Chem. Soc.* **1992**, *114*, 10288; (c) P. W. Carter, M. D. Ward, *J. Am. Chem. Soc.* **1994**, *116*, 769; (d) C. J. Brown, M. Ehrenberg, *Acta Crystallogr., Sect. C* **1985**, *C41*, 441; (e) H. Takazawa, S. Ohba, Y. Saito, *Acta Crystallogr., Sect. C* **1986**, *C42*, 1880; (f) T. H. Lu, P. Chattopadhyay, F. L. Liao, J. M. Lo, *Anal. Sci.* **2001**, *17*, 905; (g) P. Bag, C. M. Reddy, *Cryst. Growth Des.*, **2012**, *12*, 2740; (h) J. Voogd, B. H. M. Verzijl, A. J. M. Duisenberg, *Acta Crystallogr., Sect. B* **1980**, *36*, 2805; (i) M. Svärd, F. L. Nordström, T. Jasnobulka, Å. C Rasmuson, *Cryst. Growth Des.* **2010**, *10*, 195; (j) V. López-Mejías, J. W. Kampf, A. J. Matzger, *J. Am. Chem. Soc.* **2009**, *131*, 4554; (k) E. H. Lee, S. R. Byrn, M. T. Carvajal, *Pharm. Res.* **2006**, *23*, 2375.
 8. (a) K. Tam, A. Avdeef, O. Tsinman, N. Sun, *J. Med. Chem.*, **2010**, *53*, 392; (b) C. Towler, R. Davey, R. Lancaster, C. Price, *J. Am. Chem. Soc.*, **2004**, *126*, 13347; (c) V. Y. Torbeev, E. Shavit, I. Weissbuch, L. Leiserowitz, M. Lahav, *Cryst. Growth Des.*, **2005**, *5*, 2190; (d) K. Srinivasan, K. R. Devi, S. A. Azhagan, *Cryst. Res. Technol.* **2011**, *46*, 159.
 9. (a) M. Varma, I. Gardner, S. Steyn, P. Nkansah, C. Rotter, C. Whitney-Pickett, H. Zhang, L. Di, M. Cram, K. Fenner, A. El-Kattan, *Mol. Pharm.* **2012**, *9*, 1199. (b) G. Bouchard, A. Pagliara, P.-A. Carrupt, B. Testa, V. Gobry, H. Girault, *Pharm. Res.* **2002**, *19*, 1150; (c) M. Sznitowska, S. Janicki, T. Gos, *Int. J. Pharm.* **1996**, *137*, 125; (d) A. Avdeef, *Curr. Top. Med. Chem.* **2001**, *1*, 277; (e) A. Pagliara, P.-A. Carrupt, G. Caron, P. Gaillard, B. Testa, *Chem. Rev.*, **1997**, *97*, 3385.
 10. (a) K. Mazák, B. Noszál, *J. Med. Chem.* **2012**, *55*, 6942; (b) K. Mazák, G. Tóth, J. Kökösi, B. Noszál, *Eur. J. Pharm. Sci.* **2012**, *47*, 921; (c) G. Tóth, K. Mazák, S. Hosztafi, J. Kökösi, B. Noszál, *J. Pharm. Biomed. Anal.* **2013**, *76*, 112; (d) K. J. Okolotowicz, M. Dwyer, E. Smith, J. R. Cashman, *J. Biochem. Mol. Toxicol.* **2013**, *28*, 23.
 11. (a) A. O. Surov, I. V. Terekhova, A. Bauer-Brandl, G. L. Perlovich, *Cryst. Growth Des.* **2009**, *9*, 3265; (b) P. Moser, A. Sallmann, I. Wiesenberger, *J. Med. Chem.* **1990**, *33*, 2358; (c) G. L. Perlovich, A. O. Surov, L. K. Hansen,

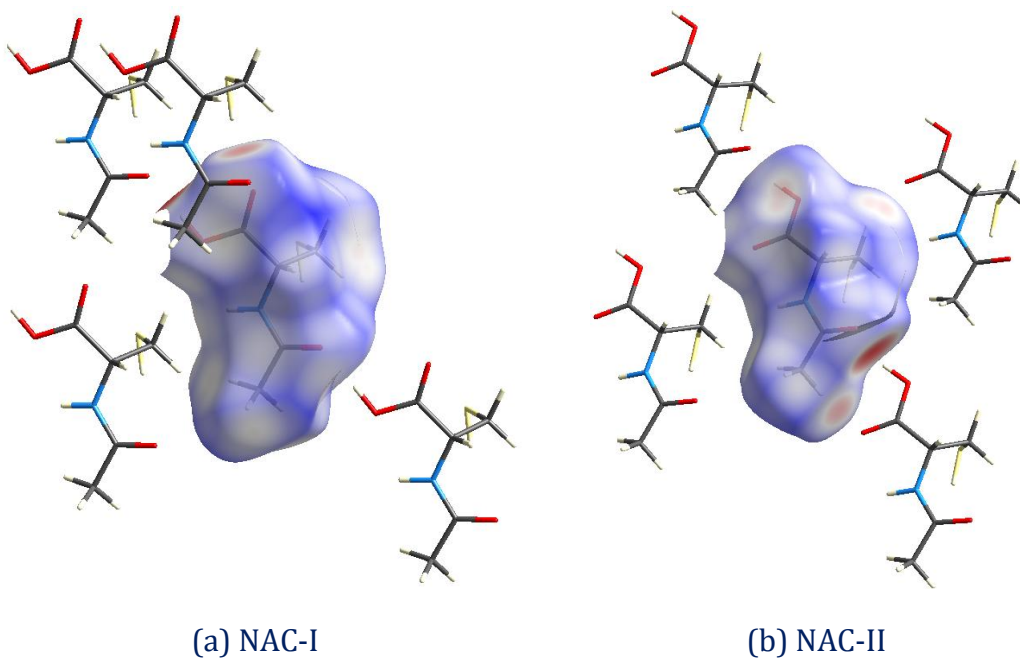
- A. B. Brandl, *J. Pharm. Sci.* **2007**, *96*, 1031; (d) E. Hee, E. H. Lee, S. X. M. Boerrigter, S. R. Byrn, *Cryst. Growth Des.* **2010**, *10*, 518; (e) A. O. Surov, P. Szterner, W. Zielenkiewicz, G. L. Perlovich, *J. Pharm. Biomed. Anal.* **2009**, *50*, 831.
12. (a) F. Bertinotti, C. Giacomello, *Acta Crystallogr.* **1954**, *7*, 808. (b) S. Kornblum, B. Sciarrone, *J. Pharm. Sci.* **1964**, *53*, 935; (c) A. Apelblat, E. Manzurola, *J. Chem. Thermodyn.* **1999**, *31*, 869; (d) V. André, D. Braga, F. Grepioni, M. T. Duarte, *Cryst. Growth Des.* **2009**, *9*, 5108; (e) R. Montis, M. B. Hursthouse, *CrystEngComm* **2012**, *14*, 5242; (f) Z. Banić-Tomišić, B. Kojić-Prodić, I. Širola, *J. Molec. Struct.* **1997**, *416*, 209; (g) R. T. Forbes, P. York, J. R. Davidson, *Int. J. Pharm.* **1995**, *126*, 199; (h) D. L.; French, J. W. Mauger, *Pharm. Res.* **1993**, *10*, 1285; (i) G. Lichtenstein, *Gastroenterol. Hepatol.* **2009**, *5*, 65.
13. (a) J. Bernstein, R. J. Davey, J. O. Henck, *Angew. Chem., Int.*, **1999**, *38*, 3441; (b) P. Munshi, K. N. Venugopala, B. S. Jayashree, T. N. G. Row, *Cryst. Growth Des.* **2004**, *4*, 1105; (c) S. Long, M. A. Siegler, A. Mattei, T. Li, *Cryst. Growth Des.*, **2011**, *11*, 414; (d) S. Long, S. Parkin, M. Siegler, C. P. Brock, A. Cammers, T. Li, *Cryst. Growth Des.*, **2008**, *8*, 3137.
14. Cambridge Structural Database, ver. 5.34, ConQuest 1.15, November 2012 release, May **2013** update, Cambridge Crystallographic Data Center, www.ccdc.cam.ac.uk.
15. (a) G. R. Desiraju, *Chem. Commun.* **1997**, 1475; (b) M. C. Etter, *Acc. Chem. Res.* **1990**, *23*, 120; (c) G. R. Desiraju, J. J. Vittal, A. Ramanan, *Crystal Engineering: A Textbook*, World Scientific, **2011**, p. 25.
16. (a) J. J. McKinnon, M. A. Spackman, A. S. Mitchell, *Acta Crystallogr. Sect. B* **2004**, *B60*, 627; (b) M. A. Spackman, D. Jayatilaka, *CrystEngComm* **2009**, *11*, 19; (c) S. S. Kumar, A. Nangia, *CrystEngComm* **2013**, *15*, 6498; (d) V. S. Minkov, N. A. Tumanov, R. Q. Cabrerabc, E. V. Boldyreva, *CrystEngComm* **2010**, *12*, 2551.
17. (a) A. Nangia, *Acc. Chem. Res.* **2008**, *41*, 595; (b) A. Nangia, *Models, Mysteries and Magic of Molecules*, Eds. J. C. A. Boeyens, and J. F. Ogilvie, Springer, **2008**, p. 63.
18. S. S. Kumar, S. Rana, A. Nangia, *Chem. Asian J.* **2013**, *8*, 1551.
19. A. J. Cruz-Cabeza, *CrystEngComm* **2012**, *14*, 6362.

20. (a) V.S. Minkov, S.V. Goryainov, E.V. Boldyreva, C. H. Görbitz, *J. Raman Spectrosc.* **2010**, *41*, 1748; (b) A. Y. Lee, I. S. Lee, A. S. Myerson, *Chem. Eng. Technol.* **2006**, *29*, 281; (c) E. Ramachandran, K. Baskaran, S. Natarajan, *Cryst. Res. Technol.* **2007**, *42*, 73; (d) A. S. Sabino, G. P. D. Sousa, C. Luz-Lima, P. T. C. Freire, F. E. A. Melo, J. Filho, *Solid State Comm.* **2009**, *149*, 1553.
21. (a) A. R. Sheth, J. W. Lubach, E. J. Munson, F. X. Muller, D. J. W. Grant, *J. Am. Chem. Soc.* **2005**, *127*, 6641; (b) M. R. Chierotti, L. Ferrero, N. Garino, R. Gobetto, L. Pellegrino, D. Braga, F. Grepioni, L. Maini, *Chem. Eur. J.* **2010**, *16*, 4347; (c) H. G. Brittain, K. Morris, D. Bugay, A. Thakur, A. Serajuddin, *J. Pharm. Biomed. Anal.*, **1993**, *11*, 1063; (d) S. Sen, P. Yu, S. Risbud, R. Dick, D. Deamer, *J. Phys. Chem. B* **2006**, *110*, 18058; (e) M. Strohmeier, D. Stueber, D. M. Grant, *J. Phys. Chem. A* **2003**, *107*, 7629; (f) H. L. Schmidt, L. J. Sperling, Y. G. Gao, B. J. Wylie, J. M. Boettcher, S. R. Wilson, C. M. Rienstra, *J. Phys. Chem. B* **2007**, *111*, 14362; (g) D. Geppi, G. Mollica, S. Borsacchi, C. Veracini, *Applied Spectro. Rev.* **2008**, *43*, 202.
22. (a) V.S. Minkov, Y. A. Chesalov, E.V. Boldyreva, *J. Struct. Chem.* **2008**, *49*, 1061; (b) Jr. A. A. Ebert, H. B. Gottlieb, *J. Am. Chem. Soc.* **1952**, *74*, 2806; (c) N. Colthup, L.H. Daly, S. E. Wiberley, *Introduction to Infrared and Raman Spectroscopy*. 3rd Ed.; Academic Press: Boston, **1990**.
23. (a) H. Wu, N. Reeves-McLaren, S. Jones, R. I. Ristic, *Cryst. Growth Des.* **2010**, *10*, 988; (b) S. Vippagunta, H. G. Brittain, D. J. W. Grant, *Adv. Drug. Del. Rev.* **2001**, *48*, 3; (c) E. Boldyreva, V. Drebuschak, I. Paukov, Y. Kovalevskaya, T. Drebuschak, *J. Therm. Anal. Calori.* **2004**, *77*, 607; (d) B. Kolesov, V. Minkov, E. V. Boldyreva, T. Drebuschak, *J. Phys. Chem. B* **2008**, *112*, 12827; (e) J. Zeitler, D. Newnham, P. Taday, T. Threlfall, R. Lancaster, R. Berg, C. Strachan, M. Pepper, K. Gordon, T. Rades, *J. Pharm. Sci.* **2006**, *95*, 2486; (f) M. Pranzo, D. Cruickshank, M. Coruzzi, M. Caira, R. Bettini, *J. Pharm., Sci.* **2010**, *99*, 3731.
24. (a) X. Yang, X. Wang, C. Ching, *J. Chem. Eng. Data* **2008**, *53*, 1133; (b) L. Lyn, H. Sze, A. Rajendran, G. Adinarayana, K. Dua, S. Garg, *Acta Pharm.* **2011**, *61*, 391; (c) R. Cantera, M. Leza, C. Bachiller, *J. Pharm., Sci.* **2002**, *91*, 2240; (d) S. Aitipamula, A. Nangia, *Polymorphism: Fundamentals and Applications. In Supramolecular Chemistry: From Molecules to Nanomaterials*, Eds. J. W. Steed and P. A. Gale, John-Wiley, pp. 2957-2974, **2012**; (e) J. Zhang, X. Tan, J. Gao, W. Fan, Y. Gao, and S. Qian, *J. Pharm. Pharmacol.* **2013**, *65*, 44; (d) M. R. Caira, S. A. Bourne, H. Samsodien, E. Engel, W. Liebenberg, N. Stieger, M. Aucamp, *CrystEngComm* **2012**, *14*,

- 2541; (f) N. Blagden, M. de Matas, P. Gavan, P. York, *Adv. Drug Del. Rev.* **2007**, *59*, 617; (g) Y. Qiu, Y. Chen, L. Liu, G. G. Z. Zhang, *Developing Solid Oral Dosage Forms: Pharmaceutical Theory and Practice*, 1st Ed., Academic Press, p. 75, **2009**; (h) J. H. Hildebrand, *Solubility*, The Chemical Catalog Company, New York, p. 206, **1924**.
25. (a) A. Newman, *Org. Process Res. Dev.* **2013**, *17*, 457; (b) J. An, W. Kim, *Cryst. Growth Des.* **2013**, *13*, 31; (c) J. An, J. Kim, S. Chang, W. Kim, *Cryst. Growth Des.* **2010**, *10*, 3044.
26. (a) S. C. McKellar, A. J. Urquhart, D. A. Lamprou, A. J. Florence, *ACS Comb. Sci.* **2012**, *14*, 155; (b) V. Lopez-Mejías, J. L. Knight, C. L. Brooks, A. J. Matzger, *Langmuir* **2011**, *27*, 7575; (c) Y. Diao, K. E. Whaley, M. E. Helgeson, M. A. Woldeyes, P. S. Doyle, A. S. Myerson, T. A. Hatton, B. L. Trout, *J. Am. Chem. Soc.* **2012**, *134*, 673; (d) S. Roy, A. J. Matzger, *Angew. Chem. Int. Ed.* **2009**, *48*, 8505.
27. (a) N. Zencirci, T. Gelbrich, V. Kahlenberg, U. J. Griesser, *Cryst. Growth Des.* **2009**, *9*, 3444; (b) J. Kendrick, R. Montis, M. B. Hursthouse, F. J. J. Leusen, *Cryst. Growth Des.* **2013**, *13*, 2906; (c) J. Cornel, C. Lindenberg, M. Mazzotti, *Cryst. Growth Des.* **2009**, *9*, 243.
28. N. Kraus, G. Nolze, Powder Cell, version 2.3, *A Program for Structure Visualization, Powder Pattern Calculation and Profile Fitting*; Federal Institute for Materials Research and Testing: Berlin, Germany, **2000**.

Chapter Four

Conformational Polymorphs of *N*-Acetyl-*L*-cysteine

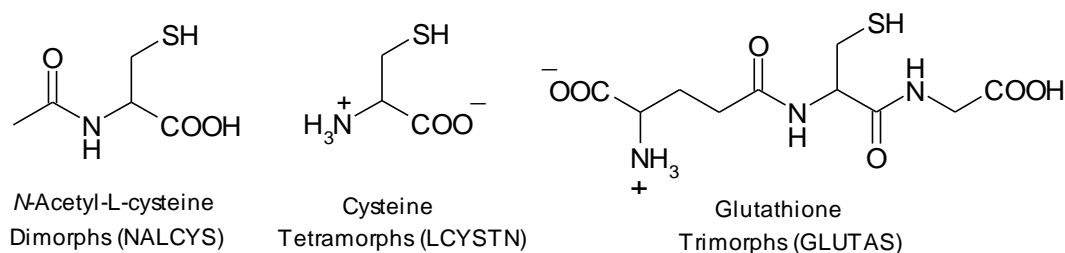


Discovery of a new polymorph of N-acetyl-L-cysteine and a rare case of differentiation based on the less common S-H...O hydrogen bond between the conformational polymorphs of NAC.

4.1 Introduction

N-Acetyl-L-cysteine, abbreviated as NAC {(2*R*)-2-acetamido-3-sulfanylpropanoic acid}, is used mainly in the treatment of acetaminophen overdose for more than 35 years. NAC (Scheme 4.1) is being sold as a dietary supplement commonly claiming antioxidant and liver protecting effects. Being an antioxidant, the drug has potential in the treatment of cancer and for preventing alcohol liver damage. It is also used for treating HIV infections, cardiovascular diseases, Alzheimer's disease, and metal toxicity.¹ It is a mucolytic agent, nutritional supplement, potent antioxidant, a scavenger for free radicals produced in cells, and a precursor of L-cysteine and glutathione. *N*-acetyl-L-cysteine (NAC) is emerging as a frontline agent in the treatment of psychiatric disorders addiction, compulsive and grooming disorders, schizophrenia and bipolar disorder.² Given its pharmaceutical significance and the fact that only one crystal structure of NAC is reported since the 1980s,³ (NALCYS and NALCYS02 in the CSD are multiple determinations of the same *P*1 structure), we decided to search for a new polymorph of NAC. Boldyreva and coworkers⁴ recently studied NAC under extreme conditions of high pressure (up to 9.5 GPa) and low temperature (down to 4 K, NALCYS10-15 in the CSD are redeterminations of the triclinic structure at different temperatures), with the idea to reduce side chain mobility, but they did not report any new crystalline phase of *N*-acetyl-L-cysteine. There were two motivations in this study at the outset: (1) the number of hydrogen bonding groups (COOH, NH-COCH₃, SH) means that possible competition for donor–acceptor pairing could lead to new polymorph; (2) being an acyclic chain backbone, there is possibility of different conformational states in crystallization. We report herein a new X-ray crystal structure of NAC (form II) and its characterization by ¹³C solid-state nuclear magnetic resonance (ss-NMR), Fourier transform infrared (FT-IR), Raman spectroscopy, powder X-ray diffraction (PXRD), and differential scanning calorimetry (DSC). Both polymorphs contain a *C*(7) chain

of $\text{COOH}\cdots\text{O}=\text{C}-\text{CH}_3$ hydrogen bonds except that the COOH group is rotated by 180° in form II to make an auxiliary $\text{C}-\text{H}\cdots\text{O}$ interaction with the methyl group in a $R_2^2(8)$ ring motif. This polymorphic set could well be the first example of the SH group engaged in $\text{S}-\text{H}\cdots\text{O}$ and $\text{N}-\text{H}\cdots\text{S}$ hydrogen bonding in form I but $\text{N}-\text{H}\cdots\text{S}$ interaction only in form II. Two sulfur-containing zwitterionic compounds, tetramorphic L-cysteine and trimorphic glutathione (Scheme 4.1) studied at variable temperature and pressure are related to NAC polymorphs in which they contain $\text{S}-\text{H}\cdots\text{O}$ and $\text{S}-\text{H}\cdots\text{N}$ interactions.⁵ Desiraju and Steiner noted that H-bonds formed by the SH group are weak, thus allowing rotation of the thiol group, leading to disorder in the structure.⁶ Both crystal structures of NAC are fully ordered. The intermolecular interactions in the two crystal structures were quantified by Hirshfeld surface analysis (d_{norm}) of 2D fingerprint plots,⁷ and 1D supramolecular constructs in XPac software.⁸



Scheme 4.1 Polymorphic set of SH containing active compounds in the CSD

4.2 Results and Discussion

4.2.1 Crystal structure analysis

Crystallization of NAC from water³ as well as common solvents (acetone, THF, dioxane, nitromethane, etc.) gave form I. Other crystallization techniques,⁹ such as melt and flash cooling, fast evaporation of solvent in a rotavap, grinding in mortar-pestle and ball mill, all gave the known triclinic cell. Crystallization of NAC from methanol gave a powdery material which was re-crystallized in MeOH/EtOH

multiple times to obtain long and thick plate morphology single crystals of a new polymorph (form II). The X-ray crystal structure was solved in orthorhombic space group $P2_12_12_1$ (see Appendix). The ORTEP diagrams are shown in Fig. 4.1. The bulk material for powder XRD was crystallized from MeOH.

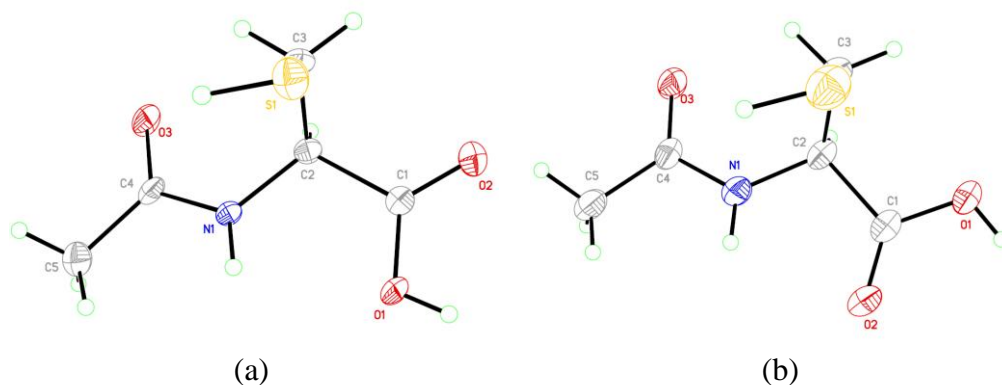


Figure 4.1 ORTEP of form I (a) and II (b) of NAC

The crystal structure of form I contains a $O1-H1\cdots O3$ catemer chain synthon¹⁰ (1.65 Å, 178°) of $C(7)$ graph set notation¹¹ between the COOH donor and $O=CCH_3$ acceptor (Fig. 4.2a). The molecular chains extend in a 2D arrangement via $C5-H9\cdots O2$ (2.72 Å, 151°) and $N1-H6\cdots S1$ (2.82 Å, 152°) interactions (Fig. 4.3a). There is an intramolecular $N-H\cdots OH$ hydrogen bond $S(5)$ motif (2.26 Å, 100°) (Fig. 4.1a). The crystal structure of form II is different in one major point, that the COOH group conformation is rotated by 180° compared to form I. So now the carbonyl acceptor of the COOH makes a $C-H\cdots O$ interaction with the CH_3 donor. Thus the catemer $C(7)$ chain of $O1-H1\cdots O3$ hydrogen bonds (1.66 Å, 164°) is stabilized by an auxiliary $C5-H7\cdots O2$ (2.36 Å, 132°), and the strong and weak interactions make a $R_2^2(8)$ ring motif (Fig. 4.2b). The 2D packing is similar to form I with $N1-H6\cdots S1$ (2.97 Å, 155°) and $C3-H4\cdots O1$ (2.56 Å, 141°) interactions (Fig. 4.3b). The intramolecular $N1-H6\cdots O2$ hydrogen bond (2.20 Å, 103°) is to a $C=O$ acceptor now.

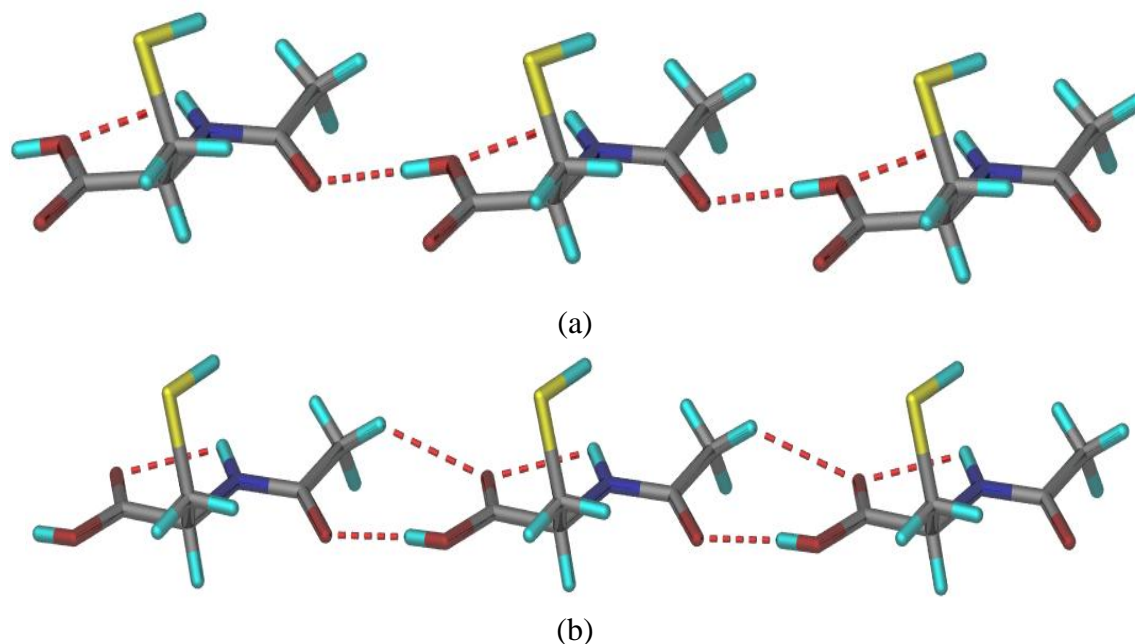


Figure 2 O–H···O hydrogen bond catemer in NAC polymorphs between COOH donor and O=C–CH₃ acceptor. (a) Form I, and (b) Form II. Note the change in conformation of COOH group and the additional C–H···O interaction in form II.

Apart from the conformational difference, another difference between forms I and II is the intermolecular hydrogen bond of the cysteine SH group. There is an S1–H5···O2 (2.15 Å, 164 °) hydrogen bond in form I (Fig. 4.4a) but such an interaction is absent in form II (Fig. 4.4b). In effect, the thiol group is acting as an H-bond donor and an acceptor in a cooperative chain, N1–H6···S1–H5···O2 motif. Even though the SH group is a significantly weaker donor than the OH group, S–H···O and N–H···S interactions have been systematically analyzed in crystal structures.¹² The SH group may be classified as a weak donor in organic structures but the degree of activation of its donor ability can become substantially strong depending on the environment in the crystal structure.⁶ Perhaps the shorter N–H···S H-bond in form I compared to that in form II (2.82, 2.97 Å) makes the SH donor slightly more activated in I to follow through with an S–H···O H-bond (Table 4.1). The SH group in form II participates only in a short contact with itself.

The contribution of intermolecular interactions to the crystal packing of form I and II was quantified by Hirshfeld surface analysis and 2D finger plots.⁷ The wings for the S \cdots H interaction penetrate deeper for form I (Fig. 4.5). Overall the plots are denser for form I than those for form II (more blue and red), due to the shorter/stronger interactions in the native crystal structure and tighter close packing. The sharp spikes in the fingerprint plot of form I and II at $d_e = d_i \approx 1.0$ Å indicates short O–H \cdots O interactions. The relative contributions of intermolecular interactions are given in Fig. 4.6a, and the Hirshfeld surfaces of neighboring molecules in form I and II are shown in Fig. 4.6b,c.

Table 4.1 Hydrogen bonds in crystal structures (neutron-normalized distances).

Interactions	H \cdots A /Å	D \cdots A /Å	\angle D–H \cdots A /°	Symmetry code
Form I				
O1–H1 \cdots O3	1.65	2.608(3)	178	-1+x,y,-1+z
S1–H5 \cdots O2	2.15	3.484(4)	164	x,y,1+z
N1–H6 \cdots O1	2.26	2.639(4)	100	Intramolecular
C3–H3 \cdots O3	2.54	3.128(3)	113	Intramolecular
N1–H6 \cdots S1	2.82	3.768(3)	152	x-1,+y,+z-1
C5–H9 \cdots O2	2.72	3.561(4)	151	x+1,+y+1,+z+1
C3–H4 \cdots O2	2.63	2.913	96	Intramolecular
Form II				
O1–H1 \cdots O3	1.66	2.611(4)	164	x,+y-1,+z
N1–H6 \cdots O2	2.20	2.614(4)	103	Intramolecular
C3–H3 \cdots O3	2.50	3.130(5)	116	Intramolecular
C5–H7 \cdots O2	2.36	3.192(5)	132	x,+y+1,+z
N1–H6 \cdots S1	2.97	3.923(3)	155	x,+y+1,+z
C3–H4 \cdots O1	2.56	3.475(4)	141	x-1/2,-y+1/2+1,-z+1

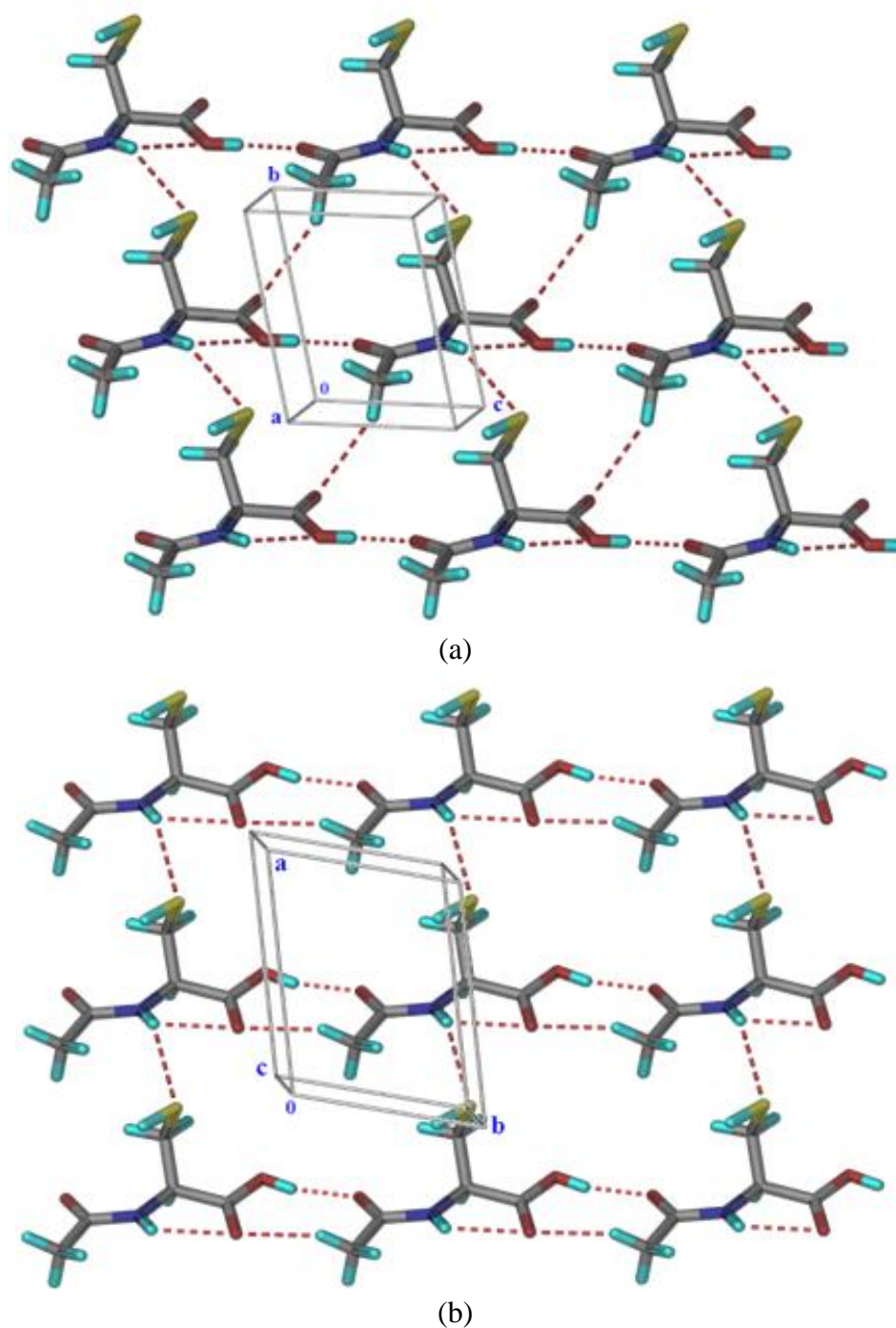


Figure 4.3 2D network of C–H \cdots O and N–H \cdots S intermolecular hydrogen bonds in form I (a) and form II (b).

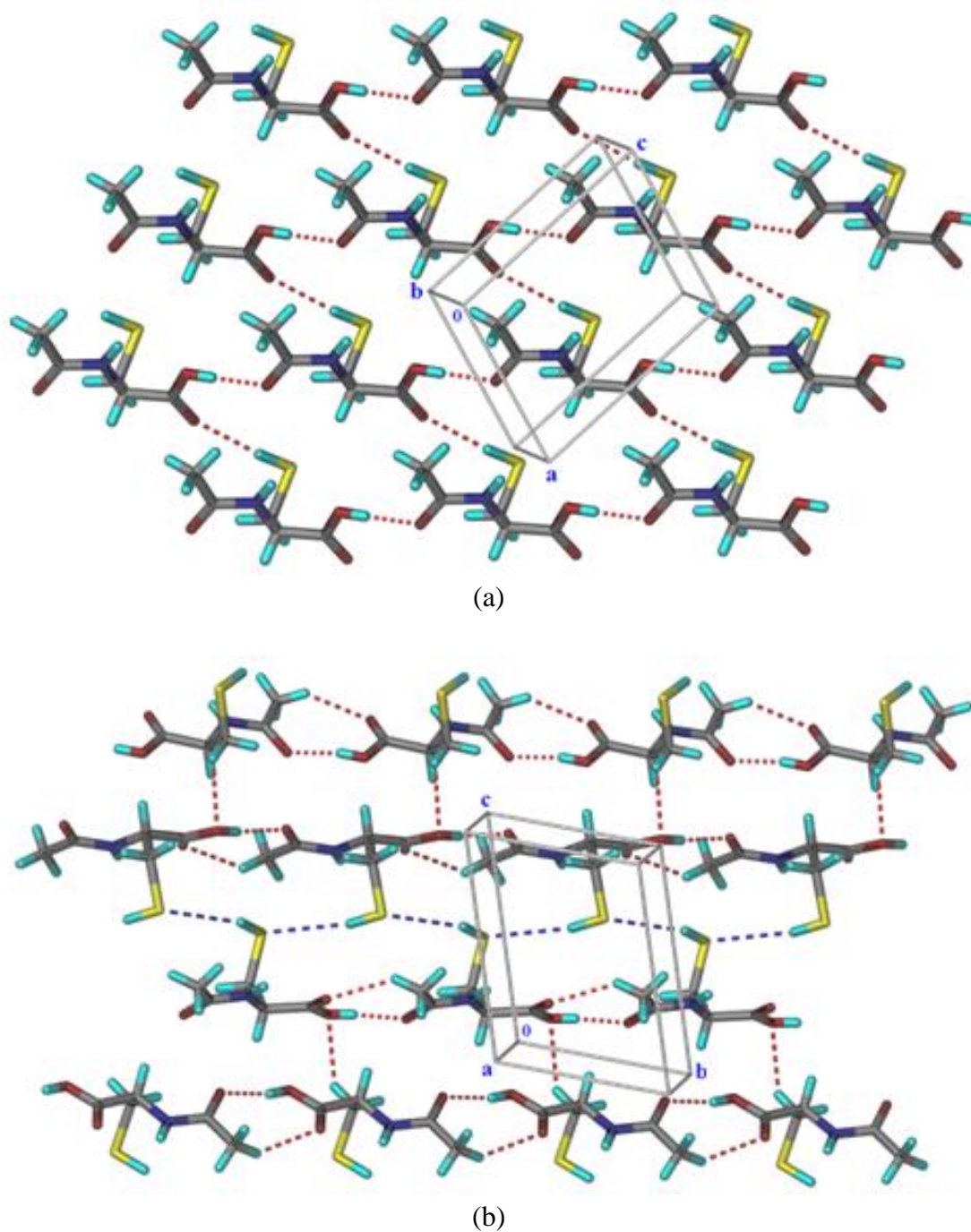


Figure 4.4 (a) 2D network of S–H \cdots O and O–H \cdots O hydrogen bonds in form I. (b) C–H \cdots O hydrogen bonds (red dots) and S–H \cdots S short contacts (blue dots) in form II.

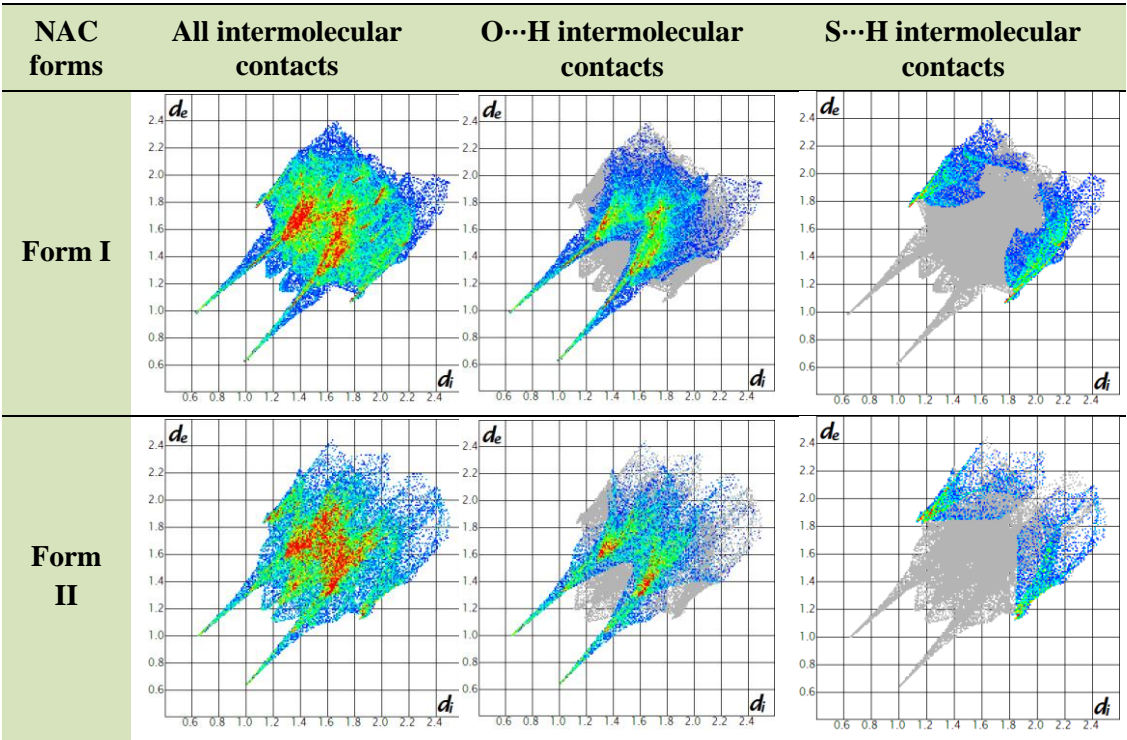
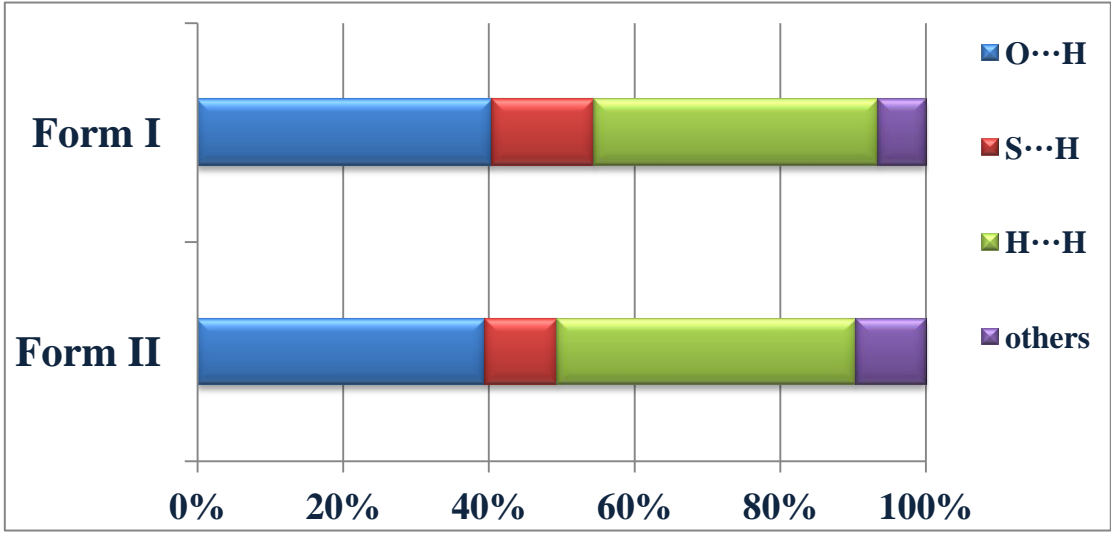


Figure 4.5 Hirshfeld surface 2D Fingerprint plots for different intermolecular interactions in form I and II of NAC.



(a)

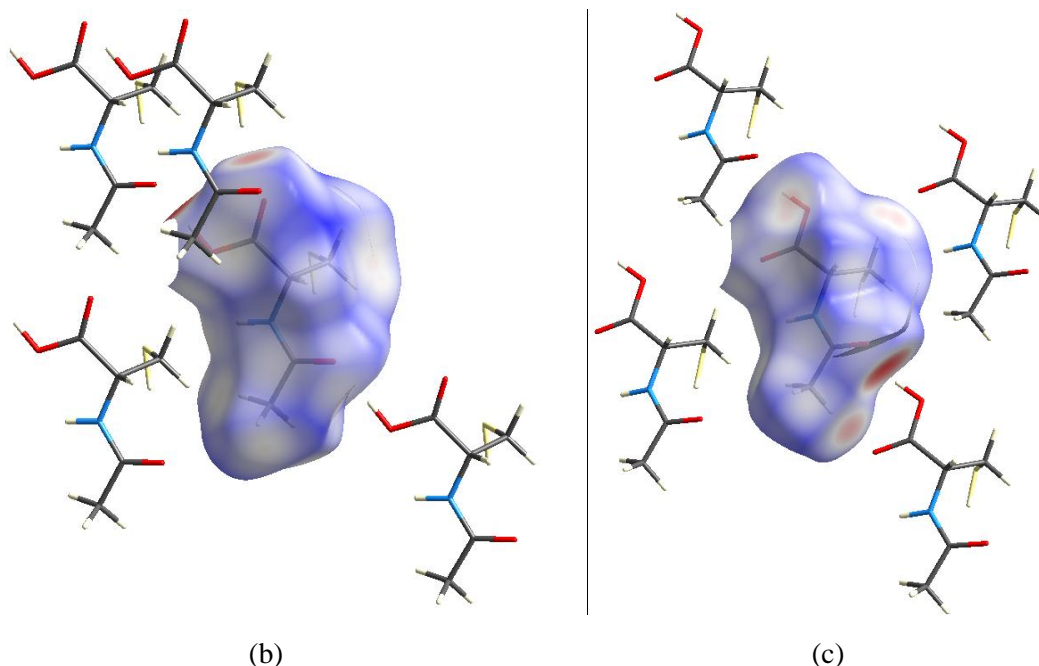
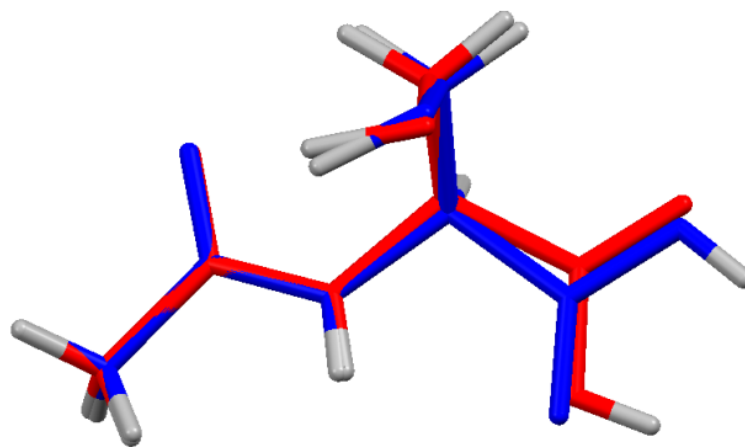


Figure 4.6 (a) The contribution of different intermolecular interactions to the Hirshfeld surface in form I and II. Hirshfeld surface maps of (b) form I and (c) form II of NAC with the neighboring molecules to show the significant intermolecular hydrogen bonds.

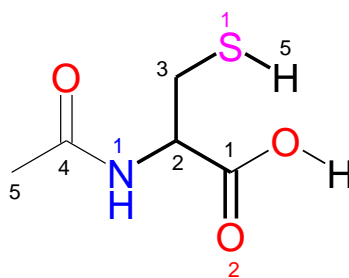
An overlay of the molecules in the two polymorphs (Fig. 4.7a) shows that the only difference is rotation of the COOH group, while the other bonds overlay nicely (torsion angles are listed in Table 4.2). The single bond rotations which cause the main conformation difference are highlighted in bold (Fig. 4.7b). The degree of similarity between the polymorphs was quantified in XPac⁸ as 5.2 (Fig. 4.8b) using the 1D supramolecular constructs of Fig. 4.8a. A value of 5.2 implies that the two polymorphs are dissimilar.

Table 4.2 Torsion angles in polymorphs.

Crystal Form	Torsion angle (°)	Torsion angle (°)	Torsion angle (°)
	τ_1 (H5–S1–C3–C2)	τ_2 (O2–C1–C2–N1)	τ_3 (C4–N1–C2–C3)
Form I	82.50(1)	177.08(1)	72.55(1)
Form II	64.99(1)	5.77(2)	68.11(1)

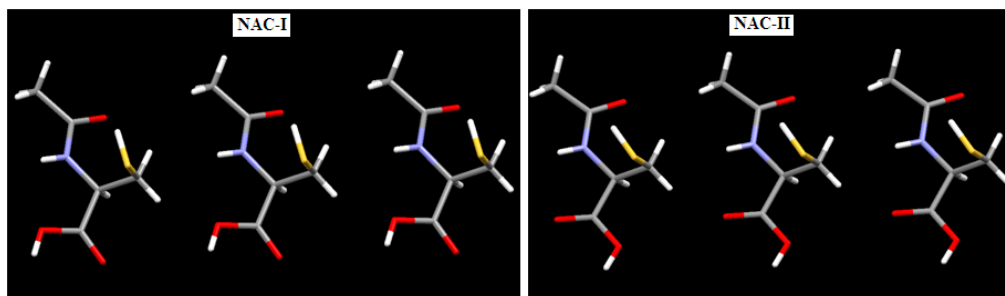


(a)

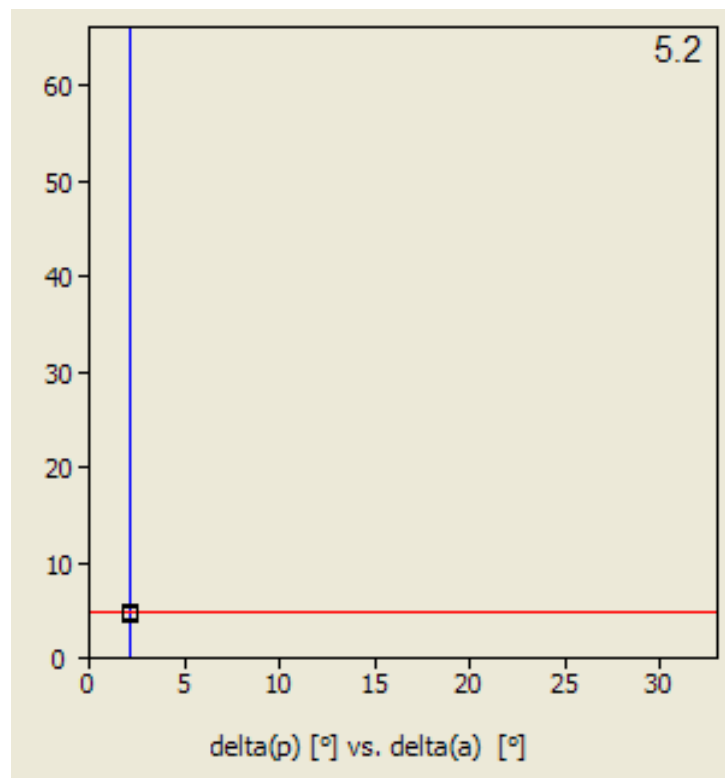


(b)

Figure 4.7 (a) Overlay of molecular conformations (red, form I; blue, form II), and (b) the main flexible rotations in the molecule are indicated by bold single bonds. Atom numbering of the crystal structure is followed.



(a)



(b)

Figure 4.8 1D supramolecular construct of form I and II (a) the plot of interplanar angular deviation vs. angular deviation ($^{\circ}$) in XPac with a similarity index of 5.2 (b).

4.2.2 Characterizations of NAC phases

The dimorphs of NAC were distinguished by ^{13}C ss-NMR and powder XRD. The chemical environment of the molecules in the solid-state is different when they adopt different molecular conformations in polymorphic structures (see Table 4.3 for chemical shift δ values). The two polymorphs showed significant differences in ^{13}C ss-NMR spectra of form I and form II for C3 and C4 carbon atoms (Fig. 4.9). The chemical shift methyl C4 moved slightly downfield in form II (172.3 ppm) compared to form I (171.6 ppm), possibly due to the electronegative environment of C5–H7 \cdots O2 interaction in form II. The chemical shift of C3 is different due to the proximal COOH group conformation change (form I 28.2 ppm, form II 25.2 ppm).

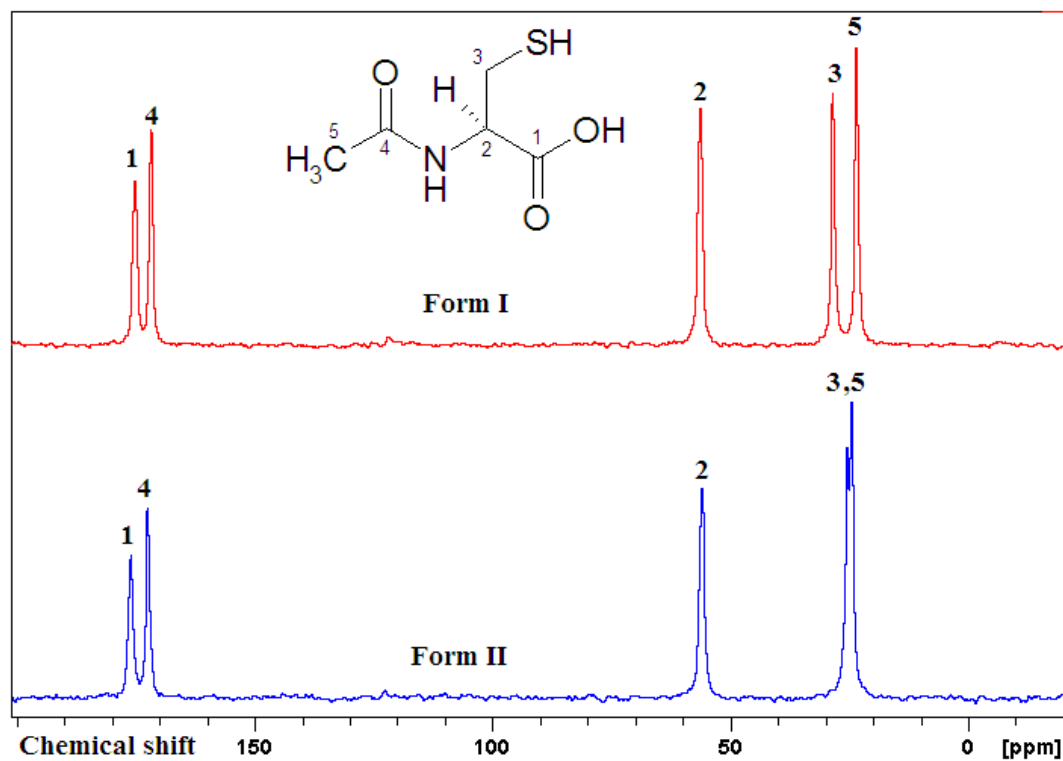


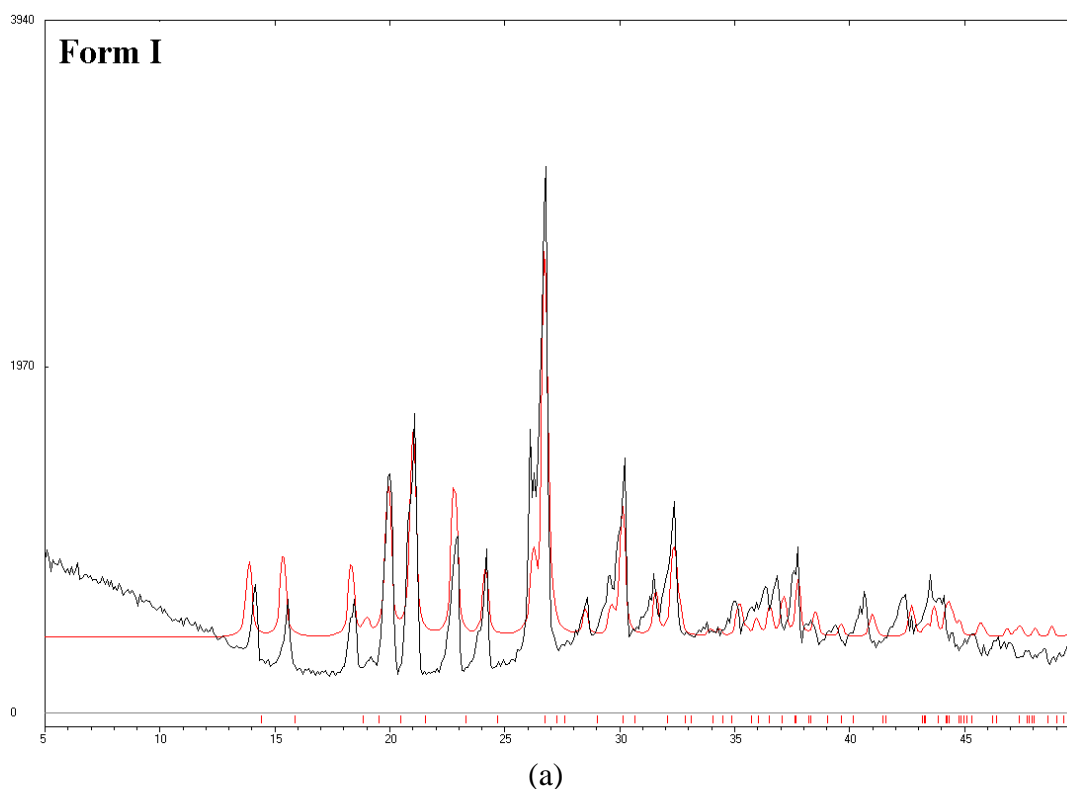
Figure 4.9 ^{13}C ss-NMR spectra of NAC polymorphs.

Table 4.3 Chemical shift (ppm) values of NAC polymorphs.

C atom	Form I	Form II
C1	175.02	175.90
C2	56.18	55.82
C3	28.29	25.24
C4	171.65	172.34
C5	23.34	24.40

The purity of the two forms was checked by powder XRD (Fig. 4.10). After confirming the bulk purity of the polymorphic materials, DSC analysis was carried out to understand their thermodynamic relationship. The T_{onset} for melting of form I

is 106.7 °C and form II at 101.5°C (Table 4.4). The two forms are enantiotropically related¹³ because the high melting polymorph I has a lower heat of fusion (16.0 kJ/mol) while the lower melting polymorph II has a higher enthalpy of fusion (20.3 kJ/mol). However, no phase transformation could be detected in DSC even at a slow heating rate of 2 °C/min (Fig. 4.11), which is contrary to the behavior for enantiotropes (it is monotropes which do not undergo phase transformation upon heating). A similar observation of enantiotropes being assigned based on enthalpy of fusion and melting point values, rather than an observable phase transition, was reported recently for metformin embonate salts.¹⁴ Hot stage microscopy visual images (Fig. 4.12) did not indicate any phase changes.



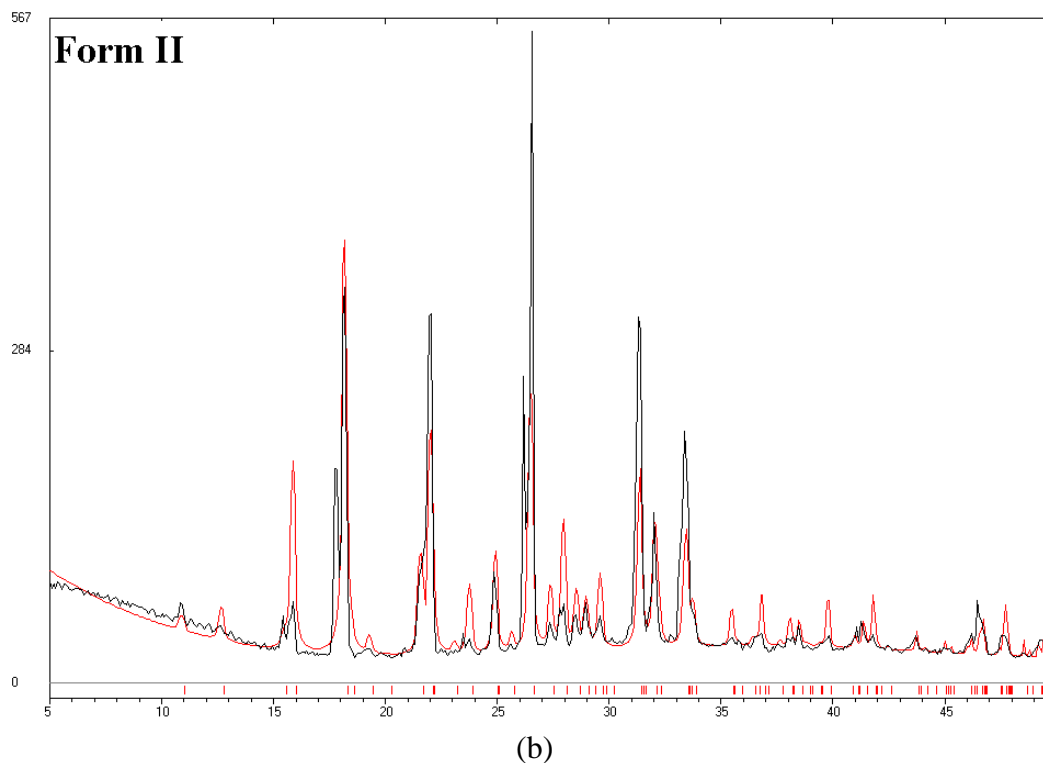


Figure 4.10 Overlay of experimental powder pattern (black) with the lines calculated - from the X-ray crystal structure (red). (a) Form I, and (b) form II.

Table 4.4 Stability parameters of NAC polymorphs.

NAC Forms	Density (g/cm ³)	Packing fraction (%)	Melting onset T _{onset} (°C)	Enthalpy of fusion H _f (kJ/mol)	Stability relation of polymorphs
Form I	1.48	70.9	106.76	16.07	Enantiotropic, form I is thermodynamic
Form II	1.46	70.2	101.58	20.37	

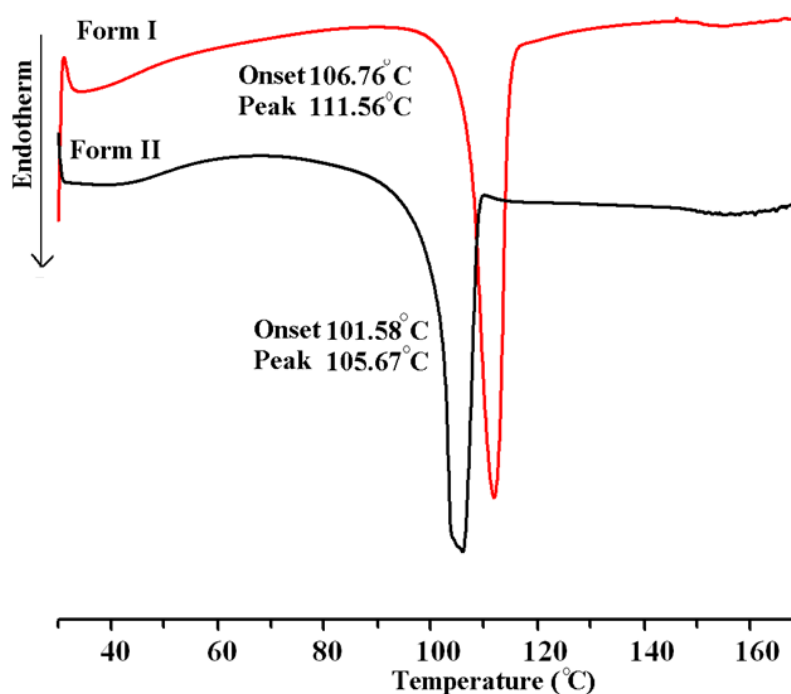


Fig. 4.11 DSC endotherms of form I and form II of NAC (heating rate 5 °C/min).

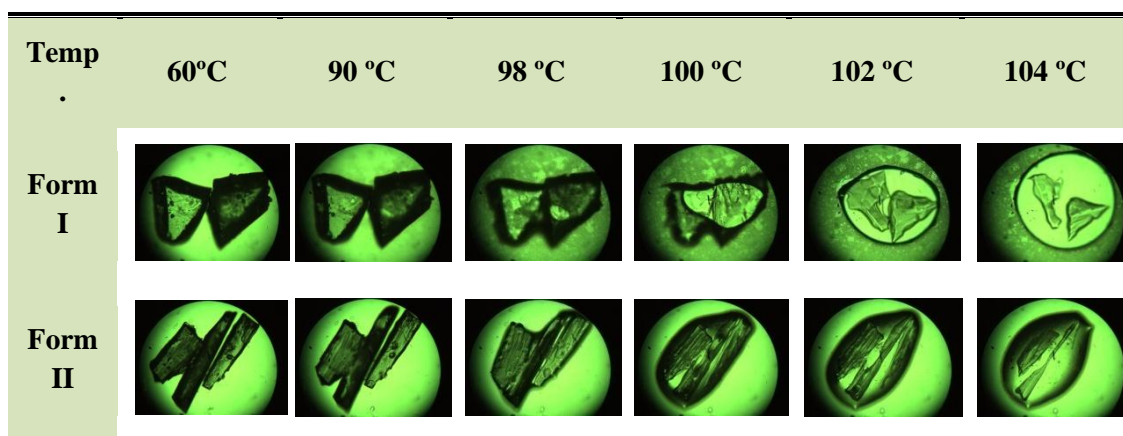


Figure 4.12 HSM images of polymorphs I and II of NAC upon heating.

4.2.3 Stability of polymorphs

The stability relation was further confirmed by FT-IR analysis. The N–H, C–H and C=O stretch are at lower wave numbers in form I compared to form II (3375,

3377 cm^{-1} ; 2925, 2930 cm^{-1} ; and 1716, 1718 cm^{-1} ; see Fig. 4.13, Table 4.5), which is consistent with shorter/ stronger intermolecular hydrogen bonds in form I, the stable modification (Table 4.1 and Hirshfeld surface analysis in Fig. 4.5). Raman frequencies of the polymorphs are given as additional spectral data (Table 4.6 and Fig. 4.14). Thus stronger hydrogen bonds, higher density and packing fraction, and higher melting point (Table 4.4), all mean that the thermodynamic modification is form I of NAC. As a final test of stability, when form II was ground in a mortar-pestle for 10-15 min or the ground slurry was stirred in n-heptane for 24 h, quantitative transformation of metastable form II to the stable form I was observed (see PXRD plots in Fig. 4.15). Polymorph II transformed to I after 3 months of storage in ambient conditions.

Table 4.5 Vibrational stretching frequency of NAC polymorphs.

FT-IR (cm^{-1})	N-H stretch	C-H stretch	Carboxylic C=O stretch	Carboxamide C=O stretch	S-H stretch	N-H bend
Form I	3375.4	2925.6	1716.4	1618.7	2547.5	1371.8
Form II	3377.4	2930.2	1717.8	1636.0	2547.8	1372.3

Table 4.6 Raman stretching frequency of NAC polymorphs.

FT-Raman (cm^{-1})	N-H stretch	C-H stretch	Carboxylic C=O stretch	Carboxamide C=O stretch	S-H stretch	N-H bend
Form I	3377.1	2935.2	1721.2	1603.8	2550.1	1375.0
Form II	3373.2	2934.8	1720.7	1587.0	2550.3	1375.6

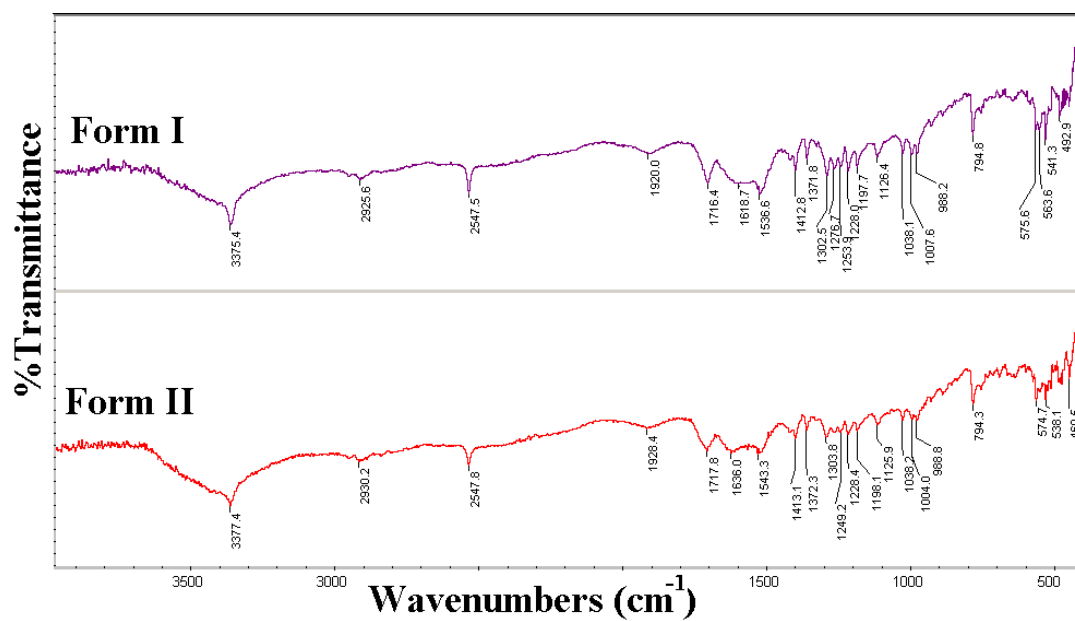


Figure 4.13 FT-IR of form I and form II of NAC.

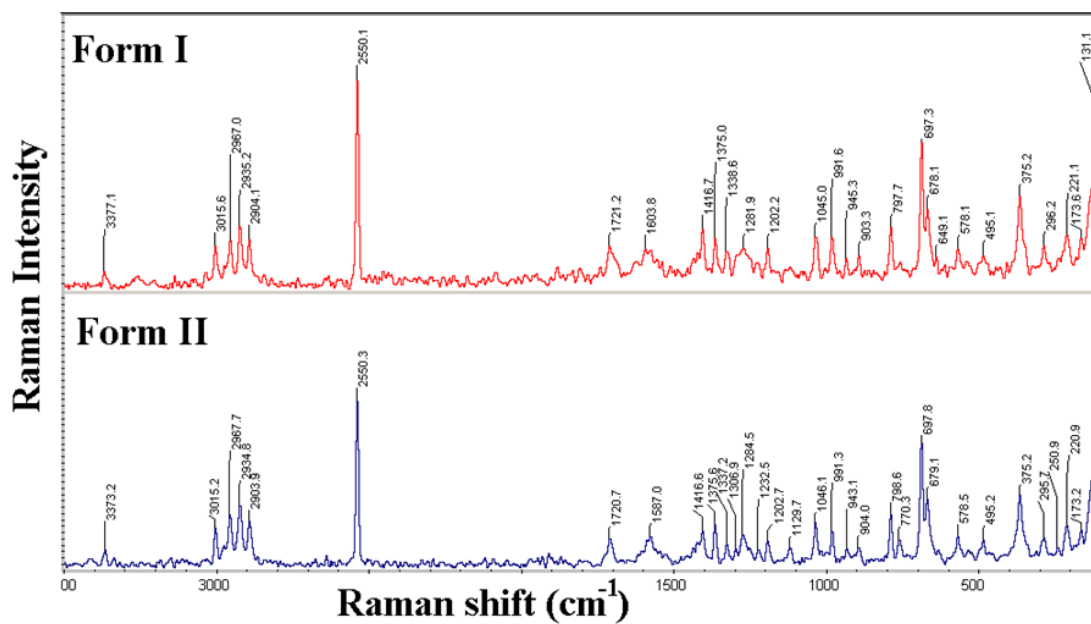


Figure 4.14 FT-Raman spectra NAC polymorphs.

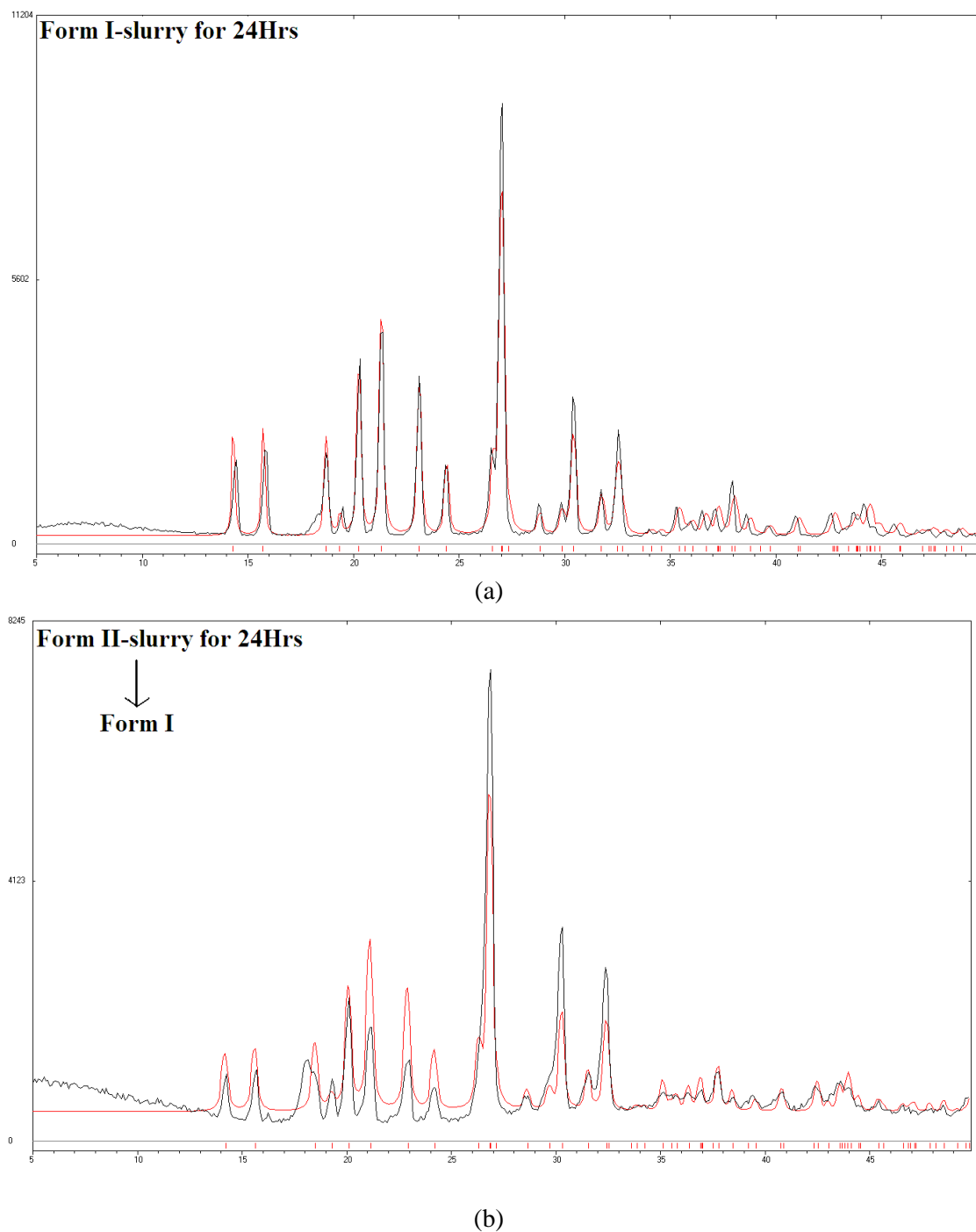


Figure 4.15 Powder X-ray diffraction pattern after slurry grinding for 24 h. (a) Form I is stable, and (b) form II transforms to stable modification I. The calculated XRD lines of polymorph I (red) are overlay for reference.

4.3 Conclusions

A new metastable polymorph of *N*-acetyl-L-cysteine was crystallized from methanol and the crystal structure was determined by X-ray diffraction. Both polymorphs contain a *C*(5) chain of O–H···O H-bonds. The NAC molecule in polymorphs I and II adopts different conformation of the COOH group. The discriminating interaction in form I is an S–H···O while form II has a C–H···O interaction. The stability of form I is understood by hydrogen bond analysis, Hirshfeld surfaces, and XPac SC. They were fully characterized by FT-IR, Raman, ¹³C ss-NMR and DSC. The thermal stability and thermodynamic relationship between polymorphs I and II was established as enantiotropic by DSC. The transformation of the new form II occurred to the thermodynamic form I in the presence of solvent by grinding, slurry or storage. The original stable polymorph I is still the preferred modification for drug formulation.

4.4 Experimental Section

Materials and Methods. Commercially available *N*-acetyl-L-cysteine (Sigma-Aldrich) matching with form I was used without further purification. All other chemicals and solvents were of analytical or chromatographic grade.

CSD search. The Cambridge Structural Database (CSD version 5.34, February 2013 update)¹⁵ was searched for S atom containing organic structures (17,266 hits) to give S–H···O in the distance range 1–4 Å (22 hits, 17 compounds), of which there are no neutral polymorphs containing an S–H···O interaction. The second search on ionic compounds S–H···O[−] (1–4 Å) gave 5 hits of which two are polymorphic, and the same two polymorph sets were retrieved in the third search on S–H···N and N–H···S interactions (1–4 Å, 7 hits). The next search using the fragment COOH···O=C–NH (26 hits) and HO–C=O···H–N (16 hits) in the distance range 1.2–3.0 Å, all organic compounds, with the word “form”, “polymorph”, “modification”, and “phase” in the

qualifier, excluding the entries for which 3D coordinates, did not furnish any hits. There are only 5 polymorph sets of O–H...O catemer chain in crystal structures, i.e. it is as such a rare synthon. These data and Refcodes are summarized in Table 7.

Table 4.7 Details of CSD searches on SH interactions and Refcodes.

4.7.1. Polymorphism in Sulfur compounds having SH group.

BOQCUF02	GLUTAS05	LCYSTN25	5 compounds are polymorphic with 13 hits in CSD
BOQCUF04	LCYSTN04	TSCARB01	
BOQCUF05	LCYSTN21	WOGKIT01	
GLUTAS03	LCYSTN22		
GLUTAS04	LCYSTN23		

4.7.2. Sulfur compounds containing neutral S–H...O interaction.

FATQIC	LAPVUU	TAPZIU*	NALCYS02 [#]	There are 17 and 22 hits in the CSD (no polymorphs)
EMANOW	LAWKIE*	TASPUY*	NALCYS11	
ESABAB	QECSAU	TAXMUA	NALCYS12	
HUDFIW	OFASOD	XEHDOF	NALCYS13	
HUKJUT	RONVAR01		NALCYS14	
HUSNEP	RONVEV		NALCYS15	

*Multi-component systems, [#] Multiple structures of NAC in VT study.

4.7.3. S–H...O[−], S–H...N and N–H...S in polymorphs.

LCYSTN03	LCYSTN23 ^{b,c}	GLUTAS03 ^{a,b,c}	S-H...O ⁻ (5 hits) S-H...N (7 hits) N-H...S (7 hits) Two polymorphic compounds L-cysteine and Glutathione
LCYSTN04 ^{a,b,c}	LCYSTN25 ^{a,b,c}	GLUTAS04 _{a,b,c}	
LCYSTN05		GLUTAS05 _{a,b,c}	
LCYSTN21		(Glutathione)	
LCYSTN22 ^{b,c}			
(L-Cysteine)			

^a S–H...O[−], ^b S–H...N and ^c N–H...S interactions.

4.7.4. Acid-amide O–H...O H-bond.

APENTN02	GLUTAS05	VAMBOA01	MUROXA	26 hits were found
----------	----------	----------	--------	--------------------

BUVKEJ	GLUTAS06	VAMBOA02	MUROXA01	with five polymorphs
DETBIO01*	INODUK*	WEFVIN*	ACOMUC	
DETBIO10	INODUK01	WEFVIN01	ACOMUC01	
GIZFIF01	MIMMOL	WEFVIN02		
GLUTAS02*	REKBUE	YIPFUY01		
GLUTAS03	SHIVOU			
GLUTAS04	VAMBOA*			

*5 polymorphs with catemer synthon

4.7.5. Acid-amide N-H...O H-bond.

APENTN02	MIMMOL	Two polymorph pairs out of 16 hits
BUVKEJ	PIMBAP04	
DETBIO01	SIHVOU	
BIHXIA*	TIPVIY	
BIHXIA01	ULAWAF	
GLUTAS03	ULAWAF01	
GLUTAS04	VAMBOA01*	
GLUTAS05	VAMBOA02	

* Polymorphs

X-ray crystallography. X-ray reflections for NAC molecule (RT data) were collected on an Oxford Xcalibur Gemini Eos CCD diffractometer using Mo-K α , radiation. Data reduction was performed using CrysAlisPro (version 1.171.33.55). OLEX2-1.0 and SHELX-TL 97 were used to solve and refine the data.¹⁶ All non-hydrogen atoms were refined anisotropically, and C–H hydrogens were fixed. N–H was located from difference electron density maps and C–H hydrogens were fixed. Packing diagrams were prepared in X-Seed.¹⁷ Crystallographic .cif files (CCDC Nos. 939816-939817) are available at www.ccdc.cam.ac.uk/data_request/cif or as part of the Electronic Supplementary Information.

Vibrational spectroscopy. Nicolet 6700 FT-IR spectrometer with an NXR FT-Raman module was used to record IR and Raman spectra. IR spectra were recorded

on samples dispersed in KBr pellets. Raman spectra were recorded with pellets of pure samples.

^{13}C ss-NMR spectroscopy. Solid-state NMR spectra were recorded on a Bruker Advance spectrometer operating at 400 MHz (100 MHz for ^{13}C nucleus). ss-NMR spectra were recorded on a Bruker 4 mm double resonance CP-MAS probe in zirconia rotors at 5.0 kHz spin rate with a cross-polarization contact time of 2.5 ms and a recycle delay of 8 s. ^{13}C CP-MAS spectra recorded at 100 MHz were referenced to the methylene carbon of glycine and then the chemical shifts were recalculated to the TMS scale ($\delta_{\text{glycine}} = 43.3$ ppm).

Thermal analysis. DSC was performed on Mettler Toledo DSC 822e module. Samples were placed in crimped but vented aluminum sample pans. The typical sample size was 3-4 mg, and the temperature range was 30-250 °C at heating rate of 5 °C/min and 2 °C/min. Samples were purged by a stream of dry nitrogen flowing at 150 mL/min.

Powder X-ray diffraction. PXRDs were recorded on a SMART Bruker D8 Advance X-ray diffractometer (Bruker-AXS, Karlsruhe, Germany) in the Bragg-Brentano geometry using Cu-K α X-radiation ($\lambda = 1.5406$ Å) at 40 kV and 30 mA. Diffraction patterns were collected over the 2θ range of 5-50° at a scan rate of 1°/min. The appearance of polymorphs for all the molecules was monitored by the appearance of new diffraction peaks. Powder Cell 2.359¹⁸ was used for overlaying the experimental XRPD pattern on the calculated lines from the crystal structure. Variable temperature mode fixed on the same instrument and recorded the phase transition with 600-1200 s delay time at a heating rate of 2 °C/min.

Ball mill grinding. Retsch-MM400 ball mill used for milling of form II in 10 min and frequency of 20 Hz for the complete conversion to form I.

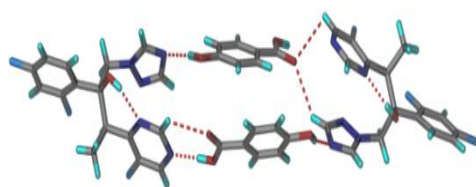
4.5 References

1. (a) M. Smilkstein, G. Knapp, K. Kulig and B. Rumack, *New Engl. J. Med.*, **1988**, 319, 1557; (b) K. Heard and J. Green, *Curr. Pharm. Biotech.*, **2012**, 13, 1917; (c) K. R. Gibson, I. L. Neilson, F. Barrett, T. J. Winterburn, S. Sharma, S. M. MacRury and I. L. Megson, *J. Cardiovasc. Pharmacol.* **2009**, 54, 319.
2. (a) O. Dean, F. Giorlando, and M. Berk, *J. Psychiatry Neurosci.*, **2011**, 36, 78; (b) R. Sansone and L. Sansone, *Innov. Clin. Neurosci.*, **2011**, 8, 10.
3. (a) F. Takusagawa, T. F. Koetzle, W. W. H. Kou and R. Parthasarathy, *Acta Cryst.* **1981**, B37, 1591; (b) W. W. H. Kou and R. Parthasarathy ACS Abstract. Papers, **1976**, 72; (c) Y. J. Lee, I. -H. Suh, *J. Korean Chem. Soc.*, **1980**, 24, 193.
4. V. S. Minkov, E. V. Boldyreva, T. N. Drebuschak, and C. H. Görbitz, *CrystEngComm*, **2012**, 14, 5943.
5. (a) S. A. Moggach, A. R. Lennie, C. A. Morrison, P. Richardson, F. A. Stefanowicz and J. E. Warren, *CrystEngComm*, **2010**, 12, 2587; (b) S. A. Moggach, D. Allan, S. Clark, M. Gutmann, S. Parsons, C. Pulham and L. Sawyer, *Acta Cryst.*, **2006**, B62, 296; (c) C. H. Görbitz and B. Dalhus, *Acta Cryst.*, **1996**, C52, 1756.
6. G. R. Desiraju and T. Steiner, *The Weak Hydrogen Bond: In Structural Chemistry and Biology*, Oxford University Press, Oxford, New York **1999**.
7. (a) J. J. McKinnon, F. P. A. Fabbiani and M. A. Spackman, *Cryst. Growth Des.*, **2007**, 7, 755; (b) F. P. Fabbiani, L. T. Byrne, J. J. McKinnon and M. A. Spackman, *CrystEngComm*, **2007**, 9, 728; (c) M. A. Spackman and D. Jayatilaka, *CrystEngComm*, **2008**, 11, 19.
8. (a) Gelbrich, T. L. Threlfall and M. Hursthouse, *CrystEngComm*, **2012**, 14, 5454; (b) T. Gelbrich, D. E. Braun, A. Ellern and U. J. Griesser *Cryst. Growth Des.* **2013**, 13, 1206.
9. (a) J. Anwar, S. Tarling and P. Barnes, *J. Pharm. Sci.*, **1989**, 78, 337; (b) P. P. Bag and C. M. Reddy, *Cryst. Growth Des.*, **2012**, 12, 2740; (c) R. J. Davey, N. Blagden, G. D. Potts and R. Docherty, *J. Am. Chem. Soc.*, **1997**, 119, 1767; (d) A. Lemmerer, N. B. Báthori, C. Esterhuysen, S. A. Bourne and M. R. Caira, *Crystal Growth Des.*, **2009**, 9, 2646; (e) A. P. Mendham, R. A. Palmer, B. S. Potter, T. J. Dines, M. J. Snowden, R. Withnall and B. Z.

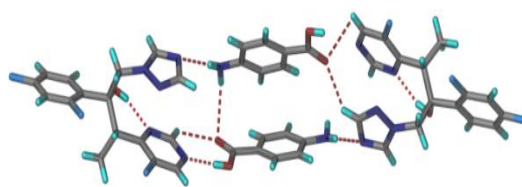
- Chowdhry J. *Raman Spectrosc.*, **2010**, *41*, 288; (f) C. Glidewell, J. Low, J. Skakle and J. Wardell, *Acta Cryst.*, **2004**, *C60*, 120.
10. G. R. Desiraju, *Angew. Chem., Int. Ed. Engl.*, **1995**, *34*, 2311.
 11. M.C. Etter, *Acc. Chem. Res.*, **1990**, *23*, 120.
 12. (a) P. Munshi and T. N. Guru Row, *Cryst. Rev.*, **2005**, *11*, 199. (b) P. Munshi, T. Thakur, T. Guru Row and G. R. Desiraju, *Acta Cryst.*, **2006**, *B62*, 118.
 13. (a) A. Burger, R. Ramberger, *Mikrochim. Acta* **1979**, *II*, 259; (b) S. Aitipamula and A. Nangia, In *Supramolecular Chemistry: From Molecules to Nanomaterials*, Eds. J. W. Steed and P. A. Gale, John Wiley, Chichester, UK, **2012**, pp. 2957-2974.
 14. J. B. Nanubolu, B. Sridhar, K. Ravikumar, K. D. Sawant, T. A. Naik, L. N. Patkar, S. Cherukuvada and B. Sreedhar, *CrystEngComm*, **2013**, *15*, 4448.
 15. Cambridge Structural Database, ver. 5.34, ConQuest 1.15, November **2012** release, Cambridge Crystallographic Data Center, www.ccdc.cam.ac.uk.
 16. G. M. Sheldrick, *SHELXS-97* and *SHELXL-97*, *Program for the Solution and Refinement of Crystal Structures*, University of Göttingen, Germany, **1997**.
 17. L. J. Barbour, X-Seed, *Graphical Interface to SHELX-97 and POV-Ray*, University of Missouri-Columbia, USA, **1999**.
 18. N. Kraus, G. Nolze, Powder Cell, version 2.3, A Program for Structure Visualization, Powder Pattern Calculation and Profile Fitting; Federal Institute for Materials Research and Testing: Berlin, Germany, **2000**.

Chapter Five

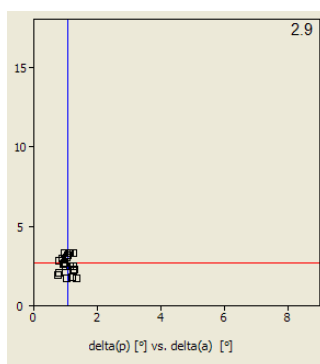
Pharmaceutical Cocrystals and a Nitrate Salt of Voriconazole



VZL-PHBA cocrystal



VZL-PABA cocrystal



XPac dissimilarity index of 2.9

VZL-PHBA and VZL-PABA cocrystals are 3D isostructural and this isomorphous VZL-PABA cocrystal is found to be ~ 3 times more soluble than VZL-PHBA cocrystal due to the more number of hydrogen bonding donors in coformer PABA.

5.1 Introduction

Cocrystals are multi-component systems consisting of two or more neutral, solid compounds held together by hydrogen bonds in a definite stoichiometry.¹ To be a pharmaceutical cocrystal, one of the components (drug) must be an active pharmaceutical ingredient (API) and the other (coformer) should be a safe compound from the GRAS list (generally regarded as safe by the US-FDA).² The idea of preparing pharmaceutical cocrystals is to alter the physicochemical properties, most often solubility and dissolution rate, of a drug without modifying its chemical structure.^{1,3} Voriconazole ((2R,3S)-2-(2,4-difluorophenyl)-3-(5-fluoropyrimidin-4-yl)-1-(1H-1,2,4-triazol-1-yl)butan-2-ol, VZL) is an antifungal drug with low aqueous solubility of 0.71 mg/mL and it is a BCS class II drug (Biopharmaceutics Classification System) of the azole family (Table 5.1). Itraconazole⁴ and fluoxetine hydrochloride⁵ are early examples of pharmaceutical cocrystals, a trail that has been followed up with several hundred publications and several excellent reviews.³ There are three examples of drug cocrystals in the market: caffeine-citric acid/ citrate,^{6a} and escitalopram-oxalic acid/ oxalate, and valproic acid/ Na-valproate.^{6b,c} A few more cocrystals are in clinical stage.^{6d} Hence, we have prepared a nitrate salt and three cocrystals of VZL with p-hydroxybenzoic acid, p-aminobenzoic acid (both are GRAS compounds) and m-nitrobenzoic acid coformers to improve physicochemical properties. All four multi-component crystals of voriconazole were obtained by solution crystallization as well as solid-state grinding and their structures were confirmed by X-ray diffraction, FT-IR, Raman, and NMR spectroscopy, and thermal techniques. VZL-PHBA and VZL-PABA are isostructural by XPac calculations and molecular packing arrangement. A notable result from a crystal engineering viewpoint is that the supramolecular synthon between the basic drug and the acidic coformer undergoes a switch based on the pK_a of the acid coformer.

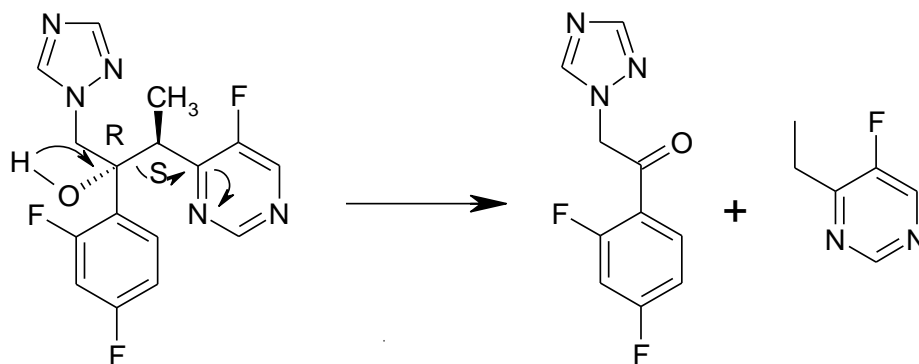
Table 5.1 Azole antifungal drugs in the market

S. No	Imidazoles	Triazoles
1	Bifonazole	Albaconazole
2	Butoconazole	Fluconazole
3	Clotrimazole	Isavuconazole
4	Econazole	Itraconazole
5	Fenticonazole	Posaconazole
6	Isoconazole	Ravuconazole
7	Ketoconazole	Terconazole
8	Luliconazole	Voriconazole
9	Miconazole	
10	Omoconazole	
11	Oxiconazole	
12	Sertaconazole	
13	Sulconazole	
14	Tioconazole	

5.2 Results and Discussion

5.2.1 Drug Profile: Voriconazole (VFEND[®], Pfizer) is an antifungal drug administered intravenously or in oral dosage formulation.⁷ Two other antifungal drugs of the azole family, itraconazole and fluconazole, have been studied for salts, cocrystals and metal complexes.^{4,8} A guest free form^{9a} and a camphor sulfonate salt^{9b} of voriconazole are reported along with nano-indentation study of the pure API.^{9c} VZL has low aqueous solubility (0.71 mg/mL) and is unstable in water due to a retro-aldol reaction (Scheme 5.1).¹⁰ Due to the presence of less basic triazole and pyrimidine rings, voriconazole is able to form salts with strong acids only, whereas with moderate organic acids it can possibly form cocrystals¹¹ (Table 5.2). A

complete list of coformers and crystallization experiments attempted is listed in Table 5.3. The successful results of nitrate salt and a few cocrystals are reported (Scheme 5.2) with the objective to analyze X-ray crystal structures and improve the physico-chemical profile of voriconazole.

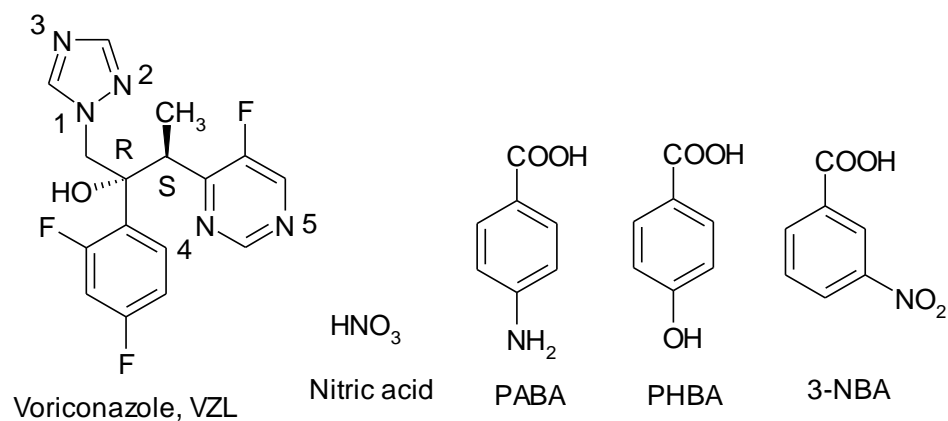


Scheme 5.1 Retro-aldol degradation pathway of voriconazole in the aqueous medium.

Table 5.2 ΔpK_a value of voriconazole and coformers.

API/Coformer	pK_a^a	Cocrystal/salt	ΔpK_a (COOH with N5- and N3-VZL)
VZL	2.27 (N3) 0.43 (N5)	-	-
HNO₃	-1.30	VZL-HNO ₃	3.57, 1.73
PHBA	3.57 (COOH)	VZL-PHBA	-1.30, -3.14
PABA	4.87 (COOH)	VZL-PABA	-2.60, -4.44
3-NBA	3.49	VZL-3-NBA	-1.22, -3.06

^a pK_a values for VZL are calculated from ChemAxon software. The pK_a values for VZL are those for the conjugate acid of the heterocycle N.



Scheme 5.2 Voriconazole and successful coformers

Table 5.3 List of experiments in the search of new VZL crystalline forms.

S.No	Coformers	Mineral acids	Polymorph screening
1	L-Ascorbic acid	HCl	Acetone
2	Saccharin	H ₂ SO ₄	Methanol
3	Glutaric acid	HNO ₃	Ethanol
4	Nicotinic acid	Formic acid	Chloroform
5	4-Hydroxybenzoic acid (PHBA)	Chlorosulphonic acid	Dichloromethane
6	4-Aminobenzoic acid (PABA)	Methanesulphonic acid	Ethylmethylketone
7	Citric acid	Sulphamic acid	Benzene
8	Benzoic acid	Acetic acid	Toluene
9	Nicotinamide		Nitromethane
10	Maleic acid		Dioxane
11	Urea		Acetonitrile
12	Salicylic acid		THF
13	4-aminosalicylic acid		Anisole
14	Fumaric acid		Xylene

15	3-nitrobenzoic acid	Mesitylene
16	3,5-dihydroxy benzoic acid	Ethylacetate
17	4-nitrobenzoic acid	Methylacetate
18	2,4-dihydroxy benzoic acid	2-propanol
19	3-methoxybenzoic acid	Isobutanol
20	4-methoxybenzoic acid	Melting/heating
21	2-methoxybenzoic acid	Rota vapor
22	Succinic acid	Sublimation

5.2.1 Crystal structure analysis

Voriconazole dinitrate salt (1:2): Voriconazole dinitrate salt was prepared by dissolving 50 mg of voriconazole in 10 mL ethanol followed by the addition of 1-2 drops of 1N HNO₃ acid solution. The mixture was boiled for a few minutes and then kept for slow evaporation at ambient conditions. Colorless plate shaped crystals were obtained whose X-ray crystal structure was solved in the orthorhombic space group $P2_12_12_1$ with one voriconazolium and two nitrate ions in the asymmetric unit (crystallographic details are mentioned in Appendix). Protons from two different nitric acid molecules are transferred to triazole N3 and pyrimidine N5 (partial transfer) of the voriconazole molecule. The fully ionized nitrate ion is sandwiched between the layers of voriconazole connected through bifurcated $N3^+-H3A\cdots O2^-$ and $N3^+-H3A\cdots O3^-$ (1.72 Å, 171° and 2.33 Å, 126°) hydrogen bonds (Table 5.4) to make of graph set motifs of notation¹² $R_1^2(3)$ (Fig. 5.1a). The second nitrate ion is connected to N5 pyrimidine through $N5^+-H6A\cdots O6^-$ interaction and a second molecule of voriconazole through weak van der Waal interactions in a zigzag tape (Fig. 5.1b).

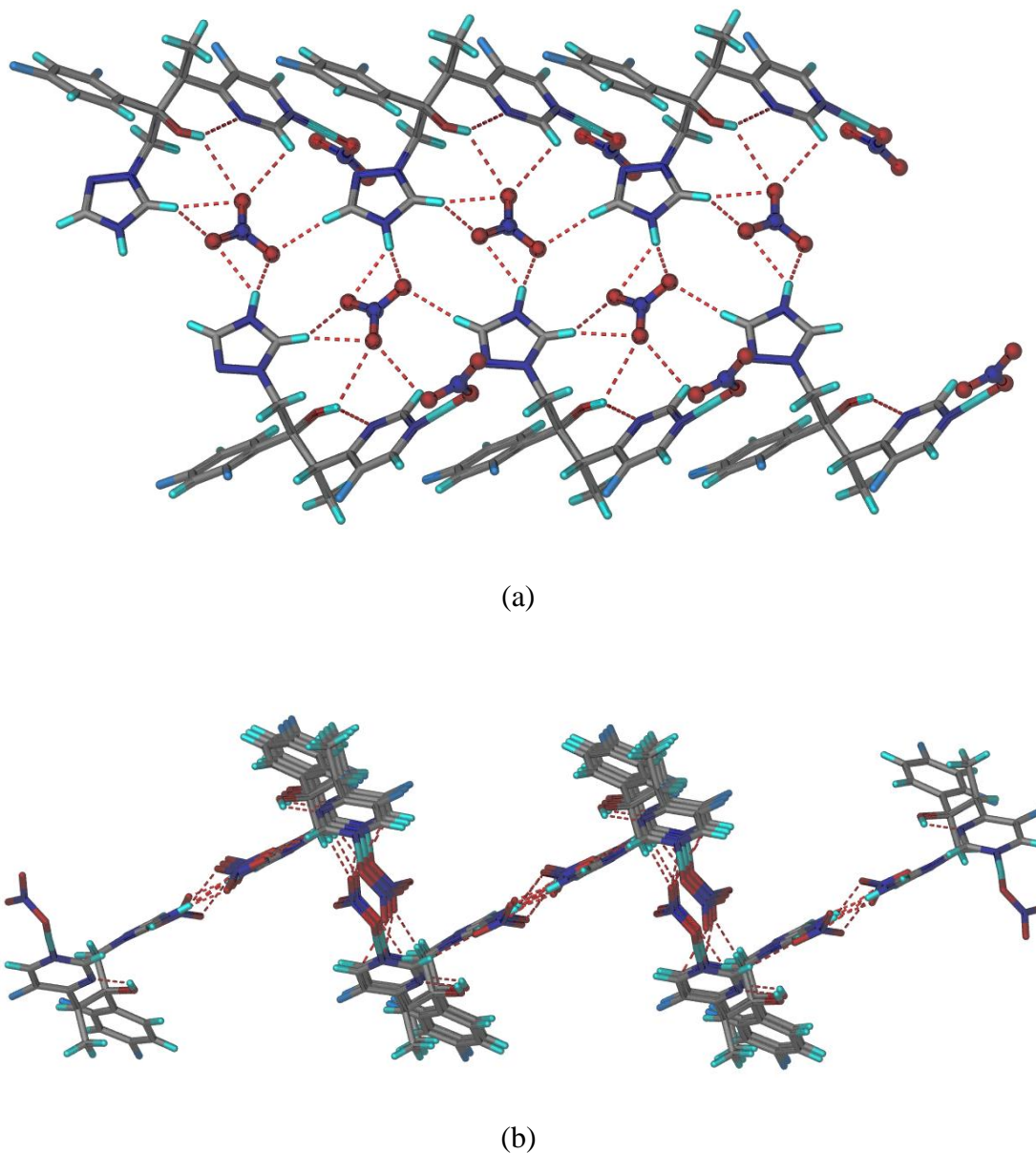


Figure 5.1 (a) Nitrate ions form strong ionic $\text{N}^+-\text{H}\cdots\text{O}^-$ and weak $\text{C}-\text{H}\cdots\text{O}$ hydrogen bonds with voriconazole molecules, and (b) $\text{C}-\text{H}\cdots\text{O}$ hydrogen bonds in the zigzag tapes of VZL molecules connected via nitrate ions.

Voriconazole–p-hydroxybenzoic acid (1:1): VZL–PHBA 1:1 cocrystal was prepared by mixing the components (0.30 mmol each) in 10 mL methanol and kept

for slow evaporation. Colorless plate-shape crystals were solved in the monoclinic space group $P2_1$. VZL and PHBA are connected in a helical chain through $O-H\cdots N$ hydrogen bonds (Fig. 5.2). The carboxyl group of PHBA forms a two-point synthon with the pyrimidine N5 of VZL rather than the N3 of triazole. The pK_a values of the two N positions suggest a strong hydrogen bond between the carboxylic acid donor and N3 of triazole as acceptor based on ΔpK_a (Table 5.2). The triazole N3 (pK_a of conjugate acid 2.72) is a stronger base than pyrimidine N5 (pK_a NH^+ 0.43). Etter's rule^{12a,b} of strong hydrogen bond donor–acceptor pairing does not seem to follow in this system. The tertiary OH group pK_a is very high (12.71) for any kind of ionization at physiological conditions. The hydroxyl group of PHBA forms $O-H\cdots N$ hydrogen bond to triazole N3.

Voriconazole is a multiple acidic/basic site molecule, and accurately determining the pK_a of each N atom is very difficult. A survey of the literature afforded two different sets of pK_a values for voriconazole. Buchanan et al.^{13a} reported 4.98 and 12.0, and Reddy et al.^{13b} reported 2.72 and 11.54. It is clear that the higher value of 11–12 refers to the OH group pK_a .^{13c} It was not mentioned in the above papers whether the 2nd pK_a number refers to that ofazole N or the pyrimidine N. We then searched the pK_a of a relatedazole drug without the pyrimidine ring, and the values for fluconazole are 11.01, 2.94, 2.65.^{13d} Therefore the value of 2.72 taken for triazole N is the correct assignment. The pyrimidine N basicity may be severely attenuated by the meta-fluoro group and so triazole N is the more basic site in voriconazole.

Table 5.4 Hydrogen bonds in crystal structures (neutron-normalized distances).

Interaction	H \cdots A /Å	D \cdots A /Å	$\angle D-H\cdots A$ /°	Symmetry code
VZL–HNO₃				
O1–H1 \cdots N4	1.89	2.703(19)	138	intramolecular
N3–H3A \cdots O2	2.33	3.038(2)	126	1/2-x,-y,-1/2+z

N3–H3A···O3	1.72	2.720(2)	171	1/2-x,-y,-1/2+z
O6–H6A···N5	1.57	2.547(2)	176	intramolecular
C1–H1A···F2	2.29	2.997(2)	121	intramolecular
C6–H6···O4	2.61	3.107 (2)	106	-x+1,+y-1/2,-z+1/2
O1–H1···O4	2.58	3.296 (2)	132	-x+1,+y-1/2,-z+1/2
C1–H1B···O7	2.45	3.514(2)	167	-1/2+x,1/2-y,-z
C1–H1A···O6	2.58	3.446(2)	136	x+1,+y,+z
C3–H3···F1	2.46	2.880(19)	101	intramolecular
C3–H3···F2	2.33	3.041(19)	122	intramolecular
C4–H4C···O3	2.45	3.528(2)	179	1+x,y,z
C6–H6···N2	2.43	3.380(2)	145	1+x,y,z
C7–H7···O1	2.44	3.259(2)	132	2-x,1/2+y,1/2-z
C9–H9···O2	2.21	3.074(2)	136	1-x,-1/2+y,1/2-z
C9–H9···O4	2.22	3.283(2)	165	-x+1,+y-1/2,-z+1/2
C10–H10···O3	2.12	3.199(2)	172	1-x,-1/2+y,1/2-z
C15–H15···O2	2.28	3.168(2)	138	-x,-1/2+y,1/2-z
C12–H12···O6	2.53	3.327(2)	129	-x,+y-1/2,-z+1/2
C10–H10···F1	2.83	3.136(2)	95	-x+1,+y-1/2,-z+1/2
VZL–PHBA				
O1–H1···N4	1.75	2.663(3)	153	intramolecular
O2–H2···N5	1.76	2.747(3)	179	-1+x,1+y,z
O4–H4···N3	1.84	2.783(4)	159	2-x,1/2+y,1-z
C1–H1A···F2	2.48	3.133(3)	118	intramolecular
C1–H1B···O4	2.41	3.438(3)	157	-x+1,+y+1/2,-z+1
C3–H3···F1	2.42	2.855(3)	102	intramolecular
C3–H3···F2	2.31	2.935(3)	115	intramolecular
C10–H10···O3	2.43	3.313(4)	138	1+x,y,z
C7–H7···O3	2.74	3.130(3)	100	-x+2,+y+1/2,-z+1

C6–H6···N2	2.54	3.432(4)	138	x,+y-1,+z
C6–H6···O3	2.69	3.452 (3)	127	-x+2,+y-1/2,-z+1
C12–H12···O1	2.24	2.655(3)	100	intramolecular
C13–H13···O2	2.41	3.418(4)	154	x,-1+y,z
C4–H4B···F2	2.87	3.418(2)	111	x,y,z
VZL–PABA				
O1–H1···N4	1.74	2.675(4)	159	intramolecular
O2–H2···N5	1.77	2.742(4)	168	-x,-1/2+y,1-z
N6–H6A···O3	2.43	3.369(6)	154	-x,1/2+y,2-z
N6–H6B···N3	2.09	3.093(6)	174	x,y,1+z
C1–H1A···N6	2.50	3.559(6)	165	1-x,-1/2+y,1-z
C1–H1B···F2	2.49	3.121(4)	116	intramolecular
C3–H3···F1	2.41	2.849(4)	103	intramolecular
C3–H3···F2	2.29	2.932(4)	116	intramolecular
C10–H10···O3	2.38	3.259(5)	137	-x,-1/2+y,1-z
C7–H7···O3	2.92	3.266(3)	98	x-1,+y-1,+z
C6–H6···N2	2.63	3.570(5)	144	x,+y+1,+z
C12–H12···O1	2.21	2.624(4)	100	intramolecular
C13–H13···O2	2.40	3.443(5)	161	1-x,1/2+y,1-z
C4–H4B···F2	2.91	3.428(5)	109	x,y,z
VZL–3-NBA				
O1–H1···N4	1.91	2.787(3)	148	intramolecular
O2–H2···N3	1.66	2.630(3)	170	1+x,y,z
O1–H1···N2	2.74	3.031(3)	98	x,+y+1,+z
C1–H1A···F2	2.16	2.938(3)	126	intramolecular
C3–H3···F1	2.36	2.882(3)	108	intramolecular
C3–H3···F2	2.50	3.117(3)	115	intramolecular
C7–H7···N5	2.45	3.506(4)	164	-x,-1/2+y,-z

C9–H9···O3	2.61	3.225(3)	114	x-1,+y,+z
C7–H7···O5	2.75	3.125(4)	99	-x,+y-1/2,-z
C6–H6···O5	2.67	3.755(4)	177	-x,+y+1/2,-z
C12–H12···O1	2.28	2.689(3)	100	intramolecular
C21–H21···O4	2.55	3.270(3)	123	x,+y+1,+z

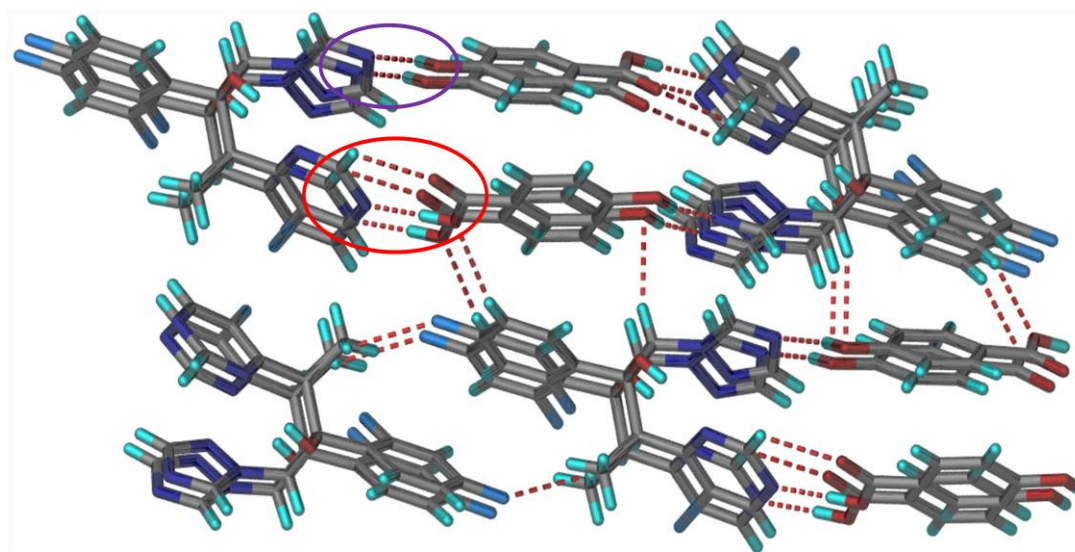


Figure 5.2 VZL forms strong O–H···N and weak C–H···O hydrogen bonds with PHBA.

Voriconazole–p-aminobenzoic acid (1:1): VZL–PABA cocrystal was crystallized from a 1:1 solution of methanol and ethanol. The colorless plates of VZL–PABA 1:1 cocrystal were solved in the monoclinic space group $P2_1$ with a helix of VZL and PABA connected via O–H···N and N–H···N hydrogen bonds (Fig. 5.3). Similar to the VZL–PHBA, VZL–PABA also is assembled via carboxylic acid-pyrimidine two-point synthon and one-point N–H···N hydrogen bond between the amino group of PABA and triazole N3 of VZL.

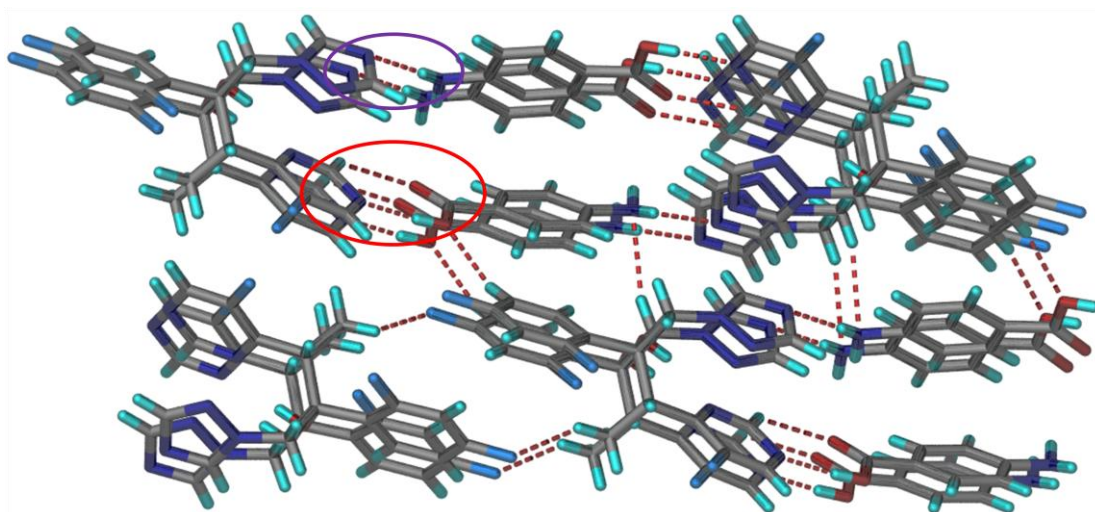
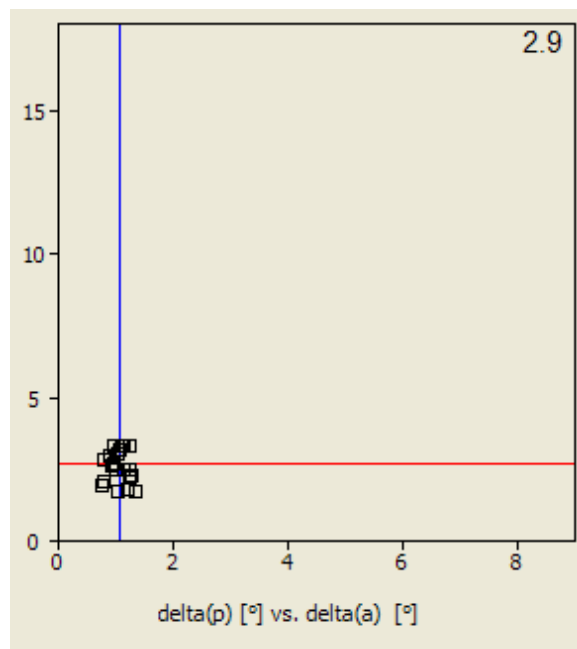
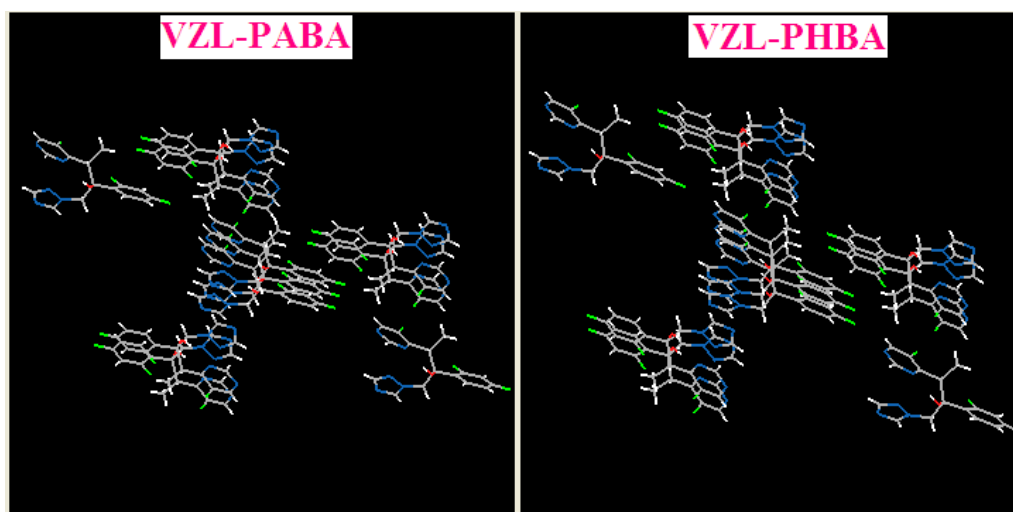


Figure 5.3 The strong acid-pyrimidine two-point synthon and amino-triazole one-point synthon is shown along with weak interactions between VZL and PABA.

The structures of VZL–PHBA and VZL–PABA have similar hydrogen bond motifs with O–H/ N–H exchange for the coformers PHBA and PABA. They are isomorphous structures. The isostructurality of single component and multi-component systems (cocrystals, solvates, and complexes) by chloro-methyl, C–H/ N–H, N–H/ O–H, C–H/ O–H, halogen exchange are well represented.¹⁴ The XPac dissimilarity¹⁵ index value of 2.9 (a small number) is indicative of 3D isostructurality between PHBA and PABA cocrystals of VZL (Fig. 5.4).



(a)



(b)

Figure 5.4 (a) The XPac dissimilarity index of 2.9 indicates similarity between PHBA and PABA cocrystals, (b) 3D supramolecular construct in VZL-PABA and VZL-PHBA.

Voriconazole–3-nitrobenzoic acid (1:1): VZL–3-NBA 1:1 cocrystal was prepared by dissolving a 1:1 mixture of voriconazole (100 mg) and 3-nitrobenzoic acid (48 mg) in acetonitrile and kept for slow evaporation at ambient conditions. Thin plate shaped colorless crystals were solved in the monoclinic space group $P2_1$. The carboxylic acid group of 3-NBA is hydrogen bonded to triazole N3 via $O-H\cdots N$ and $C-H\cdots O$ two-point synthon, consistent with Etter's¹² hydrogen bond pairing rule (Fig. 5.5). The O–H donor of VZL makes bifurcated H bonds with N4 of pyrimidine (intramolecular hydrogen bond) and triazole N2 of the next molecule in an infinite chain.

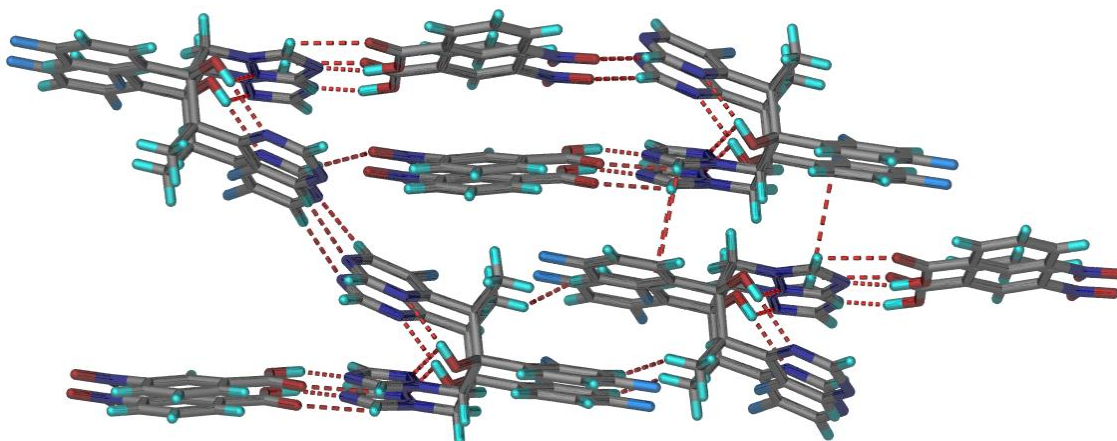


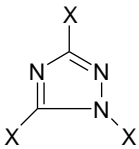
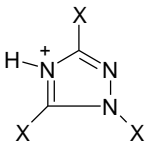
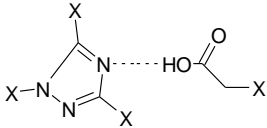
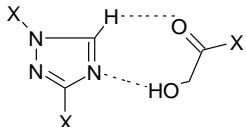
Figure 5.5 The triazole ring of VZL forms strong $O-H\cdots N$ and weak $C-H\cdots O$ hydrogen bonds with 3-NBA.

5.2.2 Supramolecular synthon and CSD search

From the four crystal structures and the reported sulphonate salt it was observed that there is a synthon switch depending on the pK_a value of the coformer. The strongly acidic 3- NO_2 -PhCOOH preferentially forms the acid–triazole synthon (eg. VZL–3-NBA cocrystal) whereas weaker acids make the acid–pyrimidine synthon (e.g. as in VZL–PHBA and VZL–PABA). Both types of heterosynths are two-point and assembled via $O-H\cdots N$ and $C-H\cdots O$ hydrogen bonds, and so it is

difficult to rationalize this switch. The very strong nitric acid gives a dinitrate with bothazole and pyrimidine N being protonated. A search of the Cambridge Structural Database¹⁶ for carboxylic acid–pyrimidine and acid–triazole two-point synthon gave only 2 hits for acid–triazole and 5 hits for acid–pyrimidine (Scheme 5.3 and Table 5.6). The number of archived crystal structures with the given motif is too small to extract a pK_a dependent synthon trend. Related searches on protonated triazole and acid–triazole single O–H \cdots N hydrogen bond gave 38 and 18 hits respectively (see details in Table 5.5). The difficulty in making cocrystals ofazole drugs with COOH is contrary to pK_a prediction, but nonetheless a fact known from the literature,^{4,9b} and the few CSD hits (Table 5.7).

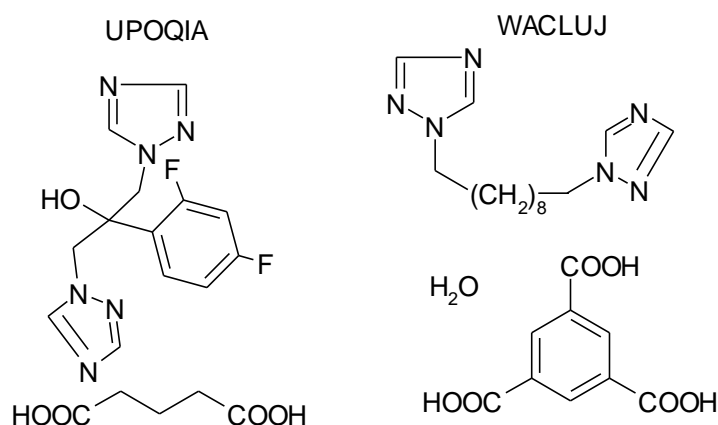
Table 5.5 CSD Search results on 1,2,4-triazole ring fragment.

Total number of 1,2,4-triazole	Protonated 1,2,4- triazole	Acid-triazole one point synthon (1,2,4-triazole)	Acid-triazole two point synthon (1,2,4-triazole)
 758 Hits	 38 Hits	 18 Hits	 2 Hits
BAHJIF01	FEDCUO	ATEYII	UPOQIA
BATWOK	XAZBUX	EPAGUY	WACLUI
BATXAX	AHUYIL	EVIMIF	
FEDCUO	AXASUO	EZEGIA	
GECLUX	AZOZIZ	GUZDEL	
LEFROF	BUHCEM	IKEQEU	
NAZREN	CINCAE	IQIHEW	
XAZBUX	CUBVOL	IQIHEW01	
ABIZAO	CUBVUR	KOPSOX	

ABOKUY	ELEPER	MOFVOT
ABUHAZ	GACNUV	NIFCIP
ADAVUX	HALHUX	ODITOL
ADIRAH	HEKSAR	QALZIO
ADIREL	KABPOU	UPOQEW
ADUPIY	KEQMAV	UPOQIA
AFOFAC	LALCOQ	WACLUI
AFOFEG	LEJRUN	ZAPMIO
AHIKIM	LERYAJ	HEBMUY
AHUYIL	MORETZ	
AJOFUB	NUJHIK	
ALAYUH	OQUJEQ	
AMIFIM	QAKNAR	
AMTAZC	QISQEP	
AMTRAZ	QULVEY	
AMTZZT	SEZHOV	
APIDUZ	TOMPAN	
APIFAH	UGARUP	
AQIJUF	UPOQAS	
AQIKIU	VOYPAA	
ATEYII	WETQES	
AVINAU	XENROY	
AXALOB	XENRUE	
AXASUO	XIXQUR	
AXEJUI	YAXFEK	
AXEKAP	ZAPGUU	

AZAKOC	ZIVROL
AZEPEA	ZIVRUR
AZOZIZ etc..	UNEROV01

Cambridge Structural Database, ver. 5.34, ConQuest 1.15, November 2012 release, May 2013 update.



Scheme 5.3 Chemical structures of CSD Refcodes with acid–triazole two-point O–H···N and C–H···O synthon.

Table 5.6 CSD refcodes for the acid–triazole synthon and calculated pK_a values.^a

Carboxylic acid–triazole two-point synthon (2 hits)	pK _a of triazole nitrogen (NH ⁺) and acid	ΔpK _a (= NH ⁺ – acid)
UPOQIA	2.03, 4.32	–2.29
WACLUIJ	1.99, 4.55	–2.56
Carboxylic acid–pyrimidine two-point synthon (5 hits)	pK _a of pyrimidine nitrogen (NH ⁺) and acid	ΔpK _a (= NH ⁺ – acid)
ABIWIT	1.78, 3.15	–1.57
POFPEF	1.58, 4.14	–2.56
XAQNOT	–0.28, 3.80	–4.08
LEJMOE	1.99, 4.37	–2.38
TENSIQ	1.19, 4.37	–3.18

^a pK_a values are calculated from ChemAxon software

5.2.3 Conformation of VZL

The presence of flexible methylene group between the heterocycle ring and the chiral center results in two clusters of conformations for voriconazole in the solid-state (Fig. 5.6). The free base and the dinitrate salt have a similar conformation whereas the cocrystals overlay in a different orientation for the triazole ring (see Table 5.7 for torsion angles).

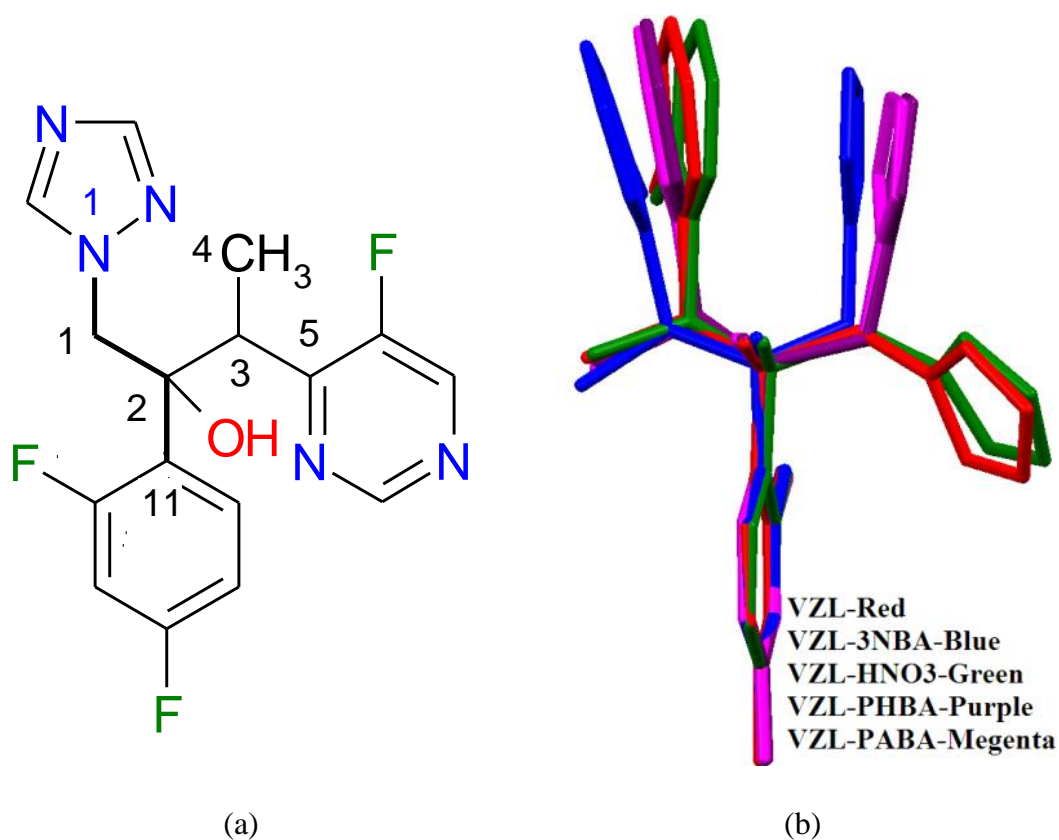


Figure 5.6 (a) Molecular structure of VZL with atom labeling considered for conformation analysis, and (b) Molecular overlay of different conformers of VZL in crystal structures.

Table 5.7 Torsion angle values of voriconazole salt and cocrystals.

Solid forms	Torsion angle (°)	Torsion angle (°)	Torsion angle (°)
	τ_1 (C11–C2–C1–N1)	τ_2 C11–C2–C3–C5)	τ_3 (C1–C2–C3–C4)
VZL (ref 9a)	55.6(4)	175.6(3)	175.0(3)
VZL–HNO ₃	61.7(2)	179.6(1)	179.8(1)
VZL–PHBA	173.4(2)	168.4(2)	164.6(2)
VZL–PABA	170.5(2)	169.1(2)	165.2(2)
VZL–3-NBA	175.18(19)	169.3(2)	167.5(2)

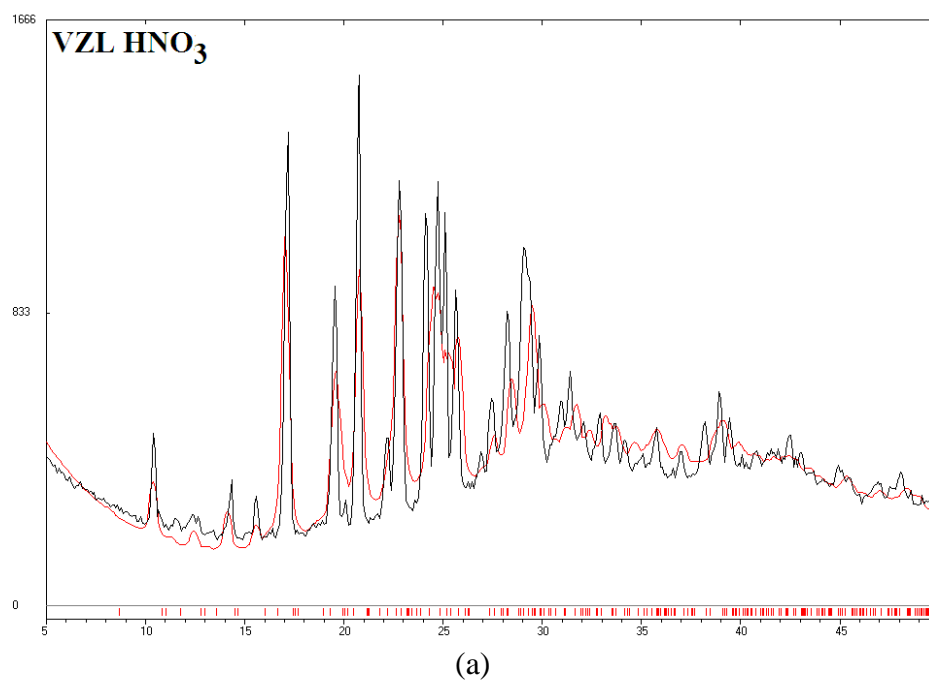
5.2.4 Characterization of VZL crystalline forms

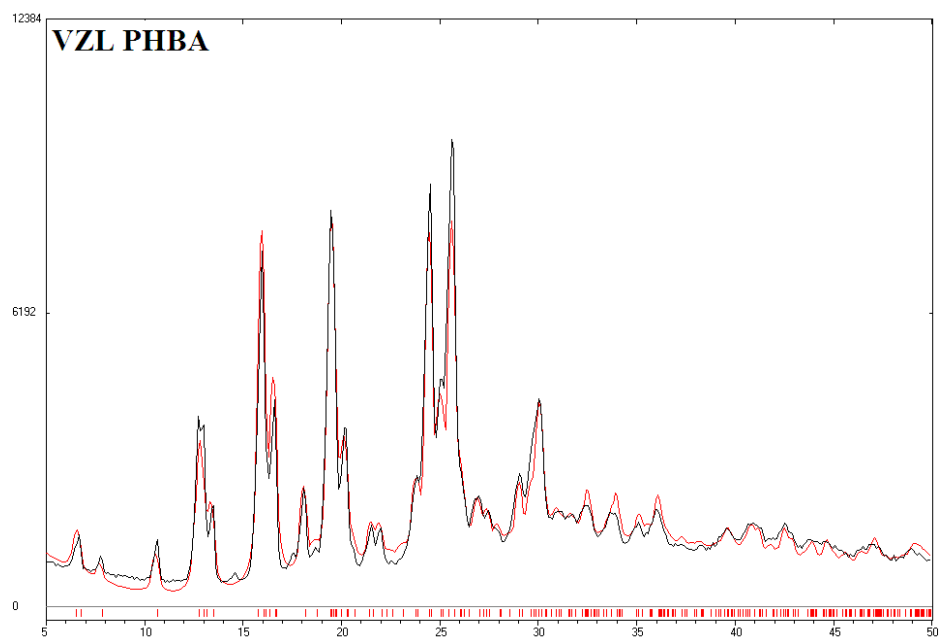
Voriconazole salt and cocrystals were prepared for spectroscopic and thermal characterization by neat and liquid-assisted grinding (LAG).¹⁷ The PXRD of the materials match well with the calculated powder pattern from the crystal structure (Fig. 5.7). ¹³C ss-NMR (Fig. 5.8), FT-IR, FT-Raman (Fig. 5.9-5.10) and differential scanning calorimetry (DSC) confirmed the bulk purity of the crystalline products (Table 5.8-5.10).¹⁸

Table 5.8 Chemical Shift values of different solid forms.

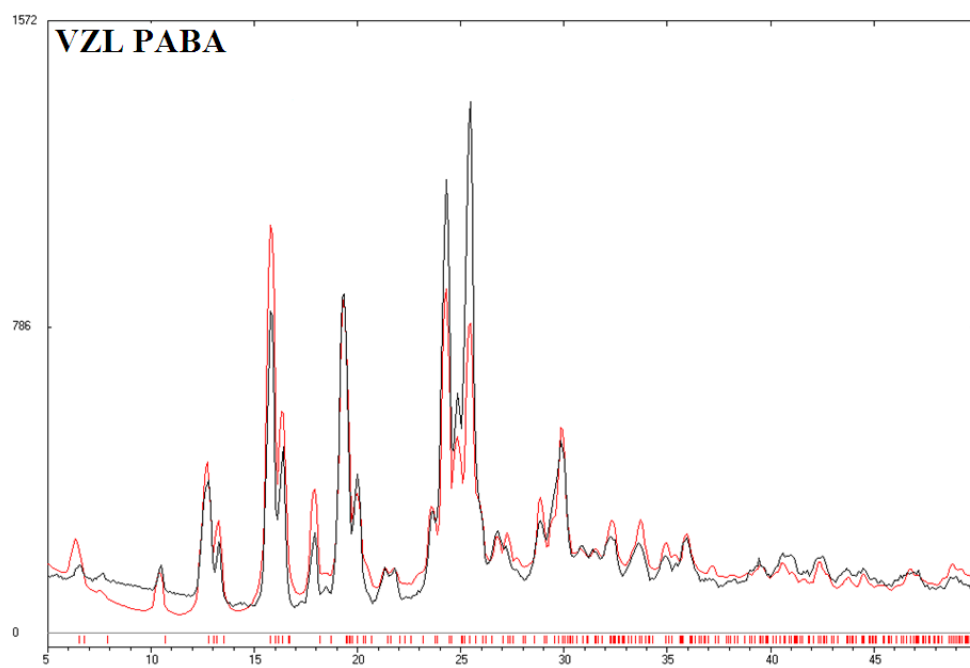
C atoms	VZL	VZL–HNO ₃	VZL–PHBA	VZL–PABA	VZL–3-NBA	PHBA	PABA	3NBA
C1	124.39	126.41	124.34	131.57	124.30	158.34	153.7	147.87
C2	101.91	104.67	102.51	102.26	103.63	133.14	131.6	133.50
C3	124.39	126.41	124.34	129.64	122.34	116.20	117.1	129.61
C4	129.59	131.41	129.90	141.49	132.90	122.15	112.4	127.35
C5	111.59	111.22	111.86	114.92	111.52	113.98	117.1	124.18

C6	129.59	131.41	132.05	143.51	132.90	133.14	131.6	127.35
C7	55.87	57.22	59.20	58.30	58.80	170.51	174.5	170.83
C8	34.69	34.77	33.86	34.23	32.89			
C9	145.80	147.03	142.46	150.24	146.90			
C10	145.59	144.14	142.46	150.52	146.90			
C11	151.18	157.80	160.89	160.25	160.56			
C12	149.86	153.44	155.74	155.91	153.04			
C13	77.11	76.58	77.60	76.92	78.31			
C14	158.80	160.93	166.92	169.74	165.57			
C15	158.80	157.80	160.89	162.93	156.39			
C16	14.40	16.59	18.15	18.09	17.33			





(b)



(c)

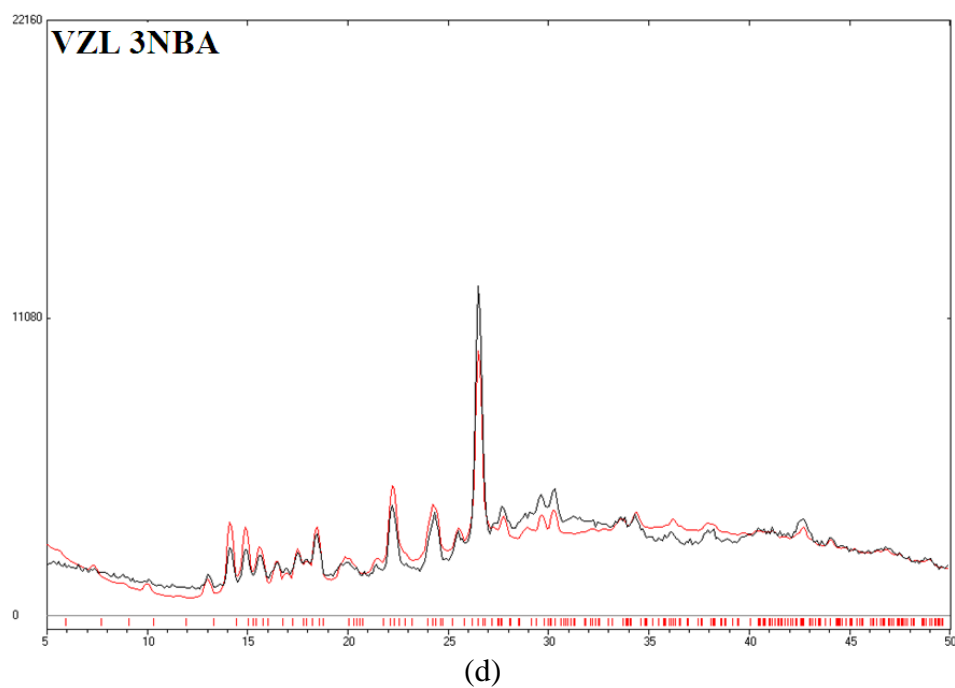


Figure 5.7 Comparison of experimental (black) and calculated (red) X-ray powder pattern of (a) Voriconazole-dinitrate salt (b) VZL–PHBA (c) VZL–PABA and (d) VZL–3-NBA cocrystals.

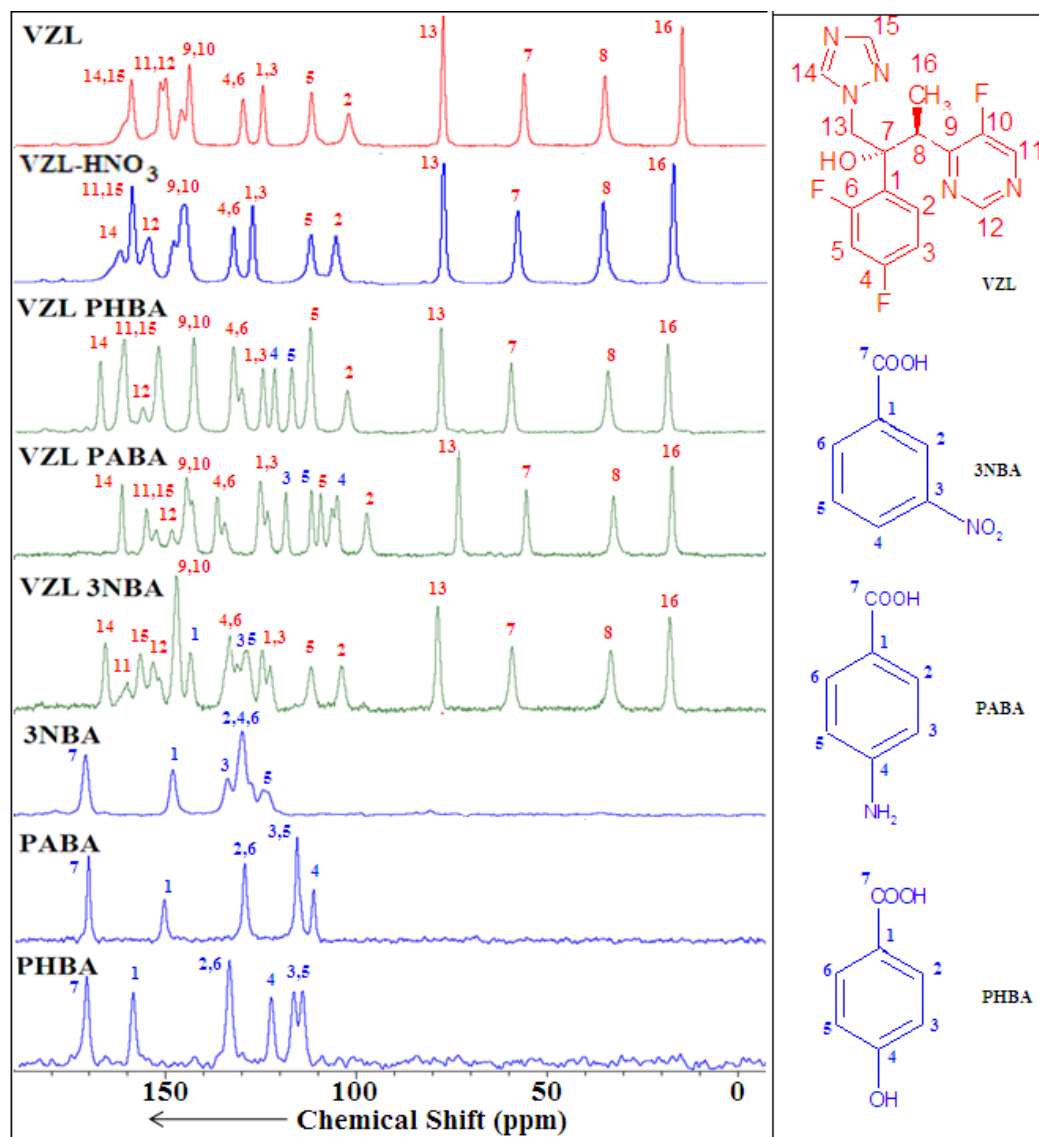


Figure 5.8 ^{13}C ss-NMR spectra of VZL dinitrate salt and cocrystals.

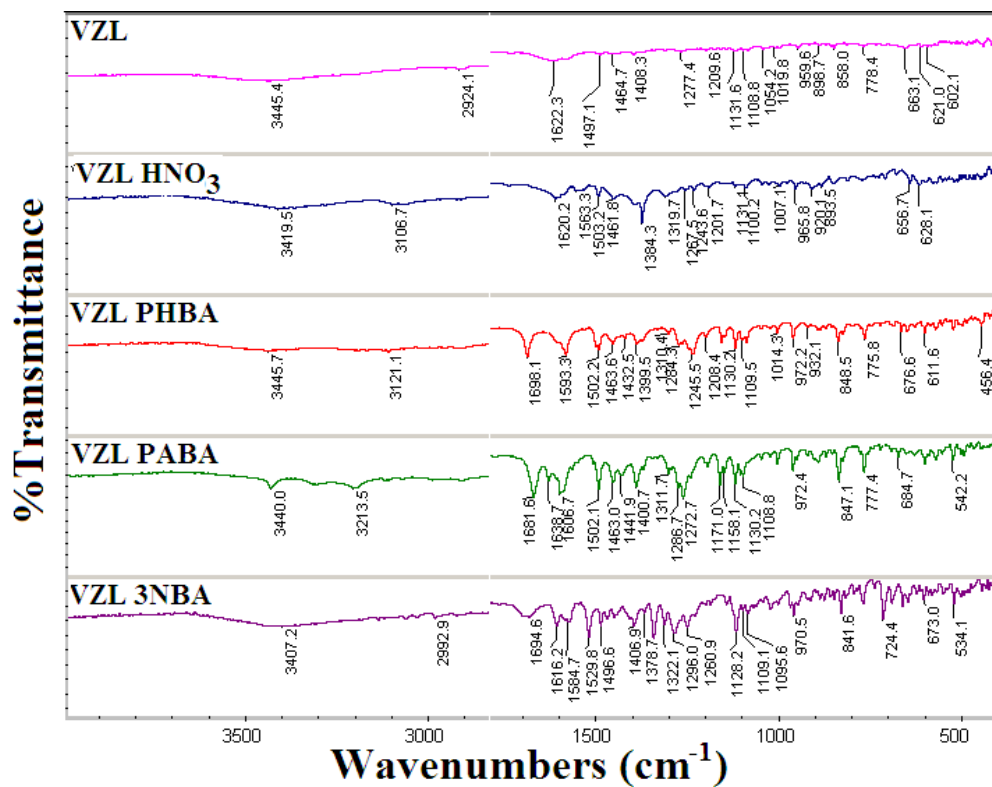


Figure 5.9 Comparison of FT-IR spectra of VZL with voriconazole-dinitrate salt and cocrystals.

Table 5.9 FT-IR stretching frequencies of solid forms (cm⁻¹).

Solid forms	O-H stretch	O-H bending (in-plane)	O-H bending (out-of-plane)	C=O stretch cocrystall (Acid group in coformer)
VZL	3445.4	1277.4	663.1	-
VZL-HNO ₃	3419.5	1243.6	656.7	-
VZL-PHBA	3445.7	1264.3	676.6	1698.1
VZL-PABA	3440.4	1272.1	684.7	1681.6
VZL-3-NBA	3407.2	1260.9	673.0	1694.6

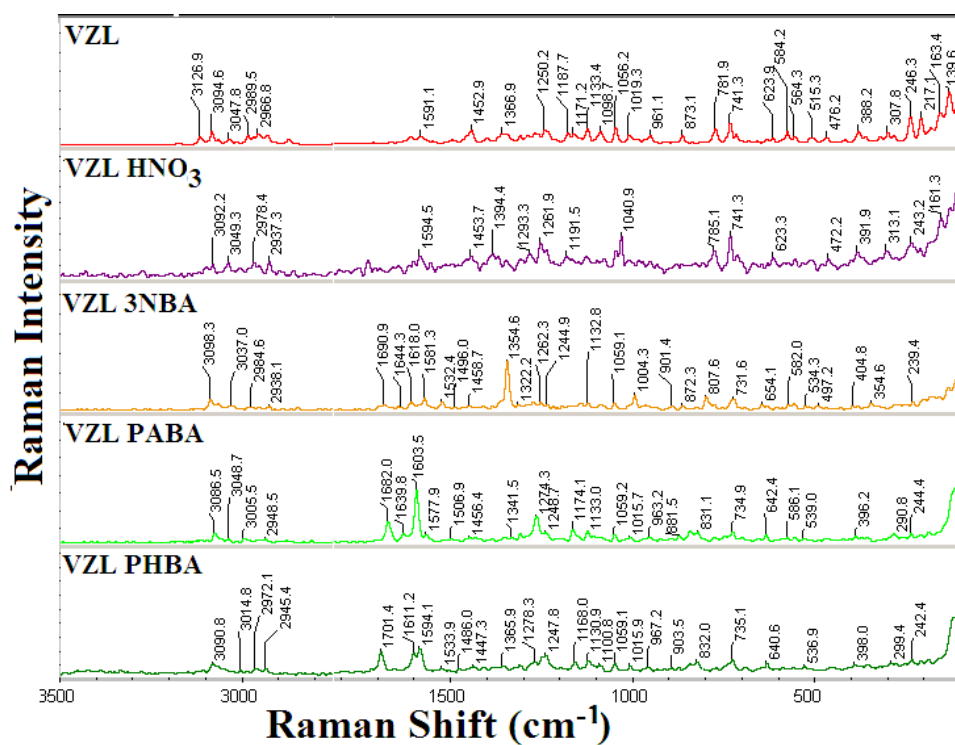


Figure 5.10 Comparison of FT-IR spectra of VZL with voriconazole-dinitrate salt and cocrystals.

Table 5.10 FT-Raman frequency of crystalline VZL forms (cm⁻¹).

Solid forms	Aromatic C-H stretch	Aliphatic C-H stretch	O-H bending (in-plane)	O-H bending (out-of-plane)	C=O stretch cocrystal (group in coformer)
VZL	3094.6	2966.8	1250.2	623.9	-
VZL-HNO ₃	3092.2	2937.3	1261.9	623.3	-
VZL-PHBA	3086.3	2938.1	1262.3	654.1	1690.9
VZL-PABA	3086.5	2948.5	1274.3	642.4	1682.0
VZL-3-NBA	3090.8	2945.4	1278.3	640.6	1701.4

5.2.5 DSC Analysis

Thermal analysis confirmed the formation of VZL salt and cocrystals. Though VZL–PABA and VZL–PHBA are isomorphous, there is a large difference in their melting points (120 °C, 152 °C). The similarity in the molecular conformation of these two isostructural cocrystals as well as their density (VZL–PHBA 1.43 g cm⁻³, VZL–PABA 1.42 g cm⁻³) suggests that the reason for difference in melting point could be hydrogen bonding. A short O–H···N hydrogen bond in VZL–PHBA of the hydroxyl donor to a triazole N (O4–H4···N3 1.84 Å, 159°) is replaced by two longer H bonds in VZL–PABA (N6–H6A···O3 2.43 Å, 154°; N6–H6B···N3 2.09 Å, 174°), while the other strong H bonds are of similar length/ strength (see Table 5.4). VZL–3-NBA has a lower melting point of 95 °C. The conformation of this cocrystal is slightly different from other two cocrystals of PABA and PHBA in the overlay of molecular conformations¹⁹ (Fig. 5.6b). Molecular conformation and melting point of carboxylic acids have been correlated in the recent literature.²⁰ DSC thermograms of VZL complexes are shown in Fig. 5.11 and the melting temperatures are mentioned in Table 5.11. The dinitrate salt melts at 151 °C and the large exotherm in the DSC indicates decomposition of the salt at 154 °C.

Table 5.11 Melting temperatures of solid forms of VZL

Solid forms	m.p. of Cocrystal/ Salt (°C)	m.p. of Coformers (°C)	Density (g cm ⁻³)
VZL	129.6	--	1.442
VZL–HNO ₃	151.0	--	1.623
VZL–PHBA	152.0	215	1.438
VZL–PABA	119.9	188	1.427
VZL–3-NBA	94.46	140	1.490

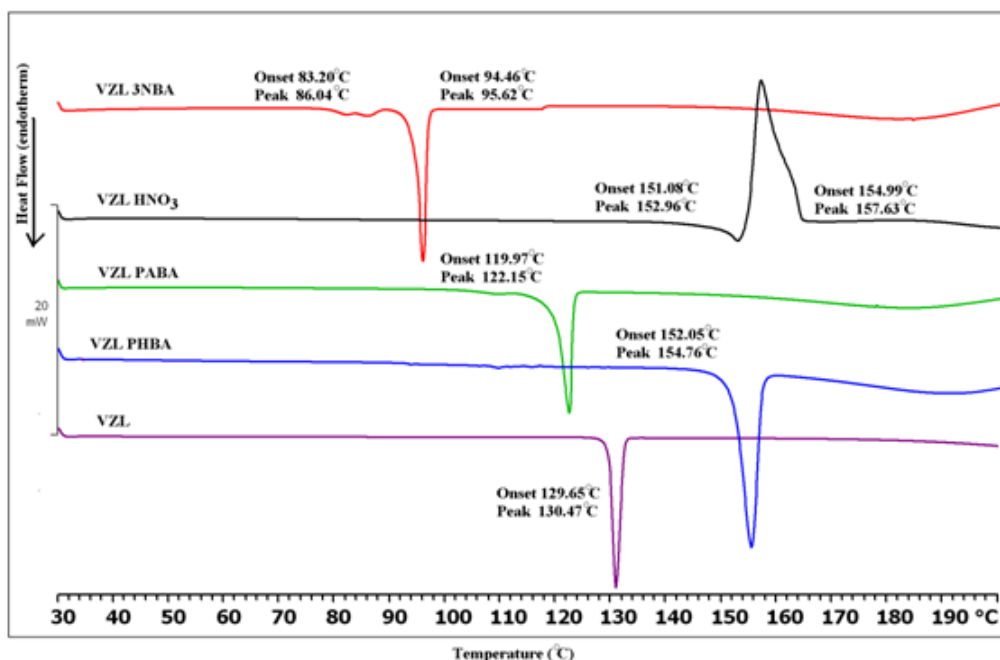


Figure 5.11 DSC comparison of VZL adducts with VZL drug.

5.3 Solubility and dissolution study

Solubility and dissolution behavior of voriconazole salt and cocrystals were measured in 0.1 N HCl. The advantage of salt preparation with respect to cocrystal is well established in the literature.²¹ However, due to the presence of less basic groups (N3 of triazole and N5 of pyrimidine) in voriconazole, salt preparation is difficult and proton transfer occurred only with the strong HNO₃. The dinitrate salt of voriconazole is about 10 times more soluble (2.5 mg/ mL) than the free base (0.26 mg/ mL) in 0.1 N HCl. The cocrystals with EAFUS coformers² (PABA and PHBA) and 3-NBA have lower solubility (1.16, 0.35 and 0.39 mg/ mL) than the dinitrate salt. It is noteworthy that the isomorphous VZL–PABA cocrystal is ~ 3 times more soluble than VZL–PHBA. The reason for the higher solubility of PABA cocrystal is due to the higher solubility of the coformer PABA (6.11 mg/mL) compared to PHBA

(4.89 mg/mL) and the presence of NH_2 (two H-bond donors) compared to OH (one H-bond donor) group, which will lead to greater hydration in solution.²²

The intrinsic dissolution²³ data follows similar trends (Table 5.12). The nitrate salt has ~ 3 times faster IDR compared to VZL base (Fig. 5.12). Some of the materials were found to be stable as confirmed by PXRD of the residue at the end of the solubility and dissolution measurements (Fig. 5.13).

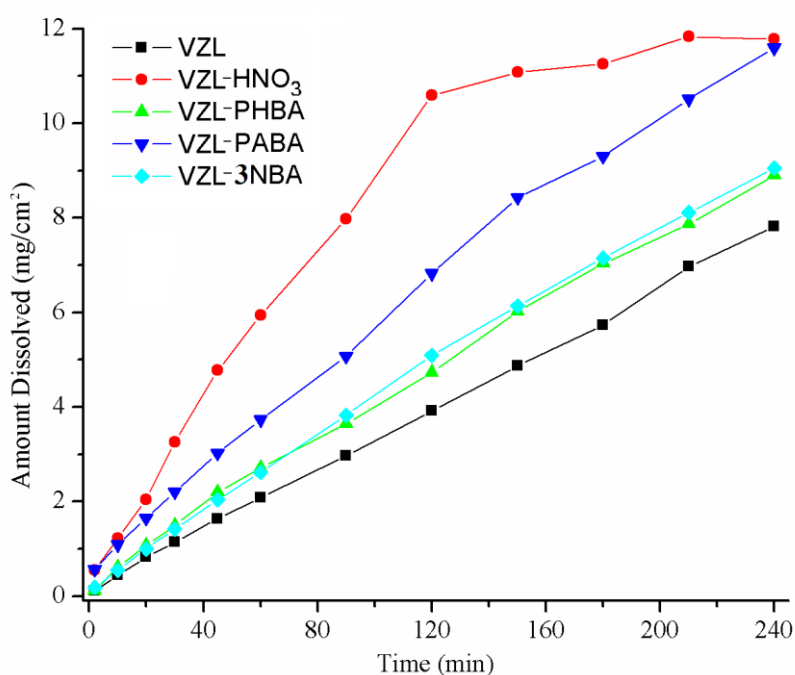


Figure 5.12 Dissolution profile of voriconazole pure base and its solid forms in 0.1N HCl solution in 4 h.

Table 5.12 Solubility and Intrinsic dissolution rate of VZL solid forms

Solid forms	λ_{max} (nm)	Absorption coefficient (ϵ), ($\text{M}^{-1} \text{cm}^{-1}$)	IDR in 0.1N HCl ($\times 10^{-2} \text{ g/cm}^2 \text{min}^{-1}$)	Solubility in 0.1N HCl (mg/mL)
VZL	257	318.37	3.27	0.26
VZL-HNO ₃	259	141.91	9.18	2.57

VZL-PHBA	258	547.70	3.86	0.35
VZL-PABA	257	187.05	5.20	1.16
VZL-3-NBA	258	337.13	3.95	0.39

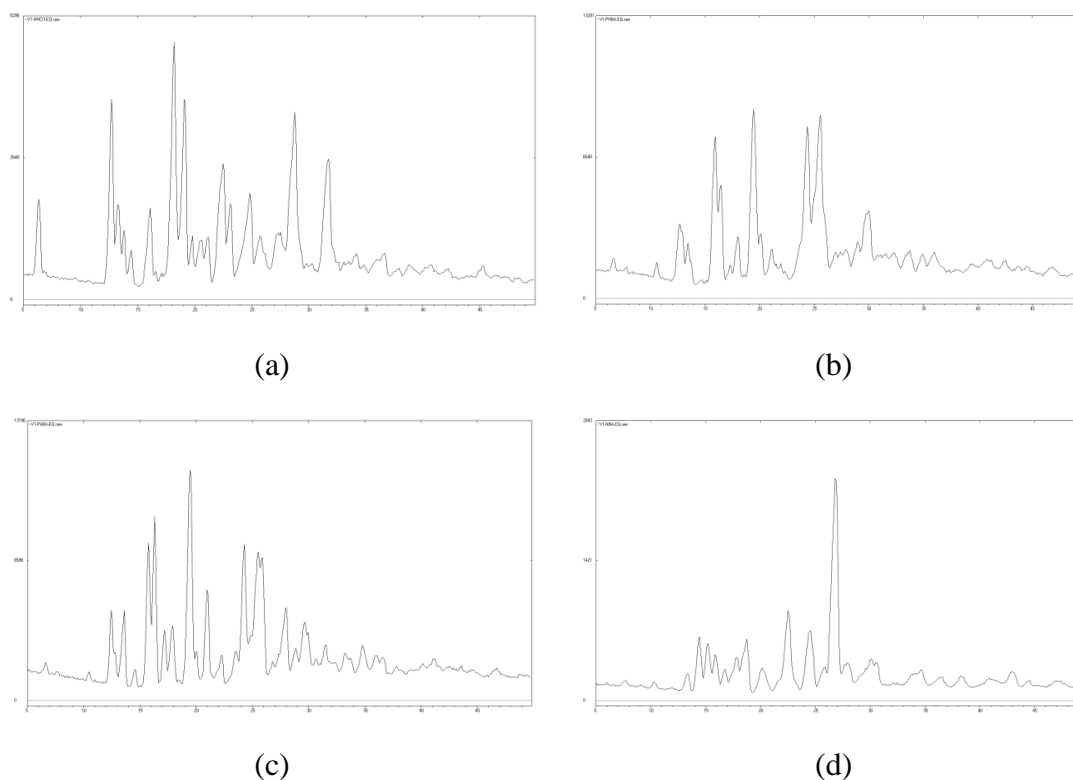


Figure 5.13 PXRD of (a) Dinitrate salt converted to HCl salt in the acid medium, (b) VZL-PHBA, (c) VZL-PABA, (d) VZL-3-NBA after slurry in solubility medium of 0.1 N HCl for 24 h.

5.4 Conclusions

A nitrate salt and three cocrystals of voriconazole with PHBA, PABA and 3-NBA were prepared in bulk as well as by solution crystallization. All the multi-component structures of voriconazole were characterized using solid-state

characterization techniques. Overall, the success rate for cocrystal/ salt formation was found to be very difficult from the 30 or so coformers/ salt formers attempted. From the crystal structures it was observed that there is a synthon switch from acid–pyrimidine to acid–triazole synthon depending on the strength of the coformer acid. The weaker PABA and PHBA are sustained by acid–pyrimidine whereas stronger 3-NBA cocrystal contains acid–triazole synthon. Both the pyrimidine and triazole N are protonated in the dinitrate salt. The occurrence of these synthons is compared with CSD statistics. There are very few reports for these two synthons and the present analysis adds structural data to the less known acid–triazole and acid–pyrimidine two-point synthons. The isostructurality between PHBA and PABA cocrystals of voriconazole was quantified by XPac. The good solubility and dissolution of VZL–PABA cocrystal is encouraging along with the dinitrate salt of voriconazole for formulation development.

5.5 Experimental Section

Materials. Voriconazole was purchased from Shanghai Xunxin Chemical Co., Ltd., China and was used without any further purification. All other coformers were of analytical or chromatographic grade and were purchased from Sigma-Aldrich (Hyderabad, India). Water altered through a double-deionized purification system (Milli Q Plus Water System from Millipore Co., Billerica, Massachusetts) was used in all the experiments. Melting points were measured on a Fisher-Johns melting point apparatus. Single crystals were obtained via slow evaporation of stoichiometric amounts of starting materials in appropriate organic solvents after solid state and liquid assisted grinding in a mortar-pestle. Cocrystals and salt were characterized by FT-IR, Raman, ^{13}C ss-NMR spectroscopy techniques, DSC, PXRD and single crystal X-ray diffraction (SC-XRD).

5.5.1 Preparation of cocrystals by liquid (solvent drop) assisted grinding

1. Voriconazole (VZL)

Voriconazole crystals were obtained from organic alcoholic solvents and the ground material of these crystals was used in the comparison of analysis and characterizations with the new solid forms. m.p. 130-132 °C.

2. VZL–PHBA (1:1) cocrystal

100 mg (0.28 mmol) voriconazole and 38.5 mg (0.28 mmol) p-hydroxybenzoic acid were ground in mortar-pestle for 15 min after adding 5 drops of EtOH, and then kept for crystallization in 10 mL ethanol. Suitable plate type crystals appeared at ambient condition after 3-4 days. m.p. 150-153 °C.

3. VZL–PABA (1:1) cocrystal

100 mg (0.28 mmol) voriconazole and 39.2 mg (0.28 mmol) p-aminobenzoic acid were ground in mortar-pestle for 15 min after adding 5 drops of EtOH, and then kept for crystallization in 10 mL 1:1 methanol-ethanol mixture. Suitable thick plate crystals were harvested at ambient condition after 3-4 days. m.p. 120-122 °C.

4. VZL–3-NBA (1:1) cocrystal

100 mg (0.28 mmol) voriconazole and 47.8 mg (0.28 mmol) PABA was ground in mortar-pestle for 15 min after adding 5 drops of EtOH/CH₃CN, and then kept for crystallization in 10 mL ethanol. Suitable block and plate type crystals were harvested at ambient condition after 3-4 days. m.p. 94-96 °C.

5. VZL–HNO₃ (1:2) salt

100 mg (0.28 mmol) voriconazole is dissolved in 10 mL of ethanol and boiled on a hot plate to reach the homogeneous solution. Few drops of diluted nitric acid

solution is added into the homogeneous solution of voriconazole, boiled for 2-3 minutes and allowed for evaporation under room temperature condition. Suitable plate crystals were harvested at ambient condition after 4 days. m.p. 152-154 °C.

X-ray Crystallography. X-ray reflections for voriconazole dinitrate salt (LT data) and voriconazole:p-hydroxybenzoic acid (RT data) were collected on a Bruker SMART APEX CCD diffractometer equipped with a graphite monochromator and Mo-K α fine-focus sealed tube ($\lambda = 0.71073$ Å). Data integration was done using SAINT.^{24a} Intensities for absorption were corrected using SADABS.^{24b} Structure solution and refinement were carried out using Bruker SHELX-TL.^{24c} X-ray reflections for voriconazole:p-aminobenzoic acid and voriconazole:3-nitrobenzoic acid (RT data) were collected on an Oxford Xcalibur Gemini Eos CCD diffractometer using Mo-K α , radiation. Data reduction was performed using CrysAlisPro (version 1.171.33.55).^{24d} OLEX2-1.0 and SHELX-TL 97 were used to solve and refine the data.^{24e} All non-hydrogen atoms were refined anisotropically, and C–H hydrogens were fixed. In case of VZL-HNO₃, the N–H location in pyrimidine ring was not stable in mapping as the proton is only partially protonated from HNO₃ to the pyrimidine ring. The reason for this partial proton transfer is due to the less basic nature of pyrimidine N compared to triazole. O–H and N–H protons were located from difference electron density maps and C–H hydrogens were fixed. Hydrogen bond distances were neutron normalized using WingGX-PLATON.^{24f} Packing diagrams were prepared in X-Seed.²⁵ Crystallographic .cif files (CCDC Nos. 971867-971870) are available at www.ccdc.cam.ac.uk/data_request/cif or as part of the Supporting Information.

CSD Search. All organic compounds, with “triazole” and pyrimidine” with the intermolecular distance of 1-3 Å with “carboxylic acid” in the qualifier, and entries for which 3D coordinates are determined were searched in Cambridge Structural Database, ver. 5.34, ConQuest 1.15, November 2012 release, May 2013 update. Two

hits for triazole–carboxylic acid and five hits for pyrimidine–carboxylic acid two point synthon of O–H···N and C–H···O hydrogen bonds were retrieved. The combination search of both triazole and pyrimidine synthons in the same distance range with carboxylic acid gave 0 hits. These data and Refcodes for CSD search are summarized in Table 3.

Vibrational Spectroscopy. Nicolet 6700 FT-IR spectrometer with an NXR FT-Raman module was used to record IR spectra. IR spectra were recorded on samples dispersed in KBr pellets. Raman spectra were recorded with the pellet of samples.

¹³C ss-NMR Spectroscopy. Solid-state NMR spectra were recorded on a Bruker Advance spectrometer operating at 400 MHz (100 MHz for ¹³C nucleus). ss-NMR spectra were recorded on a Bruker 4 mm double resonance CP-MAS probe in zirconia rotors at 5.0 kHz spin rate with a cross-polarization contact time of 2.5 ms and a recycle delay of 8 s. ¹³C CP-MAS spectra recorded at 100 MHz were referenced to the methylene carbon of glycine and then the chemical shifts were recalculated to the TMS scale ($\delta_{\text{glycine}} = 43.3$ ppm).

Thermal Analysis. DSC was performed on Mettler Toledo DSC 822e module. Samples were placed in crimped but vented aluminum sample pans. The typical sample size was 3–4 mg, and the temperature range was 30–200 °C at heating rate of 5 °C/min. Samples were purged by a stream of dry nitrogen flowing at 150 mL/min.

Dissolution and Solubility Measurements. Intrinsic dissolution rate (IDR) and solubility measurements were carried out on a USP certified Electrolab TDT-08 L dissolution tester (Electrolab, Mumbai, MH, India). A calibration curve was obtained for all the solid forms by plotting absorbance vs. concentration UV-vis spectra curves on a Thermo Scientific Evolution EV300 UV-vis spectrometer (Waltham, MA) for known concentration solutions in 0.1N HCl solutions medium. The slope of the plot from the standard curve gave the molar extinction coefficient (ϵ) by applying

the Beer-Lambert's law. Equilibrium solubility was determined in 0.1N HCl solutions medium using the shake-flask method. To obtain equilibrium solubility, 15-200 mg of each solid material was stirred for 24 h in 5-10 mL of 0.1N HCl solutions at 37 °C, and the absorbance was measured at 257-260 nm. The concentration of the saturated solution was calculated at 24 h, which is referred to as the equilibrium solubility of the stable solid form. The dissolution rates are obtained from the IDR experiments.

Powder X-ray Diffraction. PXRDs were recorded on a SMART Bruker D8 Advance X-ray diffractometer (Bruker-AXS, Karlsruhe, Germany) in the Bragg-Brentano geometry using Cu-K α X-radiation ($\lambda = 1.5406 \text{ \AA}$) at 40 kV and 30 mA. Diffraction patterns were collected over the 2θ range of 5-50° at a scan rate of 1°/min. The appearance of new solid phases was monitored by the appearance of new diffraction peaks when comparing with the starting materials. Powder Cell 2.359²⁶ was used for overlaying the experimental XRPD pattern on the calculated lines from the crystal structure.

Melting Point. Fisher-Scientific instrument is used for the determination of melting points of VZL and its solid forms. Samples were taken in less than 1 mg quantity for this study.

5.6 References

1. (a) D.-K. Bučar, G. M. Day, I. Halasz, G. G. Z. Zhang, J. R. G. Sander, D. G. Reid, L. R. MacGillivray, M. J. Duer and W. Jones, *Chem. Sci.*, **2013**, 4, 4417; (b) N. Schultheiss and A. Newman, *Cryst. Growth Des.*, **2009**, 9, 2950.
2. (a) GRAS Notices: <http://www.cfsan.fda.gov/~rdb/opa-gras.html>. (b) Food additive status list: <http://www.cfsan.fda.gov/~dms/opaappa.html>.
3. (a) H. G. Brittain, *Cryst. Growth Des.*, 2012, 12, 5823; (b) N. J. Babu and A. Nangia, *Cryst. Growth Des.*, **2011**, 11, 2662; (c) R. Thakuria, A. Delori, W. Jones, M. P. Lipert, L. Roy and N. Rodríguez-Hornedo, *Int. J. Pharm.*, **2013**,

- 453, 101; (d) S. Datta and D. J. W. Grant, *Nat. Rev. Drug Discov.*, **2004**, *3*, 42.
4. J. Remenar, S. Morissette, M. Peterson, B. Moulton, J. MacPhee, H. Guzman and Ö. Almarsson, *J. Am. Chem. Soc.*, **2003**, *125*, 8456.
 5. S. L. Childs, L. J. Chyall, J. T. Dunlap, V. N. Smolenskaya, B. C. Stahly and G. P. Stahly, *J. Am. Chem. Soc.*, **2004**, *126*, 13335.
 6. (a) S. Karki, T. Friščić, W. Jones and W. D. S. Motherwell, *Mol. Pharm.*, **2007**, *4*, 347; (b) W. T. A. Harrison, H. S. Yathirajan, S. Bindya, H. G. Anilkumar and Devaraju, *Acta Crystallogr., Cryst. Struct. Commun.*, **2007**, *C63*, 129; (c) G. Petruševski, P. Naumov, G. Jovanovski and S. Ng Weng, *Inorg. Chem. Commun.*, **2008**, *11*, 81; (d) M. Cheney, D. Weyna, N. Shan, M. Hanna, L. Wojtas and M. Zaworotko, *J. Pharm. Sci.*, **2011**, *100*, 2172.
 7. (a) J. A. Como and W. E. Dismukes, *N. Engl. J. Med.*, **1994**, *330*, 263; (b) S. Tsutsumi, M. Iida, N. Tada, T. Kojima, Y. Ikeda, T. Moriwaki, K. Higashi, K. Moribe and K. Yamamoto, *Int. J. Pharm.*, **2011**, *421*, 230.
 8. (a) Nonappa, M. Lahtinen, E. Kolehmainen, J. Haarala and A. Shevchenko, *Cryst. Growth Des.*, **2013**, *13*, 346; (b) A. Shevchenko, L. Bimbo, I. Miroshnyk, J. Haarala, K. Jelínková, K. Syrjänen, B. van Veen, J. Kiesvaara, H. Santos and J. Yliruusi, *Int. J. Pharm.*, **2012**, *436*, 403; (c) J. Kastelic, Ž. Hodnik, P. Šket, J. Plavec, N. Lah, I. Leban, M. Pajk, O. Planinšek and D. Kikelj, *Cryst. Growth Des.*, **2010**, *10*, 4943; (d) J. Kastelic, N. Lah, D. Kikelj and I. Leban, *Acta Crystallogr., Crystal Struct. Commun.*, **2011**, *C67*, 370; (e) J. Kastelic, D. Kikelj, I. Leban and N. Lah, *Acta Crystallogr., Sec. E: Struct. Reports Online*, **2013**, *E69*, 0378; (f) M. Caira, K. Alkhamis and R. Obaidat, *J. Pharm. Sci.*, **2004**, *93*, 601; (g) Y. Ling, L. Zhang, J. Li, S.-S. Fan and M. Du, *CrystEngComm*, **2010**, *12*, 604; (h) Y. Ling, L. Zhang, J. Li and A. X. Hu, *Cryst. Growth Des.*, **2009**, *9*, 2043.
 9. (a) K. Ravikumar, B. Sridhar, K. Prasad and A. B. Rao, *Acta Crystallogr., Struct. Reports Online*, **2007**, *E63*, 565; (b) R. P. Dickinson, A. S. Bell, C. A. Hitchcock, S. Narayanaswami, S. J. Ray, K. Richardson and P. F. Troke, *Bioorg. Med. Chem. Lett.*, **1996**, *6*, 2031; (c) L. J. Taylor, D. G. Papadopoulos, P. J. Dunn, A. C. Bentham, N. J. Dawson, J. C. Mitchell and M. J. Snowden, *Org. Process. Res. Dev.*, **2004**, *8*, 674.
 10. (a) S. Roffey, S. Cole, P. Comby, D. Gibson, S. Jezequel, A. Nedderman, D. Smith, D. Walker and N. Wood, *Drug Metab. Dispos.*, **2003**, *31*, 731; (b) P.

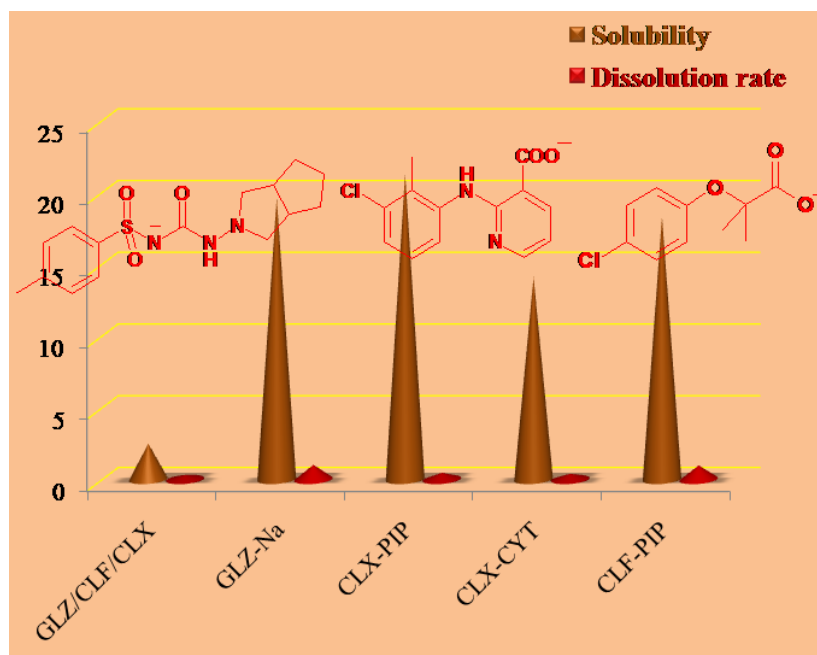
- Colomer, M. Lloret and S. Pérez, *European Patent Application* 10382204.5, EP2409699 *AI*, **2012**; (c) B. Zaludek and L. Zatloukalova, PCT/EP2011/059945, WO2012171561 *AI*, **2012**.
11. (a) B. Sarma, N. K. Nath, B. R. Bhogala and A. Nangia, *Cryst. Growth Des.*, **2009**, 9, 1546; (b) B. Sarma, R. Thakuria, N. K. Nath and A. Nangia, *CrystEngComm*, **2011**, 13, 3232; (c) S. L. Johnson and K. A. Rumon, *J. Phys. Chem.*, 1965, 69, 74; (d) S. L. Childs, G. P. Stahly and A. Park, *Mol. Pharm.*, **2007**, 4, 323.
 12. (a) M. C. Etter, *J. Phys. Chem.* 1991, 95, 4601; (b) M. C. Etter, *Acc. Chem. Res.*, **1990**, 23, 120; (c) J. Grell, J. Bernstein and G. Tinhofer, *Acta Crystallogr., Struct. Sci.*, **1999**, B55, 1030.
 13. (a) C. M. Buchanan, N. L. Buchanan, K. J. Edgar and M. G. Ramsey, *Cellulose*, **2007**, 14, 35; (b) G. N. K. Reddy, V. V. S. R. Prasad, N. Devanna and P. K. Maharana *Der Pharmacia Letter*, **2011**, 3, 249; (c) C. A. Hollingsworth, P. G. Seybold and C. M. Hadad *Int. J. Quantum Chem.*, **2002**, 90, 1396; (d) J. C. R. Corrêa, C. D. Vianna-Soares and H. R. N. Salgado, *Chromat. Res. Int.*, doi:10.1155/2012/610427.
 14. (a) N. K. Nath and A. Nangia, *Cryst. Growth Des.*, **2012**, 12, 5411; (b) N. K. Nath, B. K. Saha and A. Nangia, *New J. Chem.*, **2008**, 32, 1693; (c) S. K. Chandran, R. Thakuria and A. Nangia, *CrystEngComm*, **2008**, 10, 1891; (d) R. Thakuria and A. Nangia, *Cryst. Growth Des.*, **2013**, 13, 3672; (e) M. R. Edwards, W. Jones and W. D. S. Motherwell, *CrystEngComm*, **2006**, 8, 545; (f) D. Cinčić, T. Friščić and W. Jones, *New J. Chem.*, **2008**, 32, 1776; (g) A. Kalman, L. Parkanyi and G. Aragay, *Acta Crystallogr., Struct. Sci.*, **1993**, B49, 1039; (h) A. Anthony, M. Jaskólski, A. Nangia and G. R. Desiraju, *Chem. Commun.*, **1998**, 2537.
 15. (a) T. Gelbrich and M. B. Hursthouse, *CrystEngComm*, **2005**, 7, 324; (b) T. Gelbrich and M. B. Hursthouse, *CrystEngComm*, **2006**, 8, 448; (c) T. Gelbrich, T. L. Threlfall and M. B. Hursthouse, *CrystEngComm*, **2012**, 14, 5454.
 16. Cambridge Structural Database, ver. 5.34, ConQuest 1.15, November **2012** release, May 2013 update, Cambridge Crystallographic Data Center, www.ccdc.cam.ac.uk.
 17. (a) A. Newman, *Org. Process. Res. Dev.*, **2013**, 17, 457; (b) S. Aitipamula, A. B. H. Wong, P. S. Chow, and R. B. H. Tan, *CrystEngComm*, **2012**, 14, 8193.

18. (a) M. R. Chierotti and R. Gobetto *CrystEngComm*, **2013**, *15*, 8599; (b) T. Pawlak, P. Paluch, K. Trzeciak-Karlikowska, A. Jeziorna and M. J. Potrzebowski *CrystEngComm*, **2013**, *15*, 8680; (c) B. A. Zakharov, E. A. Losev and E. V. Boldyreva, *CrystEngComm*, **2013**, *15*, 1693.
19. (a) P. Vishweshwar, A. Nangia and V. M. Lynch, *Cryst. Growth Des.*, **2003**, *3*, 783.
20. (a) M. K. Mishra, S. Varughese, U. Ramamurty and G. R. Desiraju, *J. Am. Chem. Soc.*, **2013**, *135*, 8121; (b) S. Bhattacharya, V. G. Saraswatula and B. K. Saha, *Cryst. Growth Des.*, **2013**, *13*, 3299.
21. (a) S. M. Berge, L. D. Bighley and D. C. Monkhouse, *J. Pharm. Sci.*, **1977**, *66*, 1; (b) C. L. Cooke and R. Davey, *Cryst. Growth Des.*, **2008**, *8*, 3483; (c) M. Hawley and W. Morozowich, *Mol. Pharm.*, **2010**, *7*, 1441; (d) R. Thakuria and A. Nangia, *CrystEngComm*, **2011**, *13*, 1759.
22. (a) D. J. Good and N. Rodríguez-Hornedo, *Cryst. Growth Des.*, **2009**, *9*, 2252; (b) S. L. Childs, N. Rodríguez-Hornedo, L. S. Reddy, A. Jayasankar, C. Maheshwari, L. McCausland, R. Shipplett and B. C. Stahly, *CrystEngComm*, **2008**, *10*, 856; (c) A. T. M. Serajuddin, *Adv. Drug Deliv. Rev.*, **2007**, *59*, 603; (d) B. D. Anderson and R. A. Conradi, *J. Pharm. Sci.*, **1985**, *74*, 815.
23. (a) C. V. S. Subrahmanyam, *Textbook Of Biopharmaceutics & Pharmacokinetics, Concepts & Applications*, 1st Ed., M. K. Jain Vallabh Prakashan, **2010**; (b) Y. Qiu, Y. Chen, L. Liu and G. G. Z. Zhang, *Developing Solid Oral Dosage Forms: Pharmaceutical Theory and Practice*, 1st Ed., Academic Press, **2009**, pp. 75–86; (c) M. Abraham, A. Ibrahim, A. Zissimos, Y. Zhao, J. Comer and D. Reynolds, *Drug Discov. Today*, **2002**, *7*, 1056; (d) H. van De Waterbeemd, D. Smith, K. Beaumont and D. Walker, *J. Med. Chem.*, **2001**, *44*, 1313.
24. (a) SAINT-Plus, version 6.45; Bruker AXS Inc., Madison, WI, **2003**; (b) G. M. Sheldrick, SADABS, Program for Empirical Absorption Correction of Area Detector Data; University of Goettingen, Germany, **1997**; (c) SMART, version 5.625 and SHELX-TL, version 6.12; Bruker AXS Inc.: Madison, Wisconsin, USA, **2000**. (d) Oxford Diffraction. CrysAlis CCD and CrysAlis RED, versions 1.171.33.55; Oxford Diffraction Ltd: Yarnton, Oxfordshire, UK, **2008**; (e) O. V. Dolomanov, L. J. Bourhis, R. J. Gildea, J. A. K. Howard and H. Puschmann, OLEX2: A complete structure solution, refinement and analysis program. *J. Appl. Crystallogr.* **2009**, *42*, 339; (f) A. L. Spek, PLATON, A Multipurpose Crystallographic Tool; Utrecht

- University: Utrecht, Netherlands, **2002**. A. L. Spek, Single-crystal Structure Validation with the Program PLATON. *J. Appl. Crystallogr.* **2003**, 36, 7.
25. L. J. Barbour, X-Seed, Graphical Interface to SHELX-97 and POV-Ray; University of Missouri—Columbia, **1999**
26. N. Kraus, G. Nolze, Powder Cell, version 2.3, A Program for Structure Visualization, Powder Pattern Calculation and Profile Fitting; Federal Institute for Materials Research and Testing: Berlin, Germany, **2000**.

Chapter Six

New Pharmaceutical Salts of Gliclazide, Clonixin and Clofibric acid



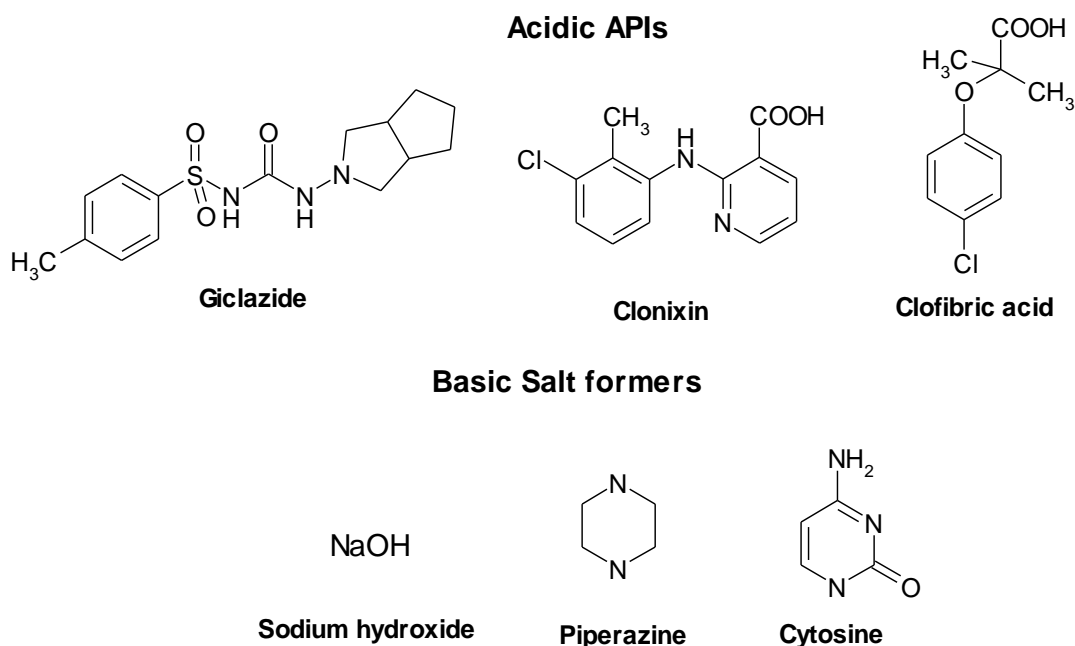
GLZ-Na, CLX-PIP and CLF-PIP salts are identified through the crystallization process and these salts are found to be ~ 10 times more soluble than that of these BCS II drugs. The organic molecular salts are of equal solubility advantage to mineral salts in this study.

6.1 Introduction

Salt formation is a common method to tune and change the desired physical and chemical properties of ionizable drug compounds.¹⁻² The main drug properties such as solubility, dissolution rate, hygroscopicity, stability, impurity profiles, and crystal habit can be regulated by variety of pharmaceutically acceptable acids or bases. Even the phase transition from polymorphism issues also is addressed by formation of salts.² Our first incentive for this drug development was polymorph screening in early development stages of any drugs because polymorphic forms differ in their crystal lattice energy that would make the impacts in different solubility and dissolution rates and eventually bioavailability. In early stages, pharmaceutical scientists and manufactures have recalled the drug products when polymorph transition occurred in the manufacture and storage.³ The selection of BCS class II drugs for salt/polymorph selection strategy is also in line with USA-FDA's year 2000 risk management and 2004 critical path initiatives.^{4a} The selection of counter ions for the formation of salts by using Orange Book Data base^{4b} consists of three drug categories such as proton acceptors I (acidic counter ion), proton donors II (basic counter ion) and no proton transfer III (non-salt) or intramolecular proton transfer (inner salt) categories by USA-FDA is also available to tune the drug properties.^{4c} There are several cocrystals reported for many drugs including ionisable^{5a-c} and non ionisable^{5d} drugs in order to improve the solubility and bioavailability but so far none of them are being approved by the USS-FDA regularity boards for further drug developments.⁵ Many other formulation techniques such as micronization, nanosizing, or complexation with cyclodextrins are also reported in the literature to increase aqueous solubility.⁶ Nevertheless, salt formulation is well developed and the only available and approved technique to change solubility property without changing the API molecule.^{6b} The salt

formulation technique is far better than the polymorph screen/cocrystal screening methods for all BCS class of drugs. It is because of different polymorphs may give same bioavailability if dissolution is not a rate limiting step such as BCS class 1 compound with high solubility and high permeability.^{4,7} Whereas the presence of different counter ions in the salt forms may impart varied safety and efficacy profiles.⁴ As a result, the salt form is usually selected prior to initiation of drug development program.^{6,7} The crystal structure of a salt is usually completely different from the crystal structure of the conjugate base or acid and also differs from one salt to another. The modification of physical chemical properties, mainly solubility and dissolution rate, may also lead to changes in biological effects such as pharmacodynamics and pharmacokinetics, including bioavailability and toxicity profile.⁸ On the basis of above ideas, we screened solid-state forms of BCS class II drugs such as Gliclazide (*N*-(hexahydrocyclopenta[*c*]pyrrol-2(1*H*)-ylcarbamoyl)-4-methylbenzenesulfonamide, GLZ), Clonixin (2-(3-chloro-2-methylanilino)pyridine-3-carboxylic acid, CLX) and Clofibric acid (2-(4-Chlorophenoxy)-2-methylpropanoic acid, CLF) listed in Scheme 6.1. These drugs are belonging to the broad classified drug categories called sulfonylurea drugs, fenamtes and fibrates (Table 6.1) and they require one general protocol to solve the drug issues such as solubility and stability. Infact these are already few low aqueous soluble drugs used for including type II diabetics as second generation sulphonylurea drug (GLZ), a non-steroid analgesic drug (CLX) and antihyperlipidemic in the BCS class II category and in the need to solve solubility issues via salt formation approach. Therefore, drugs from each category were selected and subjected into polymorph and salt screening test however they result only salts with different bases in solvent crystallization under laboratory conditions. Finally we were successful in obtaining new solid forms of these drugs with NaOH (Na salt), Piperazine (PIP) and Cytosine (CYT), and observed solubility enhancement of ~10 times higher solubility than the reference drugs.⁹ We found that the molecular salts CLX-PIP and CLF-PIP are of

equal solubility (~10 times) and stability advantage to GLZ-Na mineral salt. CLX-PIP and CLX-CYT showed even better solubility than its zwitterionic polymorph. Also CLF-PIP salt is easily crystallized reproducibly compared to cytosinium salt and it exhibits the highest solubility of 18.3 mg/mL compared to the CLF drug (2.7 mg/mL). The sodium-gliclazate showed three times improvements in dissolution rate with respect to GLZ where as the molecular salt of CLX and CLF showed two times dissolution developments with respect to CLX and CLF drugs. We report that these molecular salts are also having the equal solubility advantage and dissolution improvements to the mineral salts in this chapter. All these salts were well characterized by single crystal X-ray diffraction techniques and compared their hydrogen bonds and conformations with the parent APIs. The bulk purity of salt products was checked by powder XRD and confirmed further by solid state spectroscopy techniques ^{13}C NMR, FT-IR and Raman.¹⁰



Scheme 6.1 Low aqueous soluble drugs selected for polymorph/salt screening test and its successful salt formers are mentioned below.

Table 6.1 Drugs selected from the broad category of drug list for our study

S. No	List of sulfonylurea drugs	List of fenamates	List of fibrates
1	Carbutamide	Aceclofenac	Bezafibrate
2	Acetohexamide	Azapropazone	Ciprofibrate
3	Chlorpropamide	Clonixin	Clofibrate
4	Tolbutamide	Diclofenac	Gemfibrozil
5	Carbutamide	Etofenamate	Fenofibrate
6	Glipizide	Flufenamic acid	Etofibrate
7	Gliclazide	Flunixin	Clofibric acid
8	Glibenclamide or glyburide	Meclofenamic acid	Aluminium Clofibrate
9	Glibornuride	Mefenamic acid	
10	Gliquidone	Morniflumate	
11	Glisoxepide	Niflumic acid	
12	Glycropyramide		
13	Glimepiride		

6.2 Results and Discussion

6.2.1 Crystal Structure analysis

Gliclazide (GLZ): Gliclazide crystal was produced by dissolving 50 mg in 8 mL ethanol/acetone and solved in $P2_1/n$ space group with one molecule in the asymmetric group (see Appendix for crystallographic information).¹¹ The sulfonyl urea group of GLZ molecules is forming the linear chain of sulfonamide dimer and carboxamide dimer in alternate way in parallel to c-axis (see hydrogen bond parameters in Table 6.2). The sulfonamide $N1-H1 \cdots O1$ (2.12 Å, 141°) dimer synthon and urea carboxamide $N2-H2 \cdots O3$ (2.02 Å, 151°) dimer synthon present in the crystal structure of GLZ (Fig 6.1a) and they are subsequently forming the

hydrogen bond ring motif of $R_2^2(8)$ networks.¹² The weak bifurcated hydrogen bonds of C6–H6···O2 (2.33 Å, 151°) and C10–H10···O2 (2.46 Å, 156°) are completing the crystal packing in 2D.

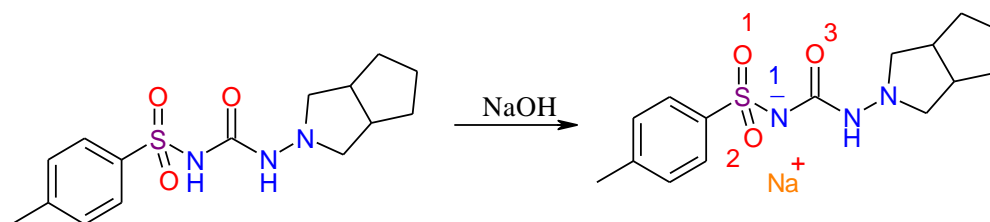
Table 6.2 Hydrogen bonds in crystal structures (neutron-normalized distances).

Interactions	H···A / Å	D···A / Å	∠D–H···A / °	Symmetry code
GLZ				
N1–H1···N3	2.30	2.681(3)	101	intramolecular
N1–H1···O1	2.12	2.976(3)	141	-x,-y,1-z
N2–H2···O3	2.02	2.949(3)	151	-x,-y,-z
C6–H6···O2	2.33	3.344(4)	156	1/2+x,-1/2-y,1/2+z
C10–H10···O2	2.46	3.386(4)	142	-1/2-x,1/2+y,1/2-z
GLZ-Na				
N2–H2···O1	1.96	2.906(3)	156	intramolecular
C7–H7···O3	2.34	3.168(4)	132	intramolecular
C7–H7···O2	2.31	3.197(4)	138	x,1/2-y,1/2+z
CLX-PIP				
N2–H2···O2	1.79	2.621(2)	137	intramolecular
N3–H3A···O1	2.53	3.240(2)	127	1/2+x,1/2-y,1/2+z
N3–H3A···O2	1.59	2.593(2)	173	1/2+x,1/2-y,1/2+z)
N3–H3B···N1	1.92	2.879(2)	158	-x+1/2,+y+1/2,-z+1/2+1
C11–H11···N1	2.28	2.879(3)	113	intramolecular
C12–H12B···Cl1	2.46	3.046(2)	113	intramolecular
C15–H15B···O1	2.42	3.438(2)	156	1/2-x,1/2+y,-1/2-z
CLX-CYT				
N2–H2···O2	1.83	2.658(4)	137	intramolecular
N4–H4A···O1	2.89	3.624(3)	128	-x+1,-y+1,-z
N4–H4A···O2	1.68	2.683(4)	172	1-x,1-y,-z
N5–H5B···O2	2.81	3.532(3)	127	-x+1,-y+1,-z

C11–H11...N1	2.14	2.851(5)	121	x,y,z
C12–H12B...Cl1	2.50	3.079(4)	112	x,y,z
C12–H12A...N5	2.69	3.173(4)	106	-x+1,-y+1,-z
C16–H16...N5	1.75	2.815(3)	165	-x,-y+1,-z
CLF				
O3–H3A...O2	1.65	2.627(16)	174	-x,-y,-z
C3–H3...O3	2.43	3.51(2)	175	1/2-x,1/2+y,1/2-z
CLF-PIP				
N1–H1A...O1	2.53	3.137(2)	119	1+x,y,z
N1–H1A...O3	1.72	2.700(2)	163	1+x,y,z
N1–H2A...O2	1.68	2.683(2)	176	x-1,+y,+z
C13–H13A...O4	2.80	3.523(11)	124	x+1/2,+y+1/2,+z
CLF-CYT.H₂O				
N5–H5B...O2	1.91	2.809(8)	146	-x,y,-z
N1–H1...O2	1.83	2.834(8)	174	x,y,z
N3–H3A...O4	1.84	2.835(10)	169	-x,y,-z
N3–H3B...O3	2.01	2.973(10)	159	-1/2+x,1/2+y,z
N4–H4A...O5	1.81	2.816(8)	174	-x,y,-z
N4–H4B...O6	1.93	2.905(9)	160	x,-1+y,z
N6–H6A...O2	1.92	2.897(9)	161	1/2-x,-1/2+y,-z
O6–H6B...O3	1.84	2.812(10)	172	x,1+y,z
O6–H6C...O2	2.12	2.905(11)	136	x,y,z
C18–H18...O4	2.00	3.085(10)	176	1/2-x,-1/2+y,-z

Sodium-gliclazate (GLZ-Na): This was prepared by dissolving 50 mg of GLZ in ethanol containing 0.1 N NaOH solutions and it is boiled for 5 minutes and then kept for slow evaporation under RT condition. Square shaped colorless crystals were separated and used for single crystal X-ray studies. The crystal structure of GLZ-Na

is solved in $P2_1/c$ space group with one molecule of anionic GLZ and one Na counter ion in the asymmetric unit. GLZ ligand has five sites which can allow chelation (Scheme 6.2) with metal ions and the chelation through N1, O2 (I) and O1, O3 (II) and N3, O3 (III) in six coordinated complex. Na^+ cation is a hard acid which binds preferentially with the hard base oxygen donors of sulfonyl urea oxygen atoms, because the nitrogen donors are softer bases, which leads to a higher probability that the ligand binds Na^+ through II mode.¹³ Furthermore, since the deprotonated nitrogen N1 is more basic than the tertiary amine nitrogen N3 chelation via site (III) was expected to form more stable complexes. The intramolecular hydrogen bonds (Fig 6.1b) are further stabilizing this complex through N2–H2···O1 (1.96 Å, 156°) and C7–H7···O3 (2.34 Å, 132°). Two molecules of GLZ anionic ligands are connected through intermolecular hydrogen bonds C7–H7···O2 (2.31 Å, 138°).



Scheme 6.2 Solid state acid-base reaction of GLZ with NaOH

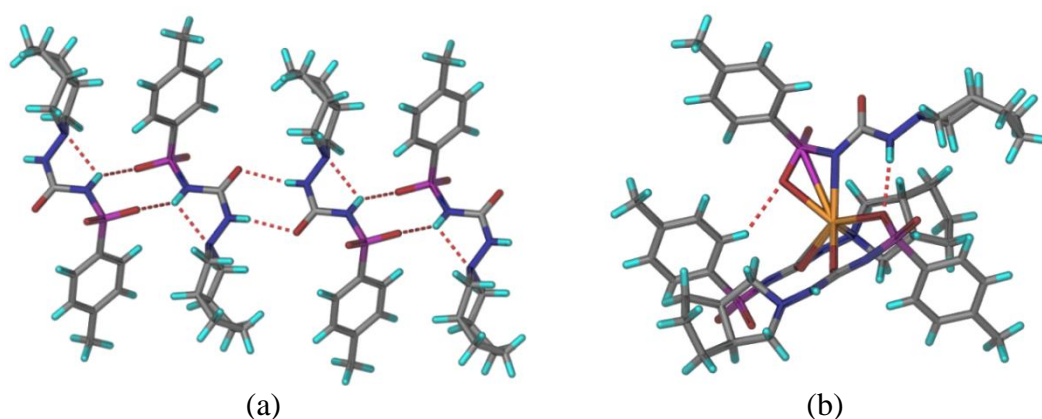


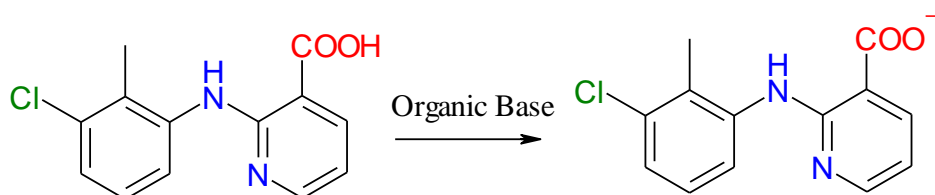
Figure 6.1 (a) Sulfonamide dimer and carboxamide dimer synthons in sulfonyl urea functionality and (b) Six coordinated chelation of Na with sulfonyl urea donors.

Clonixin: Clonixin is reported as tetramorphs¹⁴ where Form I neutral structure contains strong acid pyridine synthon ($\text{O}-\text{H}\cdots\text{N}$) where as form II ionic structure contain acid-pyridine ionic $\text{N}^+-\text{H}\cdots\text{O}^-$ interactions in crystal structures reported. The third and fourth neutral forms of clonixin are having the centrosymmetric acid ($\text{O}-\text{H}\cdots\text{O}$) dimer synthon in their crystal structures. Recently we proved that the zwitterionic form of CLX is having the twin characteristics of highest solubility and stability over neutral polymorphs.¹⁵ The same study is continued to know the effect of salt on solubility and stability of CLX.

Piperazinium-clonixate (CLX-PIP): This salt was prepared by taking the 1:0.5 mixture of clonixin and piperazine base in MeOH solvent and boiled until we get the clear solution. Then it is allowed to evaporate for three-five days in laboratory condition and the colorless crystals were separated finally for single crystal XRD study. The plate type crystals are mounted and the structure is refined in $P2_1/n$ space group. The stacking of CLX molecules are sustained by the $\text{N3}^+-\text{H3A}\cdots\text{O1}^-$ (1.59 Å, 173°) and $\text{N3}^+-\text{H3A}\cdots\text{O1}^-$ (2.53 Å, 127°) along with weak $\text{N3}^+-\text{H3b}\cdots\text{N1}$ (1.92 Å, 158°) hydrogen bonds with ionized piperazine molecules as in Figure 6.2 a. The secondary amino group is participating in intramolecular hydrogen bonding with carboxylate group through $\text{N2}-\text{H2}\cdots\text{O2}$ (1.79 Å, 137 °) interactions which is present in all four polymorphs of clonixin.

Cytosinium-clonixate (CLX-CYT): The salt of CLX and CYT was made by dissolving the mixture of 1:1 ratio of CLX and CYT in MeOH/ CH_3CN solvents and boiled for few minutes (scheme 6.3). The resulted crystal was checked in single crystal XRD and the crystal structure is refined in $C2$ space group. Two molecules of CLX are interacting through the ionic $\text{N4}^+-\text{H4A}\cdots\text{O2}^-$ (1.68 Å, 172°) and $\text{C12}-\text{H12A}\cdots\text{N5}$ (2.69 Å, 106°) interactions with cytosinium ions in crystal structure (Fig. 6.2b). The primary amino group in cytosine is connecting the two cytosinium molecules via $\text{C16}-\text{H16}\cdots\text{N5}$ (1.75 Å, 165°) and the secondary amino group in CLX

is forming the intramolecular hydrogen bonding ($\text{N2-H2}\cdots\text{O2}$, 1.83\AA , 137°) with carboxylate group.



Scheme 6.3 Solid state acid-base reaction of CLX with piperazine and cytosine bases

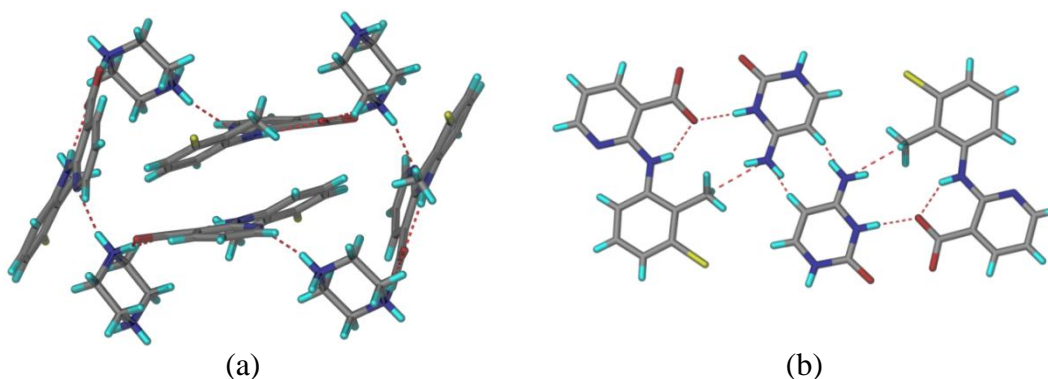


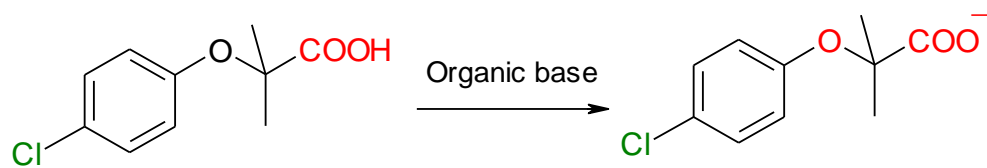
Figure 6.2 (a) Ionic $\text{N}^+-\text{H}\cdots\text{O}^-$ and $\text{N}^+-\text{H}\cdots\text{N}$ hydrogen bonds in CLX-PIP and (b) $\text{N}^+-\text{H}\cdots\text{O}^-$ and $\text{C}-\text{H}\cdots\text{N}$ hydrogen bonds in CLX-CYT molecular salts.

Clofibric acid: The crystals of clofibric acid are grown in ether solvent by solvent evaporation under ambient condition for single crystal X-ray diffraction studies. The crystal structure is solved in $P2_1/n$ space group and monoclinic crystal system. The carboxylic acid-acid dimer $R_2^2(8)$ supramolecular synthon of $\text{O3-H3A}\cdots\text{O2}$ (1.65\AA , 174°) bonds is present between two molecules of CLF in the crystal structure.¹⁶ This strong hydrogen bond is arranging the molecules in the zig-zag manner with the support of the $\text{C3-H3}\cdots\text{O3}$ (2.43\AA , 175°) weak hydrogen bonds in Fig. 6.3a. The crystal structure of clofibric acid is first reported by A.H. White et al and the carboxylic acid proton is missing in the reported crystal structure with R-factor of 0.06.¹⁶ We again report here the crystal structure of CLF with improved crystal data

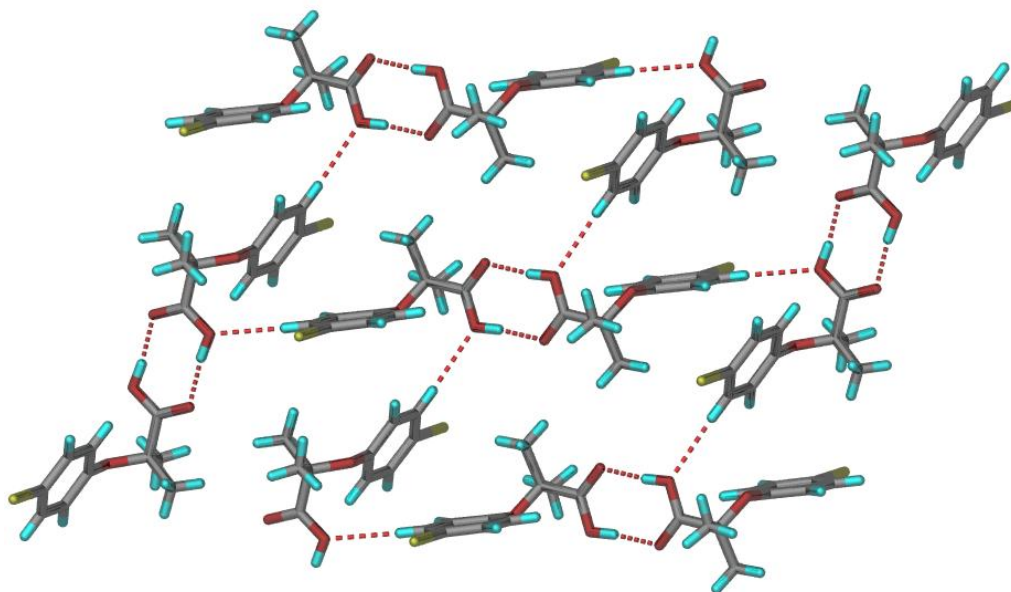
and refinement of R-factor of 0.0455 after fixing the proton. This crystal structure is considered for comparison and analysis with the crystal structures of its novel salts in the following discussions.

Piperazinium-clofibrate (CLF-PIP): The crystal structure of piperazinium-clofibrate salt was made in 1:0.5 ratios and it is crystallized in EtOH solvent (Scheme 6.4) and solved finally in $P2_1/n$ space group. The CLF molecule is interacting with piperazine molecule via strong hydrogen bonds $N1^+-H2A\cdots O2^-$ (1.68 Å, 176°) and $N1^+-H1A\cdots O3^-$ (1.72 Å, 163°) along with weak hydrogen bonds of $N1^+-H1A\cdots O1^-$ (2.53 Å, 119°) and the piperazine molecule adopted the channel between the two layers of clofibric acids as shown in Figure 6.3b. The packing of molecules in two dimension is completed by weak $C13-H13A\cdots O4$ (2.80 Å, 124°) hydrogen bonds.

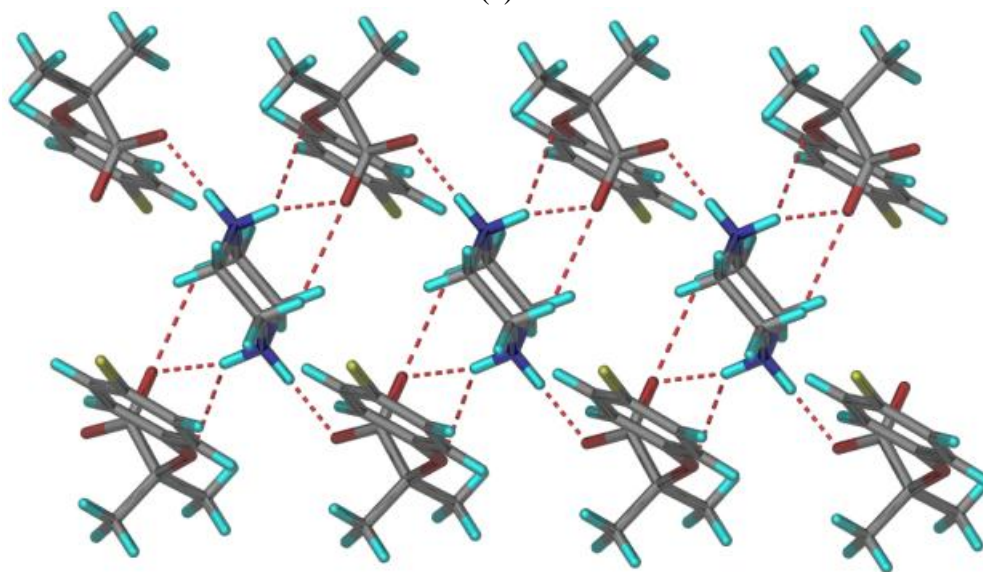
Cytosinium-clofibrate cytosine monohydrate: (CLF⁻-CYT⁺-CYT-H₂O): This salt hydrate of clofibric acid-cytosine cocrystal/salt is crystallized in acetonitrile solvent as four component in the ratio of 2:1:1 cytosine and clofibric acid with water molecule in the crystal lattice and the structure is refined in $C2$ space group. Two cytosine molecules are present as ionic and neutral in this crystal structure with one CLF molecule and water molecule. These four molecules are forming a sheet like structure along a-axis with the support of strong hydrogen bonds and two point $N^+-H\cdots O^-$ supramolecular synthon.¹² Two neutral cytosine molecules are connected via two point $N3-H3A\cdots O4$ (1.84 Å, 169°) synthon where as the ionic cytosine were connected by two point ionic synthons $N4-H4A\cdots O5$ (1.81 Å, 174°) interactions in Figure 6.3c. The neutral cytosine is connected directly to two different clofibric acid molecules by only $N1-H1\cdots O2$ (1.83 Å, 174°) and $N3-H3B\cdots O3$ (2.01 Å, 159°) interactions. The weak hydrogen bonds $O6-H6B\cdots O3$ (1.84 Å, 161°) and $O6-H6C\cdots O2$ (2.12 Å, 136°) is connecting the water molecules with CLF and the $N4-H4B\cdots O6$ (1.93 Å, 160°) interactions is bound by cytosinium ions.



Scheme 6.4 Solid state acid-base reaction of CLF with piperazine and cytosine bases



(a)



(b)

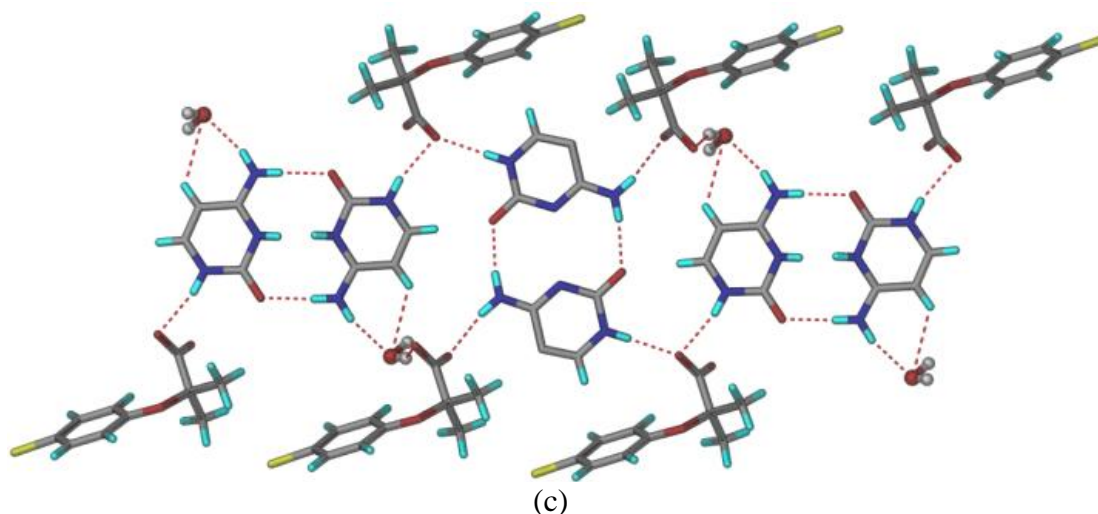
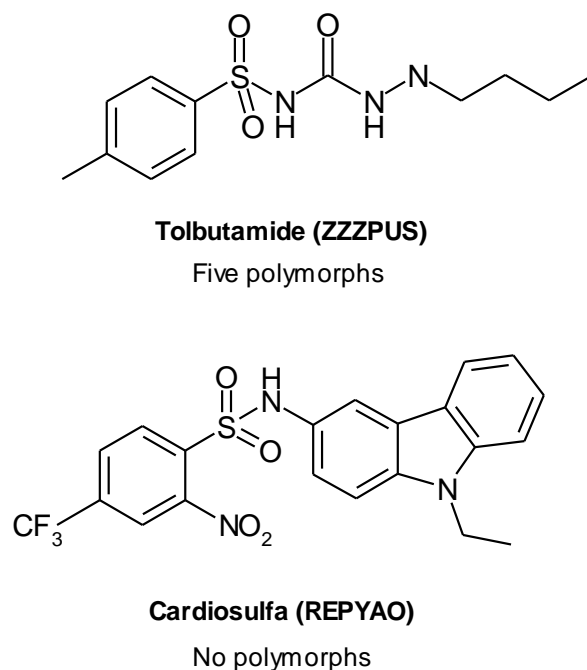


Figure 6.3 (a) Acid-acid O–H···O dimer synthon $R_2^2(8)$ in CLF (b) Ionic $N^+H\cdots O^-$ and $N^+H\cdots O^-$ hydrogen bonds in CLF-PIP and (c) Two point neutral $N-H\cdots O$ and ionic $N^+H\cdots O^-$ synthons in cytosine molecules and O–H···O in water bridge between CYT and CLF.

6.2.2 Conformational analysis: Generally, conformations are arrangements that arise by rotation about bonds ($1\text{--}3\text{ kcal mol}^{-1}$), and they may be described by specification of relevant torsion angles.^{17a} Any particular arrangement of atoms observed in a molecular crystal cannot be far from the equilibrium structure of the isolated molecule, sometimes about 8 kcal mol^{-1} for rigid molecules. The X-ray crystal structure analysis provides information about the preferred conformations of molecules although it cannot give the energy differences between conformations or the energy barriers that separate them.^{17b} In our X-ray structure analysis, Gliclazide is conformationally rigid that was strongly supported by the strong carboxamide and sulfonamide dimer synthons in the crystal structure. This rigidity is broken by crystallization with sodium hydroxide base because it removes the proton from the sulfonyl urea group and the situation for the dimer synthon formation is not available in GLZ-Na salt. The conformation of GLZ-Na showed large torsional difference of 78.22° with respect to angle of 69.38° in GLZ. This might be the reason why this molecule is not polymorphic. Tolbutamide is pentamorphic^{18a} (Scheme 6.5) whereas

GLZ is not polymorphic. The difference is the bicyclic ring in GLZ contains the N atom which is also engaged in intramolecular hydrogen bonding. This might lock the conformation of GLZ and not allowing crystallizing as conformational polymorphs, similar to Cardiosulfa^{18b} molecule where intramolecular hydrogen bonds between sulfonamide and nitro group did not allow the molecule any conformational polymorphs. In case of clofibric acid, the strong carboxylic acid O–H...O dimer synthon is not being broken by the crystallization in different solvents and heating conditions to yield any new polymorph.¹⁹ This is also supported by the salt formation with piperazine and cytosine molecules in different conformations with respect to CLF. Clonixin is tetramorph¹⁴ where the different functionalities such as carboxylic acid, pyridine, amino group and chloride present in the molecule may overcome the problems of rigidity when compared to GLZ and CLF. Torsion angle are listed in Table 6.3. The overlay of conformation of salts with drug molecules is shown in Fig. 6.4.



Scheme 6.5 Flexible Tolbutamide and rigid Cardiosulfa conformational molecules

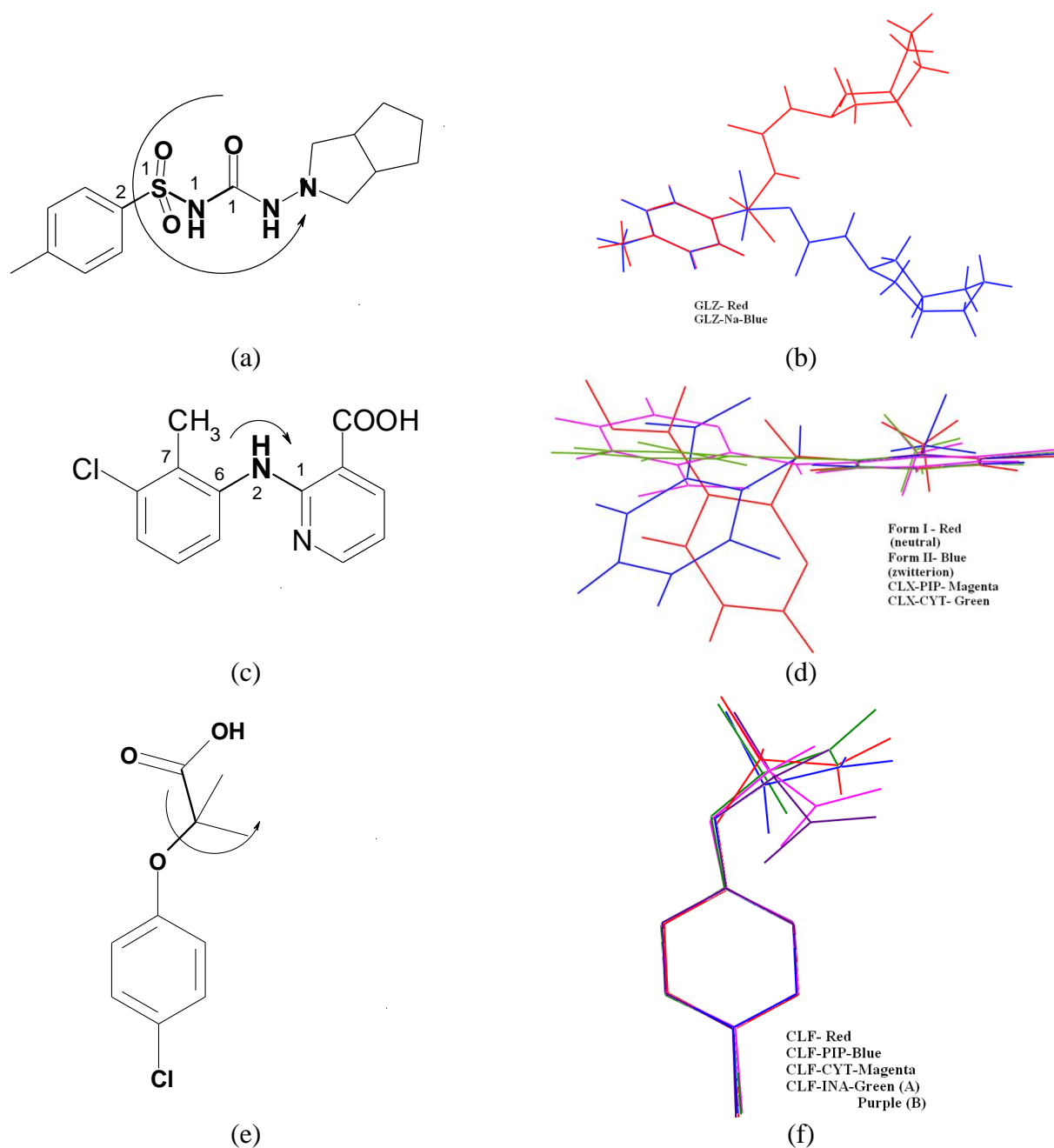


Figure 6.4 Torsional changes in GLZ (a), CLX (c) and CLF (e) overlay of different conformations in gliclazide (GLZ-red, GLZ-Na-blue), clonixin (CLX-neutral form-red, zwitterionic form-blue, CLX-PIP-magenta, CLX-CYT-green) and clofibric acid (CLF-red, CLF-PIP-blue, CLF-CYT-magenta, CLF-INA-green and purple)

Table 6.3 Torsion angles in salt/cocrystal structures of selected APIs

Compounds	Flexible bonds	Molecular torsions (°)
GLZ	C2-S1-N1-C1	69.38 (25)
GLZ-Na	C2-S1-N1-C1	78.22 (20)
CLX-I	C1-N2-C6-C7	71.27 (00)
CLX-II	C1-N2-C6-C7	140.26 (00)
CLX-PIP	C1-N2-C6-C7	161.83 (17)
CLX-CYT	C1-N2-C6-C7	174.92 (34)
CLF	C1-O1-C7-C8	78.36 (1.70)
CLF-PIP	C1-O1-C7-C8	71.64 (17)
CLF-CYT	C1-O1-C7-C8	61.62 (1.00)
CLF-INA	C1-O1-C7-C8	55.40 (00)

6.3 CSD Search and pK_a calculation

6.3.1 Sulfonylurea drugs

Carbutamide, Acetohexamide, Chlorpropamide, Tolbutamide and Tolazamide are first generation sulfonylurea drugs where as Glipizide, Gliclazide, Glibenclamide (Glyburide), Glibornuride, Gliquidone, Glisoxepide, Glycypyramide and Glimepiride are second generation sulfonylurea derivatives classified mainly as the class of antidiabetic drugs. They are used in the management of diabetes mellitus II.²⁰ Our recent search on CSD²¹ results only the n-butylammonium salt of Tolbutamide²² out of 9 hits and there are no other kind of salt reported in CSD for these low aqueous soluble sulfonylurea drugs. To our knowledge sodium-gliclazate would be the first sodium salt in this class of drugs to address the solubility issues of

sulfonylurea drugs. The pK_a values were calculated for all salt formers and APIs to know the validity of ΔpK_a rule in salts (Table 6.4). It is generally accepted that reaction of an acid with a base will be expected to form a salt if the ΔpK_a (ΔpK_a) pK_a (base) – pK_a (acid) is greater than 2 or 3. The calculated ΔpK_a is 11.8 and 5.8 (Table 6.5) for sodium-gliclazate and n-butylammonium-tolbutamidate salts and they were well validated by the ΔpK_a rule.²³

6.3.2 Fenamates

Many fenamates such as Etofenamate, Flufenamic acid, Flunixin, Clonixin, Meclofenamic acid, Mefenamic acid, Morniflumate, Niflumic acid, Tolfenamic acid and Azapropazone are reported as non-steroidal anti-inflammatory drugs having the polymorphic and solubility problem in oral dosages.^{9,24} The results extracted from CSD have shown that there are limited cocrystals and salts were reported for these drugs. There is a special need to develop these drugs via crystal engineering approach and improve the solubility by using the ΔpK_a rule.²³ Our CSD search on salt/cocrystals of fenamates gave only 16 salts out of 21 hits and 6 cocrystals out of all 63 hits. All these cocrystals and salts including the cytosine and piperazine salts of clonixin are following the ΔpK_a rule so this rule can be used to select the cofomer to improve the solubility of other fenamates.

6.3.3 Sodium, Piperazine and Cytosine salts

There are many sodium salts (794) are reported for many drugs in CSD including the anti-inflammatory drug Diclofenac sodium salt (AKOTAV) and anticonvulsant drug Sodium valproate (SITXID).²⁵ We extracted 153 hits for piperazine salts and 43 hits for cytosine salts for many organic compounds²⁶ in CSD and it indicates the number of structures reported for molecular salts is less common compared to the mineral salt drugs even though these molecular salt formers are GRAS compounds.

Table 6.4 Calculated pK_a values for APIs and coformers

APIs	pK_a^a	Coformers	pK_a^a	Nature
Gliclazide (GLZ)	4.07 (-SO ₂ -NH-)	Sodium hydroxide (Na)	15.85 (OH)	base
Tolbutamide (TBA)	4.33 (-SO ₂ -NH-)	n-Butylamine (n-BuA)	10.21 (NH ₂)	base
Clonixin (CLX)	1.88 (COOH)	Piperazine (PIP)	5.18 (N ₁ H)	base
Flunixin (FLX)	1.89 (COOH)	Cytosine (CYT)	2.35 (N ₁ H)	base
Niflumic acid (NFA)	1.88 (COOH)	4,4'-Bipyridine (Bpy)	4.44 (pyN)	base
Mefenamic acid (MFA)	3.89 (COOH)	Nicotinamide (NA)	3.63 (pyN)	base
Flufenamic acid (FFA)	3.88 (COOH)	Isonicotinamide (INA)	3.45 (pyN)	base
Tolfenamic acid (TFA)	3.88 (COOH)	Ethonalamine (EA)	9.55 (NH ₂)	base
Meclofenamic acid (MCA)	3.79 (COOH)	2-Aminopyridine (2-AP)	6.84 (pyN)	base
Phenylaminonicotinic acid (PNA)	1.89 (COOH)	4-Aminopyridine (4-AP)	8.95 (PyN)	base
2-(p-Tolylamino) nicotinic acid (TNA)	1.89 (COOH)	(2-hydroxyethyl) trimethylazanium (HT)	13.97 (OH)	acid
Clofibric acid (CLF)	3.37 (COOH)	Maleic acid (MA)	3.05 (COOH)	acid
		6-(methylamino)hexane-1,2,3,4,5-pentol (MAP)	9.11 (NH)	base
		2-amino-2-(hydroxyl methyl) propane-1,3-diol (AHP)	8.95 (NH ₂)	base

1,4,7,10-tetraaza cyclododecane (TCD)	4.81 (NH)	base
5,5,7,12,12,14-hexamethyl- 1,4,8, 11- Tetraazacyclotetradecane (TAC)	5.40 (NH)	base
1-phenylethan-1-amine (PA)	9.73 (NH ₂)	base
3-Nitrobenzoic acid (NBA)	3.69 (COOH)	acid

^apK_a values are calculated using ChemAxon (Marvin 6.0.1, 2013, ChemAxon software <http://www.chemaxon.com>).

Table 6.5 ΔpK_a value of API and its counterion molecules

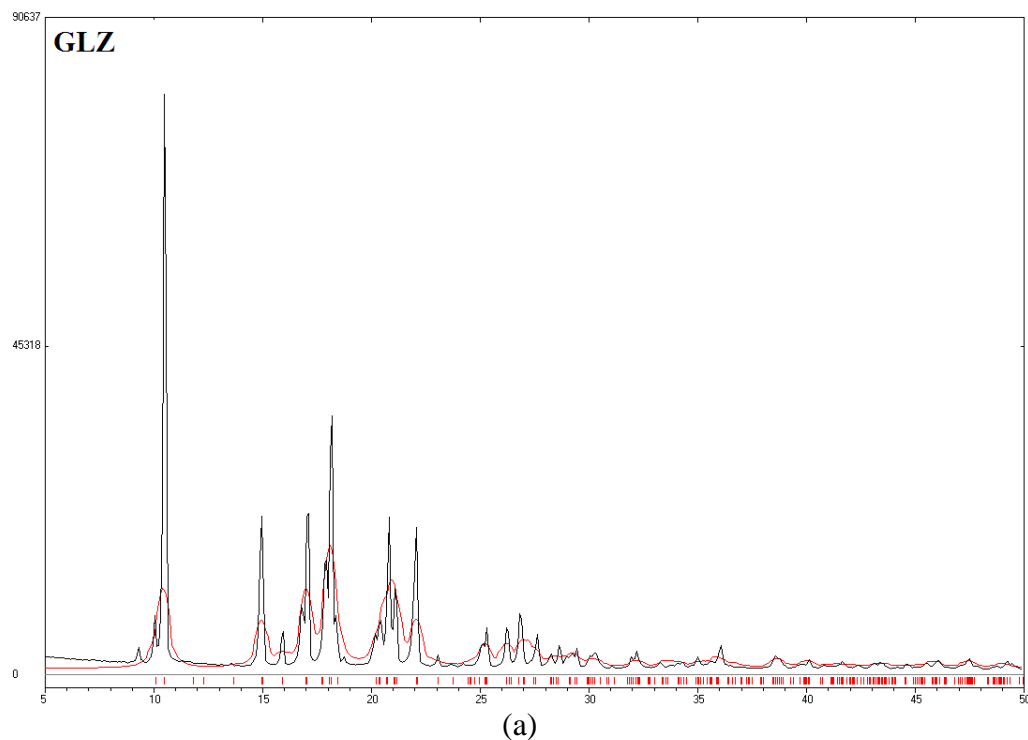
Adducts	ΔpK_a (pK _a of base- pK _a of acid)	Cocrystal/salt	CSD ref code
GLZ-Na	11.8	salt	-
TBA-BuA	5.88	salt	BENVIB
CLX-PIP	3.3	salt	-
CLX-CYT	0.47	salt	-
FLX-MAP	7.22	salt	ILIQID
NFA-PA	7.85	salt	VAKVOV
NFA-MA	2.46	salt	KIGMIX
NFA-NA	1.75	cocrystal	EXAQEA
TFA-NA	-0.25	cocrystal	EXAQIE
MCA-EA	5.76	salt	FOPMIG
MCA-HT	10.18	salt	FOPMOM

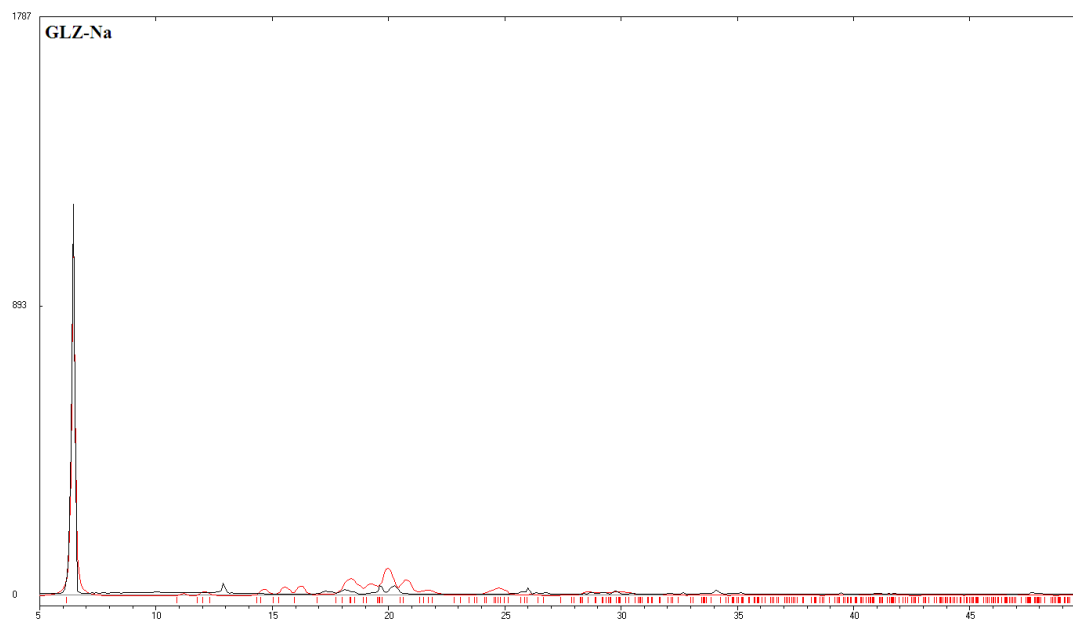
MCA-PIP	1.39	salt	SAXPOY
MCA-Bpy	0.65	salt	SAXPEO
MCA-2-AP	3.05	salt	SAXQIT
MCA-4-AP	5.16	salt	SAXQOZ
MCA-INA	-0.34	cocrystal	SAXPAK
MFA-AHP	5.06	salt	RUVNEC
MFA-TCD	0.92	salt	RUVNIG
MFA-TAC	1.51	salt	RUVNUS
MFA-PIP	1.29	salt	RUVNOM
MFA-CYT	-1.54	salt	ZAZGEO
MFA-NA	-0.26	cocrystal	EXAQOK
TNA-NBA	1.83	cocrystal	DAMQIT
TNA-2-AP	4.89	salt	DAMQEP
PNA-Bpy	2.55	cocrystal	PEFCAG
CLF-PIP	1.81	salt	-
CLF-CYT	-1.02	salt	-
CLF-INA	0.08	cocrystal	UMUYUX

6.4 Characterization of pharmaceutical salts

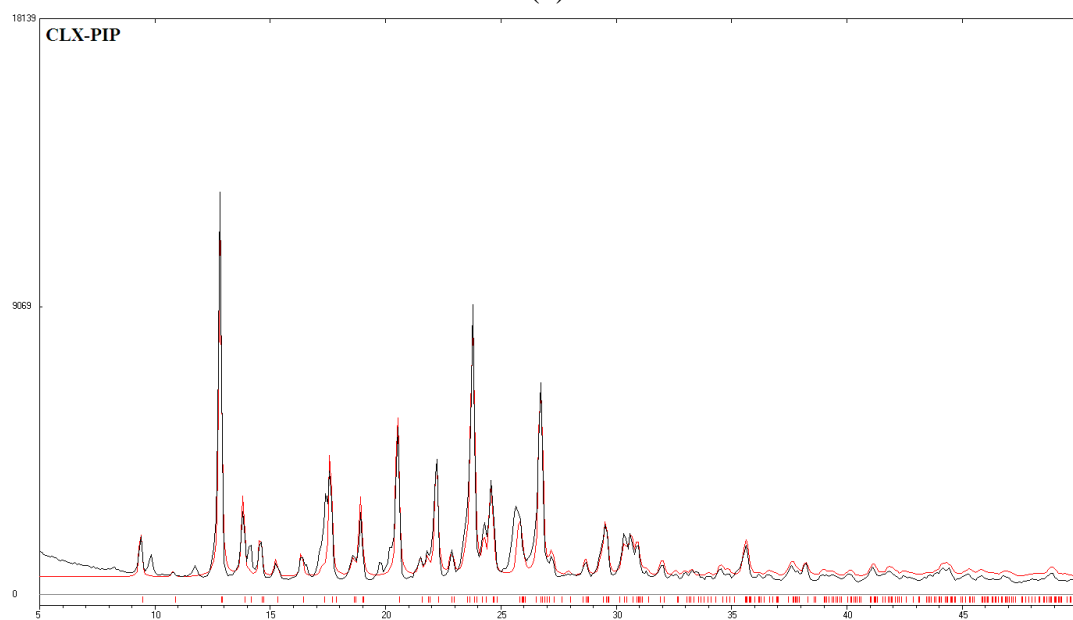
PXRD analysis: All salt materials were immediately checked after preparation from grinding or solution crystallization by PXRD and DSC to confirm the purity during salt formation experiments. The experimental PXRD patterns are matching with the

calculated pattern of the salt materials (Fig. 6.5). It confirms the integrity of the prepared materials for solubility studies. This technique is also used for analyzing the salt materials immediately after 24 hour equilibrium solubility studies to find out any solution mediated phase conversion during the slurry experiments (See, Fig. 6.12).

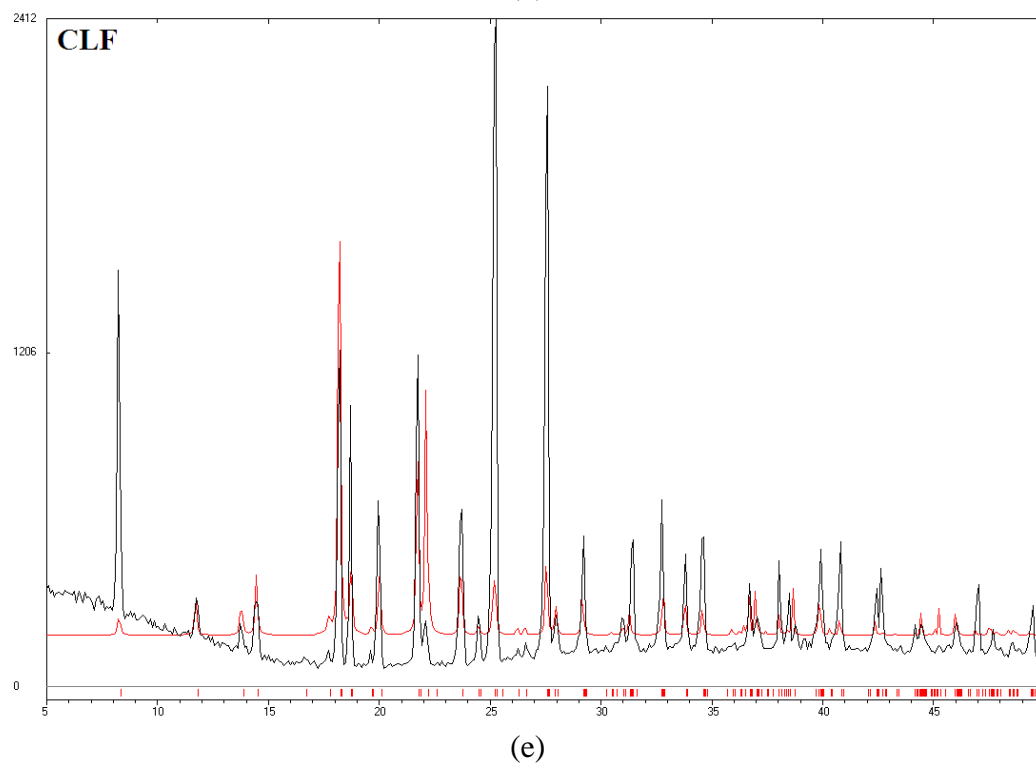
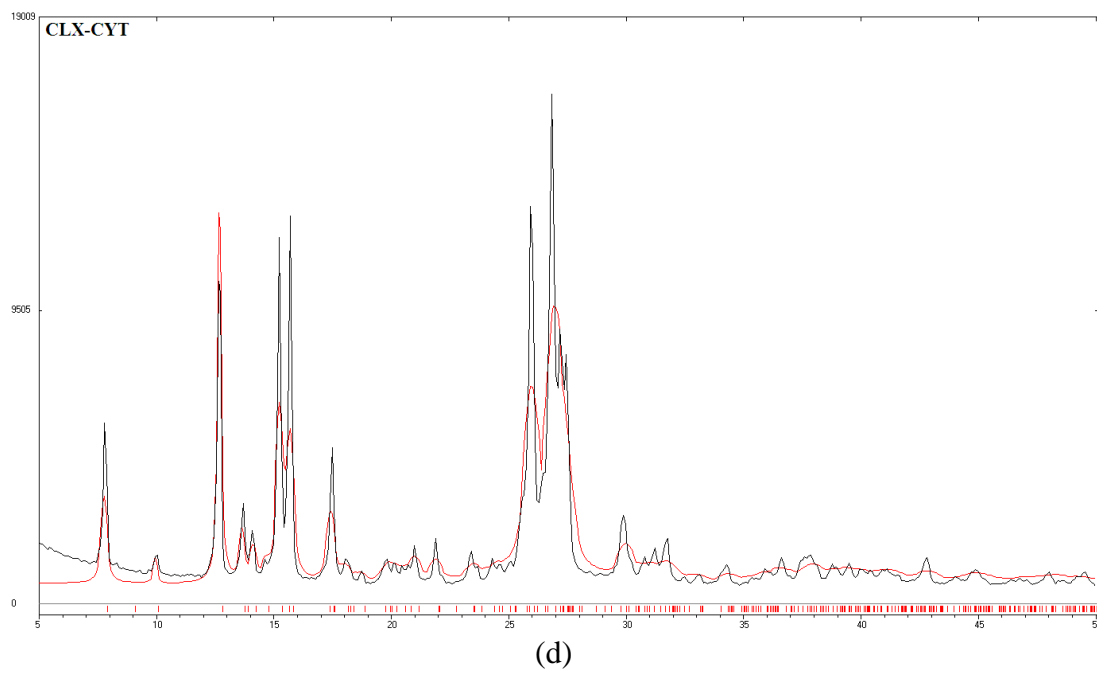




(b)



(c)



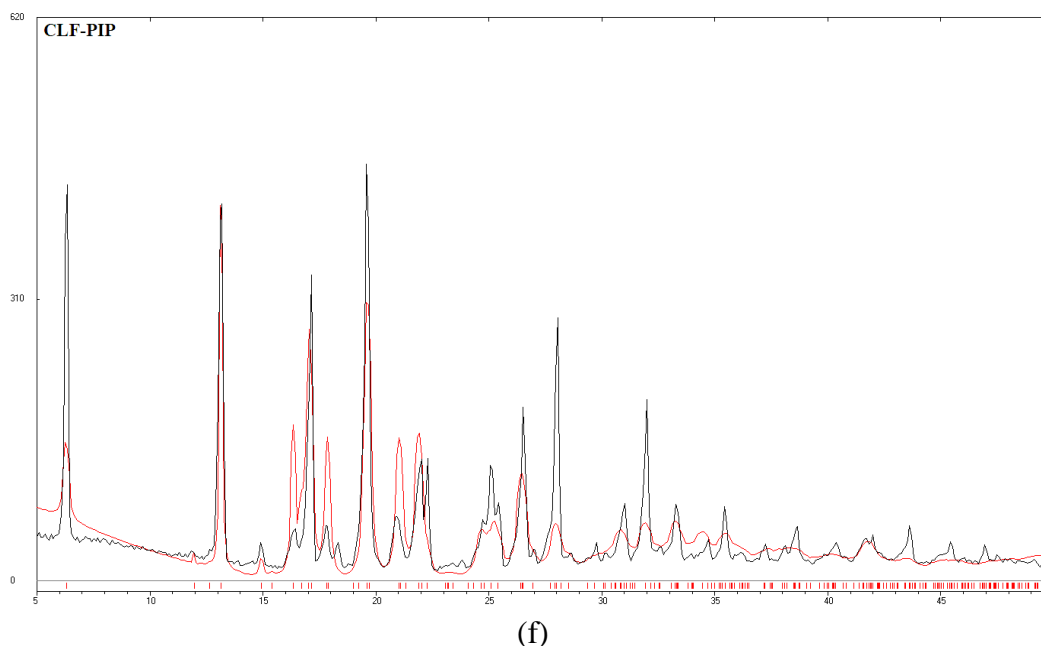
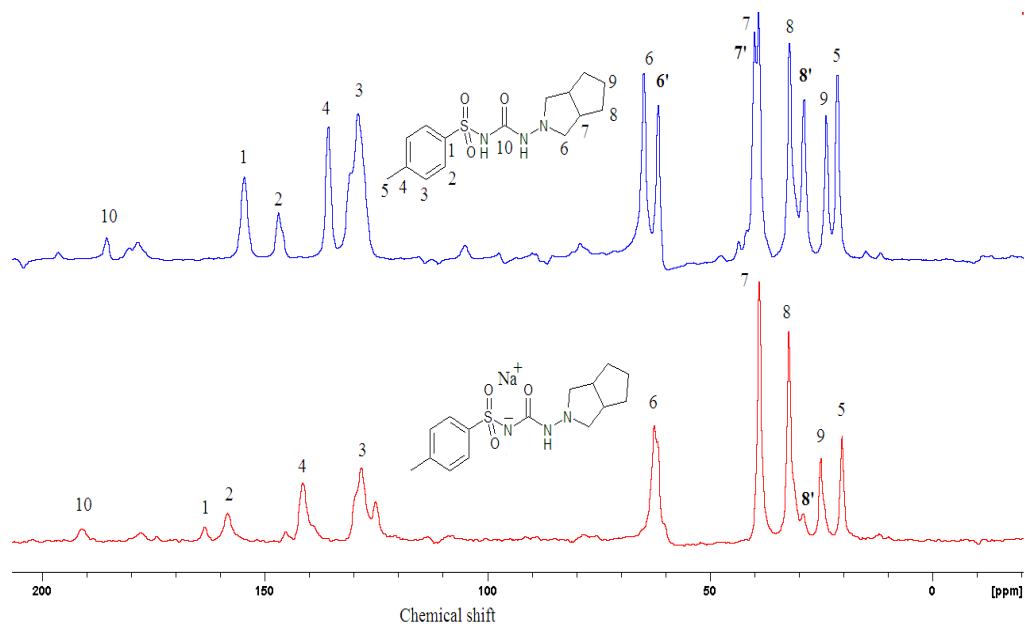
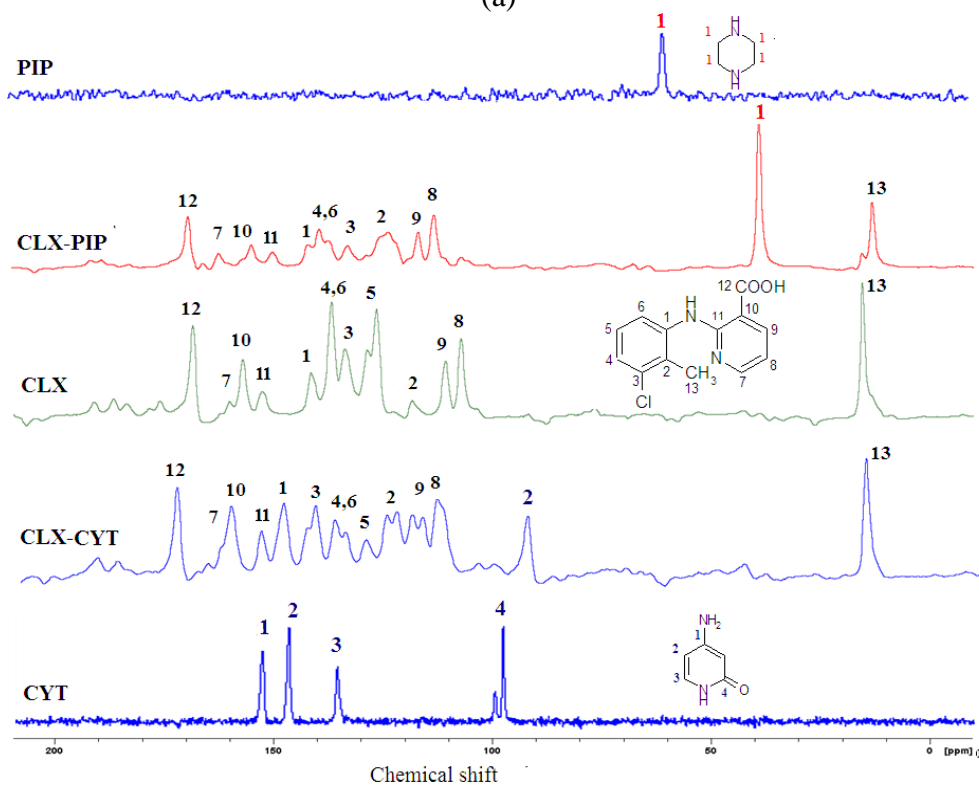


Figure 6.5 Overlay of calculated and experimental pattern of GLZ (a-b), CLX (c-d) and CLF (e-f) and its salts

6.4.1 Spectroscopy analysis: The salt materials are well differentiated by ss-NMR, FT-IR and Raman techniques. The different conformations and hydrogen bonds in the crystal structures of these new salts caused the changes in the chemical shift values with respect to the APIs in solid state NMR studies. For example, the methyl group and carbonyl groups exhibited the significant differences for GLZ and its sodium salt at 21.2 and 20.2 ppm for methyl carbons and 185.4 and 190.9 ppm for sulfonyl urea carbon atoms in Figure 6.5. For CLX, the carbonyl and methyl groups also showed variation in chemical shift values (169.3 and 15.4 ppm) compared to the salts CLX-PIP (169.5 and 13.1 ppm) and CLX-CYT (166.4 and 16.5 ppm). The detailed chemical shift values for other carbon atoms are mentioned in Table 6.6. The FT-IR and Raman spectra for all the salts and its APIs are shown in supporting information Figure 6.6-6.9. The stretching frequencies of IR spectra and the Raman shift values are given in Table 6.7-6.8.



(a)

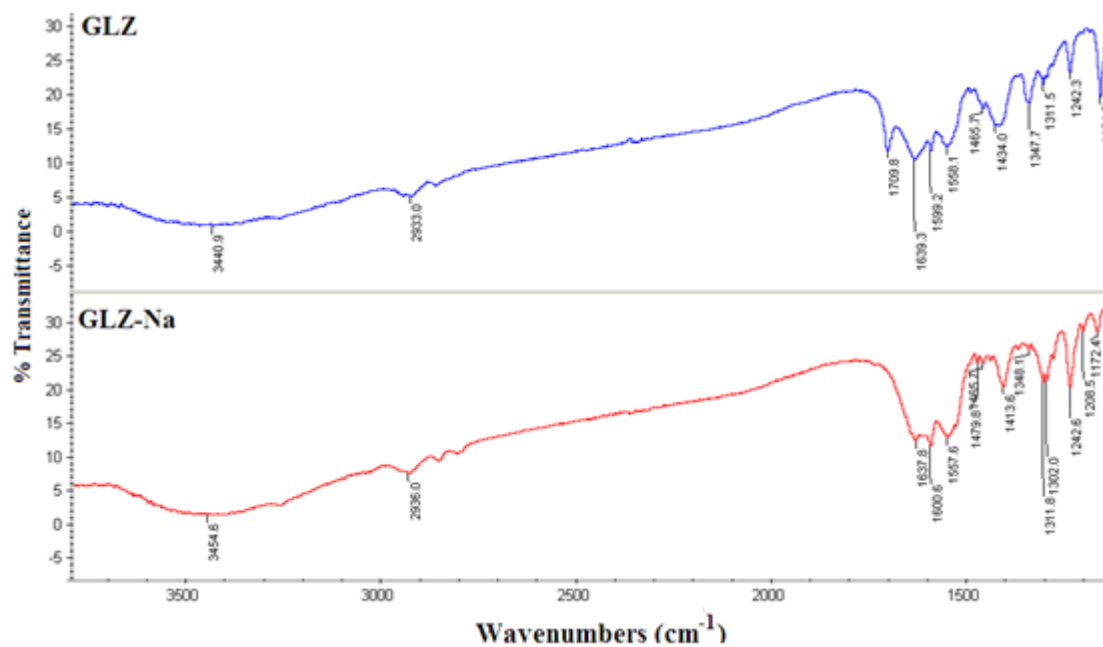


(b)

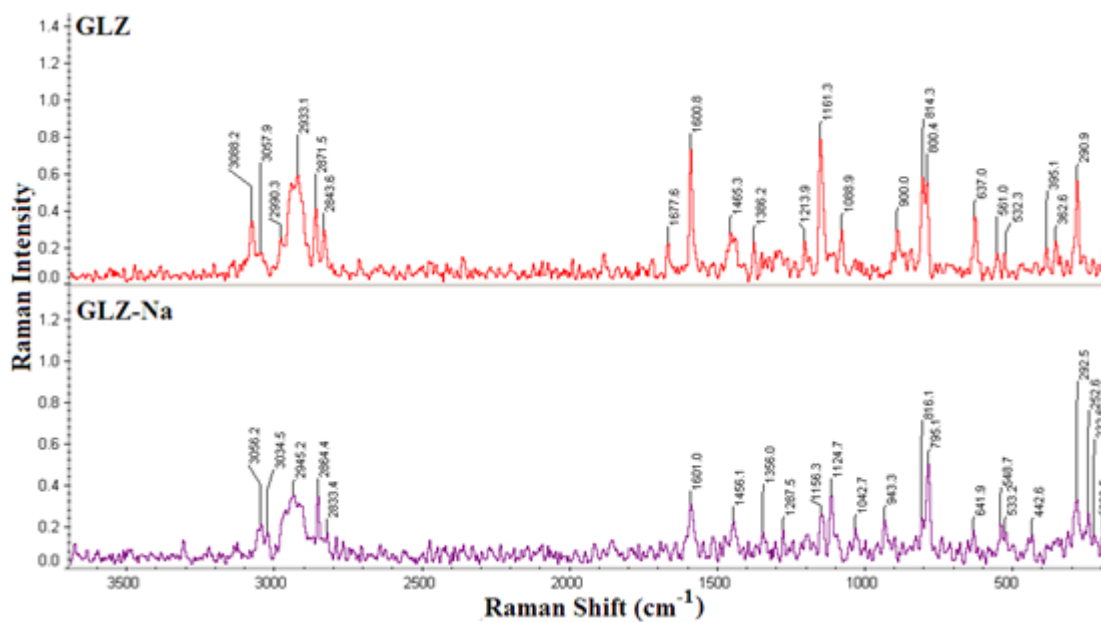
Figure 6.5 ^{13}C ss-NMR spectra of GLZ (a) and CLX (b) salts

Table 6.6 Chemical shift values for APIs and Salts

C atoms	GLZ	GLZ-Na	CLX	CLX-PIP	CLX-CYT	CYT	PIP
C1	154.5	163.3	141.5	139.5	141.9	172.4	45.4
C2	146.8	158.2	118.4	116.8	119.8	164.1	
C3	128.9	125.0, 128.2	136.8	137.4	137.4	148.9	
C4	135.6	141.3	133.7	133.0	130.0	97.2	
C5	21.2	20.2	126.6	123.8	123.3		
C6	61.5, 64.7	61.7	128.6	128.7	125.5		
C7	38.9, 39.8	38.8	160.11	162.5	166.4		
C8	28.7, 32.0	28.9, 32.1	107.2	107.1	114.1		
C9	23.7	24.9	110.82	113.3	117.4		
C10	185.4	190.9	157.1	155.0	154.2		
C11			152.6	150.2	149.1		
C12			169.3	169.5	166.4		
C13	-	-	15.5	13.1, 15.4 30.0, C1'	16.51 93.4, C2'		

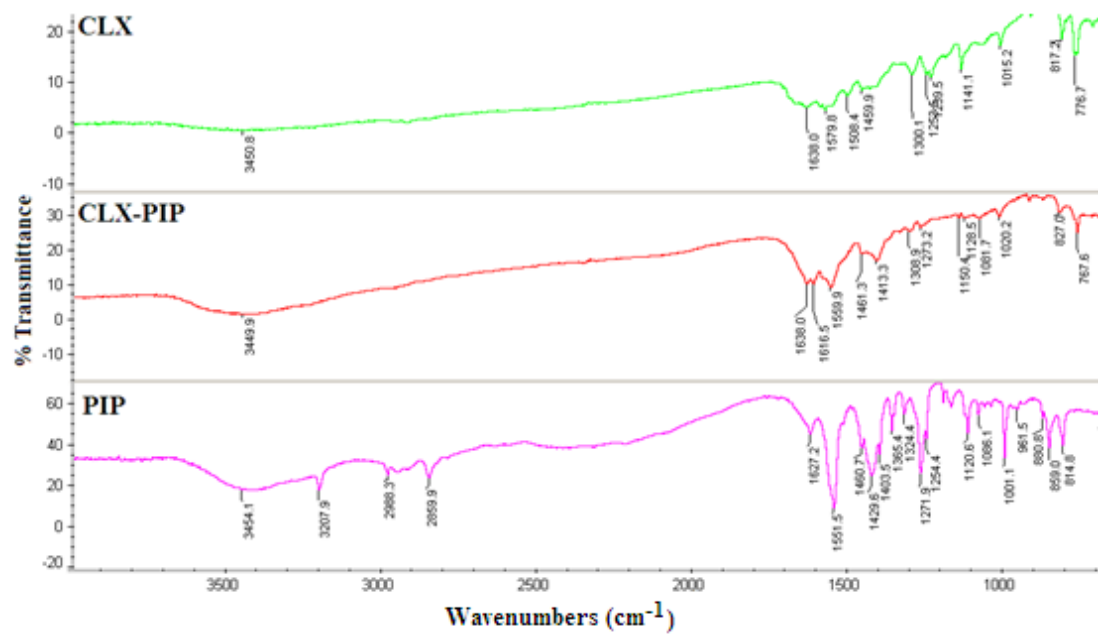


(a)

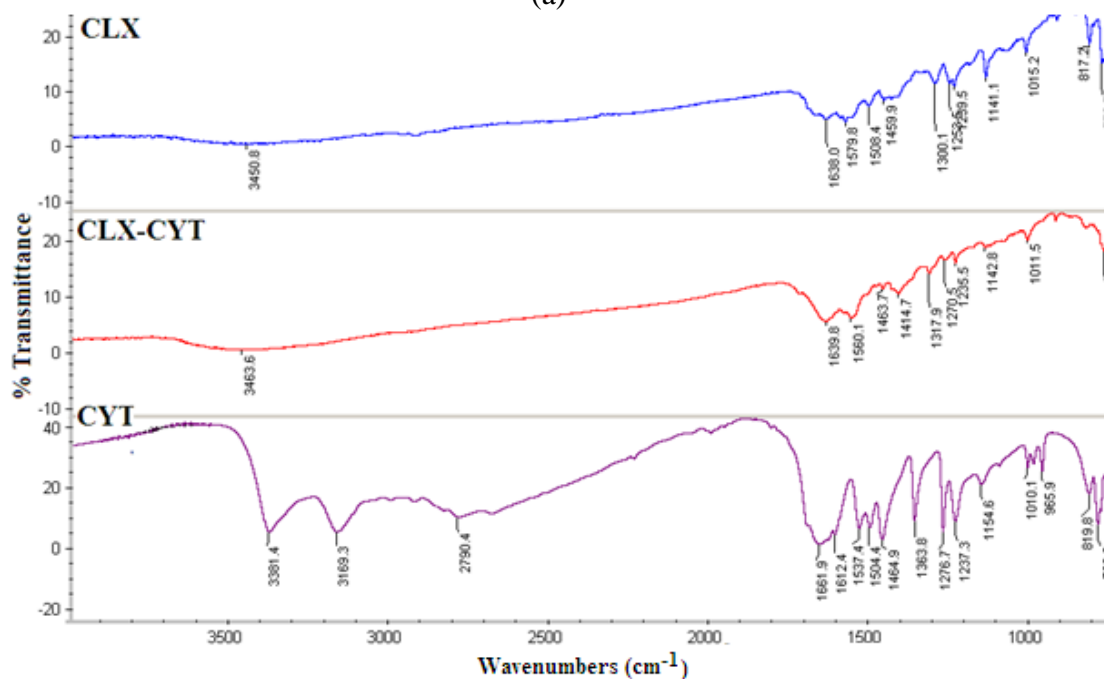


(b)

Figure 6.6 (a) FT-IR and (b) Raman spectra of GLZ and its sodium salt

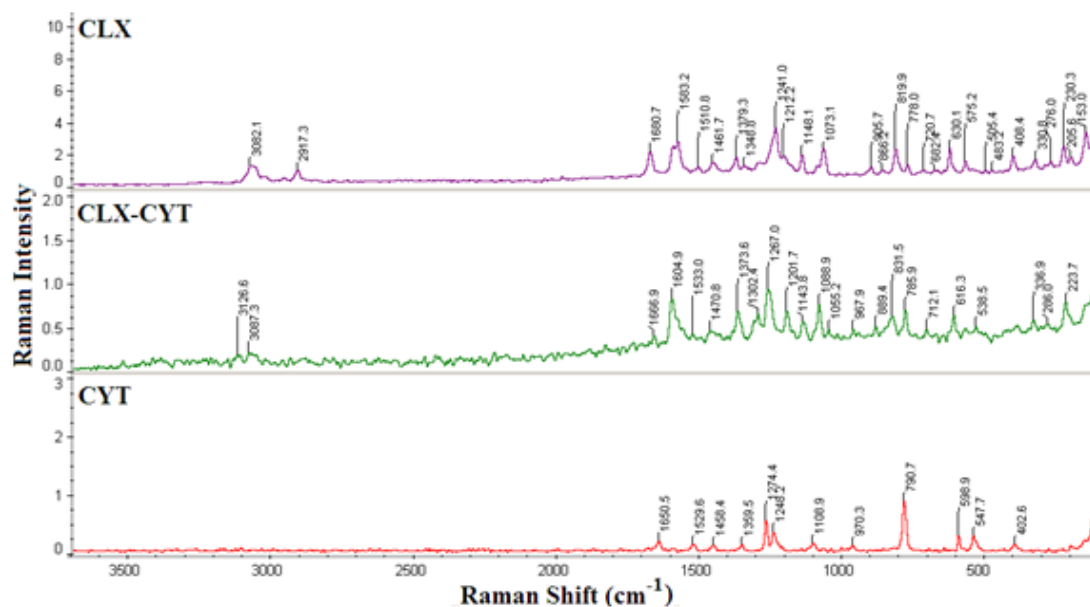


(a)

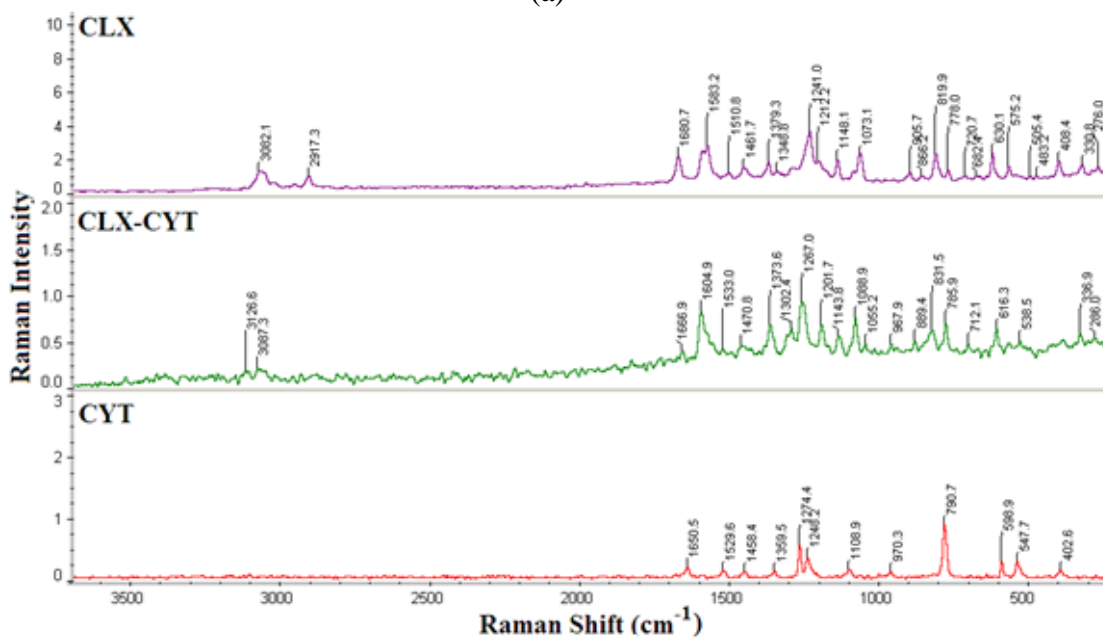


(b)

Figure 6.7 FT-IR spectra of CLX and its piperazine (a) and cytosine (b) salts

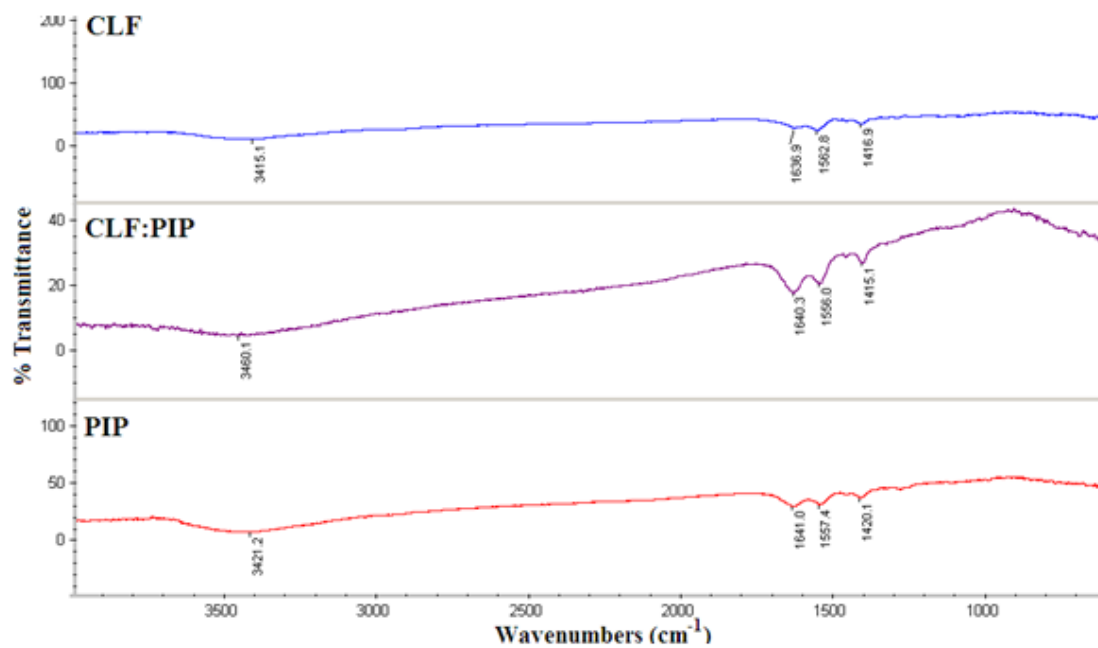


(a)

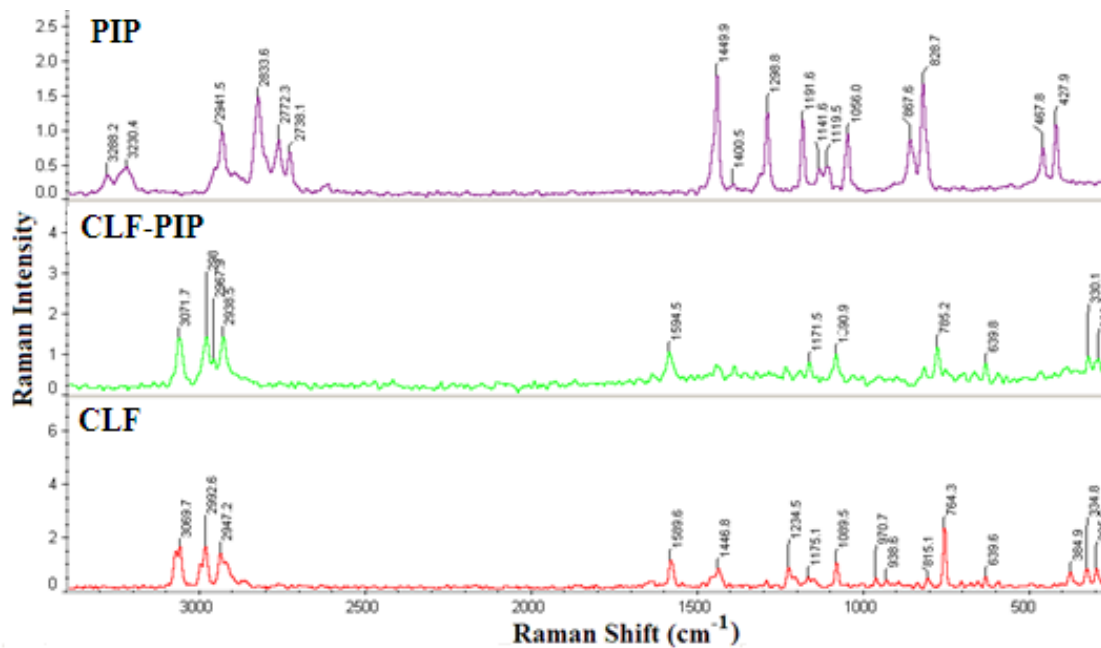


(b)

Figure 6.8 FT-Raman spectra of CLX and its piperazine (a) and cytosine (b) salts



(a)



(b)

Figure 6.9 (a) FT-IR and (b) Raman spectra of CLF and its piperazine salt.**Table 6.7** FT-IR stretching frequencies for APIs and salts

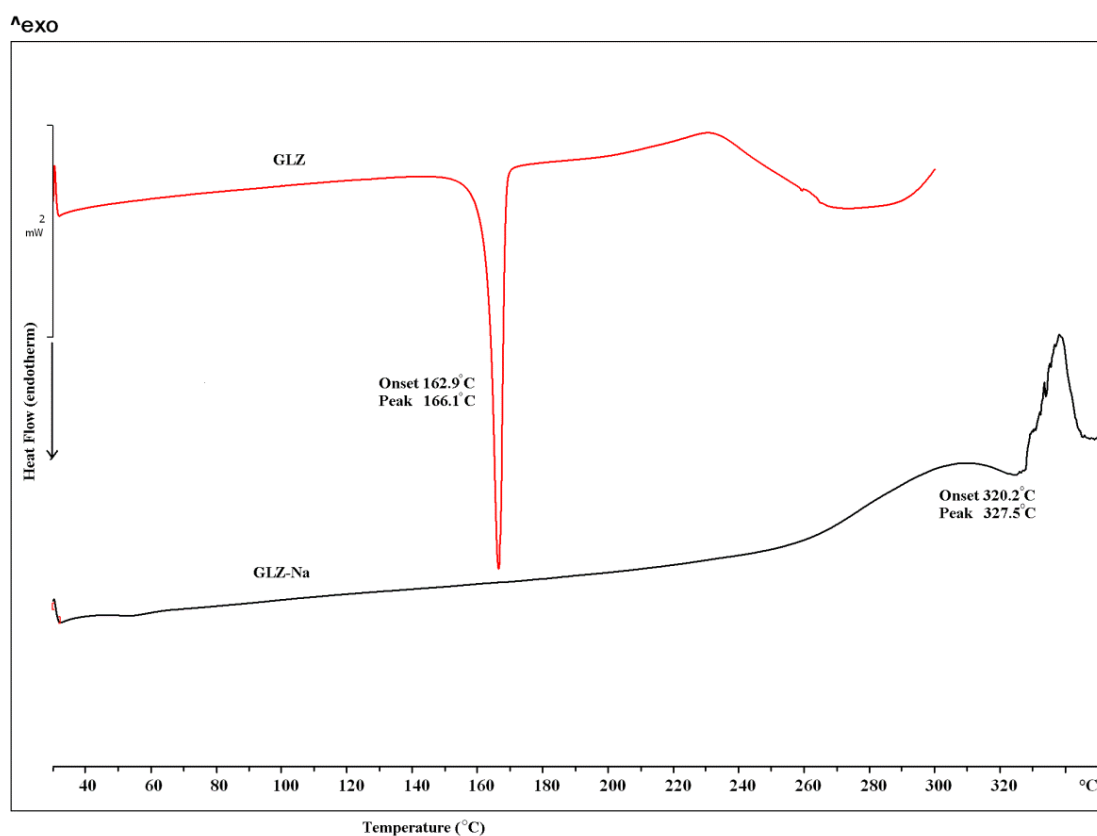
Solid forms	C=O asym/ sym stretch cm ⁻¹	N-H stretch (broad) cm ⁻¹	O-H stretch	N-H bend cm ⁻¹
GLZ	1709.8	3440.9	-	1559.2
GLZ-Na	1637.8	3454.6	-	1557.6
CLX	1638.0	3450.8	-	1579.8
CLX-PIP	1638.0	3449.9	-	1559.9
CLX-CYT	1639.8	3463.6	-	1560.1
CLF	1636.9	-	3415.1	-
CLF-PIP	1640.3	3460.1 (PIP)	-	1556.0

Table 6.8 Raman stretching frequencies for APIs and salts

Solid forms	C=O asym/ sym stretch cm ⁻¹	Aromatic C-H stretch cm ⁻¹	N-H bend cm ⁻¹
GLZ	1677.6	3088.2	1600.8
GLZ-Na	-	3056.2	1601.0
CLX	1680.7	3082.1	1583.2
CLX-PIP	-	3063.8	1594.5
CLX-CYT	1666.9	3087.3	1604.9
CLF	-	3069.7	1589.6
CLF-PIP	-	3071.7	1594.5

6.4.2 Thermal analysis: This method is generally used to confirm the material purity by checking the melting point of the formed salts after grinding. In DSC, there

was a sharp endotherm for GLZ at 162.9 °C melting temperature and some broad endotherm for GLZ-Na at 320.2 °C. This is very obvious in metal salts that the salt is always highly stable due to their strong electrostatic ionic interactions so they melt at high temperature range in Figure 6.10a. CLF-PIP salt also follows the same trend of high melting at 196.0 °C compared to CLF melts at 119.8 °C (Figure 6.10b). But in molecular salts of CLX there is no general melting trend for melting temperatures. Because the CLX-PIP melts at 170.0 °C which is the lowest melting temperature to the melting of CLX (224.9 °C) but CLX-CYT at 223.3 °C is almost equal to CLX in Figure 6.10c (Table 6.9). This may be due to the twisted conformations of CLX in salts and it favors the less packing of molecules in the crystal lattice.¹⁵



(a)

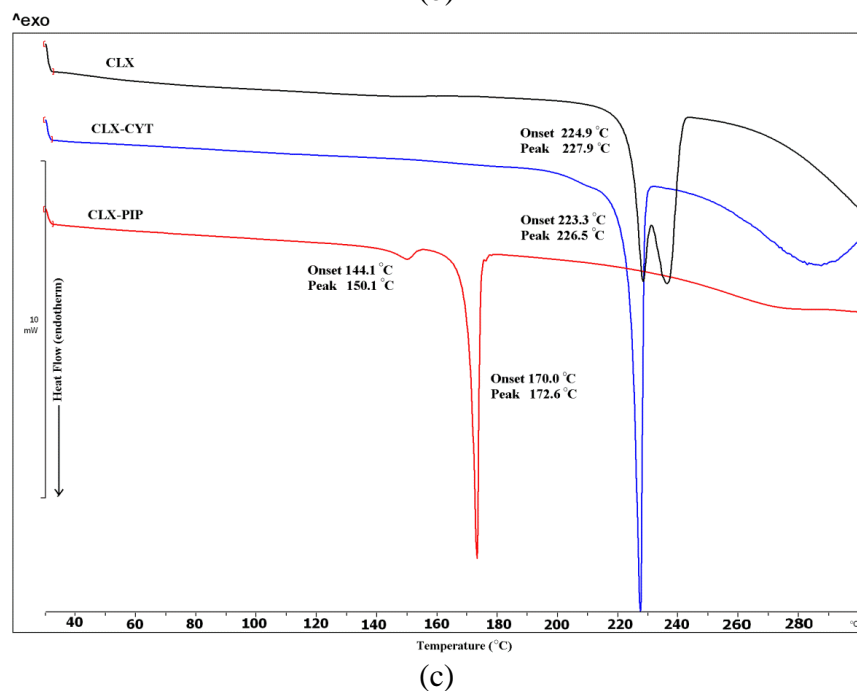
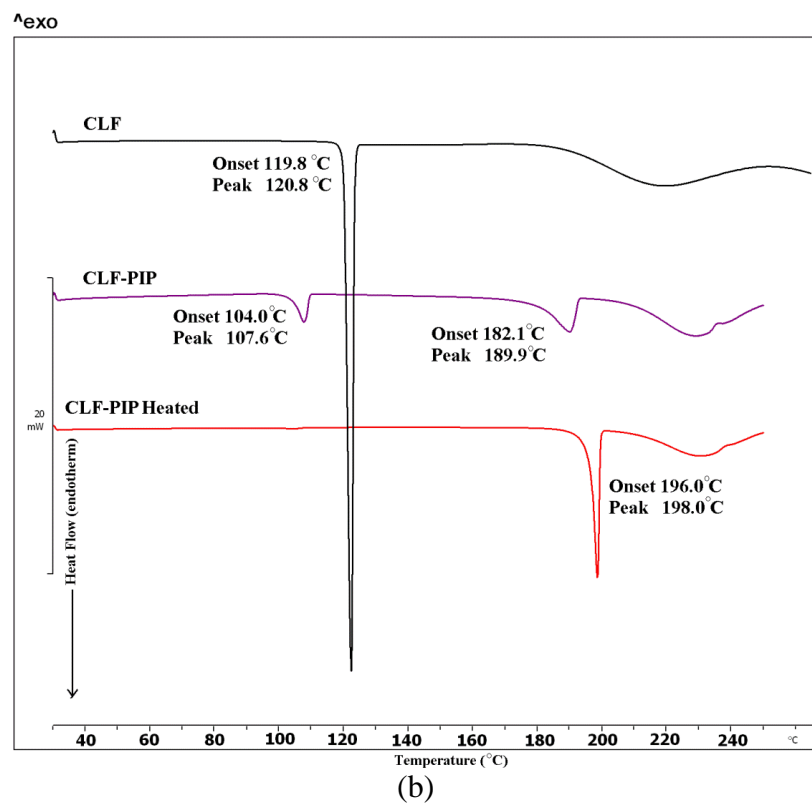


Fig. 6.10 DSC comparison of three salts of GLZ (a), CLF (b) and CLX (c).

Table 6.9 Melting temperatures of salts

Solid forms	M.P. of salt (°C)	M.P. of Coformers (°C)	Density (g cm ⁻³)
GLZ	162.9	-	1.76
GLZ-Na	320.2	318.4	1.31
CLX	224.9	-	1.41
CLX-PIP	170.0	106.0	1.45
CLX-CYT	223.3	325.0	1.50
CLF	119.8	-	1.34
CLF-PIP	196.0	106.0	1.33

6.5 Solubility and dissolution study

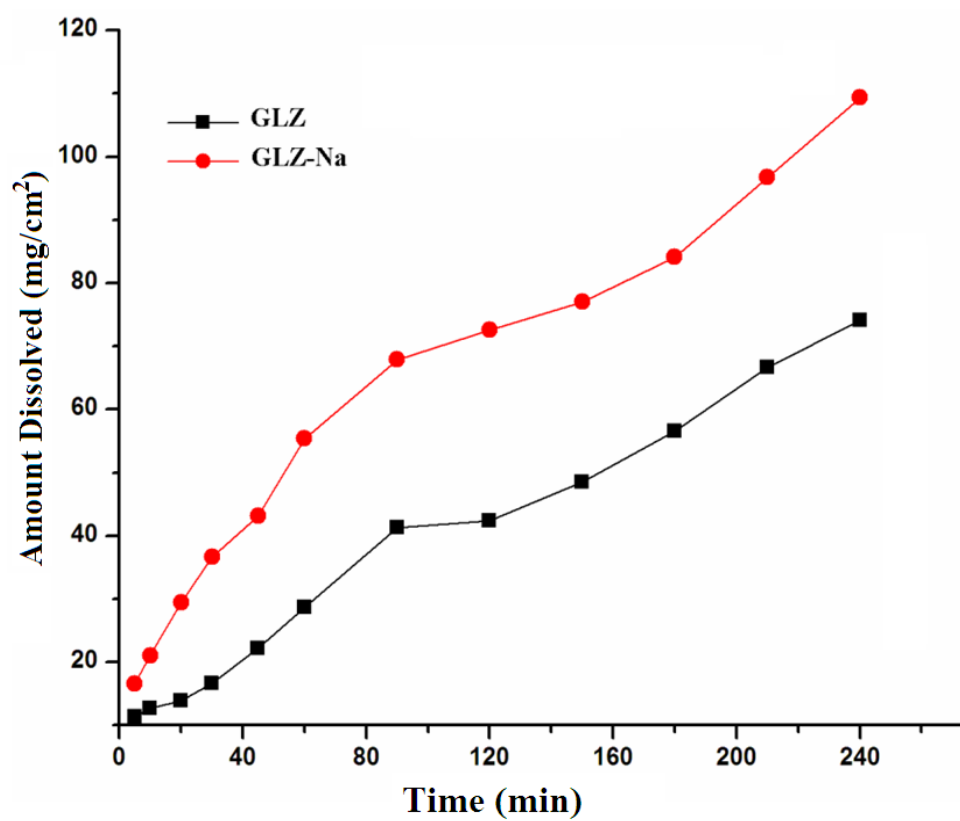
Salt formulations are practiced since long time in pharmaceutical industries to develop the stability and the solubility of low aqueous soluble drugs.^{1,27} Solubility and dissolution experiment were carried out in 50% and 60% EtOH-water mixture at 37 °C for GLZ and CLX, CLF salts. Salts are supposed to be highly soluble than the pure APIs. As expected the GLZ-Na salt is 10 times more soluble (19.6 mg/mL) and 3 times faster dissolving (1.0 mg/cm²/min) than the reference drug GLZ (2.2 mg/mL, 0.32 mg/cm²/min). The sodium-gliclazate is dissociated to GLZ and it is observed after the 24 Hrs equilibrium solubility experiments (See, Fig. 6.12). This dissociation is observed in dissolution experiments also and the solubility values are there in Table 10. The dissolution profile for three salts is listed in Figure 6.11. For CLF, the CLF-PIP exhibits the highest solubility of 18.3 mg/mL over the drug CLF solubility of 2.77 mg/mL. CLF-PIP salt (0.98 mgcm⁻²min⁻¹) is also two times faster dissolving than the CLF ref drug (0.42 mgcm⁻²min⁻¹). In case of CLX salts, the piperazine-clonixate and cytosinium-clonixate is 7 to 10 times (CLX-PIP, 21.8 mg/mL; CLX-CYT, 14.1 mg/mL) more soluble than the CLX drug (1.9 mg/mL). The dissolution

rate (0.47 mg/cm²/min, 0.40 mg/cm²/min) is also 2-3 times faster than CLX (0.14 mg/cm²/min). This piperazine salt is more soluble than the cytosine salt (Table 6.10). The reason for this high solubility is following the thermal stability and solubility relationship. In CLX-CYT, the molecules are tightly packed (1.38 g cm⁻³) than the molecules in the CLX-PIP (1.33 g cm⁻³). This is evidenced from the melting points of these two salts (m.p. CLX-CYT; 227°C, CLX-PIP; 174°C). The highest soluble salt CLX-PIP is found to be partially dissociated in equilibrium solubility experiments but the CLX-CYT salt is stable even after 24 Hrs slurry and 4 Hrs dissolution experiments (See, Fig. 6.12). In our last study on CLX solubility enhancement program we developed the method of improving the solubility by isolating/optimizing the zwitterionic form for better solubility and stability.¹⁵ However, CLX-CYT salt is the best one can be used for formulation because of its solubility and stability advantage over the zwitterionic polymorph.

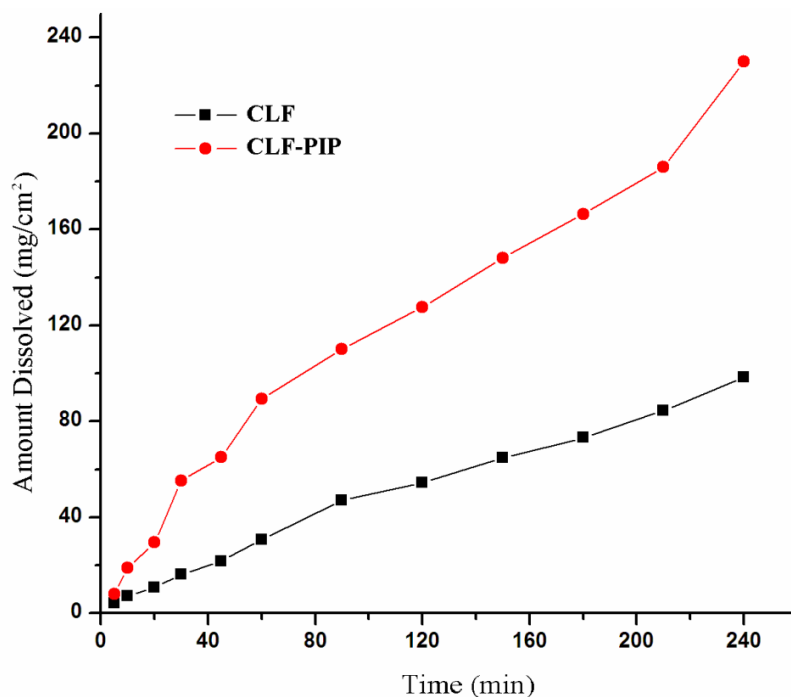
Table 10 Solubility and dissolution parameters of salts

Solid forms	Nature in solid state	Absorption coefficient (ϵ), (M ⁻¹ cm ⁻¹)	Solubility (mg/mL)	Intrinsic Dissolution rate (mgcm ⁻² min ⁻¹)
GLZ				
GLZ	Guest free	23.41	2.27	0.32
GLZ-Na	Salt	20.80	19.6	1.02
Clonixin				
Form I	Neutral	68.36	1.93	0.14
Form II	Zwitterionic	69.27	2.01	0.20
CLX-PIP	Salt	57.16	21.83	0.47

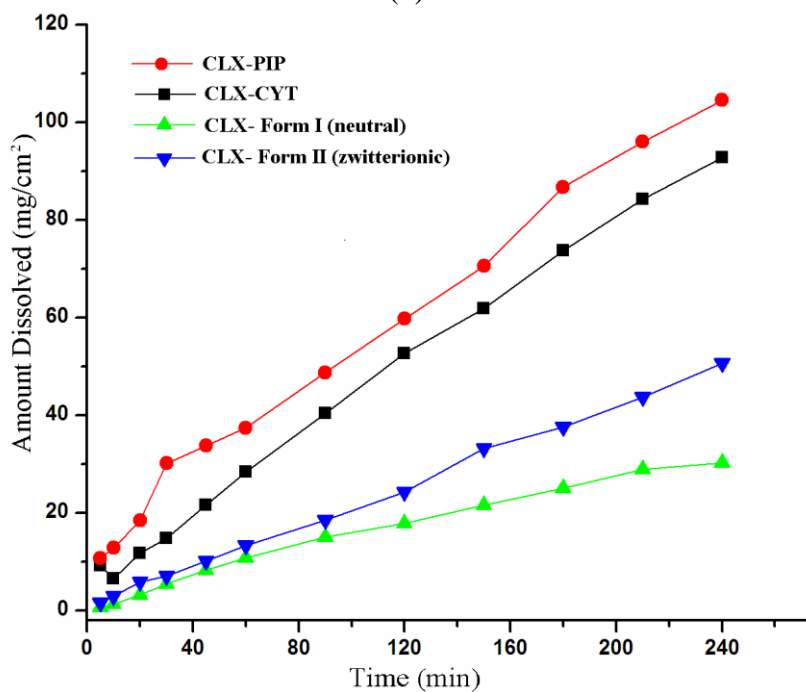
CLX-CYT	Salt	23.79	14.17	0.40
Clofibric acid				
CLF	Guest free	50.55	2.77	0.42
CLF-PIP	Salt	35.14	18.34	0.98



(a)



(b)



(c)

Fig. 6.11 Dissolution profile of pure APIs GLZ (a), CLF (b) and CLX (c) and its salts in 50%, 20% and 60% EtOH-water mixtures in 4 h at 37 °C.

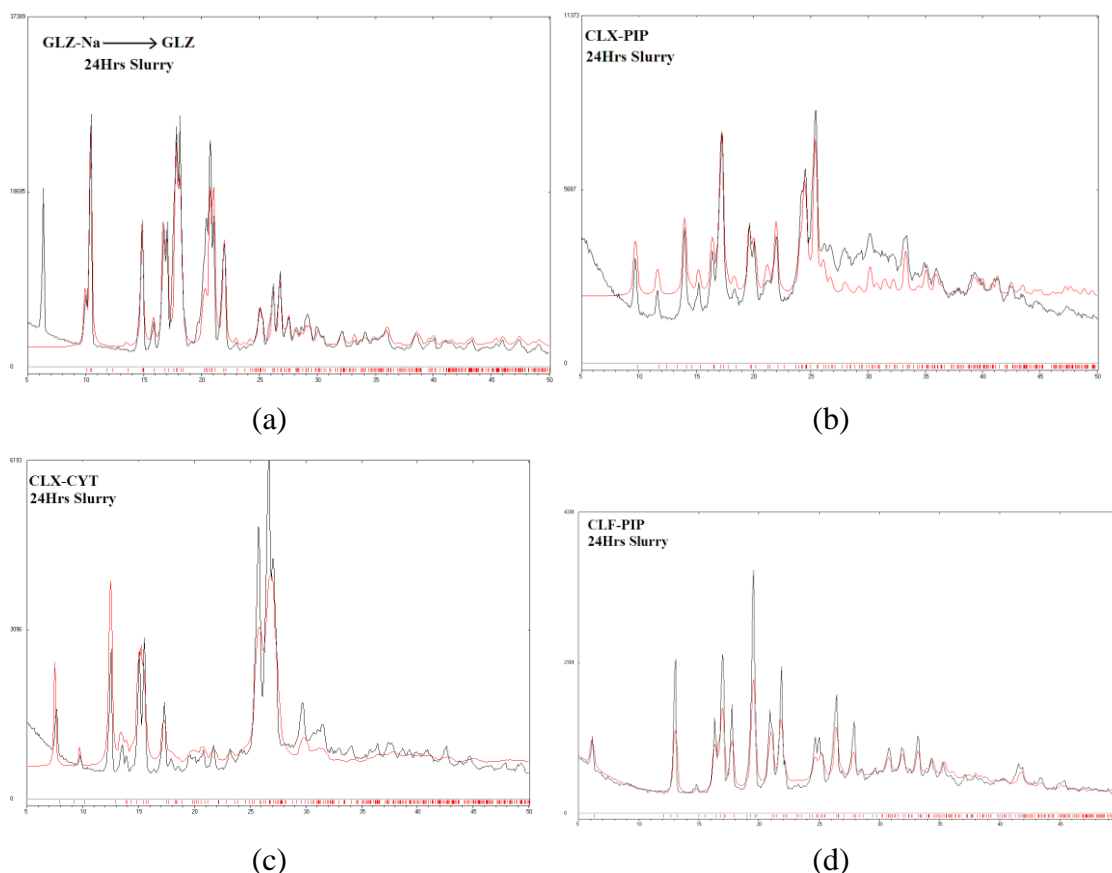


Figure 6.12 PXRDs of salts after the 24 Hrs slurry experiments of thermodynamic equilibrium solubility test. (a) GLZ-Na conversion to starting material GLZ, (b and c) CLX-CYT and CLX-CYT-no conversion, (d) CLF-PIP no conversion.

6.6 Conclusions

Some of the BCS class II drugs gliclazide, clofibric acid and clonixin were selected in this study to address the important issues associated with these drugs such as solubility and stability using the salt formation crystallization technique. Successfully, the resulted salts are consequently improved the solubility about 10 times compared to those drugs. The dissolution rate is also higher for those salts and the increment is about three times to the drugs. These salts were characterized and well differentiated by various solid state methods such as X-ray diffraction techniques (crystal and powder) and spectroscopy techniques, ss-NMR, FT-IR and

Raman methods. Thermal stability of salts was identified in DSC. The salt formulation technique is limited to traditional method but not least to improve the solubility infact there couldn't be any problem from the FDA regulatory bodies. This study provides the support of making salts over the cocrystals for safer side of improving the drug properties using the existing FDA drug guidance.

6.7 Experimental Section

Materials. The gliclazide, clofibric acid and co-formers (purity >99.8%) were purchased from Sigma-Aldrich. All other chemicals were of analytical or chromatographic grade. Clonixin was synthesized by refluxing *o*-chloronicotinic acid (315.3 mg, 2 mmol) and an equivalent amount of the 3-chloro-2-methyl aniline (1.1 equiv). The precipitated product was filtered and purified by crystallization from acetone to obtain pure clonixin (CLX) which was then characterized by ^1H and ^{13}C NMR and single crystal XRD.

Water altered through a double-deionized purification system (Milli Q Plus Water System from Millipore Co., Billerica, Massachusetts) was used in all the experiments. Melting points were measured on a Fisher-Johns melting point apparatus. Single crystals were obtained via slow evaporation of stoichiometric amounts of starting materials in appropriate organic solvents after solid state and liquid assisted grinding in a mortar-pestle. Salts were characterized by FT-IR, Raman, ^{13}C ss-NMR spectroscopy techniques, DSC, PXRD and single crystal X-ray diffraction (SC-XRD).

6.7.1 Preparation of salts by liquid (solvent drop) assisted grinding

1. APIs (GLZ, CLX and CLF)

Gliclazide, Clonixin and Clofibric acid crystals were obtained from organic alcoholic solvents and the ground material of these crystals was used in the comparison of

analysis and characterizations with the new salts. m.p. of GLZ, CLX and CLF are 165 °C, 230 °C and 122 °C.

2. GLZ-Na (1:1) Salt

100 mg (0.30 mmol) gliclazide and 12.38 mg (0.28 mmol) NaOH pellets were ground in mortar-pestle for 15 min after adding 5 drops of EtOH, and then kept for crystallization in 10 mL ethanol. Suitable plate type crystals appeared at ambient condition after 3-4 days. m.p. >300 °C.

3. CLX-PIP (1:0.5) Salt

100 mg (0.38 mmol) Clonixin and 16.39 mg (0.19 mmol) piperazine base were ground in mortar-pestle for 15 min after adding 5 drops of MeOH, and then kept for crystallization in 10 mL 1:1 methanol-ethanol mixture. Suitable thick plate crystals were harvested at ambient condition after 3-4 days. m.p. 174 °C.

4. CLX-CYT (1:1) Salt

100 mg (0.38 mmol) Clonixin and 42.21 mg (0.38 mmol) PABA was ground in mortar-pestle for 15 min after adding 5 drops of MeOH/CH₃CN, and then kept for crystallization in 10 mL ethanol. Suitable block and plate type crystals were harvested at ambient condition after 3-4 days. m.p. 227°C.

5. CLF-PIP (1:0.5) Salt

100 mg (0.46 mmol) Clofibric acid and 20.06 mg (0.23 mmol) piperazine was ground in mortar-pestle for 15 min after adding 5 drops of EtOH, and then kept for crystallization in 10 mL ethanol. Suitable block and plate type crystals were harvested at ambient condition after 3-4 days. m.p. 193 °C.

6. CLF^- - CYT^+ - CYT - H_2O (1:2:1) Salt hydrate

100 mg (0.46 mmol) Clofibric acid and 102.12 mg (0.92 mmol) cytosine was ground in mortar-pestle for 15 min after adding 5 drops of CH_3CN , and then kept for crystallization in 10 mL ethanol. Suitable block and plate type crystals were harvested at ambient condition after 3-4 days. m.p. 180 °C.

X-ray Crystallography. X-ray reflections for all salts (RT data) were collected on an Oxford Xcalibur Gemini Eos CCD diffractometer using Mo- $\text{K}\alpha$, radiation. Data reduction was performed using CrysAlisPro (version 1.171.33.55).^{28a} OLEX2-1.0 and SHELX-TL 97 were used to solve and refine the data.^{28b} All non-hydrogen atoms were refined anisotropically, and C–H hydrogens were fixed. O–H and N–H protons were located from difference electron density maps and C–H hydrogens were fixed. Hydrogen bond distances were neutron normalized using WingGX-PLATON.^{28c} Packing diagrams were prepared in X-Seed.²⁹ Crystallographic .cif files (CCDC Nos. XXXXXX) are available at www.ccdc.cam.ac.uk/data_request/cif or as part of the Supporting Information.

CSD Search. All organic compounds, “sulfonylurea with anionic nitrogen atom”, and “fenamate moiety with carboxylate ion”, and “clofibrate with carboxylate ion”, “sodium, piperazine and cytosine cation” and are taken as the molecular fragments and the entries for which 3D coordinates are determined were searched in Cambridge Structural Database, ver. 5.35, ConQuest 1.16, November 2013 release, February 2014 update. Nine hits for sulfonylurea anion, 21 hits of salts and 63 hits of cocrystals fenamates. Then also we observed 794 hits for sodium ion, 153 hits for piperazine ion and 43 hits for cytosine ion. These data and refcodes for CSD search are summarized in Table 6.5.

Vibrational Spectroscopy. Nicolet 6700 FT-IR spectrometer with an NXR FT-Raman module was used to record IR spectra. IR spectra were recorded on samples dispersed in KBr pellets. Raman spectra were recorded with the pellet of samples.

^{13}C ss-NMR Spectroscopy. Solid-state NMR spectra were recorded on a Bruker Advance spectrometer operating at 400 MHz (100 MHz for ^{13}C nucleus). ss-NMR spectra were recorded on a Bruker 4 mm double resonance CP-MAS probe in zirconia rotors at 5.0 kHz spin rate with a cross-polarization contact time of 2.5 ms and a recycle delay of 8 s. ^{13}C CP-MAS spectra recorded at 100 MHz were referenced to the methylene carbon of glycine and then the chemical shifts were recalculated to the TMS scale ($\delta_{\text{glycine}} = 43.3$ ppm).

Thermal Analysis. DSC was performed on Mettler Toledo DSC 822e module. Samples were placed in crimped but vented aluminum sample pans. The typical sample size was 3-4 mg, and the temperature range was 30-300 °C at heating rate of 5 °C/min. Samples were purged by a stream of dry nitrogen flowing at 150 mL/min.

Dissolution and Solubility Measurements. Intrinsic dissolution rate (IDR) and solubility measurements were carried out on a USP certified Electrolab TDT-08 L dissolution tester (Electrolab, Mumbai, MH, India). A calibration curve was obtained for all the solid forms by plotting absorbance vs. concentration UV-vis spectra curves on a Thermo Scientific Evolution EV300 UV-vis spectrometer (Waltham, MA) for known concentration solutions in 20%, 50% and 60% EtOH-water solutions medium for clofibric acid, gliclazide and clonixin salt forms. The slope of the plot from the standard curve gave the molar extinction coefficient (ϵ) by applying the Beer-Lambert's law. Equilibrium solubility was determined in EtOH-water solutions medium using the shake-flask method. To obtain equilibrium solubility, 15-200 mg of each solid material was stirred for 24 h in 5-10 mL of EtOH and water solutions at 37 °C, and the absorbance was measured at 229 and 289 nm for gliclazide, clofibric

acid and clonixin. The concentration of the saturated solution was calculated at 24 h, which is referred to as the equilibrium solubility of the stable solid form. The dissolution rates are obtained from the IDR experiments in the same medium at 37 °C.

Powder X-ray Diffraction. PXRDs were recorded on a SMART Bruker D8 Advance X-ray diffractometer (Bruker-AXS, Karlsruhe, Germany) in the Bragg-Brentano geometry using Cu-K α X-radiation ($\lambda = 1.5406 \text{ \AA}$) at 40 kV and 30 mA. Diffraction patterns were collected over the 2θ range of 5-50° at a scan rate of 1°/min. The appearance of new solid phases was monitored by the appearance of new diffraction peaks when comparing with the starting materials. Powder Cell 2.359³⁰ was used for overlaying the experimental XRPD pattern on the calculated lines from the crystal structure.

Melting Point. Fisher-Scientific instrument is used for the determination of melting points of VZL and its solid forms. Samples were taken in less than 1 mg quantity for this study.

6.8 References

1. (a) C. B. Aakeröy, M. Fasulo, J. Desper, *Mol. Pharmaceutics*, **2007**, *4*, 317; (b) S. Mohamed, D. A. Tocher, M. Vickers, P. G. Karamertzanis, S. L. Price, *Cryst. Growth Des.* **2009**, *9*, 2881.
2. P. H. Stahl, M. Nakano, *Pharmaceutical Aspects of the Drug Salt Form. In Handbook of Pharmaceutical Salts: Properties, Selection, and Use*; P. H. Stahl, C. G. Wermuth, Eds.; Wiley-VCH: New York, **2002**; (b) S. Morissette, Ö. Almarsson, M. Peterso, *Adv. Drug Deliv. Rev.*, **2004**, *46*, 3.
3. (a) A. Bond, R. Boese, G. R. Desiraju, *Angew. Chem., Int. Ed.* **2007**, *46*, 615; (b) M. O'Mahony, C. C. Seaton, D. M. Croker, S. Veessler, Å. C. Rasmuson, B. K. Hodnett, *CrystEngComm* **2014**, *16*, 4133.
4. (a) M. Ku, *The AAPS J.*, **2008**, *10*, 208; (b) G. Paulekuhn, J. Dressman, C. Saal, *J. Med. Chem.*, **2007**, *50*, 6665; (c) R. O. Williams III A. B. Watts, D.

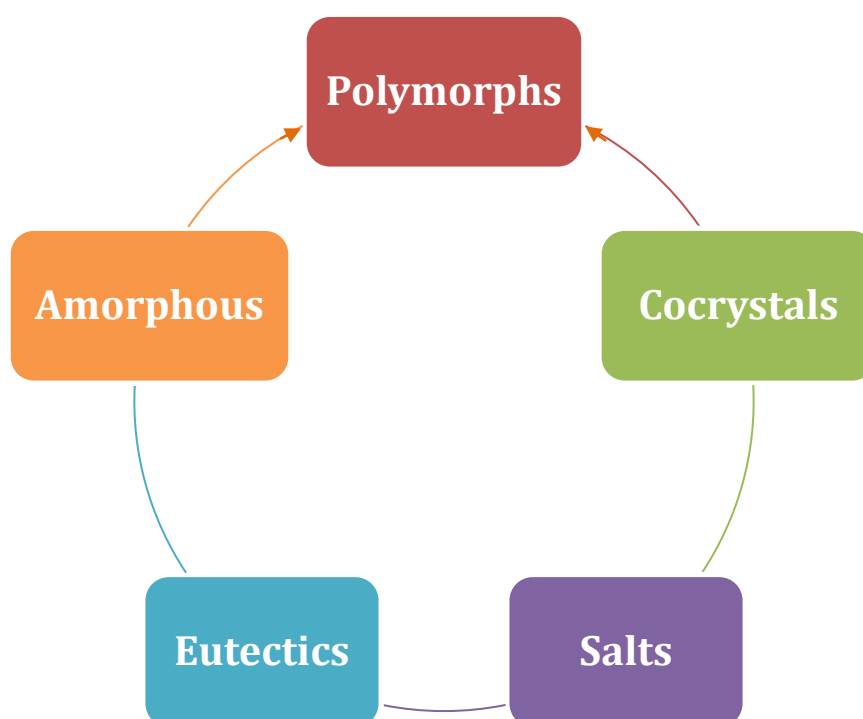
- A. Miller, *Formulating Poorly Water Soluble Drugs*, Springer: London, **2012**; Vol. 3. 1-603.
5. (a) J. Remenar, S. Morissette, M. Peterson, B. Moulton, J. MacPhee, H. Guzman and Ö. Almarsson, *J. Am. Chem. Soc.*, 2003, **125**, 8456; (b) S. S. Kumar, T. Ranjit, A. Nangia, *CrystEngComm*, **2014**, *16*, 4722; (c) S. L. Childs, L. J. Chyall, J. T. Dunlap, V. N. Smolenskaya, B. C. Stahly and G. P. Stahly, *J. Am. Chem. Soc.*, 2004, **126**, 13335; (d) P. Sanphui, S. S. Kumar, A. Nangia, *Crystal Growth & Design* **2012**, *12*, 2147.
 6. (a) A. T. M. Serajuddin, *J. Pharm. Sci.* **1999**, *88*, 1058; (b) P. L. Gould, *Int. J. Pharm.* **1986**, *33*, 201.
 7. (a) R. J. Bastin, M. J. Bowker, B. J. Slater, *Org. Proc. Res. Devel.* **2000**, *4*, 427; (b) A. Serajuddin, *Adv. Drug Deliv. Rev.*, **2007**, *59*, 603.
 8. (a) N. Blagden, M. de. Matas, P. Gavan, P. York, *Adv. Drug Deliv. Rev.*, **2007**, *59*, 617; (b) D. McNamara, S. Childs, J. Giordano, A. Iarriccio, J. Cassidy, M. Shet, R. Mannion, E. O'Donnell, A. Park, *Pharm. Res.* **2006**, *23*, 1888.
 9. (a) P. Sanphui, G. Bolla, A. Nangia, *Cryst. Growth Des.*, **2012**, *12*, 2023; (b) L. Fábíán, N. Hamill, K. Eccles, H. Moynihan, A. Maguire, L. McCausland, S. Lawrence, *Cryst. Growth Des.*, **2011**, *11*, 3522.
 10. (a) L. Rajput, P. Sanphui, G. R. Desiraju, *Cryst. Growth Des.*, **2013**, *13*, 3681; (b) R. Goud, K. Suresh, A. Nangia, *Cryst. Growth Des.*, **2013**, *13*, 1590.
 11. M. Parvez, M. S. Arayne, M. K. Zaman, N. Sultana, *Acta Crystallogr. Sec. C* **1999**, *C55*, 74.
 12. (a) G. R. Desiraju, *Angew. Chem., Int. Ed.*, **1995**, *34*, 1203; (b) C. B. Aakeröy, *Crystal Engineering: The Design and Application of Functional Solids* Ed. Seddon, K. R., Zaworotko, M. Springer, **1999**, 303–324.
 13. (a) R. Tayebjee, V. Amani, H. R. Khavasi, *Chinese J. Chem.* **2008**, *26*, 500; (b) D. Banerjee, J. B. Parise, *Cryst. Growth Des.*, **2011**, *11*, 632.
 14. M. Takasuka, H. Nakai, M. Shiro, *J. Chem. Soc., Perkin Trans. 2* **1982**, 1061.
 15. S. S. Kumar, A. Nangia, *Cryst. Growth Des.*, **2014**, *14*, 6498.
 16. C. Kennard, G. Smith, A. White, *Acta Crystallogr. Sec. B* **1982**, *B38*, 868.

17. (a) A. Nangia, *Acc. Chem. Res.*, **2008**, *41*, 595; (b) A. J. Cruz-Cabeza, J. Bernstein, *Chem. Rev.*, **2014**, *114*, 2170; (c) S. S. Kumar, A. Nangia, *CrystEngComm* **2013**, *15*, 6498.
18. (a) N. K. Nath, A. Nangia, *CrystEngComm*, **2011**, *13*, 47; (b) S. S. Kumar, S.; Rana, A. Nangia, *Chem. Asian J.* **2013**, *8*, 1551.
19. (a) G. Balendiran, N. Rath, A. Kotheimer, C. Miller, M. Zeller, N. Rath, *J. Pharm. Sci.* **2012**, *101*, 1555; (b) N. B. Báthori, A. Lemmerer, G. A. Venter, S. A. Bourne, M. R. Caira, *Cryst. Growth Des.*, **2011**, *11*, 75.
20. <http://en.wikipedia.org/wiki/Sulfonylurea>
21. Cambridge Structural Database, ver. 5.35, ConQuest 1.16, November 2013 release, Cambridge Crystallographic Data Center, www.ccdc.cam.ac.uk.
22. T. N. Drebuschak, N. A. Pankrushina, A. N. Mikheev, M. K. A. Thumm, *CrystEngComm*, **2013**, *15*, 3582.
23. (a) A. J. Cruz-Cabeza, *CrystEngComm*, **2012**, *14*, 6362; (b) S. L. Childs, G. P. Stahly and A. Park, *Mol. Pharm.*, **2007**, *4*, 323; (c) S. S.; Kumar, R.; Thakuria, A. Nangia, *CrystEngComm*, **2014**, *16*, 4722.
24. (a) S. Seethalekshmi, T. N. G Row, *Cryst. Growth Des.*, **2012**, *12*, 4283; (b) M. S. Fonari, E. V. Ganin, A. V. Vologzhanina, M. Y. Antipin, V. C. Kravtsov, *Cryst. Growth Des.*, **2010**, *10*, 3647; (c) A. Lemmerer, S. A. Bourne, M. R. Caira, J. Cotton, U. Hendricks, L. C. Peinke, L. Trollope, *CrystEngComm* **2010**, *12*, 3634; (d) S. S. Kumaresan, P.G. Seethalakshmi, P. Kumaradhas, B. Devipriya, *J. Molec. Struct.* **2013**, *1032*, 169.
25. (a) A. Llinàs, J. Burley, K. Box, R. Glen, J. Goodman, *J. Med. Chem.* **2007**, *50*, 979; (b) G. Petruševski, P. Naumov, G. Jovanovski, S. W. Ng *Inorg. Chem. Communi.* **2008**, *11*, 81.
26. C. Castellari, S. Ottani, *Acta Crystallographica. Sec. C: Cryst. Struct. Communi.* **1998**, *54*, 415.
27. (a) S. Berge, L. Bighley, D. Monkhouse, *Pharm. Sci.* **1977**, *66*, 1; (b) P. Sanphui, S. Tothadi, S. Ganguly, G. R. Desiraju, *Mol. Pharmaceutics*, **2013**, *10*, 4687; (c) P. Sanphui, G. Bolla, A. Nangia, V. Chernyshev, *IUCrJ.* **2014**, *1*, 136.
28. (a) Oxford Diffraction. CrysAlis CCD and CrysAlis RED, versions 1.171.33.55; Oxford Diffraction Ltd: Yarnton, Oxfordshire, UK, **2008**; O. V.

- Dolomanov, L. J. Bourhis, R. J. Gildea, J. A. K. Howard, H. Puschmann, OLEX2: A complete structure solution, refinement and analysis program. *J. Appl. Crystallogr.* **2009**, 42, 339; (b) G. M. Sheldrick, *SHELXS-97* and *SHELXL-97, Program for the Solution and Refinement of Crystal Structures*, University of Göttingen, Germany, **1997**; (c) A. L. Spek, PLATON, A Multipurpose Crystallographic Tool; Utrecht University: Utrecht, Netherlands, **2002**. A. L. Spek, Single-crystal Structure Validation with the Program PLATON. *J. Appl. Crystallogr.* **2003**, 36, 7.
29. L. J. Barbour, X-Seed, *Graphical Interface to SHELX-97 and POV-Ray*, University of Missouri-Columbia, USA, **1999**.
30. N. Kraus, G. Nolze, Powder Cell, version 2.3, A Program for Structure Visualization, Powder Pattern Calculation and Profile Fitting; Federal Institute for Materials Research and Testing: Berlin, Germany, **2000**.

Chapter Seven

Conclusions and Future Prospects



Several aspects of solid forms such as polymorphism, cocrytals, salts, eutectics/solid solutions and amorphous phases are available to understand and develop the physic-chemical behavior of pharmaceutical solids in the pharmaceutical form development and intellectual property management for drug commercialization.

7.1 Solid Dosage Forms and Its Formulation Techniques

The main goal in the research area of oral dose pharmaceuticals is to explore the solid-state properties of the drug formulation. Dosage forms (or unit doses) are essentially pharmaceutical products in the form in which they are marketed for use, typically involving a mixture of active drug components and nondrug components (excipients/coformers), along with other non-reusable (polymers) materials that may not be considered either ingredient or packaging (capsule shell). This property depends upon the function of the pure drug and therefore it requires the solid-state characterization of the drug substance to know the properties of the crystalline or amorphous forms. Hence the property of any drug must be thoroughly studied before the making the final dosage form. The important properties are high solubility, fast dissolution rate, good bioavailability, stability of the form, and compressibility of the tablet. The goal is to tune these properties by controlling the crystalline arrangement of molecules in the lattice. For example, polymorphs, cocrystal, salts and eutectics can have direct impact on drug properties as discussed in several chapters of this thesis. Nowadays these properties are analyzed by many characterization techniques such as microscopy, FT-IR, Raman, ss-NMR, thermogravimetric analysis (TGA), differential scanning calorimetry (DSC), Karl Fischer titration, single crystal and powder X-ray diffractometer, and surface and morphology and particle size analysis. Several of these characterizations and improvements in the drug products were investigated in the work presented in this thesis.

In chapter 2, the single crystal X-ray technique was used to identify the crystal structure of cardiosulfa and its polymorphic analogs. These X-ray structures were systematically studied and analyzed for solubility trends with respect to the molecular conformations of different active sulfonamides. A few new polymorphs were identified for many sulfonamides using powder X-ray techniques and their physical and chemical properties such as phase transitions and thermodynamic stability order were established by using the DSC. The

crystal structures of polymorphs were analyzed to find the different hydrogen bonding pattern in the structures and their impact on solubility was studied. Planar molecules pack more efficiently in the crystal lattice and consequently they are less soluble whereas molecules with a bent molecular conformation were found to have higher solubility, perhaps due to slightly loose packing. Polar hydrogen bonds in a polymorph give high solubility compared to other polymorphs having only short contacts or less polar interactions. So these structure–property comparisons of molecular conformation and hydrogen bonding pattern with solubility property could open a new strategy for controlling and improving the solubility of lead drug molecules by changing the functional groups in the discovery stage itself.

In chapter 3, many polymorphs of 2-ABA, 3-ABA (aminobenzoic acids) and Clonixin were fully identified by powder X-ray diffraction method and characterized by IR, Raman and ss-NMR spectroscopy techniques. The thermodynamic relationships and phase transition between the neutral and zwitterionic polymorphs was analyzed by DSC and VT-PXRD. The solubility and dissolution rates of neutral and zwitterionic polymorphs are taken into account because several drugs are amphoteric in nature. We expect that such a comparison will offer a better understanding of neutral and zwitterionic polymorphs for such molecules. As expected, both solubility and stability are good with zwitterionic polymorphs but normally these two properties are inversely related for many polymorphic systems. We have optimized zwitterionic polymorph for clonixin drug and other model compounds with greater stability and higher solubility. This comparison provides a direction to crystallize ionic polymorphs of amphoteric drugs for solubility enhancement. In contrast to cardiosulfa work, the solubility property can be changed using crystallization techniques without any modification of covalent bonds in the drug molecules.

Chapter 4 is about the stability comparison of two polymorphs of *N*-acetyl-L-cysteine (NAC) under thermal and ambient conditions. DSC is used to establish the thermal stability and thermodynamic relationship between NAC

forms I and II as enantiotropes. Under ambient conditions, the transformation of new polymorph NAC II to the thermodynamic stable form I by grinding, slurry or storage was noted. The difference between two polymorphs was compared by FT-IR, Raman, ^{13}C ss-NMR spectroscopy techniques. These characterization techniques are useful in this system to identify the undesirable polymorph formation during the storage of drugs. The stability of form I is due to the presence of strong hydrogen bonding in the crystal structure which is absent in form II.

Cocrystals and salts are the best methods to solve the pharmaceutical issues associated with drugs as oral dosage forms. In fact more than 50% of drugs are marketed as salts, and pharmaceutical cocrystals are in a peak developmental stage. Cocrystals and salts were successfully implemented to improve the drug property of Voriconazole (Chapter 5). All the solid forms of voriconazole were characterized by single crystal X-ray diffraction and further confirmed by powder XRD. The crystal structures are used to find out the type of synthons in the structures and there is a synthon switch from acid–pyrimidine to acid–triazole synthon depending upon the $\text{p}K_{\text{a}}$ of the coformer acid. The isomorphous/3D isostructurality between PHBA and PABA cocrystals of voriconazole provides a reason of solubility relationship with the hydrogen bonding pattern in the two cocrystals. The stability, good solubility and dissolution of VZL–PABA cocrystal and the dinitrate salt of voriconazole can be a better solution for formulation development of low solubility voriconazole drug.

Salt formulation can be widely used for all BCS classified drugs especially when other techniques failed to yield good results. For example, the application of polymorphs and cocrystals are limited to some of the drugs in improving the drug properties i.e., the effect of dissolution rate of BCS class I and III drug polymorphs on bioavailability and consideration of cocrystals as drug intermediates by FDA. In those cases, salt formation can be a better solution to make new solid forms for improving the bioavailability of drugs in I and III categories. The BCS class II/IV drugs have low solubility in water i.e., the low

aqueous soluble drugs such as gliclazide, clonixin and clofibric acid were undertaken based on this approach and improved their solubility property successfully to about 10 times higher than the parent drugs. All these salts were characterized by single crystal and powder X-ray diffraction methods. Solid-state spectroscopy was used to identify these new salts further from the drug substances. Finally, the comparison of molecular salt with mineral salts in terms of drug property suggests that these organic molecular salts are also having the equal solubility advantage to the mineral salts. The term molecular salt is taken into account in situations where both anion and cation are derived from organic acidic and basic molecules or organic electron acceptor and donor species wherein mineral salt one of the counter ion must be from inorganic elements as either cation or anion. Organic counter ions are larger in size and it contains some of the lipophilic functionalities involved in strong $\text{O}^- - \text{H} \cdots \text{N}^+$, $\text{N}^+ - \text{H} \cdots \text{O}^-$, $\text{N}^+ - \text{H} \cdots \text{N}$ hydrogen bonds in the crystal structure causes the salts to be less soluble. The metal cations or other inorganic anions are smaller in size means that a salt component can be easily split by the solvent molecules into its two ions and the dissociated ions will be surrounded by a shell of water molecules immediately after the solvation. The melting point differences between the molecular salt and mineral salt with respect to the parent molecule is high that indicated the strong ionic interactions are present in the mineral salt. The solubility of mineral salt is higher than the molecular salt and indicates inorganic ions in molecular salts are more prone solvation because of the ionic size effects.

The model compounds and drugs studied in this thesis belong to the broad category of drug classification such as sulfonamides, amphoteric compounds, amino acids, antifungal azole drugs, sulfonylureas, fibrates and fenamates and hence there is a need to explore the same structure-property relationship for these more number of drugs in each of these categories. The idea of expanding the study of polymorph screening and crystal engineering strategies to the other drugs should provide interesting directions to solve the pharmaceutical development challenges.

In the course of searching new polymorphs for some of the molecules reported in this thesis, occasionally reproducibility problems were faced and some of the drugs are non-polymorphic. New polymorphs of cardiosulfa and a few amphoteric drugs using some of the newer methods and high through put crystallization techniques can be taken up in the future, e.g. control of supersaturation level, control of nucleation temperature, solvent screening, heating and sublimation of the materials, low temperature and high temperature evaporation, rotovapor fast evaporation, seeding technology, capillary crystallization, introduction of additives, polymer-induced hetero-nucleation, nucleation confined in nanopores, heteronucleation on substrates such as ionic liquids and gels, laser-induced nucleation, etc. .

Multi-component systems such as salts, cocrystals and eutectic compositions are alternative methods to polymorphs to address the physico-chemical challenges of low aqueous solubility drugs with limited bioavailability. Salts are well established in the field to make alternate formulation dosage forms and recently cocrystals have been developed in research labs, but eutectic compositions are not well explored in this regard. Moreover, it is limited with only DSC characterization techniques and thus new analytical techniques such as atomic pair distribution function (PDF) is a possible solution. New pharmaceutical solids such as polymorphs, cocrystals, salts, eutectic composition and amorphous phases and the factors that influence their structure-property relationships will be a fruitful area for further investigations. Several formulation techniques such as micronization, nanosizing, or complexation with cyclodextrins are also reported in the literature to increase aqueous solubility and consequently improve drug bioavailability. The incorporation of works described in this thesis with these developmental studies would open a wide range of strategies to address pharmaceutical development issues in the present decade. This will be an excellent translation from crystal engineering strategies to their application in pharmaceutical formulation.

List of Publications

1. Neutral and Zwitterionic Polymorphs of 2-(*p*-Tolylamino)nicotinic Acid.
N. K. Nath, **S. Sudalai Kumar** and A. Nangia *Cryst. Growth & Des.*, **2011**, *11*, 4594.
(IUCr best poster award in ICCOSS 2011 conference)
2. Pharmaceutical Cocrystals of Niclosamide.
P. Sanphui, **S. Sudalai Kumar** and A. Nangia *Cryst. Growth & Des.*, **2012**, *12*, 4588.
3. Solid-state Form Screen of Cardiosulfa and Its Analogs.
S. Sudalai Kumar, S. Rana and A. Nangia *Chem. Asian J.* **2013**, *8*, 1551.
4. A new Conformational Polymorph of *N*-acetyl-L-cysteine, The role of S–H···O and C–H···O interactions.
S. Sudalai Kumar and A. Nangia *CrystEngComm*, **2013**, *15*, 6498.
5. Pharmaceutical Cocrystals and a Nitrate Salt of Voriconazole
S. Sudalai Kumar, R. Thakuria and A. Nangia *CrystEngComm*, **2014**, *16*, 4722.
Special Theme issue of CEC on India **IYCr 2014** Celebration.
6. A Solubility Comparison of Neutral and Zwitterionic Polymorphs.
S. Sudalai Kumar and A. Nangia *Cryst. Growth & Des.*, **2014**, *14*, 1865.
Virtual special issue **IYCr 2014** - Celebrating the International Year of Crystallography.
7. New Pharmaceutical Salts of Gliclazide, Clonixin and Clofibric acid.
S. Sudalai Kumar and A. Nangia, **2014** (Manuscript in preparation).

Activities in National and International Events

- ♣ Delivered a flash presentation on the topic of ***Structure Property Correlation of Neutral and Zwitterionic Polymorphs*** in ***K. V. Rao Award 2014*** at University of Hyderabad, India.
- ♣ Delivered a flash presentation on the topic of ***Comparison of Stability and Solubility of Neutral, Zwitterionic and Conformational Polymorphs*** in ***ChemFest 2014*** at University of Hyderabad, India.
- ♣ Delivered a flash and poster presentation on the topic of ***Polymorph Screen and Characterization of Cardiosulfa and Its Analogs*** in ***ICCOSS 2013*** at University of Oxford, Oxford, UK.
- ♣ Poster presentation on the topic of ***Characterization of Isostructural Solid Forms of APIs*** in ***MED-CHEM 2013*** conference held at IIT-Madras, India.
- ♣ Poster presentation on the topic of ***Characterization of Isostructural Solid Forms of APIs*** in ***AP Science Congress Meet 2013*** conference held at University of Hyderabad, India.
- ♣ Poster presentation on the topic of ***Solid-state Forms of Cardiosulfa and Its Analogs*** in ***ChemFest 2012*** conference held at University of Hyderabad, India.
- ♣ Poster presentation on the topic of ***Solid-state Forms of Cardiosulfa and Its Analogs*** in ***INDO-US 2012*** conference held at IIT-Delhi.
- ♣ IUCr best awards poster presentation on the topic of ***Neutral and Zwitterionic Polymorphs of 2-(p-Tolylamino)nicotinic acid (TNA)*** in international conference ***ICCOSS 2011*** held in IISc Bangalore.
- ♣ Poster presentation and participation on the topic of ***Solid-state Forms of Cardiosulfa and Its Analogs*** in ***IYC 2011*** conference and Science exhibition, demonstration and participation in ***IYC 2011*** program at School of chemistry, University of Hyderabad, India.

Appendix

Crystallographic data for the crystal structures discussed in this thesis

Compounds	1	2	3
Polymorphs	Form I	Form I	Form I
Empirical formula	C ₂₁ H ₁₆ F ₃ N ₃ O ₄ S	C ₂₁ H ₁₇ F ₃ N ₂ O ₂ S	C ₂₁ H ₁₇ F ₃ N ₂ O ₂ S
Formula weight	463.44	418.44	418.44
Crystal system	Monoclinic	Monoclinic	Triclinic
Space group	$P2_1/n$	$P2_1$	$P\bar{1}$
a (Å)	15.6328(10)	13.5320(10)	8.2089(10)
b (Å)	5.6402(4)	5.0764(3)	8.3534(10)
c (Å)	22.2846(14)	14.7251(12)	13.9725(17)
α (°)	90	90	91.917(2)
β (°)	98.2520(10)	97.781(7)	106.454(2)
γ (°)	90	90	95.941(2)
V (Å ³)	1944.5(2)	1002.21(12)	911.97(19)
D_{calcd} (g cm ⁻³)	1.583	1.387	1.524
μ (mm ⁻¹)	0.232	0.208	0.229
θ range (°)	2.63–26.08	2.78–26.31	2.46–26.05
Z/Z'	4/1	2/1	2/1
Range h	−18 to 18	−15 to 16	−10 to 10
Range k	−6 to 6	−5 to 6	−10 to 10

Range l	−26 to 26	−12 to 18	−17 to 17
Reflections collected	16101	4196	9424
Observed reflections	3421	3459	3591
Total reflections	3149	1952	3209
R_1 [$I > 2 \sigma(I)$]	0.0578	0.0769	0.0466
wR_2 (all)	0.1540	0.1648	0.1104
Goodness-of-fit	1.053	0.989	1.096
T (K)	100	298	100
X-ray diffractometer	Bruker SMART APEX	Oxford Xcalibur Gemini	Bruker SMART APEX
4	4	5	5
Form I	Form II	Form I	Form II
$C_{20}H_{17}N_3O_4S$	$C_{20}H_{17}N_3O_4S$	$C_{20}H_{17}N_3O_4S$	$C_{20}H_{17}N_3O_4S$
395.44	395.44	395.44	395.44
Orthorhombic	Triclinic	Orthorhombic	Triclinic
$Pbca$	$P\bar{1}$	$Pbca$	$P\bar{1}$
14.5064(18)	8.2781(11)	14.5064(18)	8.2781(11)
9.6887(13)	8.3657(13)	9.6887(13)	8.3657(13)
27.895(4)	13.9362(18)	27.895(4)	13.9362(18)
90	91.966(12)	90	91.966(12)
90	106.506(11)	90	106.506(11)
90	94.686(11)	90	94.686(11)

3920.5(9)	920.6(2)	3920.5(9)	920.6(2)
1.340	1.427	1.340	1.427
0.196	0.209	0.196	0.209
2.79–24.96	2.80–26.31	2.79–24.96	2.80–26.31
8/1	2/1	8/1	2/1
–17 to 14	–10 to 10	–17 to 14	–10 to 10
–11 to 11	–10 to 9	–11 to 11	–10 to 9
–33 to 27	–17 to 17	–33 to 27	–17 to 17
9500	7280	9500	7280
3463	3762	3463	3762
2032	2558	2032	2558
0.0464	0.0526	0.0464	0.0526
0.1258	0.1289	0.1258	0.1289
0.910	1.032	0.910	1.032
298	298	298	298
Oxford Xcalibur Gemini	Oxford Xcalibur Gemini	Oxford Xcalibur Gemini	Oxford Xcalibur Gemini
6	NAC-I	NAC-II	Reported NAC
Form I	Form I	Form II	Form I
C ₂₀ H ₁₈ N ₂ O ₂ S	C ₅ H ₉ N O ₃ S	C ₅ H ₉ N O ₃ S	C ₅ H ₉ N O ₃ S
350.43	163.19	163.19	163.19
Monoclinic	Triclinic	Orthorhombic	Triclinic
<i>C2/c</i>	<i>P1</i>	<i>P2₁2₁2₁</i>	<i>P1</i>

20.315(5)	5.1041(7)	6.0684(6)	5.766(1)
12.318(6)	5.9092(8)	7.6372(9)	6.433(1)
17.402(4)	6.5261(10)	16.005(2)	5.014(1)
90	96.484(12)	90	102.80(2)
125.269(15)	103.696(13)	90	102.77(1)
90	101.969(11)	90	95.81(1)
3555(2)	184.34(4)	741.74(15)	174.656(6)
1.309	1.470	1.461	1.552
0.197	0.386	0.384	0.2318
2.87–28.82	3.26–26.37	2.94–26.30	
8/1	1/1	4/1	$Z/Z' = 1/1$
–22 to 21	–6 to 5	–7 to 6	
–13 to 11	–7 to 7	–9 to 5	
–19 to 19	–5 to 8	–20 to 18	
5370	1129	2080	
1832	937	1341	
2468	887	1057	
0.0731	0.0522	0.0538	0.024
0.2185	0.1418	0.0864	
1.066	1.105	1.109	
298	298 K	298 K	T = 16 K
Oxford Xcalibur Gemini	Oxford Xcalibur Gemini	Oxford Xcalibur Gemini	Neutron diffraction

VZL–HNO ₃	VZL–PHBA	VZL–PABA	VZL–3-NBA
Salt	Cocrystal	Cocrystal	Cocrystal
C ₁₆ H ₁₆ F ₃ N ₇ O ₇	C ₂₃ H ₂₀ F ₃ N ₅ O ₄	C ₂₃ H ₂₁ F ₃ N ₆ O ₃	C ₂₃ H ₁₉ F ₃ N ₆ O ₅
475.36	487.44	486.46	516.44
Orthorhombic	Monoclinic	Monoclinic	Monoclinic
<i>P</i> 2 ₁ 2 ₁ 2 ₁	<i>P</i> 2 ₁	<i>P</i> 2 ₁	<i>P</i> 2 ₁
9.1515(9)	13.7102(5)	13.674(11)	11.5743(5)
13.1275(13)	6.04623(17)	6.085(5)	6.7286(2)
16.1908(16)	14.2265(5)	14.196(11)	14.9073(6)
90	90	90	90
90	107.314(4)	106.543(12)	97.526(4)
90	90	90	90
1945.1(3)	1125.87(7)	1132.4(15)	1150.96(8)
1.623	1.438	1.427	1.490
0.147	0.117	0.114	0.124
2.00–26.06	2.93– 24.96	2.44–22.71	2.75–26.31
4/1	2/1	2/1	2/1
–11 to 11	–16 to 10	–16 to 16	–13 to 14
–16 to 16	–6 to 6	–7 to 7	–7 to 8
–19 to 19	–16 to 16	–17 to 17	–18 to 17
20312	3814	11761	5175
3830	3071	4474	3868
3753	2831	3718	2649
0.0305	0.0345	0.0540	0.0384

0.0768	0.0933	0.1123	0.0750
1.059	1.086	1.137	0.911
100	298	298	298
Bruker SMART APEX	Oxford Xcalibur Gemini	Bruker SMART APEX	Oxford Xcalibur Gemini
GLZ	GLZ-Na	CLX-CYT	CLX-PIP
Salt	Salt	Salt	Salt
C ₁₅ H ₂₁ N ₃ O ₃ S	C ₁₅ H ₂₁ N ₃ O ₃ S Na	C ₁₇ H ₁₆ Cl N ₅ O ₃	C ₁₅ H ₁₆ Cl N ₃ O ₂
323.42	345.40	373.80	305.76
Monoclinic	Monoclinic	Triclinic	Monoclinic
<i>P</i> 2 ₁ /n	<i>P</i> 2 ₁ /c	<i>P</i> $\bar{1}$	<i>P</i> 2 ₁ /n
10.7901(14)	15.3787(13)	7.2017(8)	16.246(2)
14.299(2)	9.8248(5)	10.5681(13)	12.6435(8)
10.9828(13)	12.2850(8)	11.8941(13)	8.0873(10)
90.00	90	71.111(11)	90
106.971(13)	109.649(8)	82.807(9)	122.927(18)
90.00	90	74.951(10)	90
1620.7(4)	1748.1(2)	826.28(17)	1394.3(3)
1.769	1.316	1.502	1.457
0.216	0.226	0.261	0.282
26.370	26.370	3.19-28.40	3.26- 29.13
4/1	4/1	2/1	4/1
-12 to 13	-19 to 11	-8 to 8	-20 to 11

-9 to 17	-10 to 12	-13 to 12	-14 to 15
-13 to 13	-15 to 15	-14 to 13	-9 to 10
6063	7118	5507	5209
3301	2678	3360	2847
2131	3560	2544	2338
0.2008	0.0481	0.0748	0.0390
0.4757	0.1291	0.0922	0.1091
1.030	1.034	1.059	1.025
298	298	298	298
X- ray diffractometer Oxford Xcalibur Gemini	X- ray diffractometer Oxford Xcalibur Gemini	X- ray diffractometer Oxford Xcalibur Gemini	X- ray diffractometer Bruker SMART APEX
CLF-PIP	CLF-CYT	CLF-I	
Salt	Salt	Salt	
C ₁₂ H ₁₆ NO ₃ Cl	C ₁₈ H ₂₃ N ₆ O ₆ Cl	C ₁₀ H ₁₁ O ₃ Cl	
257.71	454.87	214.64	
Monoclinic	Monoclinic	Monoclinic	
<i>P</i> 2 ₁ / <i>n</i>	<i>C</i> 2	<i>P</i> 2 ₁ / <i>n</i>	
5.996(2)	18.957(2)	6.3269(9)	
27.929(10)	6.3853(6)	7.9567(6)	
7.867(3)	18.4827(19)	21.1046(18)	
90.00	90	90	
103.895(6)	102.917(10)	89.973(11)	

90.00	90	90
1278.9(8)	2180.6(4)	1062.4(2)
1.338	1.386	1.342
0.295	0.222	0.338
2.77 -26.17	2.69-26.36	2.73-26.36
4/1	4/1	4/1
-7 to 7	-23 to 11	-6 to 7
-34 to 34	-7 to 7	-9 to 9
-9 to 9	-20 to 23	-26 to 26
13175	4358	2964
2561	3696	1636
2103	1949	1267
0.0418	0.0976	0.0455
0.1092	0.1436	0.1117
1.026	1.110	1.074
298	298	298
X- ray diffractometer Oxford Xcalibur Gemini	X- ray diffractometer Oxford Xcalibur Gemini	X- ray diffractometer Oxford Xcalibur Gemini
